ISOMETRICA

A GEOMETRICAL INTRODUCTION TO PLANAR CRYSTALLOGRAPHIC GROUPS

in memory of Professor Rinaldo Prisco

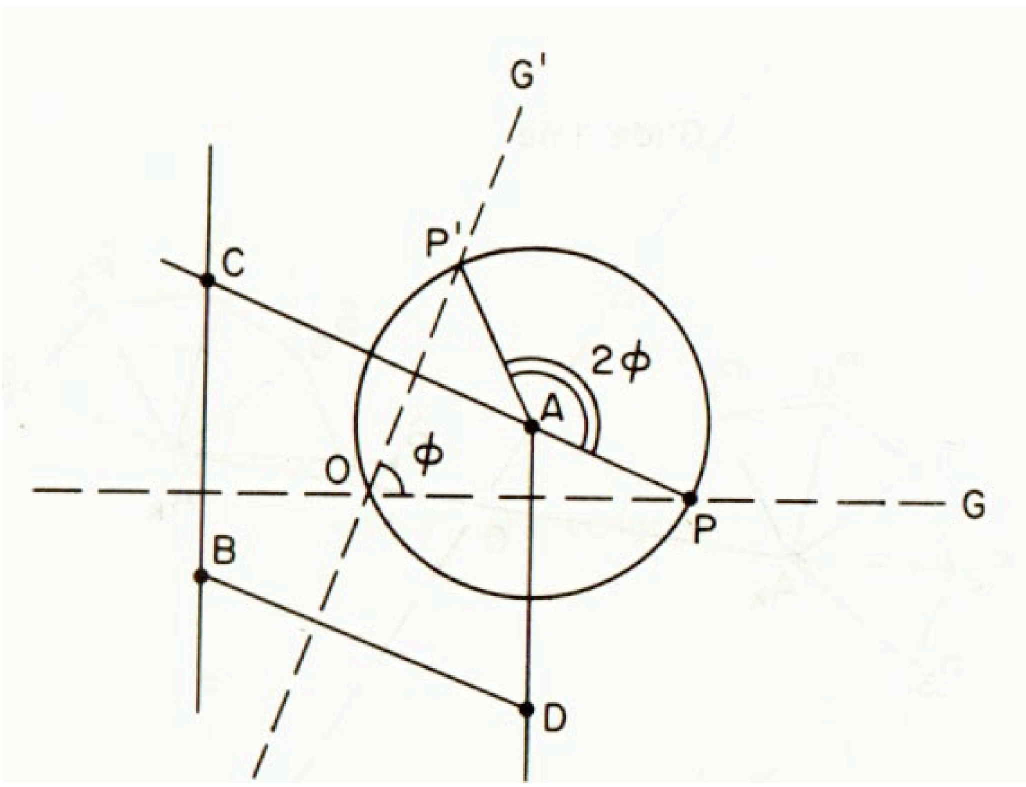

Fig. 28 Intersecting glide lines
[Arthur L. Loeb, *Color and Symmetry* (Wiley 1971, Krieger 1978)]

GEORGE BALOGLOU

SUNY OSWEGO, 2007

ISBN 978-0-9792076-0-0

ὅτι δὲ σεμνὴ ἡ ἁρμονία καὶ θεῖόν τι καὶ μέγα,
Ἀριστοτέλης ὁ Πλάτωνος ταυτὶ λέγει "ἡ δὲ ἁρμονία ἐστὶν οὐρανία τὴν φύσιν ἔχουσα θείαν καὶ καλὴν καὶ δαιμονίαν· τετραμερὴς δὲ τῇ δυνάμει πεφυκυῖα δύο μεσότητας ἔχει ἀριθμητικήν τε καὶ ἁρμονικήν, φαίνεταί τε τὰ μέρη αὐτῆς καὶ τὰ μεγέθη καὶ αἱ ὑπεροχαὶ κατ' ἀριθμὸν καὶ **ἰσομετρίαν·** ἐν γὰρ δυσὶ τετραχόρδοις ῥυθμίζεται τὰ μέρη"

Aristotle (?), Fragmenta Varia 47 (Pseudo-Plutarchus, *De Musica*)

In the study of geometry, one is constantly confronted with groups of transformations on various "spaces." Many of these groups consist simply of the symmetries of those spaces with respect to suitably chosen properties. An obvious example is furnished by the symmetries of the cube. Geometrically speaking, these are the one-one transformations which preserve distances on the cube. They are known as **"isometries,"** and are 48 in number.

Birkhoff & MacLane, *Survey of Modern Algebra* (1941), p. 127

INTRODUCTION

Symmetry is a vast subject, significant in art and nature. Mathematics lies at its root, and it would be hard to find a better one on which to demonstrate the working of the mathematical intellect. I hope I have not completely failed in giving you an indication of its many ramifications, and in leading you up the ladder from intuitive concepts to abstract ideas. – Herman Weyl, ***Symmetry*** (Princeton, 1952)

Why and how ***Isometrica***, and who would read it?

Back in Spring 1995, one of my SUNY Oswego students submitted the following one-sentence teacher evaluation: "The course was relatively easy until chapter 11 when I felt that the instructor was as lost as the students"! Chapter 11 -- typically associated with bankruptcy in the so-called 'real world' -- was in that case the symmetry chapter in Tannenbaum & Arnold's ***Excursions in Modern Mathematics***: I had casually picked it as one of two 'optional' chapters in my section of MAT 102 (SUNY Oswego's main General Education course for non-science majors, consisting of various mathematical topics).

Perhaps that anonymous student's not entirely unjustified comment was the best explanation for my decision to volunteer to teach ***MAT 103***, a General Education course devoted entirely to Symmetry, in Fall 1995: better yet, *curiosity killed the cat* -- once I started teaching ***MAT 103*** I never took a break from it, gradually abandoning my passion for rigor and computation in favor of intuition and visuality.

But where had ***MAT 103*** come from? Following a January 1991 MAA minicourse

(***Symmetry Analysis of Repeated Patterns***) by Donald Crowe at the San Francisco Joint Mathematics Meetings, my colleague Margaret Groman developed (Fall 1992) a new course (***Symmetry and Culture***) in response to our General Education Board's call for courses fulfilling the newly introduced Human Diversity requirement: after all, was Professor Groman not an algebraist keenly interested in applications of Abstract Algebra (to symmetry for example), and had Professor Crowe not co-authored a book with anthropologist Dorothy Washburn titled ***Symmetries of Culture*** (Univ. of Washington Press, 1988)?

MAT 103 ceased to fulfill the Human Diversity requirement and was renamed ***Symmetries*** in Spring 1998, but it remained quite popular among non-science majors as a course fulfilling their Mathematics requirement; it also attracts a few Mathematics majors now and then. At about the same time I set out (initially in collaboration with Margaret Groman) to write a book -- not the least because ***Washburn & Crowe*** had temporarily gone out of print -- that was essentially completed in three stages: January 1999 (chapters 1-5), January 2000 (chapter 6), and August 2001 (chapters 7 & 8). Various projects and circumstances delayed ‘official’ completion until November 20, 2006 (the day a new computer forcefully arrived), with the first six chapters posted on my ***MAT 103*** web site (***http://www.oswego.edu/~baloglou/103***) as of Fall 2003. In spite of my endless proofreading and numerous small changes, what you see here is very close in both spirit and content to the August 2001 version. [For the record, I have only added 'review' section 6.18 and subsections 1.5.3 & 4.17.4, and also added or substantially altered figures 4.73, 5.36, 6.121, 6.131, 7.44, and 8.3.]

My initial intent was to write a student-oriented book, a text that our ***MAT 103*** students -- and, why not, students and also ‘general’ readers elsewhere -- would enjoy and use: this is why it has been written in such unconventional style, and in the second person in particular; in a different direction, this is why it relies on minimal Euclidean Geometry rather than Abstract Algebra. Looking now at the finished product, I can clearly see a partial failure: the absence of exercises and other frills (available to considerable extent through the ***MAT 103*** web site), together with an abundance of detail (also spilling into the ***MAT 103*** web site), *may* have conspired toward turning a perceived student's book into a teacher's book. Beyond students and teachers, and despite its humble origins, there may also be some specialists interested in ***Isometrica***: I will attempt to address these three plausible audiences in considerable detail below; you may wish to skip these three sections at first reading and proceed to the end of the Introduction.

Comments for students and general readers

What is this book about, and how accessible is it?

Donald Crowe's 'repeated patterns', better known nowadays as frieze/border patterns and wallpaper patterns, may certainly be viewed as one of the very first mathematical (even if accidentally so) creations of humankind: long before they were recognized as the poor relatives of the three-dimensional structures so dear to modern scientists, these *planar crystallographic groups* were being discovered again and again by repetition/symmetry-seeking native artists in every corner of the world. This book's goal is therefore the gradual unveiling of the structural and the mathematical that hides behind the visual and the artistic: so chapters 2 - 4, and even chapters 5 and 6, are more eye-pleasing than mind-boggling, while chapters 7 and 8 certainly require more of the reader's attention. It is fair to say that a determined reader can read the entire book relying only on some high school mathematics.

Why is Chapter 1 here to begin with?

Good question: this is the only chapter with some algebra (read analytic geometry) in a heavily geometrical book! The simple answer is that the General Education Committee of SUNY Oswego would not approve [Spring 1998] a mathematical course without some mathematical formulas in it... And it took me a while to come up with a constructive/creative way of incorporating some formulas into ***MAT 103***, simply by providing an analytical description -- and, quite unintentionally, classification -- of the four planar isometries (that is, the four possible types of distance-preserving transformations of the plane).

So, if you are not algebraically inclined, don't hesitate to skip chapter 1 at first reading: the four planar isometries are indirectly reintroduced in the much more reader-friendly chapter 2, save for the general rotation, as well in chapters 3 and 4. (At the other end, some readers may be interested *only* in chapter 1, which is, I hope, a very accessible and engaging introduction to planar isometries, relying on neither matrices nor complex numbers.)

Any other reading tips, dear professor?

I have no illusions: most of you are going to merely browse through my book, even if you happen to be a student whose GPA depends on it... Well, save for the potentially attractive figures, this book is not browser-friendly: its conversational style may be tiring to some, and the absence of 'summary boxes' depressing to others; and let's not forget a favorite student's remark to the effect that "it is odd that in a book titled ***Isometrica*** there is no definition of isometry"! But those figures *are* there, slightly over one per page on the average, and most of them are interesting at worst and seductive at best (me thinks): so start by looking at appealing figures, then read comments related to them, then read stuff related to those comments, and ... before you know it you will have read everything! After all, this book *talks* to you -- are you willing to listen? (My thanks to another former student for this 'talking-to-me book' comment!)

Why is there no bibliography?

Both because ***Isometrica*** is totally self-contained and because suggestions for further reading are always made in the text (including this introduction) and in context. Moreover, ***Washburn & Crowe*** provides a rather comprehensive bibliography to which I would have little to add... But if you ask me for *one* book that you could or should read *before* mine, I would not hesitate to recommend Peter Stevens' ***Handbook of Regular Patterns*** (MIT Press, 1981): that is any math-phobic's dream book and, although I follow it in neither its 'kaleidoscopic' approach nor its 'multicultural' focus, several figures from ***Stevens*** have been included in ***Isometrica*** (with publisher’s permission) as a tribute.

What is there for the non-mathematically inclined?

Despite the inclusion of patterns from ***Stevens***, my book -- as well as ***MAT 103*** in both its present and past forms -- fails to address in depth the cultural aspects of those patterns and the 'inner motives' of the native artists who created them: nothing like Paulus Gerdes' ***Geometry From Africa*** (Mathematical Association of America, 1999) or Washburn and Crowe's second book (with updated bibliography), ***Symmetry Comes of Age*** (Univ. of Washington Press, 2004). Still, I must mention a telling incident: a former student made once a deal with a quilt maker friend of hers involving the exchange of her copy of ***Isometrica*** for a quilt right after the ***MAT 103*** final exam! In other words, mathematically oriented as it happens to be, ***Isometrica*** and its 'abstract' designs can still be a source of inspiration for many non-mathematically inclined readers.

Is ***Isometrica*** related to the work of Escher?

Yes and no: Escher's *symmetrical* drawings, for which he is well known, are certainly special cases of wallpaper patterns, which are ***Isometrica***'s main focus; but Escher's main achievement, the *tiling* of the plane by repeated 'real world' figures, is not discussed at all. Still, it is safe to say that those intrigued by Escher's creations are likely to be interested in ***Isometrica***; conversely, ***Isometrica*** might be a solid introduction toward a serious reading of Doris Schattschneider's classic ***M. C. Escher: Visions of Symmetry*** (Abrams, 2004).

More generally, ***Isometrica*** is not a good source for tilings of any kind; a few *obvious* planar tilings are used as standard examples, but there is no mention of hyperbolic or spherical tilings, and likewise no discussion of Penrose and other aperiodic (non-repeating) tilings. Still, the curious reader may find ***Isometrica*** to be a good starting point for such topics. (The same applies to other 'popular', loosely related topics like fractals.)

How about Alhambra?

Granada's famed Moorish palace complex that inspired Escher is barely mentioned in ***Isometrica***. For a detailed discussion of Alhambra's wallpaper aspects I would strongly recommend John Jaworski's ***A Mathematician's Guide to the Alhambra***, currently available through the ***Jaworski Travel Diaries*** at ***http://www.grout.demon.co.uk/Travel/travel.htm***.

Is ***Isometrica*** history-oriented at all?

No. Consistent with the absence of bibliography, any discussion of the subject's historical development is absent from ***Isometrica***. For such information, and a broader view as well, the interested reader is referred to both the internet and such classics as Grunbaum & Shephard's ***Tilings and Patterns*** (Freeman, 1987) and Coxeter's ***Introduction to Geometry*** (Wiley, 1980).

Comments for teachers.

Symmetry as a General Education course?

This is an eminently legitimate concern: is it fair for a course that for most of its takers is their 'final' mathematical experience to be devoted to a single subject almost devoid of 'real world' applications? My response is that students may in the end understand more about what Mathematics is about by focusing on *one* subject and its development than by being briefly exposed to a variety of subjects. (Besides, even if I wrote ***Isometrica*** for a General Education course, it may certainly be used for other classes and audiences!)

Is Symmetry just about border and wallpaper patterns?

Certainly not! In fact ***MAT 103*** does cover the isometries of the cube and the soccerball (and their compositions) toward the end, and students tend to enjoy these subjects at least as much as the rest of the course (especially when it comes to isometry composition, which is now greatly facilitated by *finiteness*). It is therefore fair to say that ***Isometrica*** may also be used for only part of a course devoted to symmetry or geometry; for example, one may spend just three to four weeks covering only chapters 2, 3, and 4, or merely two weeks on chapters 2 (border patterns) and 4 (wallpaper patterns).

What is the interplay between border patterns and wallpaper patterns?

Border patterns are planar designs invariant under translation in precisely one direction; wallpaper patterns are planar designs invariant under translation in two, therefore infinitely many, directions. This difference makes border patterns substantially easier to understand and classify. It is therefore natural to use border patterns as a stepping stone to wallpaper patterns. Further, border patterns may be seen as the building blocks of wallpaper patterns, and this is indeed an opportunity that ***Isometrica*** does not pass by; the subject is treated in depth in ***Shredded Wallpaper*** -- Bonita Bryson's 2005 honors thesis currently available at ***http://www.oswego.edu/~baloglou/103/bryson-thesis.pdf***, which may *also* be used as a quick introduction to border and wallpaper patterns.

How about covering border patterns only?

I would discourage this option, except perhaps early in high school, with the intention of covering wallpaper patterns the year after. I suspect nonetheless that several readers of ***Isometrica*** may limit their serious reading to chapter 2, which is probably the book's most successful and accessible chapter anyway!

How do border and wallpaper patterns relate to Euclidean Geometry?

The Euclidean Geometry employed in ***Isometrica*** is so minimal and elementary that a daring question emerges: would it actually be possible to develop the students' geometrical intuition through some informal exposure to border and wallpaper patterns *before* introducing them to Euclidean Geometry? Could the intense exposure to shapes and transformations enforced by the study of patterns facilitate the absorption of geometrical ideas and even arguments encountered in high school geometry? This might be a good research topic for Mathematics educators.

Could this be too easy for some students?

Yes, especially in case they happen to be visual learners. It is the teacher's responsibility to decide whether his/her students would benefit from a course based either partly or wholly on ***Isometrica***, and how much time should be spent on it (if any). I have seen students who struggled for a D in ***MAT 103***, as well as students who stated that it was the easiest course (in *any* subject) they have ever taken! Anyway, I do suspect that ***Isometrica*** could keep even the very best Mathematics/Science majors intrigued for a weekend (or at least a long Saturday afternoon), so please do not automatically give up on it simply because you happen to teach the best and brightest… [And do not forget that student's comment at the beginning of this Introduction – it *can* be a treacherous subject!]

What is the role of color?

The coverage of two-colored patterns in chapters 5 (border patterns) and 6 (wallpaper patterns) is a direct consequence of ***Isometrica***'s debt to ***Washburn & Crowe*** already alluded to. But, while for Washburn and Crowe the study of the artistically/anthropologically important two-colored patterns was an end, for me it ended up being largely a mean: indeed a careful look at chapters 5 and 6 shows how the classification of two-colored patterns is largely used as an excuse to delve into the structure of (one-colored) border and wallpaper patterns, and the compositions of their isometries in particular.

Is ***Isometrica*** written top-down or bottom-up?

The answer lies hidden in the previous paragraph! Assuming that it would be difficult for (my) students to understand *first* 'abstract' (even if geometrically presented) composition of isometries (as treated in chapter 7) and *then* pattern structure based on that (top-down approach), I opted for an indirect, if not surreptitious, introduction to isometry composition departing from various classification issues in chapters 5 and 6 (bottom-up approach). My assumption is a questionable one, so a student-friendly top-down approach may indeed be presented in a future book! (In fact such an approach is currently being tested in ***Patterns and Transformations*** (***MAT 203***), an experimental SUNY Oswego course for honors students.)

What is the significance of isometry composition?

Finding the isometries of any given pattern is a great exercise for the student, and essential for the pattern's correct classification. But it is not possible to appreciate a pattern's structure and 'personality' without understanding the way its isometries interact with each other: any two pattern isometries combined -- that is, applied sequentially -- produce a third isometry that also leaves the pattern invariant; it is for this reason that mathematicians talk about border/frieze and wallpaper *groups*, the total absence of Group Theory from ***Isometrica*** notwithstanding.

As already indicated, chapter 7 offers a thorough coverage of isometry composition in a totally geometrical context -- perhaps the most thorough (as well as accessible) coverage of compositions of planar isometries to be found in any book. It is therefore possible to use chapter 7 for a largely self-contained (despite the references to pattern structure) introduction to planar isometry composition. At the other end, section 7.0 *alone* shows how isometry composition can be studied 'empirically' in the context of multi-colored symmetrical tilings: that is in fact the way isometry composition is studied [since Spring 1997] in ***MAT 103***, definitely making for the hardest part of the course -- likened once to "pulling teeth" by one of my best students! (To make **'isometry hunting'** more fun, the instructor may even choose to initially hide from the students the helpful fact that, when it comes to isometry composition, rotations/translations and (glide) reflections act like positive and negative numbers in multiplication, respectively.)

What is the significance of isometry recovery?

Finding the isometries of a border pattern is quite easy for most students. Wallpaper patterns are a different story, complicated by more than one possible direction for glide reflection, rotations other than half turn, etc. As indicated in passing in chapter 4, the determination of all the isometries mapping a 'symmetrical' set to a copy of it -- a 'recovery' process discussed in detail in chapter 3 -- can make the isometries of a complex wallpaper pattern much more visible and 'natural': quite often the isometries mapping a 'unit' of the pattern to a copy of it are extendable to the entire pattern! This is stressed in ***MAT 103***: students are initially encouraged to reconstruct the isometries, with the hope (or rather certainty) that they will gradually become more capable of seeing them; they are in fact told that **"what you cannot see you may build"**, a guiding principle throughout the course! (A student's mother was thrilled enough by this principle to tell her daughter "now I do know that you are learning something in college" -- a very sweet comment indeed.) So, even though chapter 4 is almost entirely independent of chapter 3, I am strongly in favor of covering both.

How do students benefit from classifying patterns?

A former student told me once that "this course put some order in his mind"; and several students report in their evaluations that ***MAT 103*** made them better thinkers. For such a visual, almost playful, course these comments may appear startling at first. But the classification process, especially of two-colored patterns, is very much a thinking process; for example, and very consistently with the guiding principle cited above, the classifier will often either detect or rule out an isometry based on logical rather than visual evidence.

What is the role of symmetry plans?

Washburn & Crowe facilitates the classification of individual two-colored patterns by way of step-by-step, question-and-answer flow charts; ***Isometrica*** reaches this goal through a complete graphic description of each two-colored type's isometries *and* their effect on color (preserving or reversing). This approach has the advantage of constantly and *constructively* exposing the students to the *full* isometry structure of the 7 border patterns (through 24 two-colored types and symmetry plans at the end of chapter 5) and the 17 wallpaper patterns (through 63 two-colored types and symmetry plans at the end of chapter 6). Quite clearly, similar symmetry plans could be used for the simpler tasks of classifying one-colored border patterns (chapter 2) and one-colored wallpaper patterns (chapter 4); but I prefer a purely non-graphical description of one-colored patterns in order to test/develop the students' reading skills a bit!

Does ***Isometrica*** discriminate against glide reflection?

How did you know? You must have read the entire book! Yes, there is some discrimination ... in the sense that glide reflection is viewed as an isometry 'weaker' than reflection. This view is of course dictated by the fact that glide reflection, which may certainly be viewed as *deferred reflection*, is harder to detect in a wallpaper (or border) pattern. Further, every wallpaper pattern reflection generates translation(s) parallel to it and, therefore, "hidden glide reflection(s)": reflection 'contains' glide reflection, but not vice versa (and despite the fact that every reflection may be viewed as a glide reflection the gliding vector of which has length zero). But a careful reading of section 8.1 shows that reflection and glide reflection are simply two equivalent 'possibilities'; and the 'shifting' processes introduced in sections 4.2 - 4.4 clearly indicate that reflection is the *exception* that verifies the *rule* (glide reflection).

One way or another, the teacher must stress the curious interplay between reflection and glide reflection outlined above, and also insist that the students use dotted (read dashed) lines for glide reflection axes and vectors and solid lines for reflection axes and translation vectors, as in the symmetry plans. (There are places in ***Isometrica*** where some readers may disagree with my choice of solid or dotted lines; when a pattern reflection is combined with a parallel translation in order to create a 'hidden' glide reflection, for example, I use solid rather than dotted lines.)

What is the role of inconsistency with color?

Between the 'perfectly symmetrical' two-colored patterns of ***Washburn & Crowe*** and the randomly colored designs of the 'real world' lies a third, somewhat esoteric, class of two-colored patterns where, informally speaking, there is some order within their coloring disorders; more formally, *some* of their isometries happen to be *inconsistent with color* -- reversing colors in some instances and preserving colors in other instances -- but, otherwise, the coloring *appears* to be perfectly symmetrical, and with the two colors in perfect balance with each other in particular. Such inconsistently yet symmetrically colored patterns are largely absent from ***Washburn & Crowe***, and for a good reason: it seems that native artists, driven perhaps by instinct or intuition, largely shunned them, producing either 'perfect' or 'random' colorings!

A natural question arises: should such inconsistent colorings be avoided in teaching? Although I do cover this topic extensively in ***MAT 103*** and ***Isometrica***, my answer is a reluctant "perhaps" -- especially to those teachers who may think that two-colored patterns would already strain their students considerably. On the other hand, anyone delving into this seemingly esoteric topic will be rewarded with many fascinating (both visually and conceptually) creations; the color inconsistencies involved will often transform a 'symmetrically rich' structure into a 'lower' type, illustrating the fateful principle that **"coloring may only reduce symmetry"**. Anyway, those wishing to avoid the topic should be able to do so relatively easily, despite the presence of several color-inconsistent examples; and those venturing into it may be seduced enough to substantially enlarge ***Isometrica***'s collection of inconsistent colorings!

What is the role of the Conjugacy Principle?

The Conjugacy Principle states that the *image* of an isometry by any other isometry is an isometry of the same kind (with rotation angles or glide reflection vectors preserved modulo orientation); conversely, any two 'identical-looking' isometries are actually images of each other under a third isometry. In the context of wallpaper patterns, the Conjugacy Principle becomes an indispensable tool for their structural understanding and classification. Although formally introduced in section 6.4 (with the excuse of understanding the color effect of coexisting reflections and glide reflections) and applied throughout chapter 6, the Conjugacy Principle is thoroughly discussed and rigorously explained only in section 8.0 (paving the way for the classification of wallpaper patterns); it also appears in section 4.0 -- to the extent needed for the establishment of the *Crystallographic Restriction* (on rotation angles allowed for wallpaper patterns), which could admittedly wait until section 8.0.

What do we make of chapter 8?

This final chapter is devoted to my purely geometrical argument that there exist precisely 17 types of wallpaper patterns. It would clearly be beyond the scope of most General Education courses, and probably too sophisticated for the great majority of non-science majors as well. But it is largely self-contained -- totally self-contained in case section 4.0 and chapter 7 are assumed -- and requires mathematical maturity rather than knowledge. Interested instructors (or other readers) should probably teach/read it in parallel with ***Crystallography Now***, a web page (***http://www.oswego.edu/~baloglou/103/seventeen.html***) devoted to a more informal presentation of my classification of wallpaper patterns.

Comments for experts

Does chapter 8 really offer a classification of wallpaper patterns?

Tough question! The answer depends even on the way one defines a wallpaper pattern, and whether one believes that Group Theory has to be part of that definition in particular. Among thousands of visitors of ***Crystallography Now***, only one was kind enough to tell me that my classification is "more intuitive than others, but not at all rigorous", his main point being that "two wallpaper patterns are of the same type if and only if their isometry groups are isomorphic". Fair enough, but is it reasonable to be able to characterize such simple structures, known to humankind for thousands of years, *only* in terms of advanced mathematical concepts? How would Euclid describe -- and *perhaps* classify -- the seventeen types in the ***Elements***, had he included them there? (Just a thought!)

To be honest, a solid structural understanding of the seventeen types of wallpaper patterns was, and still is, more important to me than a rigorous/quick proof that there exist indeed precisely seventeen such types. Nonetheless, I suspect that what ***Isometrica*** offers could easily be turned into a formal proof by replacing isomorphism of isometry groups by a properly defined 'isomorphism' of symmetry plans. Such an isomorphism would certainly distinguish between solid lines (reflection) and dotted lines (glide reflection) or between hexagonal dots (sixfold centers) and triangular dots (threefold centers), etc. Under such an approach, any two symmetry plans consisting only of round dots (half turn centers) should represent the same type of wallpaper pattern (**p2**); even more frighteningly, any two wallpaper patterns having nothing but translations would be of the same type (**p1**) on account of their 'blank' symmetry plans, and so on.

More interestingly, the reader is invited to compare the way this symmetry plan approach distinguishes between **p4g** and **p4m** (section 8.3) or between **p31m** and **p3m1** (section 8.4) to the way the traditional group-theoretic approach reaches the same goals: rather than looking at their generator equations, ***Isometrica*** focuses on the two possible ways in which their (glide) reflections may 'pass through' their lattices of rotation centers.

[Note: the classification of border patterns in chapter 2 is even more 'informal' than that of wallpaper patterns, consistently with that chapter's introductory nature; the interested reader should be able to easily derive a more rigorous classification of border patterns based on symmetry plans.]

<u>Any new ideas in the proposed classification?</u>

The main new idea is the reduction of complex (rotation + (glide) reflection) types to the three rotationless types with (glide) reflection (**pg**, **pm**, **cm**) via the characterization of the latter in terms of their translations. So section 8.1, where the said characterization is achieved, may *seem* endless, but the derivation of the remaining types in the subsequent sections is swift and rather elegant (I hope).

Needless to say, the Conjugacy Principle shines throughout the classification!

<u>Any other surprises prior to chapter 8?</u>

Some readers may find a few interesting ideas lurking in my novel (non-group-theoretic) classification of two-colored patterns (which *assumes* the classification of one-colored patterns), and in the exploitation of symmetry plans in sections 6.9 and 6.11 - 6.12 in particular. Others may be delighted at the various ways of passing from one border or wallpaper type to another: although such 'transformations' are included in ***Isometrica*** mostly for educational purposes, they are bold commentaries on the ever-elusive structure of patterns, too!

Can ***Isometrica***'s ideas be extended to the three dimensions?

Before trying to explore two-colored 'sparse crystals' (blocks not touching each other and therefore not obscuring colors) I would rather try to investigate compositions of three-dimensional isometries in a geometrical context (extending chapter 7) and classify the 230 crystallographic groups geometrically (extending chapter 8). I believe that both projects are feasible, and hope to pursue them now that ***Isometrica*** has been completed; anyone interested in competing with me may like to start with ***Isometries Come In Circles*** (my 'mostly two-dimensional' novel derivation of three-dimensional isometries, currently available at ***http://www.oswego.edu/~baloglou/103/circle-isometries.pdf***).

What happens when more than two colors are involved?

This question has been answered in Tom Wieting's ***The Mathematical Theory of Chromatic Plane Ornaments*** (Marcel Dekker, 1982). I was ambitious enough to investigate multicolored types in the context of *maplike* colorings of planar *tilings*, and also without the group-theoretic tools employed by Wieting; more specifically, I was interested in the interplay between tiling structure and coloring possibilities. That was not necessarily a hopeless project, and I did/do have some interesting ideas, but I had to finally admit that my attempts -- during the summers of 2000 and 2005 -- were not that realistic: several hundred multicolored tilings later a projected ninth chapter (initially numbered as seventh) had to be abandoned, and this fascinating, literally colorful, project was postponed indefinitely... [Section 9.0 (i.e., introduction only) is available at ***http://www.oswego.edu/~baloglou/103/isometrica-9.pdf***, but has not been included in ***Isometrica***; it concludes with a 'four color' conjecture on 'symmetrically correct' coloring of tilings.]

Any other future projects related to ***Isometrica***?

It would be nice if someone with more energy and knowledge sits down and writes a book on wallpaper patterns that could be used for a mathematics capstone course! Here is how this could be achieved: start with an elementary geometrical classification of wallpaper patterns like mine and then continue with the standard group-theoretic classification (available for example in Wieting's book) *and* Conway's topological classification, developing/reviewing all needed mathematical tools along the way. The success of such a project (and course) would probably depend on the author's ability to delve into the hidden interplay among the three approaches.

[Conway's *orbifold* approach may be found, together with broadly related topics, in ***Geometry and the Imagination*** -- informal notes by John Conway, Peter Doyle, Jane Gilman, and Bill Thurston currently available at ***http://www.math.dartmouth.edu/~doyle/docs/gi/gi.pdf***; look also for ***The Symmetry of Things***, by John Conway, Heidi Burgiel, and Chaim Goodman-Strauss (AK Peters, forthcoming).]

Can we judge this book by its cover?

No way! The figure on the cover is a tribute to the great crystallographer (and not only) Arthur Loeb and his ***Color and Symmetry*** (Wiley, 1971), which offers an alternative geometrical study of wallpaper patterns. More specifically, it is a humorous reminder of Loeb's nifty derivation of the composition of two intersecting glide reflections (and that mysterious parallelogram associated with them): this important problem forms the pinnacle of my discussion of isometry composition in chapter 7, and it seems to be absent from all other books that could have discussed it; my approach is not as direct as Loeb's, but it has its own methodological advantages (such as requiring a thorough discussion of the composition of a glide reflection and a rotation, a topic not directly addressed by Loeb).

[Which ***Isometrica*** figure would be on the cover if I didn't choose to attract the reader's attention to Loeb's work and genius? Tough question, but the winner is figure 8.19 (on the 'ruling' and unexpected mirroring of half turn centers by glide reflection): in addition to capturing ***Isometrica***'s spirit, it could lead to an alternative and probably quicker discussion of half turn patterns in section 8.2. And a close second would no doubt be figure 8.39, which dispenses of the patterns with threefold/sixfold rotation and reflection by showing that their only 'factor' can be a **cm**.]

Further comments, acknowledgments, dedications.

Responding to my May 2000 talk at a Madison conference honoring Donald Crowe, H. S. M. Coxeter -- in his 90's at the time, seated in a wheelchair barely ten feet from the speaker(s) -- remarked with a wry smile that "all the two-colored types had been derived in the 1930's by a textile manufacturer from Manchester [H. J. Woods] without using any Mathematics". The eminent geometer's remark captures much of the spirit in which ***Isometrica*** has been written, as well as the subject's precarious position between Art and Mathematics. At another level, Coxeter's remark serves as a reminder of the interplay and struggle between rigor and intuition, between structure and freedom, which has certainly left its mark on ***Isometrica***.

I like to say, in hindsight, that border and wallpaper patterns are "of *limited* interest to *many* people" -- not artistic enough for artists and not mathematical enough for mathematicians... Further, and contrary to the pleasant illusions created by ***Stevens*** or ***Washburn & Crowe*** or ***Isometrica***, symmetry itself is an exception rather than a rule in the real world: I was rather flattered to hear from two former students that they think of me when they run across symmetrical figures during their New York City strolls, but how frequent, and how important after all, are such symmetrical encounters? How meaningful is abstract beauty in an increasingly tormented world? I have been caught telling friends that it is not enough for me to hear my students say that they enjoyed my course (and, by extension, book), I actually need to hear -- even if occasionally -- that it changed their life, or, less arrogantly on my part, that “it caused them see the world a little differently" (this is quoted verbatim from a former student's recent e-mail).

If you read between the lines above you already know that the teaching of ***MAT 103*** and the writing of ***Isometrica*** have certainly changed *my* life: I knew that since the first week of classes in Fall 1995, when I came up with an assignment calling for the creation of the seven border pattern types using vertical and horizontal congruent rectangles -- an assignment that looks trivial now but kept me up late that night (because the idea of 'multidecked' border patterns is not 'natural' to our minds, perhaps). Moreover, there I was, someone with absolutely no prior interest in drawing or Design, spending many hours and nights creating 'new' patterns, first by hand, then on a computer ... gradually discovering how such patterns and concepts could form a gateway to mathematical thought for students as interested in Mathematics as I once was in Design! [The term "design" is used quite narrowly here, and intentionally so: Graphic Design majors who take ***MAT 103*** tend to find its patterns rather inspiring!]

So a labor of love it was, and this is why I have largely preserved ***Isometrica*** in its original form: perhaps my preferred strategy or tactics for presenting this incredibly flexible material have changed since 2001, but I chose to preserve my initial insight and the writing adventure that ensued. For the same reason, combined with various personal circumstances, ***Isometrica*** is going straight to the internet rather than some constricting publishing house: the software packages employed (***MathWriter*** and ***SuperPaint***) were already ancient when I started, the English may seem awkward here and there, the figures are somewhat primitive and often imperfect, the overall format is kind of kinky, but you are getting the real thing, and for free at that! [You may in particular get a good sense of the struggle and discovery process that went on as the exposition revs up through the chapters: even if there is a "royal road to geometry" … I often fail to follow it ... keeping in mind that “the shortest approach is not always the most interesting”!]

My joy at having been able to preserve ***Isometrica***'s desired form is offset by the sadness of having left so much out: my plans of including everything bypassed by 'first insight' in the form of exercises had to be abandoned, but I am still hoping of creating additional web pages -- probably linked to the online version of this Introduction -- in the future, covering extra topics in detail (and color); and if this hope never materializes, with the future of ***MAT 103*** as inevitably unclear as is, I trust that enough material has been included here to inspire others toward new mathematical ideas and/or artistic creations. [Please forgive this desperate optimism about ***Isometrica*** being read and even expanded, but it is my firm belief that its informal and adventurous style is going to win it some lasting friends!]

My obvious desire to generate disciples for ***Isometrica*** has a non-obvious implication: despite the copyright notices at the beginning and ending of each chapter, I *do* allow the reproduction of my book for educational purposes; if for example a teacher anywhere in the world wishes to have hard copies (of either ***Isometrica*** in its totality or some of its chapters) for his/her students, then it is fine with me to have that school's printing service produce such copies, even if at a reasonable cost and marginal profit. So please do not write to me for permissions (concerning either ***Isometrica*** or various web pages related to it): I would love to have feedback from you, but giving me credit for the materials you have used is all that I am asking for...

For every book and completed project that sees the light of day there are several visions buried under perennial darkness: I happen to have the right personality for incompleteness, therefore I am almost ecstatic as these final lines are being written; repeatedly seduced as I was by those 'repeating patterns', the discipline often failed to match the excitement, the time and will appeared not to be there at times, the questions tended to dwarf the answers... While several friends and colleagues provided constant support, I believe that the project's completion and, I hope, success is primarily due to my ***MAT 103*** students and their enthusiasm. At the risk of being oblivious to the small but precious contributions of many, I would like to single out and thank five former students for their encouragement and inspiration: Terry Loretto (Fall 1995), Dreana Stafford (Spring 1999), Michael Nichols (Fall 1999), who also provided crucial assistance with ***SuperPaint*** in January 2000, Richard Slagle (Fall 2003), and Bonita Bryson (Spring 2004), who also wrote the aforementioned honors thesis (on the tiling of wallpaper patterns by border patterns).

As made clear in the beginning of this Introduction, there would simply be no ***Isometrica*** without Margaret Groman's original vision; I am equally grateful to her for her constant encouragement and suggestions for improvement. Likewise,

I am indebted to Mark Elmer, who has also taught ***MAT 103*** several times, for his careful reading of ***Isometrica*** and useful observations. Beyond ***MAT 103***, I am grateful to my friend and collaborator Phil Tracy, who has also read ***Isometrica*** and discussed it with me in considerable detail; and likewise to my colleagues Chris Baltus, Fred Barber, Joseph Gaskin, Michel Helfgott, and Kathy Lewis for their mathematical camaraderie over the years.

Beyond Oswego, I am grateful to a number of mathematicians and others who provided links to ***Isometrica***'s early ambassador, ***Crystallography Now***, or offered useful feedback: Helmer Aslaksen, Andrew Baker, Dror Bar-Natan, Bryan Clair, Marshall Cohen, Wis Comfort, David Eppstein (***Geometry Junkyard***), Sarah Glaz, Andreas Hatzipolakis, Dean Henderson, William Huff, Loukas Kanakis, Nikos Kastanis, Barbara Pickett, Doug Ravenel, Jim Reid, Saul Stahl, Tohsuke Urabe, Marion Walter, Eric Weisstein (***Wolfram MathWorld***), Mark Yates, and others – notably family and friends in Thessaloniki, contributors to the ***sci.math*** newsgroup, and participants of my January 2003 ***Symmetry For All*** MAA minicourse -- who should forgive me for having overlooked their input. I am also grateful to George Anastassiou, Varoujan Bedros, and Fred Linton for their advice on technical and 'legal' matters; along these lines, special thanks are also due to my friend and non-mathematical collaborator Nick Nicholas.

Back to Oswego, I am grateful to Alok Kumar, Ampalavanar Nanthakumar, and Bill Noun for their support and good advice; same applies to several other colleagues from Mathematics, Computer Science, Art and other departments (and also administration) at SUNY Oswego. Sue Fettes deserves special mention for her assistance with ***MathWriter*** (in its final years). Finally, many thanks are due to Patrick Murphy, Jean Chambers & David Vampola, and Julia & Matthew Friday for many a pleasant evening -- followed at times by all-night ***Isometrica*** writing and, inevitably, drawing -- in tranquil Oswego.

In a somber tone now ... even though ***Isometrica*** was dedicated from the beginning to the memory of our colleague Ron Prisco (Margaret Groman's Abstract Algebra teacher forty years ago, among other things), who passed away before even I started writing it but "had a lot of faith in my work", I would like to honor here the memory of a few local friends whom we lost during the last couple of years:

-- Bob Deming, whose unpublished but highly effective notes on Linear Programming provided an early model for me on classroom-generated books

-- Jim Burling, who also taught ***MAT 103*** a couple of times, organized our seminar, and was a fatherly figure for a number of younger colleagues

-- Gaunce Lewis (of Syracuse University), whose tragically untimely death was a haunting reminder of the fragility of intellectual pursuits

-- Don Michaels, who in his capacity as tireless news & web administrator contributed handsomely to the success of ***MAT 103***

Finally, ***Isometrica*** owes a lot to my late father, Christos Baloglou (1919 - 2002): a high school geometer who also taught Descriptive & Projective Geometry to Aristotle University Engineering students in the 1960's and published ***Scattered Drops of Geometry*** in 2001, he certainly influenced me to study Mathematics. My whole symmetry project may be seen as a Sisyphean effort to annul his lovely -- and, less obviously, loving -- verdict on it: "Son, this is not Mathematics"!

George Baloglou

Oswego, April 27, 2007

Table of Contents

CHAPTER 3: WHICH ISOMETRIES DO IT?

CHAPTER 4: WALLPAPER PATTERNS

CHAPTER 6: TWO-COLORED WALLPAPER PATTERNS

CHAPTER 7: <u>COMPOSITIONS OF ISOMETRIES</u>

CHAPTER 8: <u>WHY PRECISELY SEVENTEEN TYPES?</u>

Basic Index

 first draft: summer 1998

CHAPTER 1

ISOMETRIES AS FUNCTIONS

1.0 Functions and isometries on the plane

1.0.1 Example. Consider a **fixed** point O and the following 'operation': given any other point P on the plane, we send (**map**) it to a point P′ that lies on the ray going from O to P and also satisfies the equation **$|OP'| = 3 \times |OP|$** (figure 1.1). It is clear that for each point P there is precisely one point P′, the **image** of P, that satisfies the two conditions stated above. Any such process that associates precisely one image point to every point on the plane is called a **function** (or **mapping**).

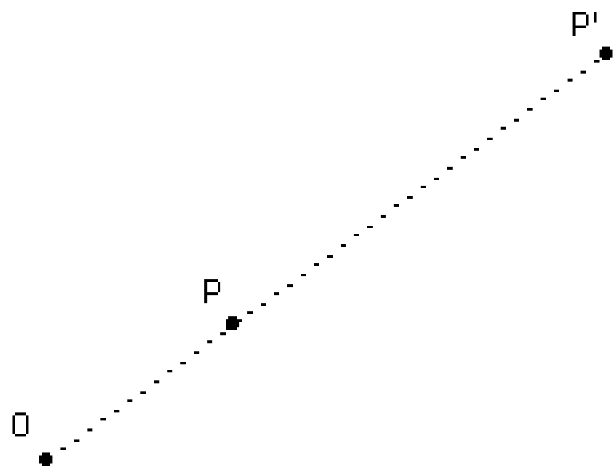

Fig. 1.1

1.0.2 Coordinates. Let us now describe the 'blowing out' function discussed in 1.0.1 in a different way, using the **cartesian coordinate system** and positioning O at the **origin**, (0, 0). Consider a specific point P with **coordinates** (2.5, 1.8). Looking at the **similar triangles** OPA and OP′B in figure 1.2, we see that $\frac{|P'B|}{|PA|} = \frac{|OB|}{|OA|} = \frac{|OP'|}{|OP|} = 3$, hence $|P'B| = 3 \times |PA| = 3 \times 1.8 = 5.4$ and $|OB| = 3 \times |OA|$

$= 3 \times 2.5 = 7.5$. That is, the coordinates of P′ are (7.5, 5.4). In exactly the same way we can show that an arbitrary point with coordinates (x, y) is mapped to a point with coordinates (3x, 3y). We may therefore represent our function by a formula: **f(x, y) = (3x, 3y)**.

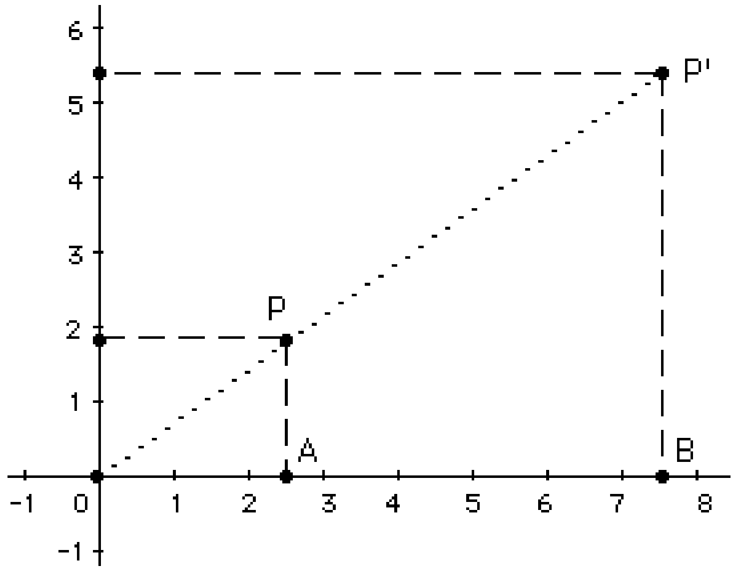

Fig. 1.2

1.0.3 <u>Images.</u> Let us look at the rectangle ABCD, defined by the four points A = (2, 1), B = (2, 2), C = (5, 2), D = (5, 1). What happens to it under our function? Well, it is simply mapped to a ‘blown out’ rectangle A′B′C′D′ -- **image** of ABCD under the ‘blow out’ function -- with vertices (6, 3), (6, 6), (15, 6), and (15, 3), respectively:

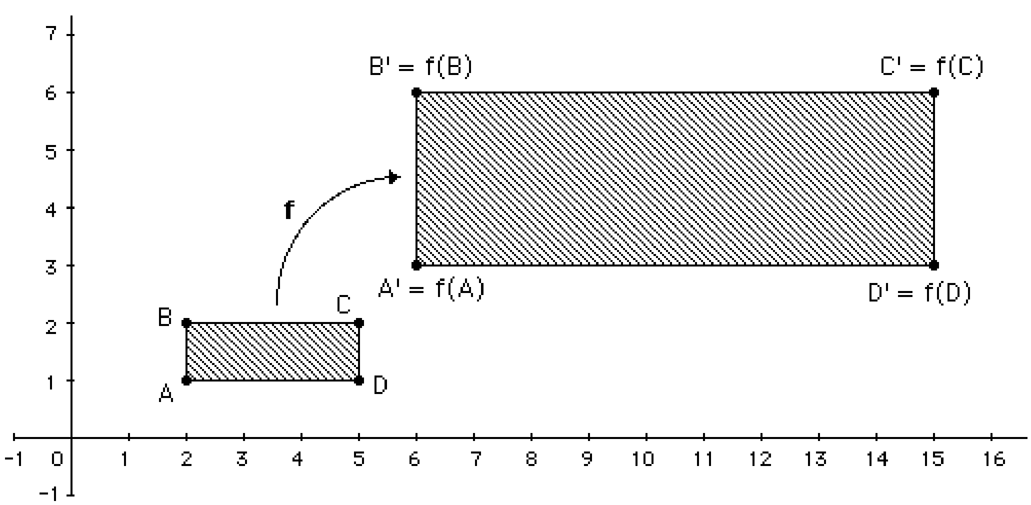

Fig. 1.3

1.0.4 <u>More functions.</u> One can have many more functions, formulas, and images. For example, **g(x,y) = (2x−y, x+3y)** maps ABCD to a parallelogram, while **h(x, y) = (3x+y, x−y^2+4)** maps ABCD to a semi-curvilinear quadrilateral (figure 1.4). We compute the images of A under g and h, leaving the other three vertices to you: g(A) = g(2, 1) = (2×2−1, 2+3×1) = (3, 5); h(A) = h(2, 1) = (3×2+1, 2−1^2+4) = (7, 5). (You may find more details in 1.0.8.)

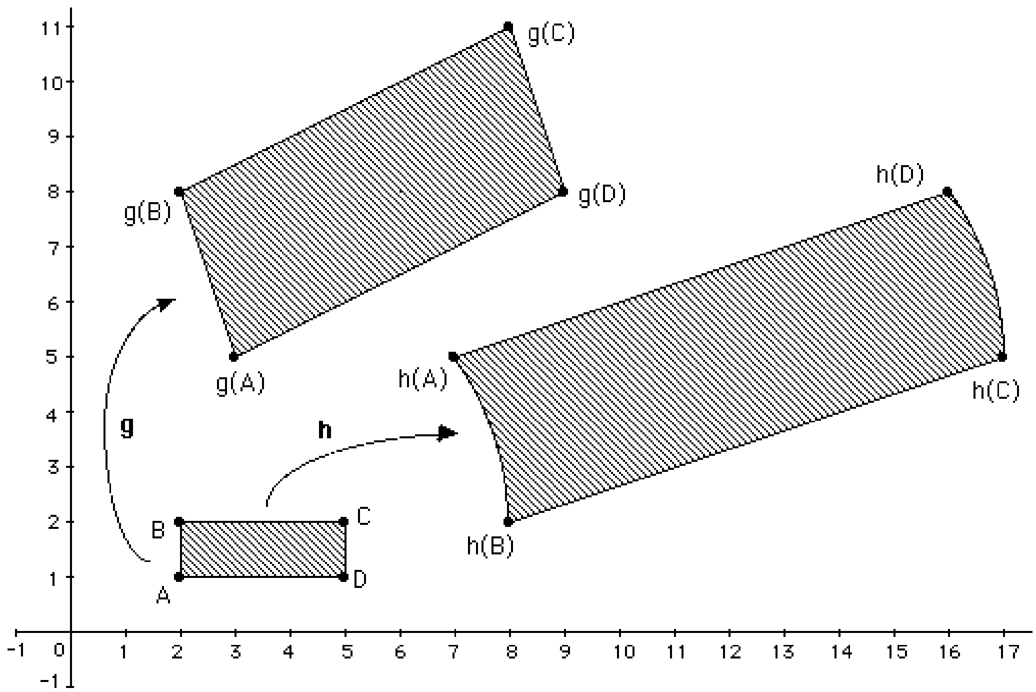

Fig. 1.4

1.0.5 <u>Distortion and preservation.</u> Looking at the three functions f, g, and h we have considered so far, we notice a progressive ‘deterioration’: f simply failed to preserve distances (mapping ABCD to a bigger rectangle), g failed to preserve right angles (but at least sent parallel lines to parallel lines), while h did not even preserve straight lines (it mapped AB and CD to curvy lines). Now that we have seen how ‘bad’ some (in fact most) functions can be, we may as well ask how ‘good’ they can get: are there any functions that preserve distances (**therefore** angles and shapes as well), satisfying **|AB| = |A′B′|** for every two points A, B on the plane?

The answer is “yes”. Distance-preserving functions on the plane do exist, and we can even tell exactly what they look like: they are defined by formulas like $\mathbf{F(x, y) = (a'+b'x+c'y, d'+e'x+f'y)}$, where a', d' are arbitrary, $b'^2+e'^2 = c'^2+f'^2 = 1$, and **either** $f' = b'$, $e' = -c'$ **or** $f' = -b'$, $e' = c'$! This is quite a strong claim, isn’t it? Well, we will spend the rest of the chapter proving it, placing at the same time considerable emphasis on a **geometric** description of the involved functions. For the time being you may like to check what happens when b' or c' are equal to 0: what is the image of ABCD in these cases? (Look at specific examples involving situations like $a' = 3$, $b' = 0$, $c' = 1$, $d' = 2$, $e' = -1$, $f' = 0$ or $a' = -2$, $b' = -1$, $c' = 0$, $d' = 4$, $e' = 0$, $f' = 1$, and determine the images of A, B, C, D.)

1.0.6 What’s in a name? You probably feel by now that such nice, distance and shape preserving functions like the ones mentioned above deserve to have a name of their own, don’t you? Well, that name does exist and is probably Greek to you: **isometry**, from ***ison*** = “equal” and ***metron*** = “measure”. The second term also lies at the root of “symmetry” = “syn” + “metron” = “plus” + “measure” (perfect measure, total harmony). In fact ancient Greek ***isometria*** simply meant “symmetry” or “equality”, just like the older and more prevalent ***symmetria***. The term “isometry” with the meaning **“distance-preserving function”** entered English -- emulating somewhat earlier usage in French and German -- in 1941, with the publication of Birkhoff & Maclane’s ***Survey of Modern Algebra***.

1.0.7 Isometries preserve straight lines! We claim that every isometry maps a straight line to a straight line. And, yes, one could prove this claim without even knowing (yet) what isometries look like, without having seen a single example of an isometry! In fact, one could prove that isometries preserve straight lines without even knowing for sure that isometries do exist!! This mathematical world can at times be a strange one, can’t it? But how do we prove such an ‘abstract’ claim?

Well, a clever observation is crucial here: it suffices to show that every isometry maps three distinct **collinear** points to three distinct **collinear** points! Indeed, let's assume this 'subclaim' for now, and let's prove right below the following: every function (**not** necessarily an isometry!) that maps every three collinear points to three collinear points must also map every straight line L to (a **subset** of) a straight line L′. Once this is done, preservation of distances shows easily that the image of L actually **'fills'** L′.

Start with a straight line L and pick any two distinct points P_1, P_2 on it. These two points are mapped by our function to distinct points P'_1, P'_2 that certainly **define** a new line, call it L′. Now every other point P on L is collinear with P_1, P_2, therefore, by our subclaim above (still to be proven!), its image P′ is collinear with P'_1, P'_2, hence it lies on L′ (figure 1.5). That is, every point P on L is mapped to a point P′ on L′, hence L itself is mapped **'inside'** L′.

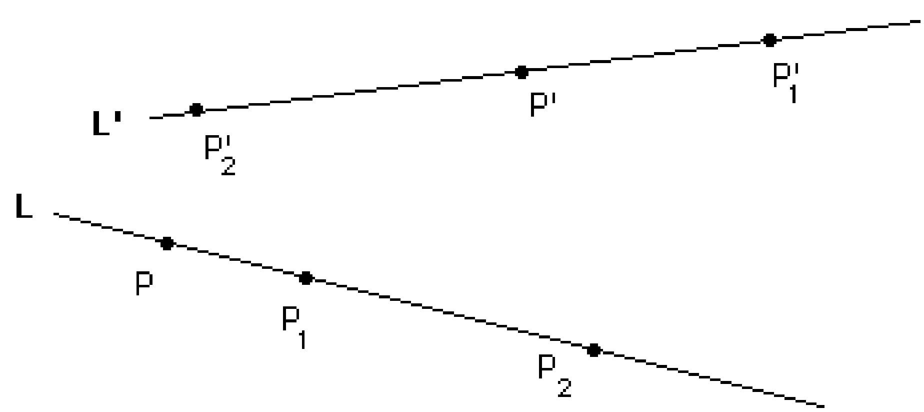

Fig. 1.5

So, how do we prove our subclaim that an isometry must always map collinear points to collinear points? Well, let A, B, C be three collinear points that are mapped to not necessarily collinear points A′, B′, C′, respectively (figure 1.6). We are dealing with an isometry, therefore $|A'C'| = |AC|$, $|A'B'| = |AB|$, and $|B'C'| = |BC|$. Since A, B, C are collinear, $|AC| = |AB| + |BC|$. But then $|A'C'| = |AC| = |AB| + |BC| = |A'B'| + |B'C'|$. We are forced to conclude that A′, B′, C′ must indeed be collinear: otherwise one side of the triangle A′B′C′ would be **equal** to the sum of the other two sides, violating the familiar **triangle inequality**.

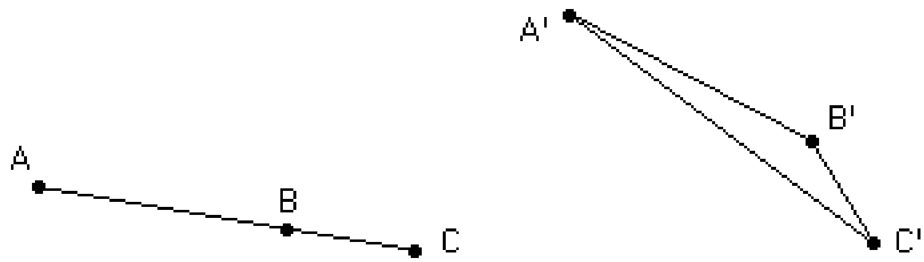

Fig. 1.6

1.0.8 Practical (drawing) issues. As you will experience in the coming sections, the fact that isometries map straight lines to straight lines makes life a whole lot easier: to draw the image of a straight line segment, for example, all you have to do is determine the images of the two **endpoints** and then **connect** them with a straight line segment. On our part, we will be repeatedly applying this principle throughout this chapter without specifically mentioning it.

On the other hand, determining the image of either a straight segment under a function that is not an isometry or a curvy segment under any function requires more work: one needs to determine the images of several points between the two endpoints and then connect them with a **rough sketch**. This is, for example, how h(AB) has been determined in 1.0.4: h(2, 1) = (7, 5), h(2, 1.2) = (7.2, 4.56), h(2, 1.4) = (7.4, 4.04), h(2, 1.6) = (7.6, 3.44), h(2, 1.8) = (7.8, 2.76), h(2, 2) = (8, 2). This is indeed a lot of work, especially when not done on a computer! Luckily, most images in this book are determined geometrically rather than algebraically; more to the point, most shapes under consideration will be quite simple geometrically, defined by straight lines.

1.0.9* How about parallel lines? Now that you have seen why isometries must map straight lines to straight lines, could you go one step further and prove that isometries must also map parallel lines to parallel lines? You can do this arguing **by contradiction**: suppose that parallel lines L_1, L_2 are mapped by an isometry to non-parallel lines L_1', L_2' intersecting each other at point K; can you then notice something impossible that happened to those **distinct** points K_1, K_2 (on L_1, L_2, respectively) that got mapped to K?

And if you are truly adventurous, can you prove, perhaps by contradiction, that whenever a function (not necessarily an isometry!) maps straight lines to straight lines it must also map parallel lines to parallel lines?

1.1 Translation

1.1.1 Example. Consider the triangles ABC, A′B′C′ below:

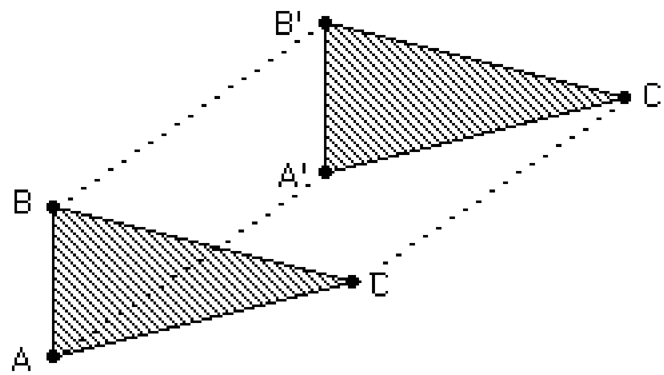

Fig. 1.7

Not only they are congruent to each other, but they also happen to be **'parallel'** to each other: AB, BC, and CA are parallel to A′B′, B′C′, and C′A′, respectively. This is a rather special situation, and what lies behind it is a **vector**.

1.1.2 Vectors. Familiar as it might be from Physics, a vector is a hard-to-define entity. It basically stands for a uniform motion that takes place all over the plane: every single point moves in the same **direction** (the vector's direction -- but have a look at 1.1.5, too) and by the same **distance** (the vector's length). In figure 1.7, for example, it is easy to see that every point of the triangle ABC has moved in the same southwest to northeast (SW-NE) direction by the same distance. We represent this motion by the 'arrow' below and call it a **translation** -- "transferring (ABC) to (A′B′C′)", in the same way a **text** is **transferred** from one language **to** another -- defined by the vector $\vec{\mathbf{v}}$:

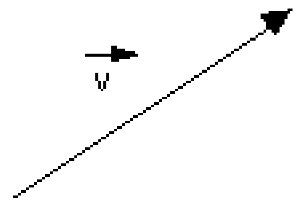

Fig. 1.8

Comparing figures 1.7 and 1.8, we easily conclude that every vector uniquely defines a translation and vice-versa. Notice also that the triangle A′B′C′ moves back to the triangle ABC by a translation **opposite** of the SW-NE one we already discussed, a translation defined by a NE-SW vector of **equal** length:

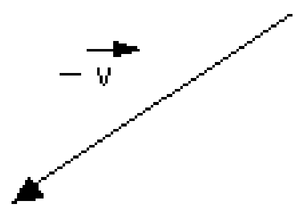

Fig. 1.9

1.1.3 <u>It's an isometry!</u> While figure 1.7 makes it 'obvious' that every translation does preserve distances, it would be nice to actually have a proof of this claim. All we need to do is to show that if points A and B move by the **same** vector $\vec{v}$ to image points A′, B′ then **|A′B′| = |AB|**. But this is easy: as AA′ and BB′ are 'by definition' **parallel** and **equal** to each other, AB and A′B′ are by necessity the opposite, therefore equal (and parallel), sides of a **parallelogram**:

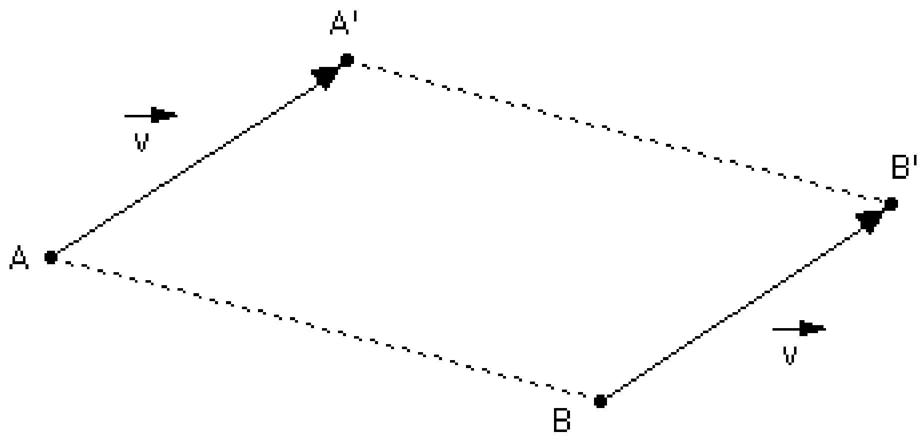

Fig. 1.10

1.1.4 Coordinates. Let us revisit 1.1.1, placing now figure 1.7 in a cartesian coordinate system, so that the coordinates of A, B, C and the **approximate** coordinates of A′, B′, C′ are as shown below:

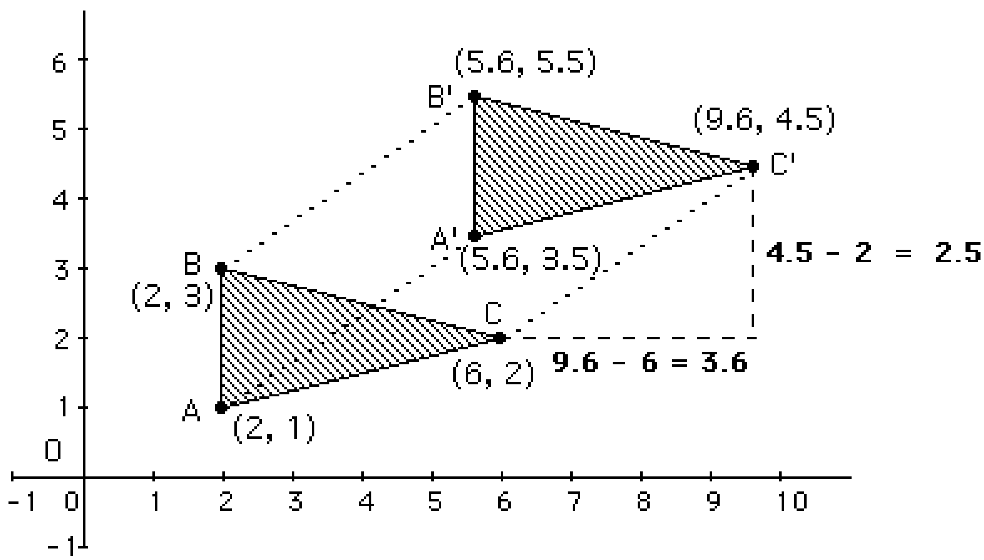

Fig. 1.11

It doesn't take long to realize that our translation simply **adds** approximately 3.6 units to the x-coordinate of every point and approximately 2.5 units to the y-coordinate of every point; this is explicitly shown in figure 1.11 for C and C′. We call these two numbers **coordinates** of the translation vector, which we may now write as $\vec{\mathbf{v}} \approx$ **<3.6, 2.5>**. By the **Pythagorean Theorem**, the vector's length is approximately $\sqrt{3.6^2 + 2.5^2} \approx 4.3$. All this is further clarified in figure 1.12, which in particular shows how the translation vector's coordinates are determined by the image O′ of **(0, 0)**:

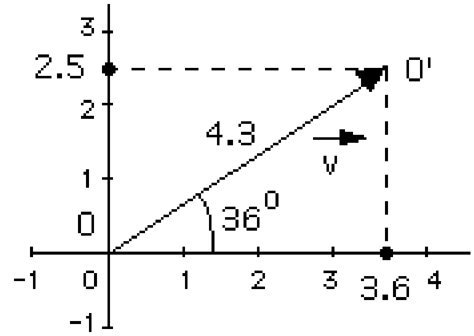

Fig. 1.12

That is, we may represent this translation employing the formula **T(x, y) = (3.6+x, 2.5+y)**. More generally, every translation on the plane may be represented by a formula of the form **T(x, y) = (a+x, b+y)**. Conversely, each formula of the form T(x, y) = (a+x, b+y) represents a translation defined by the vector **<a, b>**; sometimes we may even denote the translation itself by <a, b>. Observe that the opposite of the translation defined by the vector <a, b> is simply defined by the vector **<–a, –b>**. For example, the opposite translation of <3.6, 2.5> that we discussed in 1.1.2 is **<–3.6, –2.5>**.

1.1.5 <u>'Determining' a vector.</u> While figure 1.12 provides sufficient illustration on the relation between a vector's length, direction, and coordinates, just a bit of **Trigonometry** makes everything so much clearer! Indeed, since the vector $\vec{v}$ of length 4.3 makes a **vector-angle** of about 36^0 with the **positive** x-axis, its x-coordinate and y-coordinate are given by $4.3 \times \cos 36^0 \approx 4.3 \times .81 \approx 3.48$ and $4.3 \times \sin 36^0 \approx 4.3 \times .59 \approx 2.53$, respectively. While absolute precision has not been achieved, <3.48, 2.53> is indeed very close to <3.6, 2.5>. The quotient 2.53/3.48 ≈ .73 is the vector's **slope**, which is another quantitative way of describing the vector's direction. (Those who know a bit more know of course that this slope is equal to approximately $\tan 36^0$.)

Beware at this point of a simple, yet important, fact: while the two distinct vectors <3.6, 2.5> and <−3.6, −2.5> share the same direction, their slopes being equal (2.5/3.6 = (−2.5)/(−3.6)), they are of opposite **sense**, going opposite ways (as figures 1.8 & 1.9 demonstrate). Moreover, as we shall see in 1.4.7, **opposite** vectors have **distinct** vector-angles, in this case 36^0 and 216^0, respectively. So, it is important to remember that for every slope/direction there exist two distinct, and opposite of each other, senses. Notice at this point that any two vectors of equal length and same direction **and** sense are one and the same, while any two vectors of equal length and same direction might be either one and the same or opposite of each other.

1.2 Reflection

1.2.1 <u>Mirrors create equals.</u> Anyone who has ever successfully looked into a mirror is aware of this simple, as well as deep, natural phenomenon. Moreover, the closer you stand to a mirror, the closer you see your image in it -- another simple truth that even your cat is likely to be painfully aware of! In fact your **mirror image** lies precisely as far 'inside' the mirror as far away from it you stand: a fact used by many restaurants, bars, etc, to 'double' their perceived space. As mirrors or calm ponds cannot be included in books, we need a more abstract way of illustrating such natural observations, and we must indeed invent a 'paper equivalent' of a mirror!

1.2.2 <u>Reflection axes.</u> In order to 'touch' your mirror image inside a mirror you need to extend your hand toward the mirror **straight ahead**, so that it makes a **right angle** with the mirror, right? Well, this simple observation, together with the ones made in 1.2.1, helps us come up with the needed representation of a mirror on paper. The image P′ of a point P under **reflection** about the **axis** (mirror) L is found as figure 1.13 indicates:

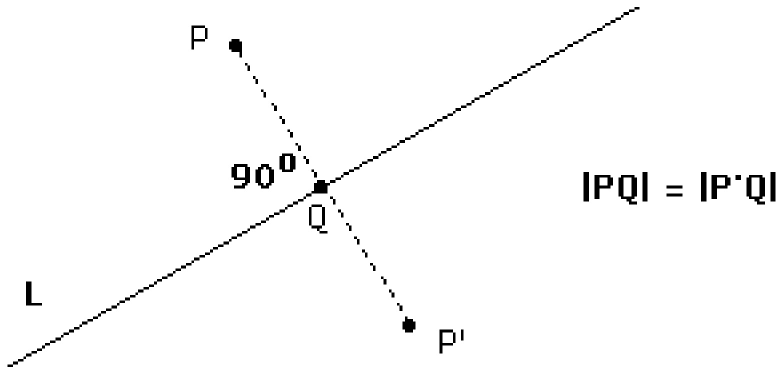

Fig. 1.13

That is, we get the same effect on P as if an actual mirror had somehow been placed perpendicularly to this page along L: you may of course go through such an experiment and see what happens!

1.2.3 Images. Let us return to triangle ABC of figure 1.7 and try to find its image under reflection by the straight line L in figure 1.14. We do that simply by determining the images A′, B′, C′ of vertices A, B, C and then connecting them to obtain the image triangle A′B′C′:

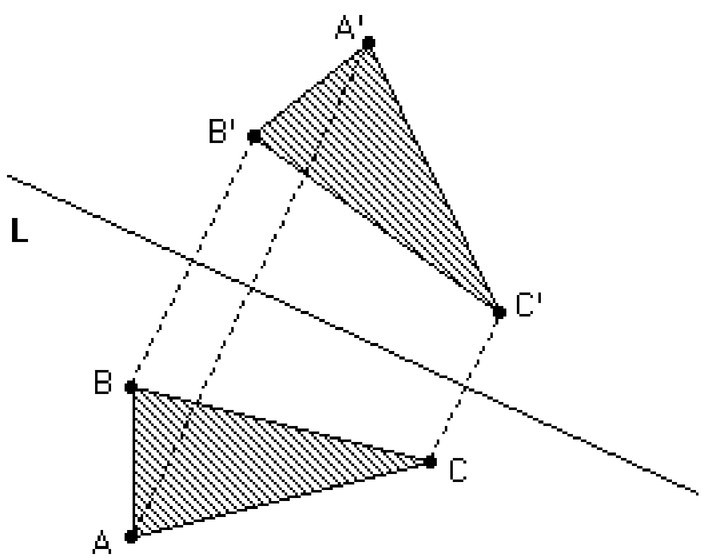

Fig. 1.14

1.2.4 <u>It's an isometry!</u> The two triangles in figure 1.14 certainly look congruent. This might not be as obvious as it was in the case of the two triangles of figure 1.7 -- we will elaborate on this in section 3.0 -- but, having three pairs of seemingly equal sides, ABC and A′B′C′ have to be congruent. How do we show that **|BC| = |B′C′|**, for example?

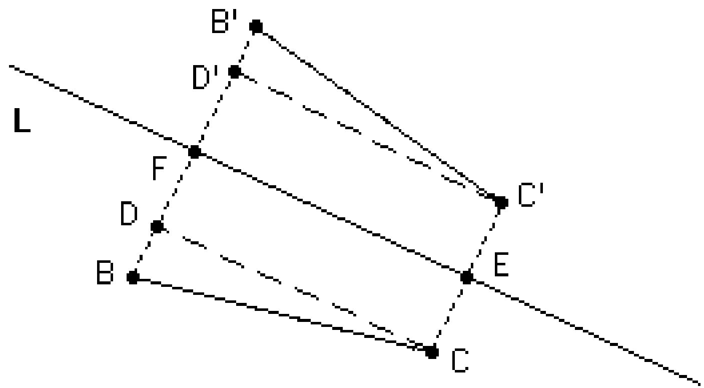

Fig. 1.15

Well, all we need to do is draw segments CD, C′D′ (both **parallel** to L and **perpendicular** to BB′, CC′) and notice, with the help of the **rectangles** FECD and FEC′D′ (figure 1.15), that |DF| = |CE| = |C′E| = |D′F|, therefore |DB| = |BF| − |DF| = |B′F| − |D′F| = |D′B′|, while |DC| = |FE| = |D′C′|: it follows that the two **right triangles** DBC and D′B′C′ are **congruent** (because |DB| = |D′B′| and |DC| = |D′C′|), hence |BC| = |B′C′|.

1.2.5 <u>Coordinates.</u> Let us now place triangles ABC, A′B′C′ and the axis L in a cartesian coordinate system (figure 1.16) and see what happens! You may use your straightedge to estimate the coordinates of A′, B′, and C′ and verify that (2, 1), (2, 3), and (6, 2) got mapped to **approximately** (5.1, 7.7), (3.6, 6.4), and (6.9, 4), respectively.

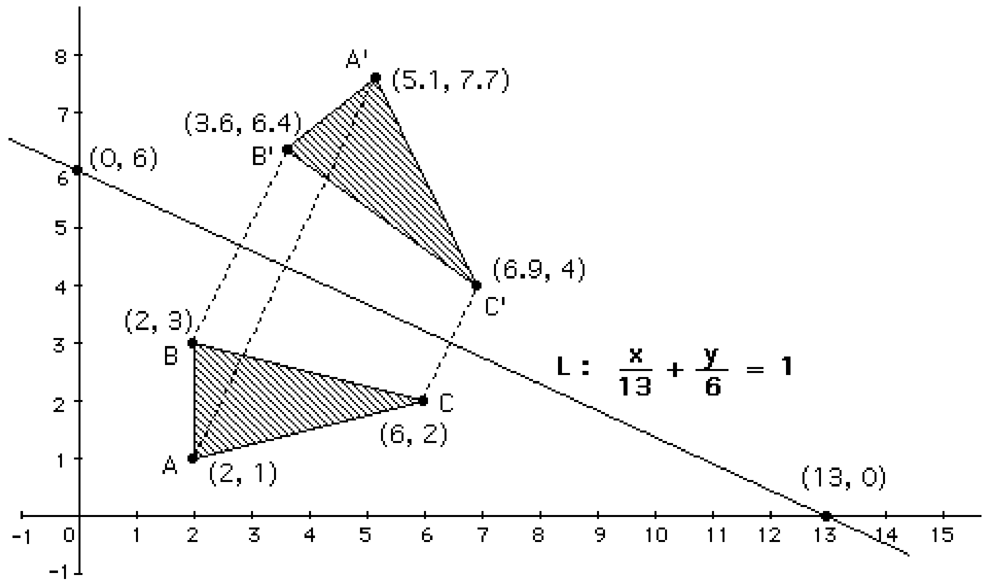

Fig. 1.16

Unlike in the case of translation, there is no obvious **algebraic** way of describing the transformation of coordinates observed above. This is of course no reason for giving up on determining the magic formula, if any, that lies behind this transformation of coordinates.

1.2.6 The reflection formula. Let L be a straight line with equation **ax + by = c** and M(x, y) be the mirror image of an arbitrary point (x, y) under reflection about L. Then ('magic formula')

M(x, y) =

$$= \left(\frac{2ac}{a^2+b^2} + \frac{b^2-a^2}{a^2+b^2}x - \frac{2ab}{a^2+b^2}y, \quad \frac{2bc}{a^2+b^2} - \frac{2ab}{a^2+b^2}x - \frac{b^2-a^2}{a^2+b^2}y\right)$$

Proof*: Let **(x′, y′)** be the coordinates of M(x, y) and **(x_1, y_1)** be the coordinates of the **midpoint Q** of the segment connecting (x, y) and (x′, y′); Q lies, of course, **on** the mirror L (figure 1.17), while $x_1 = \frac{x+x'}{2}$ and $y_1 = \frac{y+y'}{2}$.

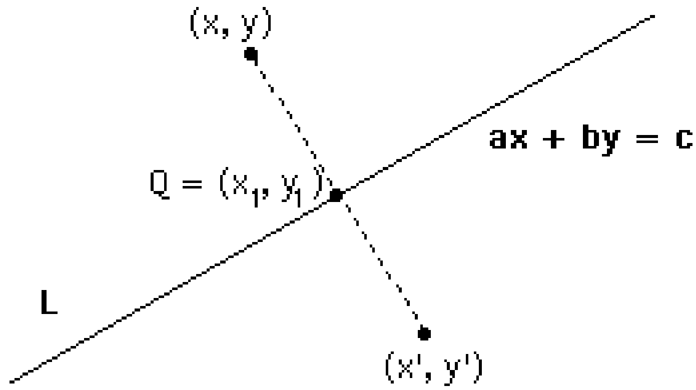

Fig. 1.17

Since $(x_1, y_1) = (\frac{x+x'}{2}, \frac{y+y'}{2})$ lies on the line $ax + by = c$, we obtain $a(\frac{x+x'}{2})+b(\frac{y+y'}{2}) = c$, therefore $a(x+x')+b(y+y') = 2c$, $ax+ax'+by+by' = 2c$, and, finally, $\mathbf{ax'+by' = 2c-ax-by}$ (I).

Next, observe that the line $ax + by = c$ (or, in equivalent form, and assuming $\mathbf{b \neq 0}$, $\mathbf{y = -\frac{a}{b}x + \frac{c}{b}}$) and the segment connecting (x, y) and (x', y') have **slopes** that are **negative reciprocals** of each other: indeed the line and the segment are **perpendicular** to each other. Since the line's slope is $\mathbf{-\frac{a}{b}}$ and the segment's slope is $\mathbf{\frac{y'-y}{x'-x}}$, we conclude that $\frac{y'-y}{x'-x} = \frac{b}{a}$, hence $a(y'-y) = b(x'-x)$, $ay'-ay = bx'-bx$ and, finally, $\mathbf{bx'-ay' = bx-ay}$ (II).

Multiplying now (I) by **a** and (II) by **b** and adding the two products we get $(a^2x'+aby')+(b^2x'-aby') = (2ac-a^2x-aby)+(b^2x-aby)$, therefore $(a^2+b^2)x' = 2ac+(b^2-a^2)x-2aby$ and $\mathbf{x' = \frac{2ac}{a^2+b^2} + \frac{b^2-a^2}{a^2+b^2}x - \frac{2ab}{a^2+b^2}y}$ (III). Very similarly (multiplying (I) by **b** and (II) by **−a**, etc) we see that $\mathbf{y' = \frac{2bc}{a^2+b^2} - \frac{2ab}{a^2+b^2}x - \frac{b^2-a^2}{a^2+b^2}y}$ (IV). Observe now that (III) and (IV) together yield the reflection formula we wished to establish.

When **b = 0**, one can see **directly** that the image of (x, y) under reflection about the **vertical** line $\mathbf{x = \frac{c}{a}}$ is M(x, y) = $\mathbf{(\frac{2c}{a} - x,\ y)}$; this observation does prove the reflection formula in the special case b = 0.

1.2.7 Let's check it out! Does an application of the reflection formula obtained in 1.2.6 confirm our empirical observations and coordinate **estimates** in 1.2.5? Well, it better, otherwise there is something wrong somewhere! Let's see: in figure 1.16 the reflection axis L passes through **(13, 0)** (x-intercept) and **(0, 6)** (y-intercept), hence its equation is $\mathbf{\frac{x}{13} + \frac{y}{6} = 1}$ or **6x + 13y = 78**; this leads to **a = 6**, **b = 13**, and **c = 78**, so that $a^2+b^2 = 6^2+13^2 = 36+169 = 205$, $b^2-a^2 = 13^2-6^2 = 169-36 = 133$, $2ab = 2 \times 13 \times 6 = 156$, $2ac = 2 \times 6 \times 78 = 936$ and $2bc = 2 \times 13 \times 78 = 2{,}028$. The reflection formula tells us that the image of a point (x, y) is given by

$$M(x, y) = (\frac{2ac}{a^2+b^2} + \frac{b^2-a^2}{a^2+b^2}x - \frac{2ab}{a^2+b^2}y,\ \frac{2bc}{a^2+b^2} - \frac{2ab}{a^2+b^2}x - \frac{b^2-a^2}{a^2+b^2}y) =$$
$$= (\frac{936}{205} + \frac{133}{205}x - \frac{156}{205}y,\ \frac{2028}{205} - \frac{156}{205}x - \frac{133}{205}y) \approx$$
$$\approx \mathbf{(4.56 + .65x - .76y,\ 9.89 - .76x - .65y)}.$$

Therefore the image of, say, **(6, 2)** 'predicted' by our formula is $(4.56 + .65 \times 6 - .76 \times 2,\ 9.89 - .76 \times 6 - .65 \times 2) = (4.56+3.9-1.52,\ 9.89-4.56-1.3) =$ **(6.94, 4.03)**, which is marvelously close to our estimates in figure 1.16! (This is the check applied to C and C′; make sure you verify the reflection formula for A, A′ and B, B′, too.)

1.2.8 Crossing a mirror? One important aspect of reflection you will have to get used to is the fact that, unlike in the real world, a mirror can **cross** through an object (set) reflected about it, and vice versa. To find the image of a set that does intersect a mirror, all you have to do is apply the 'natural rules' outlined in 1.2.1 and 1.2.2 without worrying about 'physical realities'. Here is an example:

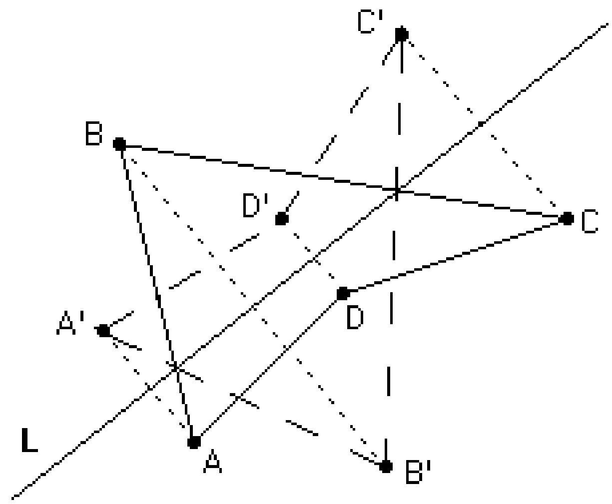

Fig. 1.18

Beware of ‘mirror-crossing’ cases where the mirror image falls back on the original set point by point: in such cases, which will become important in the rest of this book, we say that the set in question has an **internal mirror** and **mirror symmetry**. The following English letters have mirror symmetry: A, B, C, D, E, H, I, M, O, T, U, V, W, X, Y.

1.3 Rotation

1.3.1 How about a ‘time game’? Suppose that it is 9:40 (PM or AM) now that you are reading this paragraph. Take your watch in your

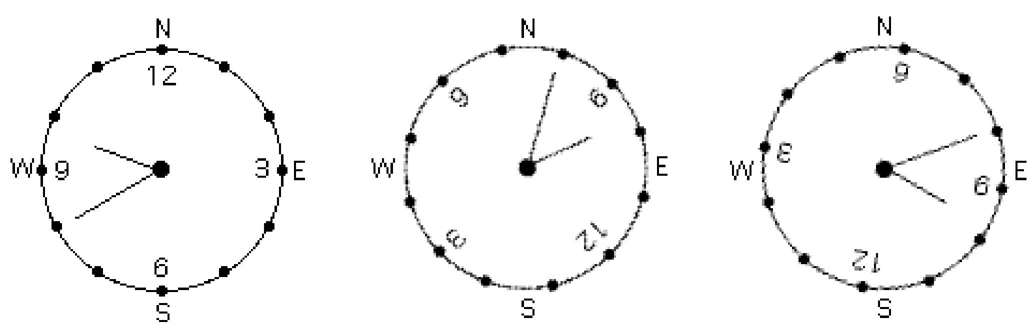

Fig. 1.19

hands, stop the time at 9:40 and start to slowly **turn** it around. You may do this on a piece of paper where you have already marked the positions of 12, 3, 6, and 9 as if on a compass (N, E, S, W); you may of course mark the other hours in between as well. There are positions where, as figure 1.19 demonstrates, your turning watch's hands will approximately show 2:00 or 4:10, right? Could you tell how much you should turn your watch in order to 'attain' these times? Well, while a precise answer would require (just like the determination of the exact attainable times) some serious mathematical thinking, you should be able to handle the question as posed: a **clockwise** ('screwing') turn by 130^0 will make the watch show a time close to 2:00 (2:01′:49″ to be precise!), while a clockwise turn by 195^0 will 'change the time' from 9:40 to approximately 4:10 (in fact 4:12′:44″, but you don't have to worry about that right now).

1.3.2 What happened to the watch? While the 'time game' described in 1.3.1 can indeed get quite complicated, especially if played with precision, some simple facts about the stopped watch's 'condition' during its turning around are simple and indisputable: its **center** remained fixed, the **angle** between the two hands remained the same (50^0), and, last but not least, the **distance** between the tips of the two hands never changed. It seems that our watch-turning game preserves distances: could in fact be some kind of isometry, then?

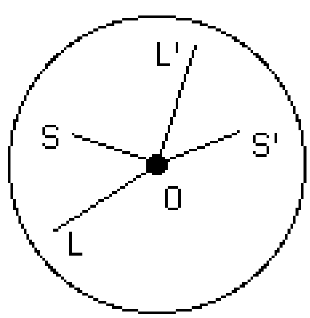

Fig. 1.20

Figure 1.20 describes the change of time from 9:40 to approximately 2:00 during our game: S and L represent the position of the tips of the watch's short and long hand, respectively, at 9:40, while S′ and L′ represent the position of those tips at about 2:00. One thing that cannot be missed is the fact that **both** angles LOL′ and SOS′ are equal to about 130^0. What really happened to the tips, and hands, and the entire watch in fact, is a clockwise **rotation** by an angle of approximately 130^0 about the point O (the watch's center).

1.3.3 <u>How does rotation work?</u> Even though figure 1.20 says it all, it would be useful to offer another example here, this time of a **counterclockwise** ('unscrewing') rotation **by** 70^0 **about** the center K shown in figure 1.21. How do we find the image P′ of any given point P under this rotation? We simply draw KP, measure it either with a ruler or with a compass, then 'build' a 70^0 angle 'to the left hand' of KP with the help of a protractor, and finally pick a point P′ on the angle's 'new' leg so that **|KP′| = |KP|**. That's all!

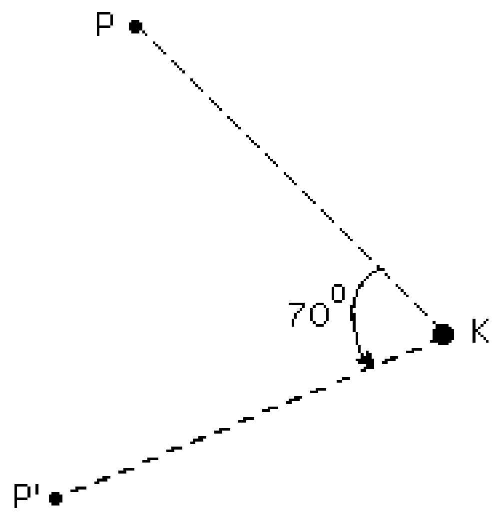

Fig. 1.21

1.3.4 <u>It's an isometry!</u> Let us now verify our conjecture in 1.3.2 and prove that every rotation is indeed an isometry. We return to our watch example and prove that **|LS| = |L′S′|**, which says that the distance between the two images L′, S′ is equal to the distance between the two original points L, S; the general case is proven in exactly the same way.

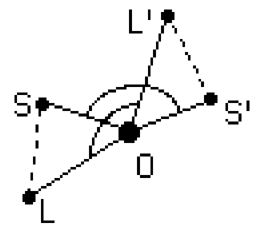

Fig. 1.22

Let us look at the two triangles OLS, OL′S′ (figure 1.22): they have two pairs of equal sides as **|OS| = |OS′|** (short hands) and **|OL| = |OL′|** (long hands). If we show the in-between angles ∠LOS and ∠L′OS′ to be equal, then the two triangles are congruent and, of course, |LS| = |L′S′|. But the equality of the two angles follows easily: ∠LOS = ∠LOL′−∠SOL′ = ∠SOS′ − ∠SOL′ = ∠L′OS′. (Note: **∠LOL′ = ∠SOS′ ≈ 130^0**.)

1.3.5 Images. Now that we know how rotation works, let us find the image of triangle ABC from 1.1.1 under rotation about the center K in figure 1.23 and by the counterclockwise 70^0 angle of 1.3.3. We do this by finding the images A′, B′, C′ of A, B, C (figure 1.23):

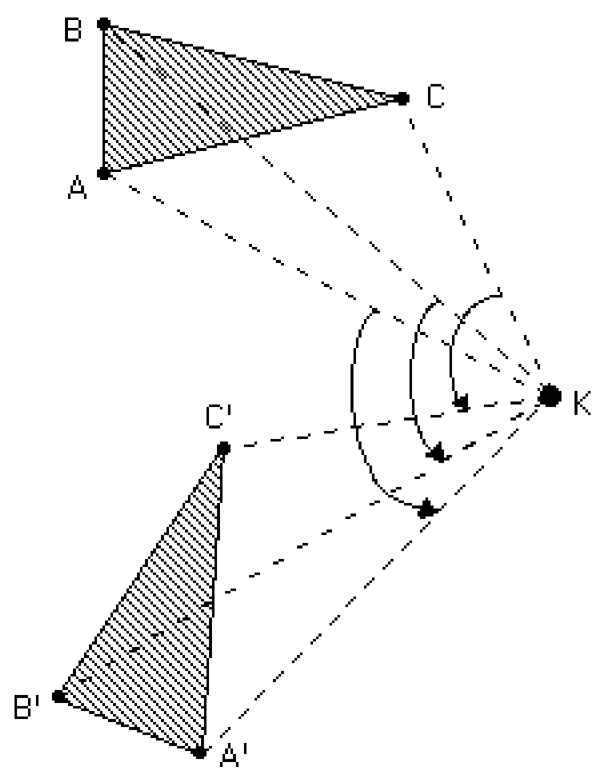

Fig. 1.23

1.3.6 Coordinates. Let us now place the triangles ABC, A′B′C′ of 1.3.5 in a cartesian coordinate system as shown in figure 1.24, so that the coordinates of A, B, C will again be (2, 1), (2, 3), (6, 2), respectively, those of the rotation center will be (8, −2). Estimating the coordinates of A′, B′, and C′ as in 1.2.5, we find them to be **approximately** (3.2, −6.8), (1.4, −6), and (3.6, −2.7), respectively.

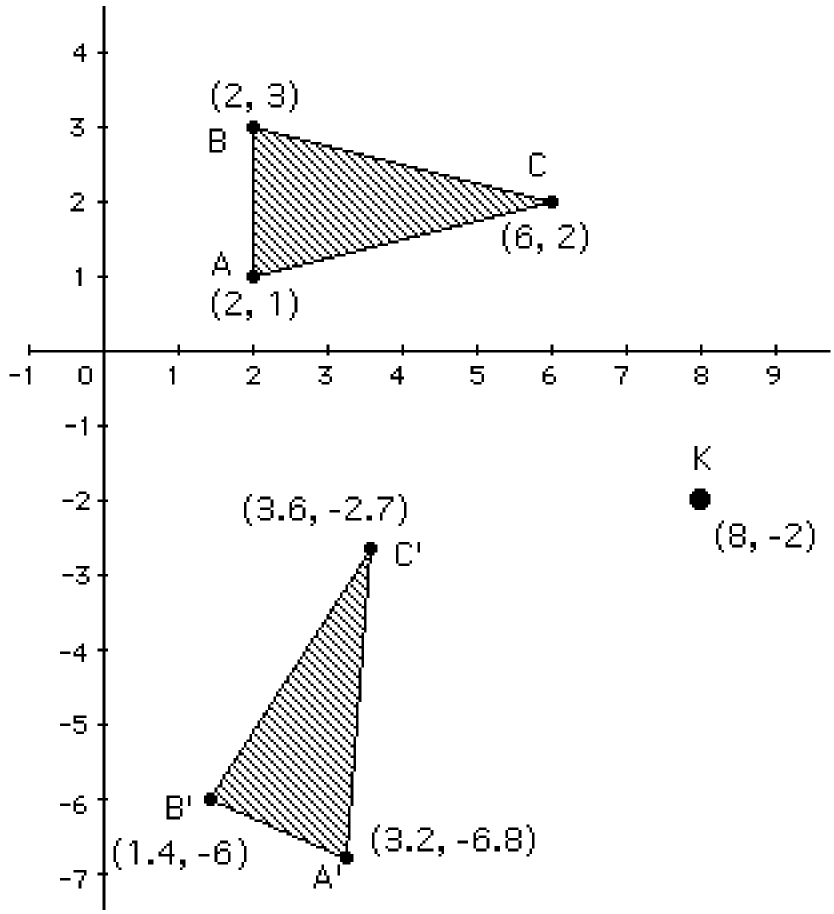

Fig. 1.24

Exactly as in 1.2.5, you might wonder whether there could possibly exist a ‘magic formula’ that could ‘predict’ the coordinates estimated above. Such a formula does exist, but its derivation is even harder than that of the reflection formula in 1.2.6 and can only be understood with some knowledge of Trigonometry.

1.3.7 The rotation formula. Let **R(x, y) = (x′, y′)** be the image of an arbitrary point (x, y) under rotation about the **rotation**

center K = (a, b) by a **rotation angle** ϕ. Then either

$$\mathbf{x' = (1-\cos\phi)a - (\sin\phi)b + (\cos\phi)x + (\sin\phi)y,}$$

$$\mathbf{y' = (\sin\phi)a + (1-\cos\phi)b - (\sin\phi)x + (\cos\phi)y}$$

(in case ϕ is **clockwise**) or

$$\mathbf{x' = (1-\cos\phi)a + (\sin\phi)b + (\cos\phi)x - (\sin\phi)y,}$$

$$\mathbf{y' = -(\sin\phi)a + (1-\cos\phi)b + (\sin\phi)x + (\cos\phi)y}$$

(in case ϕ is **counterclockwise**).

These formulas are indeed complicated, almost hard to believe, aren't they? Well, for a quick check you may like to verify that, no matter what ϕ is, both formulas yield $x' = a$ and $y' = b$ when $x = a$ and $y = b$, that is, **R(a, b) = (a, b)**: indeed the center of every rotation remains **invariant** under that rotation! Moreover, the two formulas are really one and the same: mathematicians tend to view clockwise angles as **'negative'**; so, substituting ϕ by $-\phi$ in the second formula yields the first one via $\mathbf{\cos(-\phi) = \cos\phi}$, $\mathbf{\sin(-\phi) = -\sin\phi}$.

Proof*: We offer a complete proof for the case of **clockwise** ϕ and a basic hint for the very similar case of counterclockwise ϕ. Once again, some familiarity with basic trigonometric functions and identities will be assumed; do not get discouraged if this proof seems too hard for you, and do not hesitate to ask for some help!

Let $P = (x, y)$ be a point that clockwise rotation by angle ϕ about center $K = (a, b)$ maps to a point $P' = (x', y')$, as shown in figure 1.25. Notice, referring to figure 1.25 always, that $\mathbf{|KP'| = |KP|}$, $|GK| = |CA| = |OA| - |OC|$, and $|GP| = |BD| = |OD| - |OB|$; moreover, $\boldsymbol{\theta' = 180^0-\theta-\phi}$, hence $\cos\theta' = -\cos(\theta+\phi) = -\cos\theta\cos\phi + \sin\theta\sin\phi$ and $\sin\theta' = \sin(\theta+\phi) = \sin\theta\cos\phi + \cos\theta\sin\phi$.

Now $x' = |OE| = |OA| + |AE| = |OA| + |KH| = |OA| + \mathbf{|KP'|\cos\theta'} =$
$= |OA| - \mathbf{|KP|\cos\theta}\cos\phi + \mathbf{|KP|\sin\theta}\sin\phi = |OA| - |GK|\cos\phi + |GP|\sin\phi =$
$= |OA| - (|OA| - |OC|)\cos\phi + (|OD| - |OB|)\sin\phi =$
$= a - (a - x)\cos\phi + (y - b)\sin\phi =$

$= (1 - \cos\phi)a - (\sin\phi)b + (\cos\phi)x + (\sin\phi)y$, as claimed.

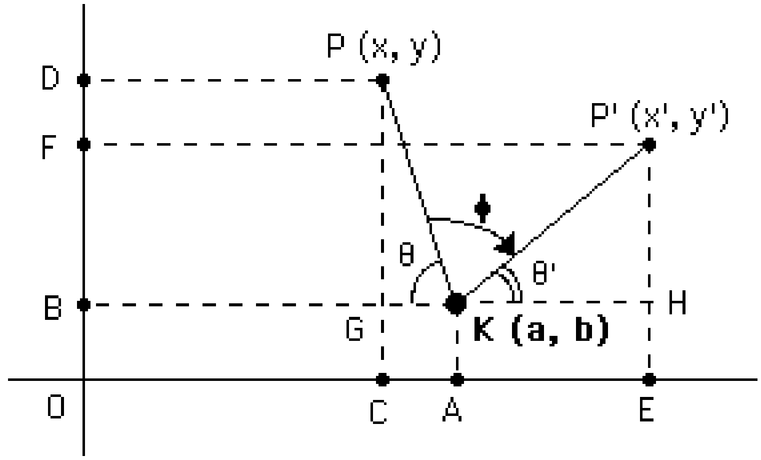

Fig. 1.25

Similarly, $y' = |OF| = |OB| + |BF| = |OB| + |HP'| = |OB| + \mathbf{|KP'|\sin\theta' =}$
$= |OB| + \mathbf{|KP|\sin\theta}\cos\phi + \mathbf{|KP|\cos\theta}\sin\phi = |OB| + |GP|\cos\phi + |GK|\sin\phi =$
$= |OB| + (|OD| - |OB|)\cos\phi + (|OA| - |OC|)\sin\phi =$
$= b + (y - b)\cos\phi + (a - x)\sin\phi =$
$= (\sin\phi)a + (1 - \cos\phi)b - (\sin\phi)x + (\cos\phi)y$, as claimed.

When ϕ happens to be **counterclockwise**, figure 1.25 changes into figure 1.26 below: now $\boldsymbol{\theta' = \theta - \phi}$, hence $\cos\theta' = \cos\theta\cos\phi + \sin\theta\sin\phi$ and $\sin\theta' = \sin\theta\cos\phi - \cos\theta\sin\phi$; $|GK| = |OA| - |OC|$ and $|GP| = |OD| - |OB|$ remain valid. You should be able to fill in the details and derive the claimed formulas for x' and y'.

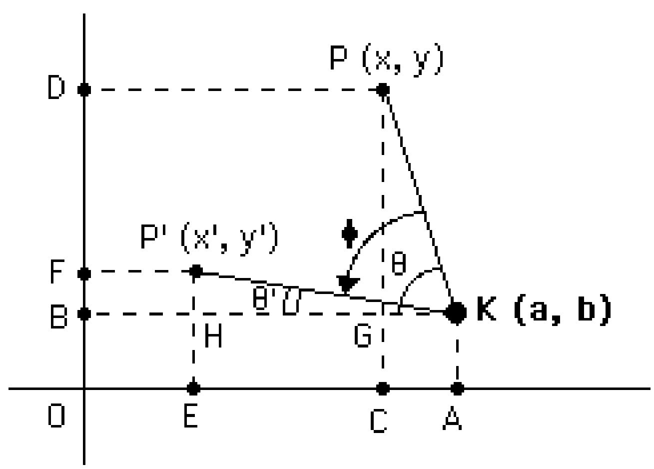

Fig. 1.26

There are in fact more cases to investigate, like when ϕ is counterclockwise and **larger** than θ, for example. Similar arguments left to you as exercises do work in all such cases, and our rotation formula works always.

1.3.8 Let's check it out! Let us now return to figure 1.24, augmented by A″B″C″, the **clockwise** image of ABC (figure 1.27). As we did in the cases of translation (1.1.4) and reflection (1.2.7), we would like to verify that **geometrical** estimates (1.3.6) and **algebraic** formulas (1.3.7) are in full agreement with each other.

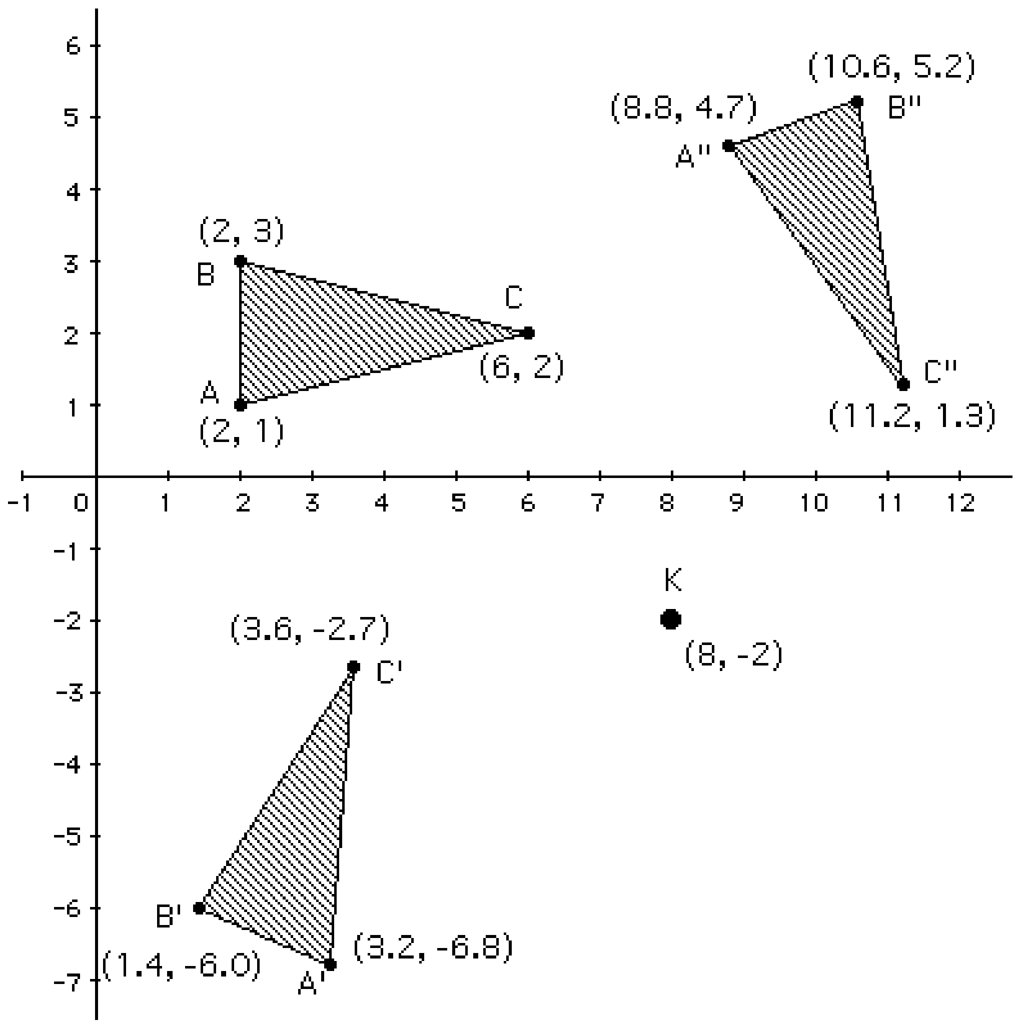

Fig. 1.27

Let's see: with $\cos 70^0 \approx .34$ and $\sin 70^0 \approx .94$, the

counterclockwise rotation formula for A = **(2, 1)** yields

$x' \approx (1-.34)\times 8 + .94\times(-2) + .34\times 2 - .94\times 1 = 5.28-1.88+.68-.94 =$ 3.14 and

$y' \approx -.94\times 8 + (1-.34)\times(-2) + .94\times 2 + .34\times 1 = -7.52-1.32+1.88+.34$ $= -6.62$,

therefore **R(2, 1) ≈ (3.1, −6.6)**, which is quite close indeed to that (3.2, −6.8) estimate in 1.3.6. Perhaps we could have achieved some greater precision with the use of more precise drawing and instruments, but such great precision will probably not be possible when you take your exam anyway...

Let us now see how things work out for A″, the **clockwise** image of A = **(2, 1)**. Coordinate estimates (figure 1.27) indicate that A″ ≈ (8.8, 4.7). The rotation formula yields

$x'' \approx (1-.34)\times 8 - .94\times(-2) + .34\times 2 + .94\times 1 = 5.28+1.88+.68+.94 =$ $= 8.78$ and

$y'' \approx .94\times 8 + (1-.34)\times(-2) - .94\times 2 + .34\times 1 = 7.52-1.32-1.88+.34 =$ $= 4.66$,

therefore **R(2, 1) ≈ (8.8, 4.7)**: our estimate (in fact our drawing) worked perfectly this time -- it happens!

By the way, a closer look at the preceding two examples should help you understand why the image of an **arbitrary** point (x, y) under rotation by 70^0 about (8, −2) is approximately **(7.16 + .34x + .94y, 6.2 − .94x + .34y)** in the clockwise case and **(3.4 + .34x − .94y, −8.84 + .94x + .34y)** in the counterclockwise case.

You should now get a bit more practice by near-matching formula outcomes and geometrical estimates for B′, C′, B″, and C″, redrawing the image triangles A′B′C′ and A″B″C″ in case you are not happy with our drawing: good luck!

1.3.9 <u>'Interior' centers.</u> Just as the reflection axis is allowed to cross a set that is reflected about it (1.2.8), the rotation center K could very well be **inside** a set rotated about it. Here is an example:

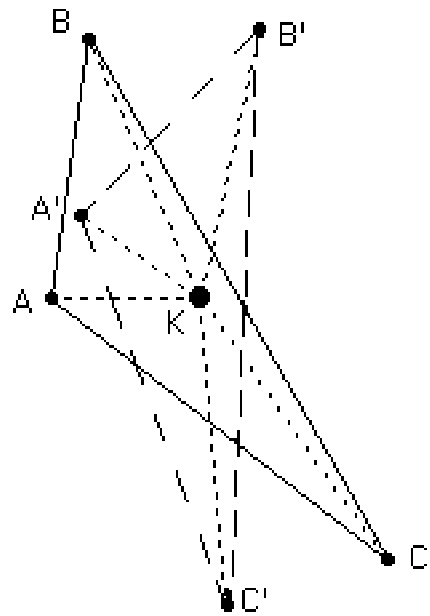

Fig. 1.28

When, in the case of such ‘internal centers’, the image falls, point by point, back on the original, we say that the figure in question has an **internal turn** and **rotational symmetry**. The following English letters have rotational symmetry (of 180^0, see 1.3.10): H, I, O, S, X, Z.

1.3.10 A ‘straight’ rotation. We have seen how important it is to know whether a rotation is clockwise or counterclockwise. There is however precisely one angle for which the distinction between clockwise and counterclockwise does not matter at all, and that is the $\mathbf{180^0}$ angle: **regardless** of which way the point P is rotated about the rotation center K, we end up with an image point P′ on the **extension** of the segment PK such that **|KP′| = |KP|** (figure 1.29).

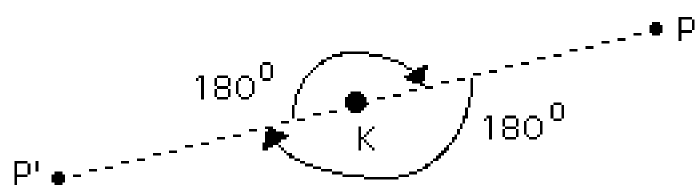

Fig. 1.29

This very special rotation by 180^0 is also known as **half turn** or **point reflection** -- we will be using either term at will -- and is destined to become very important in chapter 2 and beyond. For the time being, here is an example of half turn applied to the quadrilateral of figure 1.18:

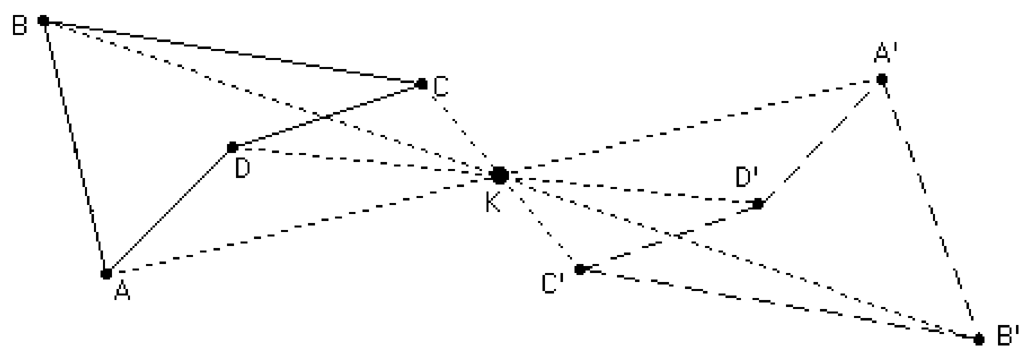

Fig.1.30

Notice here an important property of point reflection: it always maps a straight line segment to a straight line segment (equal and) **parallel** to it. You may confirm this with the help of figure 1.30 and/or a simple geometrical proof.

1.4 Glide reflection

1.4.1 Is it a 'new' isometry? Our fourth and last planar isometry is at the same time the least 'intuitive' -- you will truly understand it only after going through the next three chapters -- and the easiest one to introduce: how can this happen? The answer is simple: it is the **'combination'** of two already described isometries, translation and reflection, but it is not so clear in the beginning why anyone would ever bother to combine them!

1.4.2 Axes and vectors. All we need to describe the new isometry is, as hinted above, a reflection axis L and a translation vector $\vec{v}$ **parallel** to L: the image of an arbitrary point P is now found either by first reflecting about L to P_L and then **gliding**

(translating) along $\vec{v}$ to P′ or by first gliding along $\vec{v}$ to P_v and then reflecting about L to P′ (figure 1.31). That is, the order in which the two operations are performed does **not** affect the final outcome P′, the image of P under **glide reflection G = (L, $\vec{v}$)** by L **and** $\vec{v}$. We view glide reflection as a **'deferred reflection'** and use **dotted** lines for L (a 'half' (glided) mirror) and $\vec{v}$ (a 'half' (mirrored) glide) in order to stress their interdependence:

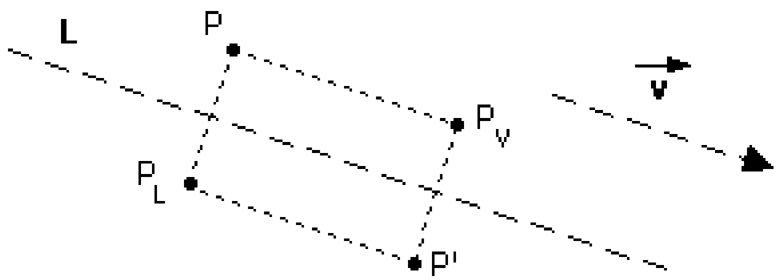

Fig. 1.31

Why do these two isometries, a reflection and a translation parallel to each other, **commute**? Figure 1.31 (and **rectangle $PP_LP'P_V$** in particular) makes that 'obvious', but it is worth stressing the role of parallelism: since $\vec{v}$ is parallel to L, the final image of P is bound to lie on a line parallel to L and at a distance from L **equal** to the distance from P to L, regardless of the order in which we performed the two operations. Observe at this point that a reflection and a translation **not** parallel to each other do **not** commute (figure 1.32);

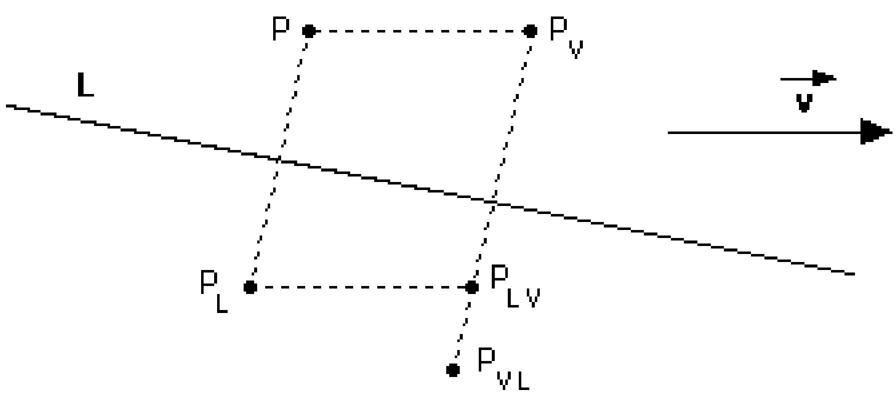

Fig. 1.32

that is generally the case whenever one tries to 'combine' any two isometries, as we will see in chapter 7. On the other hand, leaving something unchanged twice certainly preserves it: the combined effect of every two isometries is still an isometry, as each of the two isometries preserves all distances; in particular every glide reflection is indeed an isometry.

1.4.3 Images. Figure 1.33 demonstrates how one determines the image of the pentagon **S** under a glide reflection **G** = (**L**, $\vec{\mathbf{v}}$), as well as the commutativity between reflection and translation; the relation among the three isometries (translation, reflection, glide reflection) and the respective three images (**T(S)**, **M(S)**, **G(S)**) is shown clearly:

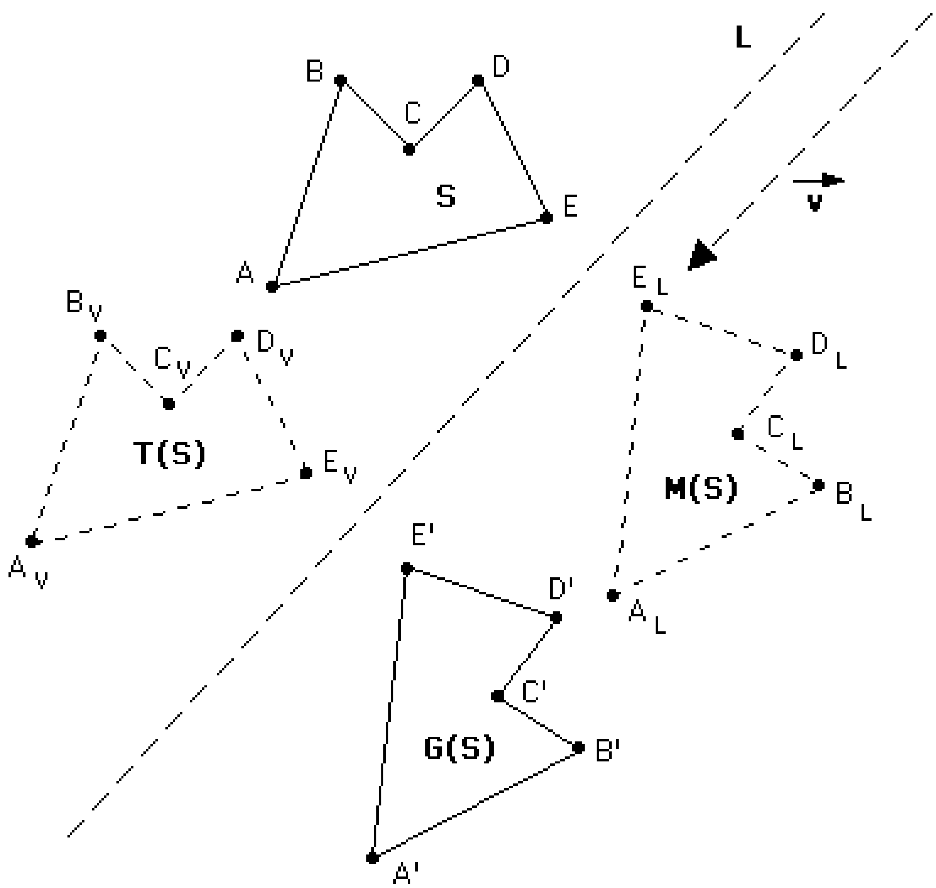

Fig. 1.33

1.4.4 Two opposite glide reflections. Let us once again revisit triangle ABC of figure 1.11, as well as the reflection axis **L** of figure 1.16, adding two vectors $\vec{\mathbf{v}}_1$ and $\vec{\mathbf{v}}_2$ (figure 1.34): these are of **equal length** and of the **same direction** (parallel to L), but of **opposite sense**. The two vectors create two glide reflections **opposite** of each other, $\mathbf{G_1} = (\mathbf{L}, \vec{\mathbf{v}}_1)$ and $\mathbf{G_2} = (\mathbf{L}, \vec{\mathbf{v}}_2)$; the images A′B′C′, A″B″C″ of ABC under $\mathbf{G_1}$, $\mathbf{G_2}$, respectively, are shown below:

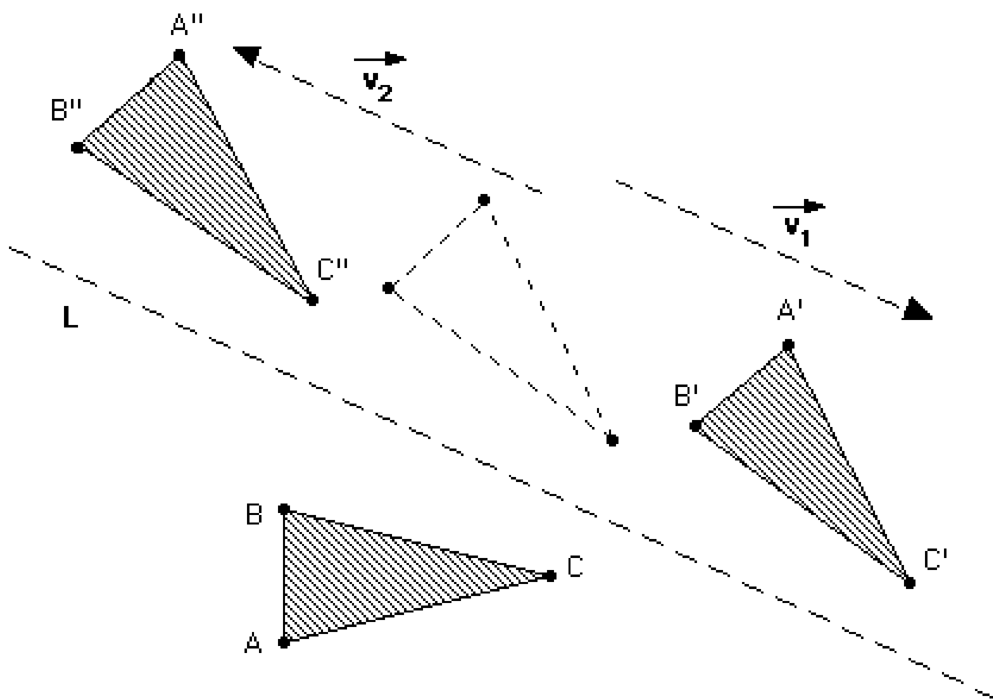

Fig. 1.34

What would have happened in case we **successively** applied $\mathbf{G_1}$ followed by $\mathbf{G_2}$ (or $\mathbf{G_2}$ followed by $\mathbf{G_1}$) to ABC? It shouldn't take you that long to realize that we would have gone first to A′B′C′ (or A″B″C″) and then back where we started from, ABC. This is why $\mathbf{G_1}$ and $\mathbf{G_2}$ are called **inverses** of each other: they simply cancel each other's effect, just as the two translations of 1.1.4 and the two rotations of 1.3.8 do. Notice by the way that every **reflection** is the **inverse of itself**, and the same holds for every **half turn**.

1.4.5 <u>The glide reflection formula.</u> Deriving a formula for the coordinates of the image point G(x, y) under a glide reflection is not that challenging in view of the work we have done in sections 1.1 and 1.2. We will in fact offer two formulas, one here (based on 1.1.4 and 1.2.6) and one in 1.4.7 (based on 1.1.5 and 1.2.6): unless you still have problems with basic Trigonometry you will probably find the formula in 1.4.7 easier to use, so you may certainly choose to read that section **first**.

Avoiding Trigonometry for now, let **ax + by = c** be the equation of the glide reflection axis L and let **<A, B>** be the glide reflection vector parallel to L. The slope **B/A** of <A, B> must be **equal** to the slope of L, which is **−a/b** (see 1.2.6); so we may and do write <A, B> as <bs, −as>, where **s** is a **parameter** that depends on the **vector's length S** via

$$S = \sqrt{A^2+B^2} = \sqrt{(bs)^2+(as)^2} = |s|\sqrt{a^2+b^2}\,.$$

That is, **<A, B> = <bs, −as>**, where $\mathbf{s = \pm\dfrac{S}{\sqrt{a^2+b^2}}}$. In the case of the vectors $\vec{\mathbf{v}}_1$ and $\vec{\mathbf{v}}_2$ of 1.4.4, a = 6, b = 13, S = 5 (see 1.2.7 and figures 1.16 & 1.35), so $s = \pm 5/\sqrt{6^2+13^2} \approx \pm.35$; now **s = +.35** yields $\vec{\mathbf{v}}_1 \approx$ <13 × .35, −6 × .35> = **<4.55, −2.1>**, while **s = −.35** leads to $\vec{\mathbf{v}}_2 \approx$ <−13 × .35, 6 × .35> = **<−4.55, 2.1>**. We obtain approximately the same coordinates for $\vec{\mathbf{v}}_1$ and $\vec{\mathbf{v}}_2$ (like **<4.6, −2.1>** and **<−4.6, 2.1>**, as in figure 1.35) following the procedures outlined in figures 1.11 or 1.12.

Now we combine the **reflection** formula from 1.2.6 and the **translation** formula from 1.1.4 to obtain **G(x, y) = (x′, y′)**, where

$$\mathbf{x' = bs + \frac{2ac}{a^2+b^2} + \frac{b^2-a^2}{a^2+b^2}x - \frac{2ab}{a^2+b^2}y,}$$

$$y' = -as + \frac{2bc}{a^2+b^2} - \frac{2ab}{a^2+b^2}x - \frac{b^2-a^2}{a^2+b^2}y.$$

So, all we did was to apply the reflection first and then **add** the translation effect coordinatewise! We still had to do a bit of work, of course, and that was the determination of the translation vector's **coordinates**.

1.4.6 Let's check it out! The game is perfectly familiar by now: we redraw figure 1.34 in a cartesian coordinate system, estimate the coordinates of points and vectors alike (figure 1.35), and use this numerical input to confirm the validity of the glide reflection formula. The work has been largely done in 1.2.7 (where we computed the quotients $\frac{b^2-a^2}{a^2+b^2}$, $\frac{2ab}{a^2+b^2}$, $\frac{2ac}{a^2+b^2}$, and $\frac{2bc}{a^2+b^2}$ for a = 6, b = 13, and c = 78 in order to derive the reflection part of the formula) and 1.4.5 (where we determined s and the two vectors of length 5 that are parallel to the axis 6x + 13y = 78). Combining everything, we obtain

$\mathbf{G_1(x,\ y)}$ = (4.55 + 4.56 + .65x – .76y, –2.1 + 9.89 – .76x – .65y) = **(9.11 + .65x – .76y, 7.79 – .76x – .65y)** and

$\mathbf{G_2(x,\ y)}$ = (–4.55 + 4.56 + .65x – .76y, 2.1 + 9.89 – .76x – .65y) = **(0.01 + .65x – .76y, 11.99 – .76x – .65y)**.

Applying these formulas to A and B, respectively, we obtain $\mathbf{G_1(2,\ 1) = (9.65,\ 5.62)}$ for A′ and $\mathbf{G_2(2,\ 3) = (-.97,\ 8.52)}$ for B″, which are quite close to our geometrical estimates below:

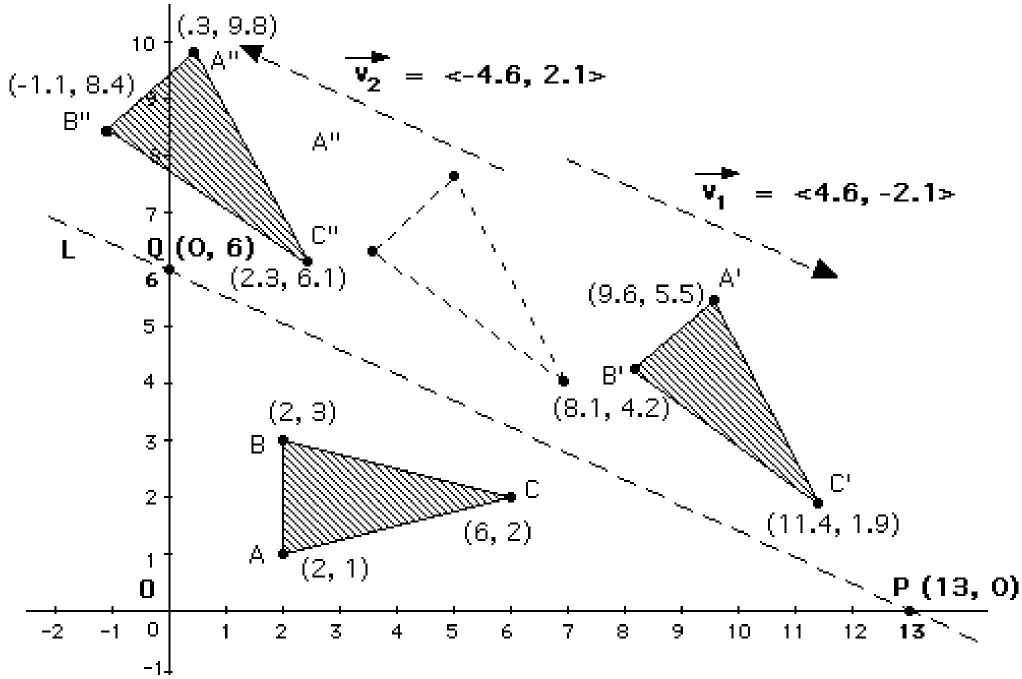

Fig. 1.35

1.4.7 Alternative formula. You certainly know that, more often than not, there is a gap between theory and practice. In the present context we point out that, while, in theory, the formula in 1.4.5 nicely expresses the glide reflection vector's coordinates in terms of the glide reflection axis' equation's coefficients, in practice determining the parameter **s** (and its **sign**) is quite complicated. It turns out that, as we promised in 1.4.5, Trigonometry offers a quick rescue.

Indeed, going back to 1.1.5, we recall that every vector may be written as **<S·cosθ, S·sinθ>**, where **S** is the vector's length and **θ** is the vector-angle, that is the **counterclockwise** angle between the vector and the **positive** x-axis. In the case of the two opposite gliding vectors $\vec{v}_1$, $\vec{v}_2$ of 1.4.5, our method is fully illustrated in figure 1.36:

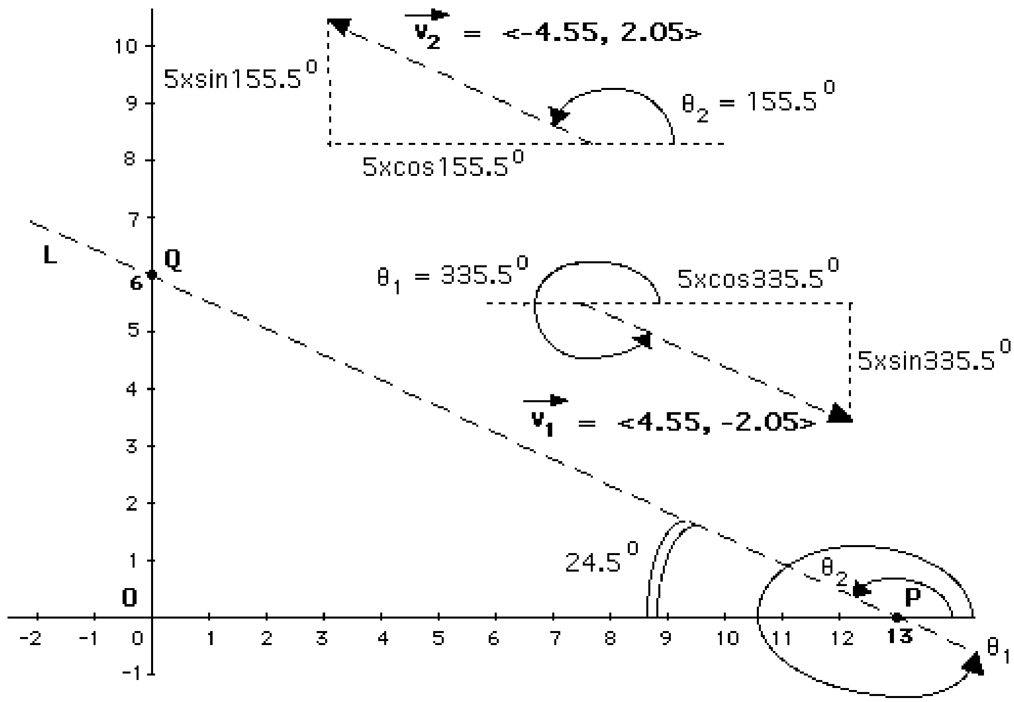

Fig. 1.36

That is, the fact that the glide reflection vectors $\vec{v}_1$, $\vec{v}_2$ are **parallel** to the glide reflection axis L **reduces** the angle's measurement, for both vectors, to simply measuring the **counterclockwise** angle between L and the **positive** x-axis (as shown in figure 1.36). As the vector-angles for $\vec{v}_2$ and $\vec{v}_1$ are $\boldsymbol{\theta_2} \approx 180^0 - 24.5^0 = 155.5^0$ and $\boldsymbol{\theta_1} = \theta_2 + 180^0 \approx 155.5^0 + 180^0 = 335.5^0$, we obtain $\cos\theta_2 \approx \cos(155.5^0) \approx -.91$ and $\sin\theta_2 \approx \sin(155.5^0) \approx .41$, so that $\cos\theta_1 = \cos(\theta_2+180^0) = -\cos\theta_2 \approx .91$ and $\sin\theta_1 = \sin(\theta_2+180^0) = -\sin\theta_2 \approx -.41$. It follows, with S = 5, that $\boldsymbol{\vec{v}_1 = <5\cdot\cos\theta_1,\ 5\cdot\sin\theta_1>} \approx <5 \times (.91),\ 5 \times (-.41)> = <4.55, -2.05>$ and $\boldsymbol{\vec{v}_2 = <5\cdot\cos\theta_2,\ 5\cdot\sin\theta_2>} \approx <5 \times (-.91),\ 5 \times (.41)> = <-4.55, 2.05>$: these are indeed very close to the vectors determined in 1.4.5.

From here on all there is to be done is to add the translation effect (as computed above) to the reflection effect (as determined in 1.2.6), obtaining **G(x, y) = (x′, y′)** with

$$\mathbf{x' = S\cdot\cos\theta + \frac{2ac}{a^2+b^2} + \frac{b^2-a^2}{a^2+b^2}x - \frac{2ab}{a^2+b^2}y},$$

$$\mathbf{y' = S\cdot\sin\theta + \frac{2bc}{a^2+b^2} - \frac{2ab}{a^2+b^2}x - \frac{b^2-a^2}{a^2+b^2}y},$$

where **S** is the gliding vector's length, θ is the gliding vector's vector-angle (as discussed right above and also in 1.1.5), and, again, **ax + by = c** is the equation of the glide reflection axis L. We leave it to you to check that, with vector-angles θ_1 and θ_2 for $\mathbf{G_1} = (\mathbf{L}, \vec{\mathbf{v}}_1)$ and $\mathbf{G_2} = (\mathbf{L}, \vec{\mathbf{v}}_2)$, respectively,

$\mathbf{G_1(x,\ y) \approx (9.11 + .65x - .76y,\ 7.84 - .76x - .65y)}$ and

$\mathbf{G_2(x,\ y) \approx (0.01 + .65x - .76y,\ 11.94 - .76x - .65y)}$:

these formulas are certainly very close to those in 1.4.6.

Of course, those with a strong Trigonometry background should have no trouble seeing the **connection** between 1.4.6 and 1.4.7: indeed $\cos155.5^0 = -\cos24.5^0 \approx -\frac{|OP|}{|PQ|} = -\frac{13}{\sqrt{13^2+6^2}} \approx -.908$ and $\sin155.5^0 = \sin24.5^0 \approx \frac{|OQ|}{|PQ|} = \frac{6}{\sqrt{13^2+6^2}} \approx .419$. Moreover, they would know that the coordinates of P and Q yield a more **exact** value for the vector-angle via $\cos^{-1}(.908) \approx \sin^{-1}(.419) \approx \tan^{-1}(6/13) \approx 24.77^0$.

1.4.8 Reflections as glide reflections. Trivial as it might seem to you right now, this is a fact that is worth keeping in mind: every reflection may be seen as a 'degenerate' glide reflection the gliding vector of which has length **zero**. Indeed setting either **s = 0** in the glide reflection formula of 1.4.5 or **S = 0** in the glide reflection formula of 1.4.7 yields the reflection formula of 1.2.6.

1.5* Why precisely four planar isometries?

1.5.1 An old claim revisited. Back in 1.0.5 we promised to show that every isometry on the plane can be expressed via a formula like $F(x, y) = (a'+b'x+c'y,\ d'+e'x+f'y)$, where a' and d' are arbitrary, $\mathbf{b'^2+e'^2 = c'^2+f'^2 = 1}$, and either $\mathbf{f' = b'}$, $\mathbf{e' = -c'}$ or $\mathbf{f' = -b'}$, $\mathbf{e' = c'}$. Before we establish this claim (and more) in 1.5.4, let us prove that every function on the plane defined by such a formula is indeed an isometry. We do this using the **distance formula**: given any two points (x_1, y_1), (x_2, y_2), the distance between their images, $F(x_1, y_1) = (a'+b'x_1+c'y_1,\ d'+e'x_1+f'y_1)$ and $F(x_2, y_2) = (a'+b'x_2+c'y_2,\ d'+e'x_2+f'y_2)$, is

$$\sqrt{((a'+b'x_1+c'y_1)-(a'+b'x_2+c'y_2))^2 + ((d'+e'x_1+f'y_1)-(d'+e'x_2+f'y_2))^2}$$
$$= \sqrt{((b'(x_1-x_2) + c'(y_1-y_2))^2 + ((e'(x_1-x_2) + f'(y_1-y_2))^2}$$
$$= \sqrt{(b'^2+e'^2)(x_1-x_2)^2 + 2(b'c'+e'f')(x_1-x_2)(y_1-y_2) + (c'^2+f'^2)(y_1-y_2)^2}$$
$$= \sqrt{(x_1-x_2)^2 + 2(b'c'-b'c')(x_1-x_2)(y_1-y_2) + (y_1-y_2)^2}$$
$$= \sqrt{(x_1-x_2)^2 + (y_1-y_2)^2}\text{, the distance between } (x_1, y_1) \text{ and } (x_2, y_2).$$

Notice at this point that, once (and if) we know that all isometries are **linear**, that is of the form $F(x, y) = (a'+b'x+c'y,\ d'+e'x+f'y)$, then it is not too difficult to show that they must be of the form conjectured in 1.0.5 (and restated above): you might be able to do this using the fact that all **three distances** among (1, 0), (0, 1), and (0, 0) must be preserved. But how do we show that every isometry is linear? One possible way to do that would be to first recall that every isometry maps straight lines to straight lines (1.0.7) and then try to prove that every planar function that preserves straight lines must indeed be linear: the latter happens to be true, but it's a real **theorem** the proof of which lies beyond the scope of this book.

We can actually show that every isometry is linear following a more direct path: first we record the particular way (**linear formula)** in which each one of the four isometries already studied is linear (1.5.2); then we show that every linear function expressed by one of the four linear formulas **must** actually be one of the four isometries already studied (1.5.3); and finally we prove that **every** isometry is expressed by one of the four linear formulas (1.5.4). That is, we will manage to show that all isometries are linear and must be one of the four isometries already studied ... **at the same time**!

1.5.2 Our bag of isometries. In the previous four sections we studied four planar functions (translation, reflection, rotation, and glide reflection) and showed each one of them to be an isometry. Our proof was purely geometrical in all four cases. Now we can provide algebraic proofs using the lemma we just established in 1.5.1! We do this by going back to the formulas derived in 1.1.4, 1.2.6, 1.3.7, and 1.4.5 and simply verifying that each of them satisfies the **isometry conditions** of 1.5.1:

Translation: $f' = b' = 1$, $e' = -c' = 0$, $a' = a$, $d' = b$.

Reflection: $f' = -b' = -\frac{b^2-a^2}{a^2+b^2}$, $e' = c' = -\frac{2ab}{a^2+b^2}$, $a' = \frac{2ac}{a^2+b^2}$, $d' = \frac{2bc}{a^2+b^2}$; $(b^2-a^2)^2 + (2ab)^2 = (a^2+b^2)^2$ implies $b'^2+e'^2 = c'^2+f'^2 = 1$.

Rotation: $f' = b' = \cos\phi$, $e' = -c' = \pm\sin\phi$, $a' = (1-\cos\phi)a + (\pm\sin\phi)b$, $d' = -(\pm\sin\phi)a + (1-\cos\phi)b$; $\cos^2\phi + \sin^2\phi = 1$ yields $b'^2+e'^2 = c'^2+f'^2 = 1$.

Glide reflection: $f' = -b' = -\frac{b^2-a^2}{a^2+b^2}$, $e' = c' = -\frac{2ab}{a^2+b^2}$,

$a' = bs + \frac{2ac}{a^2+b^2}$, $d' = -as + \frac{2bc}{a^2+b^2}$

1.5.3 'Going backwards'. The formulas summarized in 1.5.2 allow us to characterize any linear function $F(x, y) = (a'+b'x+c'y, d'+e'x+f'y)$ satisfying the isometry conditions of 1.5.1 as one of the four types of isometries we have encountered in this chapter; omitting the technical details involved (like solutions of 2×2 **linear systems**), we present the results as follows:

(I) A linear function F(x, y) = $(a'+b'x+c'y,\ d'+e'x+f'y)$ satisfying $\mathbf{f' = b' \neq \pm 1}$, $\mathbf{e' = -c' \neq 0}$, and $\mathbf{b'^2+e'^2 = c'^2+f'^2 = 1}$ is a **rotation** by (angle) $\mathbf{cos^{-1}(b')}$ about (center) $\left[\dfrac{\mathbf{(1-b')a'+c'd'}}{\mathbf{2(1-b')}},\ \dfrac{\mathbf{-a'c'+(1-b')d'}}{\mathbf{2(1-b')}}\right]$, clockwise if $\mathbf{c' < 0}$ and counterclockwise if $\mathbf{c' > 0}$; this rotation becomes a **half turn** about $\mathbf{(\frac{a'}{2},\ \frac{d'}{2})}$ when $\mathbf{c' = 0}$, $\mathbf{b' = -1}$, and is reduced to a **translation** by $\mathbf{\langle a',\ d' \rangle}$ when $\mathbf{c' = 0}$, $\mathbf{b' = 1}$.

(II) A linear function F(x, y) = $(a'+b'x+c'y,\ d'+e'x+f'y)$ satisfying $\mathbf{f' = -b' \neq \pm 1}$, $\mathbf{e' = c' \neq 0}$, and $\mathbf{b'^2+e'^2 = c'^2+f'^2 = 1}$ is a **glide reflection** about (axis) $\mathbf{2(1-b')x - 2c'y = a'(1-b')-c'd'}$ by (vector) $\mathbf{\left\langle \dfrac{a'c'+(1-b')d'}{(1-b')^2+c'^2}\cdot c',\ \dfrac{a'c'+(1-b')d'}{(1-b')^2+c'^2}\cdot(1-b') \right\rangle}$ when $\mathbf{(1-b')^2 + c'^2 \neq 0}$ and about (axis) $\mathbf{y = \frac{d'}{2}}$ by (vector) $\mathbf{\langle a',\ 0 \rangle}$ when $\mathbf{c' = 0}$, $\mathbf{b' = 1}$; this glide reflection is reduced to a **reflection** when $\mathbf{a'c' + (1-b')d' = 0}$ (first case) or $\mathbf{a' = 0}$ (second case).

You should probably try to verify the validity of these claims and formulas by revisiting our old examples, like 1.2.7 (where $a' \approx 4.56$, $b' \approx .65$, $c' \approx -.76$, and $d' \approx 9.89$ do indeed satisfy the **reflection condition** $a'c' + (1-b')d' = 0$) or 1.3.8 (where either $a' \approx 7.16$, $b' \approx .34$, $c' \approx .94$, $d' \approx 6.2$ or $a' \approx 3.4$, $b' \approx .34$, $c' \approx -.94$, $d' \approx -8.84$ do indeed yield the **rotation center** via $\left[\dfrac{(1-b')a'+c'd'}{2(1-b')},\ \dfrac{-a'c'+(1-b')d'}{2(1-b')}\right] = (8, -2)$).
More to the point, you may substitute a′, b′, c′, d′ by the ‘general’ values provided by the formulas in 1.5.2, and see what happens!

With these important observations (on the nature of the linear formulas associated with each one of the four known isometries) at hand, we are now ready to demonstrate why **every** planar isometry must be one of the four familiar ones: this is the kind of result that mathematicians affectionately call **classification theorem**.

1.5.4 Isometries and circles. Let us begin with a fundamental observation: every planar isometry is bound to map a circle of radius r to a circle of radius r. Indeed if the center O is mapped to O′, then every image point P′ must satisfy **|O′P′| = |OP| = r**. Consider now a fixed isometry that maps the unit circle, $x^2 + y^2 = 1$, to the circle $(x-a')^2 + (y-d')^2 = 1$, and the point $P_1 = (1, 0)$ to a point P_1' (figure 1.37). Isometries map straight lines to straight lines (1.0.7), so the x-axis OP_1 is mapped to a line $O'P_1'$ that makes a **counterclockwise** angle ϕ with the **positive x-axis** (figure 1.37). Consider now the points **P = (r, 0)** and **Q = (rcosθ, rsinθ)** on the circle $x^2 + y^2 = r^2$, which is mapped to the circle $(x-a')^2 + (y-d')^2 = r^2$. Since P lies on OP_1, it must be mapped to the **unique** point P′ on the intersection of $O'P_1'$ and $(x-a')^2 + (y-d')^2 = r^2$ that satisfies $\mathbf{|P'P_1'| = |PP_1|}$ (figure 1.37).

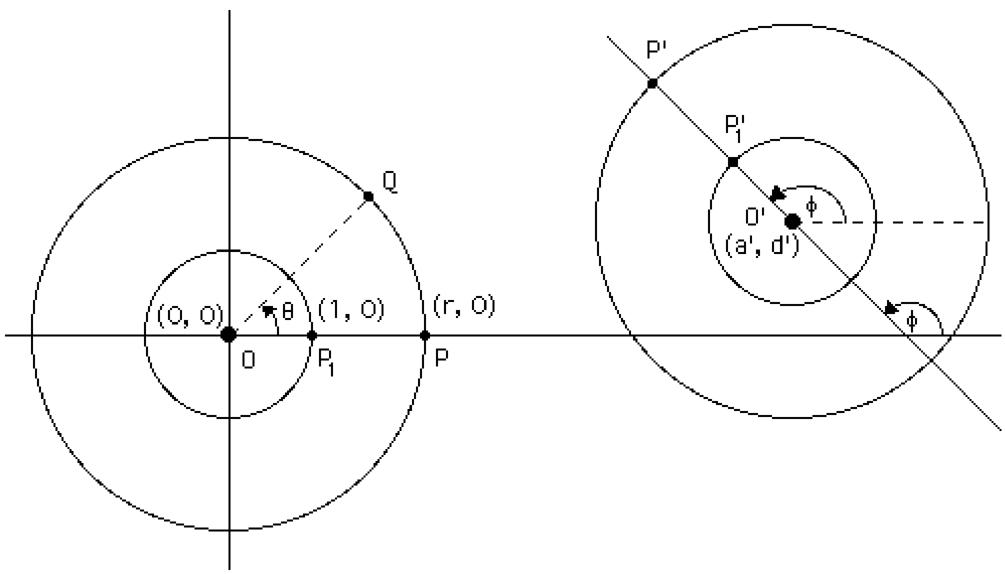

Fig. 1.37

The critical question is: where is Q mapped? Obviously to a point Q′ on $(x-a')^2 + (y-d')^2 = r^2$ such that **|P′Q′| = |PQ|**. But there isn't that much room on a circle, is there? If you are standing at P′ facing O′ and wish to move to **any** other point **on** the circle at a **given** distance from P′, how many choices do you have altogether? Precisely **two**: either you move **'to your left hand'** (making a

clockwise angle θ with $O'P'$) or you move **'to your right hand'** (making a **counterclockwise** angle θ with $O'P'$); these two possibilities are shown in figures 1.38 & 1.39, respectively. Moreover, it shouldn't take you long to realize that **all** points on $x^2 + y^2 = r^2$ are 'isometrically forced' to follow the fate of Q: we cannot have some points going clockwise and some points going counterclockwise!

In the first ('clockwise') case, $Q = (x, y) = (r\cos\theta, r\sin\theta)$ is mapped (figures 1.37 & 1.38, see also 1.3.7 and figure 1.25) to

$\mathbf{Q' = (a'+r\cos(\phi-\theta),\ d'+r\sin(\phi-\theta))}$ =

$= (a'+r\cos\phi\cos\theta+r\sin\phi\sin\theta,\ d'+r\sin\phi\cos\theta-r\cos\phi\sin\theta) =$

$= (a'+(\cos\phi)(r\cos\theta)+(\sin\phi)(r\sin\theta),\ d'+(\sin\phi)(r\cos\theta)+(-\cos\phi)(r\sin\theta))$

$= (a'+(\cos\phi)x+(\sin\phi)y,\ d'+(\sin\phi)x+(-\cos\phi)y) =$

$= (a'+b'x+c'y,\ d'+e'x+f'y)$, where $f' = -b' = -\cos\phi$, $e' = c' = \sin\phi$, $b'^2+e'^2 = c'^2+f'^2 = (\cos\phi)^2+(\sin\phi)^2 = 1$.

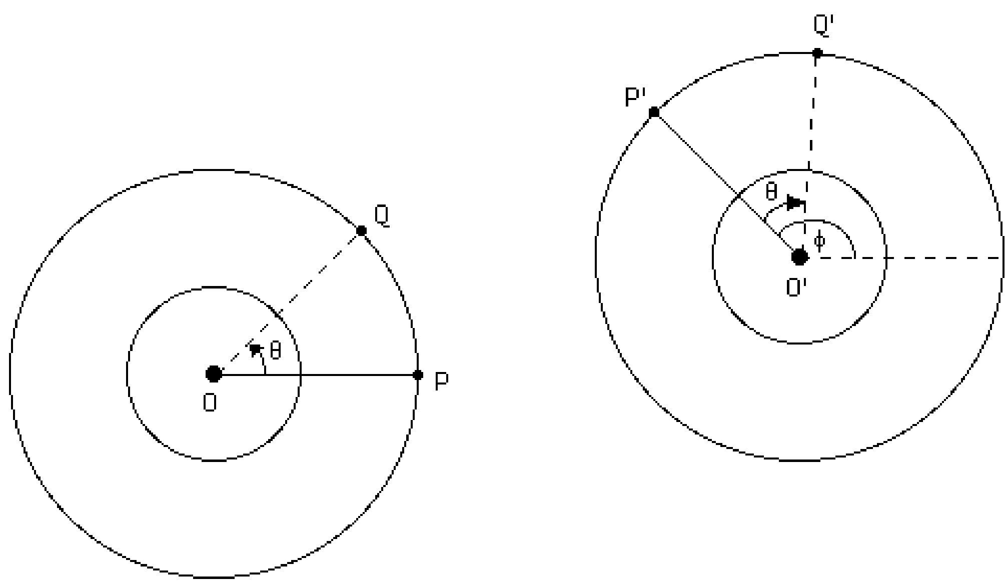

Fig. 1.38

The whole argument holds for **every r and every θ** (hence taking care of every single point (x, y) on the plane!) and is indeed very similar to what we did when we established the rotation formula in 1.3.7. At first you might even think that our isometry is in fact a rotation, but a careful look at the list of isometries in 1.5.2 shows otherwise: while rotations (and translations) satisfy

$f' = b'$ and $e' = -c'$, our isometry satisfies $\mathbf{f' = -b'}$ and $\mathbf{e' = c'}$, just as reflections and glide reflections do! To summarize, our isometry has to be either a **reflection** (in the special case $\mathbf{\tan\phi = \dfrac{2a'd'}{a'^2-d'^2}}$, as it follows from the conditions given in 1.5.3) or, far more likely, a **glide reflection** -- essentially because it maps ‘counterclockwise circles’ (think of the P-to-Q arc) to ‘clockwise circles’ (think of the P′-to-Q′ arc), formally because of our observations in 1.5.3.

In the second (‘counterclockwise’) case, $Q = (x, y) = (r\cos\theta, r\sin\theta)$ is mapped (figures 1.37 & 1.39, see also 1.3.7 and figure 1.26) to

$\mathbf{Q' = (a'+r\cos(\phi+\theta), d'+r\sin(\phi+\theta))} =$

$= (a'+r\cos\phi\cos\theta-r\sin\phi\sin\theta, d'+r\sin\phi\cos\theta+r\cos\phi\sin\theta) =$

$= (a'+(\cos\phi)(r\cos\theta)+(-\sin\phi)(r\sin\theta), d'+(\sin\phi)(r\cos\theta)+(\cos\phi)(r\sin\theta))$

$= (a'+(\cos\phi)x+(-\sin\phi)y, d'+(\sin\phi)x+(\cos\phi)y) =$

$= (a'+b'x+c'y, d'+e'x+f'y)$, where $f' = b' = \cos\phi$, $e' = -c' = \sin\phi$, $b'^2+e'^2 = c'^2+f'^2 = (\cos\phi)^2+(\sin\phi)^2 = 1$.

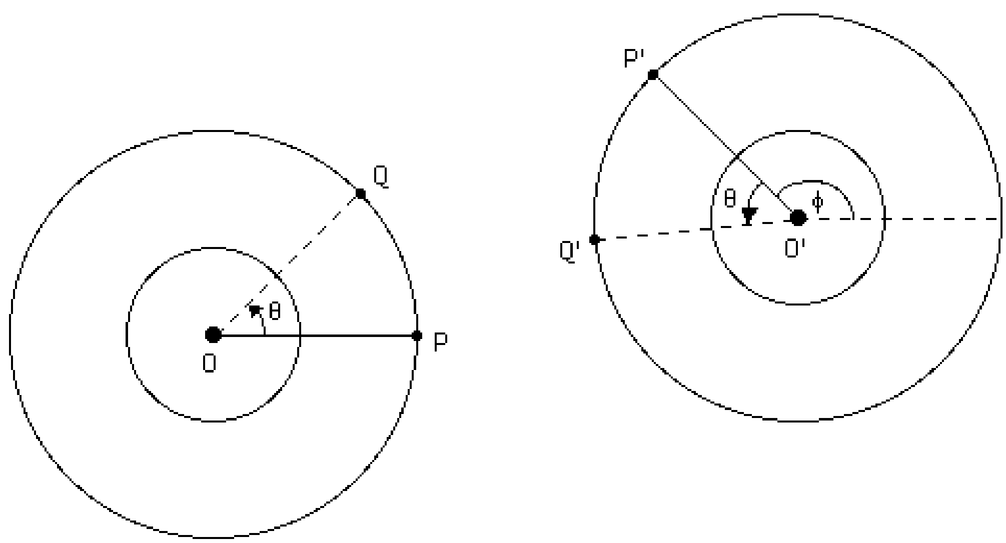

Fig.1.39

As in the first case, these computations are valid for **all r and all θ** and cover the entire plane. But this time our isometry maps ‘counterclockwise circles’ to ‘counterclockwise circles’ (think, as in figure 1.38, of the P-to-Q and P′-to-Q′ arcs) and ‘looks identical’ to a rotation! Is it one? Referring to 1.5.3 again, we see that yes, this time it is indeed a **rotation** (by angle ϕ), unless of course $\boldsymbol{\phi = 0^0}$, in which case $f' = b' = 1$, $e' = -c' = 0$ and our isometry is the **translation** $<a', d'>$ (which does **not** rotate circles at all)!

To summarize, we have shown that every planar isometry maps circles to circles and does so either **reversing circular orientation** (in which case it must be a glide reflection, or possibly a reflection) or **preserving circular orientation** (in which case it must be a rotation, or possibly a translation). We ended up both proving our claim from 1.0.5 about isometries being linear and classifying them! This is not the only way to classify isometries: probably it is not even the easiest one, see for example section 7.2. But it is a rather neat way to do it, at least for those with some familiarity with Precalculus. And those with greater such familiarity could even have more fun, like trying to determine the axis and vector (in the case of a glide reflection) or the center (in the case of a rotation) in terms of a', d', and ϕ (and in the spirit of 1.5.3), for example!

Postscript: It is possible to combine our 'circular' approach above with ideas from chapter 7 in order to provide a completely geometrical classification of isometries (not only of the plane but of space as well): please check ***Isometries Come in Circles*** at http://www.oswego.edu/~baloglou/103/circle-isometries.pdf.

first draft: summer 1998

CHAPTER 2

BORDER PATTERNS

2.0 Infinity and Repetition

2.0.1 "What goes (a)round comes (a)round". You are certainly surprised to see this familiar proverb lying near the beginning, in fact at the very root, of a mathematical book, aren't you? Well, no treatise on fate here, we are simply quoting it literally: if you are moving 'straight' on the surface of a sphere or cylinder then you are bound to return to the point where you started from, that's all... This is even more obvious to those who like to think about the structure of our **infinite** universe in terms of space and time, but we are not getting into that, either!

What we have in mind is very earthly indeed: when was the last time you noticed a certain motif **repeating** itself around a vase or belt or the margin (**border**) of a framed photo or ancient mosaic? If you do not quite recall ever having noticed such details, you better be prepared for a change after you go through this book! Such repeating motifs, called **border patterns**, have been with us for a very long time and, rather surprisingly at first, happen to be subject to mathematical rules that are accessible and profound at the same time. We investigate these rules and more with the help of many examples that might even make this book seem like an art book to you: indeed the worlds of art and mathematics are not disjoint!

Before going further, let us point out that infinity and repetition do not always go together. You may recall for example that, while some numbers with an infinite decimal portion have repeating digits after some point (like 4.7217373... = 116,863/24,750), others (like the most famous of all such numbers, **π = 3.141592654...**) come with a very unpredictable sequence of digits. And, of course, while repeating motifs abound in our finite world, infinite objects exist only in our powerful **imagination**: indeed you will have to train yourself to see the finite as infinite throughout much of this book; in the case of a border pattern, the easiest way to manage that is to simply wrap it around -- in about the same way that geometers often consider an infinite straight line as a circle of infinite radius!

2.0.2 Notation. Although border patterns will be best understood by following the examples and discussion in the following sections, we can briefly state here that they consist of a motif that repeats itself infinitely along a straight line (or finitely along a circle, in view of what we just discussed above). As we will see, there are a total of seven distinct types, each of them equipped with a special four-character **'name'** that always starts with a **p** (for "pattern"). This special notation, even though not terribly important, will be explained as we move through the next seven sections.

2.1 Translation left alone (p111)

2.1.1 Uneventful repetition. Consider the following pattern, consisting of repeated images of the letter **F**, and try to imagine it either extending itself to the right and to the left for ever or going straight around a 'short' cylinder:

Fig. 2.1

Clearly, a **horizontal translation** by the vector $\vec{\mathbf{v}}$ in figure 2.1 maps the 'first to the left' **F** to the 'second' one, the 'second' one to the 'third' one, and so on; as for that 'first to the left' **F**, you should think of it as being in turn the image of its predecessor (not shown), etc. Alternatively, we could consider the opposite translation defined by $-\vec{\mathbf{v}}$ that ‘moves’ the **F**s from right to left instead of left to right; or a translation defined by the vector $3\vec{\mathbf{v}}$ that moves every **F** to an **F** three positions to the right, etc. The possibilities for a great variety of translations are endless, and they are all allowed by the letter **F**’s **uniform repetition** along a straight line. But we will usually only consider the ‘minimal’ left-to-right translation defined by $\vec{\mathbf{v}}$, the pattern’s **minimal translation vector**.

2.1.2 More than one letters allowed. Instead of repeating a single letter, as in figure 2.1, we may create patterns by repeating two or more letters or even whole words and more:

FAMEFAMEFAME

Fig. 2.2

Notice that the (minimal) translation vector in figure 2.2 is about twice as long as the translation vector in figure 2.1: the **fundamental region** consists now of “**FAME**” instead of just “**F** ”.

2.1.3 Other motifs. Instead of repeating letters or words, we may of course repeat any geometrical or other figure of our choice and imagination. Here is an example:

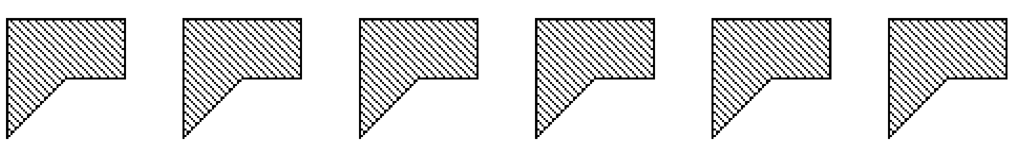

p111

Fig. 2.3

2.1.4 Attention! As we will see very shortly, repeating motifs involves 'positive risks': we may end up creating patterns with **more** symmetry (and isometries) than promised by the very title of this section! Remember, this section is devoted to patterns of **p111** type, where **p** stands for translation and the three **1**s denote the **absence** of other isometries to be revealed in the coming sections.

2.2 Mirrors galore (pm11)

2.2.1 Not all letters are created equal. What happens when we try to use the letter **M** instead of **F** in figure 2.1? Let's see:

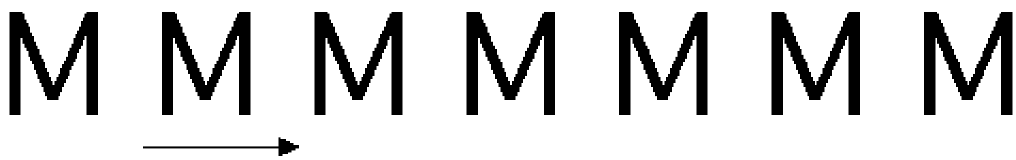

Fig. 2.4

Clearly, a vector approximately equal to the vector $\vec{\mathbf{v}}$ of figure 2.1 works as a translation vector for this pattern. But sooner or later one notices something 'extra': any vertical line either half way between any two successive **M**s or right through the middle of any **M** acts as a **vertical reflection** axis (**mirror**) for the entire pattern; that is, the whole pattern remains invariant, with each **M** being reflected onto some other **M**.

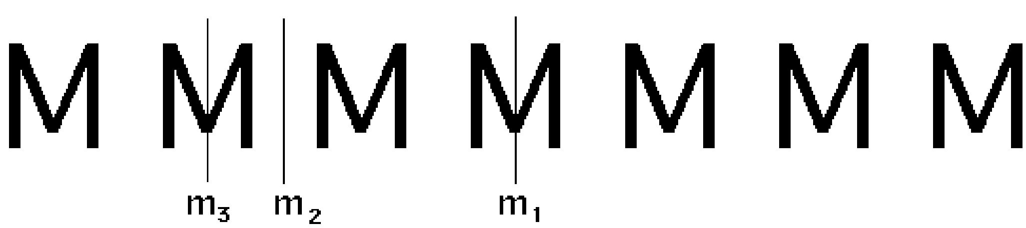

Fig. 2.5

Now you are probably ready to protest our claim and argue that only $\mathbf{m_1}$ is a legitimate reflection axis for our pattern, aren't you?

Well, if that is the case, you better hold your horses! For your protest is a sure indication that you forgot one important thing: our pattern is assumed to extend ‘for ever’ in both directions! So, there is no point in worrying that there are only two **M**s to the left of $\mathbf{m_2}$ to match the five **M**s to the right of $\mathbf{m_2}$, or only one **M** to the left of $\mathbf{m_3}$ to match the five **M**s to the right of $\mathbf{m_3}$: there are infinitely many **M**s ‘in both directions’, and our pattern is actually blessed with **infinitely many** vertical mirrors!

Patterns with vertical reflection are denoted by **pm11**, where **m** stands for “mirror (reflection)” and, again, the two **1**s mark the absence of symmetries that we still have to explore.

2.2.2 <u>What made the difference?</u> Why are there infinitely many mirrors in the **M**-pattern but none in the **F**-pattern? It all has to do with the fact that **M** itself has an **internal mirror** running through it (that maps it to itself by mapping its right half to its left half and vice versa), while **F** does **not** have such a mirror. Does that mean that in order to create a **pm11** pattern we must repeat a motif that has what we called (1.2.8) “mirror symmetry”? Yes and no: we may certainly employ two (or more) motifs without mirror symmetry, but the fundamental region itself must have it; the **pm11** pattern in figure 2.6, where the fundamental region may be taken to be either “**qp**” (of mirror $\mathbf{L_1}$) or “**pq**” (of mirror $\mathbf{L_2}$), is rather illuminating:

Fig. 2.6

2.2.3 <u>Two kinds of mirrors.</u> Our examples in 2.2.1 and 2.2.2 do indicate something interesting: there always seem to be **two kinds** of vertical mirrors in a **pm11** pattern! Indeed, there are mirrors alternatively running either through an **M** or between two **M**s in figure 2.5; likewise, mirrors alternatively running either ‘between two lines' or 'between two circles' in figure 2.6 (like $\mathbf{L_1}$ and $\mathbf{L_2}$, respectively). In more sophisticated terms, mirrors either **bisect** the fundamental region or **separate** two adjacent fundamental regions. Moreover, you may also notice something a bit more subtle: the distance between every two **successive** (hence 'different') mirrors (like $\mathbf{m_2}$ and $\mathbf{m_3}$ in figure 2.5) is equal to **half** the length of the **minimal** translation vector! All these observations are valid in every **pm11** pattern and for fairly deep reasons that will be discussed in chapters 7 and 8, specifically in 7.2.1 and 8.1.5.

2.2.4 From **p111** to **pm11**. There is a simple way of turning a **p111** pattern into a **pm11** pattern: simply 'reverse' **every other** motif (as if a mirror ran **through** it)! We illustrate this idea by getting a **pm11** pattern out of the **p111** pattern of figure 2.3:

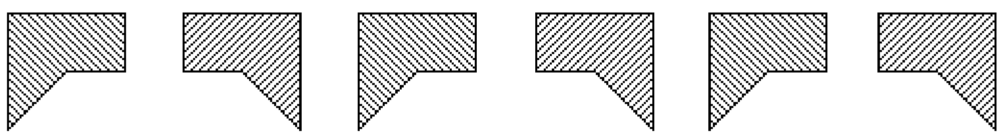

pm11

Fig. 2.7

2.3 Only one mirror (p1m1)

2.3.1 An infinite mirror. Let us now duplicate the letter **D**:

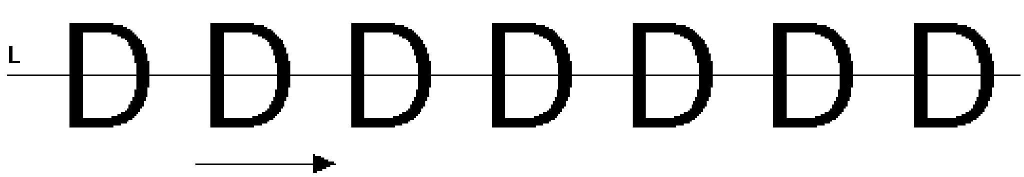

Fig. 2.8

It is obvious that the line L that runs through our **D**-pattern acts as a reflection axis for it: indeed the upper half of each **D** is mapped to its lower half (and vice versa), and that happens simply because the letter **D** itself has **mirror symmetry**. We have just created our third border pattern type, characterized by **horizontal reflection** (and only that, save for the translation of course) and denoted by **p1m1**. (Notice that **m** denotes horizontal reflection when in the third position and vertical reflection when in the second position.)

Here is another example of a **p1m1** pattern using two letters (each of them endowed with a horizontal mirror) instead of one:

D C D C D C D

Fig. 2.9

2.3.2 From **p111** to **p1m1**. It is not necessary to use motifs with horizontal mirror symmetry in order to create a **p1m1** pattern. We may in fact start with an arbitrary **p111** pattern and then reflect it across an axis **parallel** to its **'direction'** to get a perfectly legitimate **p1m1** pattern. Here is how this idea is applied to the pattern from figure 2.3:

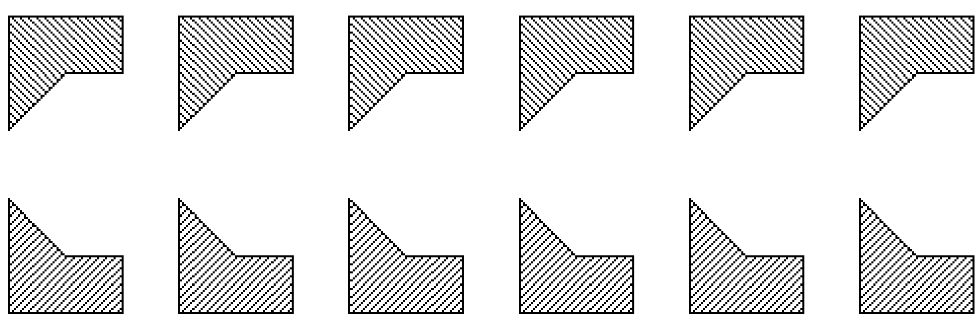

p1m1

Fig. 2.10

This example simply points to a rather obvious, yet useful, fact: in a **p1m1** border pattern the horizontal reflection axis must be the pattern's **'backbone'** (i.e., the intelligible axis that cuts the pattern into two equal halves, 'top' and 'bottom'); that is, and unlike in the case of vertical reflection, **there is only one place to look for horizontal reflection**!

2.3.3 Aesthetic considerations. We have seen in 2.2.4 and 2.3.2 how simple modifications of the **p111** pattern lead to the **pm11** and **p1m1** patterns. And we have also seen that both the **pm11** and the **p1m1** patterns are created by repetition of a motif that has mirror symmetry: we get a **p1m1** in case the repetition occurs along a direction **parallel** to the motif's internal mirror, and a **pm11** in case the repetition occurs along a direction **perpendicular** to that mirror. This simple geometrical fact bears on the visual impressions created by these patterns: using **arrows** as in figure 2.11, for example, we see that the **p1m1** creates a feeling of **motion** along the pattern's backbone, while the **pm11**'s vertical mirrors create a feeling of **stillness**; as for the **p111** type, it is not unreasonable to say that it stands somewhere between stillness and motion!

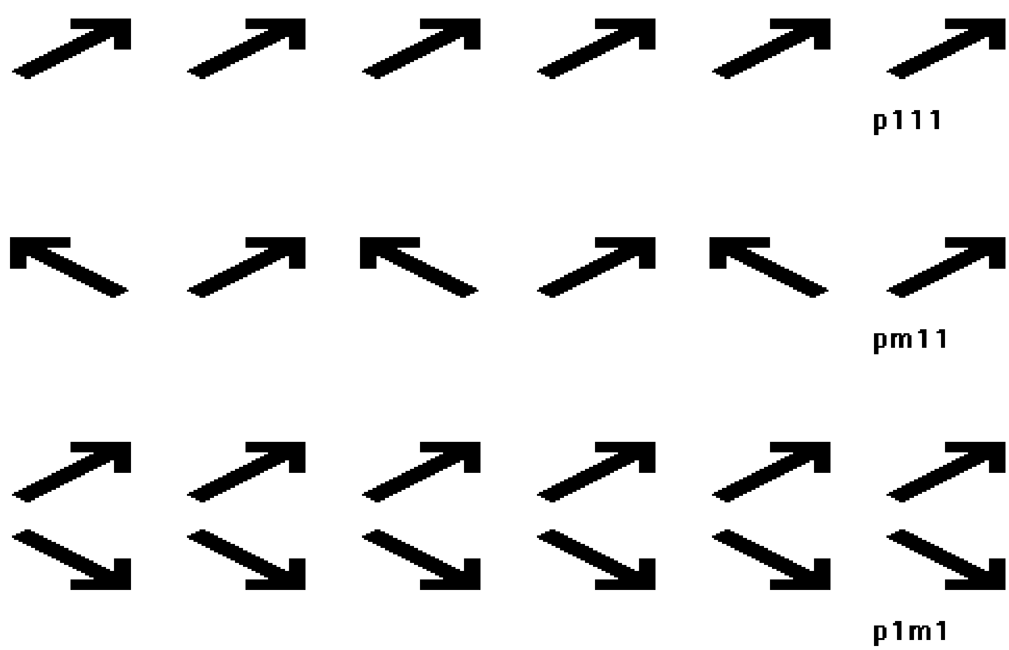

Fig. 2.11

Do you agree with our statements in the preceding paragraph? Well, do not worry in case you do not! When it comes to aesthetics, things are a bit more democratic than in mathematics, and contrasting opinions are allowed to peacefully coexist: simply consider our opinion as a starting point for developing yours! On our part, we offer a viewpoint that could support either opinion: consider each arrow in figure 2.11 as representing a **footprint** (with the arrow's tip standing for the toes); then the **pm11** pattern can be seen as a series of footprints of people standing on line **next** to each other, while the **p1m1** pattern can be seen as a series of footprints of people standing on line **behind** each other. In fact the **pm11** and **p1m1** patterns may also be created by the footprints of a **jumping** individual, and you can verify this yourself: which way would you move faster, the **pm11** way or the **p1m1** way?

2.4 Footsteps (p1a1)

2.4.1 Moving for sure now! Consider the arrow-footprint **p1m1** pattern of figure 2.11 **'cut in half'** as in figure 2.12:

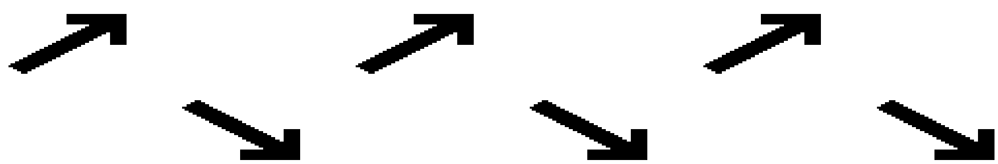

Fig. 2.12

Don't you think that the feeling of motion generated by this pattern is much stronger than the one generated by the 'full pattern' of figure 2.11? With a bit of imagination, you can view the arrows as successive positions of a kayak crossing straight through rough seas! And if you prefer to stay on land, simply return to the **arrow = footprint** equation of 2.3.3 and be proud of yourself: you actually generate that **footstep pattern** many times per day, in fact every time you resort to a straight, steady walk for a few seconds!

2.4.2 What lies between the footsteps? Recall that our 'new' pattern has been obtained by 'cutting in half' the **p1m1** pattern of figure 2.11. Moreover, we eliminated precisely those arrows that needed to be eliminated in order to **destroy** horizontal reflection and **preserve** translation at the same time. Notice however that the minimal translation vector (**solid** line) of the new pattern is precisely **twice as long** as the minimal translation vector (**dotted** line) of the 'old' **p1m1** pattern; this does make sense, as we have indeed eliminated every other arrow:

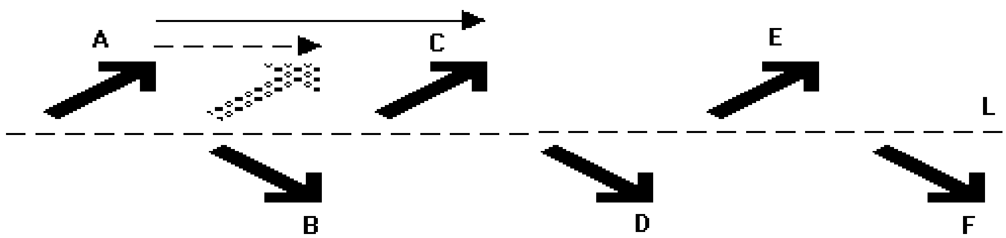

Fig. 2.13

What happens if we **translate** an arrow, say arrow **A** above, by the **'old'** vector? Nothing, unless of course we **reflect** it across that between-the-arrows line L: then it matches arrow **B**! Repeat the process to arrow **B** -- or first reflect across L and then translate by the 'old' vector -- and you get to arrow **C** (which is **A**'s translate by the **'new'** vector), and likewise from **C** to **D** (which is **B**'s translate), and so on: our footstep pattern does 'move' thanks to a **glide reflection**! We have just arrived at our fourth border pattern type, characterized by glide reflection and denoted by **p1a1**.

Summarizing our observations, we point out that the glide reflection axis in every **p1a1** pattern (typically denoted by a **dotted** line) runs parallel to the pattern's direction (and **by necessity right through its backbone**, of course); further, the minimal glide reflection vector equals **half** the pattern's minimal translation vector: this reflects on the fact that the glide reflection's **'square'** equals the translation!

2.4.3 Any good letters out there? Now that you have understood what a **p1a1** pattern is, can you create one by repeating a **single** English letter, as we did for every border pattern so far? It shouldn't take you that long to realize that this is impossible, even if you resort to letters from distant lands' alphabets or Chinese ideograms! And the reason is simple: while we used letters like **F** (no symmetries), **M** (vertical reflection), and **D** (horizontal reflection) to get the **p111**, **pm11**, and **p1m1** patterns, respectively (in 2.1.1, 2.2.1, and 2.3.1), there is no letter that has glide reflection! More to the point, **no finite figure may ever remain invariant under**

glide reflection!

Does this mean that there is no way to create a **p1a1** pattern using letters of the English alphabet? Actually not! All we need is **two** English letters mappable to each other by glide reflection:

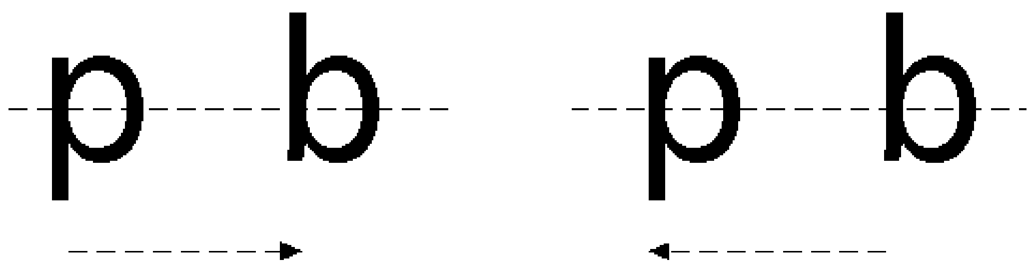

Fig. 2.14

It is not difficult now to create a **p1a1** pattern by infinite repetition of the fundamental region **"p b "**:

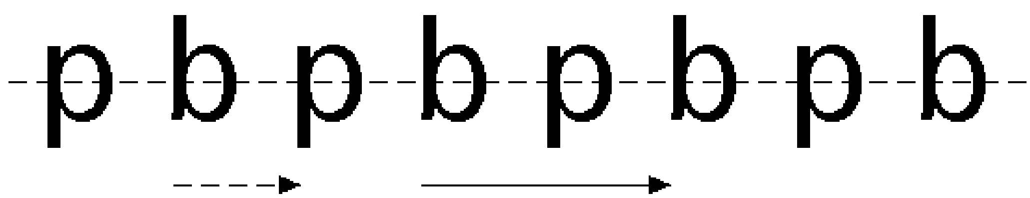

Fig. 2.15

Recall, once again, that all border patterns are **infinite** by definition, but, of course, we can only show a finite part of them on this page, leaving the rest to the imagination. In particular, the rightmost **b** above is mapped by the 'standard' left-to-right glide reflection to a **p** right next to it that is not shown, etc.

2.4.4 <u>Example.</u> Consider the following 'arrow pattern':

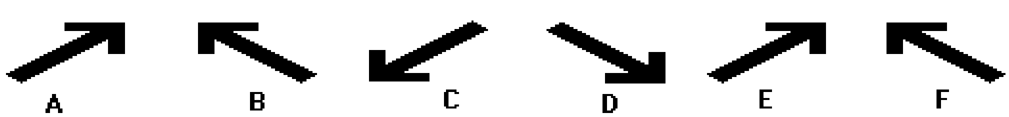

Fig. 2.16

What type is it? Does it have glide reflection? It is tempting to say “yes”: arrows **A** and **C** are mapped to arrows **D** and **F** by a **‘long’** glide reflection, arrows **B** and **D** are mapped to arrows **C** and **E** by a **‘short’** glide reflection, etc. We asked for **one** glide reflection but ended up with **two** instead! Can we still say that there exists glide reflection in our pattern ‘endowed’ with two vectors instead of just one? **No**: a glide reflection is by definition associated with precisely **one vector that works for all motifs** -- otherwise it wouldn’t be an isometry! (Indeed our ‘double vector’ pseudo-glide-reflection above fails, for example, to preserve the distance between the tips of the arrows **A** and **B**, which are ‘mapped’ to the tips of the arrows **D** and **C**, respectively.)

What type is it then? There is clearly some symmetry in our example, in particular a translation mapping **A** to **E**, **B** to **F**, and so on. Could it be just a **p111** then? No, a somewhat closer look shows that there is vertical reflection, with mirrors -- **working for the entire pattern** -- between **A** and **B**, **C** and **D**, **E** and **F**, etc: it’s a **pm11**! (Compare now this **pm11** pattern with the one in 2.3.3: what makes them differ from each other?)

2.5 Flipovers (p112)

2.5.1 <u>One more variation.</u> Let us revisit the **p1m1** and **p1a1** border patterns in figures 2.6 and 2.15, both of them starting with a **p** and continuing with either a **q** or **b**, respectively. What if we try to continue with a **d** this time? We end up with the following pattern:

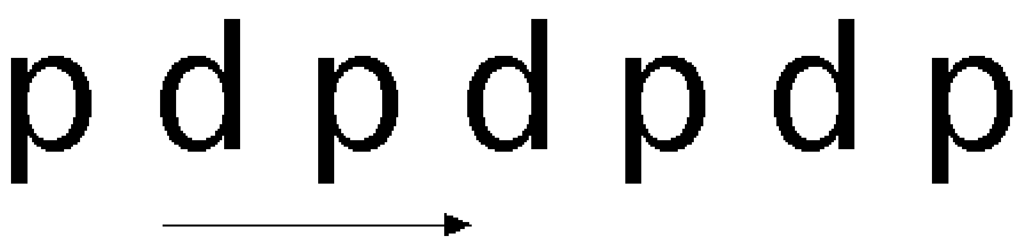

Fig. 2.17

Once again, there seems to be some symmetry involved here, and the pattern is clearly invariant under the indicated translation. You can check that no reflection or glide reflection is going to leave it invariant. There is something else going on though: what happens if you turn this page **upside down**? Does the flipped pattern look any similar to the original one? Have a classmate hold his/her copy **straight** right next to yours in case you cannot remember how the original looked like! And, if that is not possible, just **trace** the pattern and then flip it. What do you think? Is the flipped pattern the same as the original? Well, you may at first say "no": the original pattern 'begins' and 'ends' with a **p**, while the flipped one 'begins' and 'ends' with a **d**... But, do not forget: border patterns are **infinite**, so they do not 'begin' or 'end' anywhere! With this all-important detail in mind, you must now agree that the original and flipped versions are **identical**!

2.5.2 <u>How do mathematicians flip?</u> Have you really read 1.3.10 on **half turn** or had you assumed it to be little more than a footnote? Either way we suggest that you quickly review it, so that the special relation between the letters **p** and **d** illustrated in figure 2.18 will make full sense to you:

Fig. 2.18

Clearly, **p** and **d** above are images of each other under the shown half turn or **point reflection** (as the **180^0 rotation** was also called in 1.3.10). That is, all we need in order to flip a **p** into **d** or vice versa is a point reflection center, easily found by inspection. It doesn't take that long now to realize that the pattern's **backbone** in figure 2.17 is full of such centers: a half turn around each one of them leaves the **entire** pattern invariant! To confirm this you may like to trace the pattern and then rotate the tracing paper by 180^0

about your pencil's tip, held firmly at any one of the half turn centers shown in figure 2.19: every **p** on the tracing paper moves on top of a **d** and vice versa!

p·d·p·d·p·d·p·d

Fig. 2.19

In particular, our **"p d "** pattern has **half turn** and belongs to the type known as **p112**. Notice that the two **1**s in the second and third positions denote the **lack** of vertical reflection and horizontal reflection (or even glide reflection), respectively; in the same way, the **1** in the fourth position of all types we have seen so far indicated the absence of half turn. As for the **2**, that reflects on the fact that, with $\mathbf{2 \times 180^0 = 360^0}$, a half turn needs to be applied **twice** -- as its very name aptly suggests -- in order for everything to return to its original position.

2.5.3 <u>Any single letters?</u> We now ask the same question we asked in 2.4.3, providing an affirmative answer this time: it is possible to create a **p112** pattern using a single letter. All we have to do is pick a letter that has **internal half turn**, like **N** or **Z**:

Z Z Z Z Z Z Z

Fig. 2.20

Notice that the existence of half turn in the **"Z "** pattern is much more obvious than in the case of the **"p d "** pattern -- why?

2.5.4 <u>Two kinds of half turn centers.</u> The **p112** patterns in figures 2.19 and 2.20 have **two kinds** of half turn centers: between either two circles or two lines in the case of the **"p d "** pattern, right on the center of a **Z** or right between two **Z**s in the case of the "**Z** " pattern. In either case we notice that the distance between any two adjacent (hence of distinct type) half turn centers equals **half** the length of the minimal translation vector. This observation is very much in tune with our remarks in 2.2.3, and we will return to it in 7.5.2.

2.5.5 Example. We now return to the pentagon featured in 2.1.3, 2.2.4, and 2.3.2 and show how it may be built into a **p1a1** or **p112**:

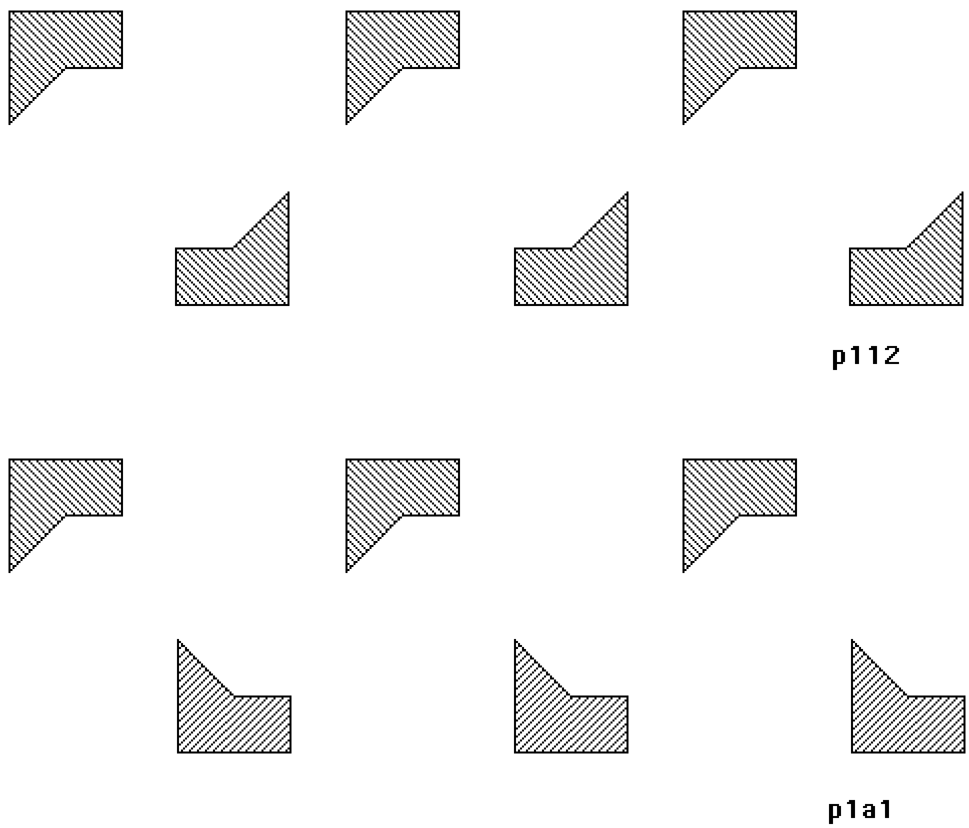

Fig. 2.21

Sometimes students confuse a **p1a1** pattern for a **p112** pattern and vice versa. Comparing the two examples above should help you understand the difference between them even at the 'intuitive' level: there is **spinning** (with lots of **parallel segments**) in **p112** as opposed to **straight motion** (and segments going **opposite ways**) in **p1a1**. Also, check what happens to each pattern when you flip it over by rotating the page by 180^0: in one case (**p112**) the new top row still 'points' to the **same** direction (right), while in the other case (**p1a1**) the new top row 'points' to the **opposite** direction (left). Further, think of what exactly you need to do in each case in order to bring a **tracing paper copy** back to the original pattern!

Anyhow, the best way to distinguish a **p1a1** type from a **p112** type is to remember the isometries that characterize them (glide reflection in **p1a1**, point reflection in **p112**) and be able to explicitly recognize them as such. You may of course wonder: isn't there any way to have **both** these wonderful isometries present in the same pattern? Well, that's the topic of the next section!

2.6 Roundtrip footsteps (pma2)

2.6.1 Are they mutually exclusive? The discussion in 2.5.5 has probably left you with the impression that glide reflection and point reflection cannot quite coexist in a border pattern. In particular, you would probably be ready to guess that the images of any given figure under a glide reflection and under a point reflection must always be distinct. This is not true: those two images could actually be one and the same in some cases! For an example, look at what happens to the letter **V** in figure 2.22:

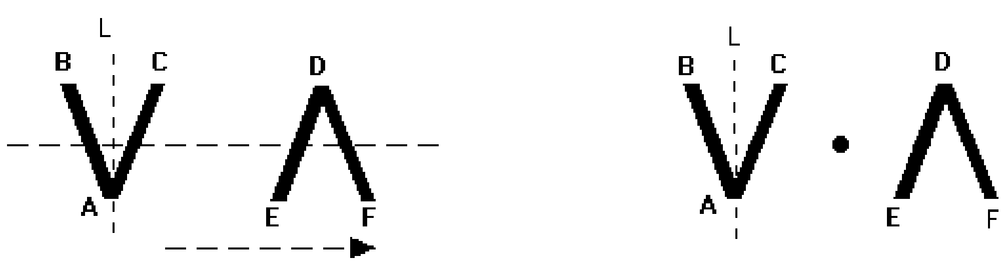

Fig. 2.22

Clearly **V** gets mapped to Λ (capital Greek Lamda) **both** by glide reflection (left) and point reflection (right)! How did that happen? Well, observe that in the case of glide reflection **AB** got mapped to **DE**, and **AC** to **DF**, while in the case of point reflection **AB** and **AC** got mapped to **DF** and **DE**, respectively; notice in the latter case that, consistently with 1.3.10, **DF** and **DE** are parallel to **AB** and **AC**, respectively. In a way, the two isometries acted on **V** in two very different ways: that should not come as a surprise in view of our remarks in 2.5.5. Were **AB** a bit longer than **AC**, for example, the two images would have been distinct. Likewise, it is important that **AB** and **AC** are not only of equal length, but also at equal distance from the vertical line L that bisects **V** and acts as an **internal mirror** for **V**. In short, the effect of the particular point reflection and the particular glide reflection on **V** are **seemingly** identical **precisely** because **V** has (vertical) **mirror symmetry**!

2.6.2 All three together now! What happens if we start **repeating** that **"V Λ "** motif created out of **V** in figure 2.22? We end up with the following border pattern:

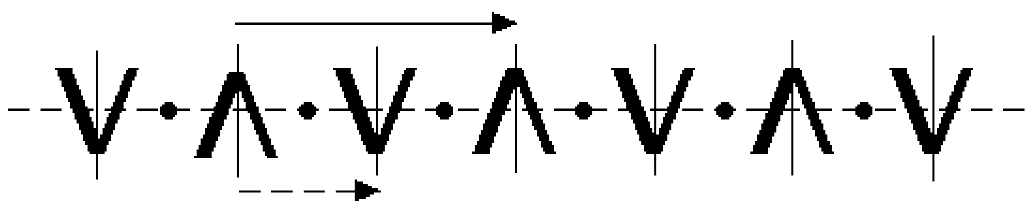

Fig. 2.23

In view of the discussion in 2.6.1, it shouldn't take you long to realize that our **"V Λ "** pattern has vertical reflection (**'inherited'** by individual motifs), glide reflection, and point reflection. Likewise, you should have no difficulty determining the vertical reflection axes, glide reflection vectors, and half turn centers, confirming both figure 2.23 and the remarks made on such entities in 2.2.3, 2.4.2, and 2.5.4. Notice in particular that **half way** between every two adjacent mirrors there exists a half turn center (and vice versa), while the distance between every two adjacent half turn centers (**or** mirrors) is **equal** to the length of the glide reflection vector. Finally, and in view of all the border pattern types and notations you have already seen, you ought to be able to guess this new pattern's 'name': **pma2**.

2.6.3 Two as good as three! Let us now apply either a half turn or a glide reflection to **pq** and then translate the outcomes repeatedly, exactly as we did in the previous section; due to the vertical symmetry of **pq**, we end up, in both cases, with the **same** **pma2** pattern (exactly as it happened with the **V** in 2.6.1 and 2.6.2):

pqbdpqbdpqbd

Fig. 2.24

We leave it to you to determine all the isometries of the **pqbd** pattern created in figure 2.24. What is important to observe is that, once again, glide reflection and point reflection seem to **'imply'** each other in the presence of vertical reflection.

What happens if we start with a motif that has point reflection, like **pd**, and then apply either glide reflection or vertical reflection to it, followed by repeated translation? We leave it to you to check that, **either way**, we end up with the **pma2** pattern of figure 2.25:

pdbqpdbqpdbq

Fig. 2.25

Again you should determine all the symmetry elements of this **pdbq** pattern and confirm the remarks made in 2.6.2. You also have the right to suspect that, in the presence of point reflection, vertical reflection and glide reflection **'imply'** each other.

What happens when we begin with a **pb** motif, known from 2.4.3 to generate a pattern with glide reflection? Will we still be able to say that, in the presence of glide reflection, point reflection and vertical reflection imply each other? Let's see... If we apply vertical reflection to **pb** and then we translate, we end up with the following pattern:

pbdqpbdqpbdq

Fig. 2.26

The vertical reflection is still there, but there are no signs of point reflection. On the other hand, the glide reflection is gone, too: this is a **pm11** pattern!

Likewise, if we apply point reflection to **pb** and then we translate, we end up with the **p112** pattern of figure 2.27:

pbqdpbqdpbqd

Fig. 2.27

That is, we came close, but have finally **failed** to produce a border pattern that would have glide reflection plus either vertical reflection without the point reflection (figure 2.26) or point reflection without the vertical reflection (figure 2.27). And for a good reason: it can be proven -- see 7.7.4, but also 6.6.2 -- that, precisely as our examples so far indicate, whenever a border pattern has **two** of these three isometries, it **must have the third one as well** (and be a **pma2**)!

Returning to our **pb** example: is there any way to get a **pma2** pattern out of it by applying either vertical reflection or point reflection followed by translation? Yes, provided that we place the mirror or half turn center between **p** and **b**, 'spacing' them appropriately! We leave it to you to verify that we end up with either the **pqbd** pattern of figure 2.24 (via vertical reflection) or the **pdbq** pattern of figure 2.25 (via point reflection): those are indeed **distinct pma2** patterns!

We conclude with a puzzle: can you create a **p1a1** pattern by translating some permutation of (**all four** of) **b**, **d**, **p**, and **q**?

2.6.4 From **p1a1** to **pma2**. There is no need for any more **pma2** examples, but we would like to justify this section's title! You may recall our 'footstep' **p1a1** example in figure 2.12. What happens if that walker returns through exactly the same route? We could very well end up with the following footprint pattern, effectively **'doubling'** our **p1a1** pattern:

pma2

Fig. 2.28

These 'roundtrip footsteps' clearly form a **pma2** pattern; glide reflection was known to be there by the pattern's very nature (and discussion in 2.4.1), while the vertical mirrors and half turn centers are even easier to see: just look **'between'** the arrows as needed!

2.6.5 From **pma2** to **p112** and **pm11**. What happens if we remove every other 'column' of arrows in the pattern of figure 2.28? We simply arrive at a **p112** pattern with **all** the half turn centers of the original **pma2** pattern preserved (figure 2.29):

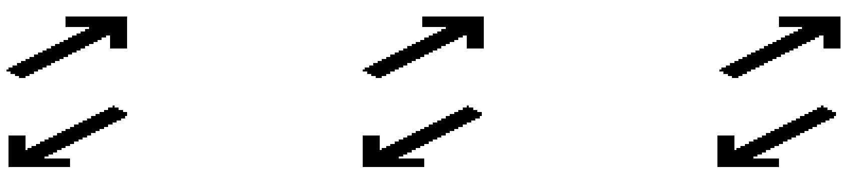

p112

Fig. 2.29

Notice also that the **upper half** of the **pma2** pattern in figure 2.28 is the familiar **pm11** pattern from figure 2.11. That is, every **pma2** pattern seems to 'contain' a **pm11**, a **p1a1**, and a **p112**: in view of the isometries involved this observation is not at all surprising and you should be able to verify it for every **pma2** pattern we have studied. How about the **p1m1** pattern then? Is it 'contained' in every **pma2** pattern? Well, as we will see right below, such a possibility is ruled out by the very nature of the patterns involved.

2.7 A couple's roundtrip footsteps (pmm2)

2.7.1 Is it a 'new' pattern? As we pointed out in 1.4.8, every reflection may be viewed as a very special glide reflection the gliding vector of which has length **zero**. What happens to a **pma2** pattern when its glide reflection is 'upgraded' to horizontal reflection? Nothing much, in a way; all other isometries will still be there, with the minimum distance between vertical mirrors and half turn centers reduced to **zero**: half turn centers are now found at the **intersections** of the pattern's **horizontal** reflection axis with every single **vertical** reflection axis! You may confirm all this by looking at a simple example of such a pattern, created by a letter that has **both** vertical and horizontal mirror symmetry:

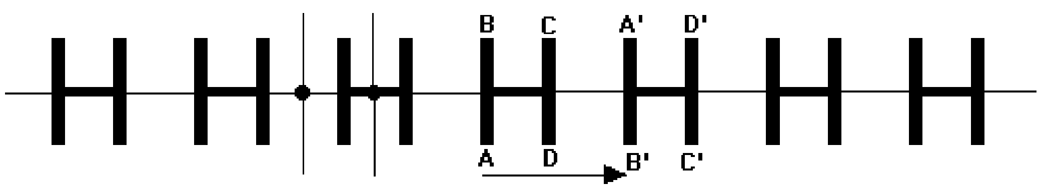

Fig. 2.30

Once again there are **two kinds** of vertical mirrors (right through **H**s and right between **H**s), hence two kinds of half turn centers as well. There isn't really too much new about this pattern, and even its name you should be able to guess: **pmm2**, with first **m** for vertical reflection, second **m** (instead of **a**) for horizontal reflection (instead of glide reflection), and **2** for point reflection.

In addition to viewing the horizontal reflection as a glide reflection with a gliding vector of zero length, we may as well employ it to create glide reflection; this is done by combining the horizontal reflection with the minimal translation vector as shown in figure 2.30: instead of **merely** reflecting each **H** back to itself, we glide it to the next **H**, too. This idea of using a reflection axis as an axis for a non-trivial, **'hidden'** glide reflection will become very important in future chapters. Notice by the way that the glide reflection of the **p1a1** pattern in figure 2.13 is none other than the 'hidden' glide reflection of the **p1m1** pattern in figure 2.11!

2.7.2 <u>The 'king' of border patterns.</u> The **pmm2** is the 'richest' type in terms of symmetry: it 'contains' both the **pma2** type (hence, as pointed out in 2.6.5, the **pm11**, **p1a1**, and **p112** types as well) and the **p1m1** type. Indeed we can 'reduce' our **pmm2** pattern to either a **pma2** or a **p1m1** pattern by cutting two 'arms' off each **H**:

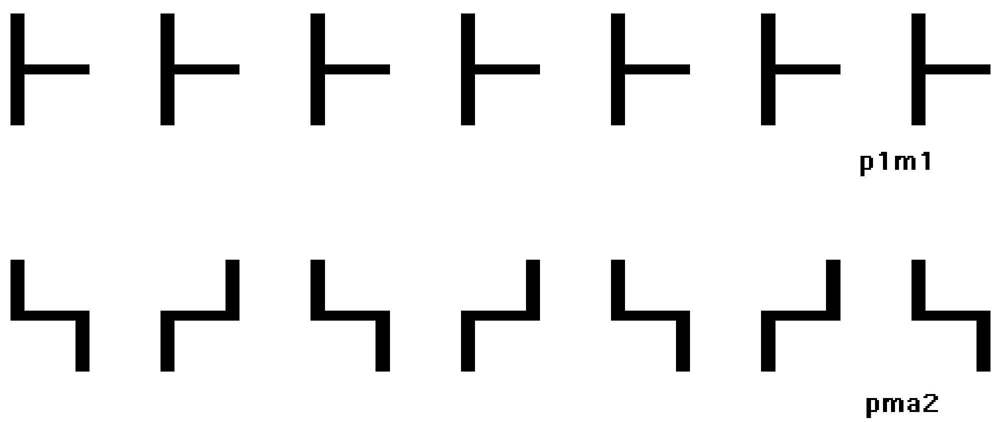

Fig. 2.31

2.7.3 <u>From **pmm2** to **pma2**.</u> We now revisit our pentagonal motif and construct **pmm2** and **pma2** patterns as shown below:

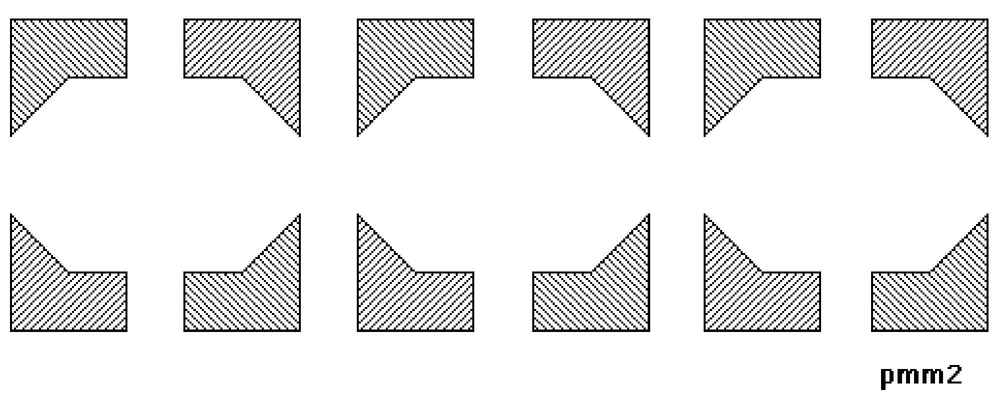

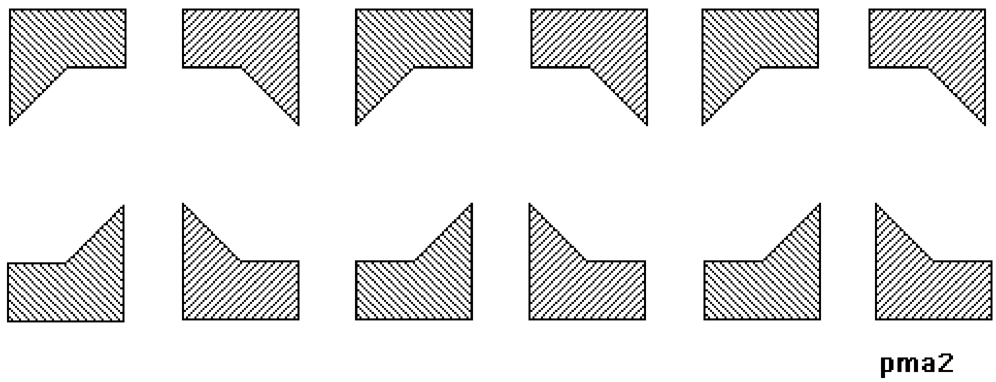

Fig. 2.32

Notice that this time we went from **pmm2** to **pma2** not by cutting the pattern in half (as in figure 2.31) but by **shifting** its bottom row. This 'shifting' will play an important role in chapter 4 and is also at the very root of the fact that the **p1m1** is not 'contained' in the **pma2**.

2.7.4 <u>More footsteps.</u> Consider the following 'arrow-footprint' pattern:

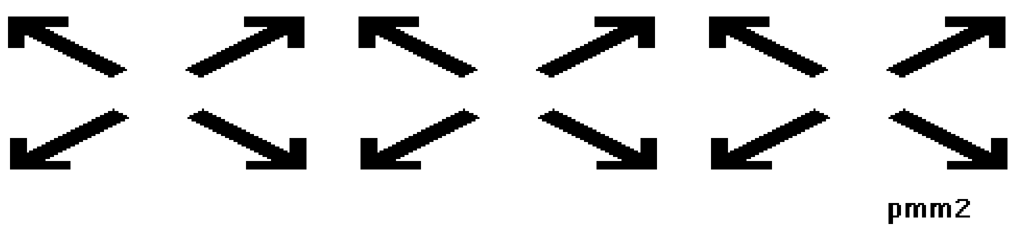

Fig. 2.33

With a little bit of thinking and imagination, you can see this **pmm2** pattern as the **roundtrip** footsteps of a couple walking together -- a bit fast perhaps -- and justify this section's title!

2.7.5 <u>Footnote.</u> Our representation of border patterns as footprints and footsteps is partially inspired by a June 24, 1996 ***What Shape Are You Into?*** lecture delivered at the Art and Mathematics conference at SUNY Albany by eminent Princeton mathematician **John Horton Conway**: he actually demonstrated how to create all seven types 'walking' alone (and barefoot)! You may like to experiment in that direction, especially when you happen to be alone; can you come up with a footprint representation of the **p112** pattern, alone or not, walking or standing?

Conway has his own **orbifold notation** for border patterns, closely related to his startling **topological** answer to the question discussed right below (and to the harder question of chapter 8, too).

2.8 Why only seven types of border patterns?

2.8.1 Brief summary. We have so far discussed the following **seven** types of border patterns (with a minimal sequence of English letters generating them (**fundamental region**) in brackets):

p111: Translation only (**common to all** seven types) [**F**]

pm11: Vertical Reflection [**M**]

p1m1: Horizontal Reflection [**D**]

p1a1: Glide Reflection [**pb**]

p112: Half Turn [**Z**]

pma2: Vertical Reflection, Glide Reflection, Half Turn [**pqbd**]

pmm2: Vertical Reflection, Horizontal Reflection, Half Turn [**H**]

Are there any other types or 'combinations' of border pattern isometries? The answer is **"no"**, and we are in a position to justify this claim without too much extra work.

2.8.2 Observations. Based on what we have observed in this chapter, and 2.7.1 & 2.6.3 in particular, we summarize here a number of useful remarks on how a certain isometry or combination of certain isometries implies the existence of another isometry:

[1] Horizontal reflection $\Rightarrow$ Glide reflection

[2] Glide reflection + Point reflection $\Rightarrow$ Vertical reflection

[3] Point reflection + Vertical reflection $\Rightarrow$ Glide reflection

[4] Vertical reflection + Glide reflection $\Rightarrow$ Point reflection

2.8.3 Classification. As we have seen in section 1.5, there exist four types of planar isometries: translation, reflection, rotation, and glide reflection. In the context of border patterns, only isometries that map the border pattern **back to itself** are allowed. That is, translation and glide reflection are allowed only along the pattern's backbone ('horizontally'), reflection may be either horizontal (along the backbone) or vertical (perpendicular to the backbone), and rotation is limited to 180^0 (half turn) with its centers lying on the pattern's backbone. Putting ever-present translation aside, we are left with four border pattern isometries, or **'four kinds of reflection'** if you wish: vertical-, horizontal-, glide-, and point-.

Now for every possible border pattern and each one of the four border pattern isometries (and reflection types) discussed above, we may, in fact must, ask a simple question: "does the border pattern have it, or not?" Clearly the answer to each one of the four possible questions is either "yes" or "no". How many possible combinations of answers are there? That will, quite simply, determine an **upper bound** for the number of possible combinations of border pattern isometries and border pattern types: there could be **at most** as many border pattern types as possible combinations of answers!

In theory there are **$2^4 = 16$** possible combinations, precisely because there are **two** possible answers ("yes" or "no") to **four** independent questions -- in the same way that, for example, there exist $6^4 = 1{,}296$ possible outcomes when four distinctly colored dice are rolled. In practice, the observations made in 2.8.2 reduce the number of possible combinations to **seven**: that is precisely how many border patterns have been recorded in 2.8.1 and studied in this chapter. In the table below you see the process of elimination, with

Y standing for “yes” and **N** for “no” (placed between **question marks** when a negative answer is in fact **impossible** because of one of the observations in 2.8.2); the number inside the parenthesis right next to “impossible” indicates the **applicable observation** from 2.8.2. Whenever a certain combination of answers happens to be impossible for more than one reasons, we cite the ‘simplest’ one.

	vertical	horizontal	glide	point	
	Y	Y	Y	Y	**pmm2**
	Y	Y	Y	?N?	impossible (4)
	Y	Y	?N?	Y	impossible (1)
	Y	N	Y	Y	**pma2**
	?N?	Y	Y	Y	impossible (2)
	Y	Y	?N?	N	impossible (1)
	Y	N	Y	?N?	impossible (4)
	Y	N	?N?	Y	impossible (3)
	N	Y	Y	N	**p1m1**
	N	Y	?N?	Y	impossible (1)
	?N?	N	Y	Y	impossible (2)
	N	N	N	Y	**p112**
	N	N	Y	N	**p1a1**
	N	Y	?N?	N	impossible (1)
	Y	N	N	N	**pm11**
	N	N	N	N	**p111**

2.9 Across borders

2.9.1 Mathematics and the artist’s imagination. Designs that belong to the seven possible types of border patterns are found all over the world, transcending borders, cultures, and historical periods. Two very different looking designs from, say, medieval Europe and pre-Colombian America, designed for very different uses and having very different cultural meanings to their creators, could very well belong to the same type of border pattern. This is not surprising: people, and artists in particular, of varying cultural and technological backgrounds are attracted to symmetry, but symmetry subjects its unsuspecting worshippers to unspoken mathematical truths and limitations that we just began to explore in this chapter.

Indeed a careful search through art books will reveal the presence of border patterns of any one of the seven types all around the world. You could find the same type around a Roman mosaic or on a Maori wood rafter, for example: different as they may look stylistically, they could very well be the same mathematically. In many cases mathematical kinship is in fact accompanied by stylistic similarity, leading perhaps to conjectures on cultural exchanges between two cultures or periods. While such exchanges and influences definitely existed, stylistic similarities are more likely to be byproducts of the mathematical limitations discussed above.

For further discussion on such issues we refer you to the book ***Symmetries of Culture: Theory and Practice of Plane Pattern Analysis***, by Dorothy K. Washburn (an archaeologist) and Donald W. Crowe (a mathematician), published by the University of Washington Press in 1988. The whole book is full of examples of designs from all over the world, while its first chapter discusses both border patterns and wallpaper patterns (which we begin to explore in chapter 4) from the **anthropological perspective**.

Less comprehensive yet brilliantly written and example-oriented is a book written by architect Peter S. Stevens, titled ***Handbook of Regular Patterns: An Introduction to Symmetry in Two Dimensions*** and published by the MIT Press in 1981. Stevens provides several pages of designs from different parts of the world for each border pattern type: going through his book will make you feel that there is nothing but perfectly symmetric designs in our world, which, fortunately or unfortunately, is not quite true. Anyhow, you should from now on be alert and keep an eye open for such 'perfect' designs around you! We give you a jump start here -- and conclude chapter 2 as well -- by citing **seven 'multicultural pages'** from Stevens' book, one for each type of border pattern, and in the same order we studied them; these pages have been included here with official permission from the MIT Press (which also covers a number of figures from Stevens' book included in chapter 4).

p111 border patterns from Peter S. Stevens' ***Handbook of Regular Patterns***, figure 12.6, p. 101 (© MIT Press, 1981):

(12.6a) French, twentieth century

(12.6b) ancient Greek

(12.6c) Roman, Pompeii

(12.6d) Chinese, eleventh century B.C.

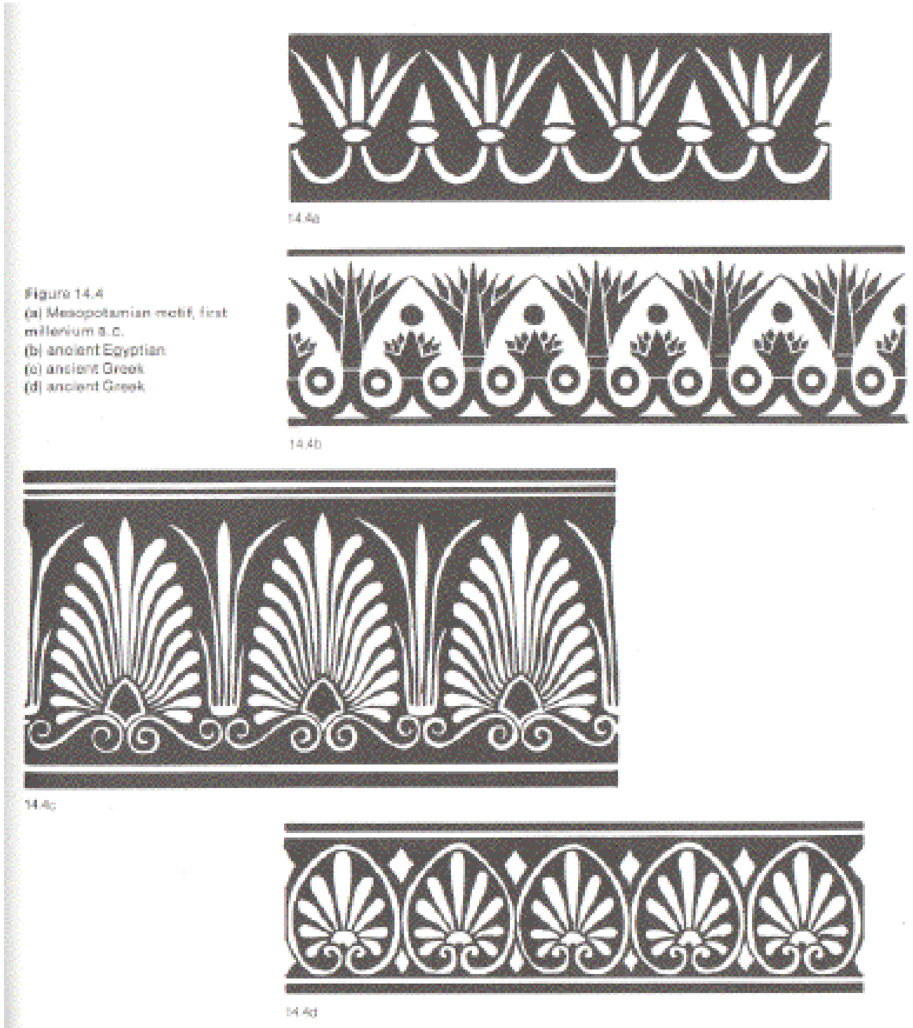

pm11 border patterns from Peter S. Stevens' ***Handbook of Regular Patterns***, figure 14.4, p. 121 (© MIT Press, 1981)

(14.4a) Mesopotamian motif, first millennium B.C.

(14.4b) ancient Egyptian

(14.4c) ancient Greek

(14.4d) ancient Greek

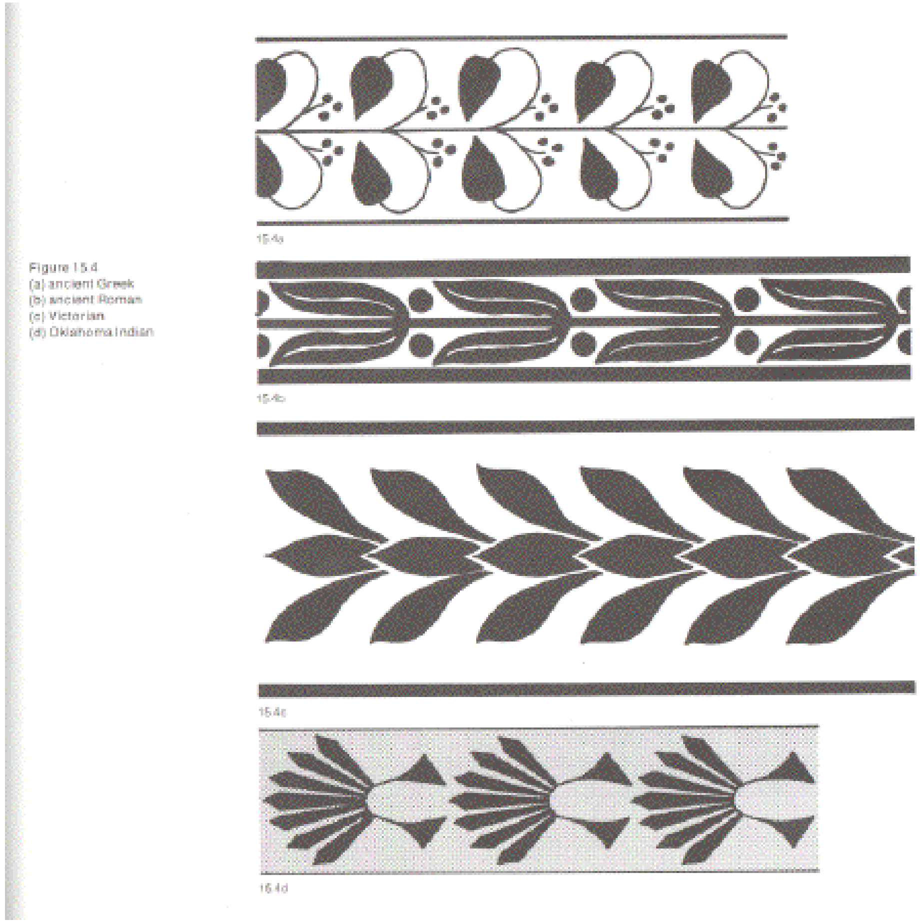

p1m1 border patterns from Peter S. Stevens' ***Handbook of Regular Patterns***, figure 15.4, p. 129 (© MIT Press, 1981)

(15.4a) ancient Greek

(15.4b) ancient Roman

(15.4c) Victorian

(15.4d) Oklahoma Indian

p1a1 border patterns from Peter S. Stevens' ***Handbook of Regular Patterns***, figure 13.8, p. 113 (© MIT Press, 1981)

(13.8a) Navaho Indian

(13.8b) Turkish design, sixteenth century

(13.8c) medieval ornament

(13.8d) Pueblo Indian design

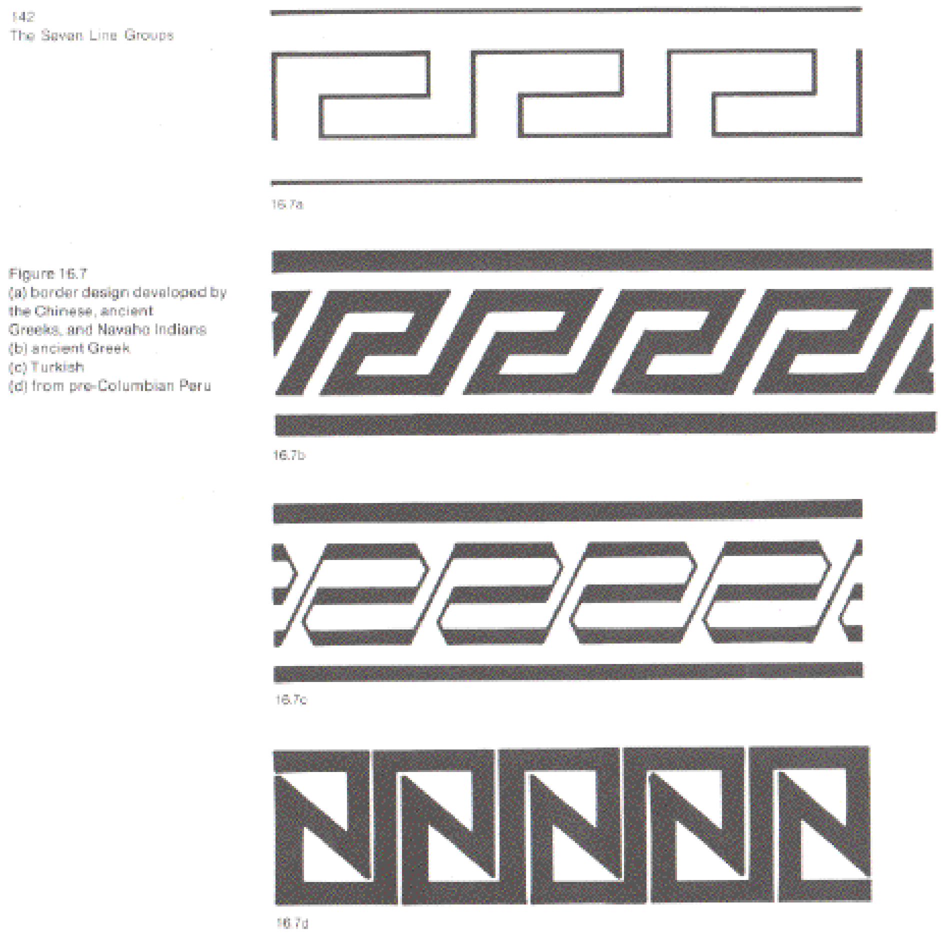

p112 border patterns from Peter S. Stevens' ***Handbook of Regular Patterns***, figure 16.7, p. 142 (© MIT Press, 1981)

(16.7a) border design developed by the Chinese, ancient Greeks, and Navaho Indians

(16.7b) ancient Greek

(16.7c) Turkish

(16.7d) from pre-Columbian Peru

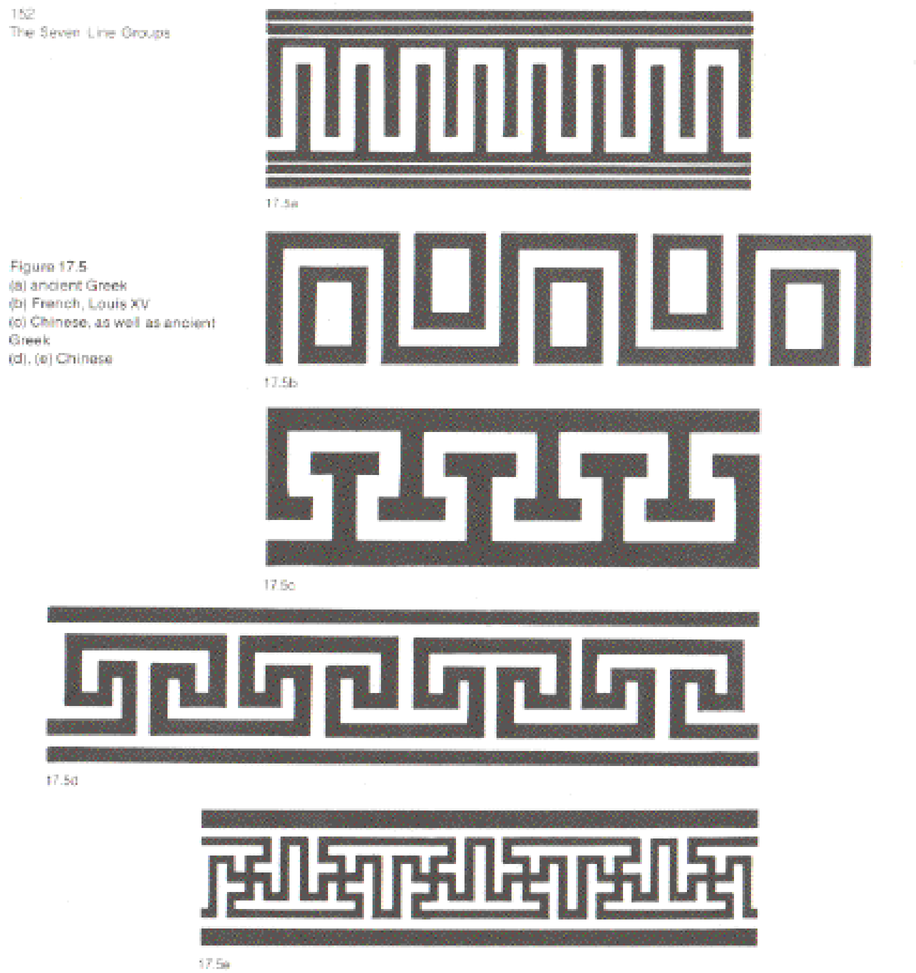

pma2 border patterns from Peter S. Stevens' ***Handbook of Regular Patterns***, figure 17.5, p. 152 (© MIT Press, 1981)

(17.5a) ancient Greek

(17.5b) French, Louis XV

(17.5c) Chinese, as well as ancient Greek

(17.5d) Chinese

(17.5e) Chinese

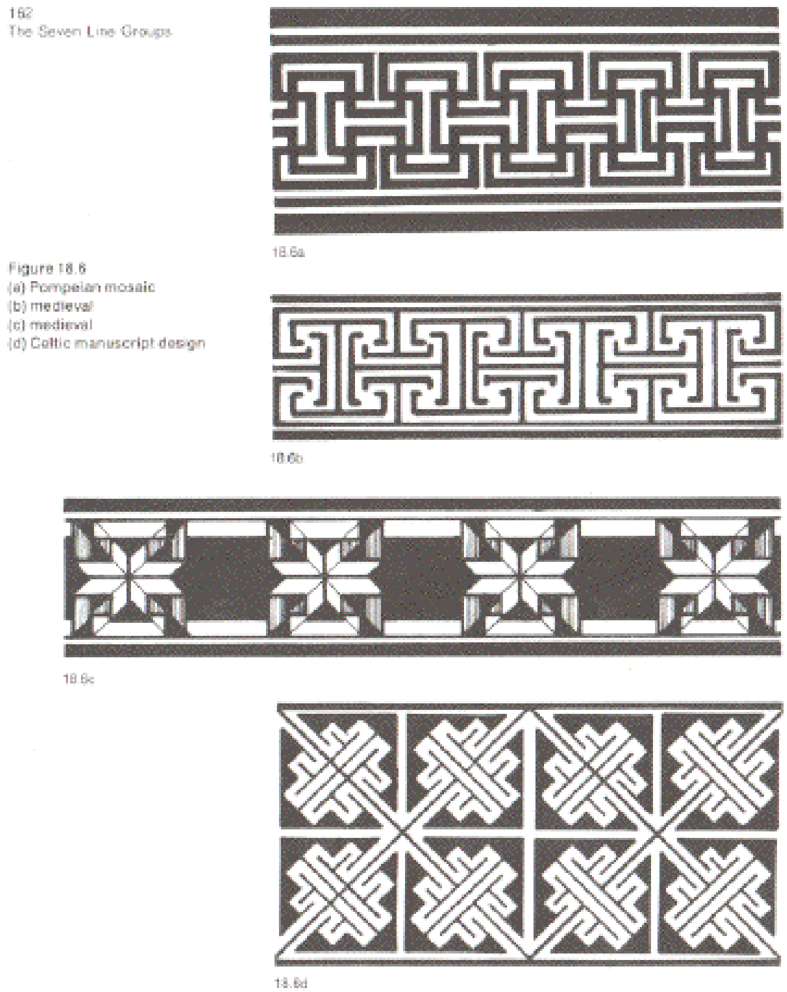
162
The Seven Line Groups

Figure 18.6
(a) Pompeian mosaic
(b) medieval
(c) medieval
(d) Celtic manuscript design

18.6a

18.6b

18.6c

18.6d

pmm2 border patterns from Peter S. Stevens' ***Handbook of Regular Patterns***, figure 18.6, p. 162 (© MIT Press, 1981)

(18.6a) Pompeian mosaic

(18.6b) medieval

(18.6c) medieval

(18.6d) Celtic manuscript design

CHAPTER 3

WHICH ISOMETRIES DO IT?

3.0 Congruent sets

3.0.1 Congruence. We call two sets **congruent** to each other if and only if there exists an isometry that maps one to the other; in simpler terms, if and only if one is a **copy** of the other. For example, this is the case with the quadrilaterals ABCD and A′B′C′D′ in either of figures 1.18 & 1.30. It is correct to say that this definition extends the familiar definition of congruent triangles and, more

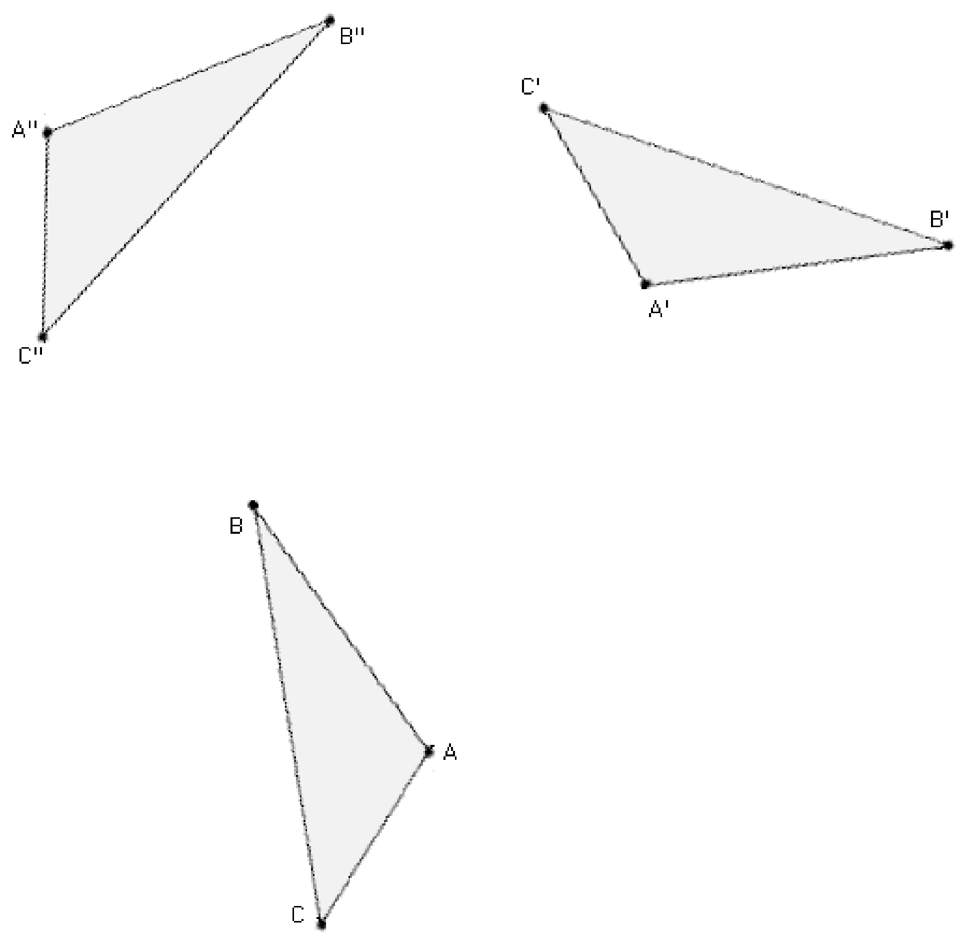

Fig. 3.1

generally, congruent polygons. In more practical terms, two sets are congruent if and only if one of them can be brought to perfectly **'match'** the other point by point. Let us for example have a look at the triangles ABC, A′B′C′, and A″B″C″ of figure 3.1: both triangles A′B′C′ and A″B″C″ are congruent to ABC as $|A''B''| = |A'B'| = |AB|$, $|A''C''| = |A'C'| = |AC|$, and $|B''C''| = |B'C'| = |BC|$. The relation of each triangle to ABC is somewhat **different** though: while A′B′C′ may be **slid** (i.e., glided and turned as needed) until it matches ABC point by point, A″B″C″ may **not** be brought back to ABC by mere sliding. How do we demonstrate the congruence of ABC and A″B″C″ in a hands-on way then? One needs to be clever enough to observe that A″B″C″ may in fact be slid back to ABC after it gets **flipped**: if that is not obvious to you, simply trace A″B″C″ on tracing paper, then flip the tracing paper and slide the flipped A″B″C″ back to ABC -- it works!

Revisiting the pairs of quadrilaterals in figures 1.18 & 1.30, we make similar observations: in figure 1.18 A′B′C′D′ (image of ABCD under reflection) must be flipped in order to be slid back to the original ABCD, while in figure 1.30 A′B′C′D′ (image of ABCD under rotation) can be slid back to ABCD without any flipping. You have probably suspected this one by now: flipping is required in the case of reflection but not in the case of rotation. But let us now take a look at the two triangles of figure 1.14, mirror images of each other:

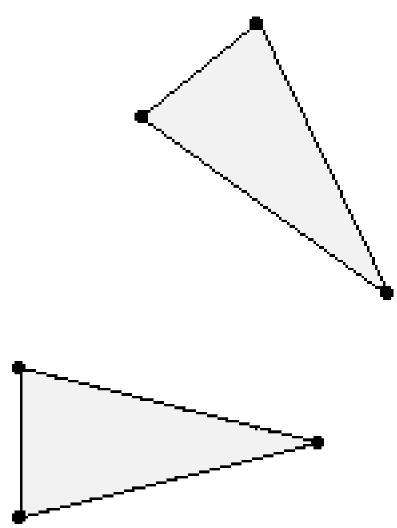

Fig. 3.2

Despite the reflection, you can easily check, using tracing paper if necessary, that the two triangles may easily be slid back to each other (without any flipping, that is). What makes the difference?

3.0.2 Homostrophy and heterostrophy. Before addressing the issues raised by figure 3.2, we need some terminology. We call two congruent sets **homostrophic** ('of same turning') if and only if they can match each other via mere sliding; and we call two congruent sets **heterostrophic** ('of opposite turning') if and only if they can only match each other via a combination of flipping and sliding. For example, ABCD and A′B′C′D′ are homostrophic in figure 1.30, but heterostrophic in figure 1.18. And, in figure 3.1 above, A′B′C′ and A″B″C″ are homostrophic and heterostrophic to ABC, respectively.

3.0.3 Labeling. Let us now return to the 'puzzle' of figure 3.2 and reinstate the vertex labels from figure 1.14 as below:

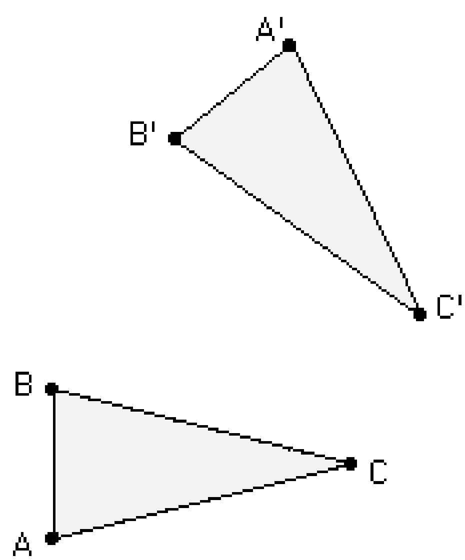

Fig. 3.3

Can you now slide A′B′C′ 'back' to ABC in a way that A′, B′, C′ 'return' to A, B, C, **respectively**? After a shorter or longer effort -- that depends on your personality -- you are bound to give up: it is simply impossible! That is, the **labeling** of the vertices has made the two congruent triangles heterostrophic: A′B′C′ needs to be flipped before it can slide to ABC. And, once again, heterostrophy seems to be associated with **reflection**.

Back in 3.0.1, and figure 3.2, you were able to slide the triangle **now** labeled A′B′C′ to match ABC. What would happen if you repeat that same sliding? The two triangles would still match each other, except that now A′ 'returns' to B and B′ 'returns' to A. This is not quite a perfect match, but it would obviously be one if we **swap** A′ and B′. Indeed such an action leads to the following situation:

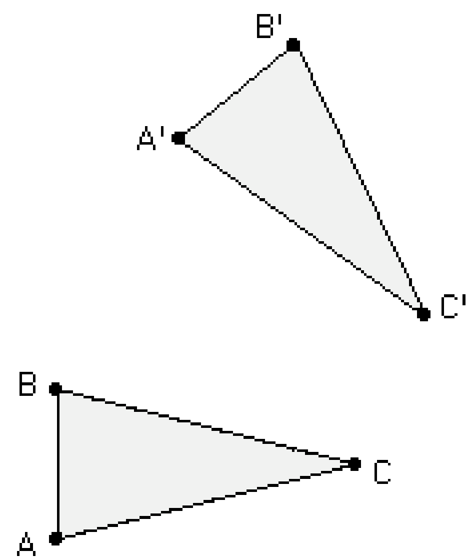

Fig. 3.4

Clearly, it is now possible to simply slide A′B′C′ to ABC: the two triangles are now homostrophic! A rushed conclusion is that **homostrophy and heterostrophy are concepts 'defined' by labeling**; this is a rule with its fair share of **exceptions**, as we will see in 3.2.6 and 3.5.4. And, in view of our entire discussion so far, an obvious question would be: is there a **rotation** that maps ABC to A′B′C′ in figure 3.4? We **knew** ahead of time, thanks to figure 1.14, of a reflection that mapped ABC to A′B′C′ in figure 3.3; it is not unreasonable now to **suspect** that there is a rotation that maps ABC to A′B′C′ in figure 3.4: but **how** do we determine such a rotation, how do we come up with a center and an angle that would work?

3.0.4 The 'reverse' problem. Let us now consider a situation similar to the one discussed in 3.0.3, departing from rotation and figure 1.24 this time; we leave the familiar triangle ABC untouched but we **swap** A′ and B′ as shown in figure 3.5 below:

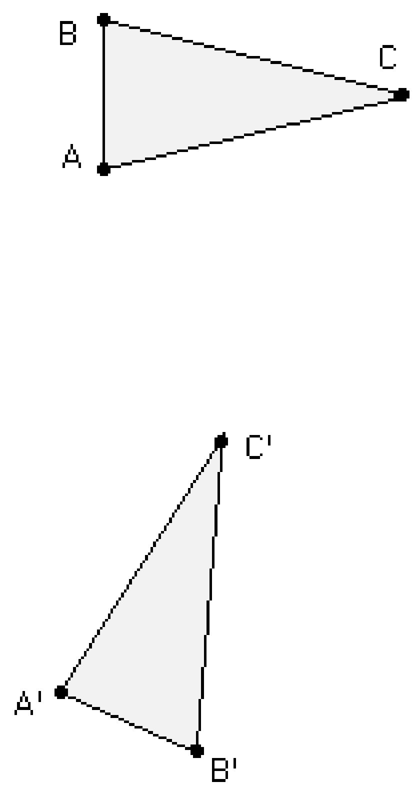

Fig. 3.5

It is clear that the homostrophy (created by rotation) in figure 1.24 has now been eliminated. Does that mean that there exists a reflection that maps ABC to A′B′C′? The answer is “no”: in every reflection the segments PP′ that join every point P of the original figure to its image point P′ are perpendicular to the reflection axis, hence they must all be **parallel** to each other; and that is clearly **not** the case in figure 3.5! For exactly the same reason there is no translation mapping ABC to A′B′C′. Nor is a rotation plausible, as we do suspect, without proof so far, that rotation is **always** associated with homostrophy. There only remains one possibility: **glide reflection**!

That glide reflection can be associated with heterostrophy is suggested by the effect of the two opposite glide reflections on ABC in figure 1.34: both A′B′C′ and A″B″C″ are easily seen to be

heterostrophic to ABC! So yes, there is hope, if not certainty, that there exists a glide reflection that maps ABC to A′B′C′ in figure 3.5; but **how** do we determine such a glide reflection, how do we come up with an axis and a vector that would work?

This last question sounds very similar to the one posed at the end of 3.0.3, doesn't it? The two questions are indeed the two faces of a broader question that **reverses** the tasks you learned in chapter 1: back then you were given a set and an isometry and you had to determine the image; here you are given the 'original' set and an 'image' set congruent to it, and you are asked to determine **all** the isometries that send the original to the image. That there may be **more than one isometries** 'between' two congruent sets should be clear in view of the examples discussed in this section, and has in fact been explicitly demonstrated in figure 2.22. Chapter 3 is devoted to this 'reverse' question.

3.1 Points

3.1.1 Infinite flexibility. Points do not take much room at all, hence they ought to be rather easy to deal with! In our context, given any two points A and A′, we can at once find not one but two isometries that map A to A′. These are a **translation** defined by the **vector AA′** and a **reflection** whose axis is the **perpendicular bisector of AA′**:

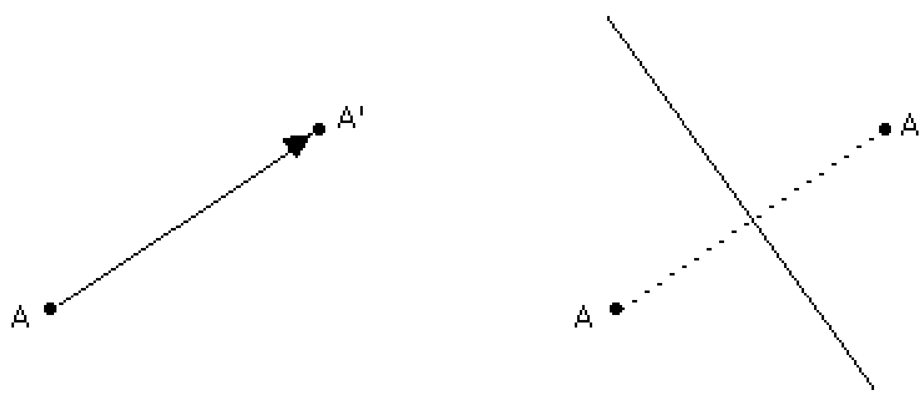

Fig. 3.6

We are much ‘luckier’ than that though! There exist in fact **infinitely many rotations** and **infinitely many glide reflections** that map A to A′. Getting them all turns out to be mostly a matter of remembering the ways of rotation and glide reflection from chapter 1: we will also need to learn to play the game backwards, and employ a bit of high school geometry as well.

3.1.2 Rotations. Let us revisit figure 1.21, where we defined rotation, and make a fundamental observation: since |KP| = |KP′|, K must lie on the **perpendicular bisector** of PP′! Indeed if M is the **midpoint** of PP′ then the two triangles MKP and MKP′ have three pairs of equal sides, hence they are congruent; but then $\angle$KMP′ = $\angle$KMP = $180^0/2 = 90^0$, hence KM is **perpendicular** to PP′:

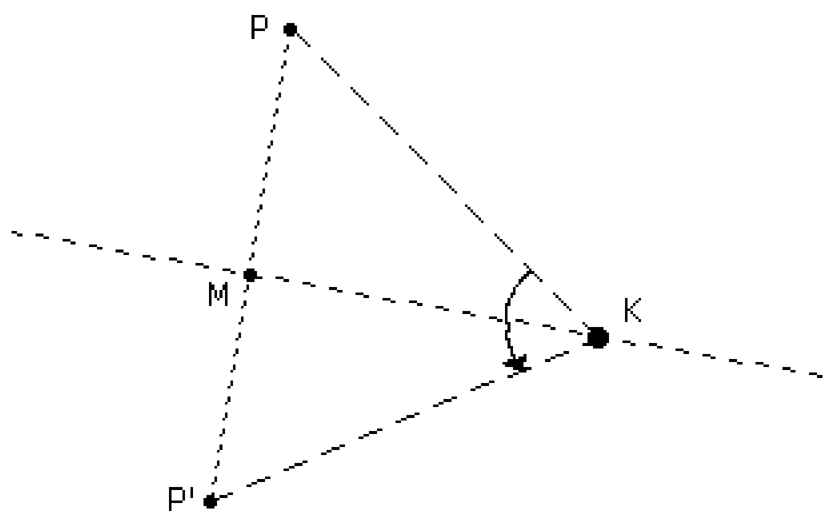

Fig. 3.7

Returning to A and A′ of 3.1.1, we may now obtain infinitely many rotations that map A to A′; simply apply the previous argument **backwards**, pick an **arbitrary** point K on the **perpendicular bisector** of AA′ to be the rotation center, and then observe that the rotation angle is none other than the **oriented angle $\angle$AKA′, opening from A toward A′ by way of K**:

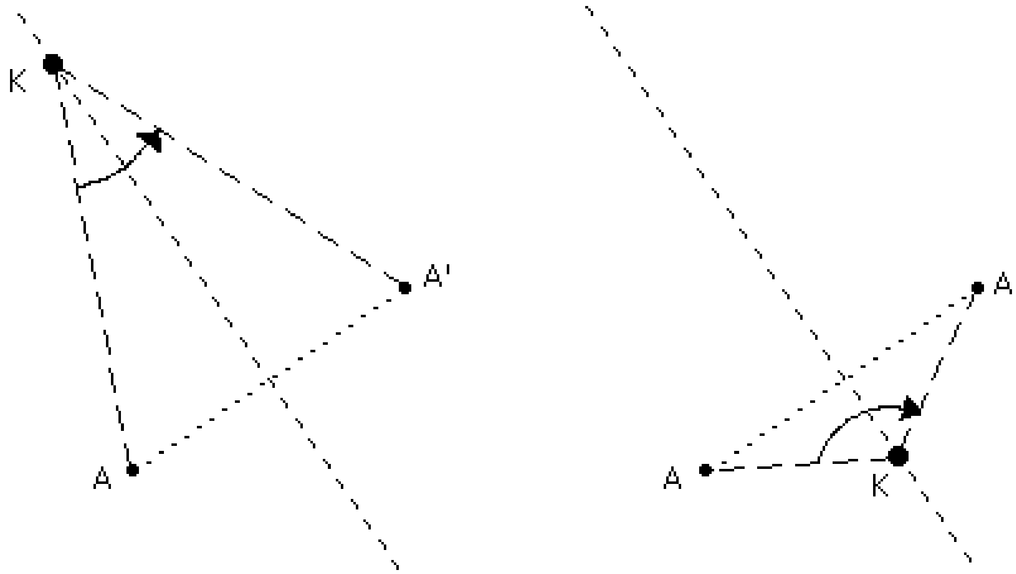

Fig. 3.8

Notice that the rotation angle could be either clockwise or counterclockwise, depending on the relative position of A, K, and A′: this information should **always** be part of your answer! Notice also that the rotation angle is 180^0 when K is the **midpoint** of AA′, and approaches 0^0 as K moves far away from (and on either side of) AA′ (with the rotation itself 'approaching' -- near AA′ at least -- the **translation** of figure 3.6).

3.1.3 Glide reflections. It's time now to revisit figure 1.31, where we defined glide reflection, and make a crucial observation: the glide reflection axis L does intersect PP′ at its **midpoint**!

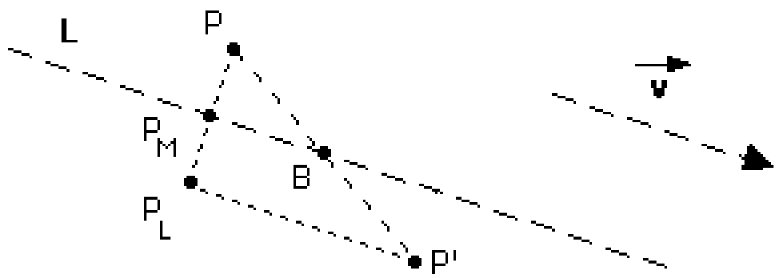

Fig. 3.9

While this is made ‘obvious’ by figure 3.9, it is not difficult to offer a rigorous proof. Indeed, since P_LP' is **parallel** to P_MB (by the very definition of glide reflection), $\frac{|PB|}{|PP'|} = \frac{|PP_M|}{|PP_L|} = \frac{1}{2}$.

How do we take advantage of this crucial observation and, in the context of 3.1.1 in particular, how could we use it to obtain glide reflections that map A to A′? All we have to do is to play the game **backwards**! Simply draw an **arbitrary** line L through the **midpoint** M of AA′ and then find the image A_L of A under reflection about L; it is easy then to check that the line L and the vector A_LA' (**pointing from the ‘intermediate’ mirror image toward the actual glide reflection image**) are the axis and vector of a glide reflection that maps A to A′:

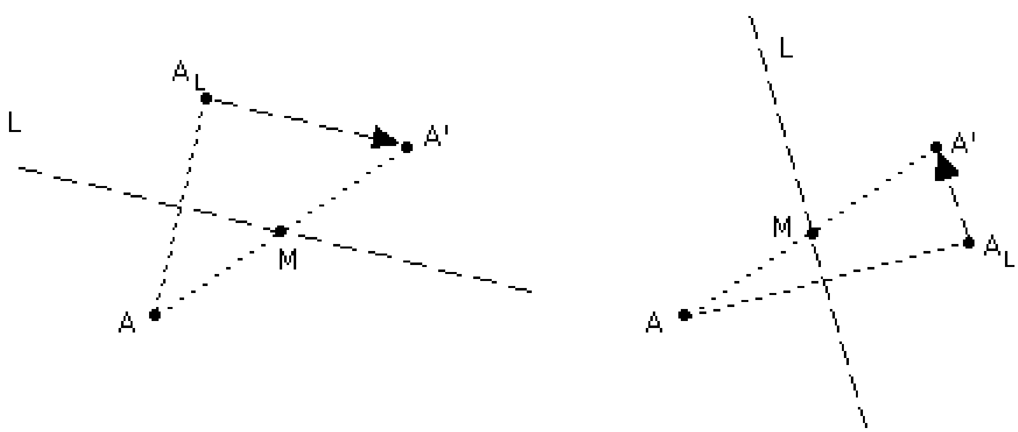

Fig. 3.10

Figure 3.10 offers two out of infinitely many possibilities for a glide reflection that maps A to A′. Notice that the glide reflection vector can be of every possible direction, but its length cannot exceed |AA′|; in the **special case** where L is the perpendicular bisector of AA′, the length of the glide reflection vector is equal to **zero** and the glide reflection is ‘reduced’ to the **reflection** of figure 3.6.

3.2 Segments

3.2.1 Two possibilities. Consider two straight line segments of **equal length**, one of them already labeled as AB:

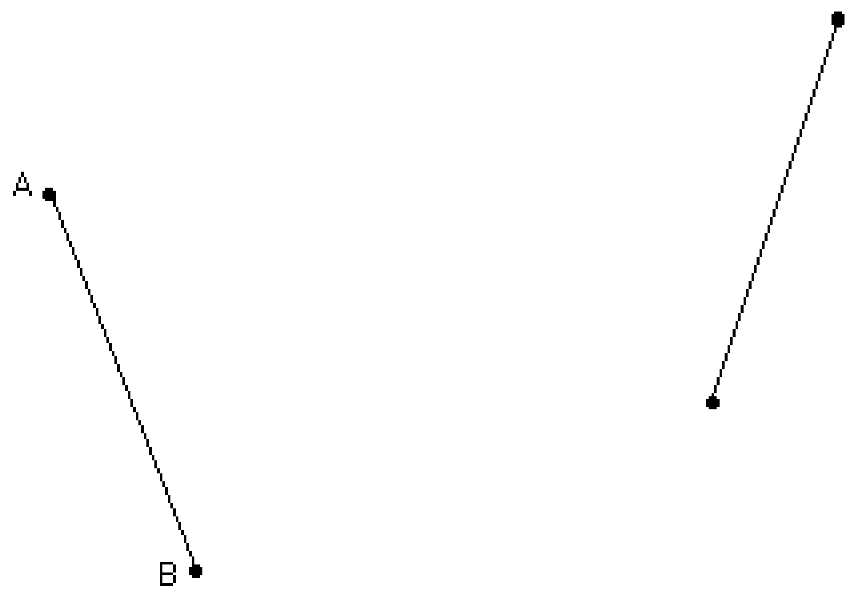

Fig. 3.11

You are probably certain that there exist isometries that map AB to the segment on the right, but you probably cannot guess how many and you are not sure how to find them, right? Well, one departing point is to realize that there exist **only two possibilities** for A and B: either A gets mapped to the 'top endpoint' and B gets mapped to the 'bottom endpoint' of the segment on the right, or vice versa. We will begin with the first possibility.

3.2.2 Two perpendicular bisectors, one center. Now that we have for the time being decided where A and B are mapped by the isometry we are trying to determine ('first possibility' in 3.2.1), we may recall (3.1.2) that there exist infinitely many **rotations** that map A to A′ and infinitely many rotations that map B to B′. The obvious question is: could some of those rotations perform **both** tasks, mapping A to A′ **and** B to B′? This question is answered if we also recall **how** all those rotations were determined! That is, let us recall (3.1.2) that the set of **centers** of all the rotations that map A to A′ is the **perpendicular bisector** of AA′, and likewise the set of centers of all the rotations that map B to B′ is the perpendicular bisector of BB′. Isn't it reasonable then to guess that the **intersection of the two perpendicular bisectors**, lying on **both** of them, will be the **unique rotation center** that achieves both goals? This guess is correct, as shown in figure 3.12, where we also determine the **rotation angle**:

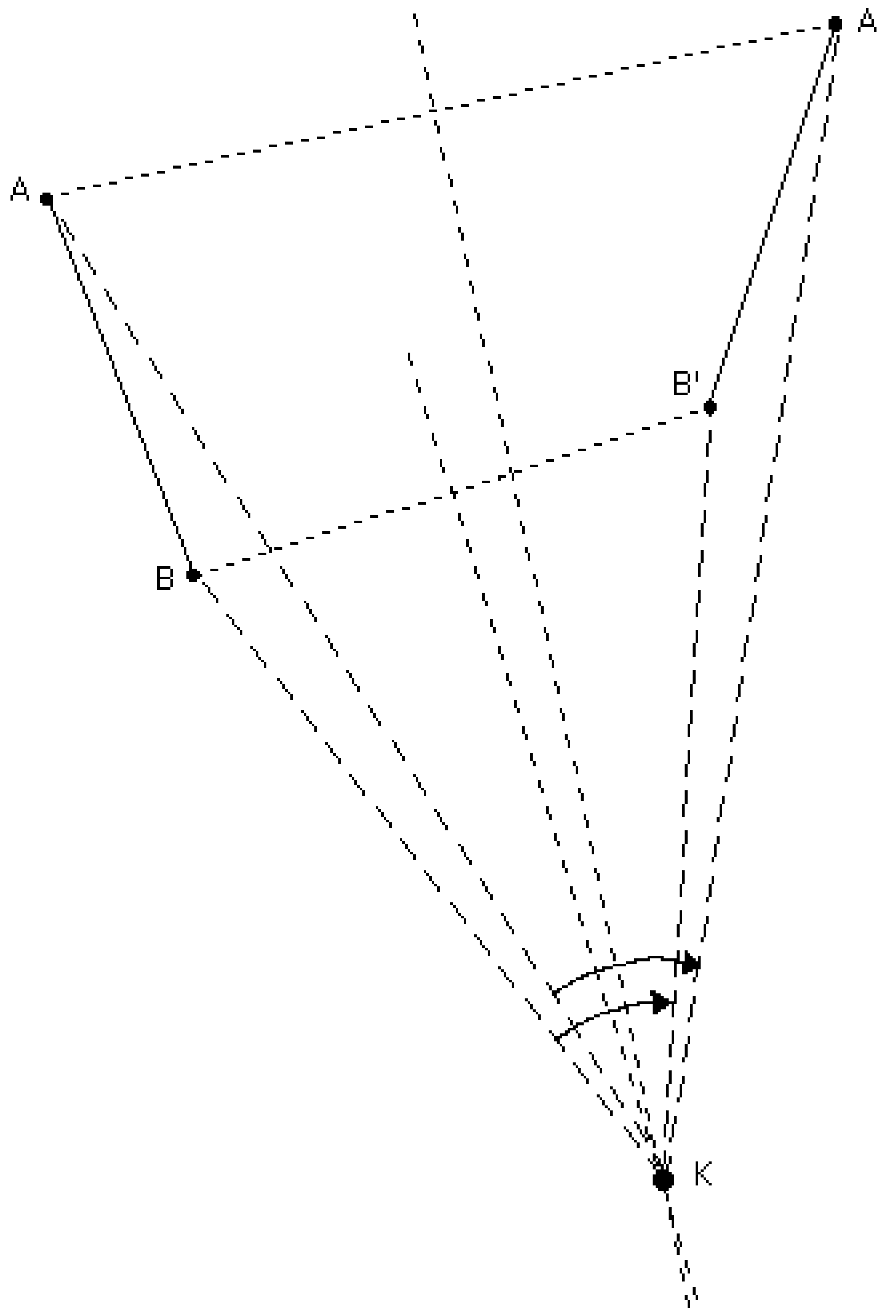

Fig. 3.12

Although it is next to impossible to achieve perfect precision, we see that approximately the same clockwise angle (and center) does indeed work for both A and B; in fact the rotation works for **all** points on AB -- we elaborate on this in 3.3.1.

3.2.3 Two midpoints, one axis. You can almost guess the game now: always sticking with that 'first possibility' of 3.2.1 (or just the placement of A′ and B′ in figure 3.12 if you wish), we would like to determine a **glide reflection** that maps **both** A to A′ and B to B′. We may at this point recall (3.1.3) that a glide reflection maps A to A′ (and B to B′) if and only if it passes through the **midpoint** of AA′ (and the midpoint of BB′). Arguing as in 3.2.2, we conclude that there exists a **unique glide reflection** mapping both A to A′ and B to B′, the axis of which is no other than the **line connecting the two midpoints**. The whole affair is presented in figure 3.13, where we also determine the **glide reflection vector**:

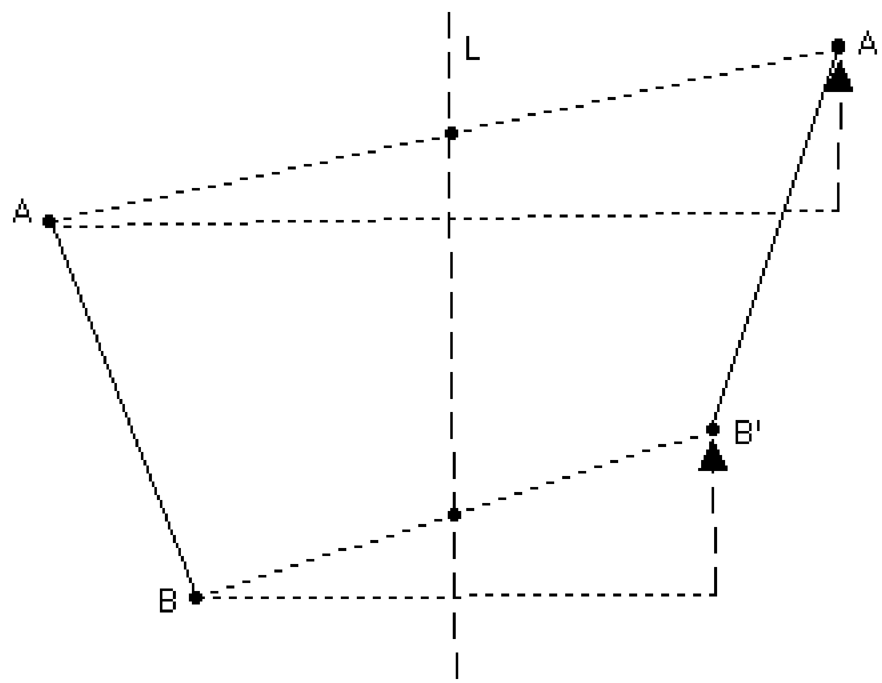

Fig. 3.13

Again we see that approximately the same S-N vector works for both A and B. The glide reflection **must** in fact work for **all** points on AB, as we are going to see in 3.3.1.

3.2.4 The 'second possibility'. We now take care of the second possible labeling of the segment on the right in figure 3.11 (3.2.1) and obtain two more isometries between the two segments as shown in figures 3.14 (rotation) and 3.15 (glide reflection):

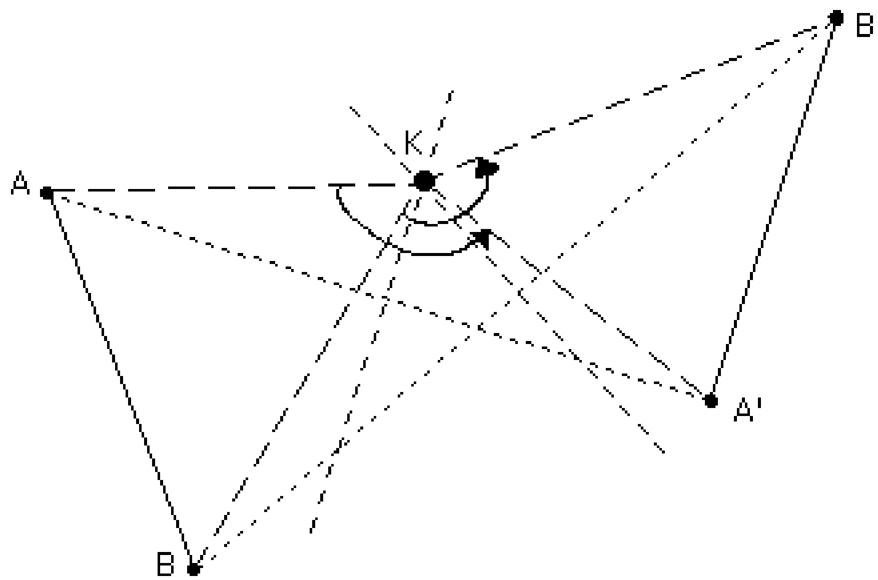

Fig. 3.14

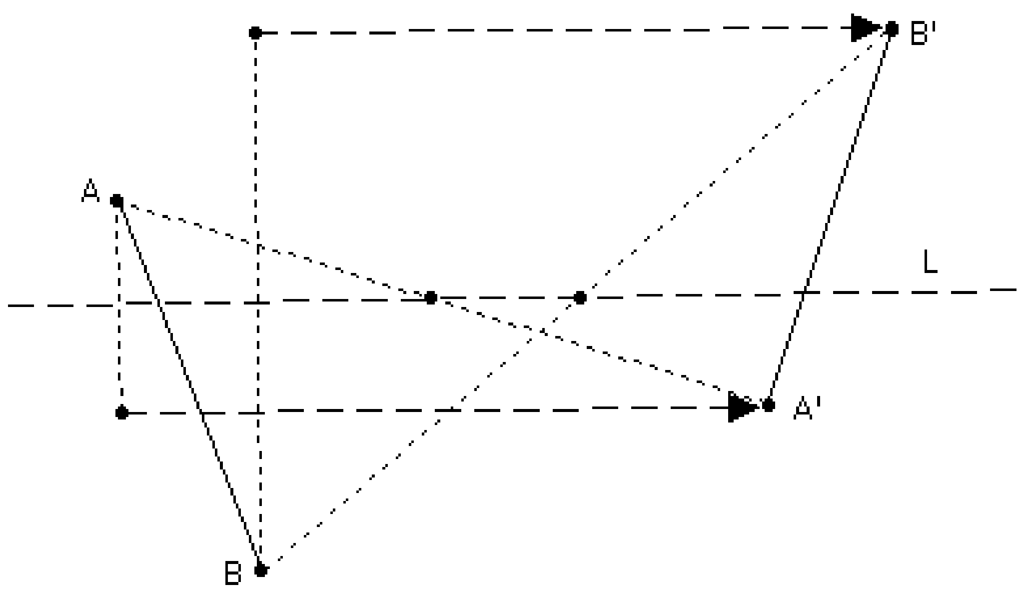

Fig. 3.15

3.2.5 Four isometries! Putting everything together, we see that there exist **two rotations and two glide reflections** mapping every two congruent straight line segments to each other. **One** of the rotations may be **'deformed'** into a **translation** (in case AB and A′B′, hence the perpendicular bisectors of AA′ and BB′ as well, are **parallel** to each other, 'meeting at infinity' -- see also concluding remark in 3.1.2); likewise, **one** of the glide reflections may be **'reduced'** to a **reflection** (in case the line connecting the midpoints of AA′, BB′ is **perpendicular** to one -- hence, by a geometrical argument, both -- of them). Both situations occur for example in the case of any two adjacent hexagons in a beehive!

3.2.6 Homostrophic segments. We conclude by pointing out that, **under either labeling**, the segment on the right (in figures 3.11 through 3.15) is homostrophic to AB. This is further indicated by the two rotations determined in figures 3.12 & 3.14, of course. But notice here that, quite uniquely as we will see later on, the segment A′B′, homostrophic to AB, is **at the same time** the image of AB under the two glide reflections determined in figures 3.13 & 3.15!

3.3 Triangles

3.3.1 Two points almost determine it all. Here is a simple question you could have already asked in section 3.2: how do we really know that each of the four isometries mapping A and B to the endpoints of the 'image segment' on the right do actually map (every point P on) the **segment** AB to (a point P′ on) the segment on the right? Good question! Luckily, circles come to the rescue of segments in figure 3.16 below.

Indeed, P′ (the image of P under whatever isometry maps A to A′ and B to B′) must lie on **both** the circle $\mathbf{C_{A'} = (A'; |AP|)}$ of **center A′** and **radius |AP|** and the circle $\mathbf{C_{B'} = (B'; |BP|)}$ of **center B′** and **radius |BP|**: the distances of P from both A and B must be preserved. But these two circles can have only one **'tangential'** point in common, **lying on A′B′**, due to $|A'B'| = |AB| = |AP| + |BP|$ (figure 3.16).

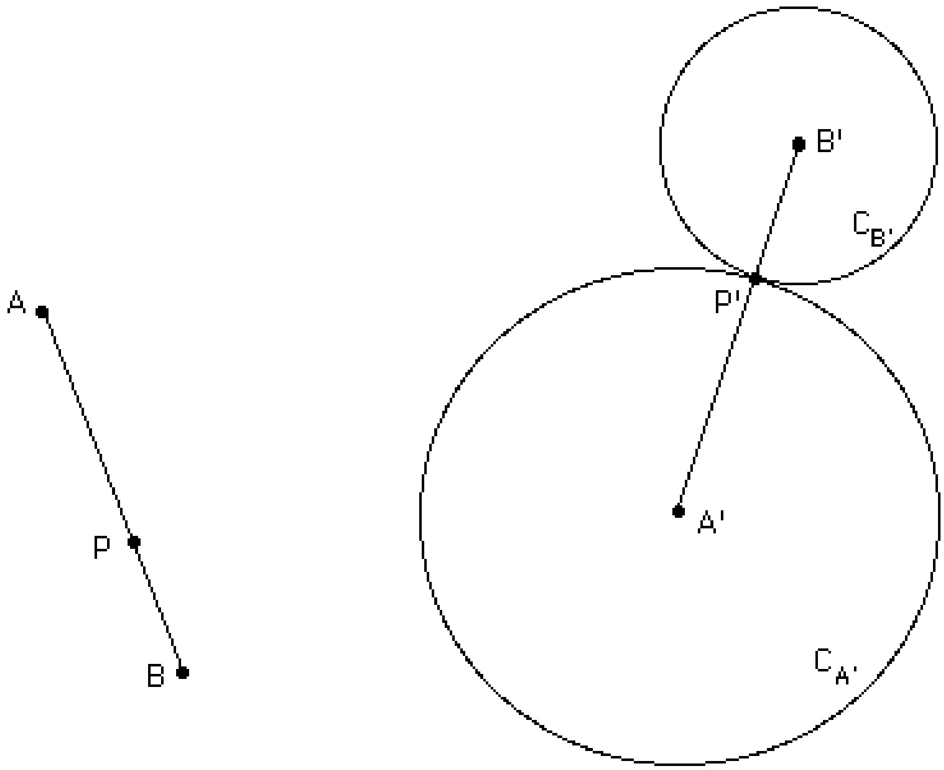

Fig. 3.16

There are of course **precisely two** possibilities for the exact location of P′ on AB's image on the right, depending on the two possibilities for A′ in 3.2.1; but in both cases every point P on AB is indeed mapped to a point P′ on A′B′ (with $|PA| = |P'A'|$ and $|PB| = |P'B'|$, of course), therefore the **entire segment** AB is mapped to A′B′.

Now that you have seen that the images of the endpoints A, B completely determine the image of every point P on the segment AB (and in fact of every point on the **entire line** of AB, thanks to a similar argument involving 'exterior points' and 'interior tangency'), you may wonder: what if P lies **outside** that line? Once again the circles $C_{A'}$ and $C_{B'}$ can be of great help, except that this time, with $|A'B'| < |AP| + |BP|$ instead of $|A'B'| = |AP| + |BP|$, they do **intersect** each other instead of being tangent to each other; hence there are **two possibilities** for P′, indicated by P'_1 and P'_2 in figure 3.17:

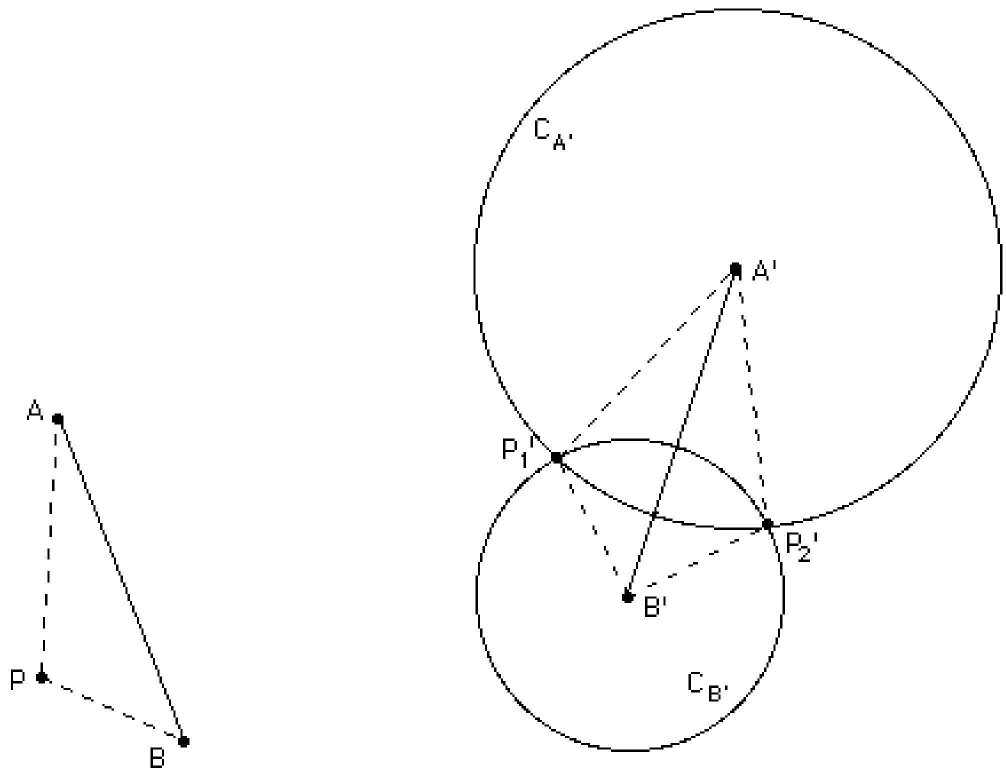

Fig. 3.17

3.3.2 <u>Congruent triangles.</u> It doesn't take long to observe that, in figure 3.17, $A'B'P'_1$ is (congruent and) **homostrophic** to ABP while $A'B'P'_2$ is (congruent and) **heterostrophic** to ABP. Reversing this observation, we notice that whenever a triangle A′B′P′ is congruent to a triangle ABP there exists **precisely one isometry** mapping ABP to A′B′P′: a rotation (or translation) in case A′B′P′ is homostrophic to ABP and a glide reflection (or reflection) in case A′B′P′ is heterostrophic to ABP. Indeed, with **A′ and B′ determined** on AB's image **by P''s position** (and $|AP| \neq |BP|$, the case $|AP| = |BP|$ being deferred to section 3.4), there are precisely two isometries mapping AB to A′B′, one rotation and one glide reflection (section 3.2): P′ may then be **only one** of the **two intersection points** of the two circles shown in figure 3.17 (and corresponding to the **two isometries** mapping AB to A′B′).

We illustrate this in figure 3.18: labeling the 'original' triangle as DEF, we easily determine the images D′, E′, F′ (homostrophic copy of DEF) and D″, E″, F″ (heterostrophic copy of DEF); it is then clear that **only one** of the two intersection points (F′) of the circles (D′; lDFl) and (E′; lEFl) corresponds to a homostrophic copy of DEF, and likewise **only one** of the two intersection points (F″) of the circles (D″; lDFl) and (E″; lEFl) corresponds to a heterostrophic copy of DEF.

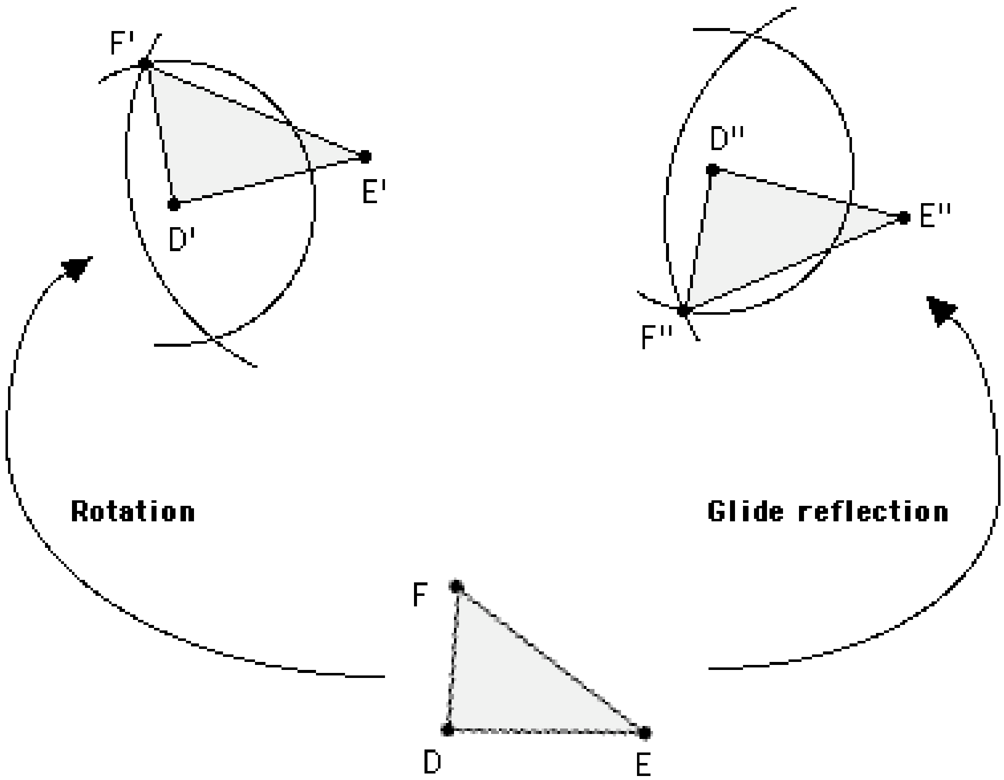

Fig. 3.18

3.3.3 Circular orientation revisited. Implicit in the discussion above is the assumption that translation and rotation are associated with homostrophy (**'same turning'**), while reflection and glide reflection are associated with heterostrophy (**'opposite turning'**). We can offer a quick justification for this assumption (and naming) as follows.

Returning to figure 3.17, let us replace the circles $C_{A'}$ and $C_{B'}$ by the three **congruent** circles C_0, C_1, and C_2, **circumscribed** to the triangles ABP, $A'B'P'_1$, and $A'B'P'_2$, respectively:

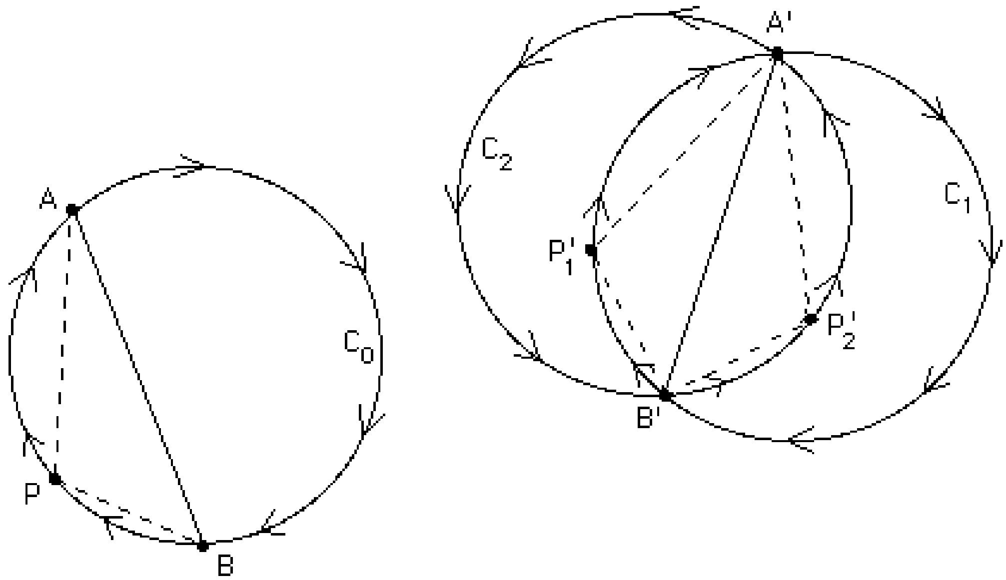

Fig. 3.19

Clearly the points A, B, P, traced **alphabetically**, are **clockwise** placed on C_0; their images are **clockwise** placed on C_1 (A', B', P'_1) and **counterclockwise** placed on C_2 (A', B', P'_2). As this **'circular order'** among A, B, P on C_0 has been **preserved** among their images on C_1 but **reversed** on C_2, it is easy to see that C_1 **can** slide back to C_0 returning images to originals, while C_2 **cannot** (without flipping, that is). So, homostrophy is associated with preservation of circular order, while heterostrophy is associated with reversal of circular order. But we have already seen in 1.5.4 -- and could certainly verify from scratch by extending section 3.1 from points to circles! -- that preservation of circular order is associated with translations and rotations, while reversal of circular order is associated with reflections and glide reflections.

3.3.4 Triangles determine everything! We just saw that, in the case of two congruent triangles, homostrophy is indeed associated with translation or rotation, and heterostrophy with reflection or glide reflection. This holds true for every pair of congruent sets on the plane, and relies on a broader fact, demonstrated in figure 3.20 below: every isometry on the plane is uniquely determined by its effect on **any three non-collinear points**!

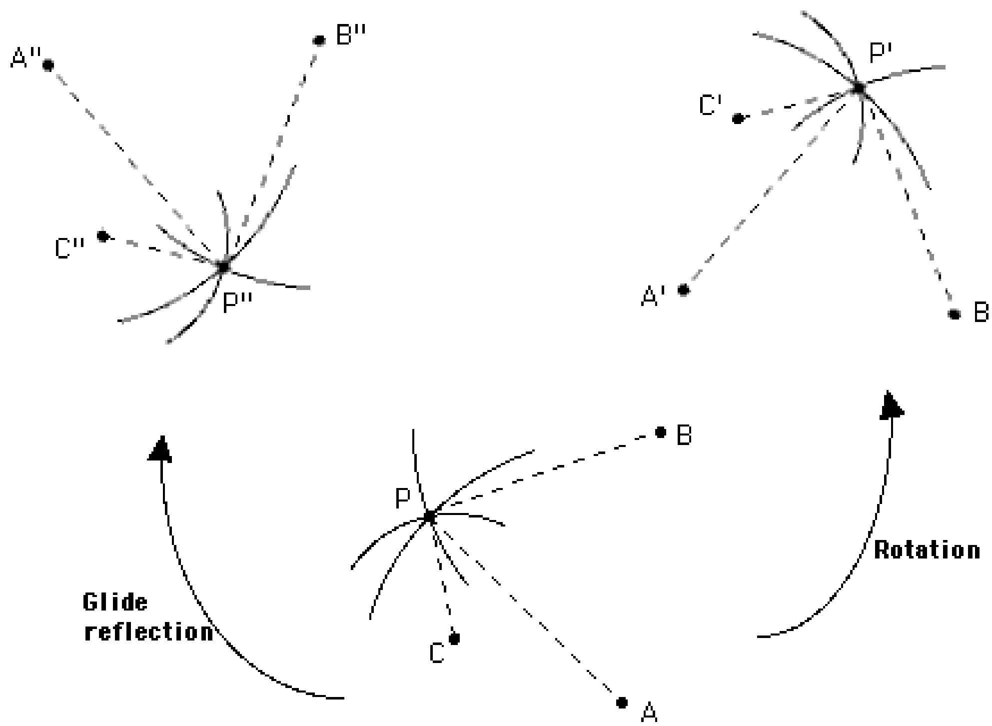

Fig. 3.20

Indeed, any ‘fourth point’ P lies at the intersection of **three circles** of centers A, B, C and radii |AP|, |BP|, |CP|, respectively. So the image of P is forced by the radius-preserving isometry to lie at the intersection of the **three image circles** (of centers A′, B′, C′ (rotation) or A″, B″, C″ (glide reflection) and radii |AP|, |BP|, |CP|); but every three circles with **non-collinear centers** can have **at most one** point in common, hence the image of P -- P′ under the rotation, P″ under the glide reflection -- is **uniquely** determined!

3.3.5 From theory to practice. Returning to section 3.0 and figure 3.1, we demonstrate in figure 3.21 how to find the **rotation** that maps ABC to A′B′C′ (homostrophic pair) and the **glide reflection** that maps ABC to A″B″C″ (heterostrophic pair).

As you can see, determining the isometries in question **reduces**, in view of 3.3.2, to picking the right type of isometry (rotation or glide reflection) that maps AB to A′B′; the rotation center or glide reflection axis is subsequently located as in section 3.2. It is always **wise** to use a **third point** (like C in figure 3.21) and its image to determine the rotation angle or glide reflection vector, as shown in figure 3.21 **--** and even **wiser** to check that the same angle or vector **indeed** works for a **fourth** point, as well as for A and B!

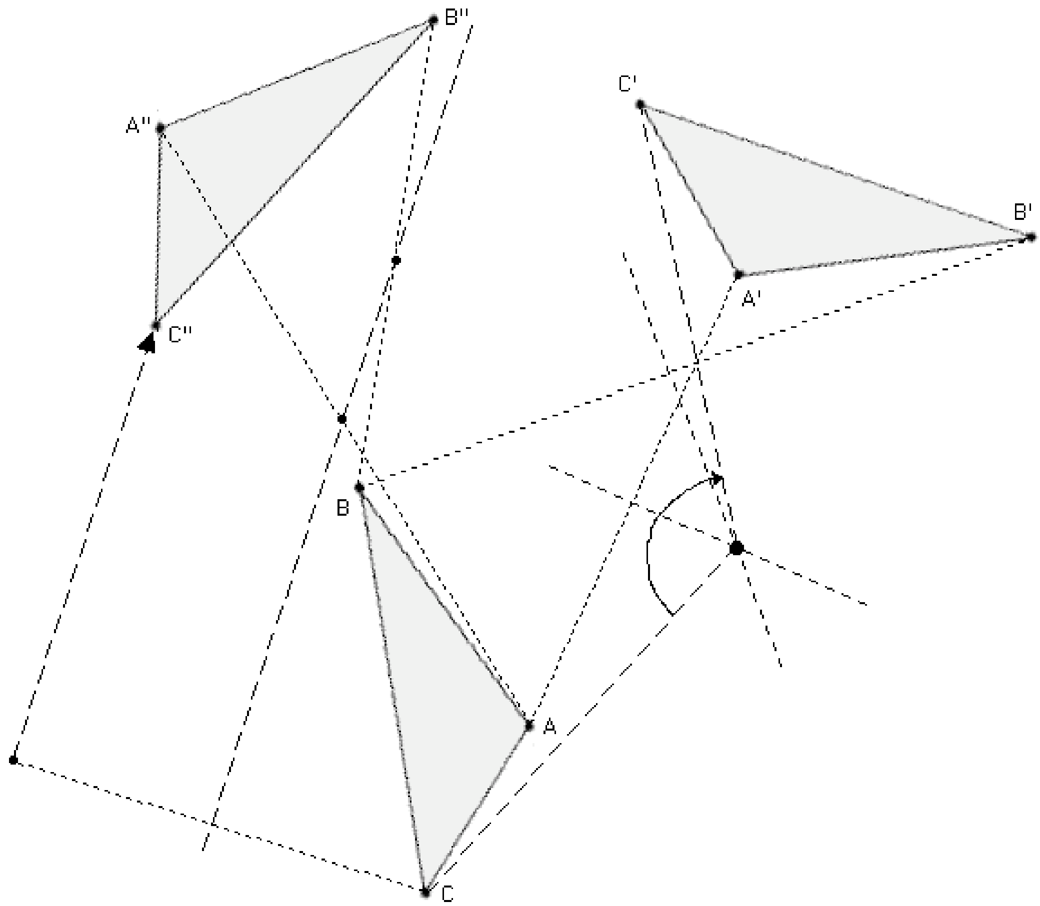

Fig. 3.21

3.4 Isosceles triangles

3.4.1 <u>The ‘second possibility’ revived.</u> As we pointed out in 3.3.2, there is generally only one isometry mapping a ‘randomly chosen’ triangle ABC to a congruent triangle A′B′C′: this is because C′ **both** allows only one possibility for the **positions** of A′ and B′ on the image of AB and determines the **kind of isometry** that maps AB to A′B′. While homostrophy/heterostrophy considerations never allow us to avoid the second limitation, it is possible to escape from the first one in case ABC happens to be isosceles (with **|AC| = |BC|**); there exist then again, as in 3.2.1, **two** possibilities for the images of A and B, associated with homostrophy (A'_1, B'_1) and heterostrophy (A'_2, B'_2). And there exist therefore one **rotation** mapping ABC to $A'_1B'_1C'$ (figure 3.22) **and** one **glide reflection** mapping ABC to $A'_2B'_2C'$ (figure 3.23), determined as in 3.3.5; but, of course, $A'_1B'_1C'$ and $A'_2B'_2C'$ are **one and the same** triangle, congruent to ABC!

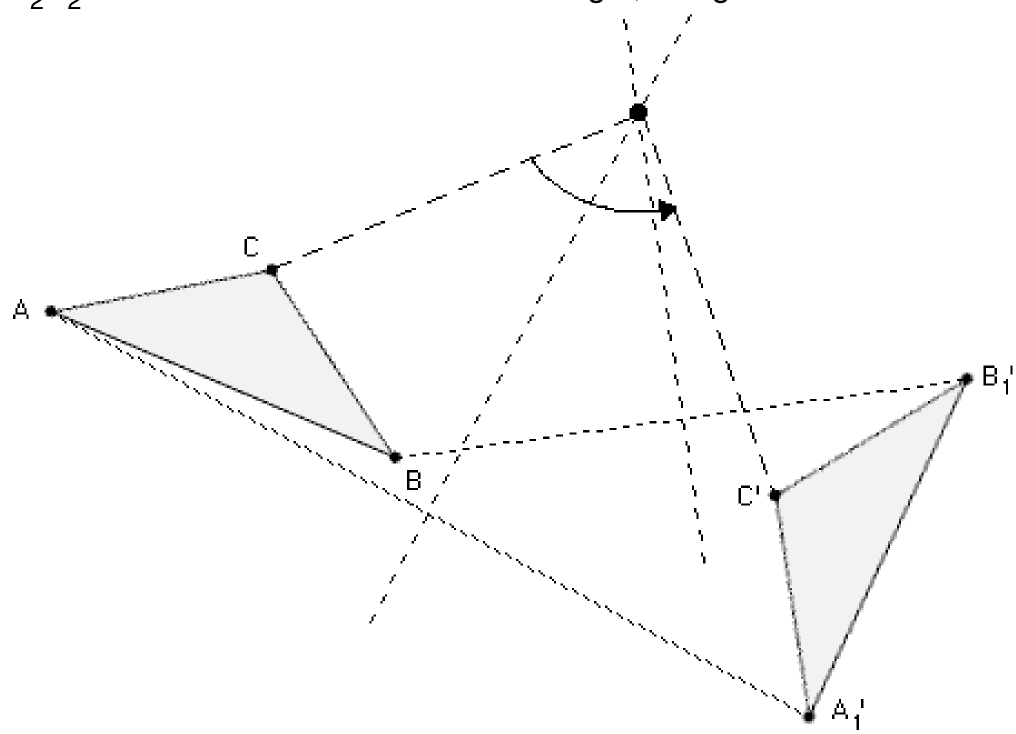

Fig. 3.22

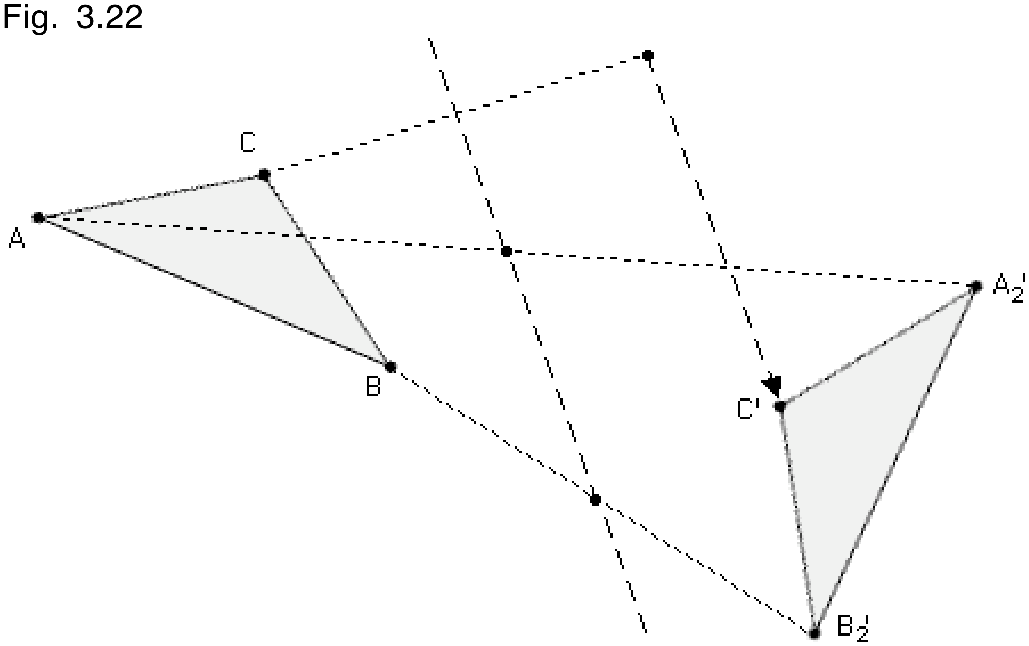

Fig. 3.23

3.4.2 <u>Old examples revisited.</u> We can at long last confirm and justify what we suspected in 3.0.3 and 3.0.4: there exists a rotation that achieves what reflection did in figure 1.14, and there also exists a glide reflection that rivals the rotation in figure 1.23. We demonstrate our findings in figures 3.24 & 3.25:

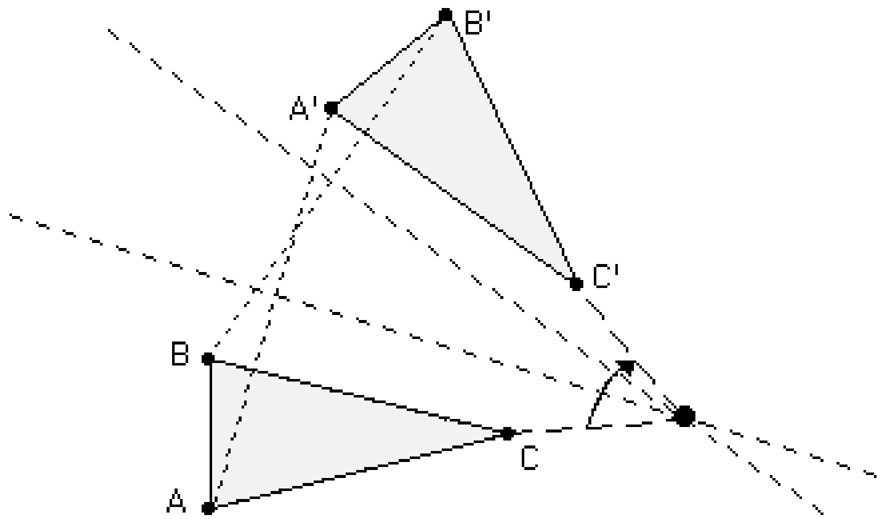

Fig. 3.24

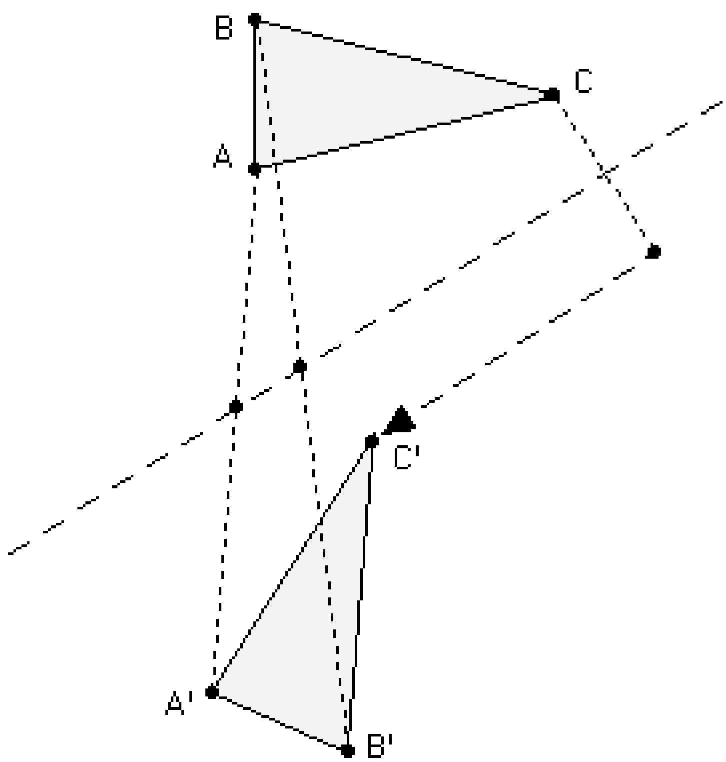

Fig. 3.25

3.5 Parallelograms, ‘windmills’, and C_n sets

3.5.1 Two triangles to go to! Consider the congruent, **heterostrophic parallelograms** ABCD, EFGH of figure 3.26:

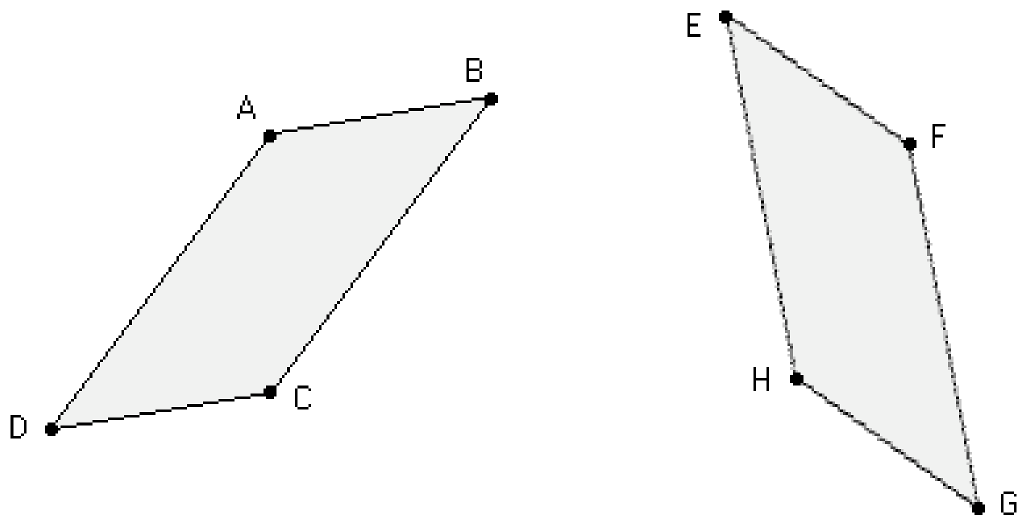

Fig. 3.26

The **congruent** triangles ABC and HGF are **heterostrophic**, so there certainly exists a glide reflection mapping ABC to HGF, hence ABCD to EFGH as well (3.3.4), obtained in figure 3.27:

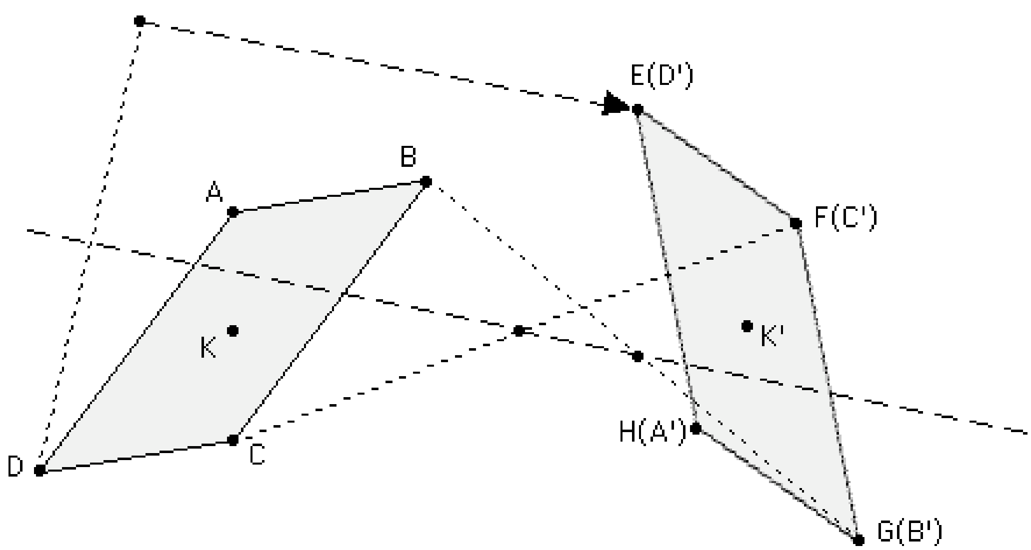

Fig. 3.27

On the other hand ... don’t you think that ABC could have gone to FEH instead? Indeed ABC and FEH **also** happen to be congruent and heterostrophic, so there must exist a glide reflection mapping ABC to FEH, hence ABCD to EFGH as well (3.3.4); and such a glide reflection is obtained in figure 3.28:

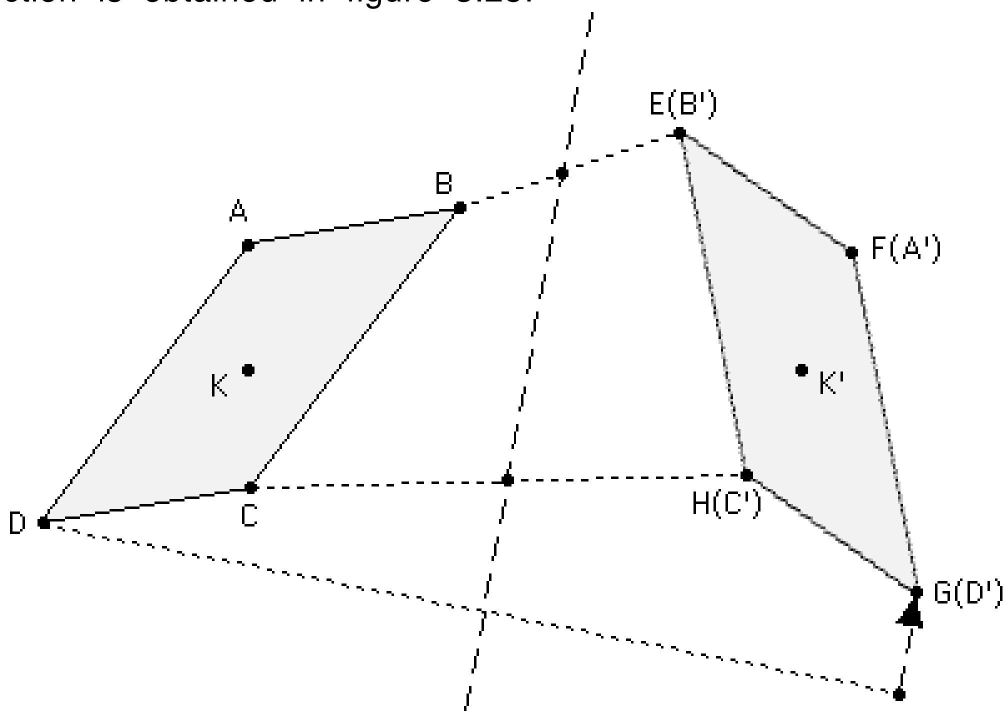

Fig. 3.28

So, there exist **two glide reflections** mapping ABCD to EFGH! What has happened? Clearly, the extra flexibility we have here is due to the existence of two **congruent** triangles **within** EFGH, HGF and FEH. Digging a bit deeper into this, what has made these two ‘components’ of the parallelogram EFGH congruent to each other? Could there be an ‘obvious’ isometry mapping one to the other? The answer is “yes”: there exists an isometry mapping HGF to FEH (or vice versa) and that is ... no other than the **half turn** about the **parallelogram’s center**, K′! To put it in more familiar terms (1.3.9), the parallelogram EFGH has **rotational symmetry**: indeed a **twofold** (180^0) rotation about K′ maps the parallelogram to itself, **swapping** HGF and FEH; and this twofold rotation is in fact **‘combined’** (section 7.8) with the glide reflection of figure 3.27 to produce the glide reflection of figure 3.28!

3.5.2 How about more triangles? It is not that difficult to come up with situations involving more than two glide reflections between two congruent sets. Indeed, and in view of the discussion in 3.5.1, all we need is two copies of a set with 'richer' rotational symmetry than that of the parallelogram, a set with more than two 'triangles' rotating around a center. How about the following pair of **heterostrophic** windmill-like sets:

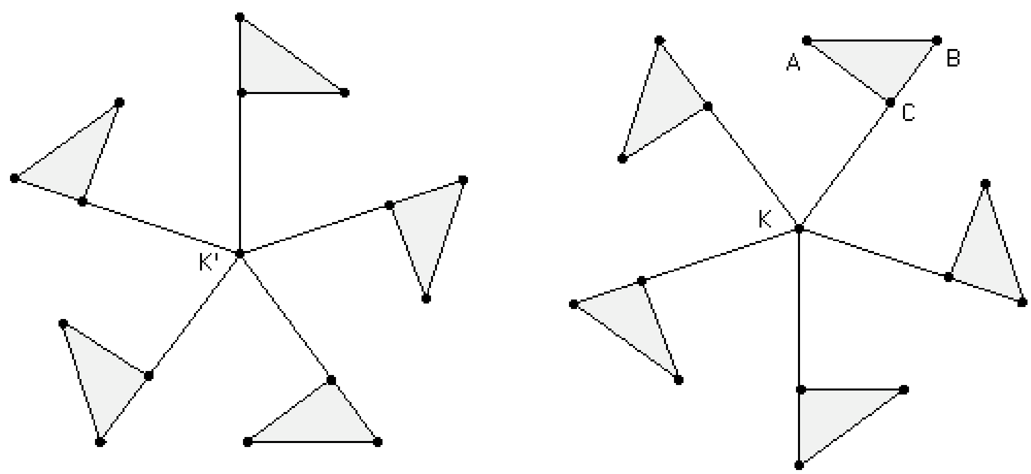

Fig. 3.29

You should have no trouble realizing that, with **five** 'options' for 'blade' ABC, there exist indeed **five glide reflections** mapping the 'windmill' on the right to the 'windmill' on the left. We leave it to you to determine these glide reflections; and if you go through this task with the great precision that is typical of you by now, you are going to see **all** five glide reflection axes **passing through the same point**, that is the **midpoint of KK′**: that should not surprise you if you care to notice that all five glide reflections **must** map K to K′! (You may of course decide to **'cheat'** by choosing K, K′ as one of your two pairs of points needed to determine each one of the five glide reflections!)

3.5.3 How about rotations? Returning to the parallelograms of figure 3.26, let us 'rectify' EFGH a bit, so that ABCD and EFGH are now **homostrophic**:

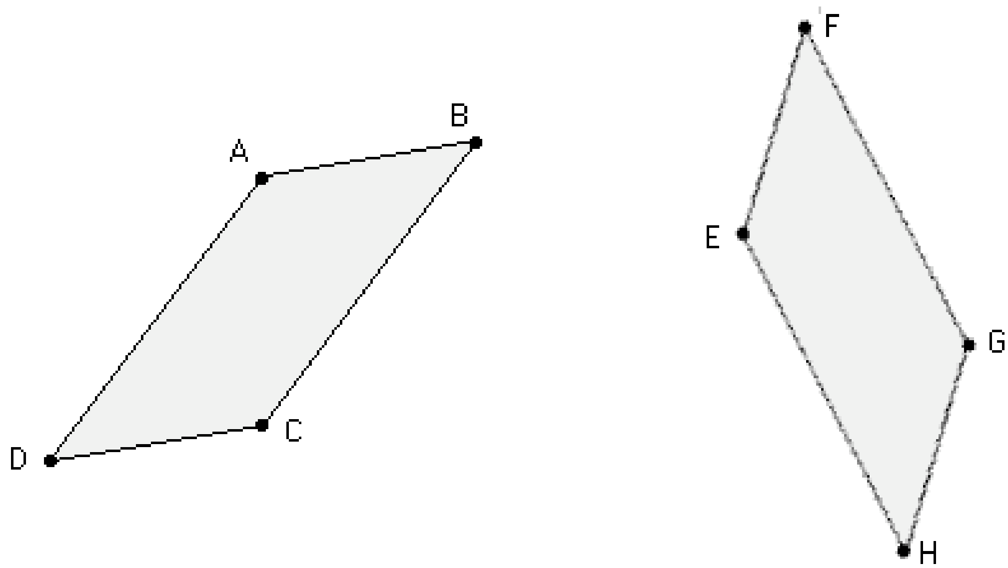

Fig. 3.30

Repeating the thought process of 3.5.1 we see that ABC is homostrophic to both GHE and EFG, hence there exist **two rotations** mapping ABCD to EFGH: one of them, by a clockwise 116^0, maps ABC to GHE (figure 3.31), the other one, by a counterclockwise 64^0, maps ABC to EFG (figure 3.32). Notice that $116^0 + 64^0 = 180^0$, in the same way, say, that the two glide reflection axes in figures 3.27 & 3.28 are perpendicular to each other: please check and, perhaps, **think** about such 'phenomena'!

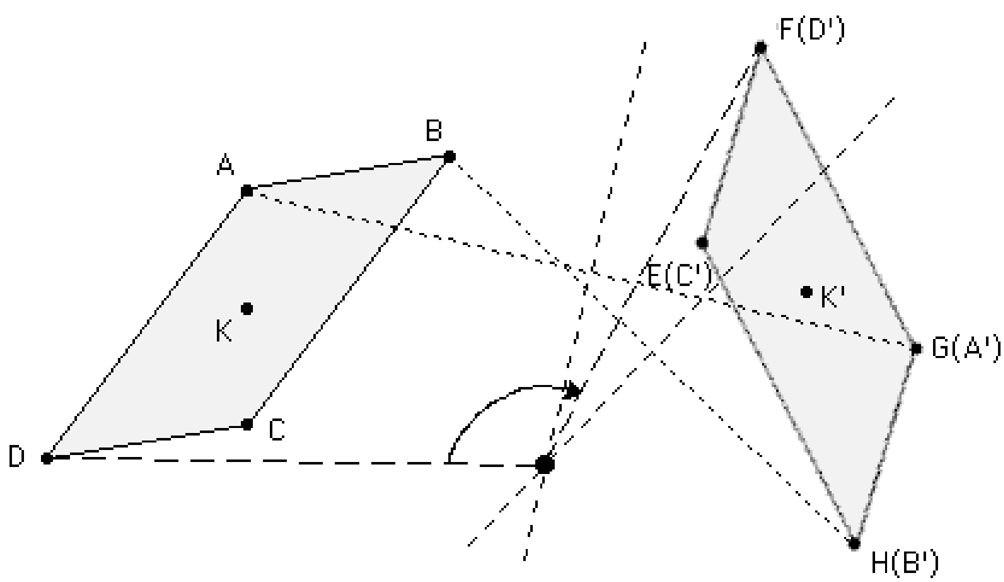

Fig. 3.31

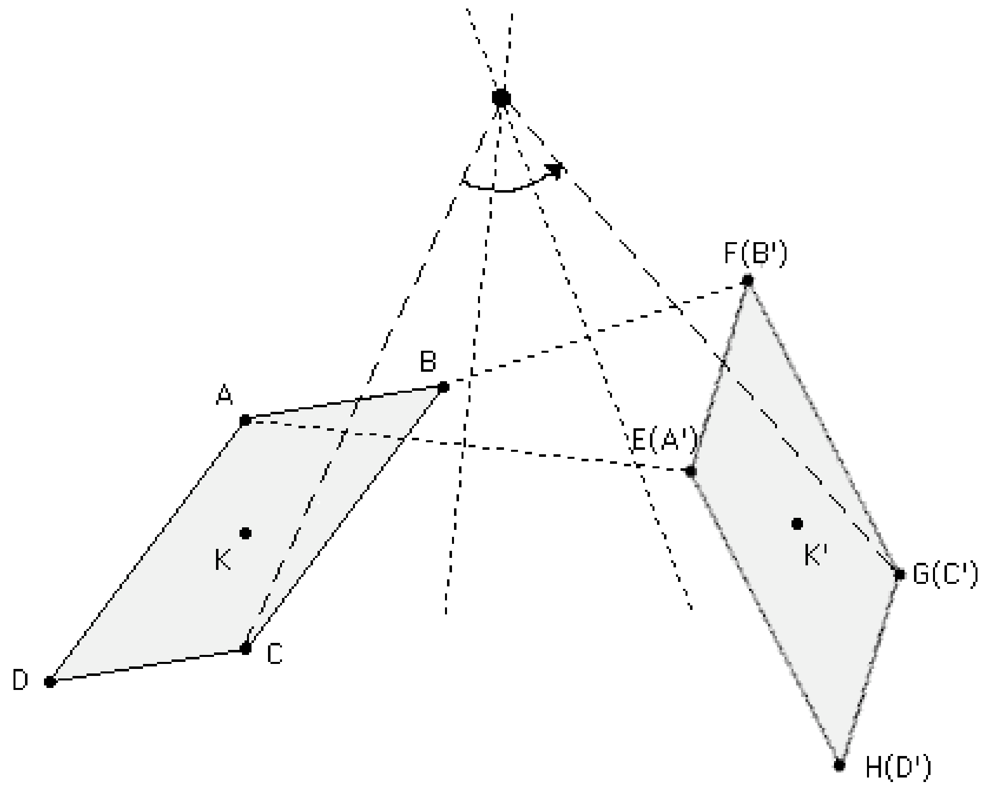

Fig. 3.32

Just as we turned the two glide reflections between the two heterostrophic parallelograms (3.5.1) into two rotations between homostrophic parallelograms, we can now turn the five glide reflections between the heterostrophic 'windmills' of figure 3.29 into **five** rotations between homostrophic 'windmills':

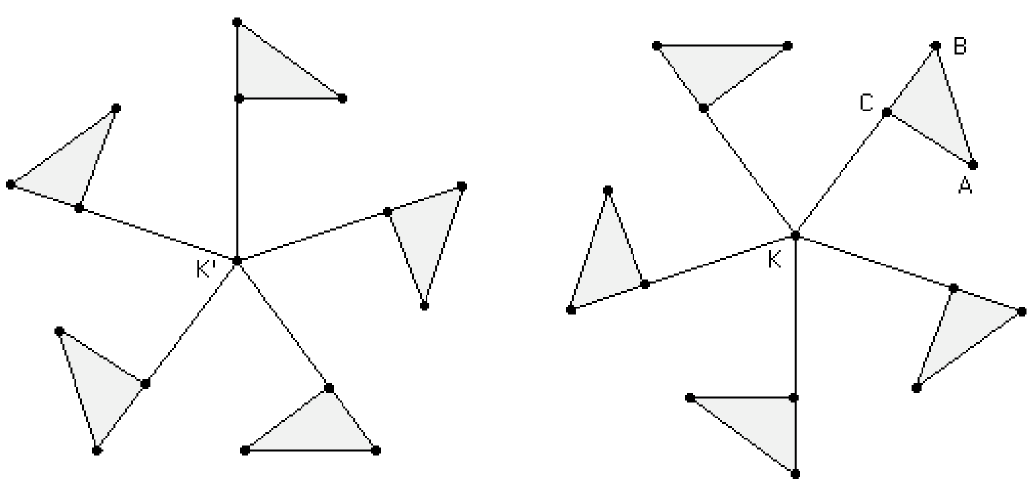

Fig. 3.33

Again, it is left to you to check that there exist **five rotations** mapping the ‘windmill’ on the right to the ‘windmill’ on the left, determined by the ‘blade’ to which ABC is mapped. As in 3.5.2, **all** five rotations **must** map K to K′, hence **all** five rotation centers must lie on the same line, the **perpendicular bisector of KK′**!

3.5.4 <u>C_n sets and the role of orientation.</u> Let us revisit figures 3.27, 3.28, 3.31, and 3.32, where we labeled EFGH as D′C′B′A′, B′A′D′C′, C′D′A′B′, and A′B′C′D′, respectively -- which, by the way, are the only possible labelings induced by isometries mapping ABCD to EFGH. Still, what made the difference was not labeling but orientation: **regardless of labeling**, we obtained a **glide reflection** between the **heterostrophic** parallelograms in **both** figure 3.27 and figure 3.28, and, likewise, a **rotation** between the **homostrophic** parallelograms in **both** figure 3.31 and figure 3.32.

Similarly, revisiting figures 3.29 & 3.33, we see that the existence of five glide reflections **or** five rotations between the two ‘windmills’ is associated **solely** with heterostrophy and homostrophy, respectively: labeling plays no role whatsoever.

Such observations always hold true between every two congruent **C_n sets**, that is, sets with **n-fold rotational symmetry without mirror symmetry**: there exist **either n rotations** mapping one to the other (in case they are **homostrophic**) **or n glide reflections** mapping one to the other (in case they are **heterostrophic**).

In addition to ‘n-blade windmills’, examples of C_n sets, known as **chiral sets** -- “hand(s)-like”, from Greek “chir” = “hand” -- in Molecular Chemistry or Particle Physics, include: non-isosceles triangles (C_1), parallelograms (C_2), the triskelion (three human legs joining each other at 120^0 angles) from, among several other places, Isle of Man (C_3), the heterostrophic and culturally unrelated Hindu and Nazi swastikas (C_4), the Star of David (C_6), etc. An excellent collection of C_n sets and likewise of D_n sets (studied in section 3.6 right below), from various regions of the world and historical periods, is available in Peter S. Stevens’ book (pages 16-93) already cited in section 2.9.

3.6 Rhombuses, 'daisies', and D_n sets

3.6.1 Two triangles and two ways. Let us consider the special case $|AB| = |BC| = |CD| = |DA|$ (hence $|FE| = |EH| = |HG| = |GF|$ as well) in **either** of figures 3.26 or 3.30; that is, let us consider the special case where each of the two congruent parallelograms is a **rhombus**:

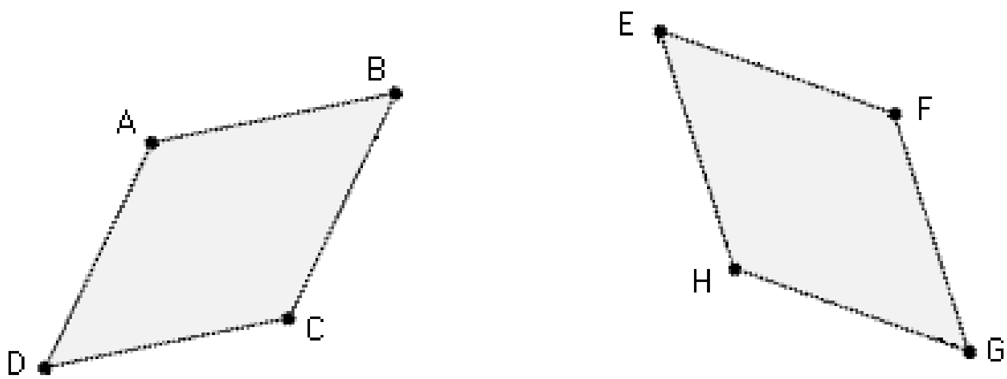

Fig. 3.34

How many isometries map ABCD to EFGH? Arguing in the spirit of section 3.5, we notice that every isometry mapping ABCD to EFGH has to map ABC to **either** FGH **or** HEF. But we also notice that ABC and either of FGH or HEF are **isosceles** triangles, and we do as well recall (section 3.4) that there always exist **two** isometries mapping an isosceles triangle to a congruent to it isosceles triangle. We conclude that there exist **two × two = four** isometries mapping ABCD to EFGH: **two rotations** (one mapping ABC to FGH (figure 3.35), another mapping ABC to HEF (figure 3.36)) and **two glide reflections** (one mapping ABC to HGF (figure 3.37), another mapping ABC to FEH (figure 3.38)); D's image is simply determined by those of A, B, C (3.3.4).

More **rigorously**, and with composition of isometries (chapter 7) in mind, we could see how, for example, the rotation in figure 3.35 is **'combined'** with the rhombus' internal reflection swapping E, G to produce the glide reflection of figure 3.38, etc.

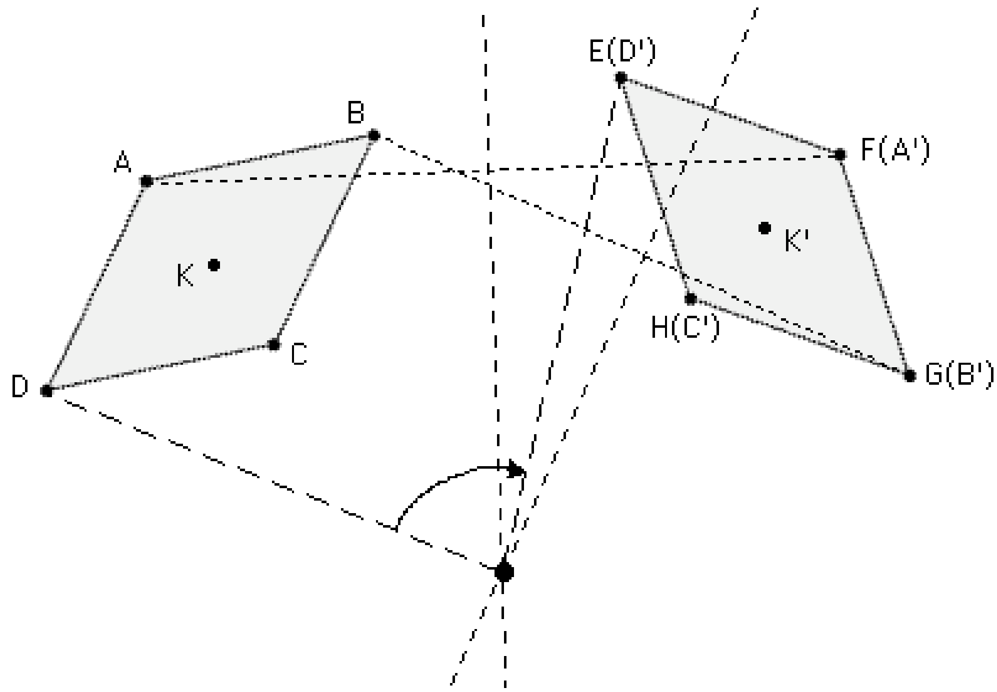

Fig. 3.35

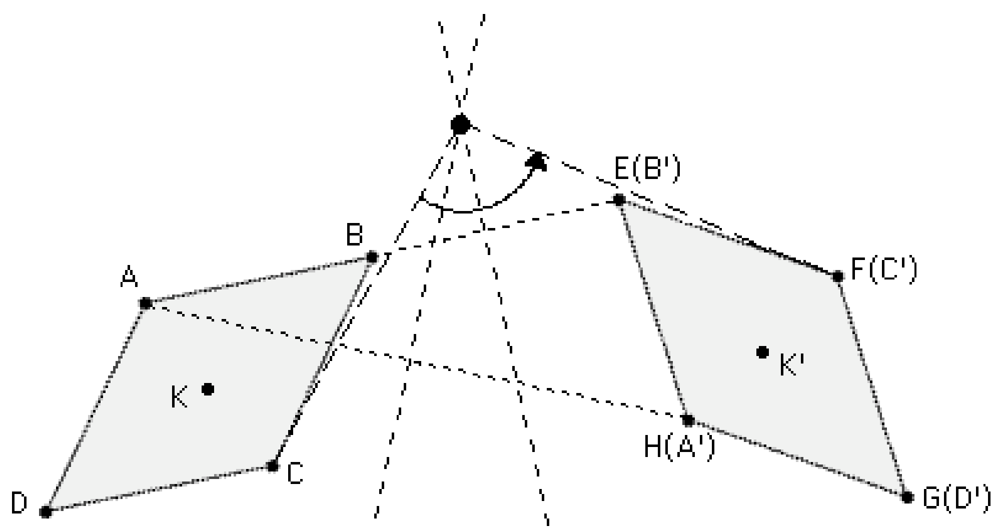

Fig. 3.36

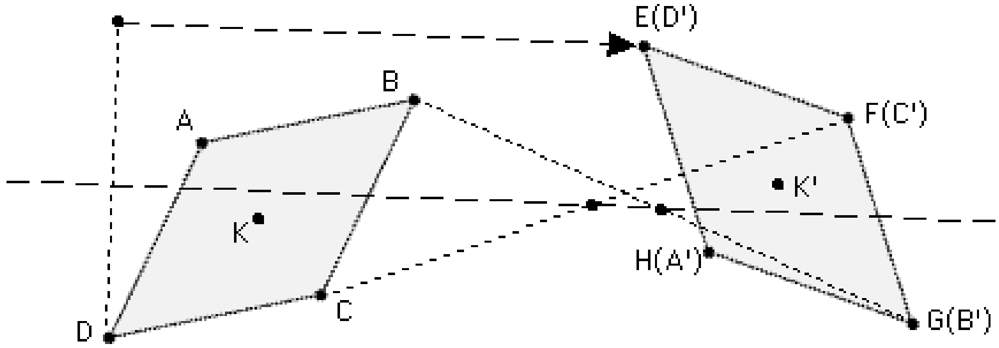

Fig. 3.37

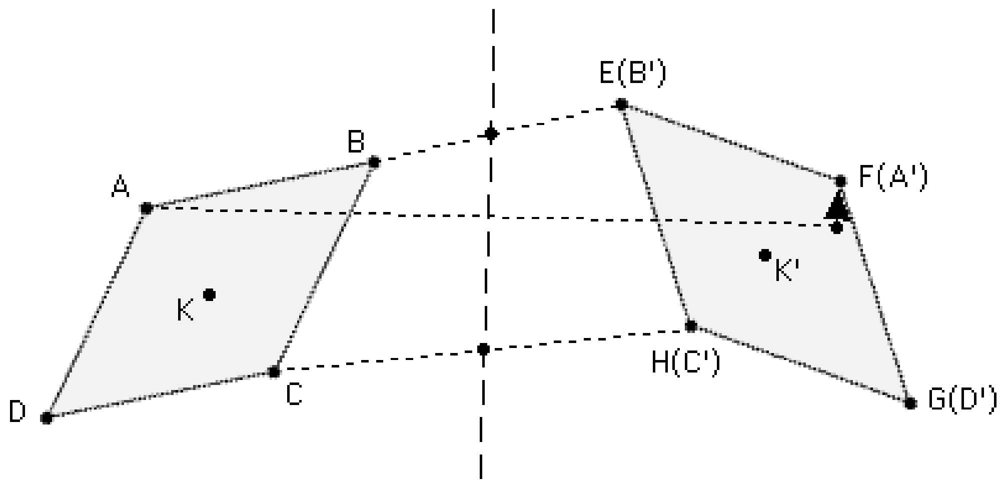

Fig. 3.38

Notice that **homostrophy or heterostrophy induced by labeling** has once again become important, just as in section 3.4: we obtained rotations in the cases of homostrophic copies (with EFGH labeled in effect as either **D′A′B′C′** (figure 3.35) or **B′C′D′A′** (figure 3.36), both of them **homostrophic to ABCD**) and glide reflections in the cases of heterostrophic copies (with EFGH labeled in effect as either **D′C′B′A′** (figure 3.37) or **B′A′D′C′** (figure 3.38), both of them **heterostrophic to ABCD**).

3.6.2 Everything in double! What happens if we apply the same ‘symmetrization’ process applied to the parallelograms of figures

3.26 & 3.30 to those **'5-blade windmills'** of figures 3.29 & 3.33? We need to **replace** non-isosceles triangles by isosceles ones, arriving at a pair of congruent **'5-petal daisies'**:

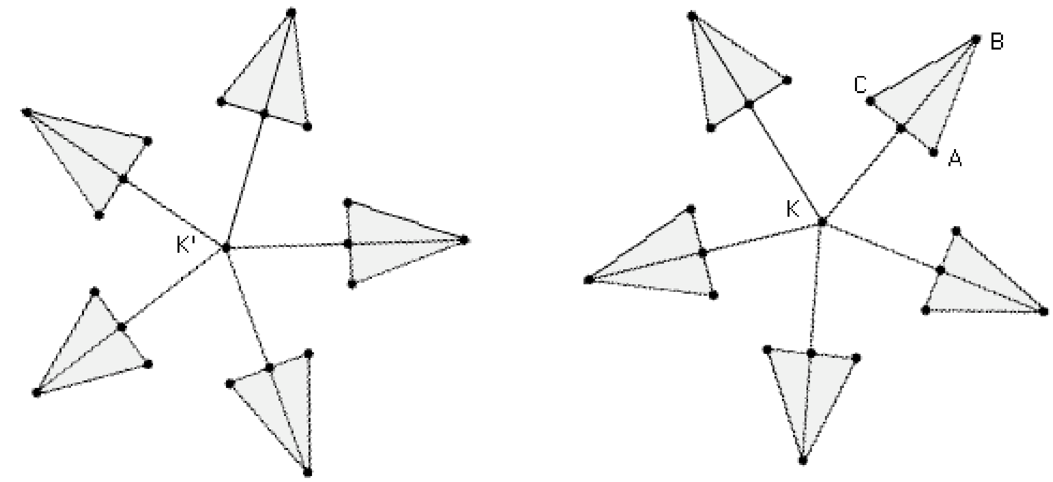

Fig. 3.39

How many isometries map the 'daisy' on the right to the 'daisy' on the left? Well, you almost know the game by now: there are **five** 'petals' to which 'petal' ABC can be mapped, and in each case this can be done by **both** a rotation and a glide reflection mapping the 'daisy' on the right to the 'daisy' on the left; putting everything together, we see that there exist **five × two = ten** isometries between the two congruent 'daisies', **five rotations and five glide reflections**! We leave it to you to provide the right labeling for each one of these ten isometries: you should then be able to check that all five glide reflection axes pass through the midpoint of KK′ (3.5.2) and that all five rotation centers lie, despite falling off this page on occasion, on the perpendicular bisector of KK′ (3.5.3).

3.6.3 D_n sets and the role of labeling. A closer look at 3.6.1 and 3.6.2 explains the abundance of isometries between the rhombuses and the '5-petal daisies': in addition to **rotational symmetry** (by 180^0 and 72^0, respectively), they are both blessed by at least one **isosceles triangle** the reflection axis of which acts as a reflection axis for the entire set -- that is, they also have **mirror symmetry**!

Summarizing and generalizing our findings in this section, we may say that between every two congruent **D_n sets**, that is, sets with **both mirror symmetry and n-fold rotational symmetry**, there exist **n rotations** (allowed by 'homostrophic labeling') **and n glide reflections** (allowed by 'heterostrophic labeling').

In addition to 'n-petal daisies', examples of D_n sets, known to scientists as **achiral sets**, include: isosceles triangles (D_1), rhombuses and straight line segments (D_2), equilateral triangles (D_3), squares and the Red Cross symbol (D_4), the 'pentagram' (D_5), snowflakes (D_6), regular n-gons (D_n), circles and points (D_∞), etc.

3.6.4 'Practical' issues. You must have observed by now that, once we know what type of isometry (rotation or glide reflection) between two congruent sets we are looking for, and any and all issues of homostrophy/heterostrophy and labeling have been decided, the actual determination of the isometry simply reduces to constructing one between two congruent **segments** and choosing the relevant **endpoints**. Such an observation is of course a natural consequence of our discussion in the entire chapter; see in particular 3.3.5.

When looking for a rotation, it is advisable to choose two pairs of points such that the perpendicular bisectors of the corresponding segments will **not** be **'nearly parallel'** to each other. The idea here is that tiny, almost inevitable, errors in the location of the two midpoints and/or the direction of the perpendicular bisectors are propagated in case the two lines run nearly parallel to each other, hence the rotation center could be greatly misplaced. For example, choosing to work with B, B′ and C, C′ would have been a bad idea in figure 3.36 but not in figure 3.35.

Likewise, in the case of a glide reflection, it is **not** advisable to work with two segments the midpoints of which are **'too close'** to each other: again, tiny, almost inevitable, errors in the location of the two midpoints are likely to lead to a considerably misplaced glide reflection axis; this has in fact happened to some extent with B, B′ and C, C′ in figure 3.37 (why?), but probably not in figure 3.38.

Prior to choosing your pair of points, you should decide whether you need a rotation or a glide reflection. If both are possible, then homostrophy/heterostrophy issues become important. You must carefully choose your **labeling** so that it will be both **possible** (avoid a disaster situation where, for example, $|A'B'| \neq |AB|$!) and **appropriate** (homostrophic or heterostrophic as needed) for the isometry you are looking for. Figures 3.35-3.38 should provide sufficient illustration in this direction. Another useful tip for labeling the image set, suggested by **Erin MacGivney** (Spring 1998), is this: trace the original set, including original labels (A, B, C, ...) on tracing paper, then slide it in every possible way until it matches (and labels!) the image set, **with or without flipping** the tracing paper (and inducing heterostrophic or homostrophic labeling, respectively).

Various 'labeling' errors can often be caught with the use of a **'third point'** (in determining the rotation angle or glide reflection vector) already advocated in 3.3.5: **watch out** in particular for **unequal** angle legs or for an axis and vector **not parallel** to each other!

Of course, you should first of all answer the following question about the given pair of congruent sets: **are they C_n sets or D_n sets, and what is n?** If they are **C_n sets** then you must decide whether they are homostrophic or heterostrophic, allowing for **either n rotations or n glide reflections**, respectively. If they are **D_n sets** you should keep in mind that, with fully developed labeling skills, you ought to be able to get all **n rotations and n glide reflections** between the two sets; and keep in mind that **one** rotation could be 'reduced' to a translation (in case the two sets are side-by-side **'parallel'** to each other) and **one** glide reflection might 'merely' be a reflection (3.2.5).

3.7* Cyclic (C_n) and dihedral (D_n) groups

3.7.1 <u>'Turning the windmills'.</u> Let us revisit that '5-blade windmill' C_5 set of figure 3.29, redrawn and relabeled in figure 3.40 below; more specifically, the five 'blades' are now labeled as T_0, T_1, T_2, T_3, and T_4.

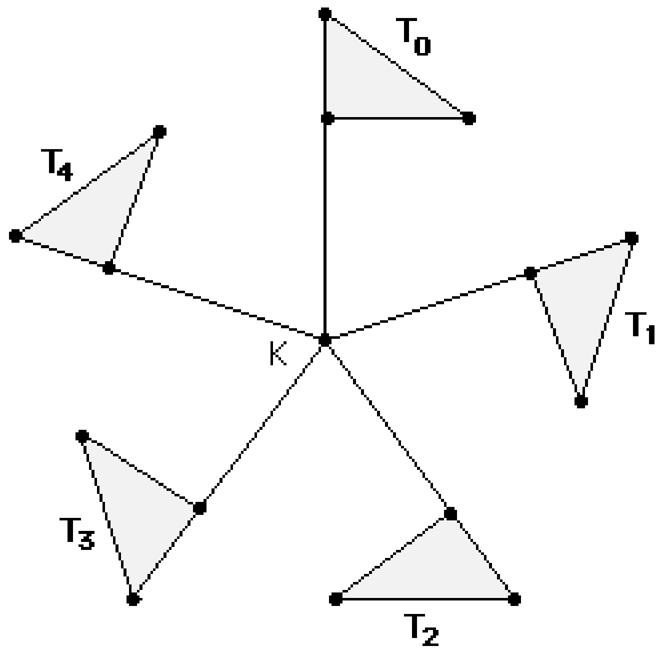

Fig. 3.40

As we noticed in 3.5.2, a clockwise $360^0/5 = 72^0$ rotation **r** about K maps the 'windmill' to itself by moving the 'blades' T_s around according to the formula $\mathbf{r}(T_s) = T_{(s+1)\mathrm{mod}5}$, where, for every integer t, **tmod5** is the **remainder** of the division of t by 5. For example, $\mathbf{r}(T_2) = T_3$, $\mathbf{r}(T_4) = T_0$, etc. What happens when we apply **r** **twice in a row**? Clearly, $\mathbf{r}(\mathbf{r}(T_2)) = \mathbf{r}(T_3) = T_4$, $\mathbf{r}(\mathbf{r}(T_4)) = \mathbf{r}(T_0) = T_1$, and so on; we write $\mathbf{r}^2(T_2) = T_4$, $\mathbf{r}^2(T_4) = T_1$, and so on, and we notice that $\mathbf{r}^2$ is a clockwise rotation by $2 \times 72^0 = 144^0$, 'rigorously' defined via $\mathbf{r}^2(T_s) = T_{(s+2)\mathrm{mod}5}$. And likewise we can go on and define $\mathbf{r}^3$ and $\mathbf{r}^4$ as clockwise rotations by $3 \times 72^0 = 216^0$ and $4 \times 72^0 = 288^0$, respectively, subject to the rule, for l = 3 and l = 4, respectively, $\mathbf{r}^l(T_s) = T_{(s+l)\mathrm{mod}5}$. For example, for l = 3 and s = 4, (s+l)mod5 = 7mod5 = 2, therefore $\mathbf{r}^3(T_4) = T_2$, a result that you may certainly confirm **geometrically** (by rotating T_4 about K by a clockwise 216^0).

All this extends naturally to the ‘n-wing windmill’ (of ‘blades’ T_0, T_1, ... , T_{n-1}), where the clockwise $360^0/n$ rotation **r** satisfies $\mathbf{r^l}(T_s) = T_{(s+l)modn}$ for all integers s, l between 0 and n−1. We may in fact extend this formula for all l ≥ n; for **l = n**, in particular, we notice that (s+n)modn = (s+0)modn, hence $\mathbf{r^n}(T_s) = T_s$ for all s: that is, $\mathbf{r^n} = \mathbf{r^0} = \boldsymbol{I}$ is a ‘dead’ rotation (***Identity map***) that leaves all the ‘blades’ unchanged. Moreover, we can easily compute the **product** of the rotations $\mathbf{r^k}$ and $\mathbf{r^l}$ (a clockwise rotation of $l \times 360^0/n$ followed by a clockwise rotation by $k \times 360^0/n$) via $\mathbf{r^k * r^l}(T_s) = \mathbf{r^k}(\mathbf{r^l}(T_s)) = \mathbf{r^k}(T_{(s+l)modn}) = T_{(s+l+k)modn} = \mathbf{r^{k+l}}(T_s)$; that is, $\mathbf{r^k * r^l = r^{(k+l)modn}}$, due to (s+l+k)modn = (s+(l+k)modn)modn: please check!

You may also verify this ‘rotation multiplication’ by **adding the angles** via $l \times 360^0/n + k \times 360^0/n = (l+k) \times 360^0/n$ and noticing that a $(l+k) \times 360^0/n$ rotation is the same as a $((l+k)modn) \times 360^0/n$ rotation. Moreover, you may certainly confirm this multiplication rule geometrically by returning to our ‘5-blade windmill’ and checking that, for example, the $\mathbf{r^3}$ rotation of 216^0 followed by the $\mathbf{r^4}$ rotation of 288^0 does indeed produce the $\mathbf{r^2}$ rotation of 144^0, precisely as (4+3)mod5 = 2 would predict!

The relations $\mathbf{r^n} = \mathbf{r^0} = \boldsymbol{I}$ and $\mathbf{r^k * r^l = r^{(k+l)modn}}$ derived above define the **cyclic group of order n**, denoted by $\mathbf{C_n}$: an algebraic structure whose elements are $\boldsymbol{I}$, **r**, ..., $\mathbf{r^{n-1}}$ and whose importance in Mathematics is inversely proportional to its simplicity! It is in fact a **commutative** group: the order of ‘multiplication’ does not matter ($\mathbf{r^k * r^l = r^l * r^k = r^{(k+l)modn}}$). Its identity element is the ‘dead map’ (rotation) $\mathbf{r^n} = \boldsymbol{I}$ we already discussed, and the **inverse** of $\mathbf{r^l}$ is simply $\mathbf{r^{n-l}}$ (with $\mathbf{r^l * r^{n-l} = r^{n-l} * r^l = r^0} = \boldsymbol{I}$).

3.7.2 <u>‘Bisecting the daisies’.</u> Let us now apply the notation of 3.7.1 to the ‘leaves’ of that ‘5-petal daisy’ from figure 3.39, drawing its reflection axes (‘bisectors’) at the same time; we end up with the axis $\mathbf{m_s}$ bisecting ‘petal’ T_s for s = 1, 2, 3, 4, and with axis $\mathbf{m_5}$ bisecting ‘petal’ T_0:

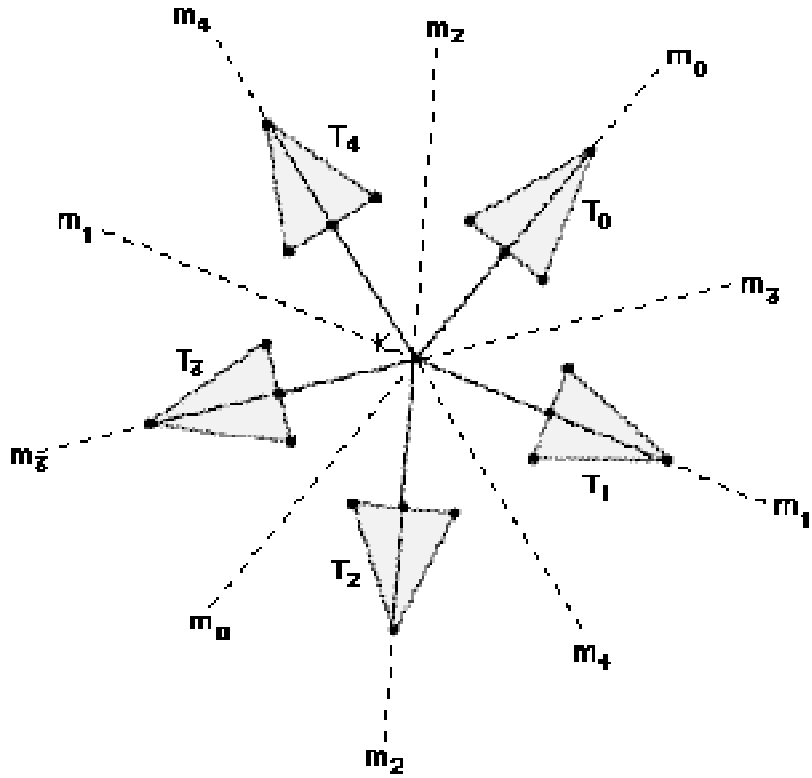

Fig. 3.41

In addition to the reflections, our '5-petal daisy' has five rotations, including the trivial one, all 'inherited' from 3.7.1. In total, there are ten isometries mapping the daisy to itself: $\boldsymbol{I}$, $\mathbf{r}$, $\mathbf{r^2}$, $\mathbf{r^3}$, $\mathbf{r^4}$, $\mathbf{m_1}$, $\mathbf{m_2}$, $\mathbf{m_3}$, $\mathbf{m_4}$, and $\mathbf{m_5}$. Could these isometries possibly form a group? The answer would be "yes" if we could show that the product (successive application) of every two of them is still one of the ten isometries listed above, and that each one of the ten isometries has an inverse. Starting from the latter, recall (1.4.4) that every reflection is the inverse of itself, hence the inverse of $\mathbf{m_s}$ is $\mathbf{m_s}$ with $\mathbf{m_s * m_s} = \boldsymbol{I}$ for s = 1, ... , 5; moreover, the inverse of $\mathbf{r^l}$ for l = 1, ... , 4 is $\mathbf{r^{5-l}}$ (3.7.1), and $\boldsymbol{I}$ is of course the inverse of itself. Observe next that the product of every two rotations is indeed a rotation, with $\mathbf{r^k * r^l = r^l * r^k = r^{(k+l)mod5}}$ (3.7.1), and same holds for the product of every two reflections (as we will see in section 7.2 and as you could probably verify even now). Keeping the latter in mind and observing also that $\mathbf{m_t}(T_s) = T_{(2t-s)mod5}$, let us now compute $\mathbf{m_t * m_s}(T_0) = \mathbf{m_t}(\mathbf{m_s}(T_0)) = \mathbf{m_t}(T_{(2s-0)mod5}) = \mathbf{m_t}(T_{2smod5}) = T_{(2t-2s)mod5} = \mathbf{r^{(2t-2s)mod5}}(T_0)$ -- the last step follows from $\mathbf{r^k}(T_0) = T_k$ -- and conclude that $\mathbf{m_t * m_s = r^{(2t-2s)mod5}}$: if two **rotations** have the same effect on any one of the ‘petals’ (in this case T_0) then they must be one and the same! ‘Multiplying’ both sides of the derived identity by $\mathbf{m_t}$ (from the left) and by $\mathbf{m_s}$ (from the right), we obtain, with some details omitted, the identities $\mathbf{r^l * m_s = m_k}$ (where $\mathbf{2k = (2s+l)mod5}$) and $\mathbf{m_t * r^l = m_k}$ (where $\mathbf{2k = (2t-l)mod5}$), respectively. (You may not be able to derive the missing details right now, but you can certainly verify them **geometrically**: for $l = 3$ and $s = 2$, for example, $k = 1$ satisfies $2k = (2s+l)mod5$, hence the product $\mathbf{r^3 * m_2}$ (reflection bisecting T_2 followed by clockwise 216^0 rotation) ought to be $\mathbf{m_1}$ (reflection bisecting T_1), etc.)

Replacing 5 by **any odd n**, we can extend the results and formulas of the preceding paragraph to arbitrarily large groups of 2n elements (and yet very similar structure). For **even n** some slight modifications, as well as a ‘6-petal daisy’, are in order:

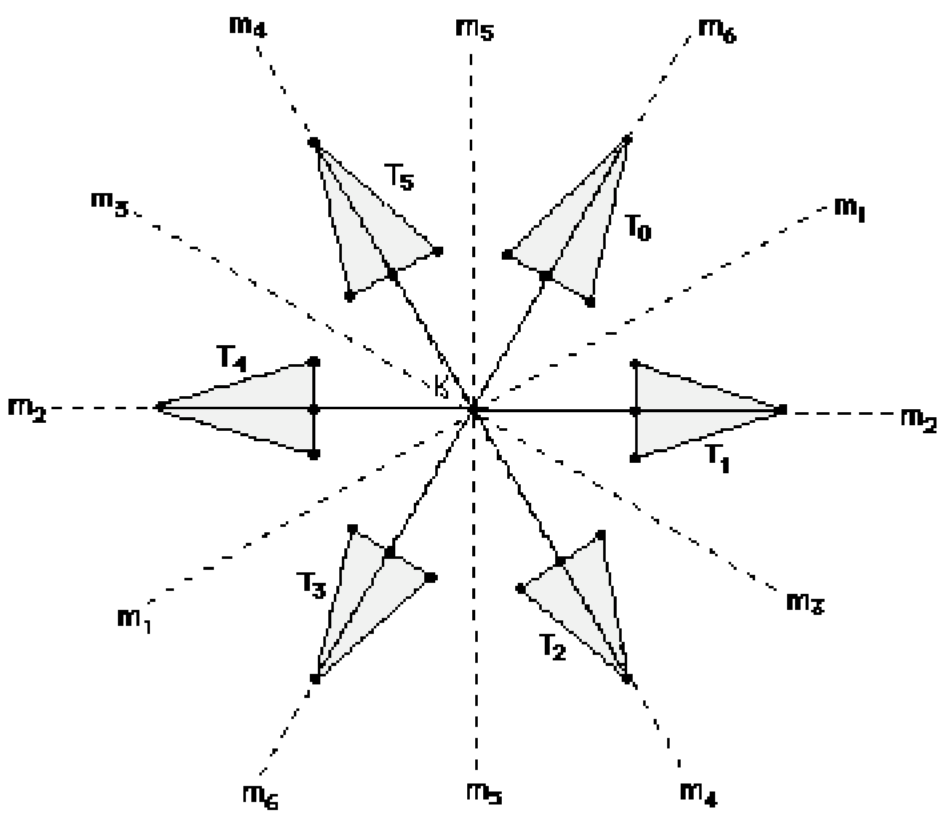

Fig. 3.42

Observe that our new 'daisy' is now bisected in two different ways, with some axes ($\mathbf{m_2}$, $\mathbf{m_4}$, $\mathbf{m_6}$) cutting through 'petals' and other axes ($\mathbf{m_1}$, $\mathbf{m_3}$, $\mathbf{m_5}$) passing right between 'petals'. The effect of the reflections on the 'petals' is now somewhat different, with $\mathbf{m_t}(T_s) = T_{(2t-s)\mathrm{mod}5}$ replaced by $\mathbf{m_t}(T_s) = T_{(t-s)\mathrm{mod}6}$; that leads in turn to $\mathbf{m_t * m_s = r^{(t-s)mod6}}$, as opposed to $\mathbf{m_t * m_s = r^{(2t-2s)mod5}}$. At the same time, $\mathbf{r^k * r^l = r^l * r^k = r^{(k+l)modn}}$ (3.7.1) remains intact, while the other two kinds of products are in fact **simplified**: proceeding as in the preceding paragraph, we now establish $\mathbf{r^l * m_s = m_{(s+l)mod6}}$ and $\mathbf{m_t * r^l = m_{(t-l)mod6}}$. (Once again you should be able to verify these formulas **geometrically**; for example, $\mathbf{m_3 * r^4}$ (clockwise $4 \times 360^0/6 = 240^0$ rotation followed by 'in-between' bisection $\mathbf{m_3}$) ought to be equal to $\mathbf{m_{(3-4)mod6} = m_{(-1)mod6} = m_5}$, another 'in-between' bisection.) Notice that all formulas obtained in this paragraph for n = 6 can be easily modified for **arbitrary even n**.

To summarize, we have just proven, by going through two distinct cases (odd n and even n), that, for every n, the set of 2n isometries $\{\boldsymbol{I}, \mathbf{r}, ..., \mathbf{r^{n-1}}, \mathbf{m_1}, ... , \mathbf{m_n}\}$ forms indeed a **group** under **composition of isometries**, subject to the rules and formulas established in this section. This **non-commutative** group, which contains $\mathbf{C_n}$ as a **subgroup**, is well known in the literature as **dihedral group of order 2n,** denoted by $\mathbf{D_n}$. It may be shown -- see for example chapter 8 in George E. Martin's ***Transformation Geometry: An Introduction to Symmetry*** (Springer, 1982) -- that every **finite group** of isometries in the plane **must** be $\mathbf{C_n}$ or $\mathbf{D_n}$ for some n: this result is attributed to none other than Leonardo da Vinci and is known as **Leonardo's Theorem**!

[How about **infinite** such groups? Well, those are actually studied in chapters 2 and 4, but our approach tends to be informal and geometrical (even in chapter 8) rather than group-theoretic -- a group-theoretic approach is available in Martin's book above, as well as in several **Abstract Algebra** texts, such as M. A. Armstrong's ***Groups and Symmetry*** (Springer, 1997), for example.]

first draft: fall 1998

CHAPTER 4

WALLPAPER PATTERNS

4.0 The Crystallographic Restriction

4.0.1 Planar repetition. Even if you don't have one in your own room, you probably see one often at a friend's place or your favorite restaurant: it fills a whole wall with the same motif **repeated** all over in an **'orderly manner'**, creating various visual impressions depending on the particular motif(s) depicted, the background color, etc. And likewise you must have noticed the **tilings** in many bathrooms you have been in: they typically consist of one square tile repeated all over the **bathroom wall**, right? Well, as you are going to find out in this chapter, we can do much better than simply repeating square tiles (plain or not) all over: tilings (and other **repeating designs** as well), be it on Roman mosaics, African baskets, Chinese windows or Escher drawings, can be wonderfully complicated!

You can certainly imagine the wall in front of which you are standing right now extended in **'all directions'** without a bound, thus turning the wallpaper or tiling you are looking at into an **infinite design**; for the sake of simplicity we call any and all such **two-dimensional** (planar) infinite designs that repeat themselves in all directions and 'in an orderly manner' **wallpaper patterns**. For example, the familiar **beehive**, consisting of hexagonal 'tiles', is still viewed here as a wallpaper pattern -- once extended to cover the entire plane, that is. More technically, a wallpaper pattern is a design that covers the entire plane and is **invariant under translation in two distinct**, **non-opposite**, **directions**; check also our definition at the end of 4.0.7 and discussion in section 4.1. Notice at this point that motif repetitions, however 'imperfect' mathematically, are not that rare in nature: think of a leopard's skin or certain butterflies' wings, for example. Moreover, there are zillions of such repetitions and 'orderly packings' to be seen in three dimensions, and in particular when one looks at a **crystal** through a microscope: although this is where this section's title (but not content) comes from, we will not dare venture into three-dimensional symmetry in this book!

4.0.2 <u>Taming the infinite.</u> As we have seen in 2.0.1, infinite border patterns may be 'finitely represented' by strips going around the lateral side of a **'short' cylinder**. Notice at this point that, precisely because they do have a certain finite width, border patterns are, strictly speaking, **'one-and-half'** dimensional: a truly one-dimensional pattern would be something as dull as the infinite repetition of a **Morse signal** (__ . __ . _ _ _ _ . . .), while two-dimensional patterns could only be represented on the lateral side of a **cylinder of infinite height**. But, in the same way an infinite strip can be 'wrapped around' into a 'short' cylinder (of finite height equal to the strip's width), a cylinder of infinite height can be 'wrapped around' into a **torus**: before you get somewhat intimidated by this 'abstract' geometrical term, be aware that this is a familiar item on the breakfast table, be it in the form of a doughnut or a bagel! Yes, you could draw all the wallpaper patterns you will see in this book on a bagel!

Representations of wallpaper patterns by polyhedra may at least be considered. Think of the **soccer ball**, for example, which looks like a beehive consisting of pentagonal and hexagonal 'tiles'; known to chemists as "carbon molecule C_{60}", it does not correspond to a planar (wallpaper) pattern: it is in fact **impossible** to tile the plane with such a combination of regular pentagons and hexagons! Another trick, familiar to map makers and crystallographers, is the **stereographic projection**, that is the representation of the entire plane on a sphere (as in figure 4.1); it clearly maps every point on the plane to a point on the sphere (hence every wallpaper pattern to a 'spherical design'), but it leads to great distortion and problems around the **'north pole'**:

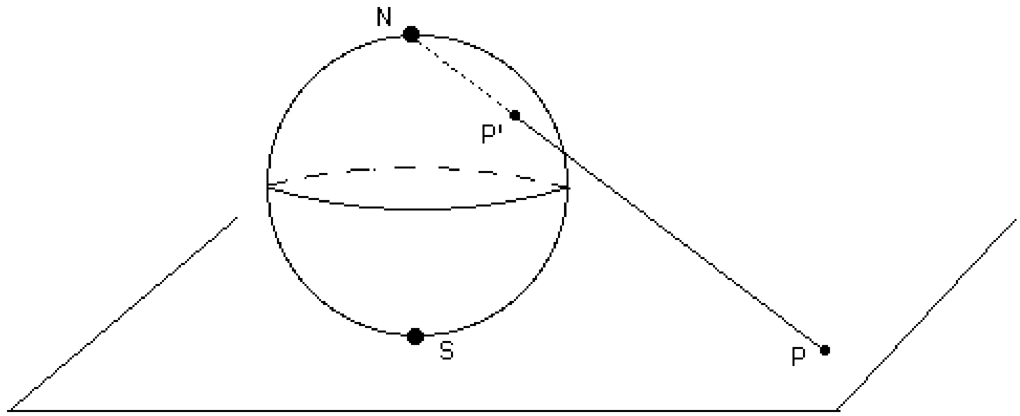

Fig. 4.1

Well, our brief excursion into the three dimensions is over. From here on you will have to keep in mind that, unless otherwise stated, the finite-looking designs in this book are in fact infinite, extending in every direction **around the page** you are looking at; it may not be easy at first, but sooner or later you will get used to the concept!

4.0.3 How about rotation? Let's have a look at the beehive and bathroom wall patterns we mentioned in 4.0.1:

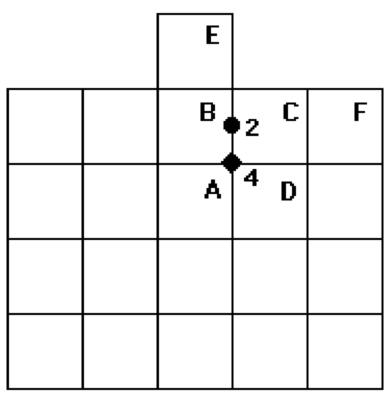

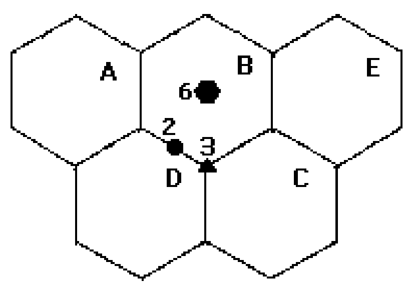

Fig. 4.2

Clearly, a sixfold (**60^0**) clockwise rotation about **6** maps the entire (infinite!) beehive to itself: B is mapped to itself, E to C, C to D, D to A, etc; every hexagonal tile is clearly mapped to another one, and, overall, the entire beehive remains **invariant**. Likewise, a threefold (**120^0**) clockwise rotation about **3** leaves the beehive invariant, mapping B to C, C to D, D to B, A to E, etc; and, a twofold (**180^0**) rotation about **2** does just the same, mapping D to B (again!), A to C, etc. We describe these facts by saying that the beehive has 60^0 rotation (about **6** and all other hexagon centers), 120^0 rotation (about **3** and all other hexagon vertices), and 180^0 rotation (about **2** and all other midpoints of hexagon edges). Notice that the existence of 60^0 rotation in a wallpaper pattern always implies the existence of 120^0 and 180^0 rotations about the same center: for example, applying **twice** the 60^0 rotation centered at **6** yields a 120^0 rotation (mapping E to D, C to A, etc), while a **triple** application leads to a 180^0 rotation (mapping E to A, etc). Further, the existence of 60^0 centers **implies** the existence of **'genuine'** 120^0 and 180^0 centers (7.5.4).

Visiting the bathroom wall now, we see that it has both **90^0** and **180^0** rotation. Indeed a clockwise fourfold (90^0) rotation about **4** leaves it invariant (mapping A to B, B to C, C to D, D to A, E to F, etc), and so does a twofold (180^0) rotation about **2** (mapping B to C, D to E, etc). In fact the middle of every square is **also** the center of a 90^0 rotation (as well as a 180^0 rotation via a **double** application of the 90^0 rotation), while the midpoint of every square edge is the center of a 180^0 rotation (but **not** a 90^0 rotation!).

So, we have just seen that wallpaper patterns can have twofold, threefold, fourfold, and sixfold rotations (by 180^0, 120^0, 90^0, and 60^0, respectively). More precisely, we have seen examples of wallpaper patterns where the **smallest rotation** is 60^0 (beehive) or 90^0 (bathroom wall). As we will see in the rest of this chapter, there also exist wallpaper patterns with smallest rotation 120^0 (somewhat exotic) and 180^0 (very common), as well as wallpaper patterns with no rotation at all. A very important question is: are there any other 'smallest' rotations besides those by 60^0, 90^0, 120^0, and 180^0? Are there any wallpaper patterns with **fivefold** rotation (**72^0**), for example? The answer to these questions is negative, and we devote the rest of this section to establish this important fact, known in the literature as the **Crystallographic Restriction** and central in proving that there exist **precisely seventeen types of wallpaper patterns**. (We describe these types in the rest of chapter 4, but we defer their classification to chapter 8.)

4.0.4 Rotation centers translated. In section 1.4 we defined glide reflection as the combination of a reflection and a translation parallel to each other, and we observed that the two operations commute with each other only when the reflection axis and the gliding vector are parallel to each other (1.4.2).

Asking the same question about rotation and translation leads **always** to a negative answer. We may confirm this in the context of the bathroom wall of figure 4.2 placed now in a coordinate axis (figure 4.3): consider for example **R**, the clockwise 90^0 rotation about (0, 0), and **T**, the translation by the vector <1, 1>; it can be verified, using techniques from either chapter 3 (see right below) or chapter 1, that **R∗T** (**T** followed by **R**) is the clockwise 90^0 rotation about (−1, 0), while **T∗R** (**R** followed by **T**) is the clockwise 90^0 rotation about (1, 0).

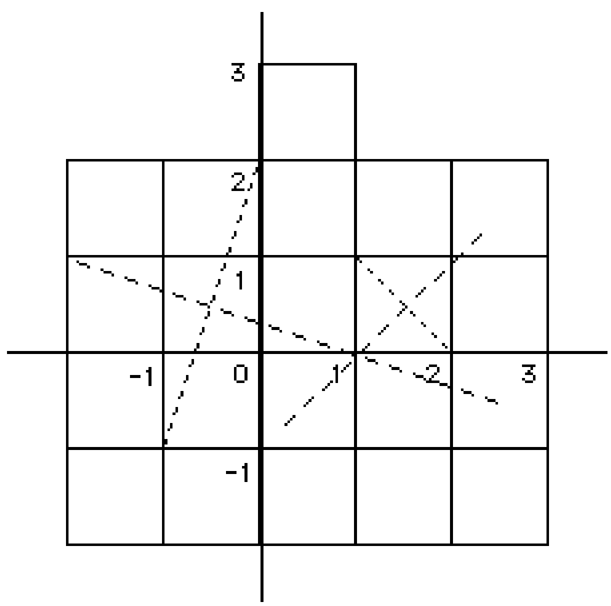

Fig. 4.3

Concerning the latter, notice that **R** maps (−1, −1) to (−1, 1), and subsequently **T** maps (−1, 1) to (0, 2); likewise, (1, 1) is mapped by **R** to (1, −1), which is in turn mapped by **T** to (2, 0). So **T∗R**, which **must** be a rotation (why?), maps (−1, −1) to (0, 2) and (1, 1) to (2, 0). With the perpendicular bisectors of the segments joining (−1, −1), (0, 2) and (1, 1), (2, 0) intersecting each other at (1, 0) (figure 4.3), it is easy from here on to verify that **T∗R** is indeed the clockwise 90^0 rotation about (1, 0).

At this point, you may ask: how come **T∗R** is **not** $\mathbf{R_T}$, the **'translated'** clockwise 90^0 **rotation** about (1, 1)? Shouldn't the translation **T** 'translate' the entire rotation **R** the same way it **translates** its **center** (0, 0) to (1, 1)? Well, we already proved in the preceding paragraph, and may further confirm here, that this is not the case: for example, $\mathbf{R_T}$ maps (0, 2) to (2, 2) instead of its image under **T∗R**, which is (3, 1). But **observe** at this point that the one point that $\mathbf{R_T}$ maps to (3, 1) is no other than the point (1, 3), which happens to be the image of (0, 2) under translation by **T**! Likewise, if we **first translate** (0, 1) **by T** to (1, 2) and **then rotate** (1, 2) **by** $\mathbf{R_T}$ we end up mapping (0, 1) to (2, 1), exactly as **T∗R** does! And so on.

Putting everything together, it seems that $\mathbf{R_T * T}$, that is **T** followed by $\mathbf{R_T}$, has the same effect as **R** followed by **T**, that is **T∗R**: in the language of Abstract Algebra, $\mathbf{R_T * T = T * R}$. 'Multiplying' both sides by $\mathbf{T^{-1}}$ (**T**'s **inverse**, that is a translation by a vector **opposite** -- see 1.1.2 -- to that of **T** that **cancels T**'s effect), we obtain $\mathbf{R_T = T * R * T^{-1}}$; in even more algebraic terms, we have shown that $\mathbf{R_T}$ is the **conjugate** of **R** by **T**. Switching to Geometry and moving away from the bathroom wall, we offer a 'proof without words' (figure 4.4) of the following fact: for every translation **T** and every rotation $\mathbf{R = (K, \phi)}$, the **'product'** $\mathbf{T * R * T^{-1}}$ is indeed the rotation $\mathbf{R_T = (T(K), \phi)}$, that is, **R 'translated' by T**. (You may of course provide a rigorous geometrical proof, especially in case you are aware of the fact that any two isosceles triangles of equal bases and equal top angles must be congruent!)

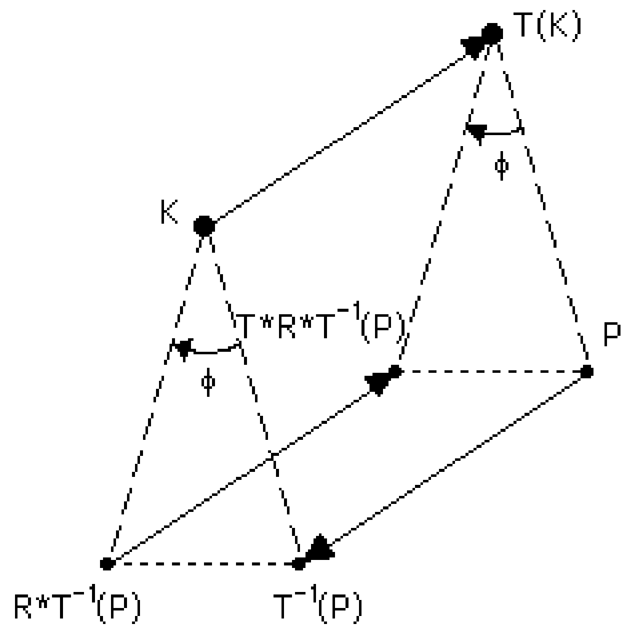

Fig. 4.4

Since compositions of isometries leaving a wallpaper pattern invariant leave it invariant, too, we conclude that we may indeed assume the following: in every wallpaper pattern, the image of the center of a rotation **R** by a translation **T** is the center for a new rotation (**T∗R∗T^{-1}** rather than **T∗R** or **R∗T**) by the **same angle**. This follows from the more general fact depicted in figure 4.4, was empirically confirmed in the case of the bathroom wall, and may be further verified in the cases of the beehive and the other wallpaper patterns you are going to see in this chapter.

It follows that the existence of a single rotation center in a wallpaper pattern implies the existence of infinitely many rotation centers all over the plane! Indeed, there exist two distinct, non-opposite translations in our pattern, say <p, q> and <r, s>, hence translating the rotation center by the four distinct translations <p, q>, <r, s>, <–p, –q>, and <–r, –s> -- notice that if a translation leaves a wallpaper pattern invariant then so does its opposite -- we produce four new rotation centers around the old one. Repeating this process to all new centers again and again we end up with an **infinite lattice** of rotation centers, shown in figure 4.5 below for the cases of the beehive and the bathroom wall. Observe that there exist in fact **three lattices in one** in the case of the beehive, consisting of 60^0, 120^0, and 180^0 centers, and **two lattices in one** in the case of the bathroom wall, consisting of 90^0 centers and 180^0 centers. (There is more than meets the eye here: there really are two kinds of 90^0 centers in the bathroom wall -- only one of which was shown in figure 4.2 -- the translations of which may transport us from one kind to another only in a rather 'indirect' manner (7.6.3); and similar remarks apply to the beehive's 120^0 centers and to the 180^0 centers of both the beehive and the bathroom wall.)

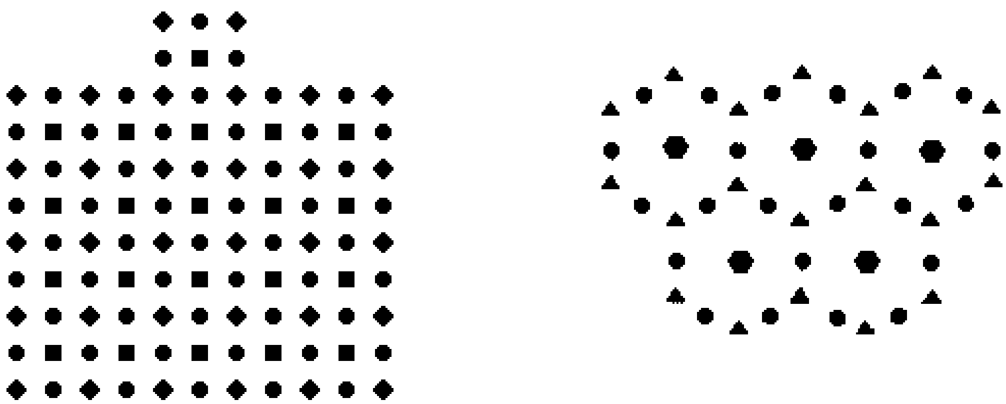

Fig. 4.5

Notice the lack of rotation centers other than the ones shown in figure 4.5: in a wallpaper pattern rotation centers cannot be arbitrarily close to each other, in the same way that translation vectors **cannot be arbitrarily small** -- this is what Arthur L. Loeb calls **Postulate of Closest Approach** in his ***Concepts and Images*** (Birkhauser, 1992). For a challenge to this principle and further discussion you may like, if adventurous enough, to have a look at 4.0.7. It seems in fact that there is an interplay between translation vectors and distances between rotation centers, to the extend that you might venture to guess that every vector starting at a rotation center and ending at a center for a rotation by the **same angle** is in fact a translation vector for the entire pattern: this is true for 60^0 centers but not for 90^0, 120^0, or 180^0 centers, as you may verify for yourself (and has been hinted on at the end of the preceding paragraph); still, there are interesting facts relating the **distances** between rotation centers to the **lengths** of translation vectors that you should perhaps explore on your own!

4.0.5 Rotation centers rotated. Let's have another look at the beehive pattern and its various rotation centers, as featured in figure 4.2 (entire pattern) or figure 4.5 (centers only). It seems clear that the rotation about a randomly chosen center (be it for 60^0, 120^0, or 180^0) of **every** other center (be it for 60^0, 120^0, or 180^0) moves it to another center (for a rotation by the **same angle**); for example, rotating a 120^0 center about a 60^0 center (by 60^0, of course) we get another 120^0 center, rotating a 60^0 center about a 180^0 center (by 180^0) we get another 60^0 center, etc. Similar observations may be made for the bathroom wall and, in fact, every wallpaper pattern that has one, therefore infinitely many, rotation centers: wallpaper patterns are indeed wonderful!

Moving away from the harmonious world of wallpaper patterns, we must ask: is it true in general that rotations always rotate rotation centers to rotation centers? To be more specific, consider two rotations, $\mathbf{R_1 = (K_1, \phi_1)}$ and $\mathbf{R_2 = (K_2, \phi_2)}$: is it true that $\mathbf{R_1(K_2)}$, that is $\mathbf{K_2}$ rotated about $\mathbf{K_1}$ by ϕ_1, is a center for a rotation by ϕ_2? The answer is "yes", and the rotation in question is no other than $\mathbf{R_1{*}R_2{*}R_1^{-1}}$, the **conjugate** of $\mathbf{R_2}$ by $\mathbf{R_1}$: the same algebraic operation employed in 4.0.4 to express the translation of a rotation works here for the **rotation of a rotation**! While a computational proof using the rotation formulas of section 1.3 certainly works, the easiest way to demonstrate this wonderful fact is a **geometrical** 'proof without words' (figure 4.6 below) in the spirit of figure 4.4; we take both ϕ_1 and ϕ_2 to be clockwise, but you may certainly verify that this is an unnecessary restriction.

We should note in passing that 4.0.4 and 4.0.5 (and figures 4.4 & 4.6 in particular) are special cases of a broader phenomenon that we will encounter again and again in chapter 6 (starting at 6.4.4) and section 8.1 (and the rest of chapter 8): the **'image' of an isometry** by another isometry is again an isometry; we should probably remember this fact under a name like **Mapping Principle**, but we will later call it **Conjugacy Principle** on account of the algebraic realities discussed above.

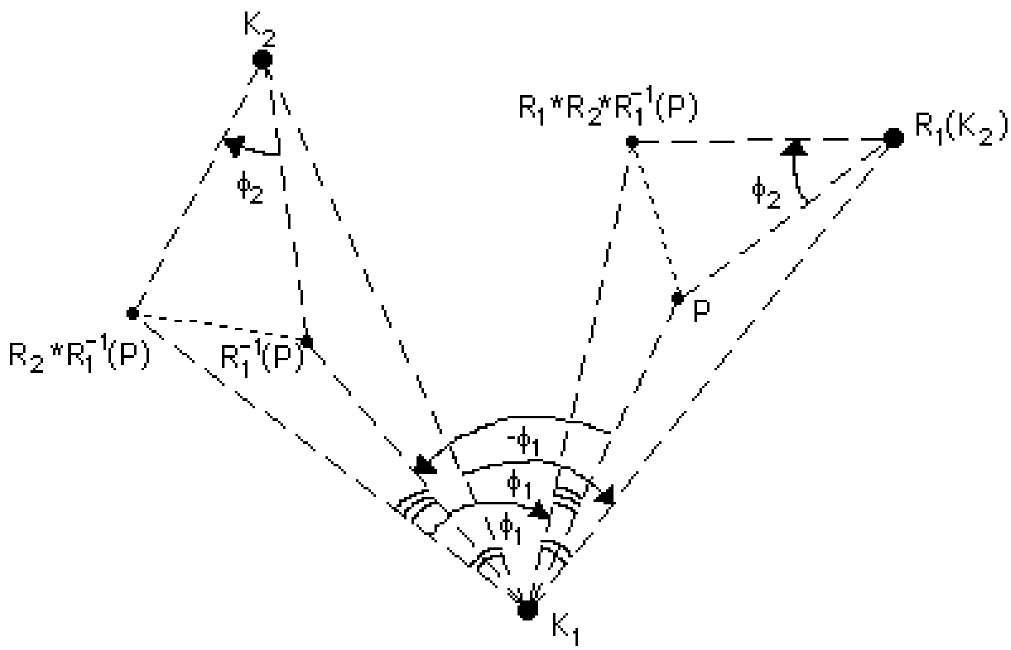

Fig. 4.6

As in 4.0.4, we must stress that the rotations $\mathbf{R_1{*}R_2}$, $\mathbf{R_2{*}R_1}$, and $\mathbf{R_1{*}R_2{*}R_1^{-1}}$ are all distinct: we will thoroughly examine such compositions of rotations and other isometries in chapter 7.

4.0.6 Only four angles are possible! At long last, we are ready to **establish** the Crystallographic Restriction. Assume that a certain wallpaper pattern remains invariant under rotation by an angle ϕ, and pick two centers at the **shortest possible distance** (4.0.4) from each other, K_0 and K_1. Let us also assume that $\mathbf{0^0 < \phi \leq 180^0}$: in case $\phi > 180^0$ we can work with the angle $360^0 - \phi$, which also leaves the wallpaper pattern invariant. We may now (4.0.5) **rotate $\mathbf{K_1}$** by a counterclockwise ϕ **about $\mathbf{K_0}$** in order to get a new center K_2, and then rotate K_2 (about K_0 and by counterclockwise ϕ always) to obtain yet another center K_3, and so on. For how long can we continue this way, producing new centers on the **'rotation center circle'** (figure 4.7) of center K_0 and radius $|K_0K_1|$? In theory (and absence of the assumption that $|K_0K_1|$ is the minimal possible distance between any two distinct rotation centers) for ever; in practice not for too long, as **no** center is allowed to fall within an **'arc distance'** of **less**

than 60^0 from K_1, unless it returns to K_1: otherwise we would have two rotation centers at a **distance smaller than $|K_0K_1|$** from each other! (Think of an isosceles triangle K_0K_1K where K is the multi-rotated K_1 and $|K_0K_1| = |K_0K|$; if the angle $\angle K_1K_0K$ is smaller than 60^0 then the other two angles are bigger than 60^0, therefore $|KK_1|$ would be smaller than $|K_0K_1|$.)

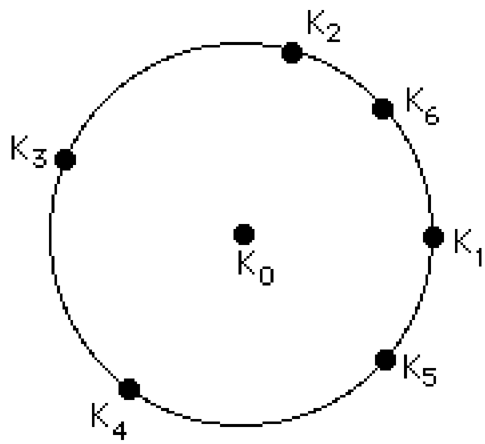

Fig. 4.7

Let now N be the unique integer such that **$N\times\phi \leq 360^0 < (N+1)\times\phi$**: that is, N records how many rotations are required for K_1 to either **return** to K_1 ($N\times\phi = 360^0$) or **bypass** K_1 ($N\times\phi < 360^0 < (N+1)\times\phi$).

In the latter case (**$N\times\phi < 360^0$**) we must also assume, in order to avoid the **'forbidden arc'**, the inequalities **$360^0 - N\times\phi \geq 60^0$** and **$(N+1)\times\phi - 360^0 \geq 60^0$**; these inequalities lead to $300^0/N \geq \phi$ and $\phi \geq 420^0/(N+1)$, respectively. It follows that $300/N \geq 420/(N+1)$, so $300\times(N+1) \geq 420\times N$ and $300 \geq 120\times N$; we end up with **$N \leq 2.5$**, hence either $N = 1$ or $N = 2$. The case $N = 1$ is ruled out by $\phi \leq 180^0$, while in the case $N = 2$ the inequalities $300^0/N \geq \phi$ and $\phi \geq 420^0/(N+1)$ yield **$140^0 \leq \phi \leq 150^0$**. But if K_2 lies on the arc $[140^0, 150^0]$ then K_3 lies on the arc $[280^0, 300^0]$, K_4 on the arc $[60^0, 90^0]$, K_5 on $[200^0, 240^0]$, and K_6 on $[340^0, 390^0]$ = **$[-20^0, 30^0]$**, which is part of the 'forbidden arc': K_1's trip ends up in a disaster, **unless perhaps $\phi = 144^0$** (the solution of the **'return equation'** $5\times\phi = 2\times360$), in which case K_1 quietly returns to itself with $K_6 \equiv K_1$ (figure 4.8). But in that case a (counterclockwise) rotation by 144^0 applied twice certainly yields a (counterclockwise) rotation by 288^0, hence a (clockwise) rotation by $360^0 - 288^0 = \mathbf{72^0}$, a rotation that will be ruled out further below.

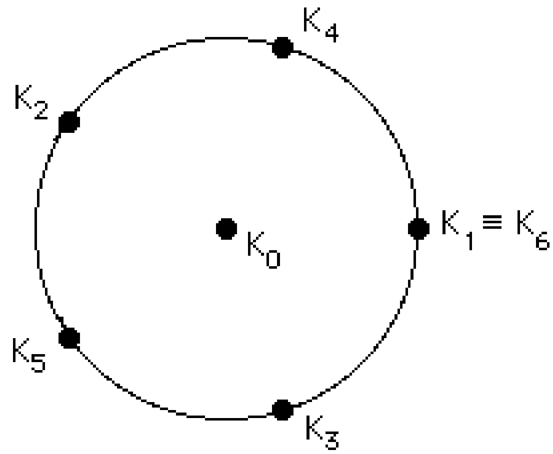

Fig. 4.8

In the former case ($\mathbf{N\times\phi = 360^0}$) we substitute $\phi = 360^0/N$ into the inequality $(N+1)\times\phi - 360^0 \geq 60^0$ to get $(N+1)\times360/N - 360 \geq 60$ and, eventually, $\mathbf{N \leq 6}$; more intuitively, we must have $\boldsymbol{\phi \geq 60^0}$ or else K_2 would fall into that 'forbidden arc' discussed above. After discarding the case N = 1 ($\phi = 360^0$ -- no rotation), we are left with the cases N = 2 ($\phi = 180^0$), N = 3 ($\phi = 120^0$), N = 4 ($\phi = 90^0$), N = 5 ($\phi = 72^0$), and N = 6 ($\phi = 60^0$); 'global rotations' by all these angles are possible and familiar to you by now, **except for** $\boldsymbol{\phi = 72^0}$ (the angle that tormented many artists only a few centuries ago!). To render a rotation by 72^0 impossible for a wallpaper pattern, we simply rotate $\mathbf{K_0}$ **about** $\mathbf{K_1}$ by **clockwise** $\mathbf{72^0}$ to a rotation center $\mathbf{K'_0}$ (figure 4.9): it is obvious now that $\mathbf{|K_2K'_0|}$ **is smaller than** $\mathbf{|K_0K_1|}$, thus violating the assumption on the minimality of $|K_0K_1|$! (To be precise, trigonometry yields $|K_2K'_0| = (\sin18^0/\sin54^0) \times |K_0K_1| \approx .38 \times |K_0K_1|$.)

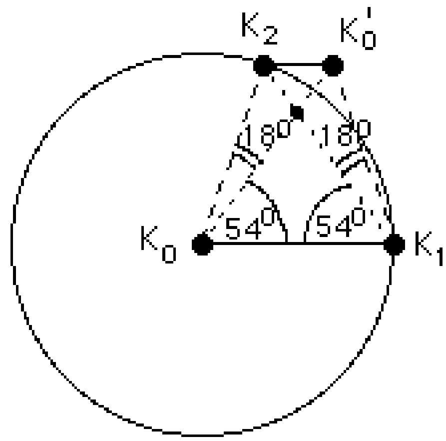

Fig. 4.9

We conclude that a wallpaper pattern either has no rotation at all or that the smallest rotation that leaves it invariant can only be by one of the four angles that we couldn't rule out: **60^0**, **90^0**, **120^0**, **180^0**. Based on this fact, we naturally split wallpaper patterns into **five families**: those that have no rotation at all (or, equivalently, smallest rotation 360^0), and those of smallest rotation 60^0, 90^0, 120^0, and 180^0, respectively; this greatly facilitates their classification into **seventeen distinct types** (chapter 8), as well as their descriptions in this chapter (sections 4.1 through 4.17).

4.0.7* <u>An 'exotic' pattern and a definition.</u> Most available proofs of the crystallographic restriction seem to follow, in one way or another, **W. Barlow**'s proof, published in Philosophical Magazine in 1901; such is the case, for example, with both H. S. M. Coxeter's ***Introduction to Geometry*** (Wiley, 1961) and David W. Farmer's ***Groups and Symmetry: A Guide to Discovering Mathematics*** (American Mathematical Society, 1996). These proofs assume **both** Loeb's Postulate of Closest Approach (4.0.4), which guarantees a minimum distance between rotation centers, also assumed in our proof, and the fact that a wallpaper pattern's smallest rotation angle is of the form **$360^0/n$** (where n is an integer), which we did **not** assume. Our example below presents a clear challenge to both these assumptions.

Let **S** be the set of all **rational points** in the plane, that is, the set of all points both coordinates of which are rational numbers; notice that S is **dense** in the plane, in the sense that every circular disk, no matter how small, contains **infinitely many** elements of S. What if we consider S to be a wallpaper pattern? It certainly has **translations in infinitely many directions**: for every pair of rational numbers, a and b, T(x, y) = (a+x, b+y) defines a translation <a, b> that leaves S invariant! Observe also that S has 180^0 rotation about every point (c, d) in S, defined by R(x, y) = (2c−x, 2d−y); this already shows that rotation centers of S can indeed be arbitrarily close to each other. Moreover, S has **rotation about each point of S by infinitely many angles**: every angle both the sine and the cosine of which are rational would map a rational point to a rational point, as the rotation formulas of 1.3.7 would demonstrate; and for every pair of integers m, n, such an angle is actually defined via $\sin\phi = \frac{2mn}{m^2+n^2}$ and $\cos\phi = \frac{m^2-n^2}{m^2+n^2}$, thanks to $|2mn| \leq m^2+n^2$, $|m^2-n^2| \leq m^2+n^2$, and the **Pythagorean identity** $(2mn)^2 + (m^2-n^2)^2 = (m^2+n^2)^2$!

So, S is indeed a pattern invariant under rotation by angles other than $360^0/n$ that has rotation centers at arbitrarily small distances from each other. In case you protest the fact that S consists of single points, we can easily modify it to look more 'pattern-like'. For example, we can augment every rational point (a, b) to a square 'frame' defined by the points (a−r, b−r), (a−r, b+r), (a+r, b−r), and (a+r, b+r), where r is an arbitrary **rational** number. As each such 'frame' contains many points with one or two irrational coordinates, you may protest that the union of all the 'frames' (over all (a, b) and all r) is no other than the entire plane: that turns out not to be the case, because each 'frame' is **'thin'** (in the sense that it contains no full disks) and a theorem in **Topology** -- many thanks to **Robert Israel**, who helped this former topologist recall his first love by way of a sci.math discussion! -- called **Baire Category Theorem** states that the plane cannot be a **countably infinite** union of such 'thin' sets. This much you could perhaps see even without this heavy-duty theorem -- the union of all 'frames' contains no points **both** coordinates of which are irrational! -- but you would need the theorem in case our 'extended pattern' contains not only the 'frames' described above but their images by **all** rotations of S described in the preceding paragraph as well: yes, this extended pattern **S#** that inherits all the translations and rotations of S and seems to be everywhere is **still a countable union of 'thin' sets**, hence not the entire plane! (There is of course a bit more to this Baire Category Theorem, as you may find out by checking any undergraduate Topology book; one suggestion is George F. Simmons' ***Introduction to Topology and Modern Analysis*** (McGraw-Hill, 1963).)

'In practical terms' now, exotic wallpaper patterns such as S and S# cannot quite exist (as art works) in the real world: for every bit of paint (or even ink) contains a miniscule full disk -- recall **Buckminster Fuller**'s statements about "every line having some width and structure" and "every circle being a polygon with enormously many sides" (***Loeb***, p. 126) -- and, **'reversing'** the Baire Category Theorem, we easily conclude that every pattern containing such disks **and** having arbitrarily small translations must equal/blacken the entire plane! That is, art works -- which cannot be infinite to begin with -- cannot have arbitrarily small translations, hence, less obviously, must also satisfy that **Postulate of Closest Approach** (no arbitrarily small distances between rotation centers): indeed, as we will see in 7.5.2, one can always 'combine' two rotations (by the same angle but of opposite orientations) to produce a translation (of vector length not exceeding twice the distance between the two centers).

A broader way of ruling out arbitrarily small translations is the following definition (certainly satisfied by art works): a wallpaper pattern S is a **countable union of congruent sets S_n** that is invariant under translation in two distinct, non-opposite directions, and has also the property that **every disk intersects at most finitely many S_ns**. (In the case of the beehive and the bathroom wall the S_ns are (boundaries of) regular hexagons and squares, respectively; and in the case of the sets S and S# -- not accepted as wallpaper patterns under this definition due to failure of the **finite intersection property** -- the S_ns are rational points and rational points surrounded by those rationally rotated concentric rational square frames, respectively.)

4.1 360^0, translations only (p1)

4.1.1 Stacking **p111**s. What happens when we fill the plane with copies of a **p111** border pattern placed right above/below each other in **'orderly'** fashion, whatever that means? We obtain wallpaper patterns like the ones shown below:

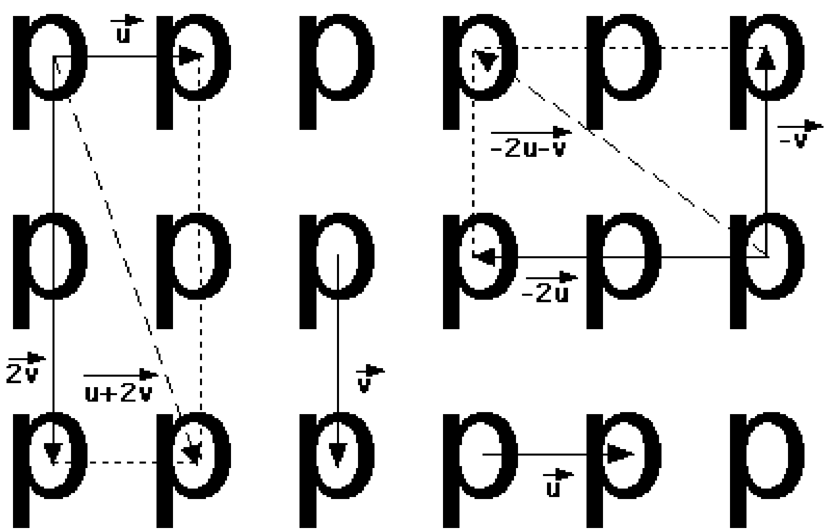

Fig. 4.10

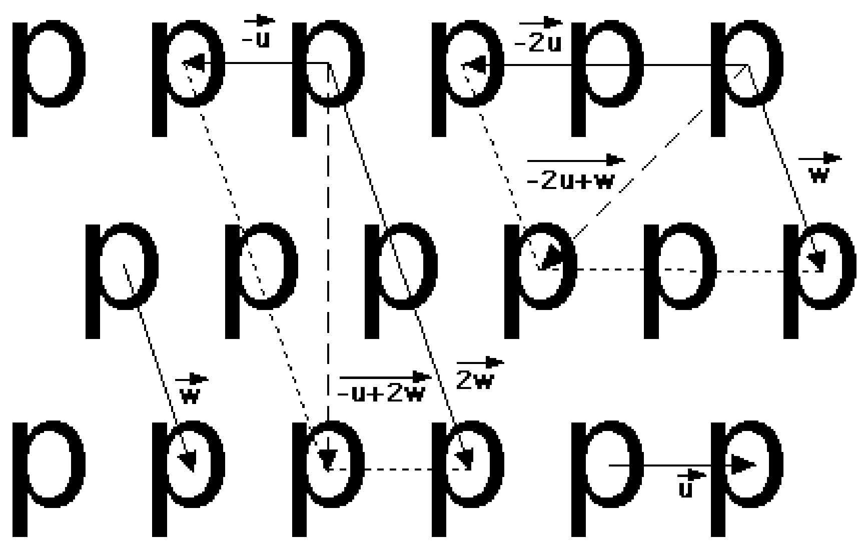

Fig. 4.11

While looking different from each other, these two wallpaper patterns are ‘mathematically identical’: they both have translation in two, thus **infinitely many** directions, and no other isometries. It is only their **minimal translation vectors** that separate them: horizontal $\vec{u}$ and vertical $\vec{v}$ (figure 4.10) versus horizontal $\vec{u}$ and diagonal $\vec{w}$ (figure 4.11); notice that the two patterns share many translation vectors, like $\vec{u}$, $\vec{u}+2\vec{v} = 2\vec{w}$, $-\vec{u}+2\vec{w} = 2\vec{v}$, etc. (Vectors are added following the **parallelogram rule** familiar from Physics, see figures 4.10 & 4.11; and it is this addition’s nature that leads to the infinitude of translations alluded to right above.) Such wallpaper patterns are denoted by **p1** and are the simplest of all.

Is it possible to stack copies of the **“p ”** border pattern in some kind of **‘disorderly’** fashion so that the end result is **not** a wallpaper pattern? The answer is “yes”, and here is an example:

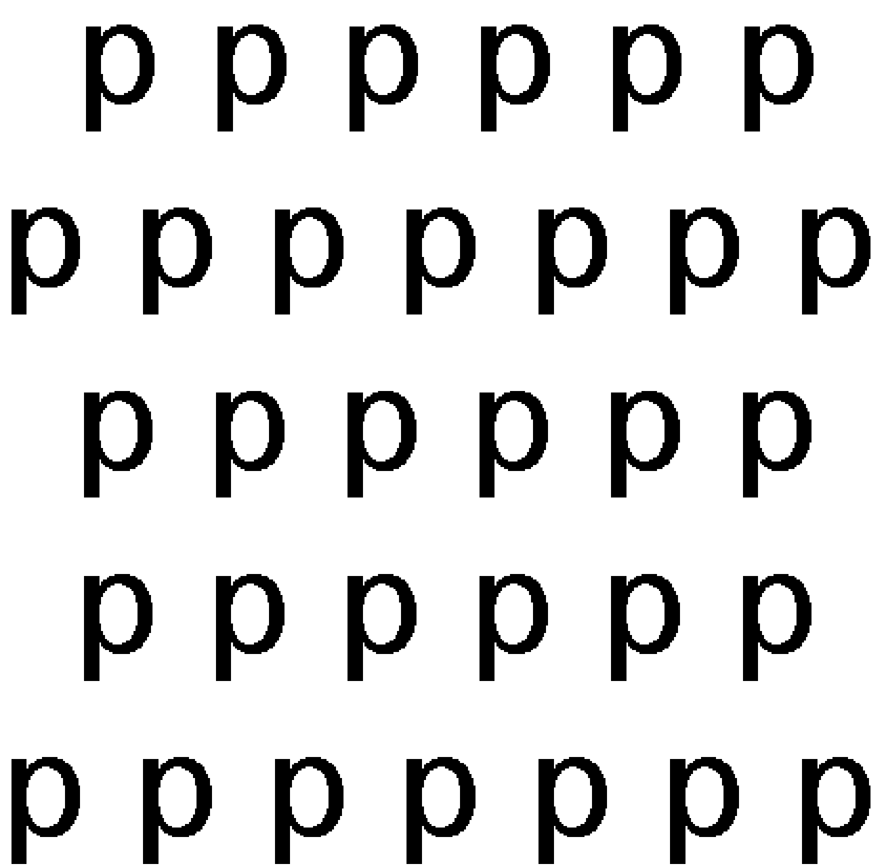

Fig. 4.12

What went wrong with the design in figure 4.12? To answer this question you have to know, if you have not guessed it already, what the rest of the design is! Recall that all wallpaper patterns are infinite, and you must always be able to imagine their extension beyond the page you are reading! This ‘extension’ is normally not that difficult to see (as long as you remember that you have to, of course), but in the case of the ‘pathological’ pattern of figure 4.12 you may need some help: we start with a copy of the **“p ”** border pattern, then place **one** ‘shifted’ copy right below it, continue with **two** ‘straight’ copies underneath, then **one** shifted copy below them, then **three** straight copies again, then **one** shifted copy, and so on; the same process applies to all rows above the top one in figure 4.12. We leave it to you to verify that this ...32123...-like design is **not** a wallpaper pattern: all you have to do is to verify that it has **translations in only one direction**, the horizontal one.

4.1.2 Pis all the way! Below you find another design that fails to be a wallpaper pattern by having translation in only one direction, in this case the vertical one; unlike the one in figure 4.12, built by disorderly stacking of a border pattern, this one is built by orderly stacking of an one-dimensional design that is **not** a border pattern:

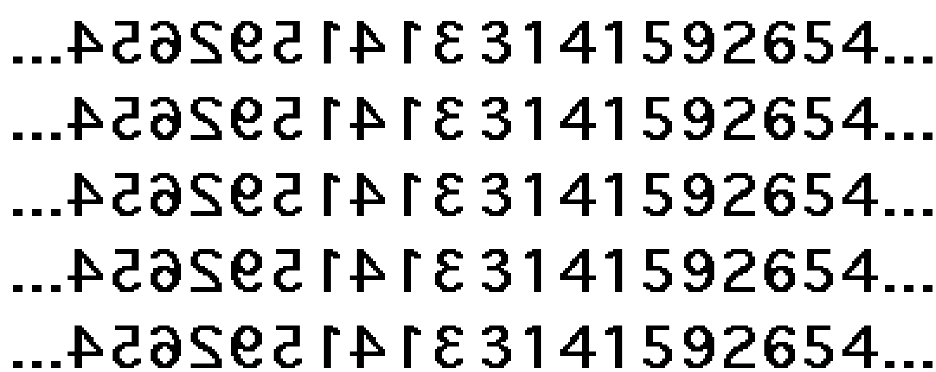

Fig. 4.13

In case you haven’t noticed, the protagonist here is no other than **$\pi \approx$ 3.141592654...**, well known to have an infinite, non-repeating decimal expansion: don’t be fooled, **one** reflection alone (right in the middle) cannot produce a translation!

4.1.3 From the land of the Incas. Here is a very geometrical Inca design that, in spite of its geometrical beauty and complexity, has no isometries other than translations, therefore it is classified as a **p1** wallpaper pattern (***Stevens***, p. 180):

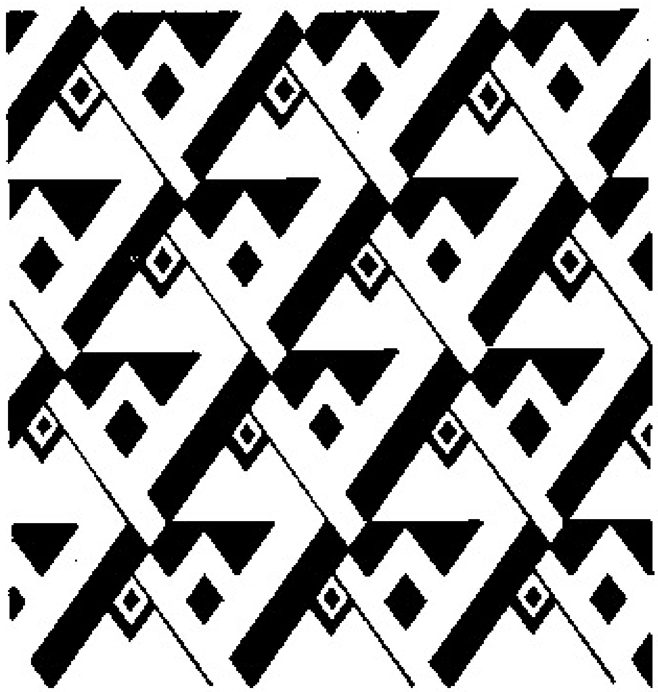

Fig. 4.14

4.2 360^0 with reflection (pm)

4.2.1 Straight stacking of **pm11**s. You have certainly noticed that the design in figure 4.13 has mirror symmetry. Due to the lack of horizontal translation, however, there exists one and only one reflection axis that works. To obtain a wallpaper pattern with infinitely many reflection axes (all **parallel** to each other), we can resort to the process of 4.1.1, stacking copies of a **pm11** border pattern this time:

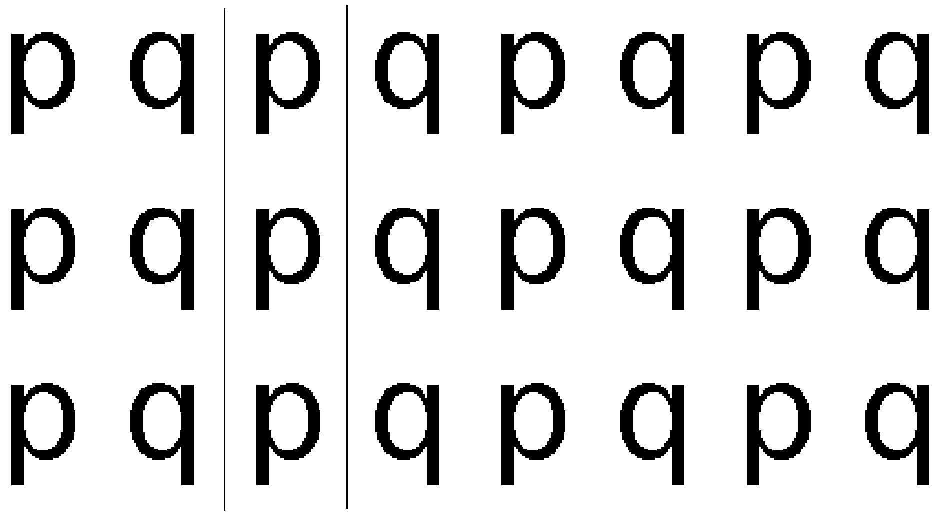

Fig. 4.15

You recognize of course the **“p q ”** border pattern of 2.2.2 and figure 2.6. The wallpaper pattern in figure 4.15 has automatically inherited all its symmetries (like vertical reflection and horizontal translation) in a rather obvious manner; in addition to those, **‘straight’** stacking -- **every p straight above a p and every q straight above a q** -- has created vertical translation.

Such wallpaper patterns generated by straight stacking of a **pm11** border pattern and having reflection in one direction (and no rotation of course) are denoted by **pm**.

4.2.2 <u>Two kinds of mirrors.</u> Just like **pm11** border patterns, all **pm** wallpaper patterns have two kinds of reflection axes; this is for example the case with the wallpaper pattern of figure 4.15. We illustrate this phenomenon with a more geometrical example, stressing once again the fact that reflection axes are allowed to go **through** the motifs (in this case being identical to the trapezoids’ own reflection axes):

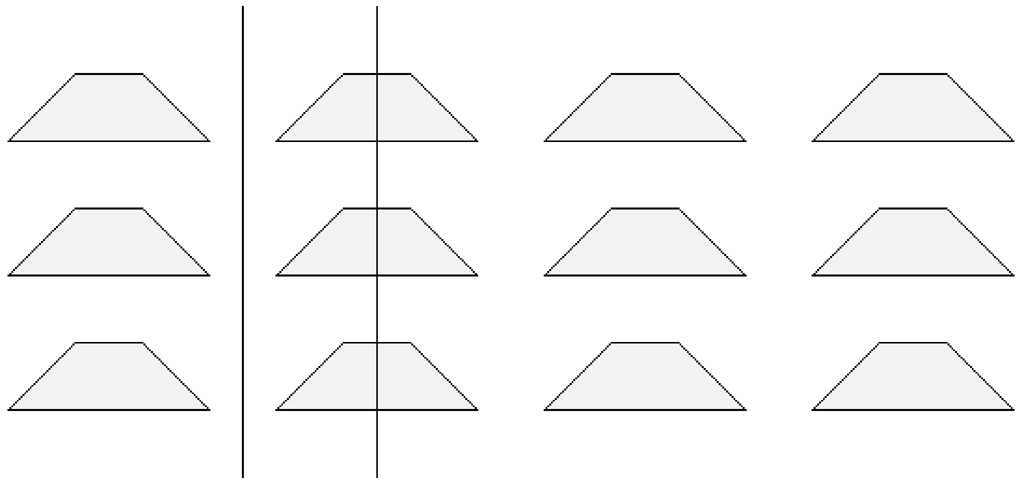

Fig. 4.16

4.2.3 Ancient Egyptian oxen. The following example of a **pm** pattern (***Stevens***, p. 193) is dominated by the stillness that tends to characterize the **pm** patterns (as well as oxen in general):

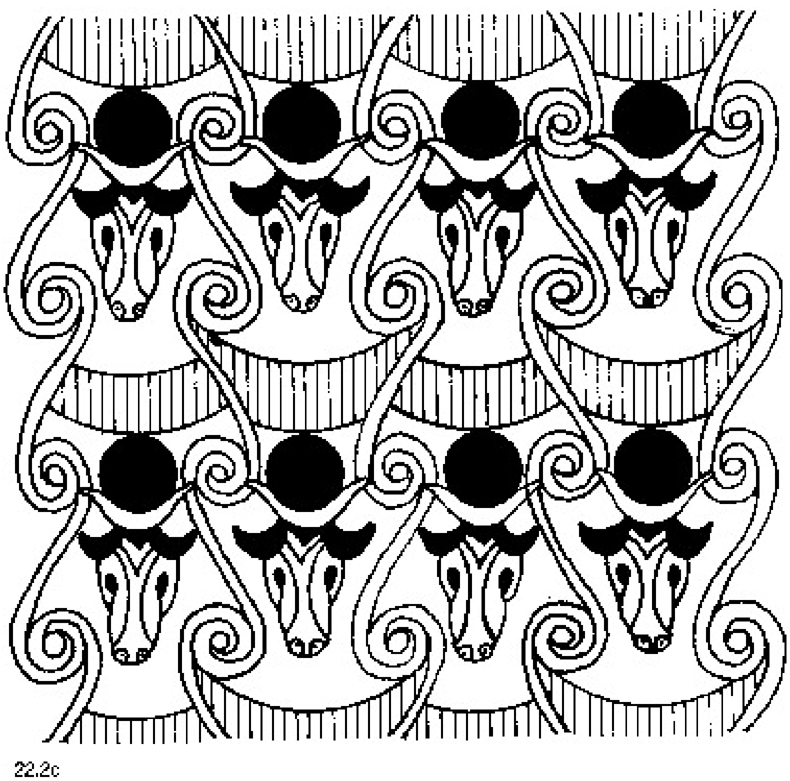

Fig. 4.17

Thanks to the **cascading spires** between the oxen, there are still **two kinds** of reflection axes, even though they all ‘dissect’ the oxen!

4.3 360^0 with glide reflection (pg)

4.3.1 <u>Shifted stackings of **pm11**s.</u> What happens when we stack the **“p q ”** pattern in a ‘disorderly’ manner, as shown right below?

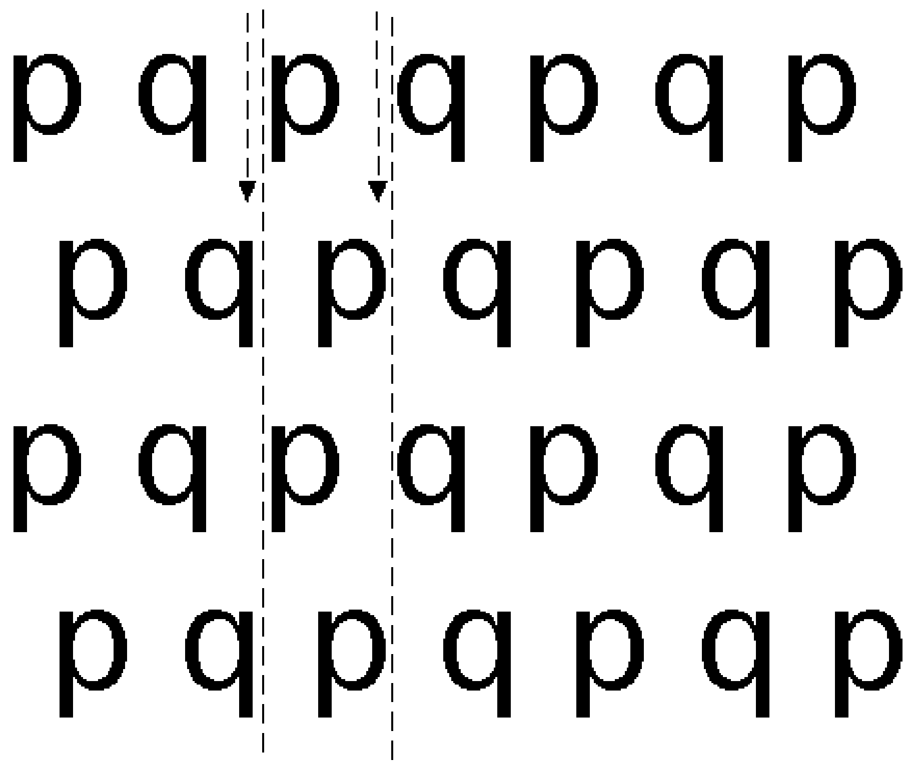

Fig. 4.18

Clearly, the **shifting of every other row** has eliminated any possibility for reflection, but it has generated **two kinds** of vertical **glide reflection**, as shown in figure 4.18. Such rotationless wallpaper patterns with glide reflection are denoted by **pg**; they may be obtained either as a shifted stacking of a **pm11** border pattern (figure 4.18) or by shifting every other row in a **pm** wallpaper pattern, as the following modification of figure 4.16 (and determination of glide reflection axes based on chapter 3 methods) demonstrates:

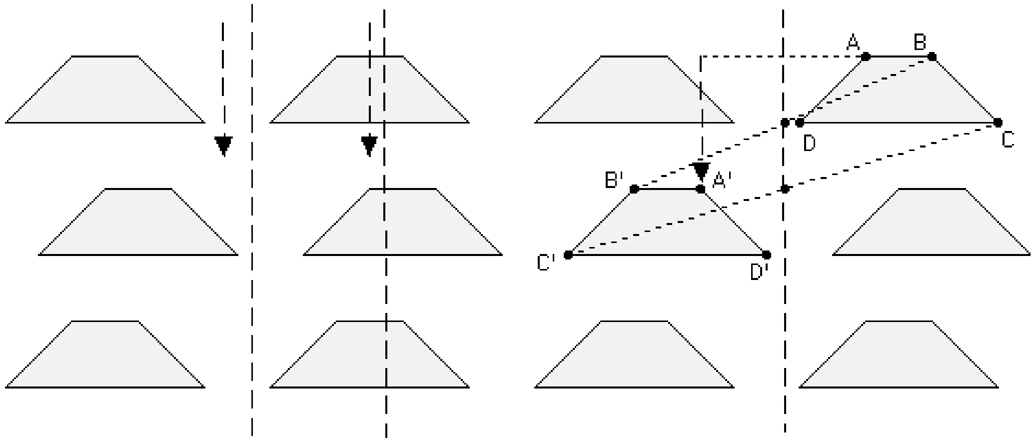

Fig. 4.19

4.3.2 <u>Straight stackings of **p1a1**s.</u> Can we get a **pg** wallpaper pattern by stacking copies of a border pattern with glide reflection?

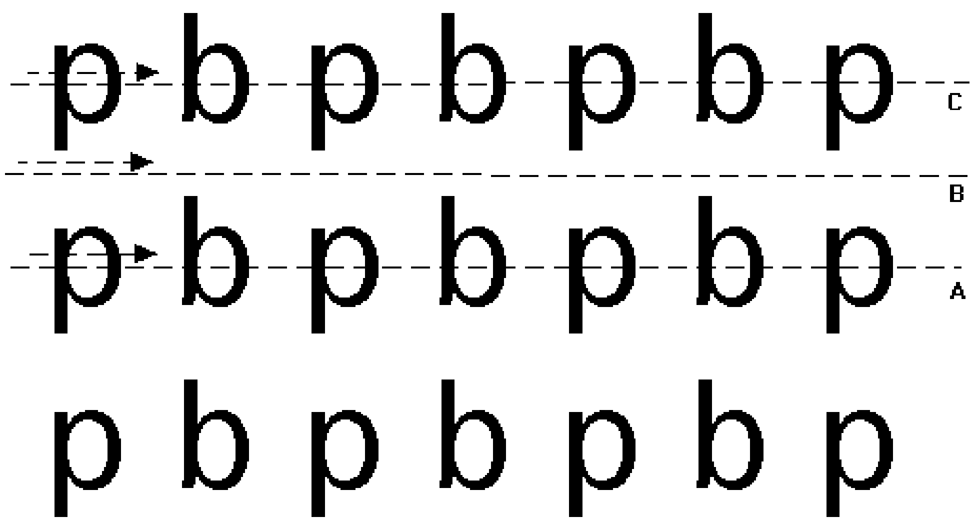

Fig. 4.20

As figure 4.20 illustrates, this is certainly possible: our pattern inherits the **horizontal** glide reflection from the **p1a1** border pattern of figure 2.15 (crossing right **through** the stacks, like lines **A** and **C**), and it has its own, ‘stack-gluing horizontal glide reflection (with axes running right **between** the stacks, like line **B**).

4.3.3 <u>Between **pg** and **p1**.</u> What kind of wallpaper pattern is the one obtained via a **shifted** stacking of copies of **"p b "**?

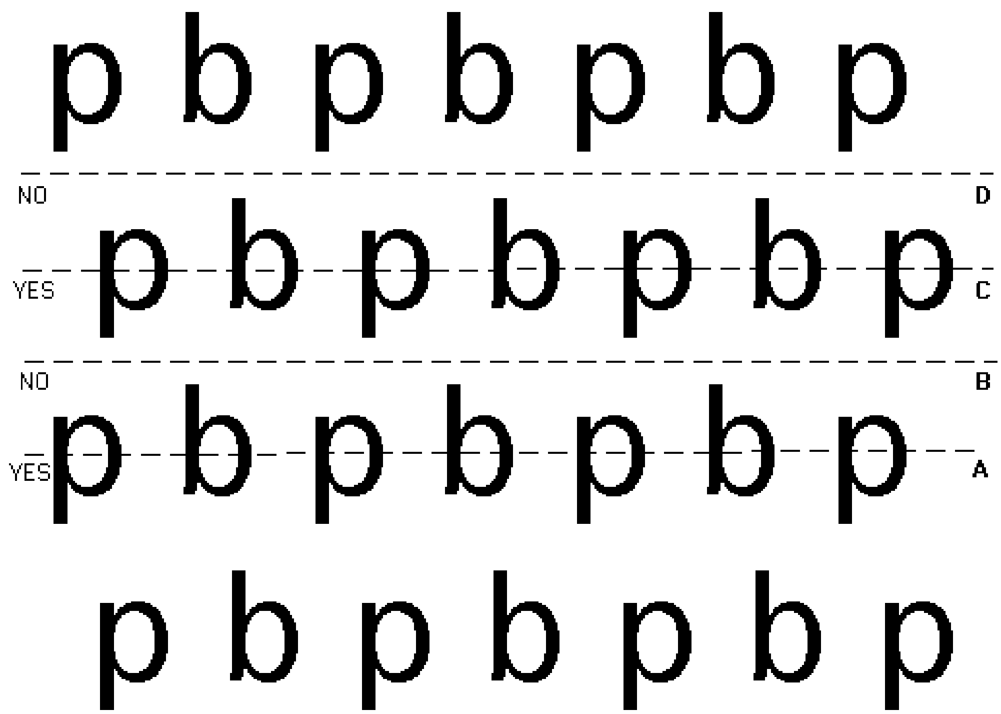

Fig. 4.21

The wallpaper pattern shown in figure 4.21 is a 'complicated' one: it has glide reflection along the lines **A** and **C**, exactly as the pattern in figure 4.20, but **not** along lines **B** or **D**! Indeed line **B** (or **D**) fails to be a glide reflection axis for the same reason that the border pattern in figure 2.16 does not have glide reflection: it would require **two distinct vectors** -- short vector sending C-letters to A-letters, long vector sending A-letters to C-letters -- in order to work as a glide reflection axis! So, and unless one checks **only** axes like **B** or **D**, our pattern is classified as a **pg** rather than a **p1**. Interestingly, this **pg** pattern may be viewed as a straight stacking of a **p111** border pattern (consisting of the strip between two **B**-like axes, for example)!

How does one 'see' glide reflection in a wallpaper pattern where **not** all motifs are **homostrophic**, distinguishing between **pg** and **p1**? One trick is suggested by our observation in 2.4.2 that remains valid for wallpaper patterns, too: the glide reflection vector is always equal to **half** of a translation vector -- but not vice versa, as the **pg** has glide reflection in **only one** direction and translation in **infinitely many** directions... So, first you use your intuition to pick the **'right' direction**, next you translate a motif by half the minimal translation vector in that direction, and finally you look for a reflection axis that maps it to another motif: for example, trapezoid ABCD in figure 4.19 is first vertically translated right across the reflection axis from trapezoid A′B′C′D′.

4.3.4 Peruvian birds. We conclude this section with an example of a Peruvian **pg** pattern from ***Stevens*** (p. 188):

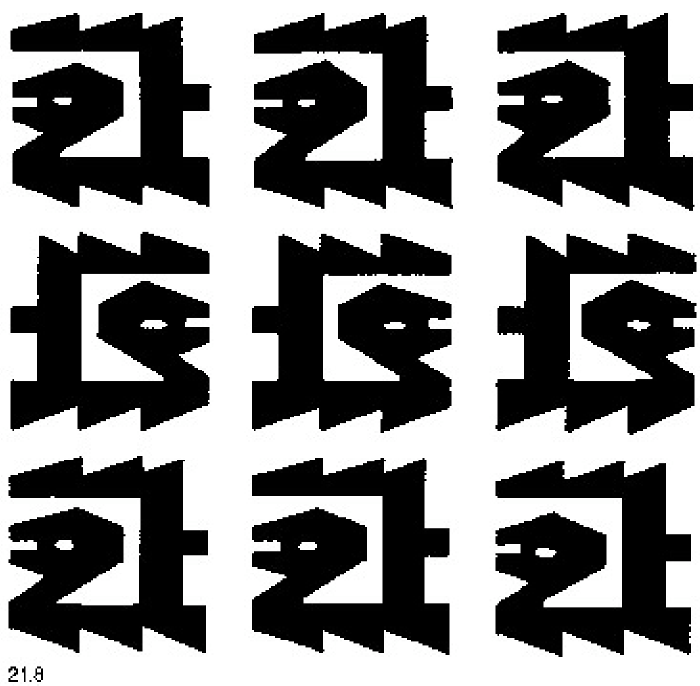

Fig. 4.22

Clearly, there are two flocks of birds 'flying' in opposite directions, and that feeling of 'opposite' movements **perpendicular** to the direction of the glide reflection is quite common in **pg** patterns; you can see that in the wallpaper pattern of figure 4.20, for example (especially if you turn the page sideways), but not quite in those of figures 4.18 or 4.19 -- can you tell why?

4.4 360^0 with reflection and glide reflection (cm)

4.4.1 <u>A ‘perfectly shifted’ stacking of **pm11**s.</u> What if we shift every other row in the pattern of figure 4.18 a bit further, pushing **every p straight above a q and vice versa**? Here is the result:

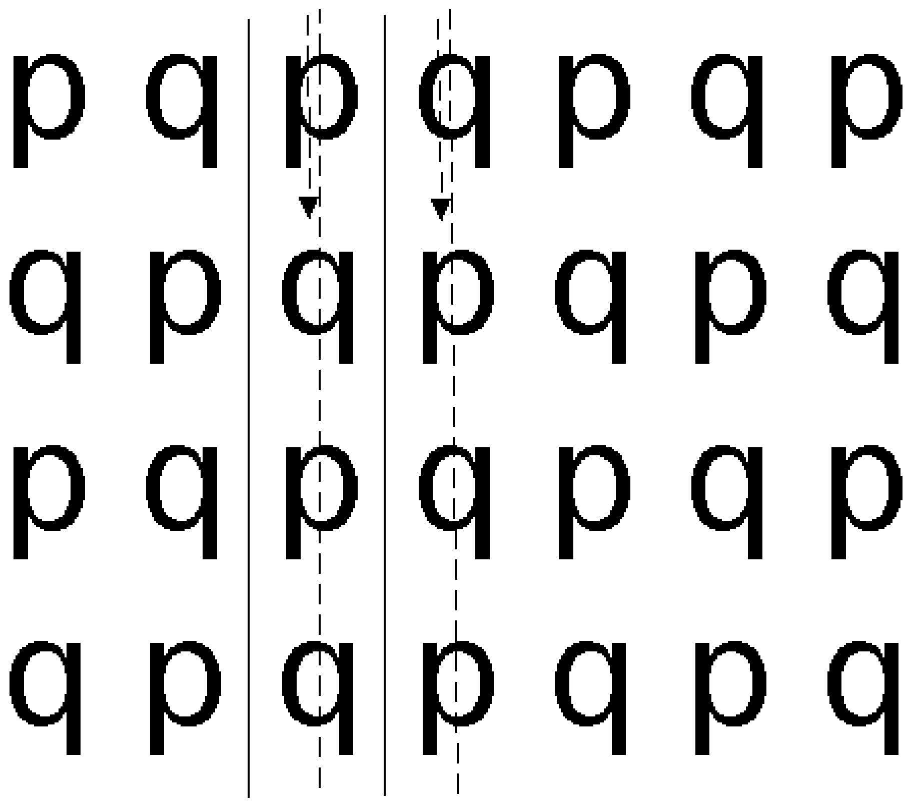

Fig. 4.23

The wallpaper pattern in figure 4.23 looks like **‘both’** a **pm** and a **pg**, as reflection axes alternate with glide reflection axes: it is in fact a ‘new’ type, known as **cm**.

4.4.2 <u>More perfectly shifted stackings.</u> What has made the patterns of figures 4.15, 4.18, and 4.23 different? Well, a straight stacking of the **pm11 “p q ”** border pattern simply preserved the border pattern’s reflection and created a **pm** wallpaper pattern in figure 4.15; a **'random'** shifting of every other row 'replaced' the reflection of the **pm** pattern by glide reflection and created a **pg** pattern in figure 4.18; and, finally, a **'perfect'** shifting of every other row 'preserved' the glide reflection of the **pg** pattern **and** 'revived' the lost reflection, creating a **cm** pattern. But, what do we mean by "perfect shifting"? Well, the following example may help you answer this question:

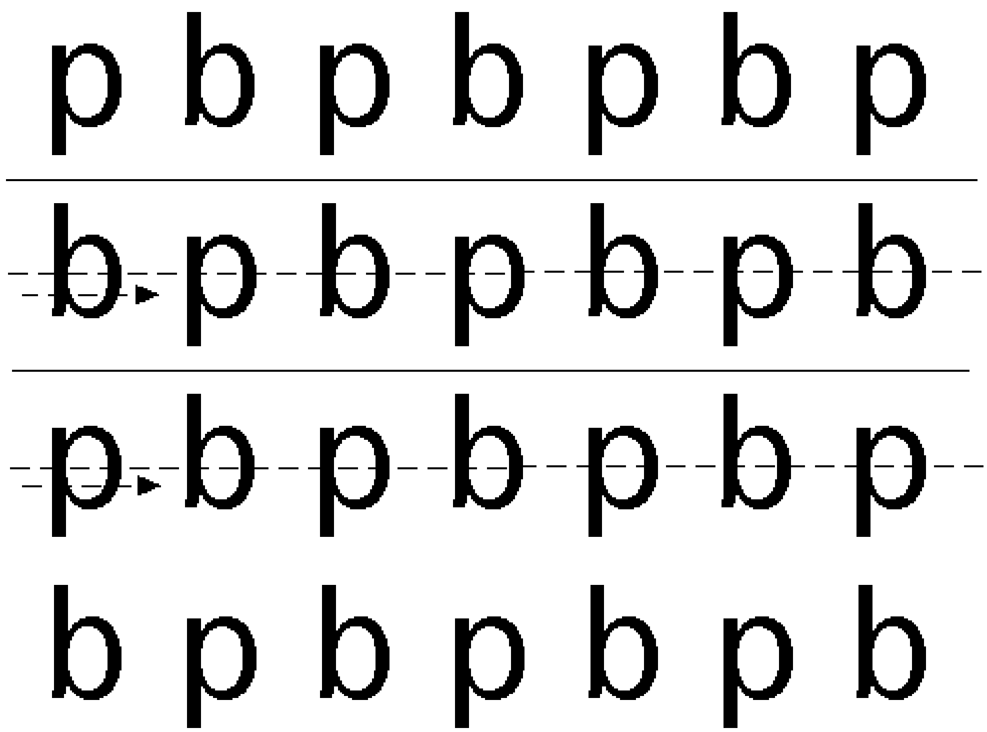

Fig. 4.24

We just obtained another **cm** wallpaper pattern, this one with horizontal reflection and glide reflection, stacking copies of the **"p b " p1a1** border pattern: just as in figure 4.23, placing every **p** straight below a **b** and vice versa allows for some reflection that we couldn't possibly have in the patterns of figures 4.20 & 4.21 (consisting of straight stackings and randomly shifted stackings of that **"p b "** border pattern, respectively). A closer look reveals that it was crucial to shift every other row by a vector equal to **half the minimal translation vector** of the original border pattern! That's what we mean by "perfect shifting", as opposed to "random shifting" (by a vector of length either strictly smaller or strictly bigger than half the minimal translation vector's length). By the way, the pattern in figure 4.11 is the result of a perfect shifting!

We leave it to you to check that perfectly shifted stackings of **p1m1** border patterns are **cm** wallpaper patterns, while their randomly shifted stackings are **pm** wallpaper patterns: you may of course use the **D**-pattern of figure 2.8 to verify this.

4.4.3 In-between glide reflection. Consider the following trapezoid-based wallpaper pattern:

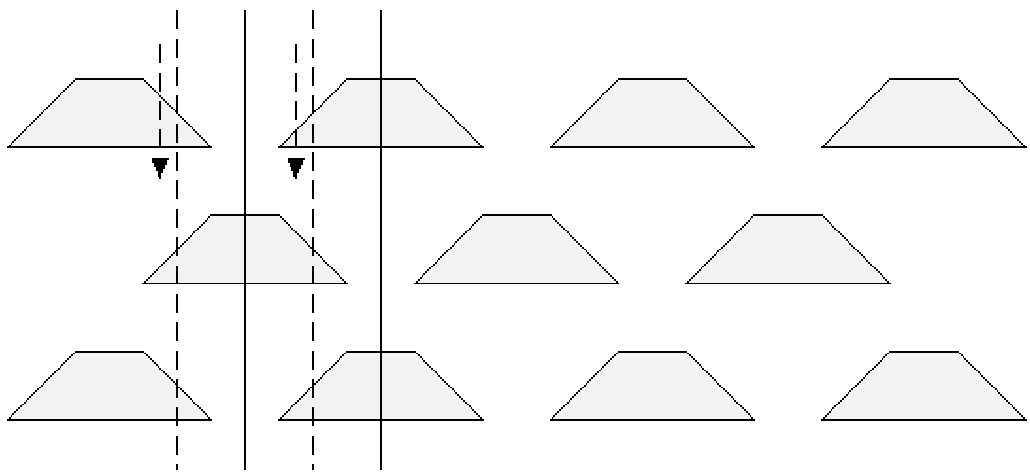

Fig. 4.25

Many students will typically see either all the reflections or half of them and quickly classify it as a **pm** pattern. Having just gone through 4.4.2, you are of course likely to recognize it as either a perfectly shifted version of the **pm** pattern of figure 4.16 or a perfectly shifted stacking of a **pm11** border pattern: either way, it is clearly a **cm** pattern!

Are there any ways of seeing the glide reflection **'directly'**? One could employ the machinery of chapter 3, as we did in 4.3.1, or resort to the idea discussed in 4.3.3. An easier approach takes advantage of the very structure of the **cm** type and the fact that its glide reflection axes always run **half way** between two nearest reflection axes: once you have determined the reflection axes in what seems to be a **pm** pattern, draw a line half way between them and check whether or not there is a vector that makes it work: if yes your pattern is a **cm**, if not your pattern 'remains' a **pm**. In short, every time you see reflections in a wallpaper pattern **check** whether or not there exists **in-between glide reflection**.

4.4.4 Phoenician funerary 'crowns'. The following design from a Phoenician tomb in Syria (***Stevens***, p. 202) shows that the **cm** type has been with us for a very long time; but this is the case with most, if not all, types of wallpaper patterns...

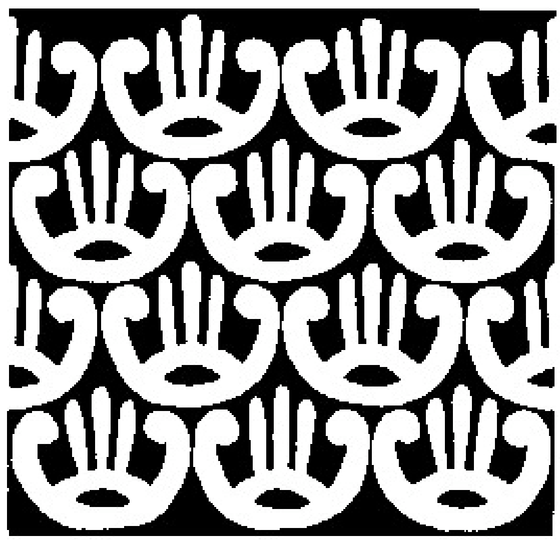

Fig. 4.26

The Phoenicians were a naval superpower more than twenty five centuries ago, but the **cm** remains popular with our times' superpower: next time you stand **close** to the Star-Spangled Banner, have a **careful** look at its stars!

4.4.5 Diagonal axes. Reflection and glide reflection axes do not always have to be 'vertical' or 'horizontal'; they may certainly run in every possible direction, and the concept of direction is a **relative** one, as it changes every time you rotate the page a bit! Here we present an interesting example of a **cm** pattern with easy-to-see **'diagonal'** reflection and more subtle in-between glide reflection:

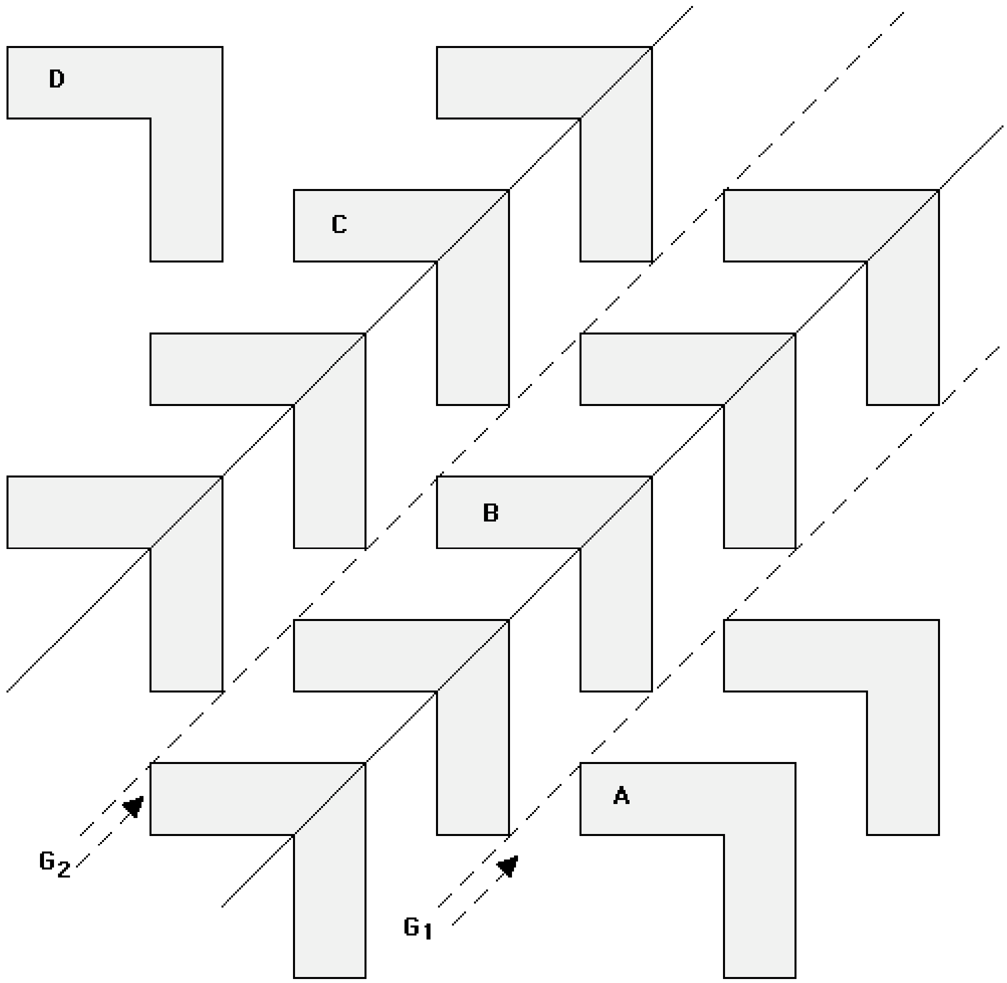

Fig. 4.27

Under glide reflection $\mathbf{G_1}$, for example, **A** is mapped to **B**, while glide reflection $\mathbf{G_2}$ maps **A** to **D** and **B** to **C**, etc.

4.4.6 Only one kind of axes! While our examples in sections 4.2 and 4.3 show that there are always two kinds of reflection and glide reflection axes in **pm** and **pg** wallpaper patterns, respectively (both in the same direction, of course), all the examples in this section clearly indicate that every **cm** wallpaper pattern has only **one** kind of reflection axes and only **one** kind of glide reflection axes as well. We elaborate on this observation in 6.4.4 and 8.1.5, as well as in 4.11.2. For the time being we would like to point out that, in the case of the **cm**, it seems that whatever we **gained** in terms of symmetry we **lost** in terms of diversity! In other words, whenever all vertical reflection axes look the same to you, look out for that in-between glide reflection: your pattern is probably not a **pm** but a **cm**! Likewise, if all the glide reflection axes in a seemingly **pg** pattern look the same to you, then either you have **missed the 'other half'** of the glide reflection or you have **achieved the impossible**: you saw the glide reflection without seeing the reflection ... and your pattern is probably a **cm** rather than a **pg**!

4.5 180^0, translations only (p2)

4.5.1 <u>Stacking **p112**s.</u> Replacing the **"p "** border pattern of 4.1.1 by the **"p d "** border pattern, we obtain the following wallpaper patterns, direct analogues of the **p1** patterns in figures 4.10 & 4.11:

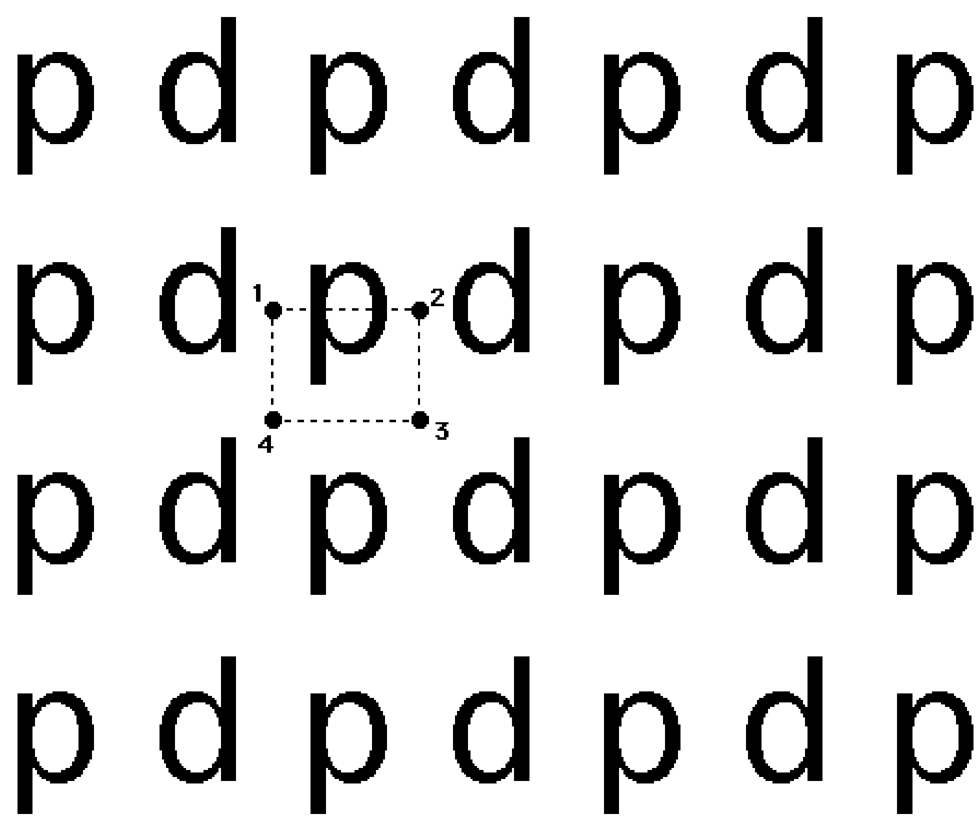

Fig. 4.28

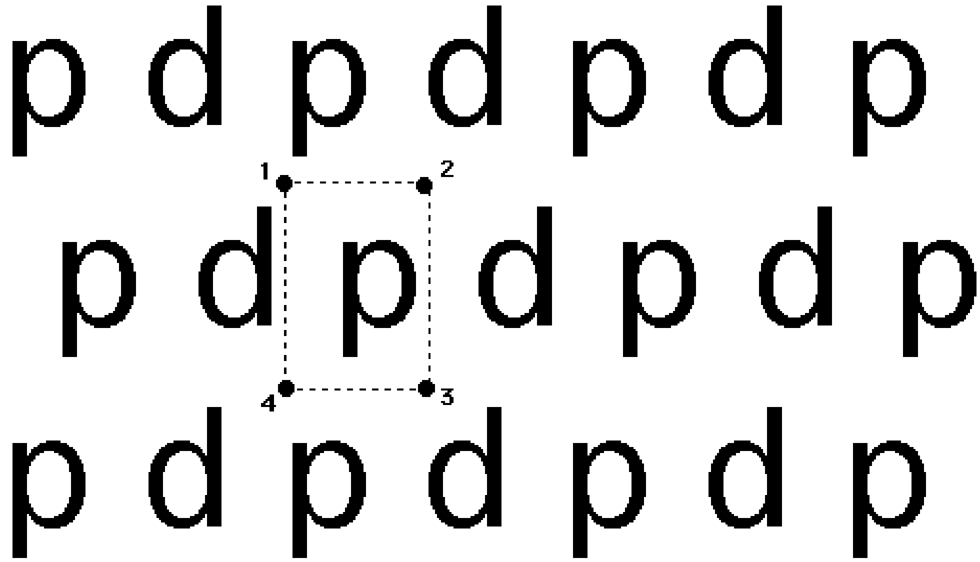

Fig. 4.29

Such patterns, having nothing but **half turn** -- in addition to translation, always -- are known as **p2**. As you can see, there exist **four kinds** of rotation centers, nicely arranged at the **vertices of rectangles** (and numbered **1**, **2**, **3**, **4**). These rectangles are usually mere **parallelograms** -- as in figure 8.18, think for example of a **p2 tiling** of the plane by copies of a single parallelogram -- but they may on occasion be rhombuses or even squares:

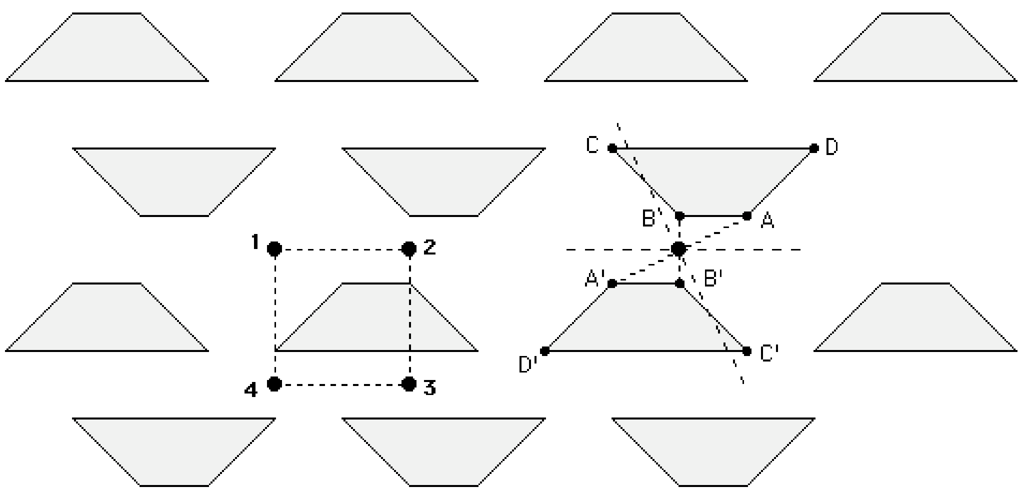

Fig. 4.30

4.5.2 When is the twofold rotation there? How could you tell that the wallpaper pattern in figure 4.28 has 180^0 rotation without some familiarity with the **p112** border pattern that created it? Well, the easiest way is to turn the page upside down and decide whether or not the pattern still looks the same ... keeping always in mind the fact that all patterns are **infinite**. It is always better, on the other hand, to be able to determine some 180^0 rotation centers: this you can do either based on your intuition and experience or following methods from chapter 3, as shown in figure 4.30; and then you can always confirm your findings using tracing paper!

As we will see in the next four sections, it is easier to find the twofold rotation centers when the given pattern happens to have some (glide) reflection: then the location of the rotation centers is, more or less, **predictable**. Within the **p2**, once you have found **one** center, you can use the pattern's **translations** to locate **all** the others: indeed a look at figures 4.28-4.31 will convince you that the lengths of the sides of those 'center parallelograms' are equal to **half the length** of the pattern's **minimal translation vectors** (to which the sides themselves are **parallel**); more on this in 7.6.4!

4.5.3 Italian curves. How about finding all four kinds of 180^0 rotation centers in this modern Italian ceramic (***Stevens***, p. 213)?

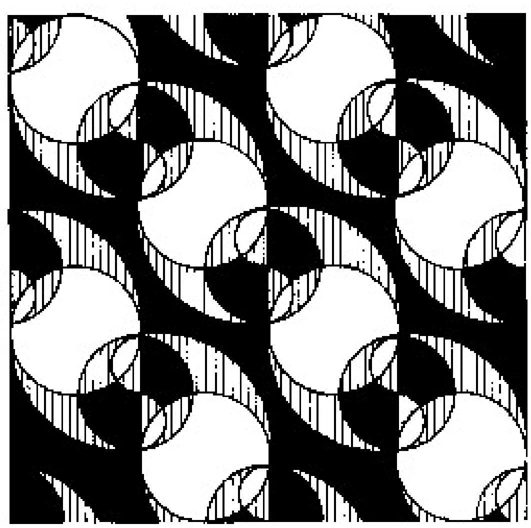

Fig. 4.31

4.6 180^0, reflection in two directions (pmm)

4.6.1 <u>Stacking **pmm2**s.</u> Rather predictably in view of what we saw in earlier sections, straight stackings of **pmm2** border patterns have both 180^0 rotation and reflection in **two** directions:

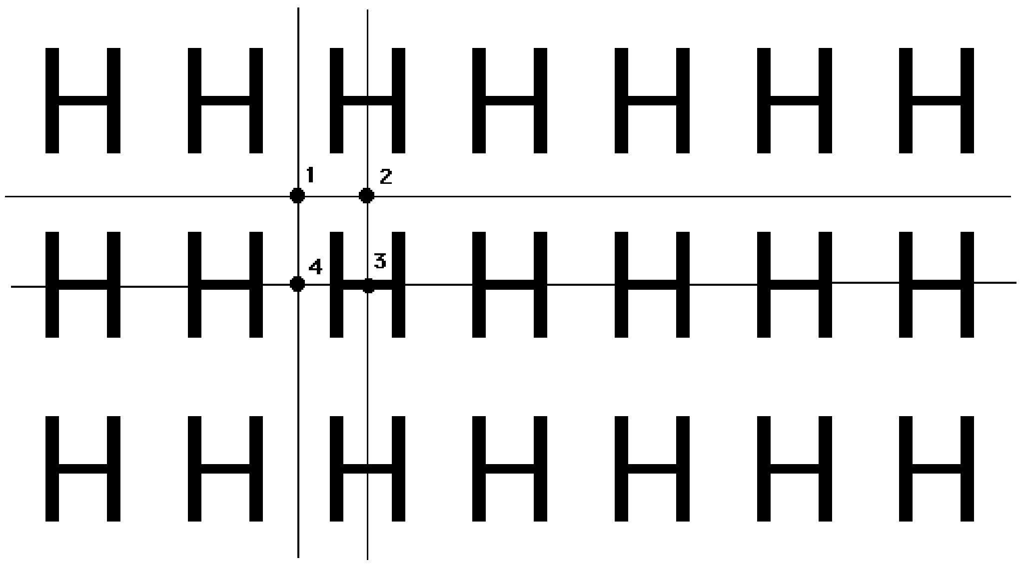

Fig. 4.32

There is nothing too tricky about this new type of wallpaper pattern, known as **pmm**: it has reflection axes (of two kinds) in **two perpendicular directions** and four kinds of 180^0 rotation centers, all of them located at the **intersections of reflection axes**. This last observation gives you a chance to practice your geometry a bit and try to explain why, as first noticed in 2.7.1, the intersection of two perpendicular reflection axes yields a 180^0 rotation center: this is a special case of a more general fact discussed in 7.2.2!

4.6.2 <u>Native American 'gates'.</u> Here is a Nez Perce′ **pmm** pattern from ***Stevens*** (p. 244), not quite dominated by the **pmm**'s stillness:

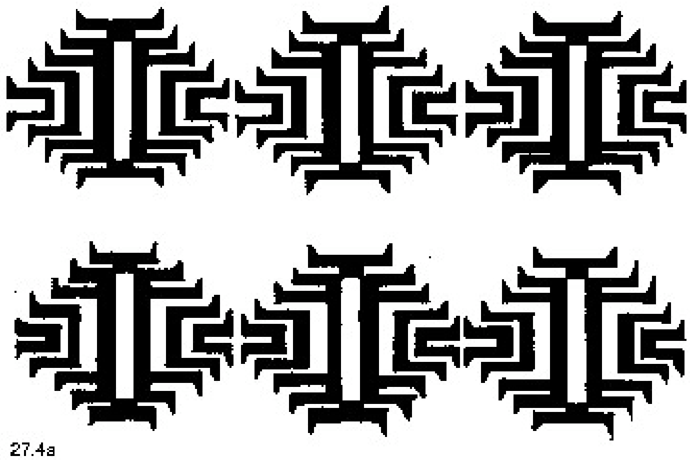

Fig. 4.33

4.6.3 More examples. While the ‘building blocks’ in the wallpaper patterns of figures 4.32 & 4.33 had a lot of symmetry themselves ($\mathbf{D_2}$ sets), it is certainly possible to build **pmm** patterns employing less symmetrical motifs (still creating $\mathbf{D_2}$ fundamental regions though), as figures 4.34 & 4.35 demonstrate:

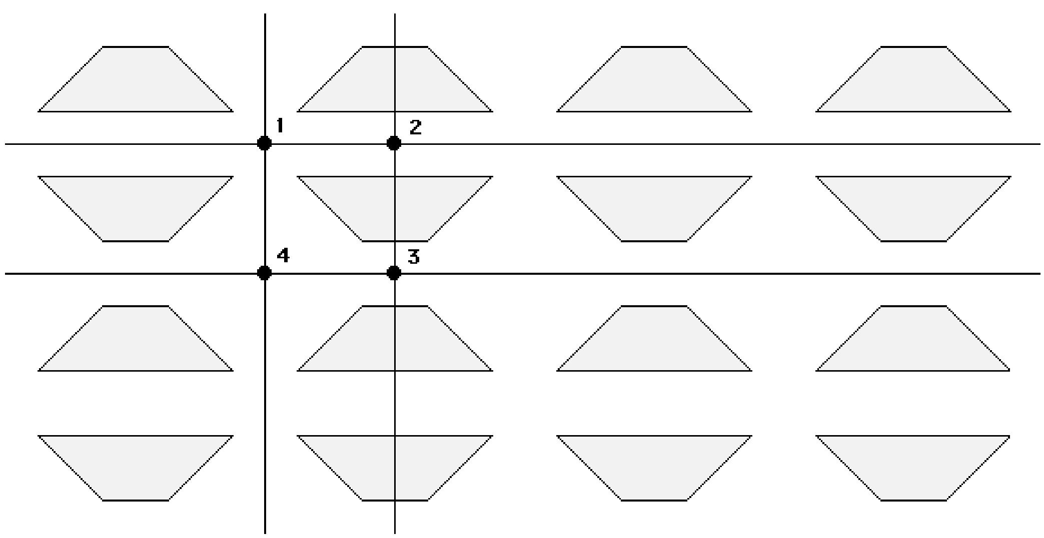

Fig. 4.34

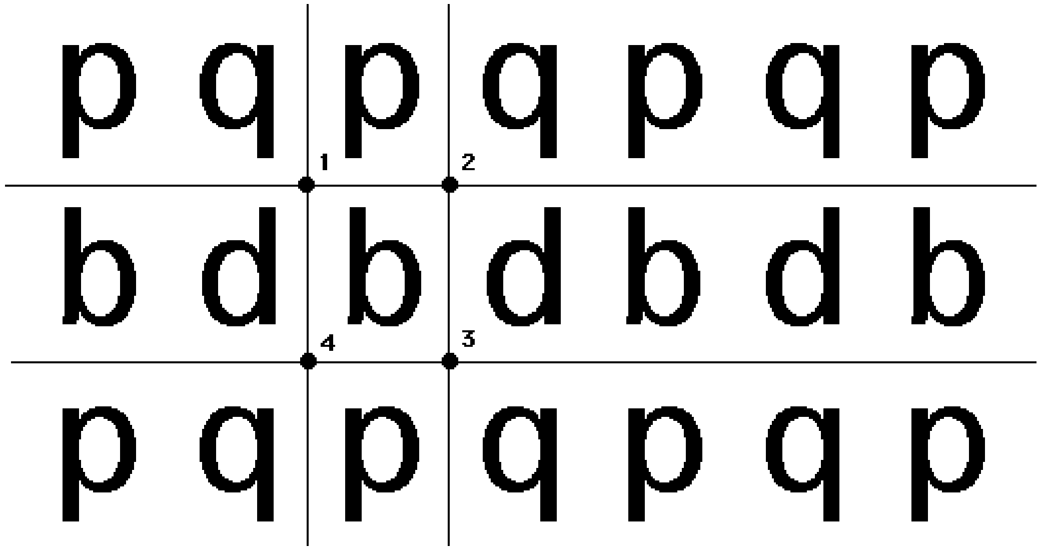

Fig. 4.35

4.7 180^0, reflection in one direction with perpendicular glide reflection (pmg)

4.7.1 <u>Shifted stackings of **pmm2**s.</u> Let’s look at a randomly shifted stacking of the **“H ”** border pattern employed in figure 4.32:

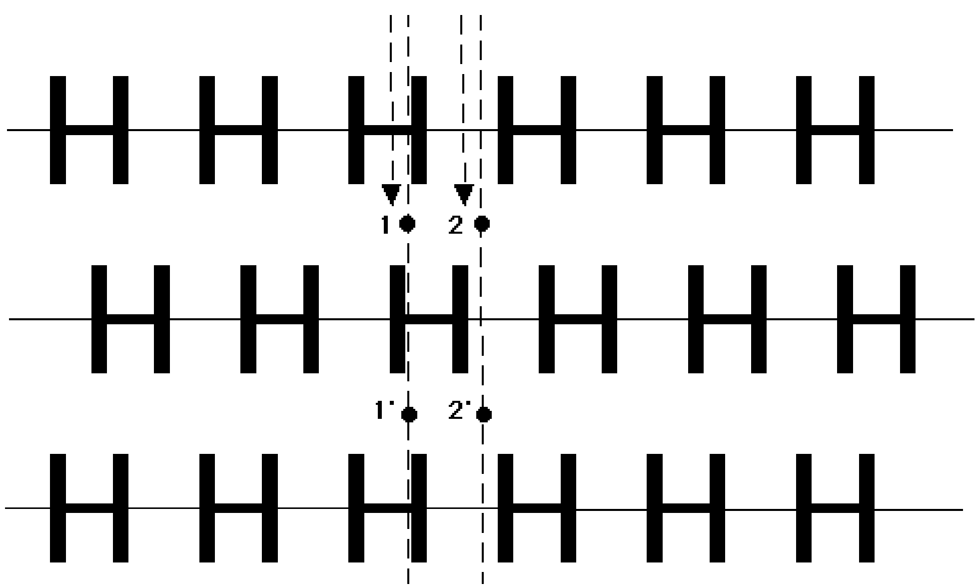

Fig. 4.36

4.7.2 <u>Straight stackings of **pma2**s.</u> Let's also look at a straight stacking of a **pma2** border pattern similar to the one in figure 2.24:

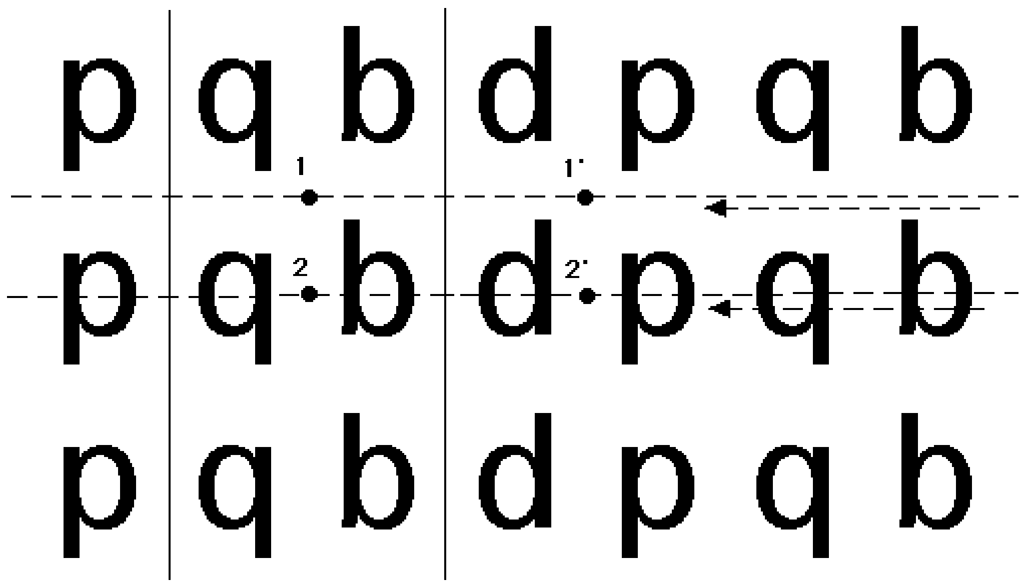

Fig. 4.37

4.7.3 <u>What is going on?</u> As we have indicated above, both wallpaper patterns created have 180^0 rotation, reflection in one direction (horizontal in figure 4.36, vertical in figure 4.37), and glide reflection in one direction as well (vertical in figure 4.36, horizontal in figure 4.37). In both cases, the directions of reflection and glide reflection are **perpendicular** to each other, with **all the rotation centers on glide reflection axes**, **half way between two reflection axes**: this type of 180^0 wallpaper pattern is known as **pmg**. Here are two more examples employing, once again, trapezoids:

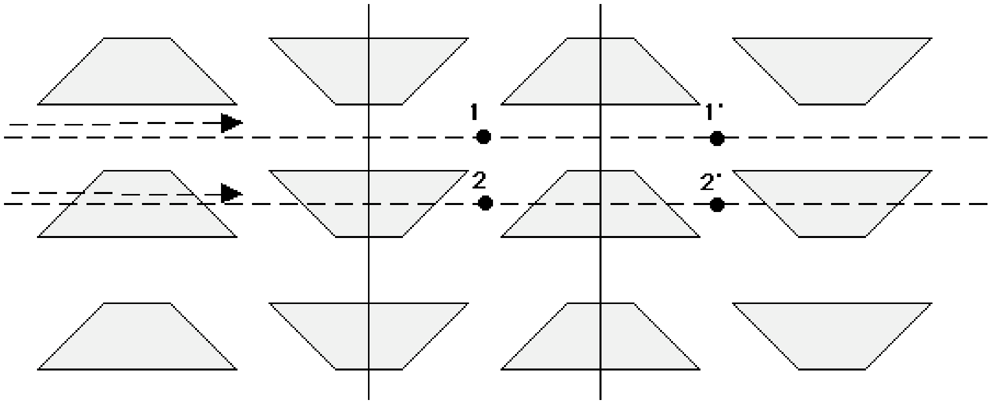

Fig. 4.38

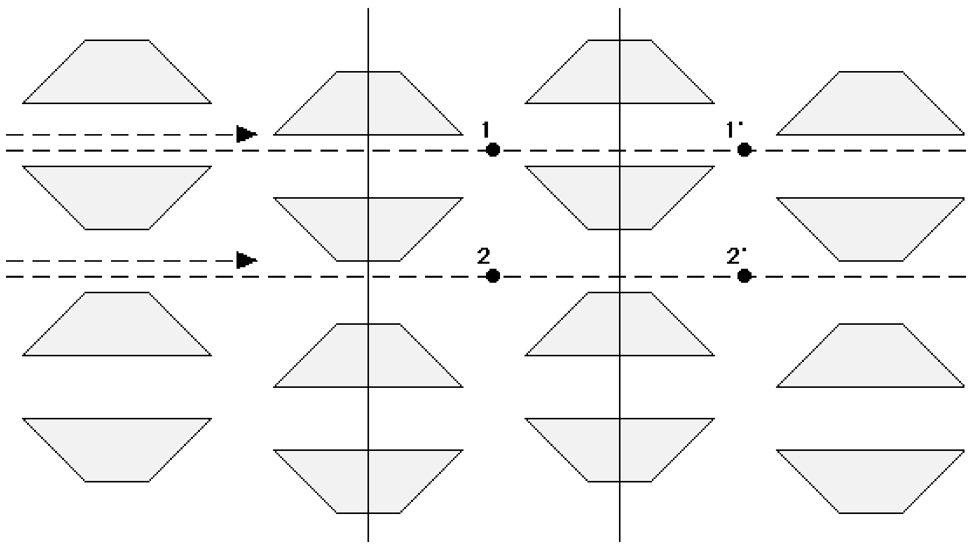

Fig. 4.39

While all four wallpaper patterns in figures 4.36-4.39 belong to the same type (**pmg**), they do not necessarily 'look' the same; for example, the ones in figures 4.36 & 4.39 (**randomly** shifted stackings of a **pmm2** border pattern) create a feeling of a wave-like motion, while the ones in figures 4.37 & 4.38 (straight stackings of a **pma2** border pattern) create an impression of two flows in opposite directions. More significantly, there are **glide reflection axes of two kinds** in all four examples. It is tempting to say the same about reflection axes (especially in figures 4.37 & 4.38), but not quite so if we are 'cautious' enough to **turn** the patterns upside down: we elaborate further on this in 4.11.2. (Likewise concerning the **numbering** of half turn centers in figures 4.36-4.39!)

How does one recognize a **pmg** pattern? Basically, look for a 180^0 pattern with **reflection in only one direction** -- as we are going to see the **pmg** is the **only** 180^0 wallpaper pattern with reflection in only one direction -- and then use all the other observations made in this section for confirmation.

4.7.4 Chinese pentagons. The following **pmg** example of a Chinese window lattice (***Stevens***, p. 221) comes close to a famous **impossibility** (tiling the plane with **regular** pentagons):

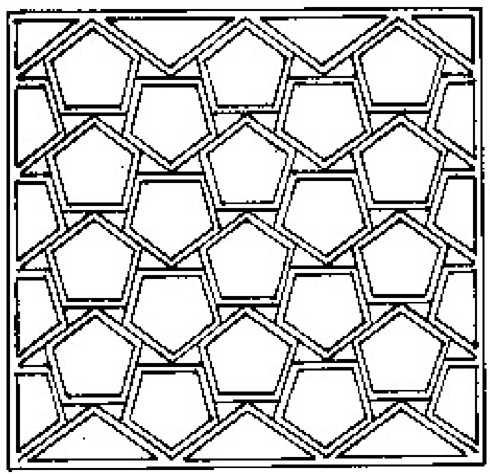

25.7n

Fig. 4.40

4.8 180^0, glide reflection in two directions (pgg)

4.8.1 Shifted stackings of **pma2**s. In the same way that going from straight to shifted stackings of **pmm2**s substituted reflection by glide reflection in **one** of the two directions (and 'reduced' the symmetry type from **pmm** to **pmg**), going from straight to shifted stackings of **pma2**s replaces the reflection by glide reflection and 'reduces' the symmetry type from **pmg** to **pgg**:

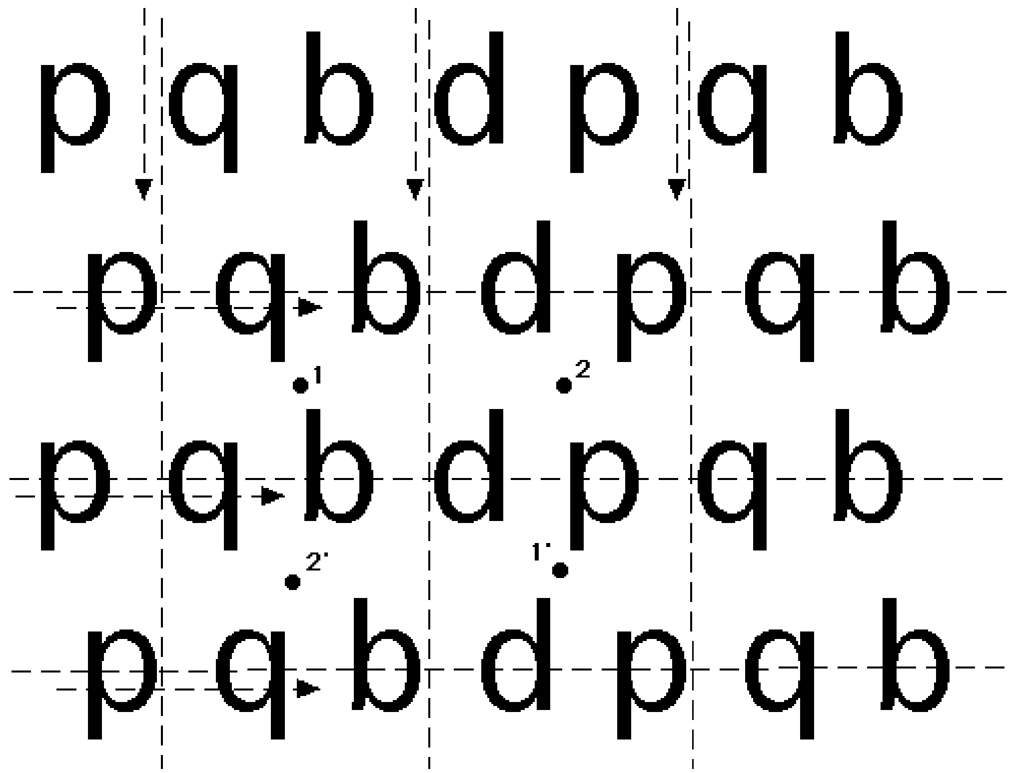

Fig. 4.41

A brief review of figures 4.18 & 4.21 would make it easier for you to realize that the wallpaper pattern in figure 4.41 has the indicated glide reflections, in **two perpendicular directions**. It should also be easy for you by now to locate the 180^0 rotation centers (of **two** kinds, actually) and confirm that each of them lies **right between four glide reflection axes**. There is no reflection. Wallpaper patterns of this type are known as **pgg**.

4.8.2 Between **p2** and **pgg**. Distinguishing between **p2** and **pgg** -- especially in the presence of **'rectangularly ruled'** half turn centers characteristic of glide reflection (8.2.2) -- is not that easy. Reversing our advice in 4.8.1, we suggest that every time you determine **all** the 180^0 rotation centers in a wallpaper pattern you should subsequently check the lines passing **right between rows or columns of rotation centers**: those **could** be glide reflection axes! In general, the presence of **heterostrophic motifs** in a pattern (such as **p** and **q** in figures 4.18 & 4.41) is a major indication in favor of glide reflection (4.3.3). Things can get a bit trickier in case the pattern's 'building blocks' are $\mathbf{D_1}$ (rather than $\mathbf{C_1}$) sets:

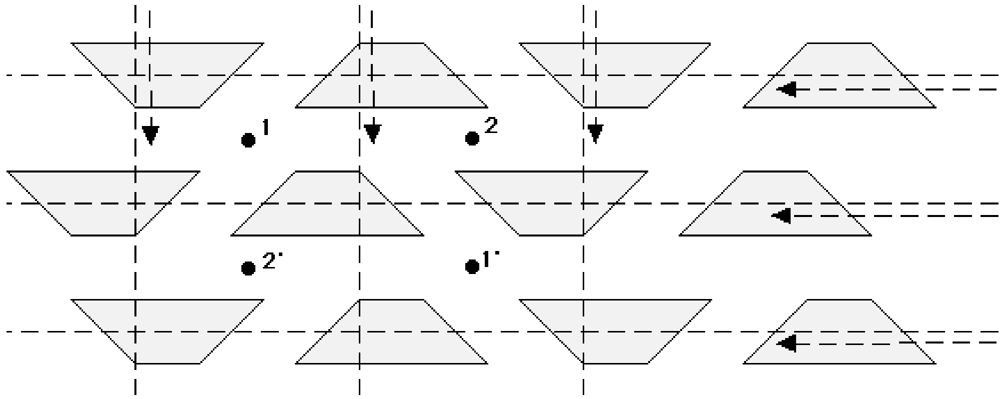

Fig. 4.42

4.8.3 <u>Two kinds of axes?</u> Observe that the **pgg** patterns in figures 4.41 & 4.42 **appear** to have two kinds of vertical glide reflection axes: we must stress at this point that remarks similar to the ones made in 4.7.3 do apply! Anyway, returning now to $\mathbf{C_1}$ motifs, or cutting the trapezoids of the pattern in figure 4.42 in half if you wish, here is a **pgg** pattern that **appears** to have two kinds of glide reflection axes in **both** directions:

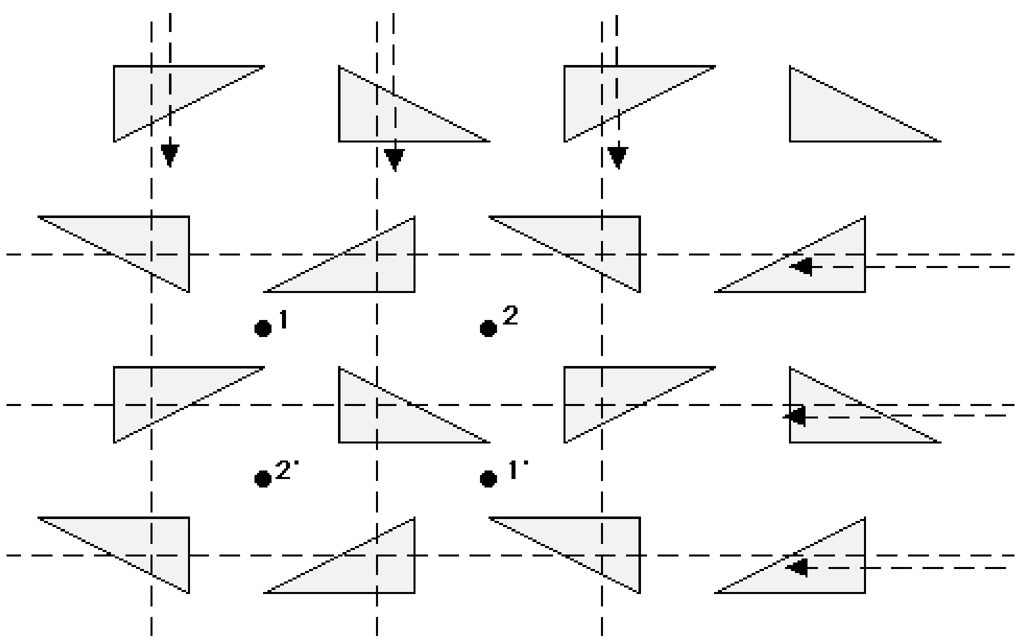

Fig. 4.43

4.8.4 Congolese parallelograms. The following **pgg** example from ***Stevens*** (p. 236), full of **heterostrophic parallelograms**, should allow you to practice your skills in determining glide reflection axes:

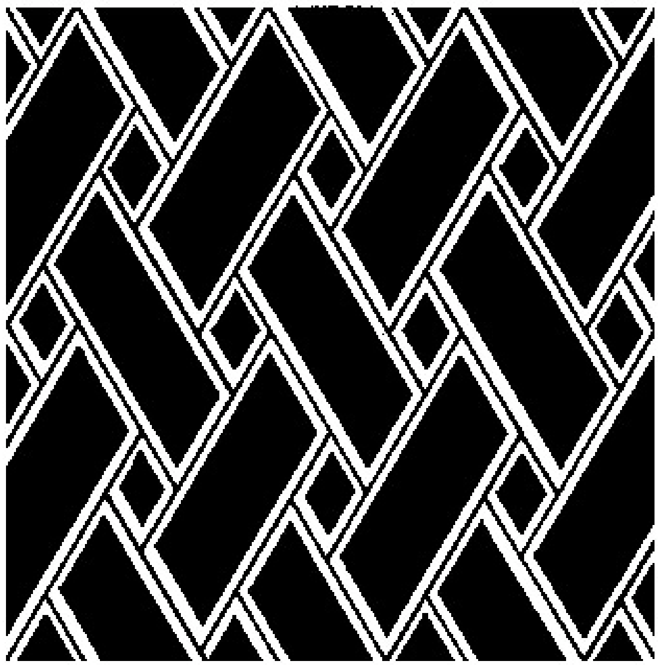

26.6a

Fig. 4.44

4.9 180^0, reflection in two directions with in-between glide reflections (cmm)

4.9.1 Perfectly shifted stackings of **pma2**s and **pmm2**s. In the same way perfectly shifted stackings of **pm11**, **p1a1**, and **p1m1** border patterns created a 'new' type of wallpaper pattern (**cm**) in section 4.4, perfectly shifted stackings of **pma2** and **pmm2** border patterns create a two-directional analogue of **cm** as shown below:

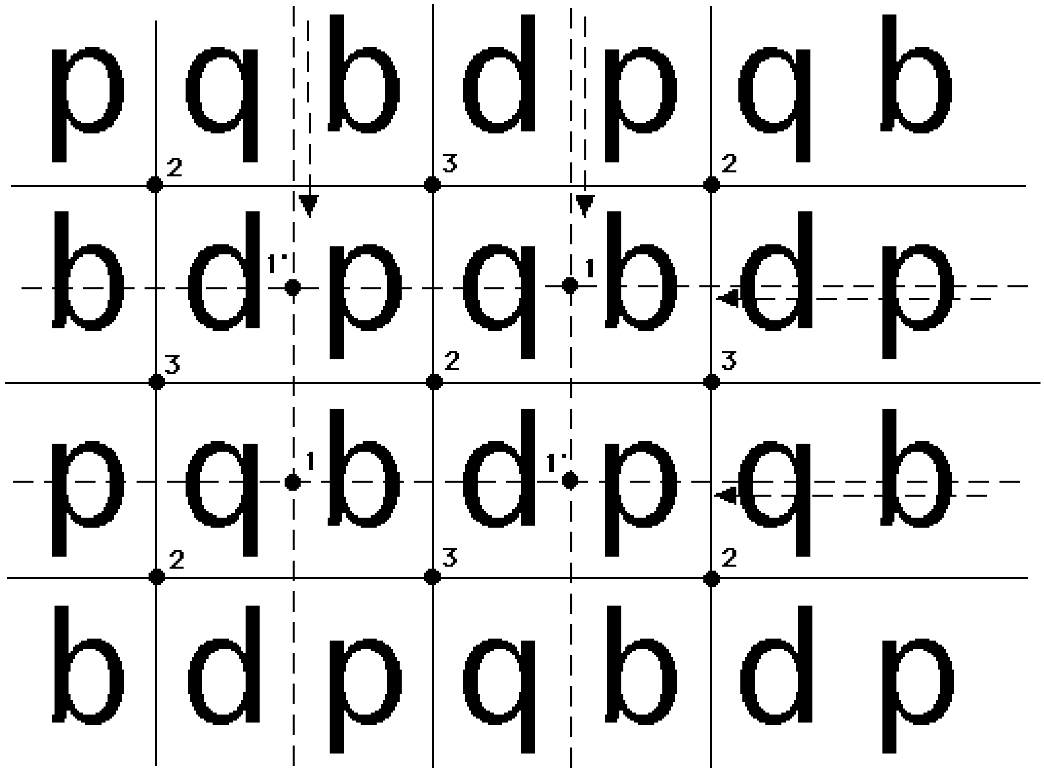

Fig. 4.45

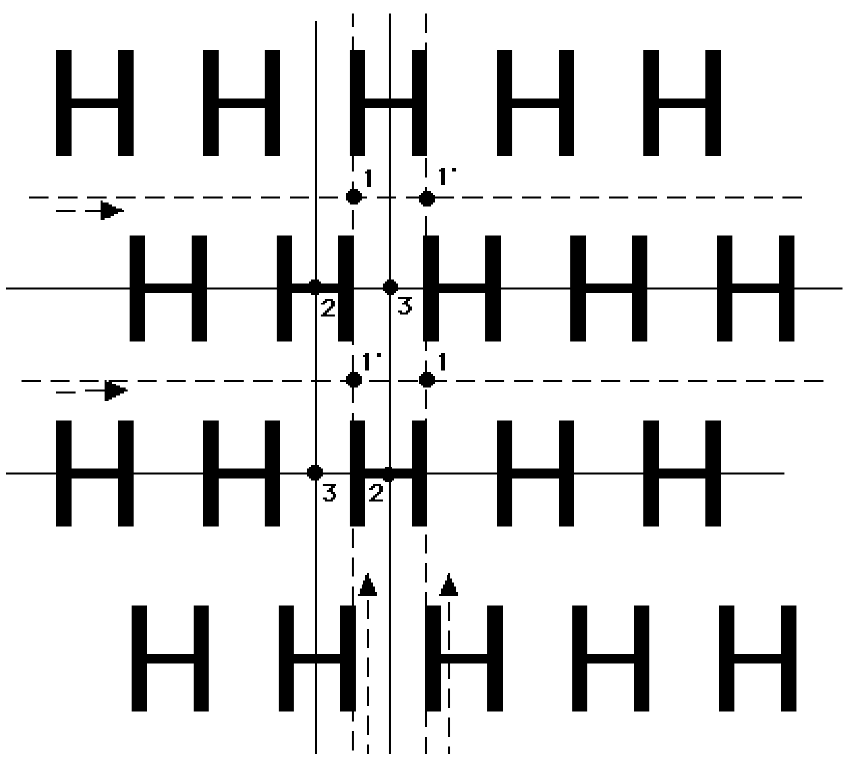

Fig. 4.46

There is nothing too surprising about this new type of wallpaper pattern to those familiar with the **cm** and **pmm** patterns: there is reflection and in-between glide reflection in **two perpendicular directions**; within each direction, both reflection and glide reflection axes are of **one kind only**; 180^0 rotation centers are found at the intersections of reflection axes and -- the only new element -- at the **intersections of glide reflection axes** as well. This new type, very rich in terms of symmetry, is known as **cmm**, and its last property is perhaps the easiest way to distinguish it from the **pmm** type: in the **pmm** pattern **all** rotation centers lie on reflection axes, in the **cmm** pattern **half** of them do **not**. Since locating the rotation centers can at times be trickier than finding the glide reflection axes, another obvious way of distinguishing between **pmm** and **cmm** is the latter's in-between glide reflection. Either way, once **all** reflection axes have been determined, you know where to look for both glide reflection axes and rotation centers!

4.9.2 Shifting back and forth to other types. Quite clearly, the **cmm** pattern of figure 4.45 is a close relative, or a 'shifted version', if you wish, of the **pmg** pattern in figure 4.37 and the **pgg** pattern in figure 4.41. Likewise, the **cmm** pattern of figure 4.46 is related to the **pmm** pattern of figure 4.32 and the **pmg** pattern of figure 4.36. Here are two more, trapezoid-based, **cmm** patterns the 'shifting relations' of which to previously presented examples you may like to investigate:

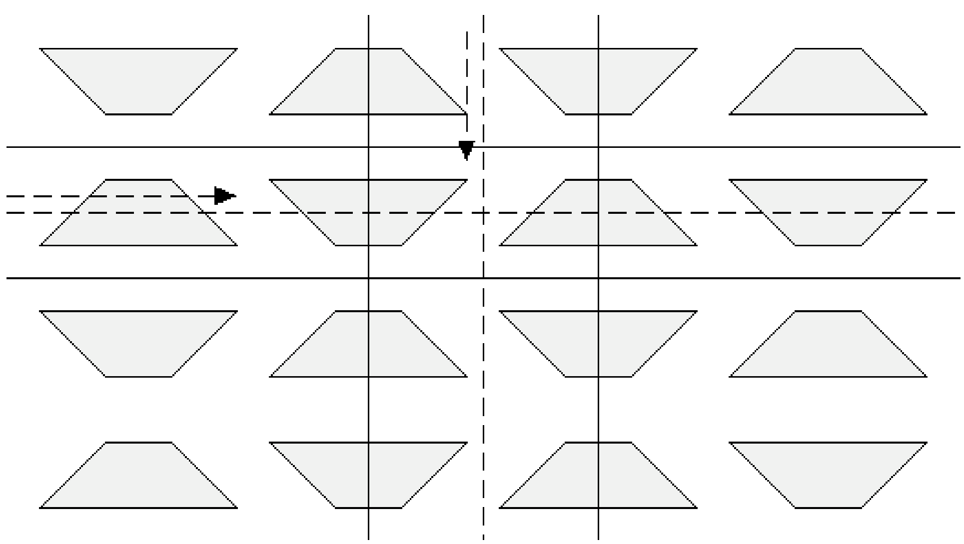

Fig. 4.47

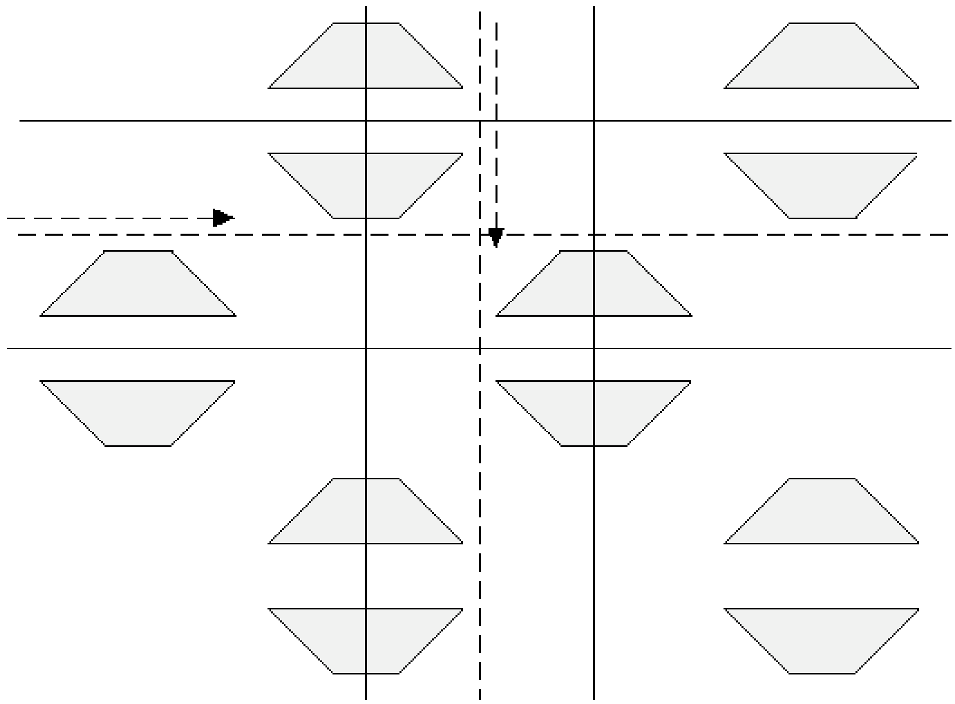

Fig. 4.48

4.9.3 Turkish arrows. Here comes our long-awaited real-world example of a **cmm** pattern, a 16th century Turkish design from ***Stevens*** (p. 250); make sure you can find all the rotation centers!

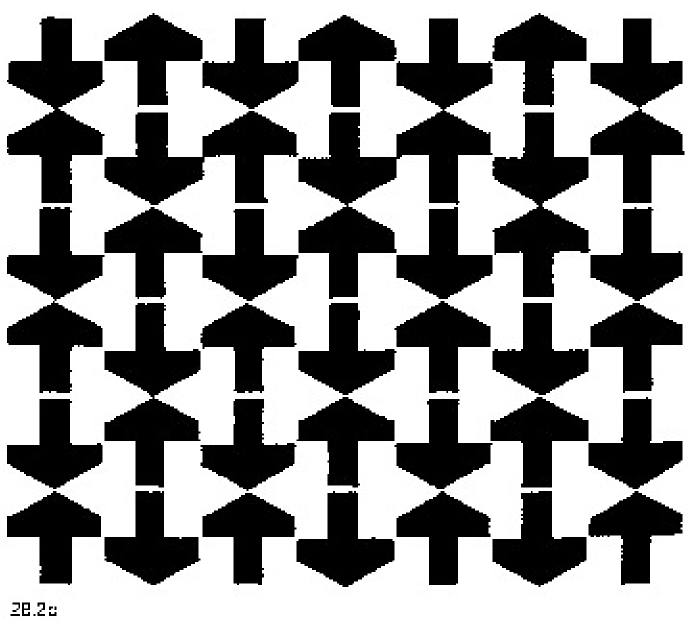

Fig. 4.49

4.9.4 <u>The world's most famous **cmm** pattern ...</u> is no other than the all-too-familiar **brick wall**:

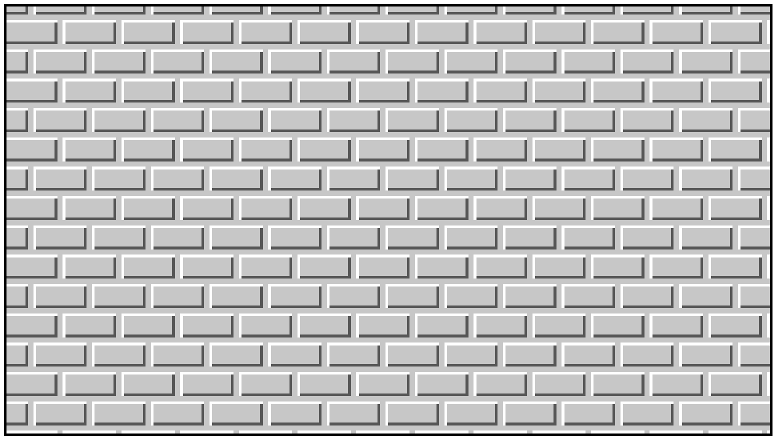

Fig. 4.50

We have already discussed the **bathroom wall** in section 4.0**:** as you will see right below, the two walls **are** mathematically distinct!

4.10 90^0, four reflections, two glide reflections (p4m)

4.10.1 <u>The bathroom wall revisited.</u> How would one classify the bathroom wall in case he or she misses its 90^0 rotation, already discussed in 4.0.3? It all depends on which reflections one goes by! Indeed, looking at its vertical and horizontal reflections only, the bathroom wall would certainly look like a **pmm**: two kinds of axes, no in-between glide reflection... If, on the other hand, one focuses only on the diagonal reflections, then the bathroom wall looks like a **cmm**: for there does indeed exist some 'unexpected' (yet **in-between**) glide reflection, as demonstrated in figure 4.51:

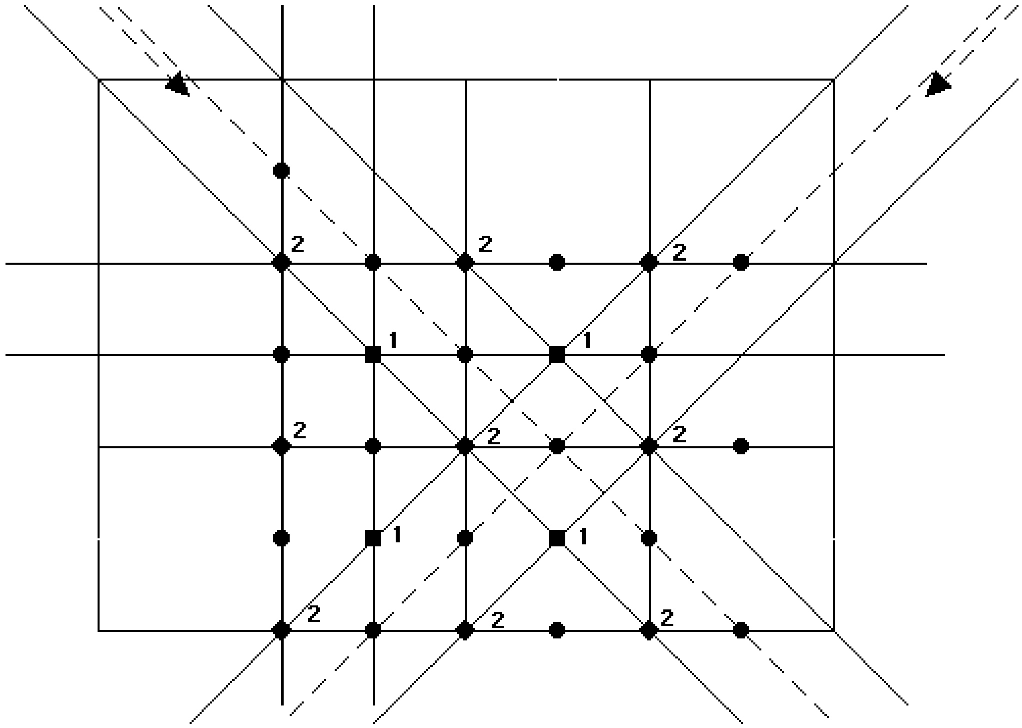

Fig. 4.51

Well, our 180^0 dreams are over! The bathroom wall is clearly full of 90^0 rotation centers, as pointed out in 4.0.3 and shown in figures 4.5 & 4.51. Moreover, 180^0 patterns may have reflection in at most two directions, and, as we will see in section 7.2, the intersection point of two reflection axes intersecting each other at a 45^0 angle is always a center for a 90^0 rotation. On the other hand, the bathroom wall has many 180^0 rotation centers, too: again, we first noticed that in 4.0.3, where it was also pointed out that there are **two kinds** of fourfold (90^0) centers, as opposed to only **one kind** of 180^0 centers; notice also the 90^0-45^0-45^0 triangles formed by two fourfold centers (one of each kind) and one twofold center (figure 4.51), something that will be further analysed in 6.10.1 and 7.5.1. Finally, observe that 90^0 and 180^0 centers are always at the intersection of **four** and **two** reflection axes, respectively. Wallpaper patterns having all these remarkable properties are known as **p4m**, and they are the only ones having **reflection in precisely four directions**.

4.10.2 <u>The role of the squares.</u> Do we always get 90^0 rotation in wallpaper patterns formed by square motifs? The answer is a flat "no", as demonstrated by a familiar floor tiling:

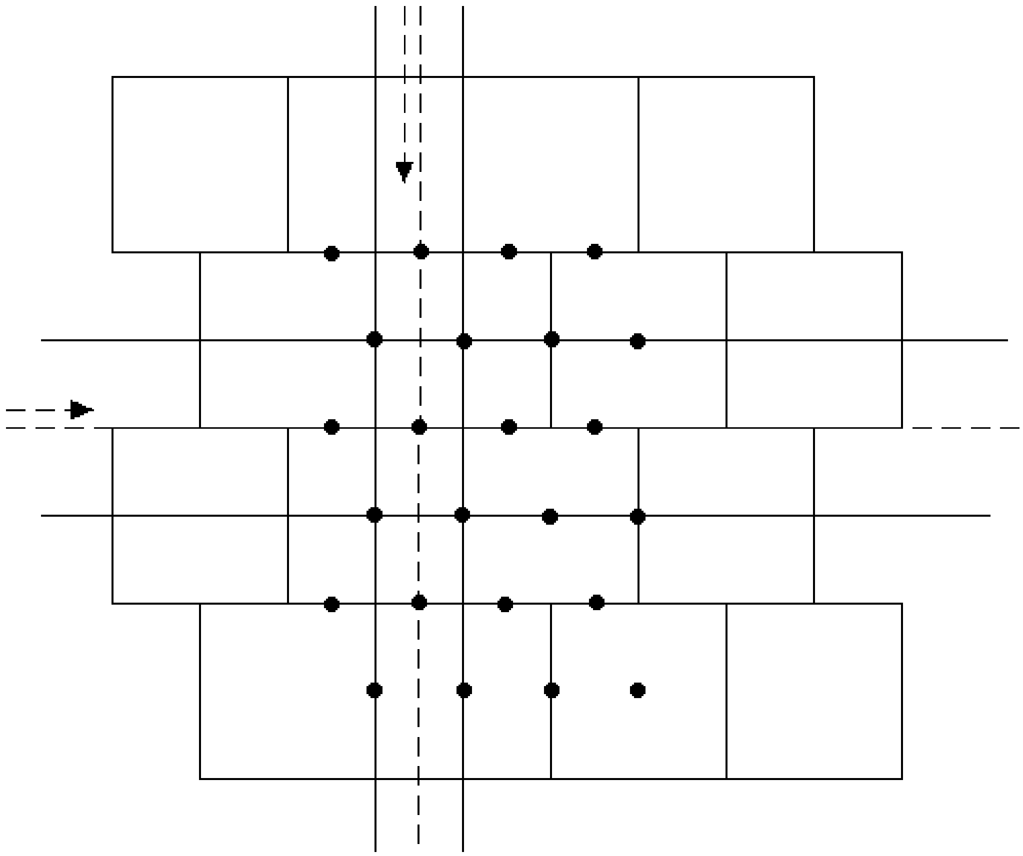

Fig. 4.52

The pattern in figure 4.52 is somewhere between the bathroom wall and the brick wall of 4.9.4, a perfectly shifted version of the former yet much closer to the latter mathematically: they both belong to the **cmm** type. Other shiftings of the bathroom wall will easily produce **pmg** patterns, and you should also be able to produce the other 180^0 (or even 360^0) wallpaper patterns using square motifs by being a bit more imaginative!

Reversing the question asked two paragraphs above, can we say that **p4m** patterns are always formed by square motifs? The answer is again "no", and the following modification of the **cmm** pattern of figure 4.48 provides an easy counterexample:

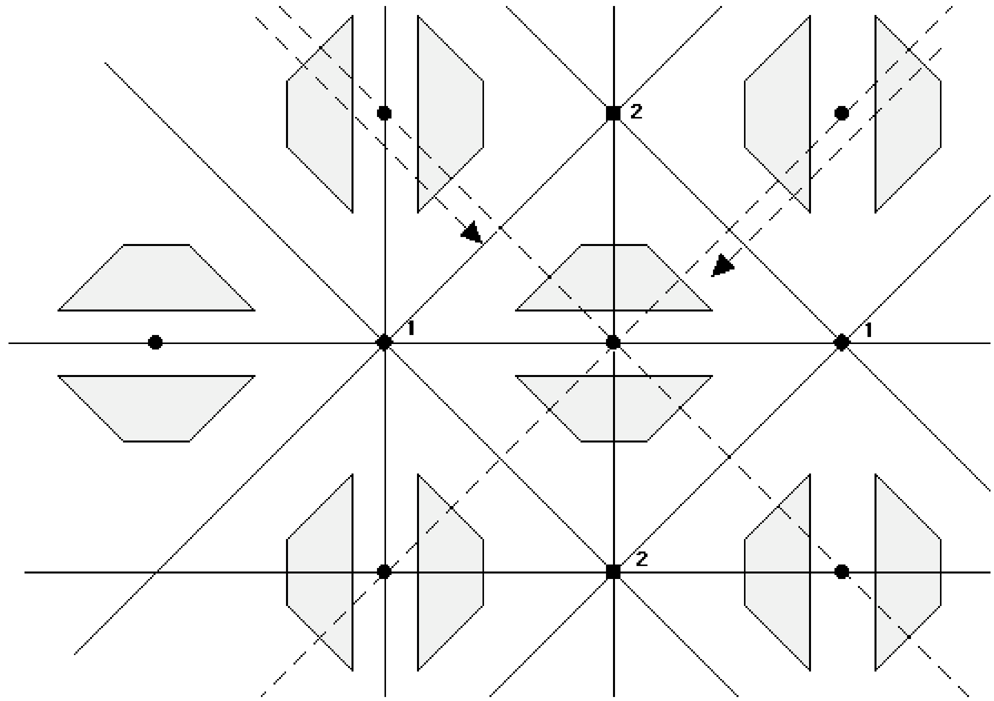

Fig. 4.53

4.10.3 Byzantine squares. The following example from ***Stevens*** (p. 308) stresses the **p4m**'s glide reflections:

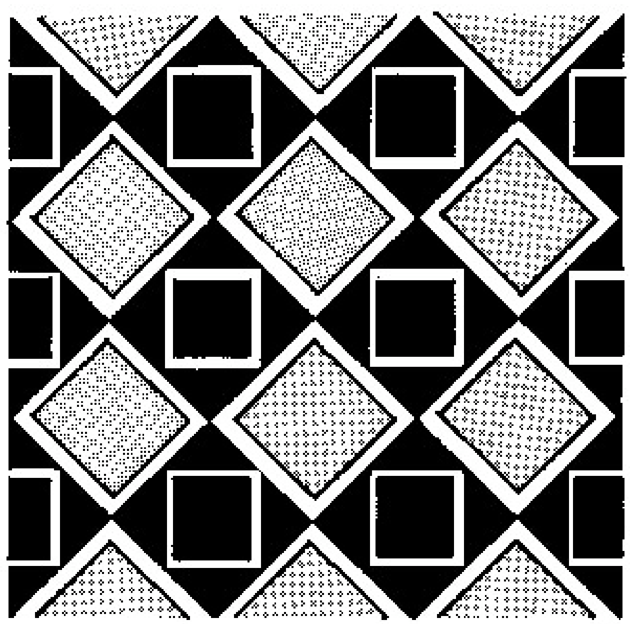

Fig. 4.54

4.11 90^0, two reflections, four glide reflections (p4g)

4.11.1 Similar processes, different outcomes. In 4.10.2 we rotated the motifs in **every other column** of the 'squarish' **cmm** pattern of figure 4.48 by 90^0 and ended up with the **p4m** pattern in figure 4.53. Here is what happens when we rotate the motifs in **every other 'diagonal'** of the **pmm** pattern of figure 4.34:

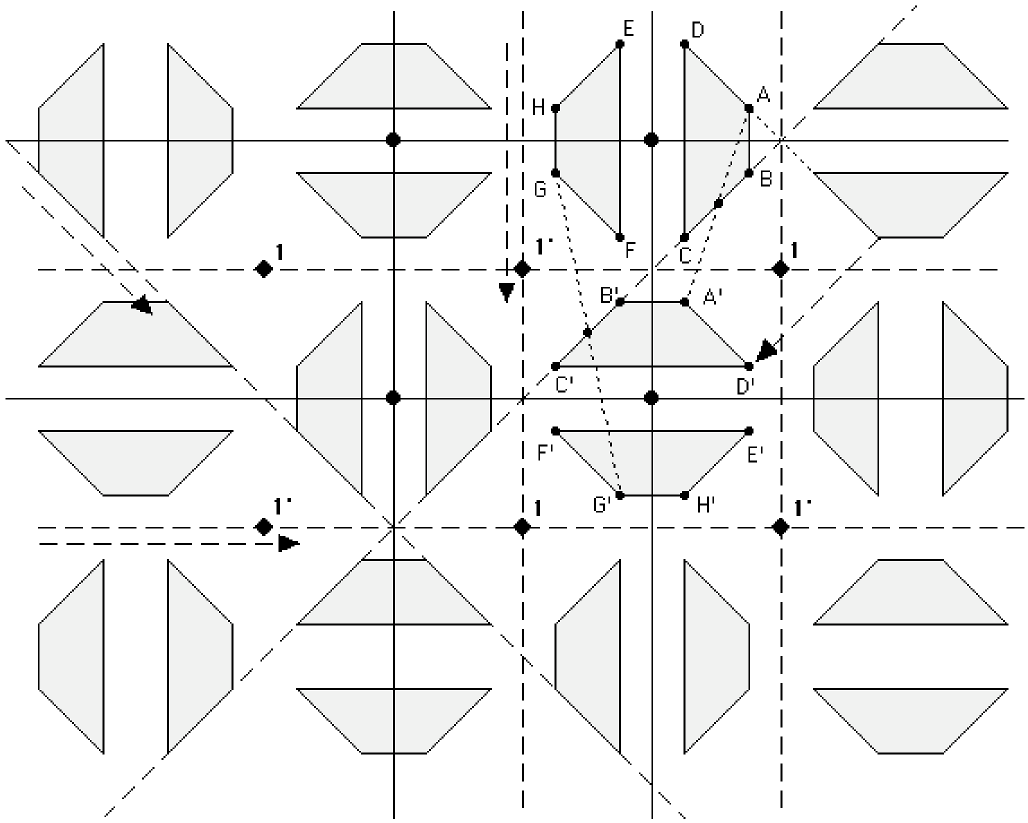

Fig. 4.55

The derived pattern looks very much like a **cmm**, having vertical and horizontal reflection and in-between glide reflection. There are, **as always** (4.6.1), 180^0 rotation centers at the intersections of perpendicular reflection axes. What happens at the **much less predictable** intersections of perpendicular **glide** reflection axes?

Well, those intersections are centers for **90^0**, rather than just 180^0, rotations: no chance for a **cmm**, which has by definition a **smallest** rotation of 180^0! And the surprises are not over yet: as in figure 4.53, every pair of trapezoids is a **'square' D_2** set, hence (3.6.3) there exist two rotations **and** two glide reflections between every two adjacent, perpendicular pairs of trapezoids (such as ABCD/EFGH and A′B′C′D′/E′F′G′H′); we already know the two 90^0 rotations that do the job, but where are the glide reflections? Using methods from chapter 3 once again (figure 4.55), we see that our new pattern has **glide reflection in two diagonal directions**; these are the 'subtle' glide reflections we were looking for, passing half way through two adjacent rotation centers (for 90^0 and 180^0, alternatingly) **in every single row and column of centers**!

Wallpaper patterns with the properties discussed above are known as **p4g**; they are the only 90^0 patterns with **reflection in precisely two directions**. They are easy to distinguish from the **p4m** patterns: one has to simply look at the number of directions of reflection (or even glide reflection, if adventurous enough).

4.11.2 How about rotation centers? Although there seem to be two kinds of 90^0 rotation centers in figure 4.55, marked by **1** and **1′**, we still declare that, unlike **p4m** patterns, every **p4g** pattern has just **one kind** of fourfold centers: indeed every 90^0 rotation center of **type 1′** is the **image** of a **type 1** 90^0 rotation center under one of the pattern's isometries (glide reflection or reflection), and vice versa; and, for reasons that will become clear in 6.4.4, but have also been discussed in 4.0.5, we tend to view any two isometries that are images of each other as 'equivalent' (read **"conjugate"**).

Likewise, we view all the 180^0 centers in either a **p4g** or a **p4m** pattern as being of the same kind: any two of them are images of each other by either a 180^0 rotation (possibly about a 90^0 center) or a 90^0 rotation! This also confirms that the **cm** has only 'one kind' of reflection axes (4.4.6): every two adjacent reflection axes are images of each other under the **cm**'s glide reflection or translation! More subtly, all reflections in the **pmg** (4.7.3) and all the glide reflections (of same direction) in the **pgg** (4.8.3) are 'of the same kind': indeed every two adjacent **pmg** reflection axes and every two adjacent, parallel **pgg** glide reflection axes are, as we indicated in 4.7.3, images of each other under a 180^0 rotation! Finally, we leave it to you to confirm that there exist **two**, rather than four, kinds of 180^0 centers in the **pgg** and **pmg** types, and **three** kinds of 180^0 centers in the **cmm**.

4.11.3 <u>More on 'diagonal' glide reflections.</u> The **p4g** wallpaper pattern in figure 4.56 should be compared to the **pgg** pattern of 4.8.4, which may be viewed as a 'compressed' version of it. On the other hand, every **p4g** pattern may be viewed, with some forgiving imagination, as a **'special case'** of a **pgg** pattern: just 'overlook' the 90^0 rotation and all reflections and in-between glide reflections ... and focus on the 180^0 rotations and the diagonal glide reflections!

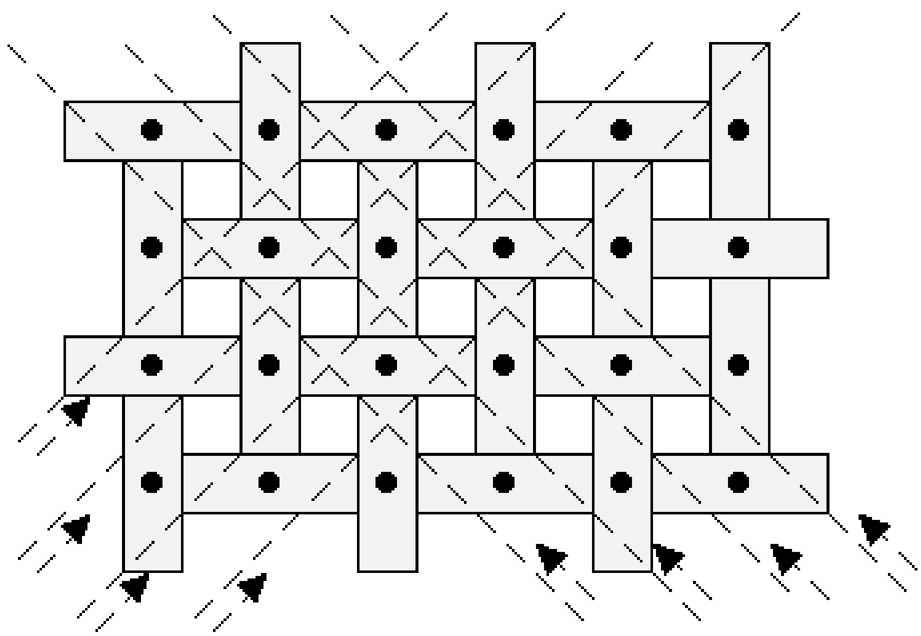

Fig. 4.56

Every **p4g** pattern may also be viewed as the union of two disjoint, **'perpendicular' cmm patterns** mapped to each other by any and all of the **p4g**'s diagonal glide reflections; this is best seen in the following 'relaxed' version of the previous **p4g** pattern (where the two **cmm**s consist of the vertical and the horizontal motifs, respectively):

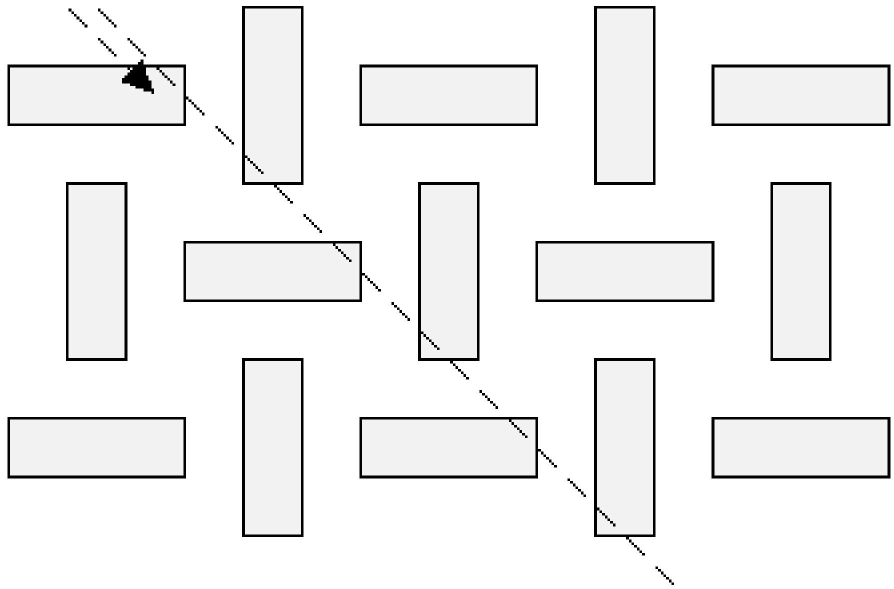

Fig. 4.57

4.11.4 Roman semicircles. In the following **p4g** example from ***Stevens*** (p. 294), every two nearest 90^0 centers are nicely placed at the centers of heterostrophic $\mathbf{C_4}$ sets:

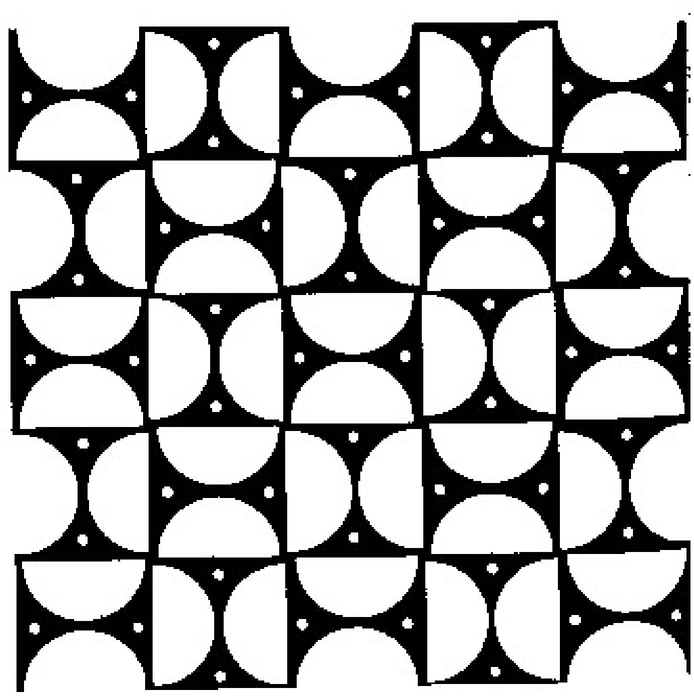

Fig. 4.58

4.12 90^0, translations only (p4)

4.12.1 Still the same centers! Let's have a look at the following 'distorted' version of the **p4g** pattern of figure 4.57, obtained via an 'up and down, left and right' process:

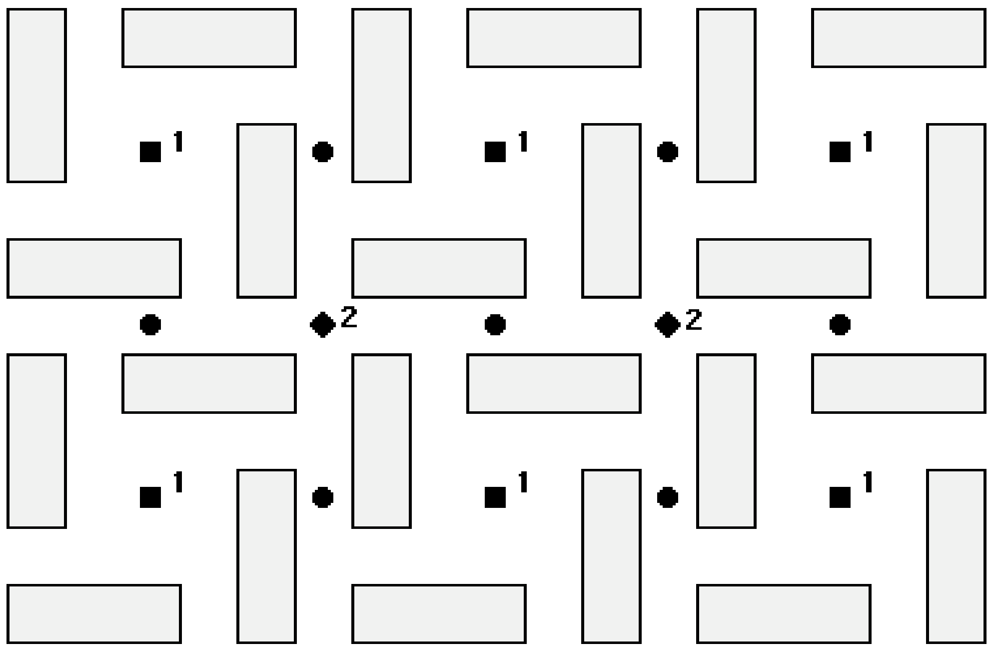

Fig. 4.59

In terms of rotations, the wallpaper pattern in figure 4.59 is identical to a **p4m** pattern: **two kinds** of 90^0 centers, **one kind** of 180^0 centers, and exactly the same lattice of rotation centers that we first saw in figure 4.5. What makes this new pattern different is that it has no reflections or glide reflections: the absence of the former is obvious, some candidates for the latter would require two or more gliding vectors each in order to work. Such patterns, having only 90^0 (and 180^0, of course) rotation (plus translation, always), are known as **p4**.

4.12.2 On the way back to **p4m**. Pushing the 'process' that led from the **p4g** pattern of figure 4.57 to the **p4** pattern of figure 4.59 one more step we obtain the following **p4** pattern:

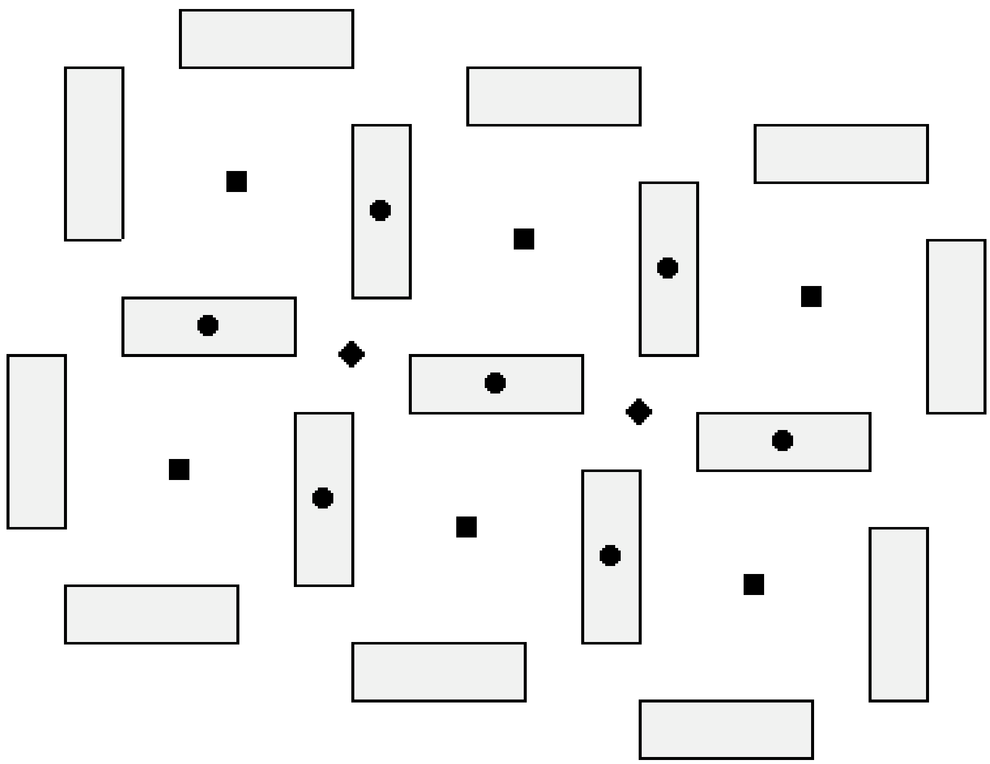

Fig. 4.60

You can probably guess at this point the next step in the process, a step that will result into a **p4m** pattern: all these 90^0 types are close relatives indeed!

4.12.3 Two kinds of Egyptian 'flowers'. In this remarkable **p4** design from ancient Egypt (***Stevens***, p. 284), the two kinds of 90^0 centers are cleverly placed inside two slightly different types of flower-like $\mathbf{D_4}$ figures; were the two kinds of 'flowers' one and the same, this design would still be a **p4**, except that the other kind of 90^0 centers would have to move to the 'swastikas':

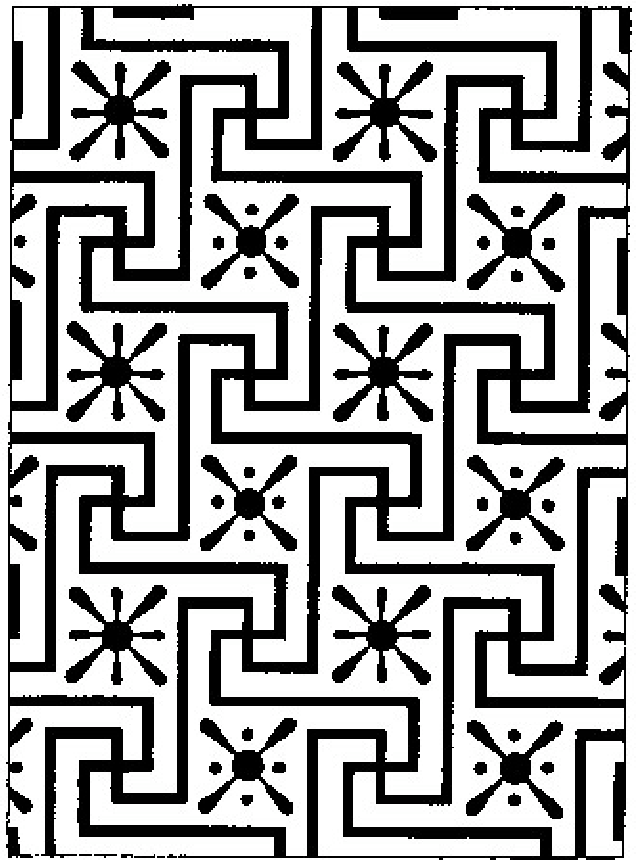

Fig. 4.61

4.13 60^0, six reflections, six glide reflections (p6m)

4.13.1 Bisecting the beehive. We have already discussed the lattice of rotation centers of the beehive (figure 4.5), and are aware of its three rotations (60^0, 120^0, 180^0). Figure 4.62 stresses **some** of its rather obvious reflections (of two kinds and in six directions), as well as its **in-between** glide reflections (again, of two kinds and in six directions):

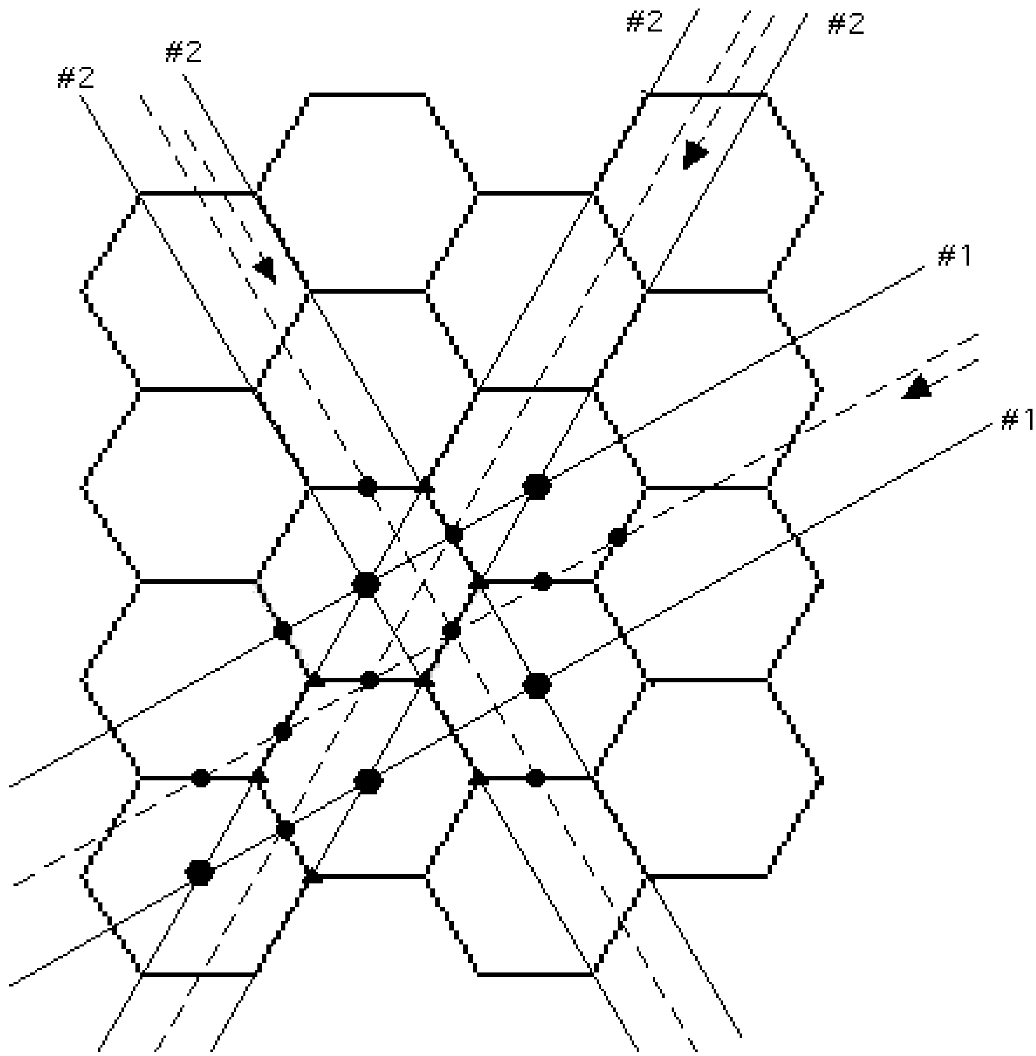

Fig. 4.62

So, while some reflection axes (**#1**) pass through sixfold and twofold centers only, others (**#2**) pass through all three kinds of centers. As for glide reflection axes, they all pass through **twofold centers only**, but they are of two kinds as well, having gliding vectors of different length (figure 4.62). Wallpaper patterns with these properties are denoted by **p6m**, a type that can justifiably be branded "the king of wallpaper patterns": indeed not only is **p6m** very rich in terms of symmetry, but, as we will see in the coming sections, many other types are 'contained' in it or 'generated' by it. (The downside of this is that some times one may miss the 60^0 rotation and underclassify a **p6m** as a **cmm** or even **cm**).

4.13.2 <u>From hexagons to rhombuses.</u> It is easy to get a **'dual'** of the pattern in figure 4.62 that features **rhombuses** instead of hexagons and yet preserves all its isometries:

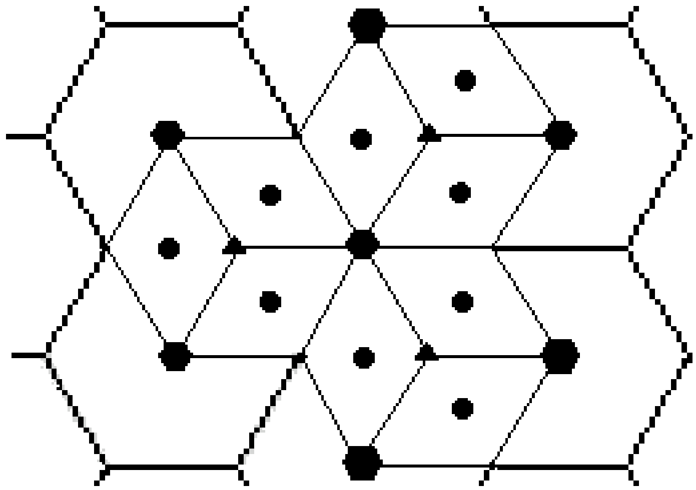

Fig. 4.63

4.13.3 <u>Arabic rectangles.</u> Here are two complex, 'rectangular' **p6m** patterns from ***Stevens*** (p. 330); can you see how to derive them from the beehive by attaching **rectangles** to the hexagons?

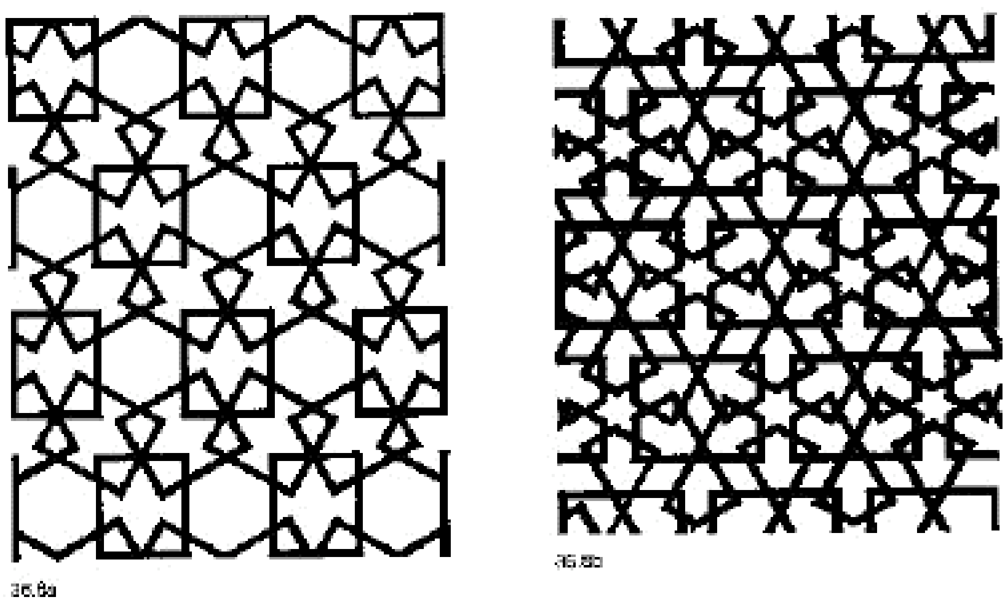

Fig. 4.64

4.14 60^0, translations only (p6)

4.14.1 'Adorning' the rhombuses. What happens when one starts 'enriching' the 'plain' rhombuses in the **p6m** pattern of figure 4.63? The following Arabic design (***Stevens***, p. 318) provides an answer:

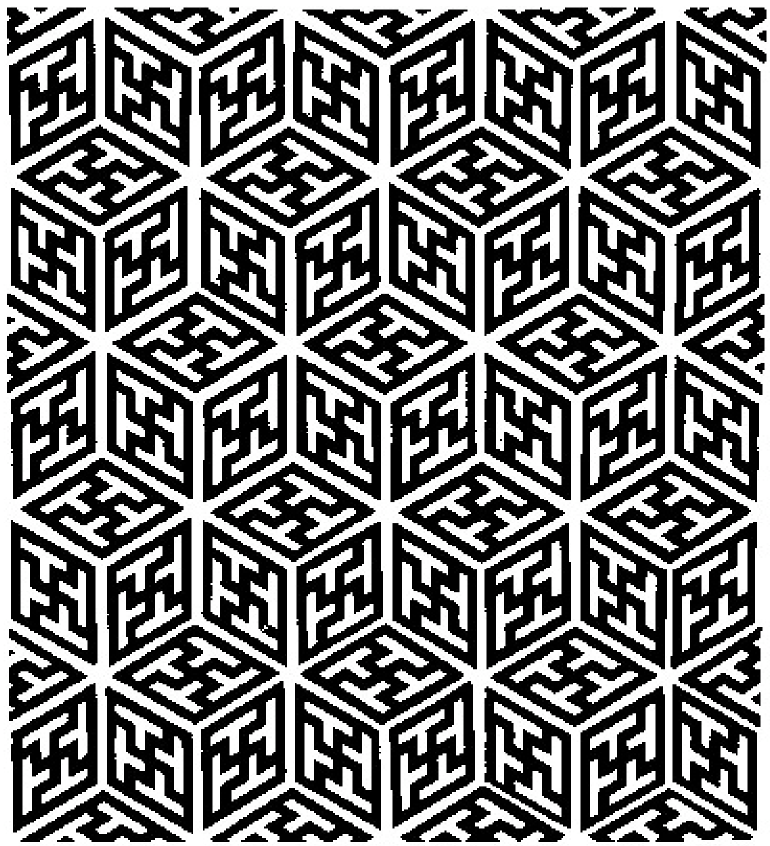

Fig. 4.65

The **T**-like figures inside the rhombuses have turned them from $\mathbf{D_2}$ sets into homostrophic $\mathbf{C_2}$ sets, destroying all possibilities for (glide) reflection, and yet preserving the rotations: the lattice of centers from figure 4.5 remains intact, with twofold, threefold, and sixfold centers placed at the vertices of 90^0-60^0-30^0 triangles (on which you may read more in 6.16.1 and 7.5.4). Such multi-rotational, rotation-only patterns are denoted by **p6**.

4.14.2 <u>Hexagons with ‘blades’.</u> One can get a **p6** pattern directly from the beehive by cleverly turning the hexagons from $\mathbf{D_6}$ sets into homostrophic $\mathbf{C_6}$ sets; here is one of many ways to do that, turning three out of every four old sixfold centers into twofold centers (and eliminating three quarters of the old threefold centers as well):

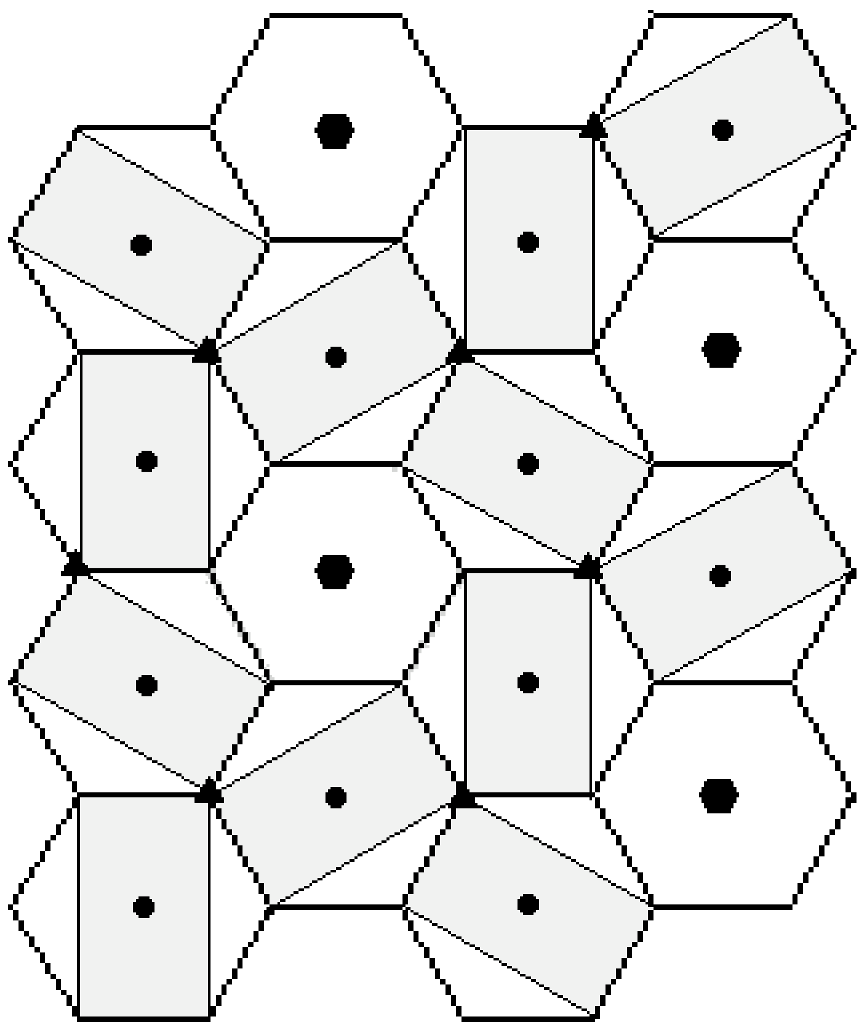

Fig. 4.66

4.15 120^0, translations only (p3)

4.15.1 <u>Further rhombus ‘ornamentation’.</u> Let’s have a look at the following Arabic design from ***Stevens*** (p. 260), similar in spirit to the **p6** pattern of figure 4.65:

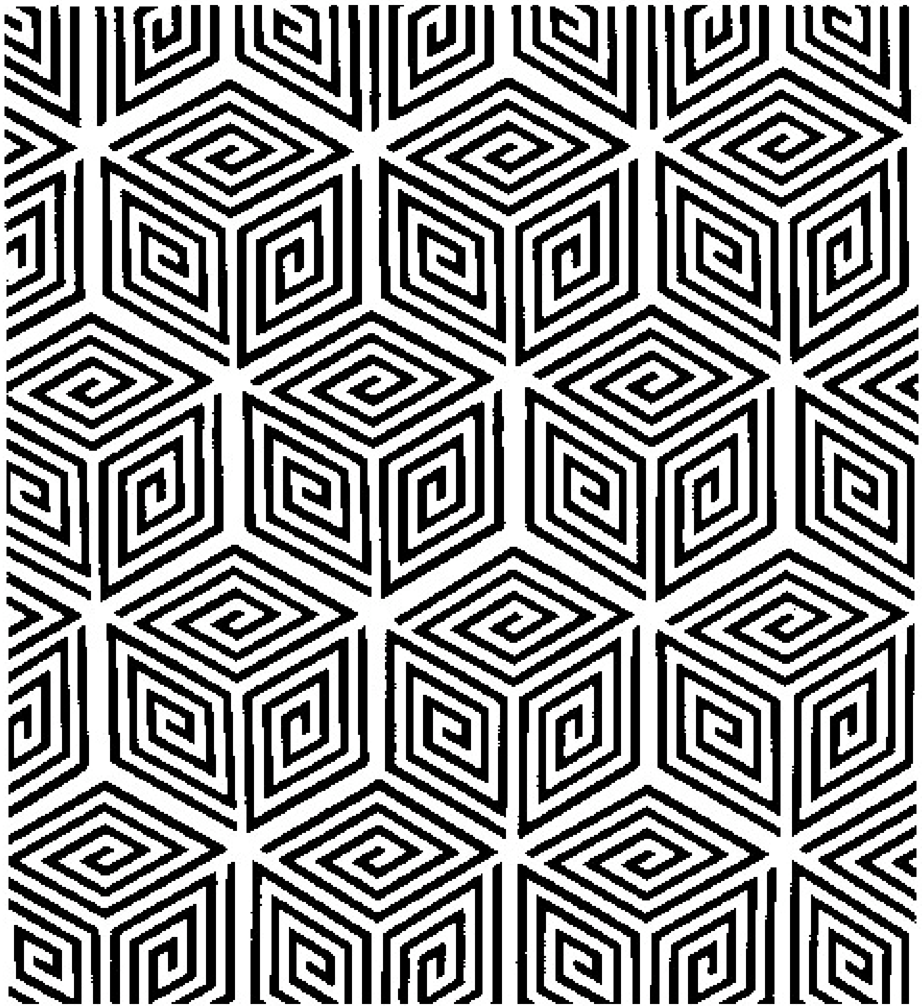

Fig. 4.67

Both patterns create a **three-dimensional** feeling, consisting of **cube-like** hexagons split into three rhombuses rotated to each other via 120^0 rotation, but that's where their similarities end. Indeed, while the rhombuses in figure 4.65 are homostrophic $\mathbf{C_2}$ sets (allowing for **two rotations** between any two adjacent rhombuses, one by 60^0 and one by 120^0), the rhombuses in figure 4.67 are homostrophic $\mathbf{C_1}$ sets allowing for **only one rotation** between any two adjacent ones, the 120^0 rotation already mentioned: there goes our 60^0 rotation, with the old 60^0 centers **reduced** to 120^0 centers!

It seems that we will have to settle for a wallpaper pattern having no other isometries than 120^0 rotations and translations: such patterns are known as **p3**.

4.15.2 Three kinds of rotation centers. There is a little bit of compensation for this reduction of symmetry: unlike **p6m** or **p6** wallpaper patterns, every **p3** pattern has **three kinds** of 120^0 rotation centers; this is perhaps easier to see in the following direct modification of the beehive than in the pattern of figure 4.67:

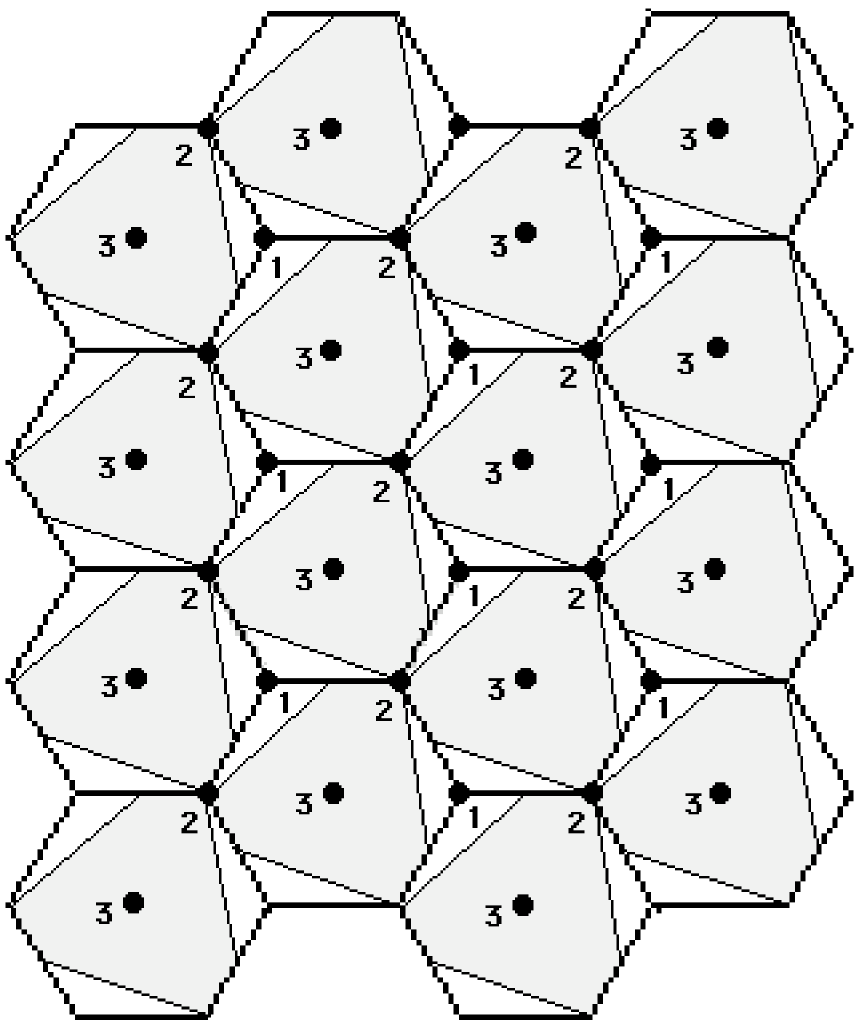

Fig. 4.68

4.16 120^0, three reflections, three glide reflections, some rotation centers off reflection axes (p31m)

4.16.1 Regaining the reflection. All the **p6** and **p3** patterns we have seen so far may be viewed as modifications of the beehive, with $\mathbf{D_6}$ sets (hexagons) replaced by homostrophic $\mathbf{C_6}$ and $\mathbf{C_3}$ sets, respectively: twelve (or just six) rhombuses 'build' a $\mathbf{C_6}$ set in figure 4.65, while only three suffice for a $\mathbf{C_3}$ set in figure 4.67. What happens when $\mathbf{D_6}$ sets turn into $\mathbf{D_3}$ sets? Here is an answer:

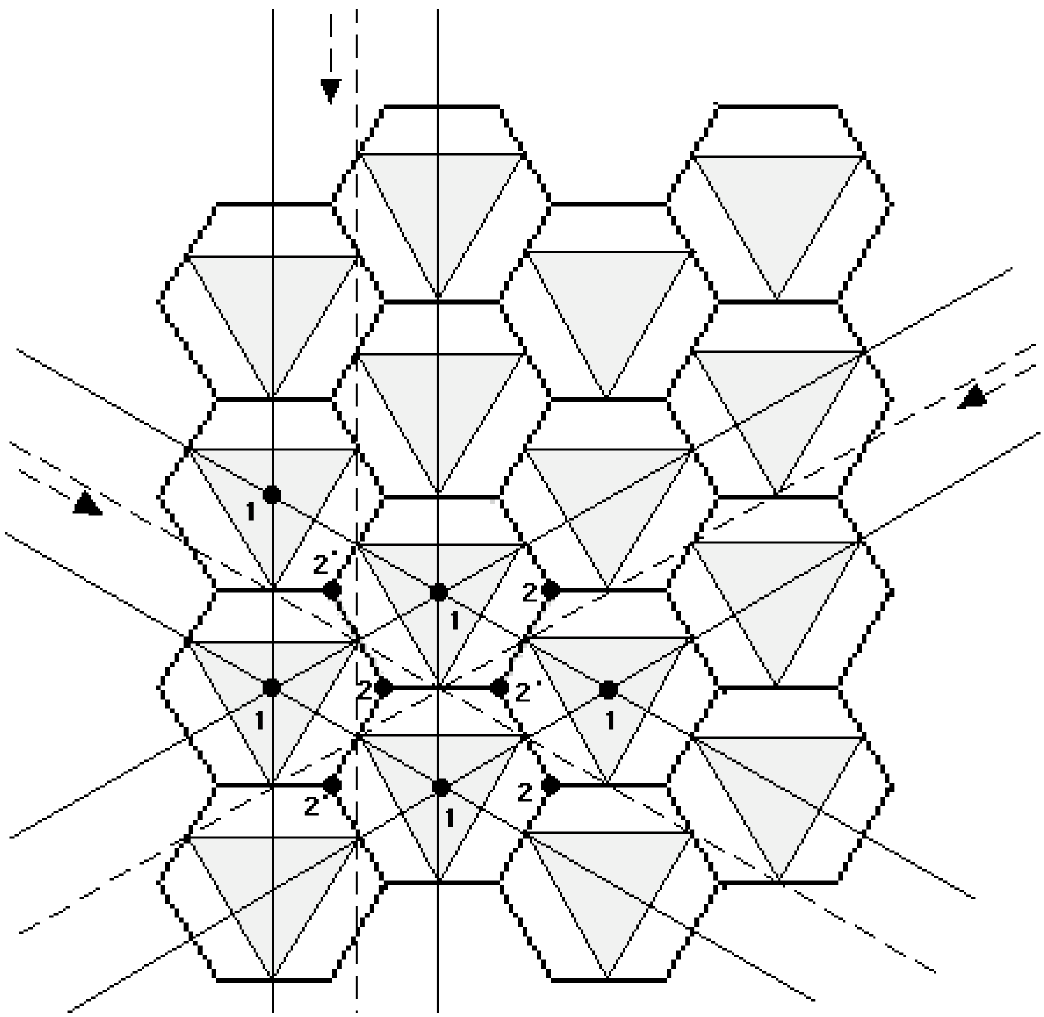

Fig. 4.69

Rather luckily, the reflections of the $\mathbf{D_3}$ sets (hexagons with an **inscribed equilateral triangle**) have survived, producing a wallpaper pattern with reflection and in-between glide reflection in three directions; notice that these reflections are precisely the **type 1** reflections of the original **p6m** pattern, passing through its sixfold and twofold, but not threefold, centers (4.13.1).

Which other isometries of the original **p6m** pattern (beehive) have survived, and how? Well, all sixfold centers have turned into threefold centers, and all threefold centers have remained intact! One may say that there are **two kinds** of 120^0 rotation centers: those -- denoted by **1** in figure 4.69 and always mappable to each other by translation -- **at the intersections of three reflection axes** (old sixfold centers); and those -- denoted by **2** or **2′** in figure 4.69 and mappable to each other by either (glide) reflection (**2** to **2′**) or translation/rotation (**2** to **2** or **2′** to **2′**) -- **on no reflection axis** (old threefold centers). All **type 2** reflections and glide reflections are gone -- in this example at least (see also 4.17.4). Wallpaper patterns of this type are known as **p31m**.

4.16.2 Japanese triangles. In our next example from ***Stevens*** (p. 274) the off-axis 120^0 centers are hidden inside curvy triangles:

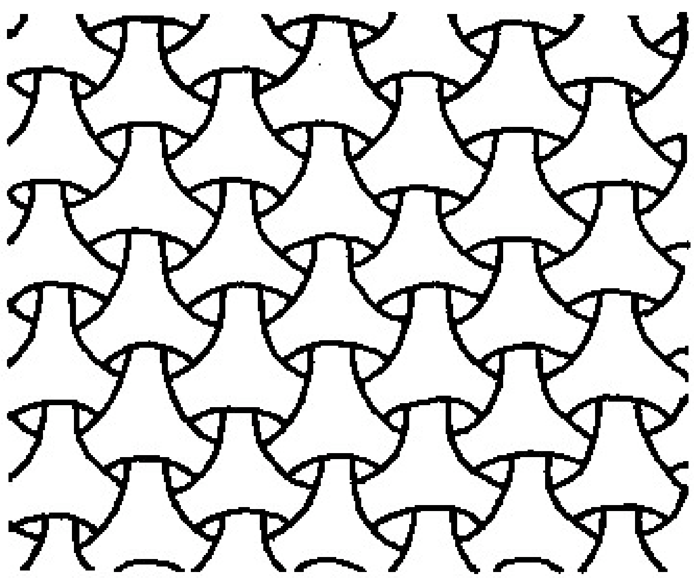

Fig. 4.70

4.17 120^0, three reflections, three glide reflections, all rotation centers on reflection axes (p3m1)

4.17.1 Thinning things out a bit. Consider the following diluted version of the wallpaper pattern in figure 4.69:

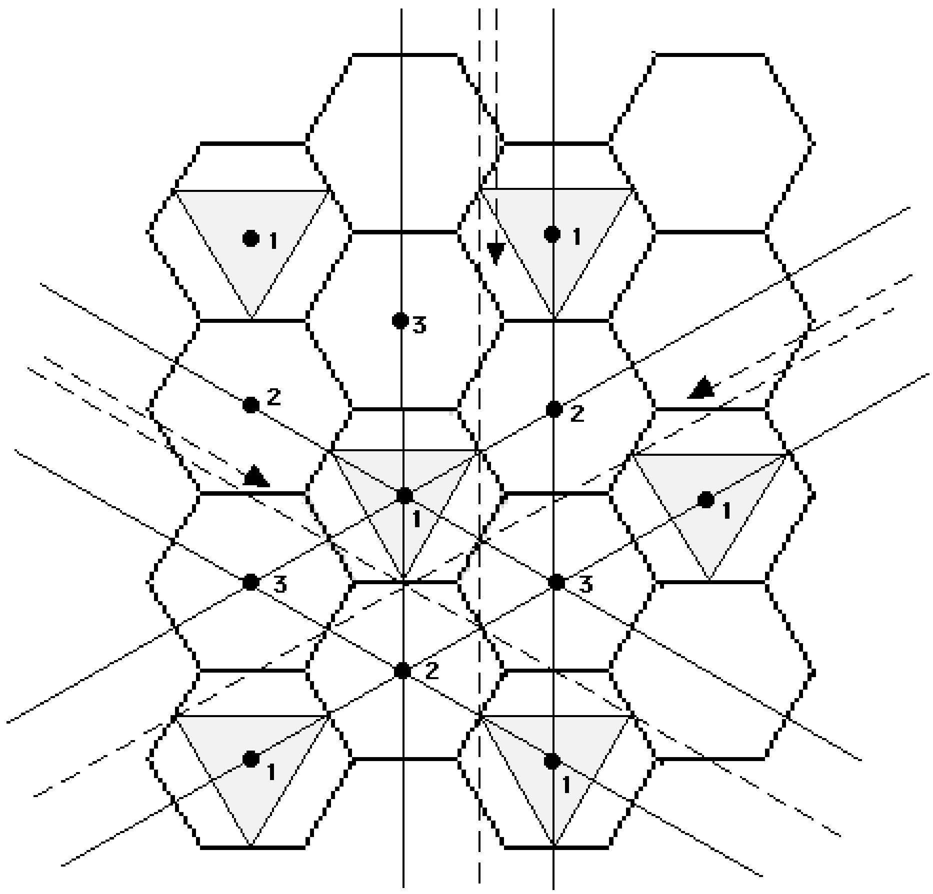

Fig. 4.71

This new pattern is of course very similar to that of figure 4.69: they both have rotation by 120^0 only, and they both have reflection and in-between glide reflection in three directions. What, if anything, makes them different in that case? To simply say that the one in figure 4.69 is 'denser' than the one in figure 4.71 is certainly not that precise or acceptable mathematically! (See also 4.17.4 below.) Well, a closer look reveals that, unlike in the case of the **p31m** type, **all** the $\mathbf{120^0}$ centers in the new pattern were $\mathbf{60^0}$

centers in the beehive and lie at the intersection of three reflection axes: such patterns are known as **p3m1**, our 'last' type.

4.17.2 How many kinds of threefold centers? In a visual sense, the pattern in figure 4.71 has three kinds of 120^0 rotation centers: one at the center of a triangle (**1**), one between three vertices (**2**), and one between three sides (**3**). From another perspective, all rotation centers are the same: they are all old sixfold centers, lying on reflection axes, and **at the same distance from the closest glide reflection axis**. More significantly though, and in the spirit of 4.11.2, the three kinds of centers are distinct because no isometry maps centers of any kind to centers of another kind. Either way, **p3m1** patterns (**three or one** kinds of centers, depending on how you look at it) are distinguishable from **p31m** patterns (**two** kinds of centers)!

4.17.3 Persian stars. In the following **p3m1** example from ***Stevens*** (p. 267), six-pointed stars and hexagons give the illusion of a **p6m** pattern, but you already know too much to be fooled (and miss the 'tripods' that turn the $\mathbf{D_6}$ sets into $\mathbf{D_3}$ sets):

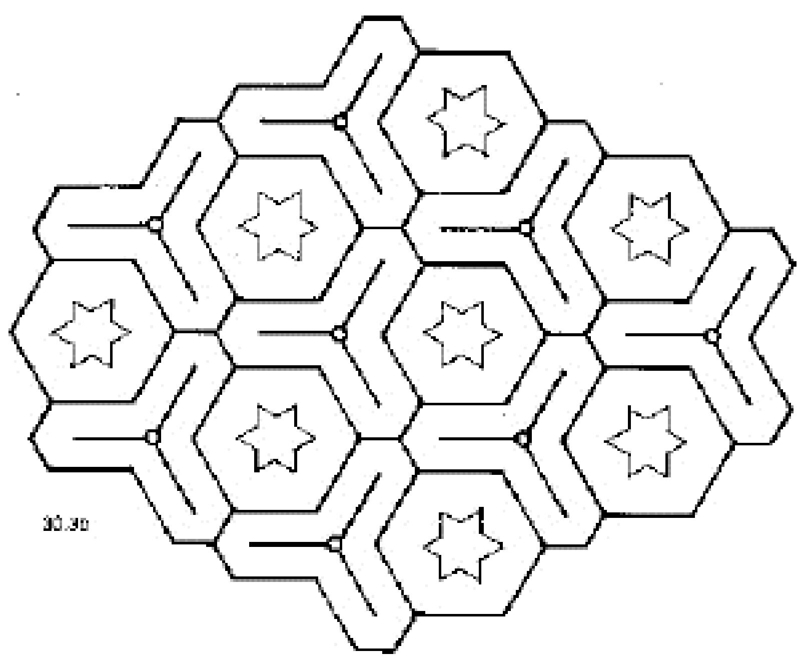

Fig. 4.72

4.17.4 <u>More on (glide) reflection.</u> The reflections and in-between glide reflections in both figures 4.69 (**p31m**) and 4.71 (**p3m1**) are none other than those **type 1** (glide) reflections inherited from the beehive pattern in figure 4.62. This may give you the impression that the beehive's **type 2** (glide) reflections can never survive in a 120^0 pattern. But as figure 4.73 demonstrates, it is possible to 'build' a **p3m1** pattern 'around' **type 2** (glide) reflection; and we leave it to you to demonstrate the same for **p31m** patterns -- a simple way to do that would be to modify figure 4.71 so that the vertices of the triangles would be each hexagon's vertices rather than edge midpoints!

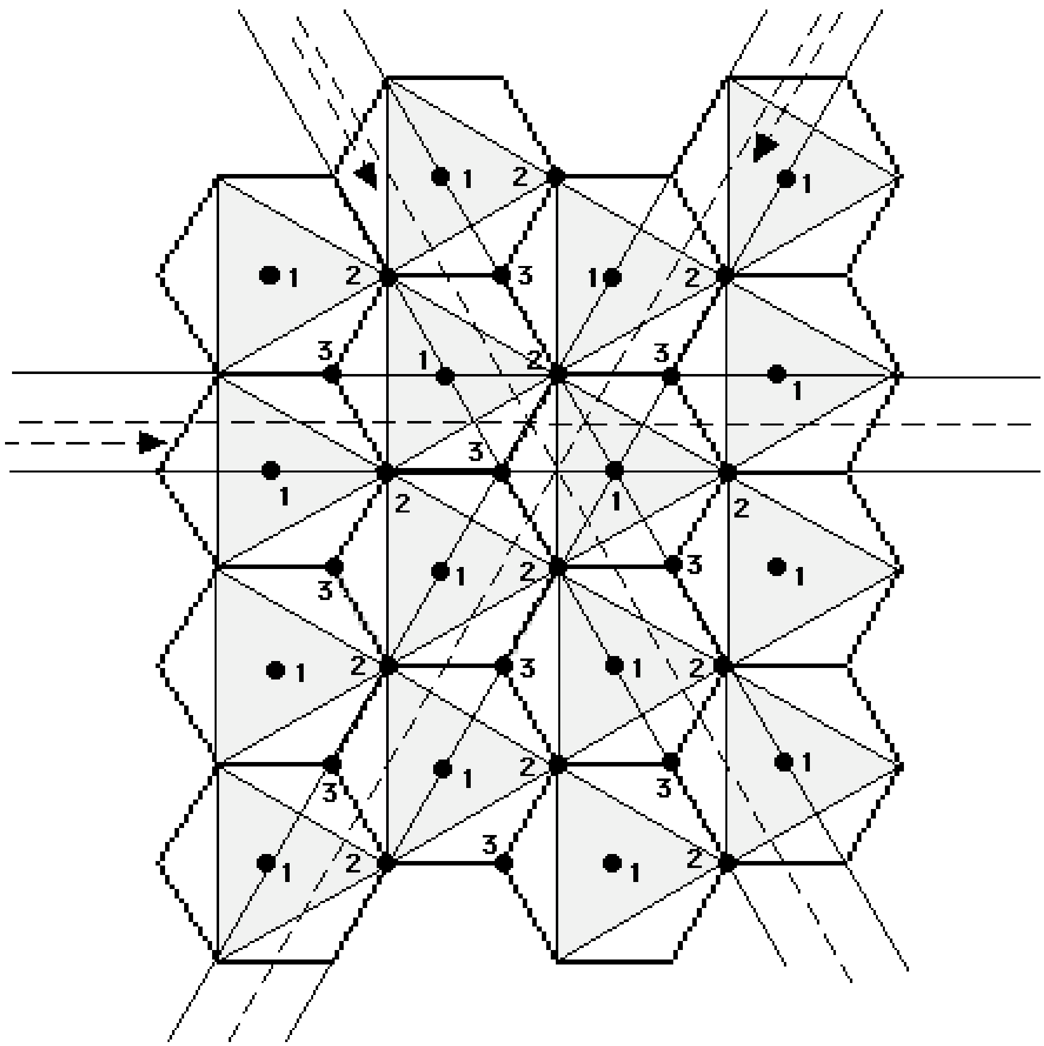

Fig. 4.73

As we indicate in 8.4.3 (and figure 8.41 in particular), and as you may verify in figures 4.69-4.73, the real difference between **p3m1** and **p31m** has to do with the **placement** of their (glide) reflection axes with respect to their lattice of rotation centers; for example the **ratio** of the glide reflection vector's length to the distance between two nearest rotation centers equals $\sqrt{3}/2$ in the case of the **p31m** as opposed to 3/2 in the case of the **p3m1**.

A medieval design very similar to the pattern in figure 4.73 was actually at the center of a famous controversy regarding whether or not **all seventeen** types of wallpaper patterns (and the **p3m1** in particular) appear in the Moorish **Alhambra Palace** in Spain: indeed the pattern in figure 4.73 may be viewed as a **two-colored** pattern of **p6m** (rather than **p3m1**) type, more specifically a **p6′mm′** (described, among other two-colored **p6m** types, in section 6.17)! This can be avoided simply by starting with a **'sparse'** beehive (i.e., one from which two thirds of the hexagons have been removed, in such a way that no two hexagons touch each other): see figures 6.132 & 6.133, as well as the 60^0 & 120^0 examples in ***Crystallography Now*** (http://www.oswego.edu/~baloglou/103/seventeen.html, a web page devoted to a geometrical classification of wallpaper patterns in the spirit of chapters 7 and 8).

4.18 The seventeen wallpaper patterns in brief

(I) Patterns with no rotation (360^0)

p1 : nothing but translation (common to all seventeen types)

pg : glide reflection in one direction; no reflection

pm : reflection in one direction; no in-between glide reflection

cm : reflection in one direction, in-between glide reflection

(II) Patterns with smallest rotation of 180^0

p2 : 180^0 rotation only

pgg : glide reflection in two perpendicular directions, no reflection; no rotation centers on glide reflection axes

pmm : reflection in two perpendicular directions, no in-between glide reflection; all rotation centers at the intersection of two perpendicular reflection axes

cmm : reflection in two perpendicular directions, in-between glide reflection; all rotation centers either at the intersection of two perpendicular reflection axes or at the intersection of two perpendicular glide reflection axes

pmg : reflection in one direction (with no in-between glide reflection), glide reflection in a direction perpendicular to that of the reflection; all rotation centers on glide reflection axes, none of them on a reflection axis

(III) Patterns with smallest rotation of 90^0

p4 : 90^0 rotation only; distinct 180^0 rotation, too

p4m : reflection in four directions; in-between glide reflection in two out of those four directions; all 90^0 rotation centers at the intersection of four reflection axes; all 180^0 rotation centers at the intersection of two reflection axes and two glide reflection axes

p4g : reflection in two directions; in-between glide reflection in both of those directions; additional glide reflection in two more (diagonal) directions; all 90^0 rotation centers at the intersection of two perpendicular (vertical and horizontal) glide reflection axes, none of them on a reflection axis or a diagonal glide reflection axis; all 180^0 rotation centers at the intersection of two perpendicular reflection axes

(IV) Patterns with smallest rotation of 120^0

p3 : 120^0 rotation only

p3m1: reflection in three directions with in-between glide reflection; all rotation centers at the intersection of three reflection axes; no rotation center on a glide reflection axis

p31m: reflection in three directions with in-between glide reflection; some rotation centers at the intersection of three reflection axes; some rotation centers on no reflection axis; no rotation center on a glide reflection axis

(V) Patterns with smallest rotation of 60^0

p6 : 60^0 rotation only; distinct 120^0 and 180^0 rotations, too

p6m : reflection in six directions with in-between glide reflection; all 60^0 (120^0) rotation centers at the intersection of six (three) reflection axes, none of them on a glide reflection axis; all 180^0 rotation centers at the intersection of two reflection axes and four glide reflection axes

first draft: fall 1998

CHAPTER 5

TWO-COLORED BORDER PATTERNS

5.0 Color and colorings

5.0.1 Design, color, and background. Color is present everywhere, even on this page: it is the contrast between black ink and white **background** that makes this page visible! One could even talk about 'active' design colors and 'passive' background colors; in more complex situations it is not so clear what belongs to the design and what belongs to the background -- nor is such a differentiation always important or even possible, of course. But it is often crucial in discussions of '**colored patterns**'.

Consider the following **pma2** border pattern:

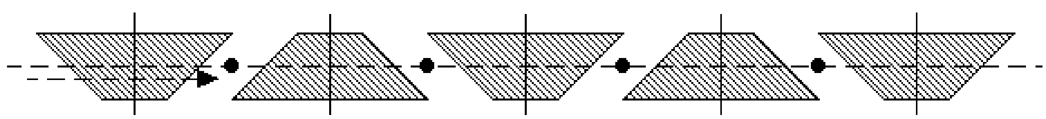

Fig. 5.1

One can certainly talk about three colors being present here: the trapezoids are 'grey', their boundaries are black, and the background is, of course, white; since we generally ignore the boundary lines' color, we can safely talk about two colors being present and deal with an **'one-colored'** (grey) **pattern** on white background.

5.0.2 Colorings. Let us now leave blank (white) the pattern of figure 5.1, planning to color it in two colors as indicated below:

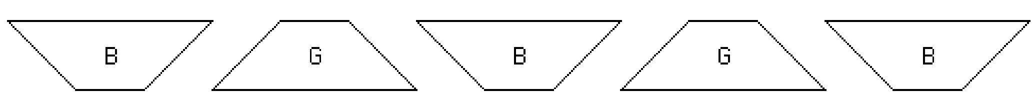

Fig. 5.2

In figure 5.2, **B** and **G** could stand for blue and green, or any other pair of distinct colors: if you feel that blue and green are too close to each other or that they do not get along that well, whatever, you are free to use, for example, red for **B** and yellow for **G**, etc. (The choice of the two colors is not an entirely trivial matter, as it could in fact affect perception of space and interaction between shapes.) For our purposes, and in an effort to keep printing costs low, we limit ourselves to black for **B** and grey for **G** (in this and the next chapters, where, with the exception of 5.0.4 below, only two colors are involved). In particular, our coloring of figure 5.2 yields the following **'two-colored'** border pattern:

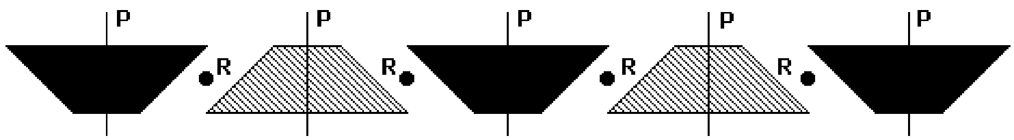

Fig. 5.3

5.0.3 <u>Color preservation and reversal.</u> Does the border pattern in figure 5.3 look the same if you flip this page (or if you trace it and flip the tracing paper)? Your first response might be "no", as the black trapezoids that were 'inverted' in figure 5.3 are now 'upright':

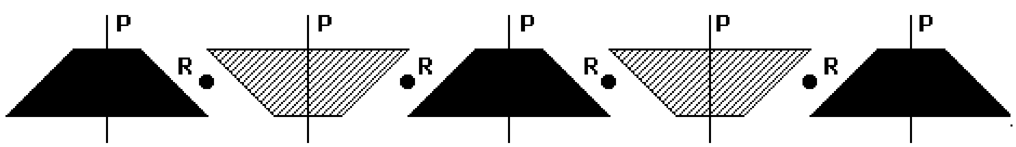

Fig. 5.4

In other words, it is tempting to say that the pattern in figure 5.3 (or 5.4) does not have half turn. But then the question arises: what happened to the half turn of the original pattern, and to the rotation centers indicated in figure 5.1, in particular? A closer look at figures 5.3 & 5.4 shows that a 180^0 rotation (half turn) about each of those rotation centers maps **every** black trapezoid to a grey one and vice versa! In the language that we will be using from here on, each half turn in figures 5.3 & 5.4 **reverses colors**. We end up saying that our pattern has **color-reversing half turn**, indicating this fact by placing a capital **R** right next to each rotation center: indeed those **R**s that you see right next to the rotation centers in figures 5.3 & 5.4 do not stand for “rotation” but for “reverses”!

How about the vertical reflections of our pattern? In figures 5.3 & 5.4 you see a **P** right next to each reflection axis, standing for “preserves”: indeed vertical reflection about each axis maps **every** black trapezoid to a black one (possibly even itself) and **every** grey trapezoid to a grey one! In our new language we say that the pattern in figures 5.3 & 5.4 has **color-preserving vertical reflection**.

So, every half turn in the border pattern of figures 5.3 & 5.4 reverses colors, while every vertical reflection preserves colors. Does that mean that, in such two-colored border patterns, half turns always reverse colors and vertical reflections always preserve colors? **Not at all**: as you are going to see in what follows, all combinations are possible; further, it is possible for a single border pattern to have **both** color-preserving and color-reversing half turns, or **both** color-preserving and color-reversing vertical reflections. On the other hand, a border pattern can have only one glide reflection or horizontal reflection: so these isometries, if there to begin with, must be either color-preserving or color-reversing; but wait until section 5.8, too!

5.0.4 More than two colors? Let’s have a look at a few colorings -- indicated by letters rather than real colors -- of another **pma2** border pattern:

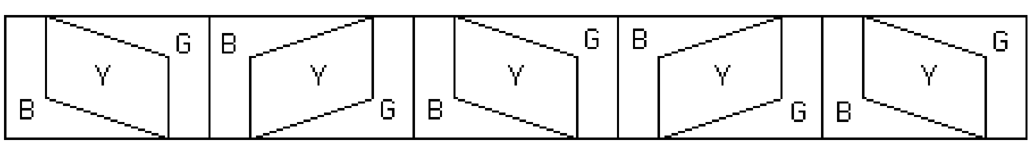

Fig. 5.5

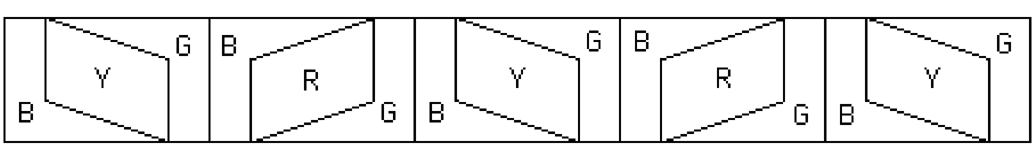

Fig. 5.6

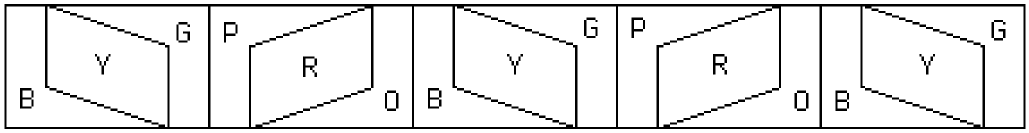

Fig. 5.7

In the pattern of figure 5.5, there are two colors 'in balance' with each other (blue and green) and a third color (yellow) not 'in balance' with either of the other two: it is more reasonable then to describe the pattern as two-colored (blue-green) **pma2** on yellow-white background; at the same time, one could 'see' an one-colored **pma2** border pattern (yellow) on three-colored (blue-green-white) background!

Much more so, it is not clear what the background is in figure 5.6, so one could easily talk of **two** two-colored **pma2** border patterns, a blue-green one **and** a yellow-red one, on white background: indeed yellow and red are as much 'in balance' with each other as blue and green are! Finally, it does make sense to talk of a **four-colored** (blue-green-purple-orange) **pma2** border pattern **and** a two-colored (yellow-red) **pma2** border pattern in figure 5.7!

Complicated, isn't it? Well, in this and the next chapter all border and wallpaper patterns will be simple enough to be viewed as two-colored, with no room for confusion; one or more **background colors** might be there from time to time, but it will be clear that those are indeed background colors. The concept of background color is more important in the context of **'real world'** patterns, found in textiles, mosaics, and other artifacts.

But what is, after all, and in our context of border or wallpaper patterns always, that "background (color)"? It is reasonable to say that, in the presence of more than one colors in a pattern, a color is viewed as background if and only if the pattern has **no isometry that swaps it with another color**. Under this definition, the situation is certainly clear in figure 5.5 (yellow is background) but not quite so clear in figures 5.6 & 5.7: it would be best to view those border patterns as four-colored and **six-colored** patterns, respectively. (On another note, this definition resolves the

‘Alhambra controversy’ of 4.17.4 by rendering the ‘entrapped white’ in figure 4.73 a **second color**!)

5.0.5 One-colored or two-colored? Motivated by the discussion in 5.0.4, we say that a border or wallpaper pattern is **two-colored** if and only if **precisely two** of its colors are **swapped by at least one isometry** that maps the pattern to itself. In particular, this definition implies that the two colors are **‘in balance’** with each other: for example there is as much grey as black in figures 5.3 & 5.4 (with grey and black swapped by half turn), and as much blue as green in figure 5.5 (with blue and green swapped by both vertical reflection and half turn).

For a change, let’s have a look at the following border pattern:

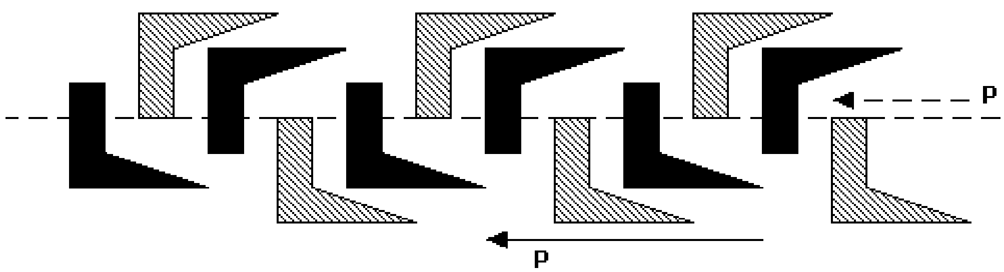

Fig. 5.8

How many isometries do you see that swap black and grey? None! Our pattern has color-preserving translation and color-preserving glide reflection, and that’s about it! On the other hand, it is clear that black and grey are in perfect balance with each other: is it a two-colored pattern, then? No, under our sound definition the border pattern in figure 5.8 is **one-colored**, classifiable in fact as a **p1a1**!

Confused? Well, don’t worry, the next seven sections will be relatively straightforward; patterns such as that of figure 5.8 are indeed rare... (Can you create any others, by the way? Having, for example, only color-preserving translation and color-preserving vertical reflection?) For the rest of the chapter we will be dealing mostly with ‘genuine’ two-colored patterns, colorings in fact of the seven types of one-colored patterns we studied in chapter 2. Now things can at times go a bit ‘wrong’ with those colorings, too, but you will have to wait until section 5.8 to see how that can happen!

5.1 Colorings of p111

5.1.1 Color-reversing translation. All border patterns presented in section 5.0 have color-preserving translation, common in fact **by definition** to **all** border patterns, but none of them has **color-reversing translation**. Does that mean that no translation can be color-reversing? Not at all, in fact sometimes a color-reversing translation is the **only** isometry that makes a border pattern two-colored! This will have to be the case in this section: if you start with a border pattern that has only translation (**p111**), coloring it in two colors can at most make it have **both** color-reversing and color-preserving translation instead of just color-preserving translation; **coloring may not increase symmetry!** Here is an example of two distinct colorings of the same **p111** pattern:

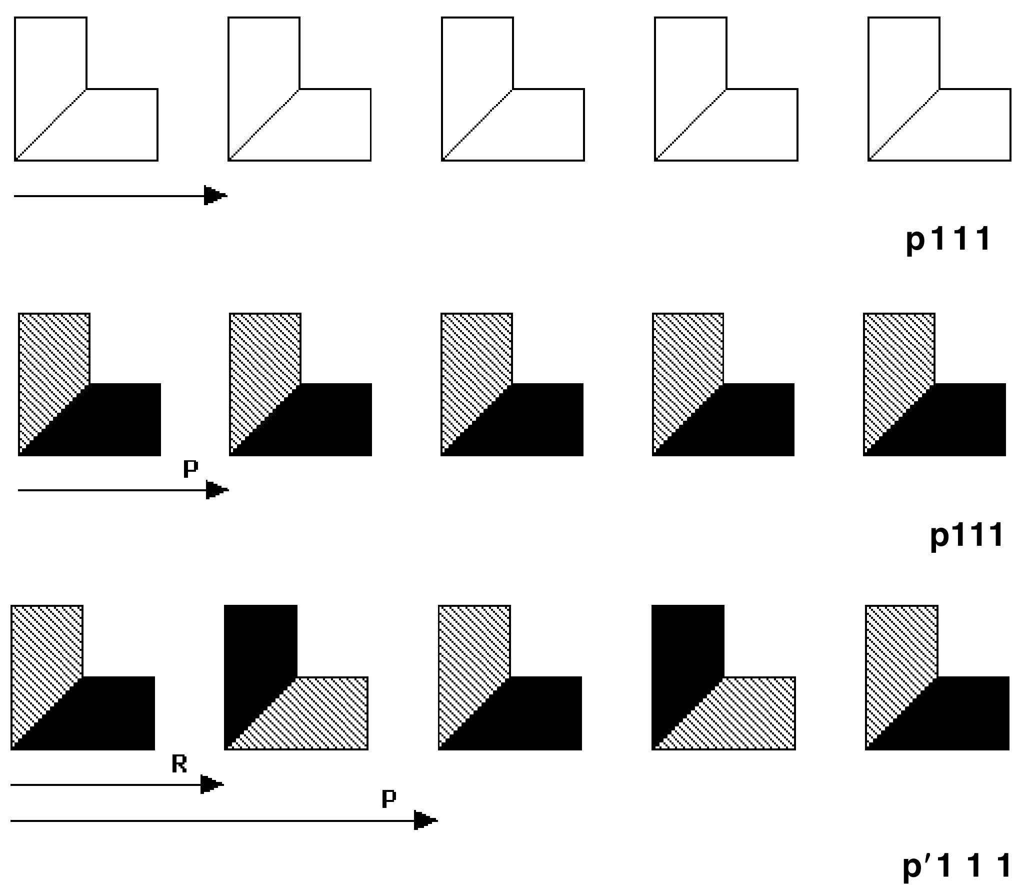

Fig. 5.9

Only the second coloring above allows for color-reversing translation (indicated by **R**–vector), in addition of course to color-preserving translation (indicated by **P**–vector, **twice as long** as the **R**–vector): this yields a **two-colored** pattern known as **p′111**. The first and second patterns in figure 5.9, despite looking like colorless and two-colored, respectively, are **both** classified as **p111**: they both have color-preserving translation and nothing else!

5.1.2 <u>A word on notation.</u> That little **'accent'** (like the one above **p** in **p′111**) will always indicate a **color-reversing isometry** in this and the next chapter; in particular, **p′** always stands for **color-reversing translation**. In figure 5.9 we indicated color-reversing translations with **R**–vectors and color-preserving translations with **P**– vectors. From here on we will no longer bother to indicate color-preserving translations: they are present in **all** border patterns, be them one-colored or two-colored; moreover, the **doubling** of any color-reversing translation vector produces a color-preserving one! Here is an example, again of two distinct colorings of the same border pattern, illustrating this approach:

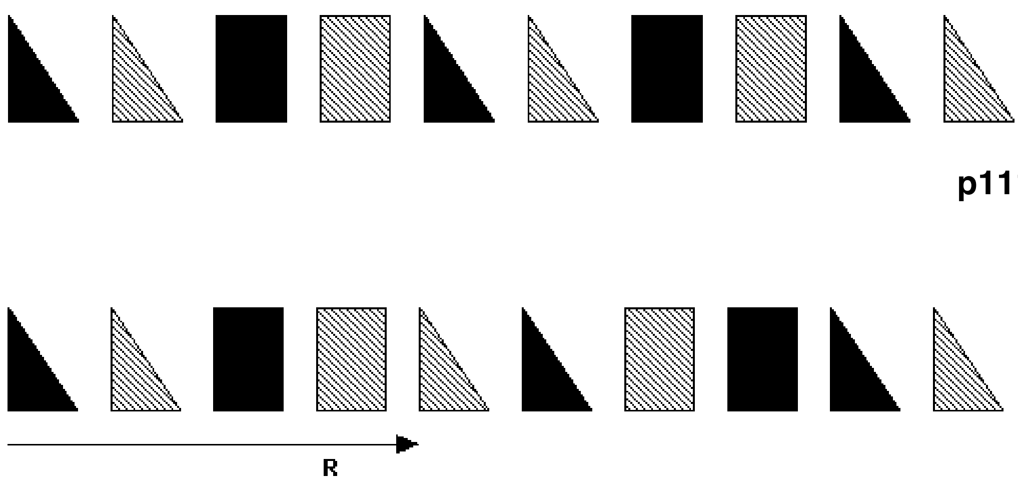

p111

p′1 1 1

Fig. 5.10

5.2 Colorings of pm11

5.2.1 Color-reversing vertical reflection. Let us now start with a ‘colorless’ **pm11** border pattern and color it following the colorings employed in figure 5.9:

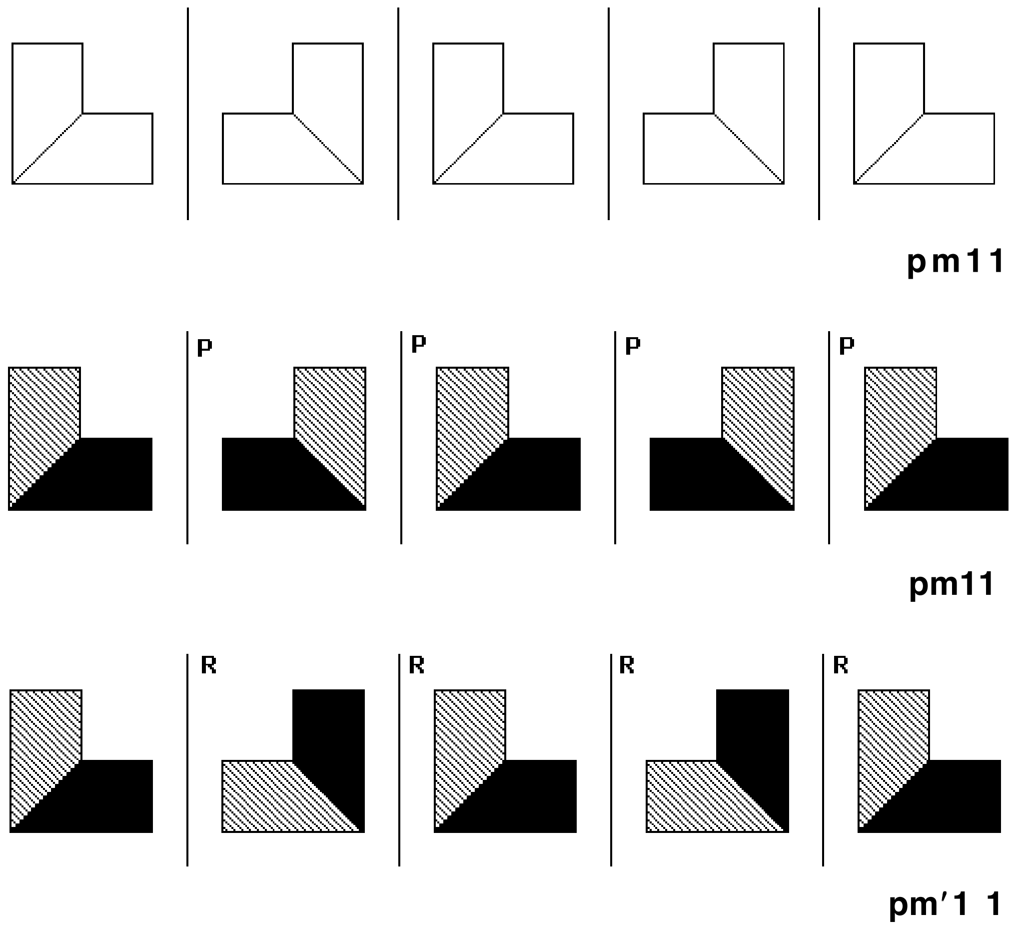

Fig. 5.11

Once again, only the third pattern is two-colored, not because of color-reversing translation (which it doesn’t have) but because of its **color-reversing vertical reflection**: such border patterns, having only color-reversing vertical reflection (in addition, of course, to that ubiquitous color-preserving translation) are denoted, rather predictably in view of 5.1.2, by **pm′11**.

5.2.2 How about color-reversing translation? Can we ‘force’ the third pattern in figure 5.11 to also have color-reversing translation? One thing to try is to reverse the colors in **every other pair** of motifs ... and see what happens:

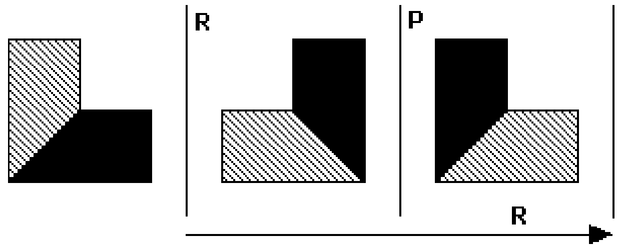

p′m11

Fig. 5.12

Clearly, color-reversing translation has been achieved. How about vertical reflection? Well, here we got a bonus: instead of color-preserving vertical reflections **only** or color-reversing vertical reflections **only**, as in the second (**pm11**) and third (**pm′11**) patterns in figure 5.11, respectively, our new pattern has **both** color-preserving (**P**) and color-reversing (**R**) vertical reflections; such border patterns are known as **p′m11**, in honor (**p′**) of the color-reversing translation that actually allows for the two kinds of vertical reflections ... and is in turn implied by them!

5.2.3 Two kinds of mirrors. As we pointed out in 2.2.3, every **pm11** border pattern has two kinds of vertical reflection axes (mirrors). This is nicely illustrated in the context of figure 5.12, where one kind of reflection axes preserve colors and the other kind of reflection axes reverse colors. Can we get the two kinds of axes to have the exact opposite effect on color? Surely we can, in fact the same process that led from the third pattern of figure 5.11 to the pattern of figure 5.12 leads from the second pattern in figure 5.11 to the following border pattern:

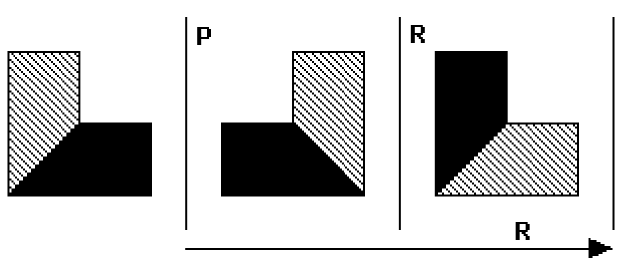

p′m11

Fig. 5.13

While the two-colored patterns in figures 5.12 & 5.13 are **distinct to the eye**, they are mathematically identical (**p′m11**): each of them has color-reversing translation and **both kinds** of vertical reflection (color-preserving and color-reversing). In more mathematical terms, we may say, never forgetting that all border patterns are infinite, that the patterns in figures 5.12 & 5.13 share the same **symmetry plan**:

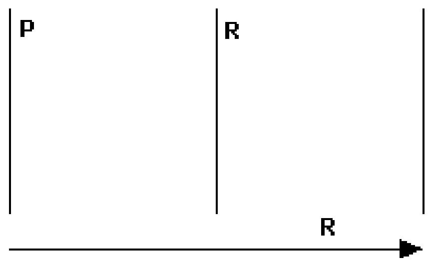

Fig. 5.14

Symmetry plans will be revisited in full in section 5.9.

5.2.4 How many colorings? There are two kinds of reflection axes in every **pm11**-like pattern and two possibilities for each kind of reflection axis (color-preserving and color-reversing), hence there should be two × two = four **possible** types all together. In view of our remarks in 5.2.3, however, two of those four types are viewed as identical, hence there exist four minus one = three types of **pm11**-like border patterns: **pm11**, **pm′11**, and **p′m11** (each of them discussed and exhibited already).

Another way of arriving at this conclusion follows the approach employed in 2.8.3 for classifying all one-colored border patterns:

Color-reversing translation	Color-reversing vertical reflection	Border pattern type
Y	Y	**p′m11**
Y	N	impossible
N	Y	**pm′11**
N	N	**pm11**

The ruling out of the second possibility above relies on the following observation: the existence of color-reversing translation in a border pattern with vertical reflection **implies** the existence of color-reversing vertical reflection; check also 7.3.1 and 5.6.2!

5.2.5 Further examples. Here are a couple of suggested colorings further illustrating the role of **pm11**'s two kinds of vertical reflection:

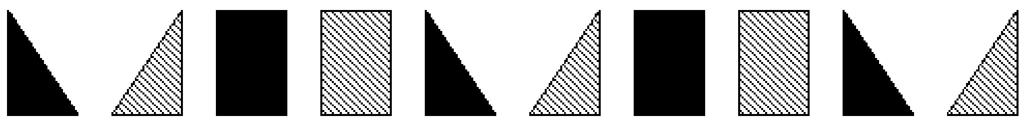

pm′1 1

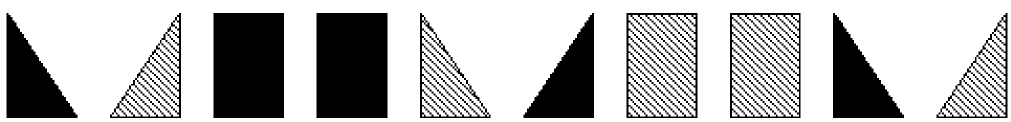

p′m 1 1

Fig. 5.15

5.3 Colorings of p1m1

5.3.1 Four possibilities. The **p1m1** border pattern may of course be viewed as a **pm11** pattern with vertical reflection **'replaced'** by horizontal reflection. Replacing "vertical" by "horizontal" in the table of 5.2.4 we obtain the following list of possibilities and border pattern types:

Color-reversing translation	Color-reversing horizontal reflection	Border pattern type
Y	Y	**p′1a1**
Y	N	**p′1m1**
N	Y	**p1m′1**
N	N	**p1m1**

In other words, we claim that this time **all** two × two = four types are indeed possible. In particular there is no problem having color-reversing translation without color-reversing horizontal reflection in a **p1m1**-like border pattern. The best way to establish this claim is of course to provide examples for each one of the four possibilities: one picture is worth one thousand words! To do that, we start with a 'colorless' **p1m1** border pattern and then we color it in two colors and in every possible way, exactly as in the two preceding sections:

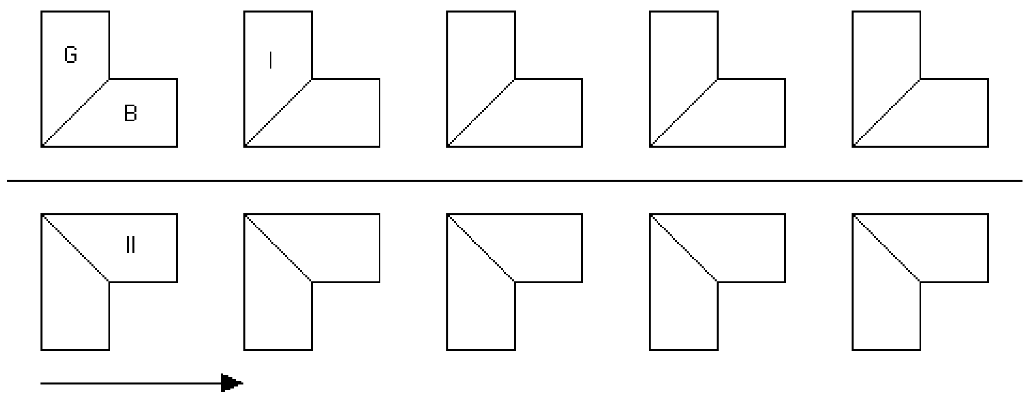

p1m1

Fig. 5.16

Now if we start by coloring the first two 'cells' grey (**G**) and black (**B**) as indicated in figure 5.16, then there exist **two** choices (**G** or **B**) for **each** of the two 'adjacent' cells I and II; so there exist indeed four possibilities altogether shown in figures 5.17-5.20.

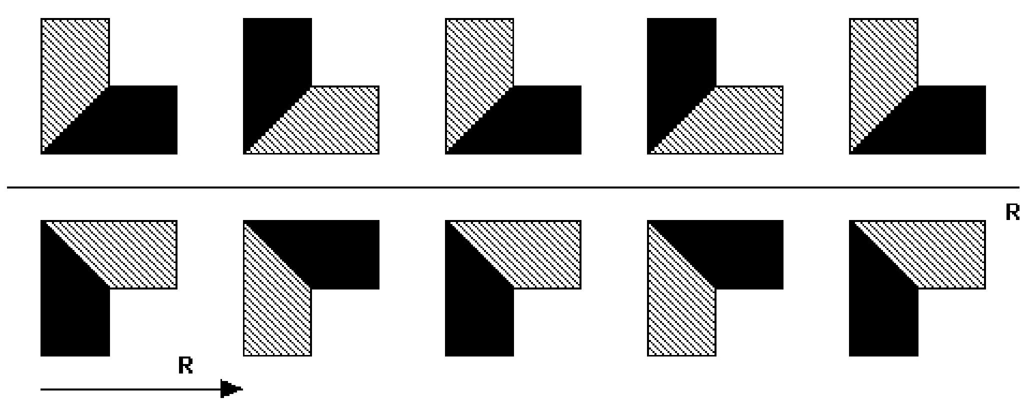

(I = **B**, II = **G**) **p′1a1**

Fig. 5.17

This type is known as **p′1a1**, ‘in honor’ of the **color-preserving** glide reflection (**a**) implied ‘automatically’ by the horizontal reflection (and the translation) in the spirit of 2.7.1. It should more appropriately be denoted by “p′1m′1”, perhaps, but the **crystallographic notation** has its own little secrets!

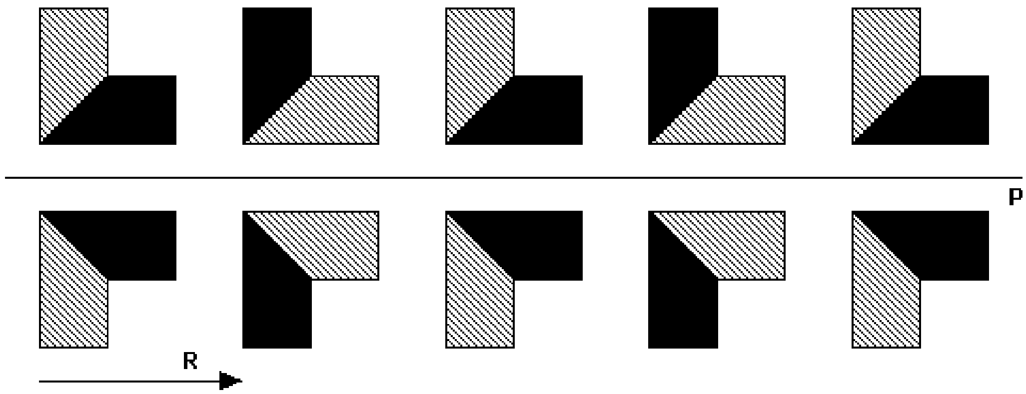

(I = **B**, II = **B**) **p′1m1**

Fig. 5.18

This type is known as **p′1m1** and may be viewed as a ‘doubled’ version of a **p′111**, with the bottom half being a mirror image of a **p′111** border pattern at the top.

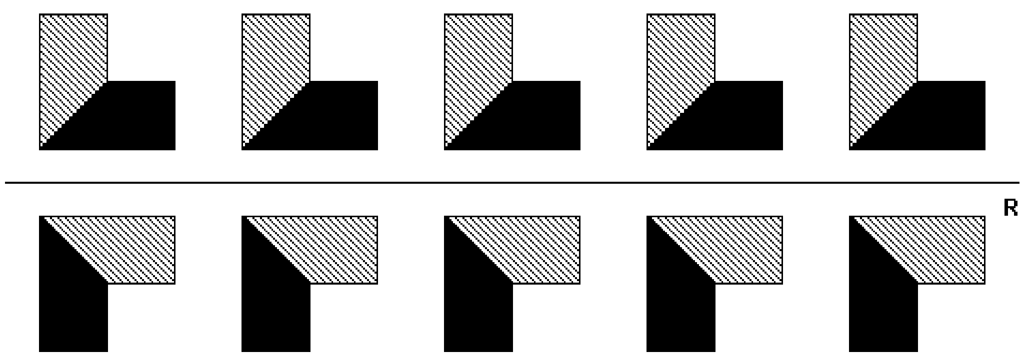

(I = **G**, II = **G**) **p1m′1**

Fig. 5.19

This type is known as **p1m′1**; it could also be called “p1a′1”, thanks to its ‘hidden’ color-reversing glide reflection and in conformity with the **p′1a1** type’s naming above, except that ... this ‘name’ is reserved for a type we will introduce in the next section!

Finally, we get the standard two-colored looking, one-colored classifiable border pattern that is found in every group, a **p1m1**:

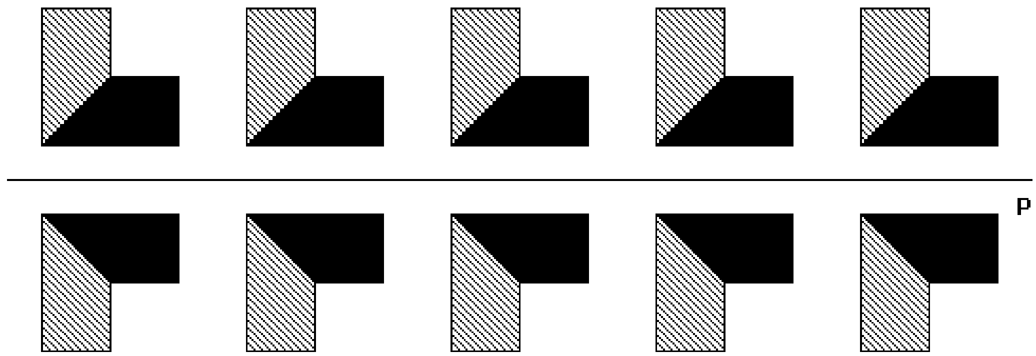

(I = **G**, II = **B**) **p1m1**

Fig. 5.20

5.3.2 <u>Further examples.</u> Here are three colorings illustrating the three new members of the **p1m1** group:

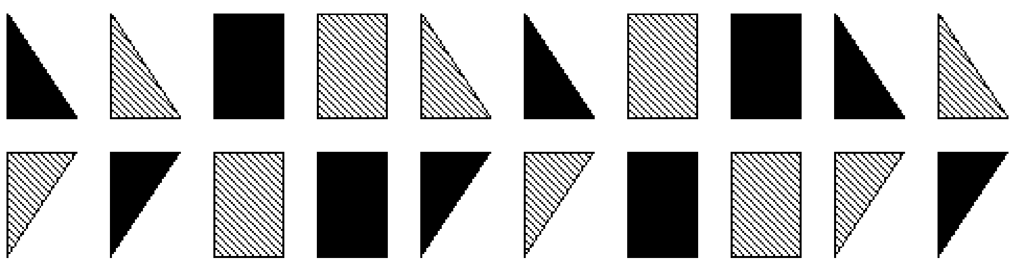

p′1a1

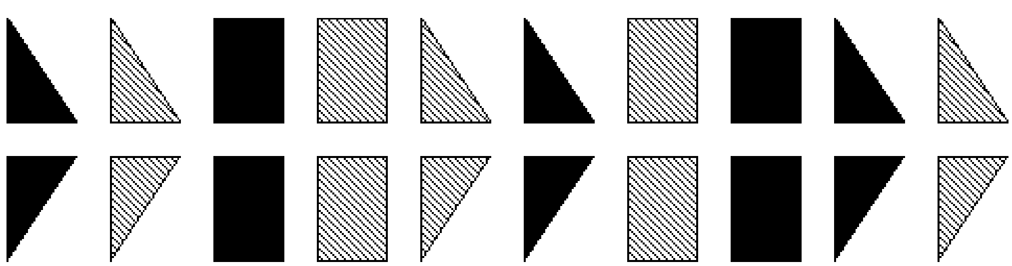

p′1 m 1

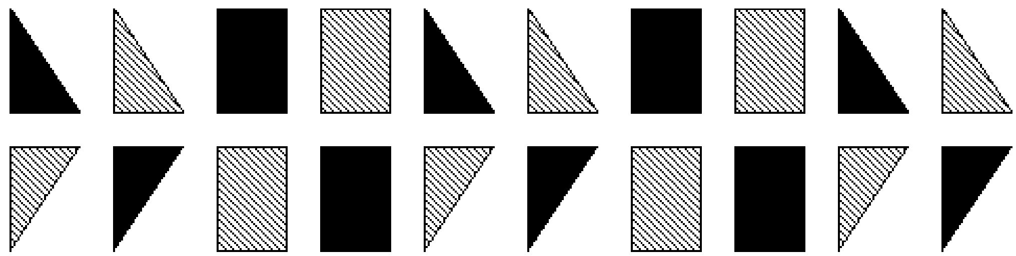

p1m′1

Fig. 5.21

5.4 Colorings of p1a1

5.4.1 Only two possibilities. In 2.4.2 we observed that the glide reflection vector in every **p1a1** border pattern is equal to **half** the pattern's minimal translation vector. Pushing that observation one step further we see that a **double** application of the **p1a1**'s minimal glide reflection results in the **p1a1**'s minimal translation. You may verify that yourself for the following 'colorless' **p1a1** pattern:

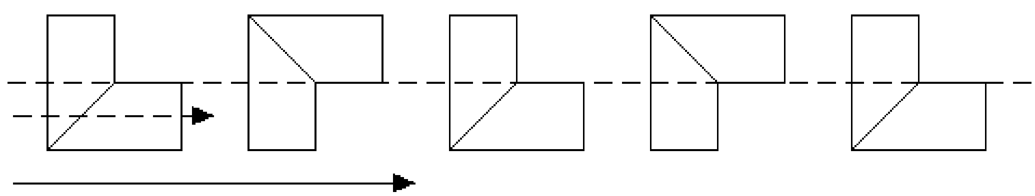

p1a1

Fig. 5.22

Our observation has a crucial implication: no matter how one colors a **p1a1** border pattern, the resulting two-colored pattern cannot possibly have color-reversing translation! Indeed, the **p1a1**'s translation is the **'square'** of either a color-preserving glide reflection or a color-reversing glide reflection: in either case, that 'square' **must** be **color-preserving**, in the same way that the square of every non-zero number must be positive. But this means that there is **only one question** to ask ("does the pattern have color-reversing glide reflection?”) and as many types of **p1a1**-like two-colored patterns as possible answers to that question:

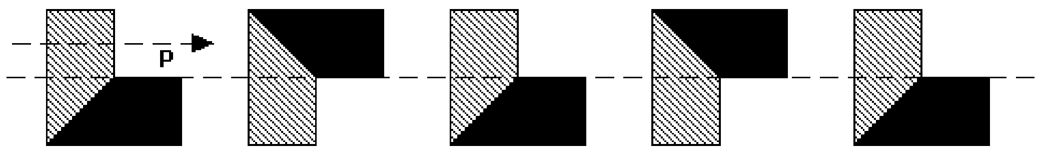

p1a1

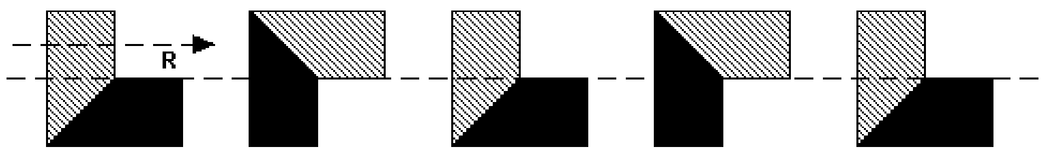

p1a′1

Fig. 5.23

So we have only one genuinely two-colored pattern in the **p1a1** group, characterized by color-reversing glide reflection (**p1a′1**).

5.4.2 Example. Our usual coloring example follows, involving two distinct but closely related **p1a′1**s:

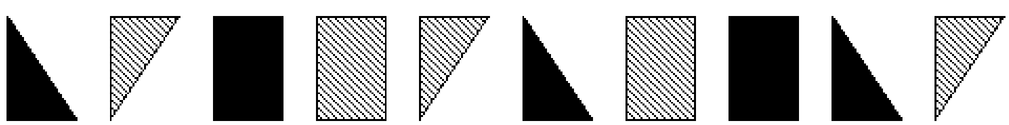

p1a′1

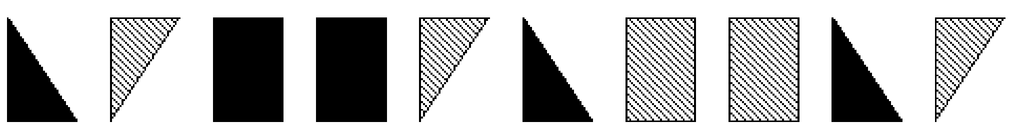

p1a′1

Fig. 5.24

5.5 Colorings of p112

5.5.1 A familiar story! Back in 2.5.4 we alluded to a certain similarity between vertical mirrors (in the **pm11** type) and half turn centers (in the **p112** type). This similarity is in fact so strong that virtually all our observations in section 5.2 remain valid when “vertical reflection” is replaced by “half turn”. In particular, color-reversing translation in a **p112**-like border pattern **implies** color-reversing half turn -- check also 7.6.4 -- and that table from 5.2.4 migrates here as follows:

Color-reversing translation	Color-reversing half turn	Border pattern type
Y	Y	**p′112**
Y	N	impossible
N	Y	**p112′**
N	N	**p112**

That is, there are precisely three types of patterns in the **p112** group, only two of them genuinely two-colored, shown right below:

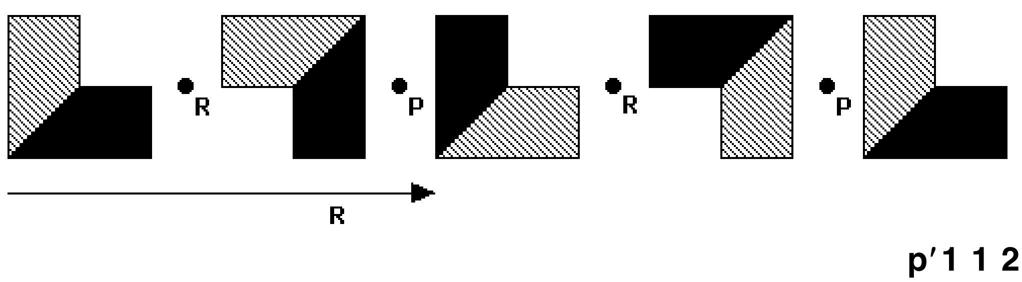

Fig. 5.25

This type, known as **p′112**, has **both** color-reversing and color-preserving half turn centers, thanks to color-reversing translation. But why is color-reversing translation associated with two adjacent half turn centers (or vertical reflection axes) of **opposite** effect on color? Well, the easiest way to see this right now is to argue as in 5.4.1, observing in particular that the successive application (‘**product**’) of two adjacent half turns (or vertical reflections) yields the pattern's minimal translation; check also 7.5.3 (and 7.2.1)!

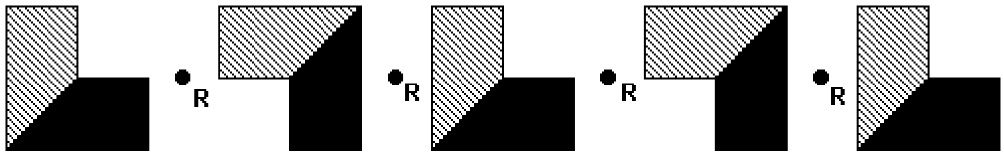

p112′

Fig. 5.26

This type, known as **p112′**, has only color-reversing half turn: now **both** types of centers correspond to color-reversing half turns.

As usual, we are 'tolerant' enough to include a 'two-colored looking' one-colored pattern in our collection:

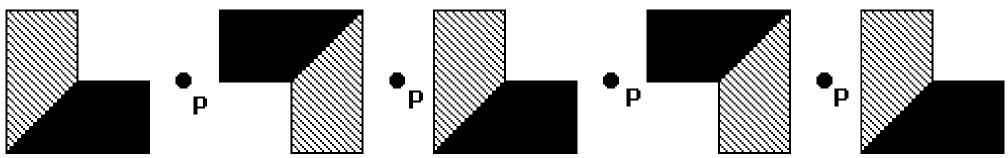

p112

Fig. 5.27

5.5.2 Examples. Here are two colorings of a **p112** pattern that should be compared to the colorings of **pm11** in 5.2.5 (as well as the colorings of **p1a1** in 5.4.2):

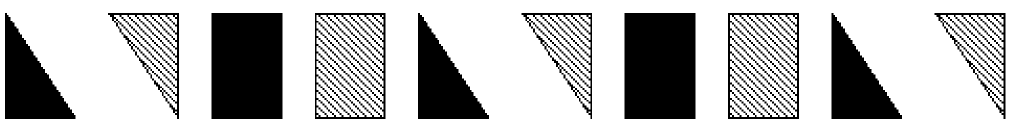

p112′

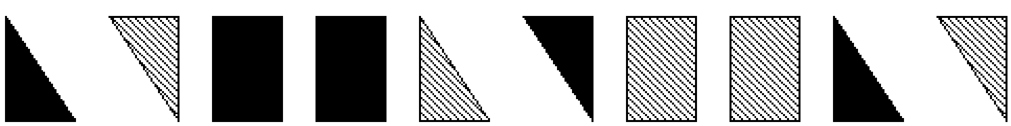

p′1 1 2

Fig. 5.28

5.6 Colorings of pma2

5.6.1 Half turns and mirrors of one kind only! Combining the discussions in 5.4.1 and 5.5.1 we are forced to conclude that in every **pma2**-like two-colored pattern **all** half turns must be either color-preserving or color-reversing, and likewise for vertical reflections. Indeed, the 'combination' of two adjacent half turn centers or vertical reflections of opposite effect on color would produce a color-reversing translation, which is ruled out by the presence of glide reflection!

5.6.2 Another kind of multiplication. As we are going to see in 6.6.2 and 7.7.4, and have already hinted on in 2.6.3, the **pma2**'s glide reflection may be viewed as the 'product' (successive application) of the pattern's half turn and vertical reflection. This means that the glide reflection's effect on color is **completely determined** by those of the half turn and the vertical reflection: if both are either color-preserving (**P**) or color-reversing (**R**), then the glide reflection has to be color-preserving (**P × P = P**, **R × R = P**); and if one is color-preserving (**P**) and the other one is color-reversing (**R**), then the glide reflection must be color-reversing (**P × R = R**, **R × P = R**). This **'multiplication rule'**, partially introduced in 5.4.1 and 5.5.1, is something you should be able to verify on your own: for **P** × **R** (color-reversing isometry **followed** by color-preserving isometry), for example, **B** → **G** → **G** and **G** → **B** → **B**, hence **B** → **G** and **G** → **B**. You may also draw an analogy with ordinary multiplication, thinking of **P** as **'positive'** and **R** as **'negative'**!

5.6.3 Precisely four possibilities. The discussion in 5.6.1 and 5.6.2 allows for a quick determination of all the **pma2** colorings. Indeed it suffices to look only at the pattern's half turn and vertical reflection, each of which has a well defined effect on color (either **P** or **R**), and the following table captures all two × two = four types:

Half turn	Vertical reflection	Pattern type	Glide reflection
P	**P**	**pma2**	**P** × **P** = **P**
P	**R**	**pm′a′2**	**P** × **R** = **R**
R	**P**	**pma′2′**	**R** × **P** = **R**
R	**R**	**pm′a2′**	**R** × **R** = **P**

Once again, we better provide one example per type in order to show that each type is indeed possible:

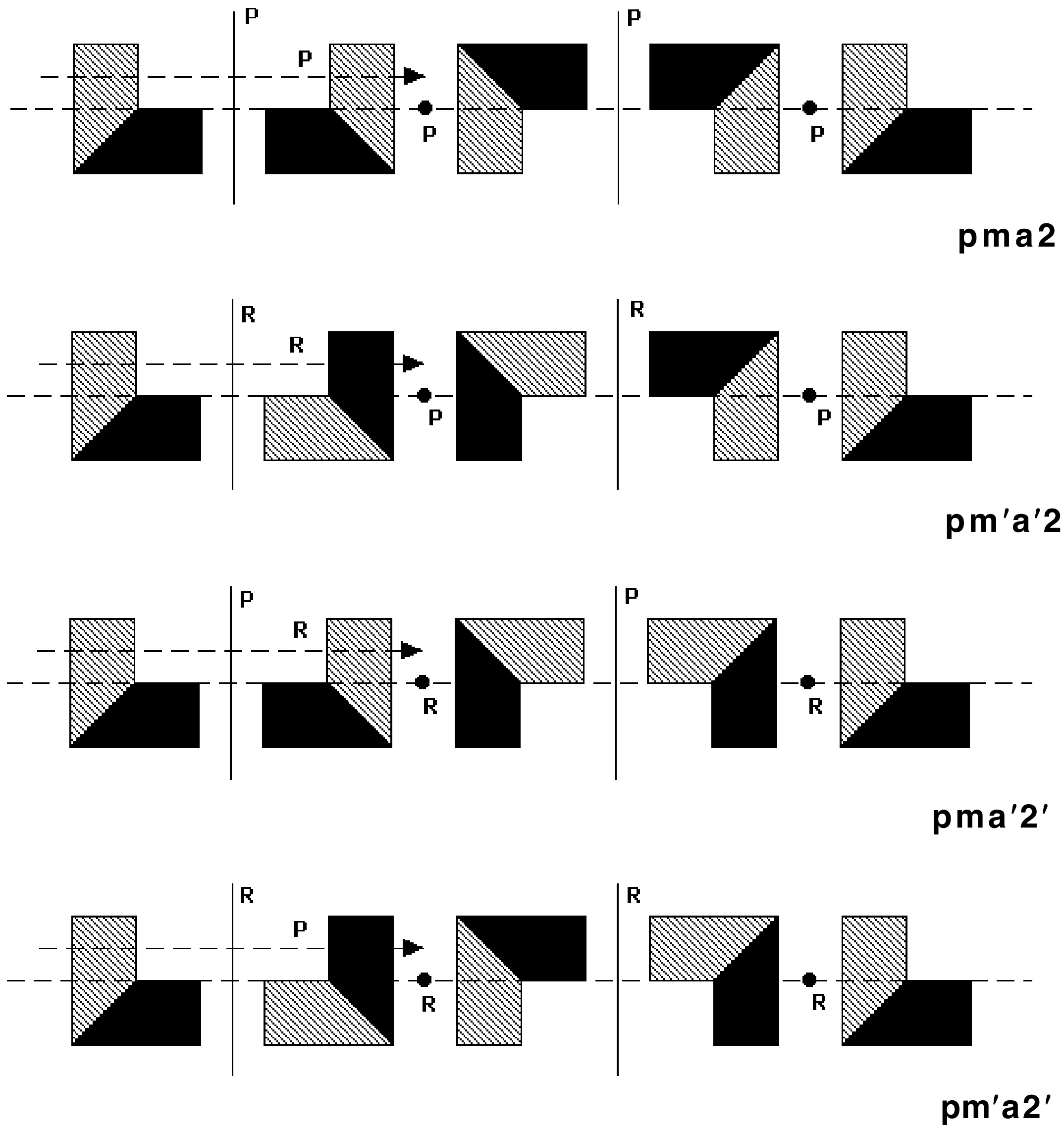

Fig. 5.29

Now you can go back to section 5.0, practice what you just learned and confirm that the two-colored patterns presented there indeed belong to the **pma2** family as follows: **pma′2′** (figures 5.3 & 5.4 (black-grey)), **pm′a2′** (figures 5.5 & 5.6 (blue-green)), and **pm′a′2** (figures 5.6 & 5.7 (yellow-red)).

5.6.4 Further examples. Three more **pma2**-like border patterns:

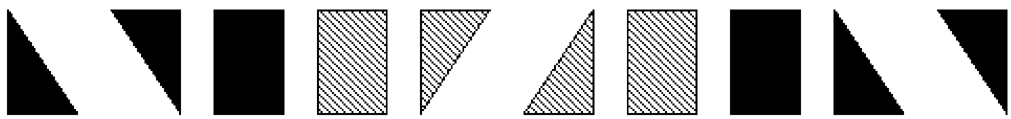

pm′a′2

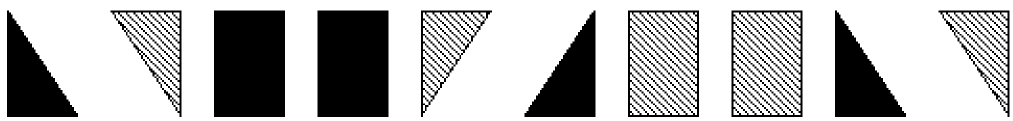

pma′2′

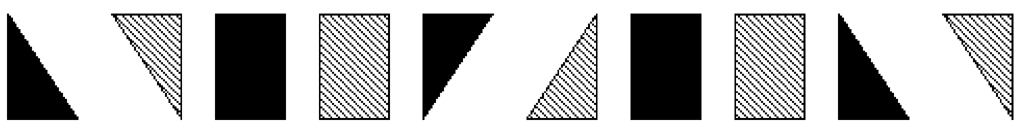

pm′a2′

Fig. 5.30

5.7 Colorings of pmm2

5.7.1 ‘Multiplying’ two types now! As we noticed in 4.6.1, the half turn of the **pmm2** border pattern may be seen as the ‘product’ of that pattern’s vertical and horizontal reflections, with the half turn centers found at the **intersection points** of the horizontal reflection axis with the vertical reflection axes. That is, the effect of a two-colored **pmm2**'s half turns on color is determined by the effect on color of its horizontal reflection and vertical reflections, following again the 'multiplication' rules of 5.6.2. It follows that we only need to focus on the effect on color of the horizontal reflection (viewing for a moment our **pmm2** pattern as merely a **p1m1** one), the vertical reflection (now treating the **pmm2** pattern as merely a **pm11** one), and the translation (present of course in both **'factor types'**). Focusing on whether or not **both** 'factors' have color-reversing translation or not, as well as on the color effect of their reflections, we build a **'multiplication table'** as follows:

color-reversing translation	**p1m1** 'factor'	**pm11** 'factor'	**pmm2** type	half turn (H.R.×V.R.)
N	**p1m1**	**pm11**	**pmm2**	**P** only
N	**p1m′1**	**pm11**	**pmm′2′**	**R** only
N	**p1m1**	**pm′11**	**pm′m2′**	**R** only
N	**p1m′1**	**pm′11**	**pm′m′2**	**P** only
Y	**p′1m1**	**p′m11**	**p′mm2**	**P** and **R**
Y	**p′1a1**	**p′m11**	**p′ma2**	**P** and **R**

There are many things one could say about this complicated 'multiplication', but we would rather let you discover those on your own and verify our table with the help of the following examples:

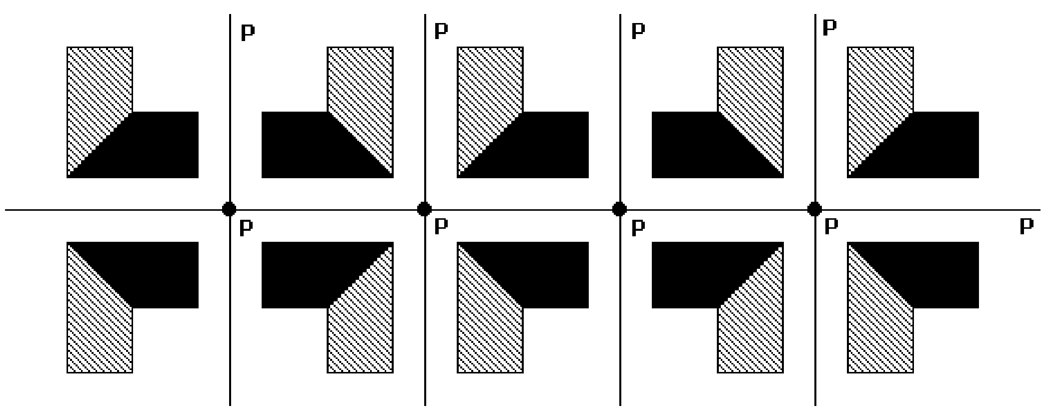

pmm2

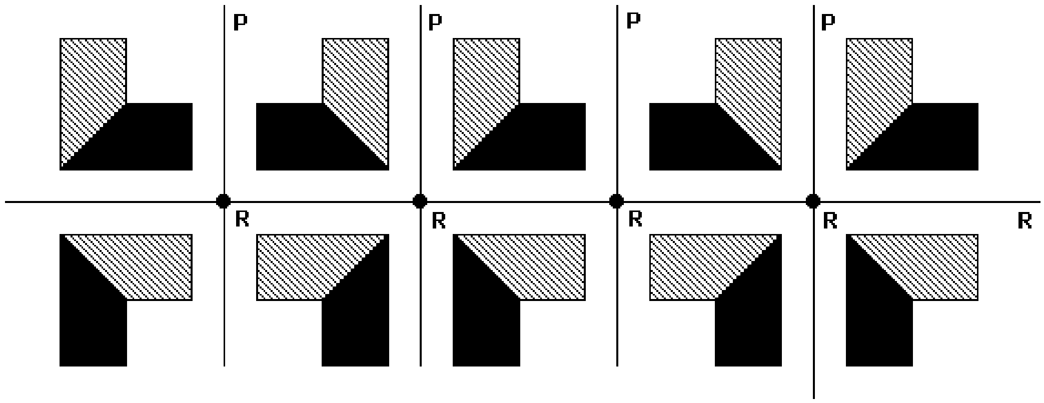

pmm′2′

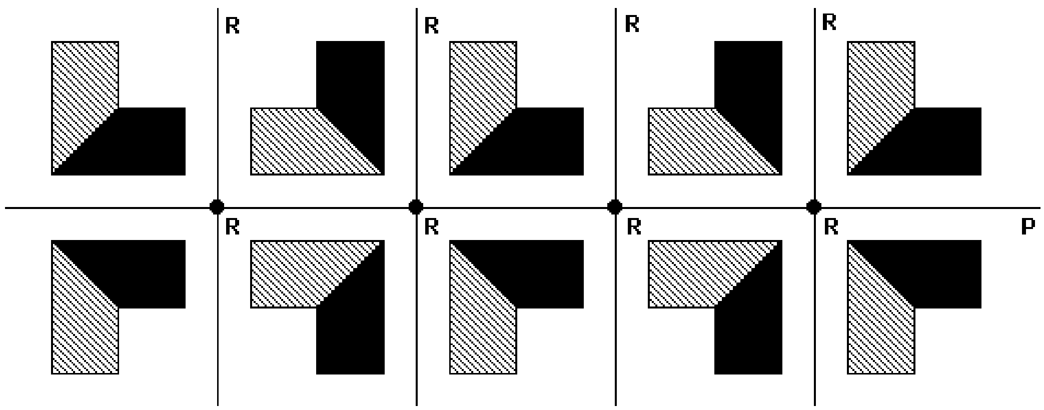

pm′m 2 ′

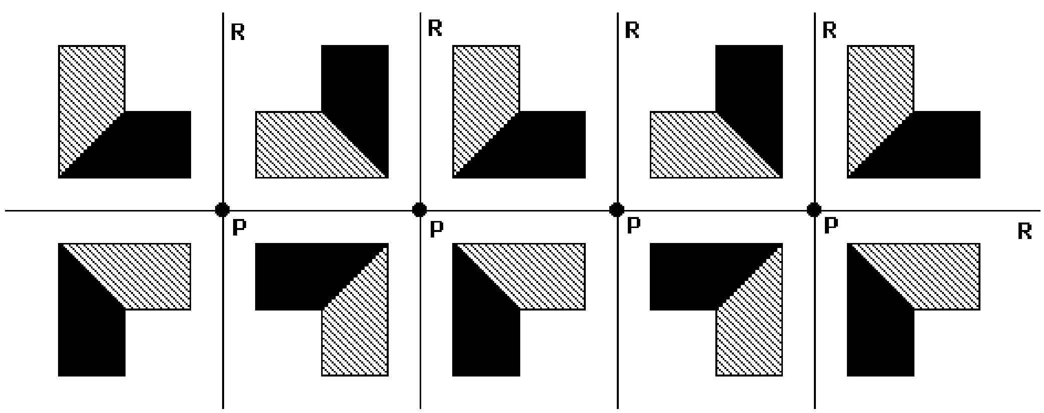

pm′m ′2

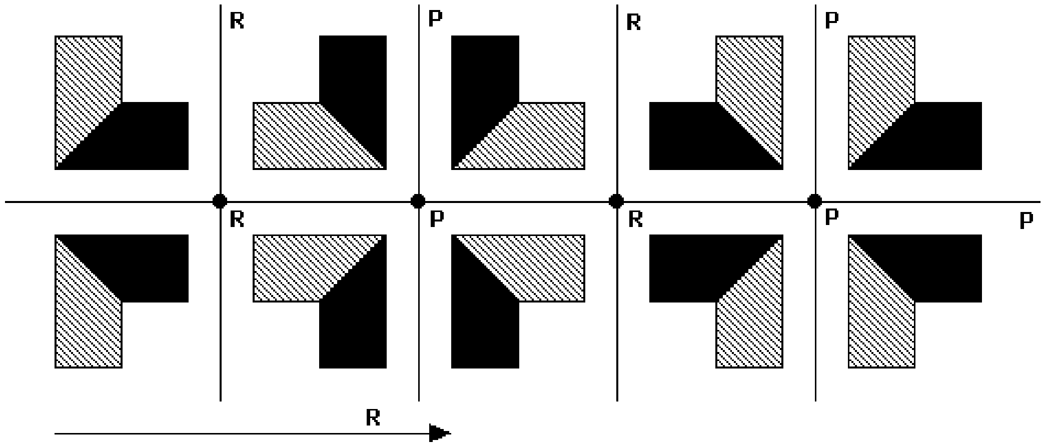

p′m m 2

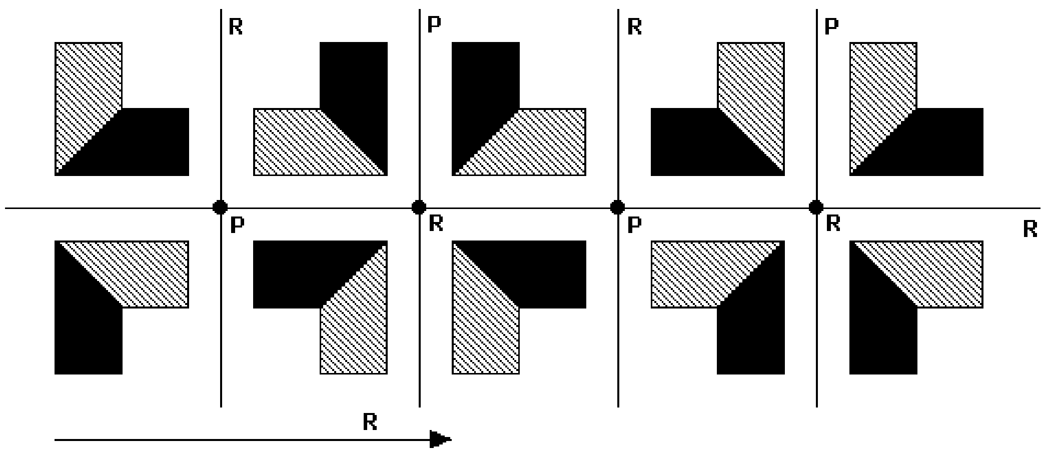

p′ma2

Fig. 5.31

5.7.2 Further examples. Once again, here are five colorings, corresponding to each one of the five new **pmm2**-like patterns:

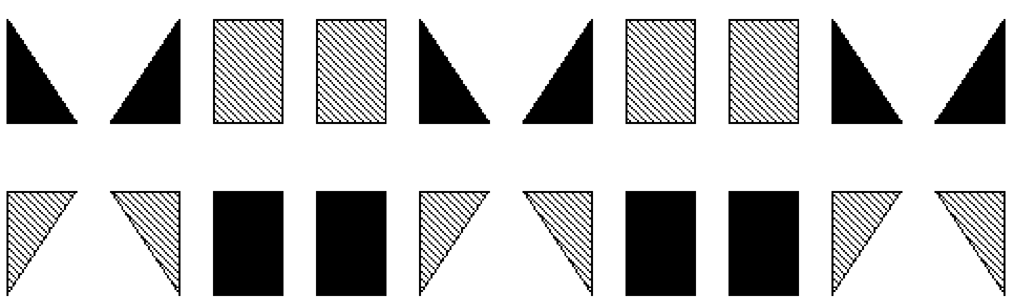

pmm′2′

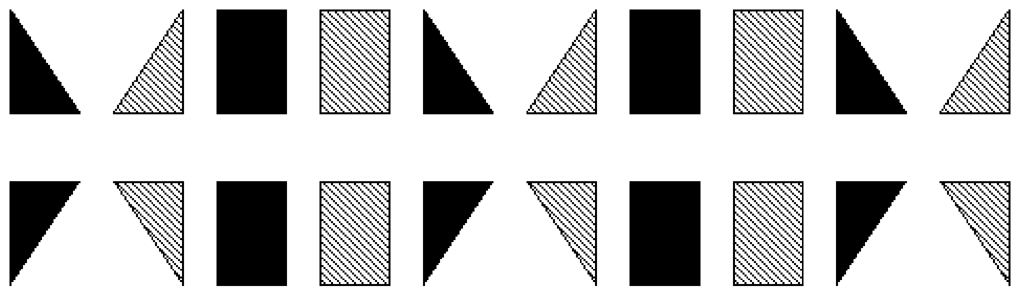

pm′m 2 ′

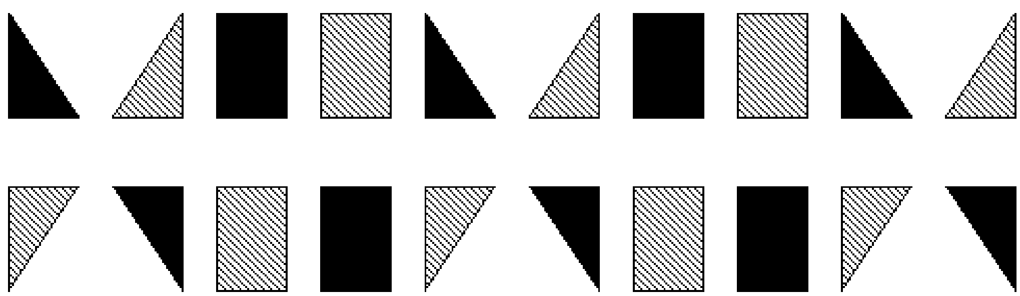

pm′m ′2

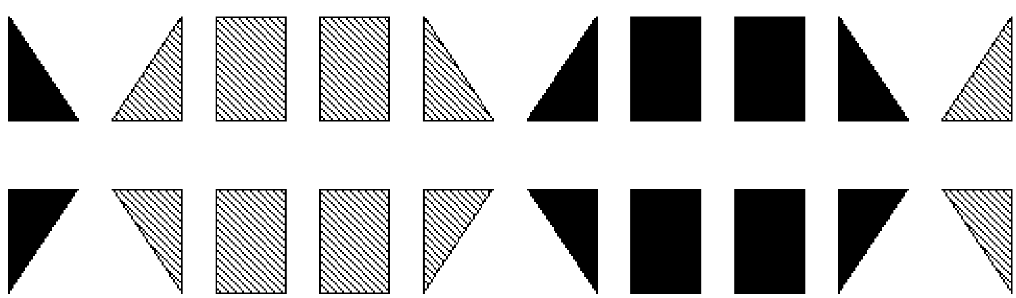

p′m m 2

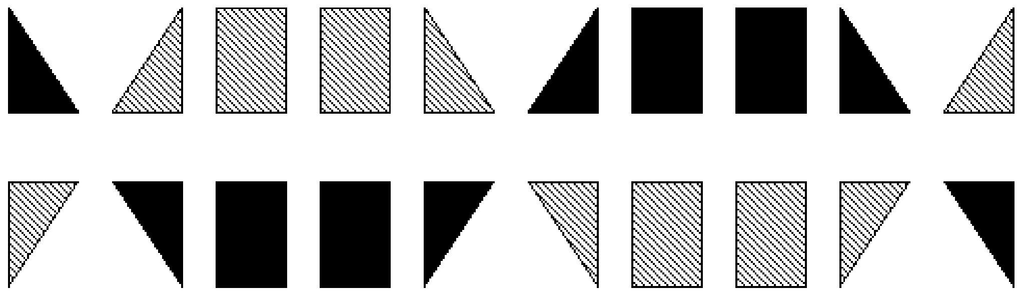

p′m a 2

Fig. 5.32

5.8 Consistency with color

5.8.1 What happened to that reflection? Let's try a coloring for the **pma2** pattern of figures 5.1 & 5.2 a bit different from the one featured in figures 5.3 or 5.4:

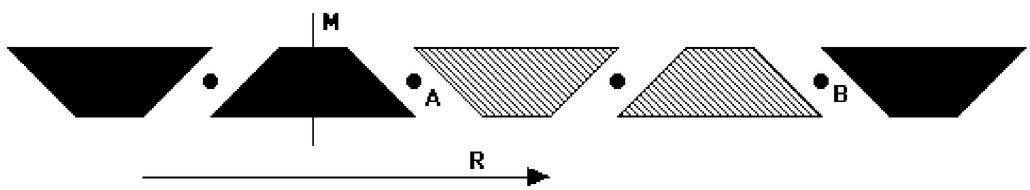

Fig. 5.33

Do the vertical reflection axes carried over from figure 5.1 preserve or reverse colors? The answer is neither "yes" nor "no": looking at axis **M**, for example, we see that it leaves the black trapezoid it bisects inevitably unchanged, but it maps the black trapezoid to its left to the grey trapezoid to its right. One might say that our reflection axis acts **inconsistently** with respect to color, preserving it in some instances and reversing it in others. And it doesn't take long to notice that all reflection axes in figure 5.33 'behave' the same way, being **inconsistent with color**.

How would you classify the pattern in question? First, you would certainly not think of vertical reflection anymore (our pattern **looks** now like a row of **homostrophic** black and grey **parallelograms**, leaving no room for reflection or even glide reflection), but you would probably notice the **color-reversing half turns** centered at **A** and **B** and nothing else: a **p112′**, then? Well, if you remember or review section 5.5 and also notice the pattern's **color-reversing translation**, you will disagree: **p112′** does not have color-reversing translation, hence our pattern must be a **p′112**. But every **p′112** has both color-reversing and color-preserving centers: where are the **color-preserving half turn centers**, in that case? Well, a bit of experience would have led you to look right at the center of each **parallelogram-like pair of trapezoids** of same color, the 'internal' half turn of which naturally extends to the entire border pattern. Alternatively, both color-preserving and color-reversing half turn centers have been 'inherited' from the original **pma2** pattern, hence they should not be missed. One way or another, we have reached a conclusion: the pattern in figure 5.33 is a **p′112**.

5.8.2 Coloring, symmetry, and perception. Back in 5.1.1 we made an 'innocent' remark to the effect that coloring cannot increase symmetry. We are now in a position to complete that remark by stating that **coloring may only decrease symmetry**. Indeed the example discussed in 5.8.1 is an appropriate illustration of this principle, in both **visual** and **conceptual** terms: the two-coloring of a **pma2** border pattern **'eliminated'** its vertical reflection -- and glide reflection, as you should verify on your own -- by rendering it inconsistent with color and reduced it to a **p′112** pattern; and instead of trapezoids, the viewer is now more likely to **'see'** parallelograms!

More generally, the rule born out of the discussion in 5.8.1 is: when classifying a two-colored border pattern, **discard every isometry that is inconsistent with color**.

5.8.3 Inconsistent half turns? Now you might ask: isn't the half turn in the 'trapezoidal' pattern discussed in 5.8.1 inconsistent with color? Do not half of the 180^0 centers reverse colors while the other half preserve them? **Attention!** When you examine consistency with color, you should focus on **one isometry at a time!** Indeed if you think of any individual half turn center in the pattern of figure 5.33, you will confirm for yourself that **it either preserves colors** (mapping every black trapezoid to a black one and every grey trapezoid to a grey one) **or it reverses colors** (mapping every black trapezoid to a grey one and vice versa); that is, every half turn in figure 5.33 is **consistent with color**, one way or another.

Does this mean that half turns are always consistent with color? Not at all! Here is another coloring of the original **pma2** pattern -- to be precise, of a **'partitioned'** version of it (in which every trapezoid is cut into two equal halves) -- that produces a **p′m11** pattern:

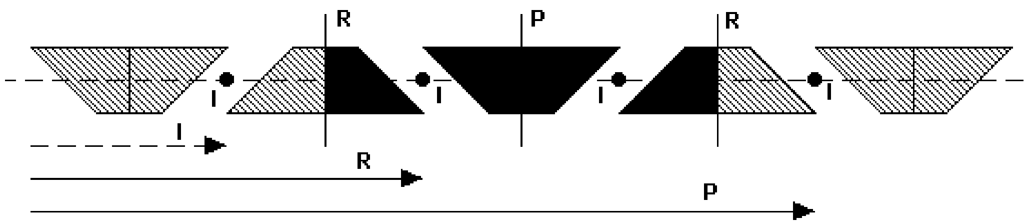

Fig. 5.34

Indeed all half turns are inconsistent with color (a fact denoted by an **I** right next to every half turn center), hence **discarded** (likewise for glide reflection); at the same time, vertical reflection axes alternate between color-preserving (**P**) and color-reversing (**R**).

5.8.4 <u>Both kinds together.</u> Here is yet another coloring of the original **pma2** pattern, producing a **pm′11** this time:

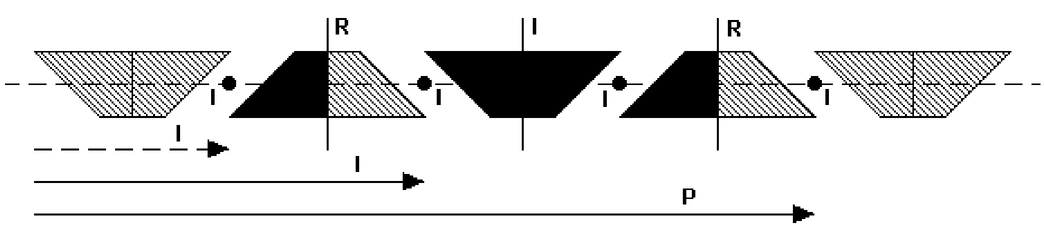

Fig. 5.35

Now **only half** of the vertical reflections in figure 5.35 are consistent, that is color-reversing (**R**); the other half are inconsistent (**I**), hence **discarded** together with the half turns, glide reflection, and even inconsistent translation! (There is still a color-preserving translation, of course, but the color-reversing one in figure 5.34 has been rendered inconsistent by our modification of coloring.)

5.8.5 Consistent glide reflection? Both colorings of the **pma2** pattern presented in 5.8.3 and 5.8.4 eliminated its glide reflection by rendering it inconsistent with color: are there any colorings that eliminate the pattern's half turn **and** vertical reflection but preserve its glide reflection? The answer is "yes", but such colorings are a bit harder to come up with; here is a coloring that reduces the **pma2** to a **p1a′1**, exhibited on a 'compressed' version of the original pattern (with the length of each trapezoid cut in half):

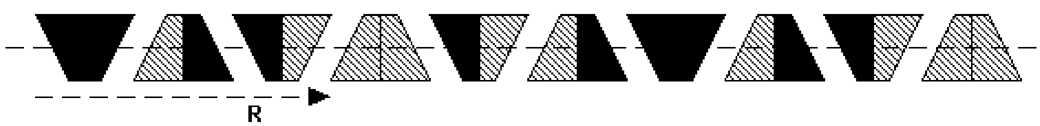

Fig. 5.36

5.8.6 Further examples. Here are some inconsistent colorings reducing a 'partitioned diamond' **pmm2** pattern to 'lower' types:

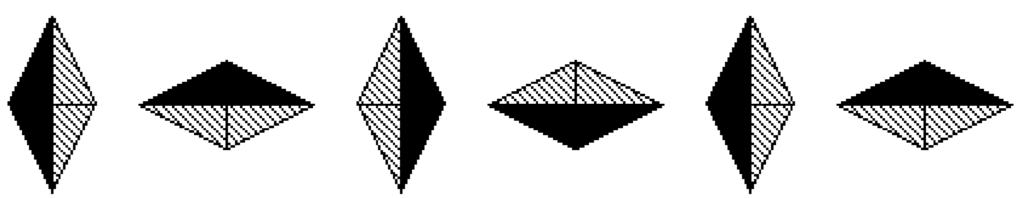

p′m11

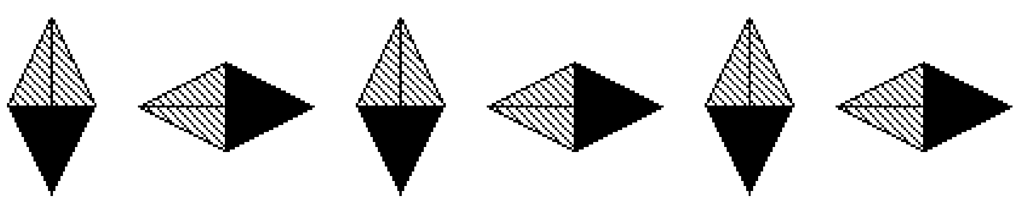

p112′

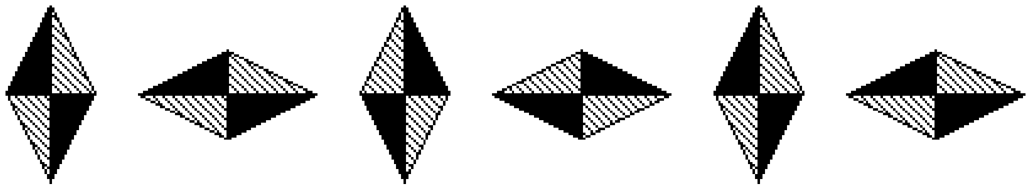

p′1 a 1

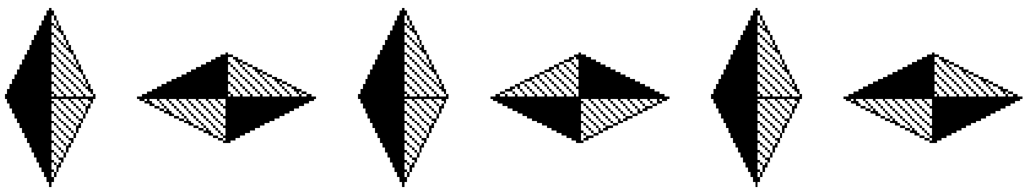

pm′a 2′

Fig. 5.37

5.9 Symmetry plans

5.9.1 The abstract way of looking at it. As we indicated in 5.2.3, from the purely mathematical point of view, and for mere classification purposes, all that matters in a border pattern is its symmetry elements (isometries) and their effect on color, captured in what we called **symmetry plan**. Here we present symmetry plans for all **twenty four** types of two-colored border patterns: seventeen genuinely two-colored ones (introduced in this chapter) and seven one-colored ones (introduced in chapter 2); it is of course the various colorings of these seven **'parent types'** (presented below in bold face print) that generate the other seventeen types, hence the latter are appropriately grouped under the former.

When trying to classify a border pattern, you should first locate its parent type and then match it with one of the parent type's 'offspring'. Do not forget that **isometries inconsistent with color --** which should **still** be marked with an **I -- are not taken into account at all**: there are no **I**s in the symmetry plans below!

Symmetry Plan notation: **solid** lines represent **translation** vectors (indicated even when color-preserving) and **reflection** axes; **dotted** lines represent **glide reflection** vectors and axes.

p111

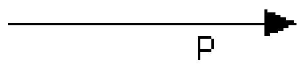

p'111

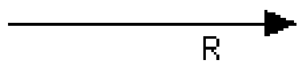

pm11

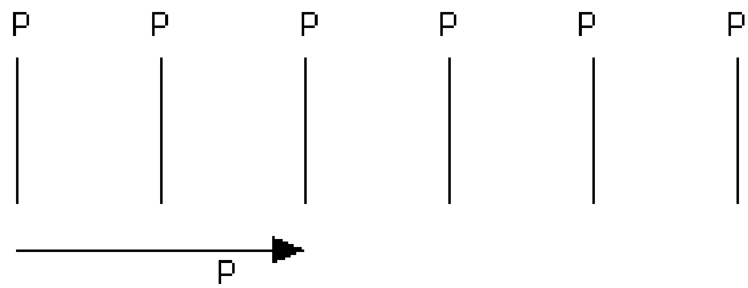

pm'11

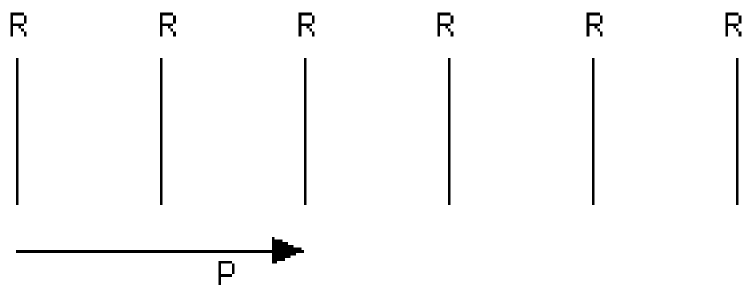

p'm11

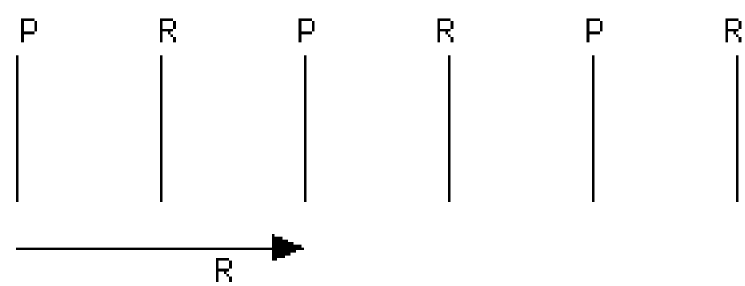

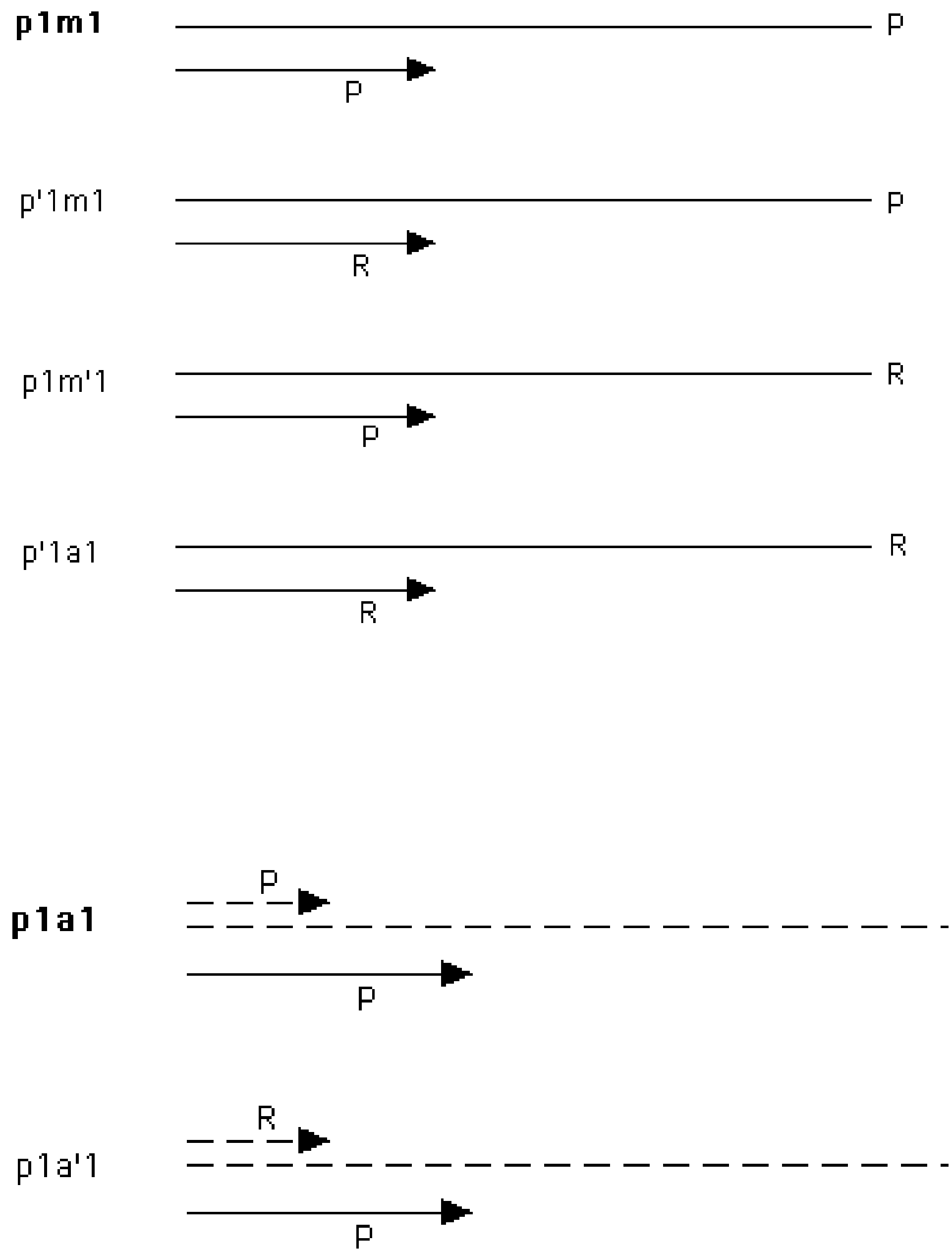
p1m1
P
P
p'1m1
P
R
p1m'1
R
P
p'1a1
R
R
p1a1
P
P
p1a'1
R
P

p112

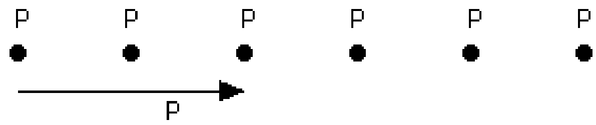

p112'

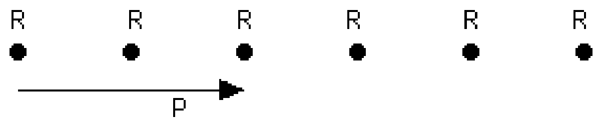

p'112

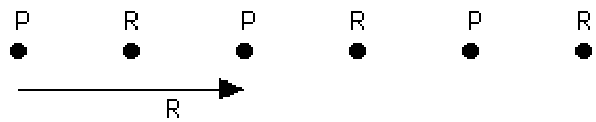

pma2

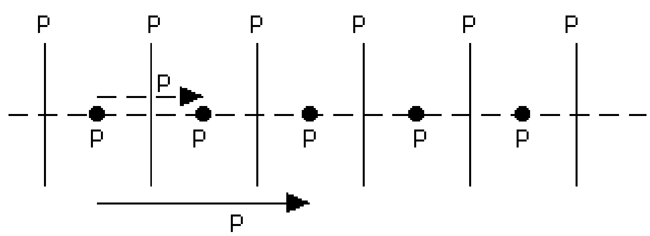

pm'a'2

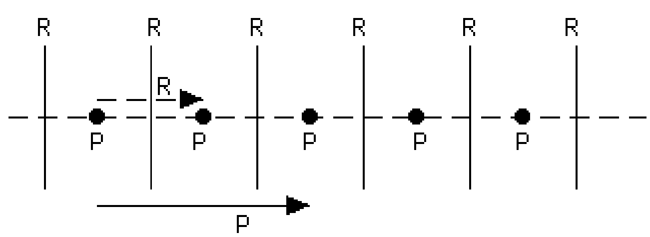

pma'2'

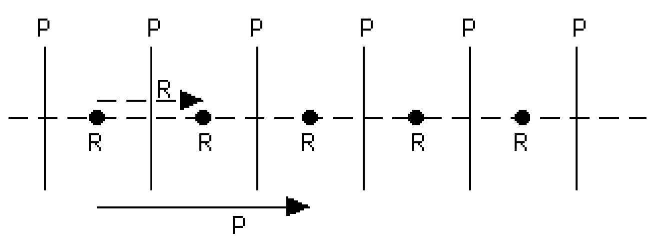

pm'a2'

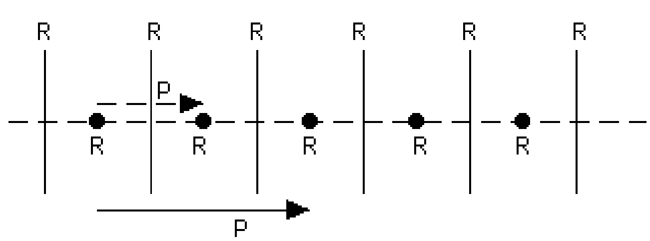

pmm2

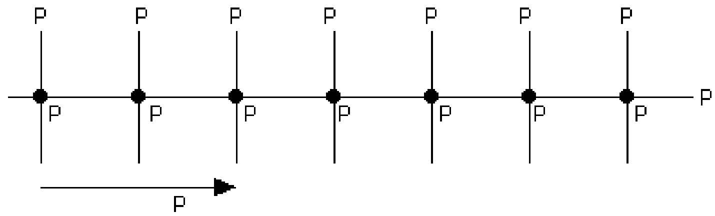

pmm'2'

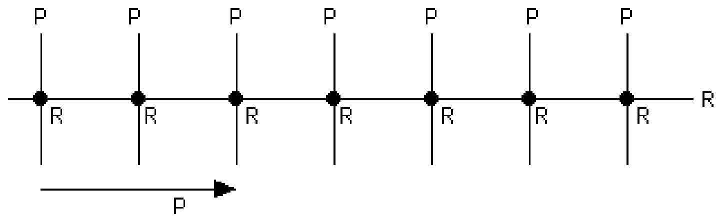

pm'm2'

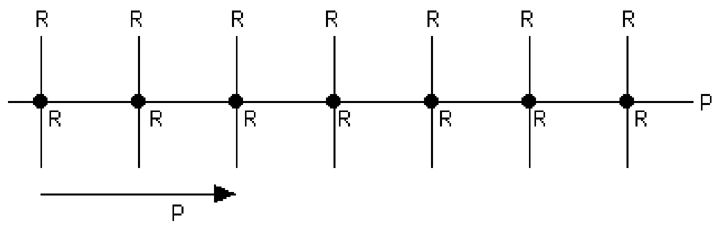

pm'm'2

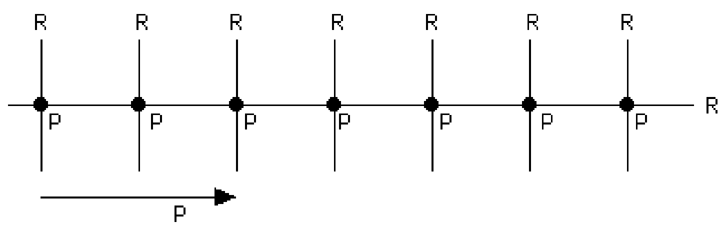

p'mm2

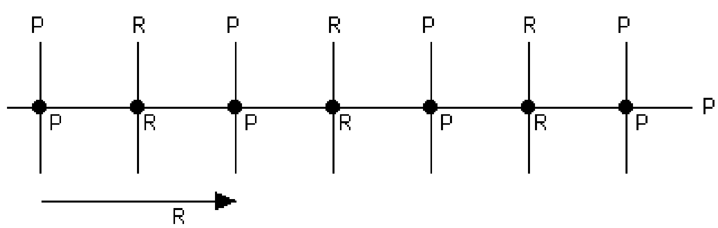

p'ma2

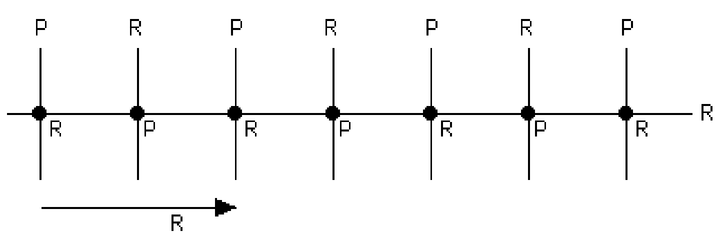

first draft: winter 1999

CHAPTER 6

TWO-COLORED WALLPAPER PATTERNS

6.0 Business as usual?

6.0.1 Consistency with color. All concepts and methods pertaining to two-colored border patterns discussed in detail in chapter 5 extend appropriately to two-colored wallpaper patterns. Once again, and due to induced color inconsistencies, **coloring may only preserve or decrease symmetry**. As an example, the following coloring of the **cm** pattern in figure 4.27 eliminates **both** its reflection and its glide reflection by way of color inconsistency:

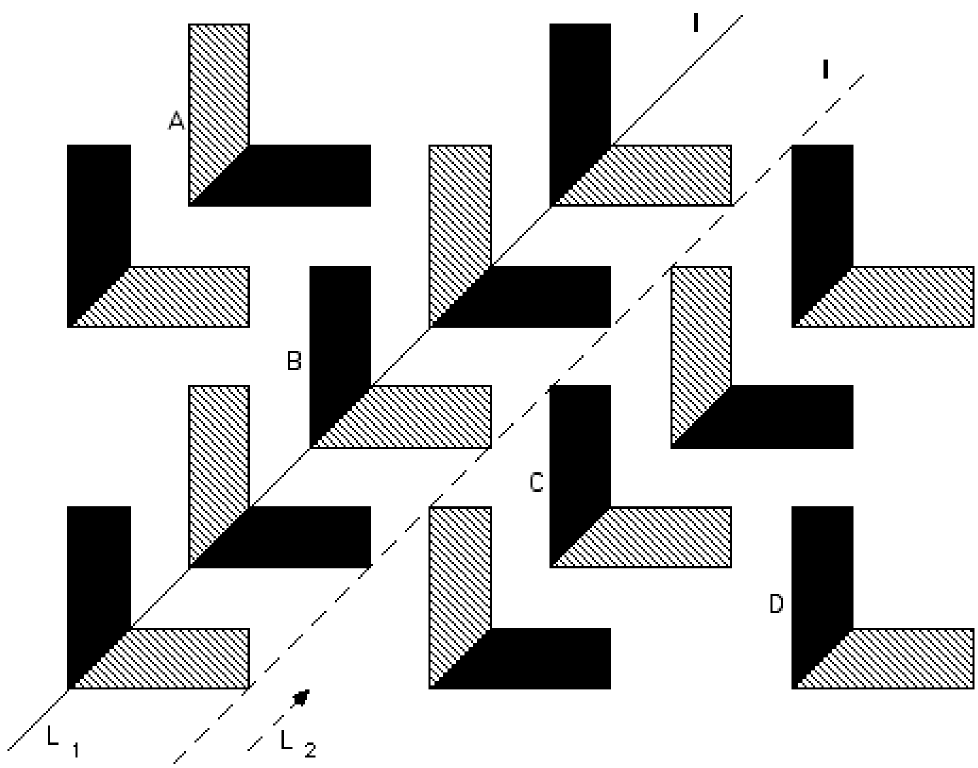

Fig. 6.1

Indeed, the reflection axis $\mathbf{L_1}$ reverses colors as it maps B to itself but preserves colors as it maps A to C; and the shown **upward** glide reflection along $\mathbf{L_2}$ reverses colors as it maps B to C but preserves colors as it maps A to D. (An important lesson drawn out of this example that you should keep in mind throughout this chapter is this: whenever you check a reflection or glide reflection axis for consistency with color, make sure that you look **both** at motifs on or **'near'** that axis and at motifs **'far'** from that axis -- "far" and "near" depending on the fundamental (repeated) region's size.)

6.0.2 <u>The smallest rotation angle.</u> As in the case of one-colored wallpaper patterns (chapter 4), the most important step in classifying two-colored wallpaper patterns is the determination of the pattern's smallest rotation angle; again, coloring may eliminate certain rotations by rendering them inconsistent with color, and it is appropriate to state here that **coloring may only preserve or increase the smallest rotation angle**. As an example, the following two colorings (figures 6.2 & 6.3) of the **p4g** pattern in figure 4.57 do increase the **smallest rotation angle consistent with color** from 90^0 to 180^0 (color-reversing) and 360^0 (none), respectively; and this change most definitely affects our **visual perceptions** of these 'new' wallpaper patterns:

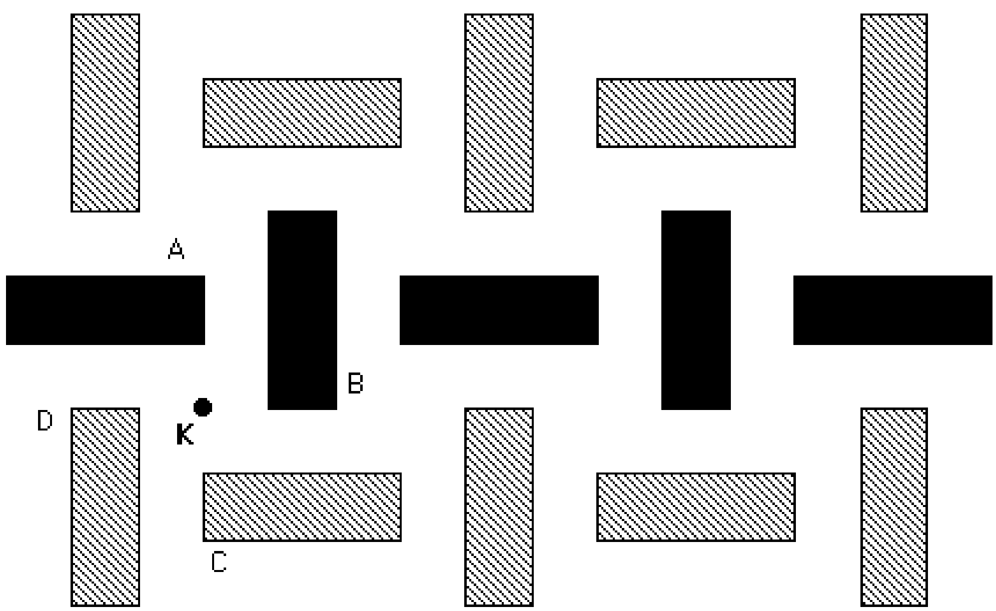

Fig. 6.2

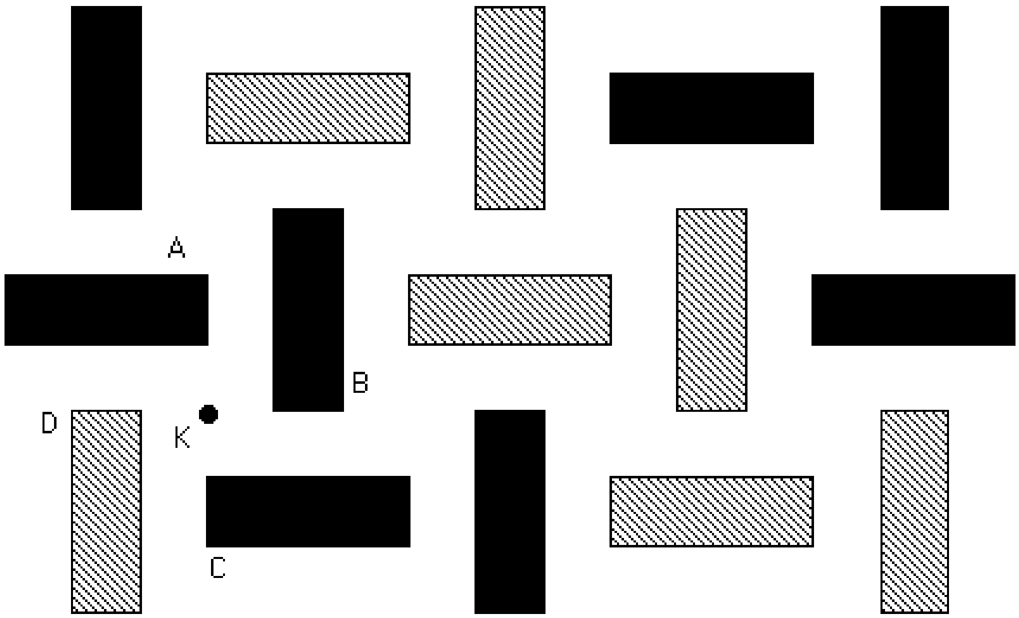

Fig. 6.3

In the pattern of figure 6.2, clockwise 90^0 rotation about **K** maps black A to black B but black B to grey C (inconsistent), while 180^0 rotation about **K** maps **all** black units to grey ones and vice versa (consistent): that is, the initial 90^0 rotation is gone but the induced 180^0 rotation -- recall (4.0.3) that applying a 90^0 rotation **twice** trivially generates a 180^0 rotation -- survives. And in the pattern of figure 6.3 clockwise 90^0 rotation about **K** maps black A to black B but black C to grey D (inconsistent), while 180^0 rotation about **K** maps black A to black C but black B to grey D (inconsistent): that is, **both** the 90^0 and 180^0 rotations about **K** have been rendered color-inconsistent by the original **p4g** pattern's coloring -- which has in fact 'destroyed' **all** rotation centers, twofold and fourfold alike. In a nutshell, the pattern in figure 6.2 is a two-colored **180^0** pattern, while the pattern in figure 6.3 is a two-colored **360^0** pattern.

6.0.3 <u>When the two colors are 'inseparable'.</u> As in chapter 5, it is possible for a 'two-colored looking' pattern to be classifiable as one-colored because it has **no color-reversing isometry**. Here are two such 'exotic' examples featuring **color-preserving translation** -- present in **all** two-colored patterns, hence not mentioned -- together with **color-preserving glide reflection** (a

pg, figure 6.4) or **color-preserving half turn** (a **p2**, figure 6.5); of course one may view these two patterns as unions of two **'equal and disjoint'**, black and grey, **pg** and **p2** patterns, respectively.

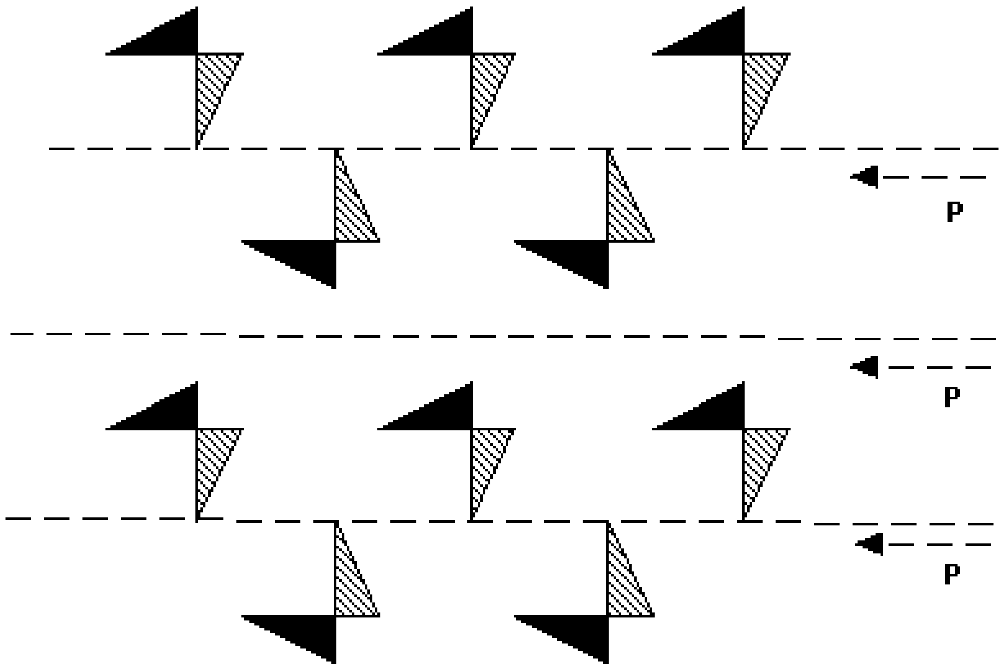

pg

Fig. 6.4

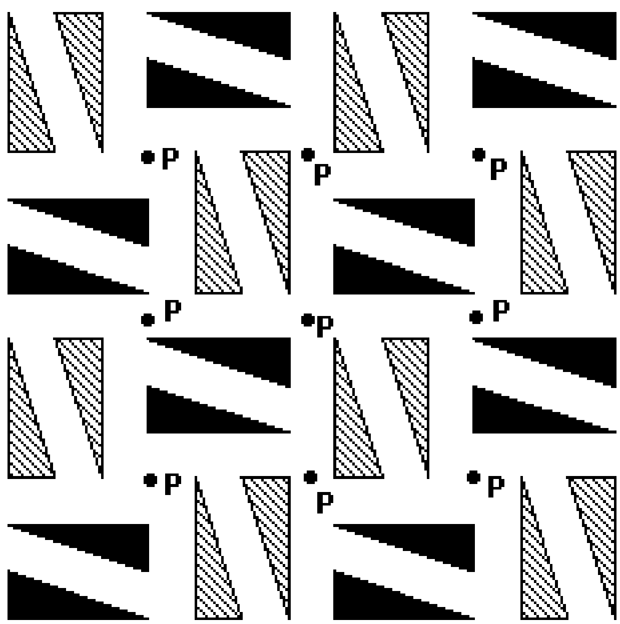

p2

Fig. 6.5

6.0.4 Symmetry plans and types. Tricky two-colored wallpaper patterns such as the ones presented so far, as well as easier ones, are not that difficult to classify once the smallest rotation angle consistent with color has been determined. Indeed there are **symmetry plans** available at the end of most sections, focused on those symmetry elements that are essential for classification purposes; all notation introduced in 5.2.3 and employed in section 5.9 remains intact. As in chapter 4, little attention is paid to the crystallographic notation's mysteries: simply try to comprehend symmetry plans instead of memorizing **sixty three** type names!

In each of the next seventeen sections we will be looking not only at all possible ways of coloring each one of the seventeen wallpaper types in two colors, but also at all possible two-colored types sharing the same isometries (be them color-preserving or color-reversing) with each of the seventeen parent types. For example, the two-colored patterns in figures 6.2 & 6.3 are no longer associated with the **p4g** parent type, but rather with 180^0 and 360^0 parent types to be determined -- stay tuned! Moreover, the number of two-colored possibilities associated with each parent type will be not only artistically and empirically determined, but also **mathematically justified and predicted**: and it is precisely through this 'prediction process' that you will begin to understand the mathematical structure of the seventeen wallpaper pattern types, and how their isometries **interact** with each other, effectively building each type's symmetry and **'personality'**!

Here is the number of two-colored types associated with each of the seventeen parent types, **including** in each case the one-colored parent type itself (which is justified by our discussion in 6.0.3):

p1:	2	**pmg**:	6	**p3**:	1
pg:	3	**pmm**:	6	**p31m**:	2
pm:	6	**cmm**:	6	**p3m1**:	2
cm:	4	**p4**:	3	**p6**:	2
p2:	3	**p4g**:	4	**p6m**:	4
pgg:	3	**p4m**:	6		

As promised above, the grand total is **63**: the journey begins!

6.1 p1 types (p1, p'_b1)

6.1.1 One direction is not enough! A two-colored wallpaper pattern must by definition have translation consistent with color in **two**, therefore (4.1.1) **infinitely many**, directions. Notice here, as in 5.1.2, the existence of color-preserving translation in **all** two-colored patterns (already mentioned in 6.0.3): since the successive application of any translation that leaves the pattern invariant produces a **double** translation that also leaves the pattern invariant, the **R** x **R** = **P** rule of 5.6.2 allows us to get a color-preserving translation out of every color-reversing translation.

On the other hand, color-reversing translation in **one** direction (with no other color-consistent translations in sight) does **not** make a wallpaper pattern! Combining ideas from section 4.1 (figures 4.12 & 4.13), we use **vertical p′111** border patterns to built the following **'non-pattern'** that has vertical color-reversing translation (hence black and grey **in perfect balance** with each other):

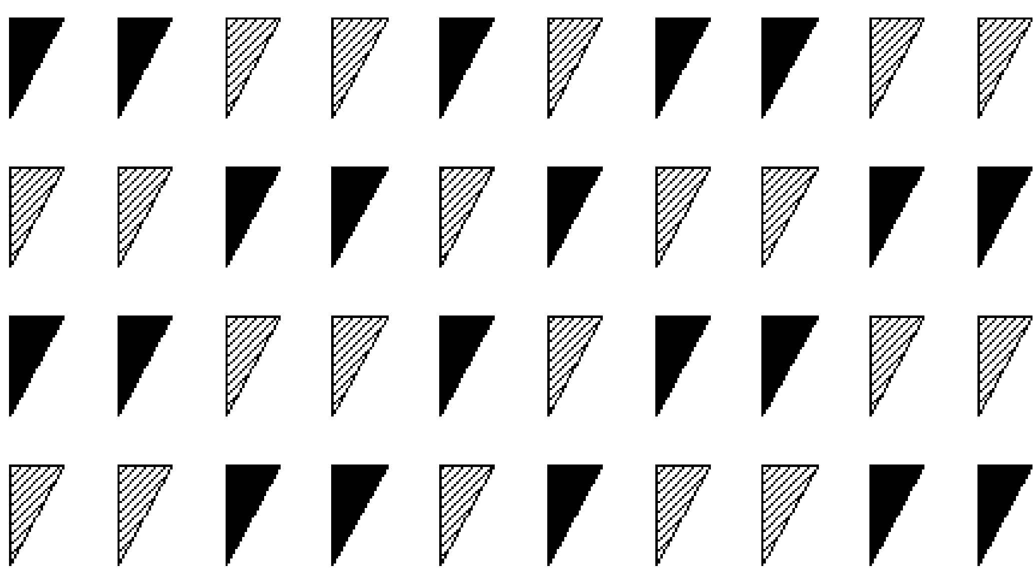

Fig. 6.6

6.1.2 Infinitely many color-reversing translations. Leaving the 'non-pattern' of figure 6.6 behind us, let's have a look at the two-colored wallpaper pattern of figure 6.1: it clearly has no rotation, and we have already pointed out in 6.0.1 that all its reflections and glide reflections are gone due to color inconsistency. In view of our discussion in 6.0.3, you have every right to ask: is it 'truly' two-colored? That is, does it have any isometries that **swap** black and grey? Yes, if you remember to think of **translations**! Indeed, you can easily see that there is an 'obvious' horizontal **color-reversing translation** and three less obvious **'diagonal'** color-reversing translations, mapping A to B, C, and D, respectively; and you can probably see by now that there exist such translations in **infinitely many directions**. This property of the pattern in figure 6.1 should not surprise you in view of our discussions in 4.1.1, 6.1.1, and the **R** x **P** = **R** rule of 5.6.2: every two-colored wallpaper pattern that has color-reversing translation in one direction must have color-reversing translation in infinitely many directions.

The observation we just made holds true for every two-colored wallpaper pattern: all patterns you are going to see in this chapter have color-reversing translation in **either none or infinitely many directions**. Patterns that have nothing but color-reversing translation (and color-preserving translation, of course) are known as $\mathbf{p'_b1}$ patterns. Here are three examples of such patterns **simpler** in underlying structure than the one in figure 6.1:

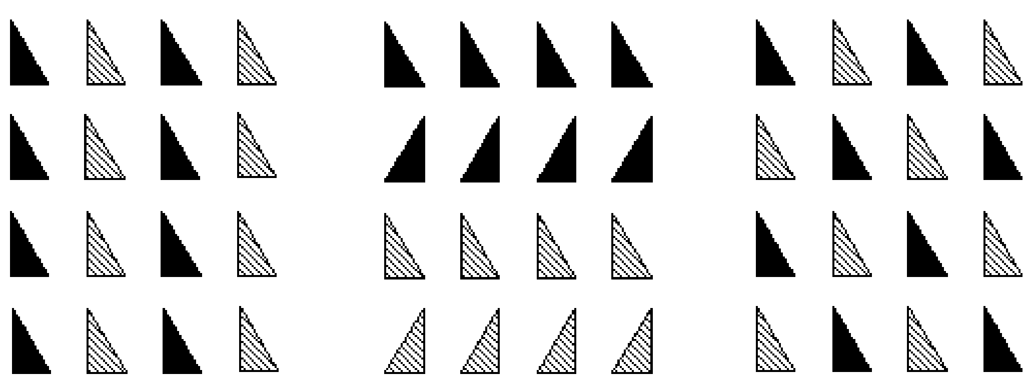

$\mathbf{p'_b1}$ $\mathbf{p'_b1}$ $\mathbf{p'_b1}$

Fig. 6.7

6.1.3 No color-reversing translations. The only wallpaper pattern type simpler than the $\mathbf{p'_b1}$ is the one that has the only isometry **common to all** wallpaper patterns (**color-preserving translation**) and nothing else: this is the **p1** type, familiar of course from section 4.1. But how about a **p1** pattern that, just like the **p2** and **pg** patterns in 6.0.3, looks like a 'genuine' two-colored pattern, having black and grey in perfect balance with each other? Here is such an example:

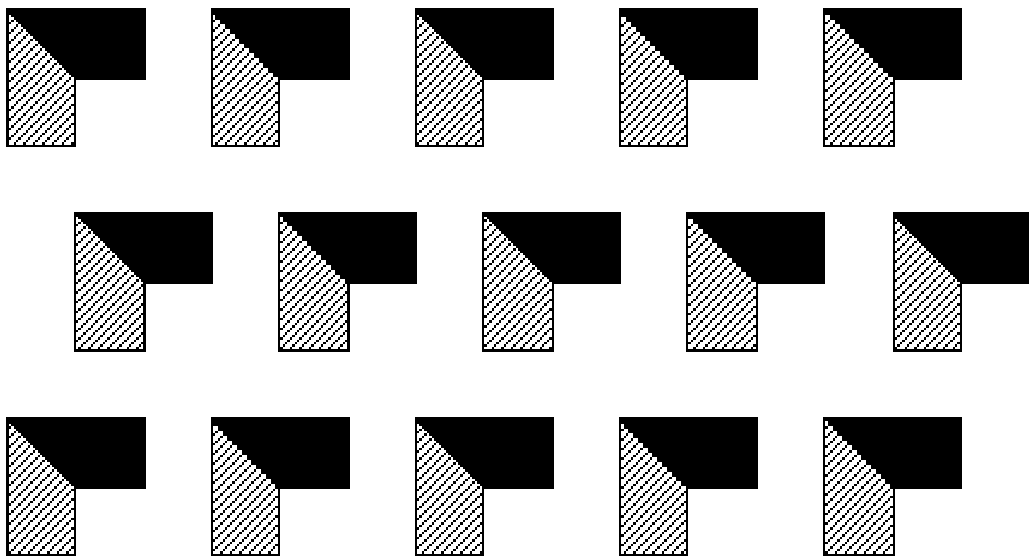

p1

Fig. 6.8

We leave it to you to compare this pattern to the $\mathbf{p'_b1}$ pattern of figure 6.1 and verify its **p1** classification: notice in particular that there are no 'underlying' reflections or glide reflections; or, if you wish, they were dead before they were born, ruled out by **structure** and **position** rather than inconsistency with color.

6.2 pg types (pg, $\mathbf{p'_b1g}$, pg′)

6.2.1 Those elusive glide reflections. While the pattern in figure 6.2 clearly has vertical and horizontal color-preserving reflections and in-between color-reversing glide reflections, as well as 180^0

rotations of both kinds, the corresponding isometries of the pattern in figure 6.3 are **all** inconsistent with color; the only consistent with color isometries that the pattern in figure 6.3 seems to have are **translations**, and in particular vertical and horizontal color-reversing translations. So, are we to conclude that the pattern in question is a $\mathbf{p'_b1}$? Well, as in every context in life, some knowledge of **'history'** can only help. Going back to the pattern's progenitor in figure 4.57, we see the standard **p4g** 'diagonal' glide reflection: we leave it to you to check that the particular **NW-SE** axis shown in figure 4.57 (passing through **bottoms** of vertical rectangles) provides a **color-preserving** glide reflection; and that the NW-SE glide reflection axes right next to it (passing through **tops** of vertical rectangles) provide **color-reversing** glide reflections. So the pattern in figure 6.3 is not a $\mathbf{p'_b1}$, but rather what is known as a $\mathbf{p'_b1g}$: color-reversing translation ($\mathbf{p'_b1}$) plus glide reflection, **both** color-preserving and color-reversing (**g**).

6.2.2 Let's change those triangles a little! A slight modification of the **pg** pattern in figure 6.4 yields another example of a $\mathbf{p'_b1g}$:

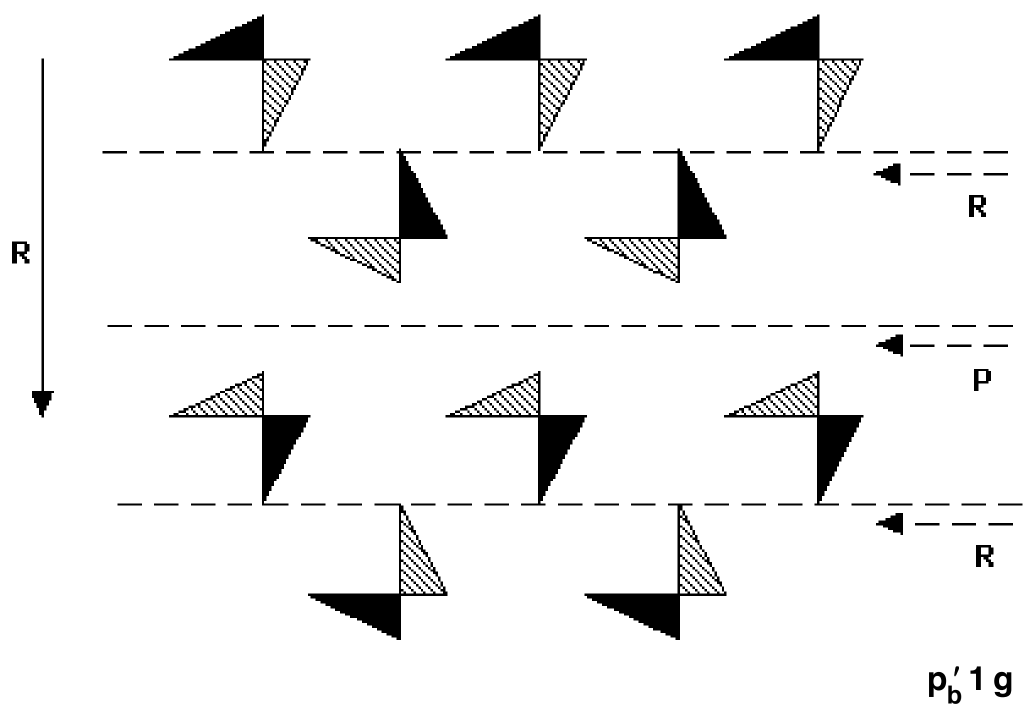

Fig. 6.9

The visual difference between the 'two kinds' of glide reflection axes is much more clear than the one in the example discussed in 6.2.1, so it is even less surprising that one kind of axes preserve colors while the other kind reverse colors.

6.2.3 Hunting for the third type. As we have seen in 5.2.1 and 5.5.1, it is possible to have **both kinds** of vertical reflection axes or half turn centers **reverse** colors in a two-colored border pattern. Therefore it is very reasonable to expect to have patterns in the **pg** family where **all** glide reflection axes **reverse** colors. Could a coloring of the familiar **p4g** pattern of figure 4.57 produce such an example? Well, a closer look at the NW-SE glide reflection of the $\mathbf{p'_b1g}$ pattern in figure 6.3 suggests this attempt:

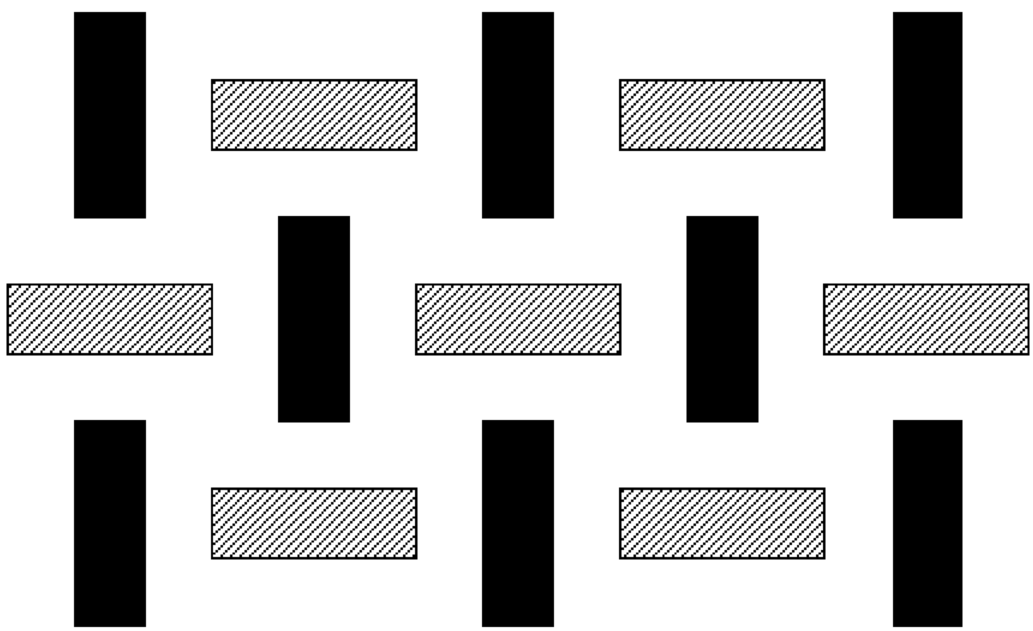

Fig. 6.10

Indeed all NW-SE glide reflections reverse colors. But so do the NE-SW glide reflections (which were in fact inconsistent with color in figure 6.3)! Could such a pattern ever belong to the **pg** family? As we will point out in sections 7.2, 7.9, and 7.10, and as you may already have observed in chapter 4, whenever a pattern has reflection and/or glide reflection in **two distinct directions** it **must** also have **rotation**: indeed our pattern above has color-reversing $\mathbf{90^0}$ rotation -- not to mention its color-preserving reflections and glide reflections -- and it belongs to the **p4g** family (see 6.11.2).

The lesson drawn out of this example is that some times we get **more** symmetry than desired, especially when we try to **'hide'** a rich underlying structure by way of coloring. This is a lesson worth remembering, but what about our original quest for a **pg** kind of pattern with **color-reversing** glide reflection **only**? Well, perhaps it is time to be less adventurous, avoid 'structural traps', and look for a more down-to-earth example; not that it is the simplest way out, but, once again, a modification of the **pg** pattern in figure 6.4 works:

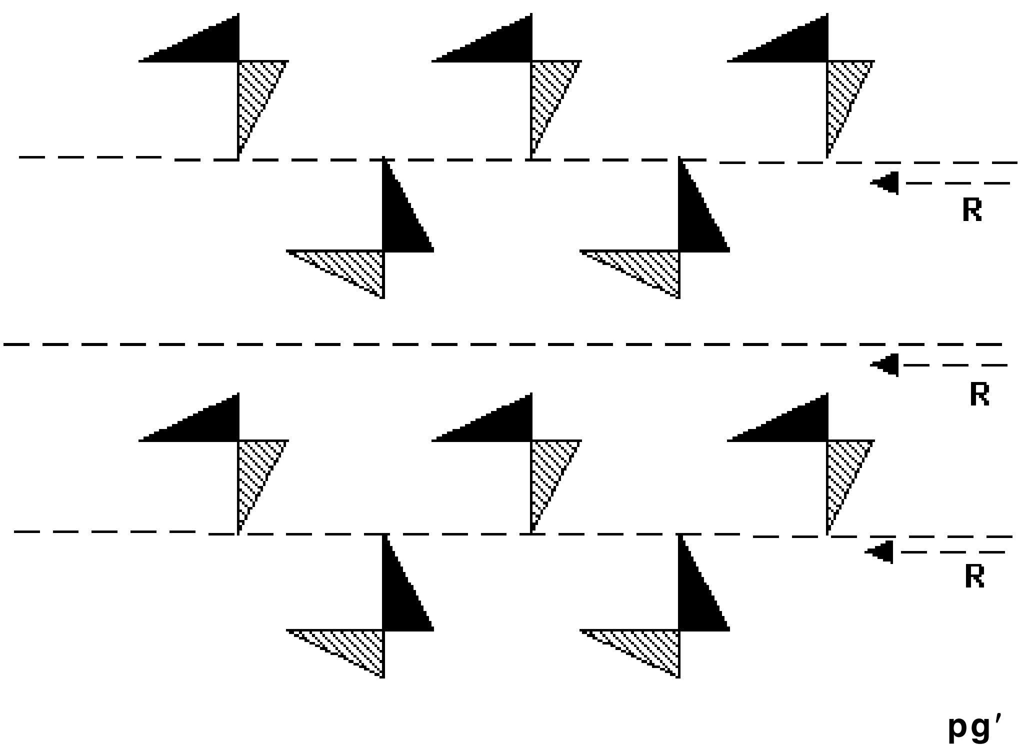

Fig. 6.11

Patterns such as the one in figure 6.11 are known as **pg′**.

6.2.4 Examples. These colorings should be compared to the **p1** colorings employed in figure 6.7:

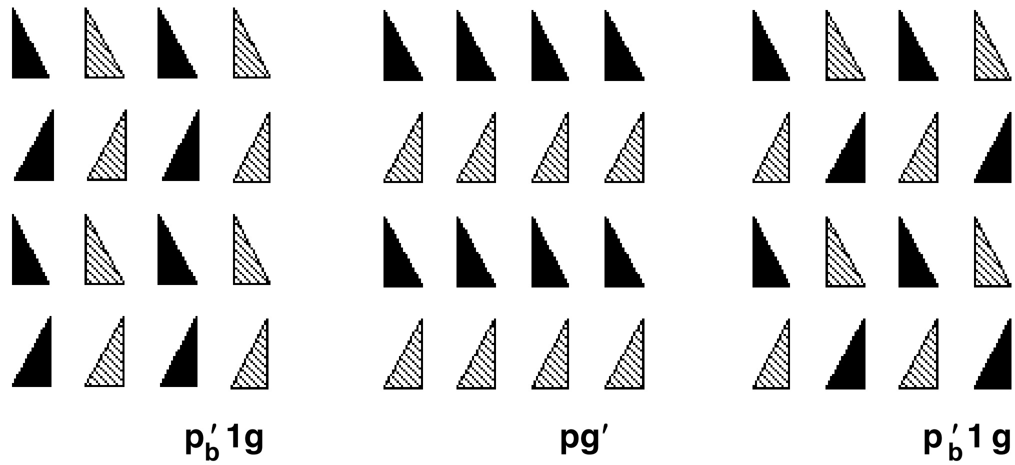

Fig. 6.12

6.2.5 <u>Are there any more **pg** types?</u> The three look-alikes in figures 6.4, 6.9, and 6.11 represent the three types (**pg**, $\mathbf{p'_b1g}$, **pg′**, respectively) discussed so far in this section: they all have glide reflection in a single direction, and what makes them distinct is the effect of their glide reflections on color. Could there be other such types? Well, in the absence of rotations and reflections, the only other isometry that could split the three types into subtypes is **translation**. At first it looks like we could have three × two = six cases: **three** possibilities for glide reflection (color-preserving only (**PP**) or both color-preserving and color-reversing (**PR**) or color-reversing only (**RR**)), and **two** possibilities for translation (color-preserving only (**PP**) or both color-preserving and color-reversing (**PR**), see section 6.1).

But a pattern's glide reflections and translations are **not independent** of each other: as we will prove in section 7.4, and as you can see in figure 6.13 right below, a glide reflection (mapping A to B) and a translation (mapping B to C) **combined** produce another glide reflection (mapping A to C) **parallel** to the first one (G × T = G); moreover (see figure 6.21 further below), the **combination** of two **parallel** glide reflections of **opposite vectors** is a translation **perpendicular** to their axes (G × G = T).

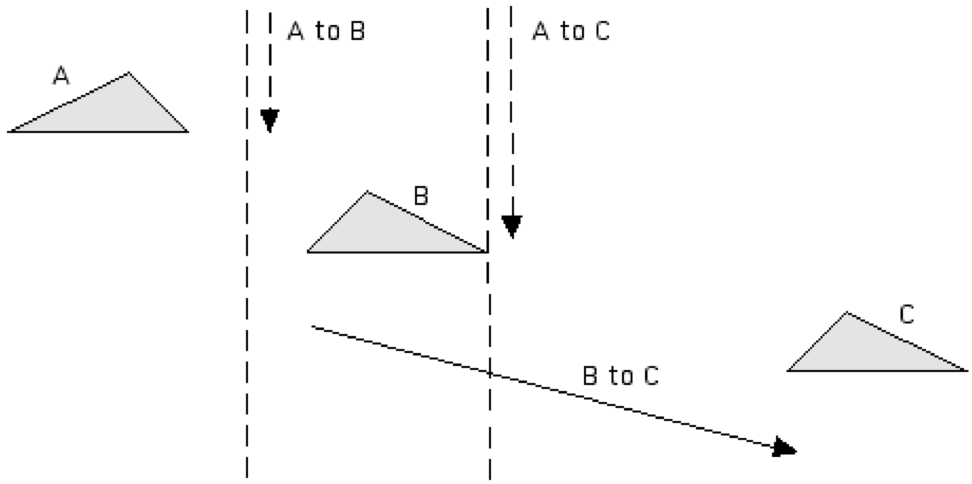

Fig. 6.13

In view of these facts, the multiplication rules of 5.6.2 analyse the six cases mentioned above as follows:

G(**PP**) × T(**PP**) = G(**PP**), G(**PP**) × G(**PP**) = T(**PP**): **pg**
G(**PP**) × T(**PR**) = G(**PR**), G(**PP**) × G(**PP**) = T(**PP**): impossible
G(**PR**) × T(**PP**) = G(**PR**), G(**PR**) × G(**PR**) = T(**PR**): impossible
G(**PR**) × T(**PR**) = G(**PR**), G(**PR**) × G(**PR**) = T(**PR**): $\mathbf{p'_b1g}$
G(**RR**) × T(**PP**) = G(**RR**), G(**RR**) × G(**RR**) = T(**PP**): **pg′**
G(**RR**) × T(**PR**) = G(**PR**), G(**RR**) × G(**RR**) = T(**PP**): impossible

So, there are no more types in the **pg** family after all. Using the examples of this section you can certainly confirm that the only member of the **pg** family that has both kinds of translations (color-preserving and color-reversing) is the one that has both kinds of glide reflections ($\mathbf{p'_b1g}$), just as the above equations indicate. And an important byproduct of the entire discussion, quite useful to remember throughout this chapter, is this: in the presence of (glide) reflections, **translations play no role** at all when it comes to classifying two-colored wallpaper patterns; indeed a pattern with (glide) reflection has translations of both kinds **if and only if** it has both kinds of (glide) reflections! (Recall (1.4.8) that every reflection may be viewed as a **special case** of glide reflection.)

6.2.6 Symmetry plans. We capture the structure of the three **pg** types as follows:

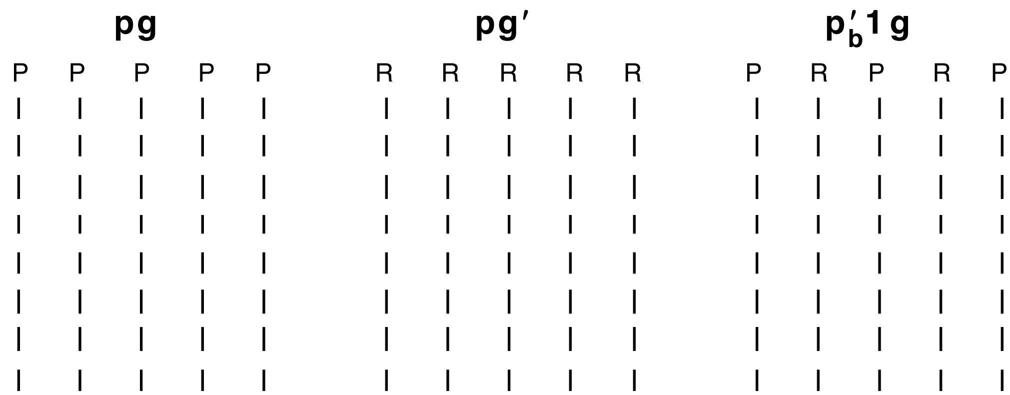

Fig. 6.14

In these symmetry plans glide reflection vectors are not shown for the sake of simplicity, but you **must** indicate them in your work!

6.3 pm types (pm, pm′, p'_b1m, p′m, p'_bg, c′m)

6.3.1 Upgrading the glide reflection to reflection. Employing an old idea from 2.7.2 -- where we viewed a **pma2** pattern as ‘half’ of a **pmm2** pattern -- in the opposite direction, we are now ‘doubling’ the three **pg**-like patterns in figures 6.4, 6.9, and 6.11 into **pm**-like patterns by **‘fattening’** the glide reflections into reflections; that is, we reflect the pattern across every glide reflection axis without gliding the image. This process is bound to produce **six** two-colored **pm**-like patterns having **reflection** in **one** direction: indeed as we reflect across the glide reflection axes we have the **option** of a color effect either opposite to or same as that of the glide reflection (see also 6.3.2 and 6.3.5), so we end up with three × two = six **pm** types. We illustrate the process in the following six figures, indicating in each case the ‘original’ **pg**-like pattern and providing the name for the ‘new’ **pm**-like pattern. Make sure you can rediscover the old **pg**-like pattern inside the richer structure of the new pattern; there is more than mere nostalgia in our call: the old glide reflection is alive and well, **‘hidden’** under the new reflection and ready to play an important role in the classification process!

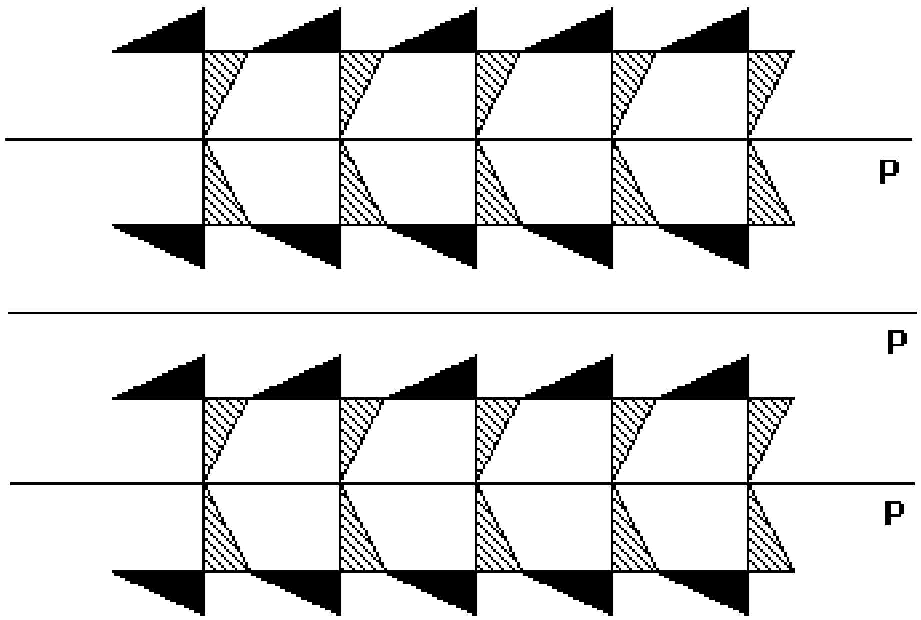

pg → pm

Fig. 6.15

All reflections and hidden glide reflections preserve colors, so the new pattern is classified as a **pm**, despite being two-colored.

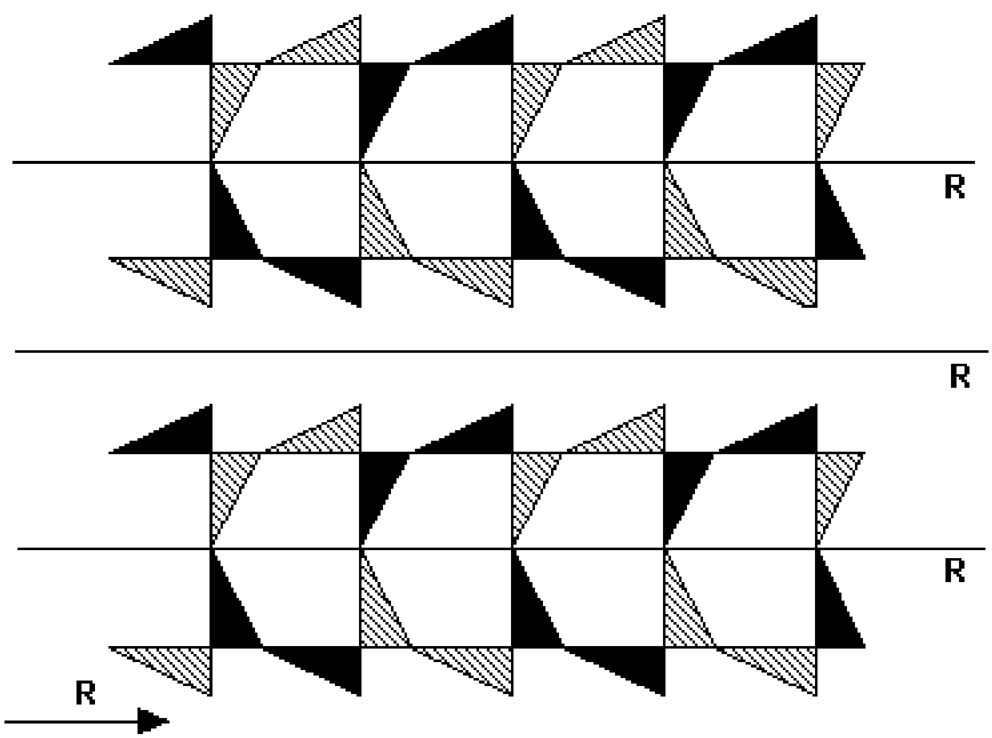

pg → $p'_b g$

Fig. 6.16

Reflections reverse colors, hidden glide reflections preserve colors (**g**); there exists **color-reversing translation** along the reflection axes ($\mathbf{p'_b}$). Such patterns are known as $\mathbf{p'_b g}$.

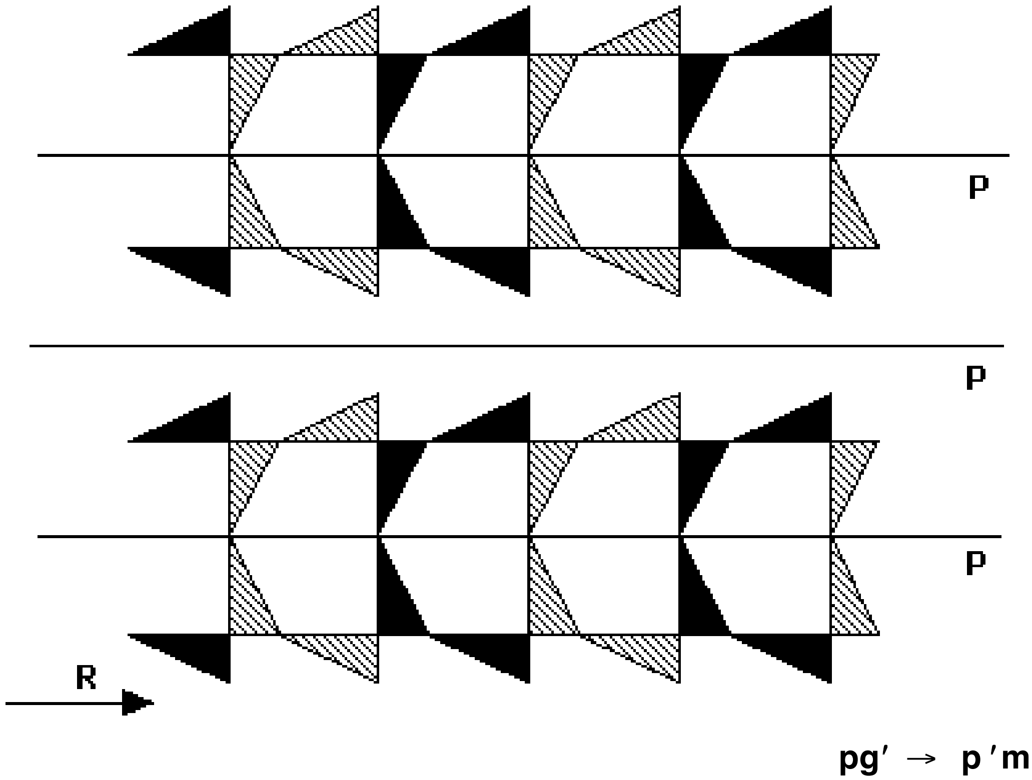

Fig. 6.17

Once again we get color-reversing translation along the reflection axes (**p′**), all of which preserve colors (**m**): the new pattern is known as **p′m**.

Comparing the two patterns in figures 6.15 & 6.17 we see that they are similar not only in name, but in structure as well; in fact the only thing that makes them **distinct** is that the **p′m** has color-reversing translation while the **pm** doesn't. But didn't we promise back in 6.2.5 that "in the presence of (glide) reflection translation will play no role in the classification process"? Well, there is indeed another, more subtle way of distinguishing between **pm** and **p′m**, and that is their **hidden** ('old') **glide reflection**, which of course preserves colors in the case of the **pm** (an 'offspring' of **pg**) but reverses colors in the case of the **p′m** (an 'offspring' of **pg′**)!

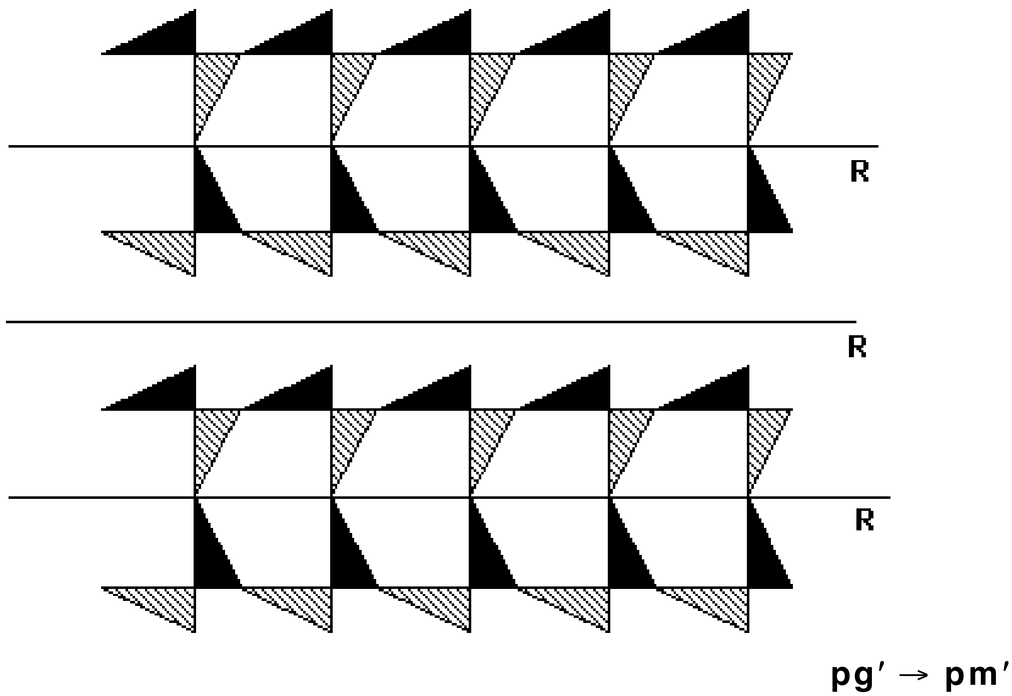

Fig. 6.18

All reflections and hidden glide reflections in this **pm′** pattern do reverse colors (**m′**). Notice the absence of color-reversing translation.

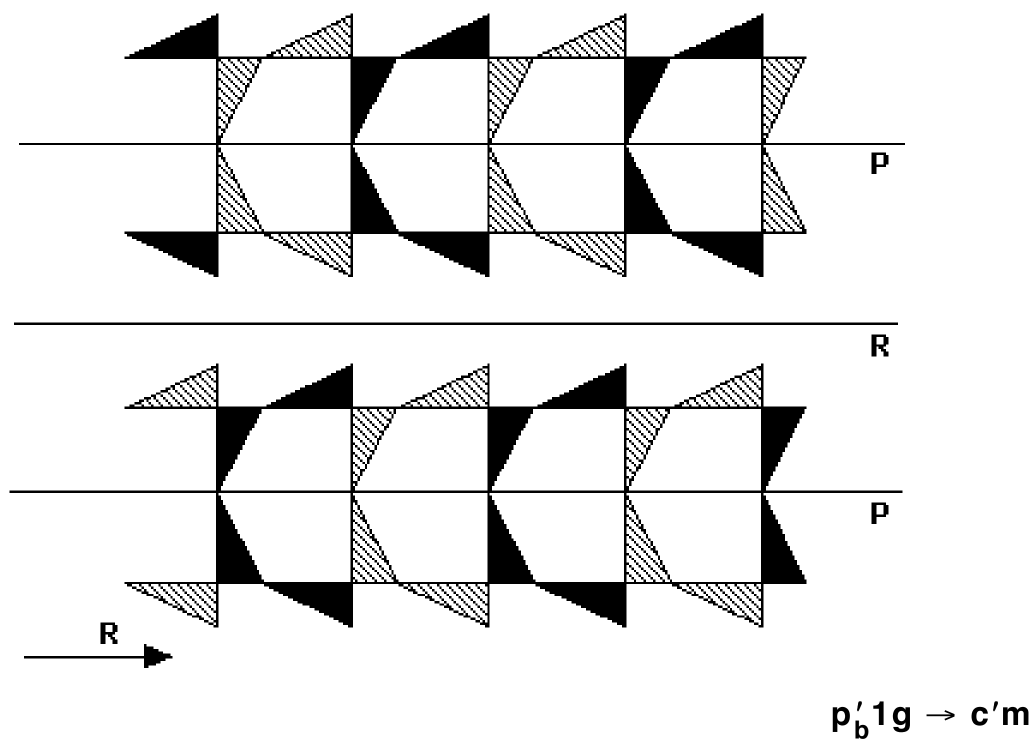

Fig. 6.19

Things started getting a bit complicated! Unlike the previous four types, this pattern has **both** color-preserving and color-reversing reflection, and likewise both color-preserving and color-reversing hidden glide reflection; notice that each reflection and hidden glide reflection associated with it have **opposite** effect on color. And, for the first time, we get color-reversing translation in directions **both** parallel and perpendicular to that of the reflection. **Visually**, the effect of all this is a feeling that every other **column** in our pattern has been **shifted** (like in the case of the **cm** patterns of section 4.4), hence its somewhat unexpected name (**c′m**).

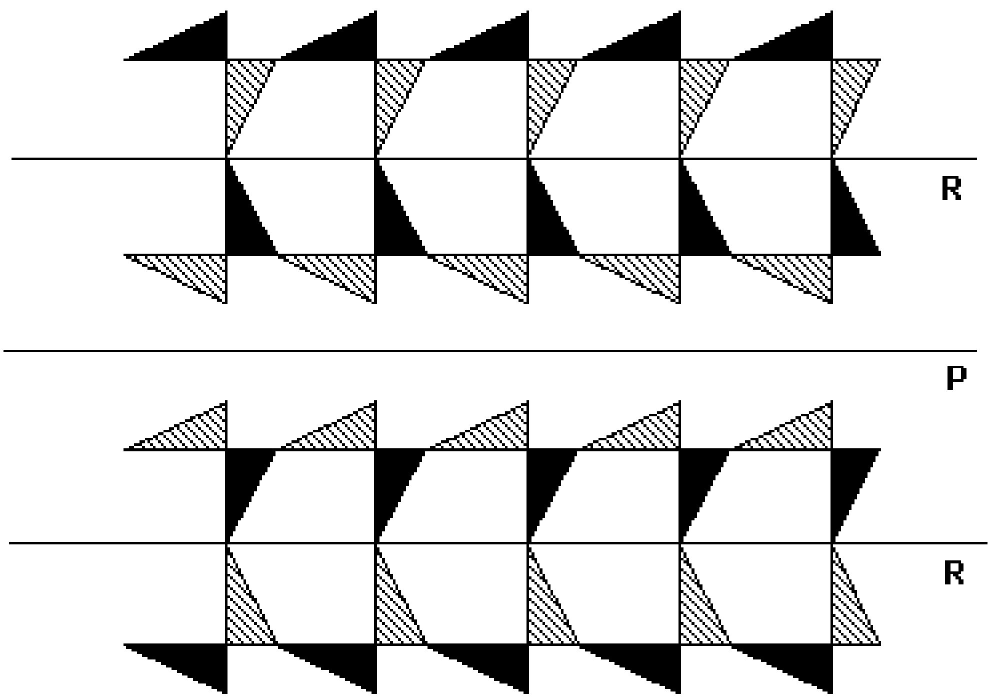

$\mathbf{p'_b1g \rightarrow p'_b1m}$

Fig. 6.20

Just as in the case of the other ‘offspring’ of $\mathbf{p'_b1g}$ we just discussed (**c′m**, figure 6.19), this new pattern, known as $\mathbf{p'_b1m}$, has **both** color-preserving and color-reversing reflections. Unlike in the case of the **c′m**, however, the hidden glide reflection of the $\mathbf{p'_b1m}$ always has the same effect on color as the corresponding reflection.

6.3.2 Are there any other types? The process employed in 6.3.1

produced six **pm**-like two-colored wallpaper patterns out of the three **pg**-like patterns of section 6.2. We must ask: could there be any more types in the **pm** family, 'unrelated' perhaps to **pg** types? Well, looking back at the new types we constructed, we can **fully** describe them in terms of the effect on color (**R** or **P**) of their 'two kinds' of reflection (R) **and** hidden glide reflection (G) as follows:

pm:	R(**PP**)/G(**PP**)
$\mathbf{p'_bg}$:	R(**RR**)/G(**PP**)
p′m:	R(**PP**)/G(**RR**)
pm′:	R(**RR**)/G(**RR**)
c′m:	R(**PR**)/G(**RP**)
$\mathbf{p'_b1m}$:	R(**PR**)/G(**PR**)

It becomes clear that the only possible extra types we could get would be of a form like R(**PR**)/G(**RR**) or R(**RR**)/G(**PR**), etc. That is, we 'need' types where the hidden glide reflection has the same effect on color as the corresponding reflection in the case of **every other** reflection axis, and the opposite effect on color of that of the corresponding reflection in the case of all other reflection axes. In other words, we 'need' situations like the one pictured right below:

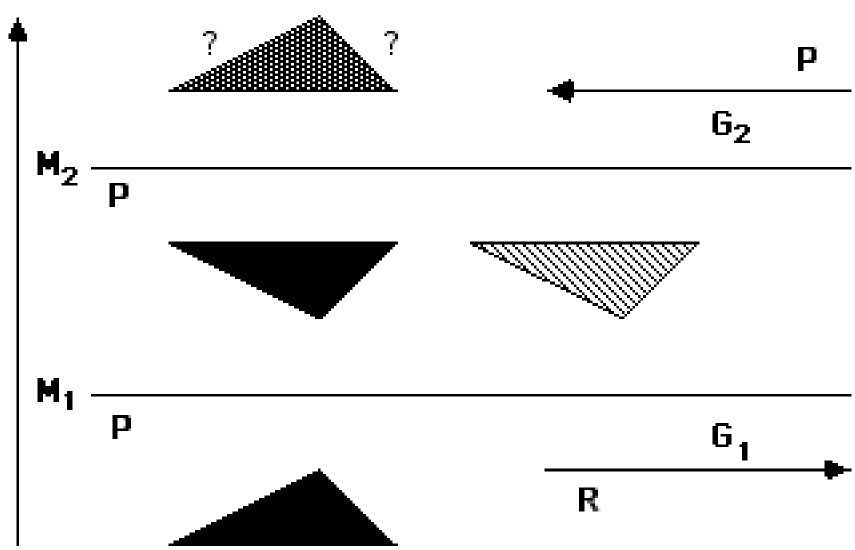

Fig. 6.21

But this is an impossible situation! Indeed the bottom reflection ($\mathbf{M_1}$) followed by the top one ($\mathbf{M_2}$) produce the shown **vertical** translation which must be **color-preserving** (**P** × **P** = **P**); but the **same translation** is produced by combining the corresponding hidden glide reflections (**G_1** followed by **G_2**) of the shown **opposite vectors**, hence it has to be **color-reversing** (**P** × **R** = **R**), too!

The **contradiction** we have arrived at shows that there cannot possibly be any **pm**-like two-colored wallpaper patterns other than the **six** types already derived in 6.3.1.

6.3.3 Examples. You should pay special attention to the sixth example, which should belong to the **cm** family but is in fact a **p'_b1m** because its in-between glide reflection is **inconsistent** with color:

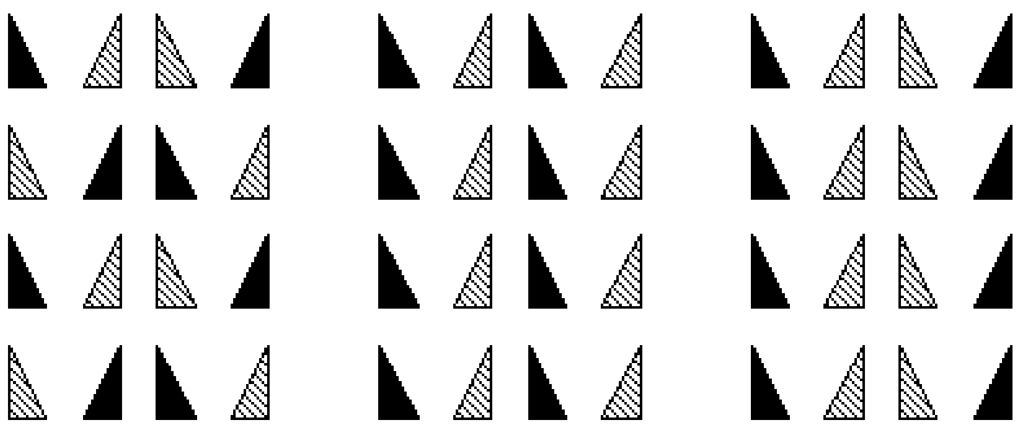

$c'm$ **pm'** **p'_b1m**

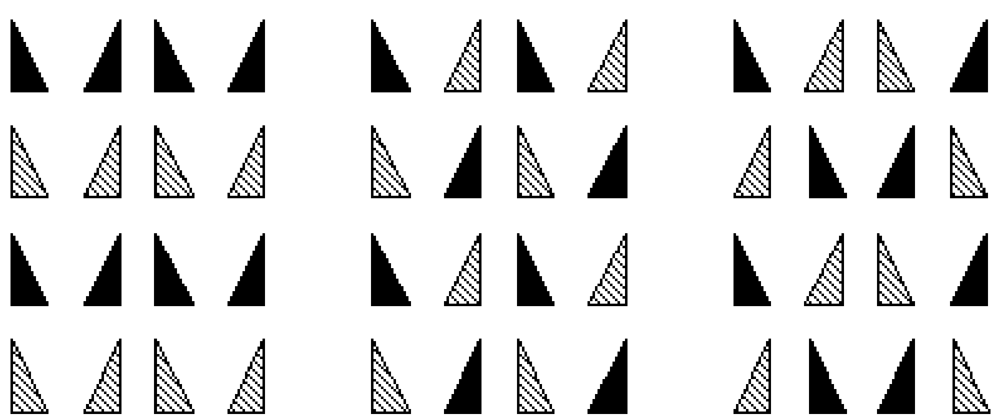

$p'm$ **p'_bg** **p'_b1m**

Fig. 6.22

6.3.4 Translations and hidden glide reflections revisited. The examples in 6.3.1 and 6.3.3 make 'visually obvious' the fact that there always exists a glide reflection employing the same axis as any given reflection. Such a 'hidden' glide reflection exists because a translation **parallel** to the reflection axis is **always** there (just as in the case of **p1m1** and **pmm2** border patterns); and it is easy to see that the hidden glide reflection's minimal gliding vector is always **equal** to the minimal translation vector along the reflection axis.

But **why** should such a parallel translation be there, after all? The double application of every glide reflection produces a parallel translation of vector **twice** as long as the gliding vector (2.4.2, 5.4.1), but why should a 'vectorless' reflection carry the obligation to produce a translation **parallel** to itself? This is best explained through a 'proof without words':

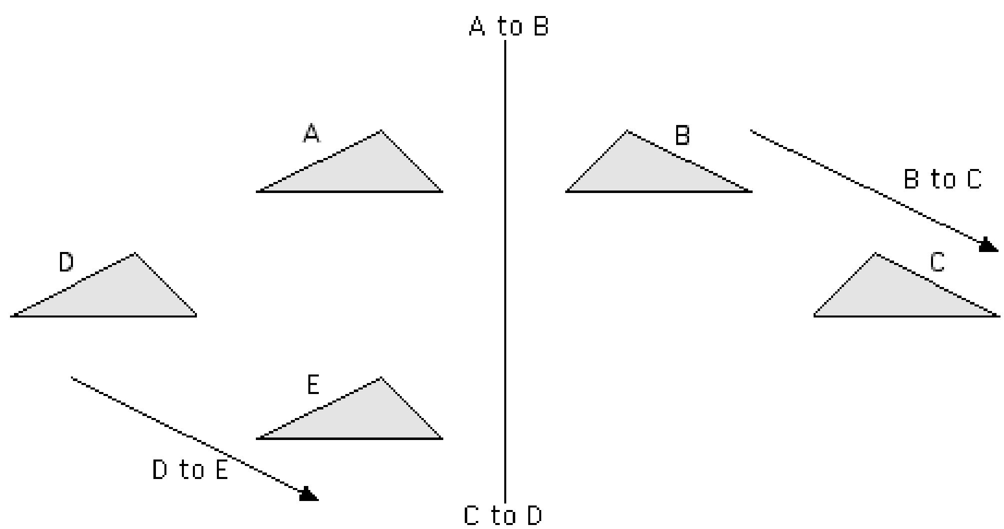

Fig. 6.23

[Since every wallpaper pattern has translations in **at least two** directions, pick one in a direction **non-perpendicular** to that of the reflection axis; then subsequent application of reflection (A to B), translation (B to C), reflection (C to D), and translation (D to E) produces a parallel to the reflection translation (mapping A to E)!]

Once we know that a translation vector parallel to the reflection axis **exists**, then it is possible to pick the **minimal** such vector -- recall that wallpaper patterns do **not** have arbitrarily small translations (4.0.4) -- which is easily shown to be the minimal gliding vector of a (hidden) glide reflection along the reflection axis. You should verify all these ideas for the examples in 6.3.1 and 6.3.3; you may in particular verify that the vertical translation guaranteed by the process in figure 6.23 is actually **twice as long** as the pattern's minimal vertical translation.

6.3.5 Symmetry plans. Even though we classified the **pm** types looking at their reflections and hidden glide reflections, we prefer to provide their symmetry plans based on reflections and parallel to them **translations**. It is of course easy to see that there exists a **color-reversing** translation parallel to the reflection axis if and only if the reflection and the corresponding hidden glide reflection have **opposite** effect on color.

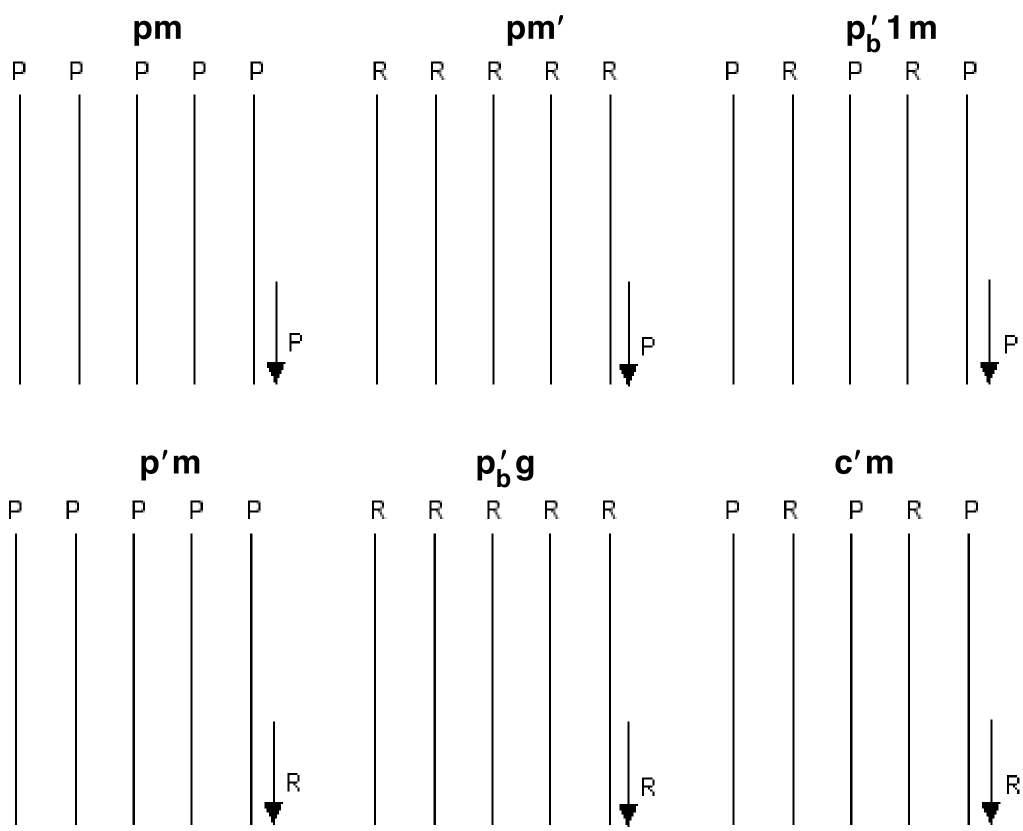

Fig. 6.24

6.4 cm types (cm, cm′, p'_cg, p'_cm)

6.4.1 Playing that old game again. As we have seen in 4.4.3, every **cm** pattern can be seen as a **pm** pattern every other row of which has been **shifted**. Therefore it is reasonable to assume that the application of that process to the two-colored **pm**-like patterns of 6.3.1 -- shifting columns rather than rows, of course -- is bound to produce two-colored **cm**-like patterns. This turns out to be largely true, with a couple of exceptions: the 'standard' shifting process leads from the **c′m** and the **p'_b1m** 'back' to **p'_b1g** (due to induced **color inconsistencies**). We illustrate all this in the following six figures:

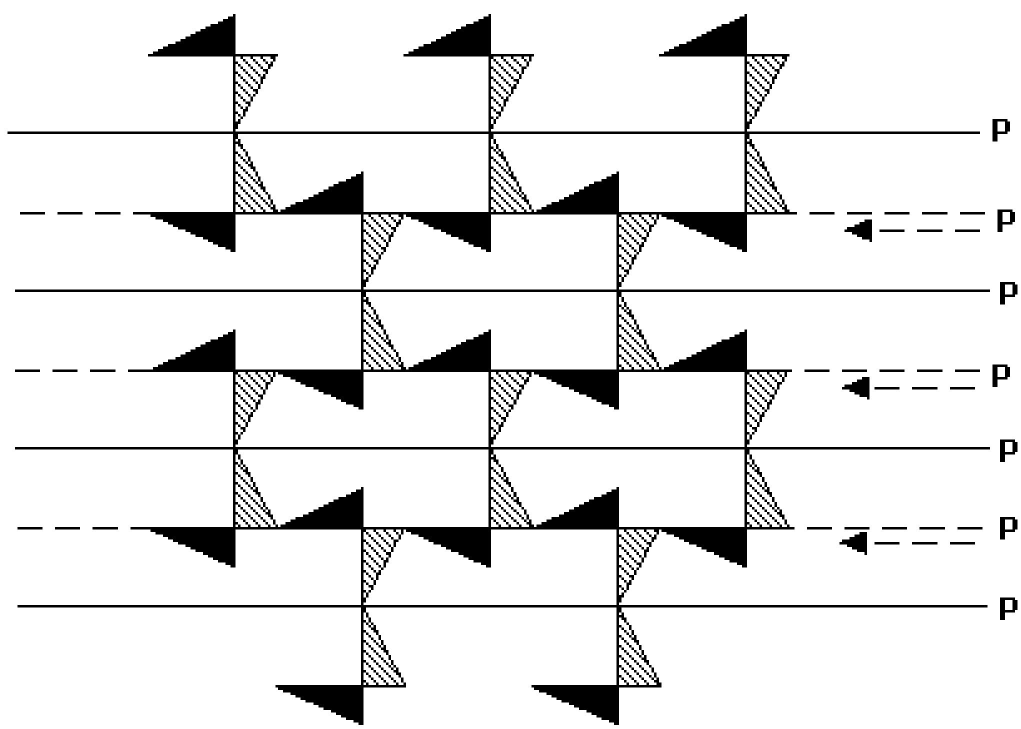

pm → cm

Fig. 6.25

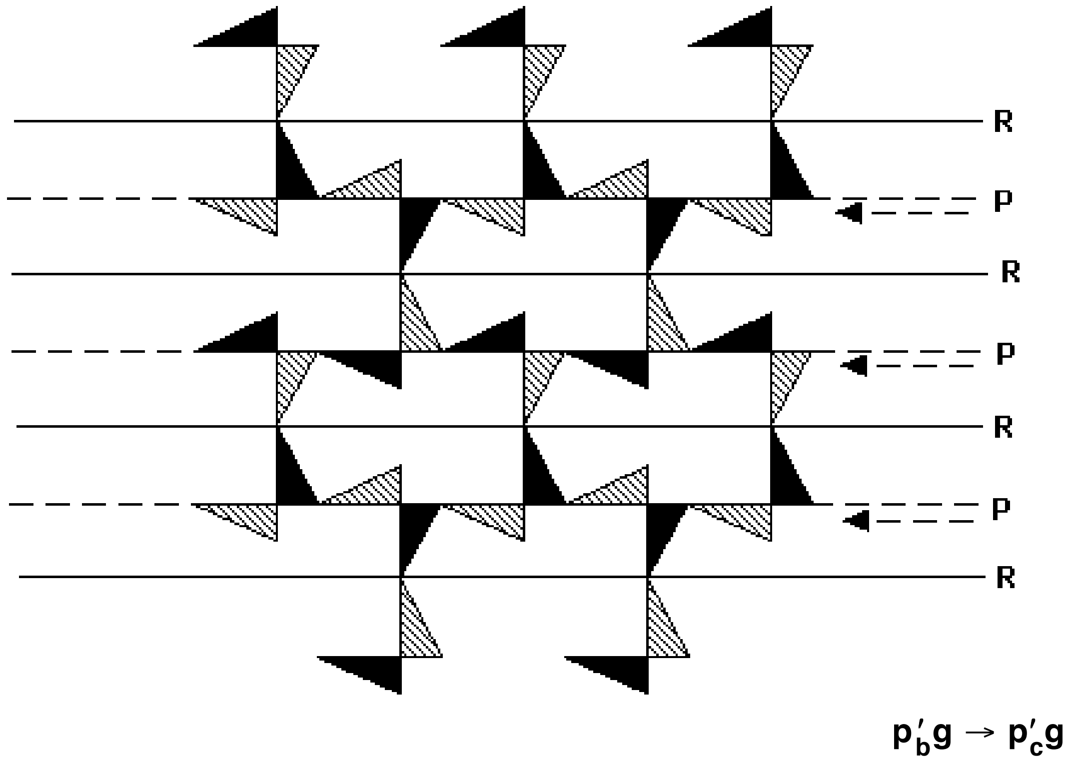

Fig. 6.26

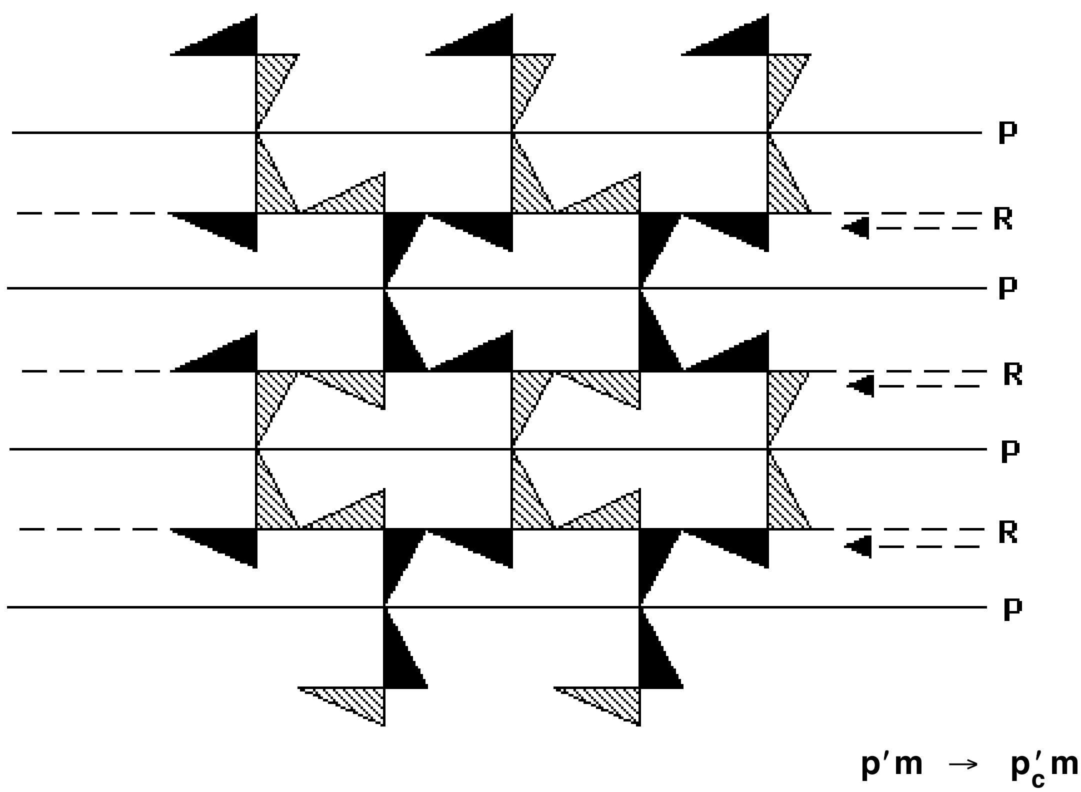

Fig. 6.27

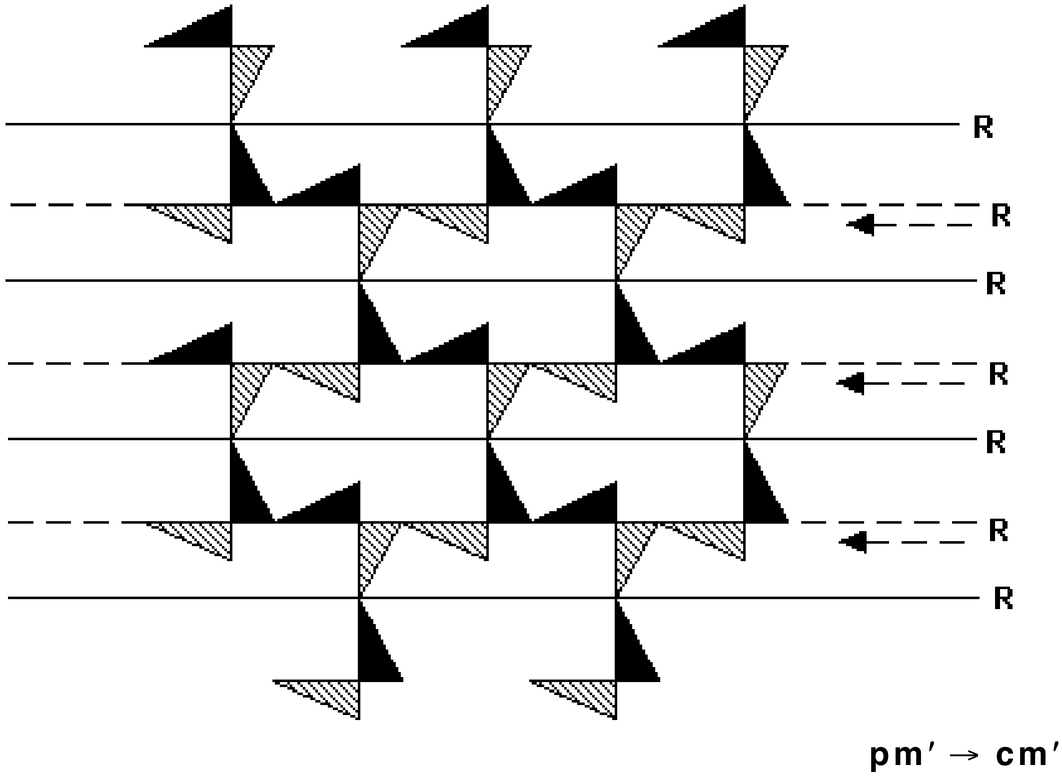

Fig. 6.28

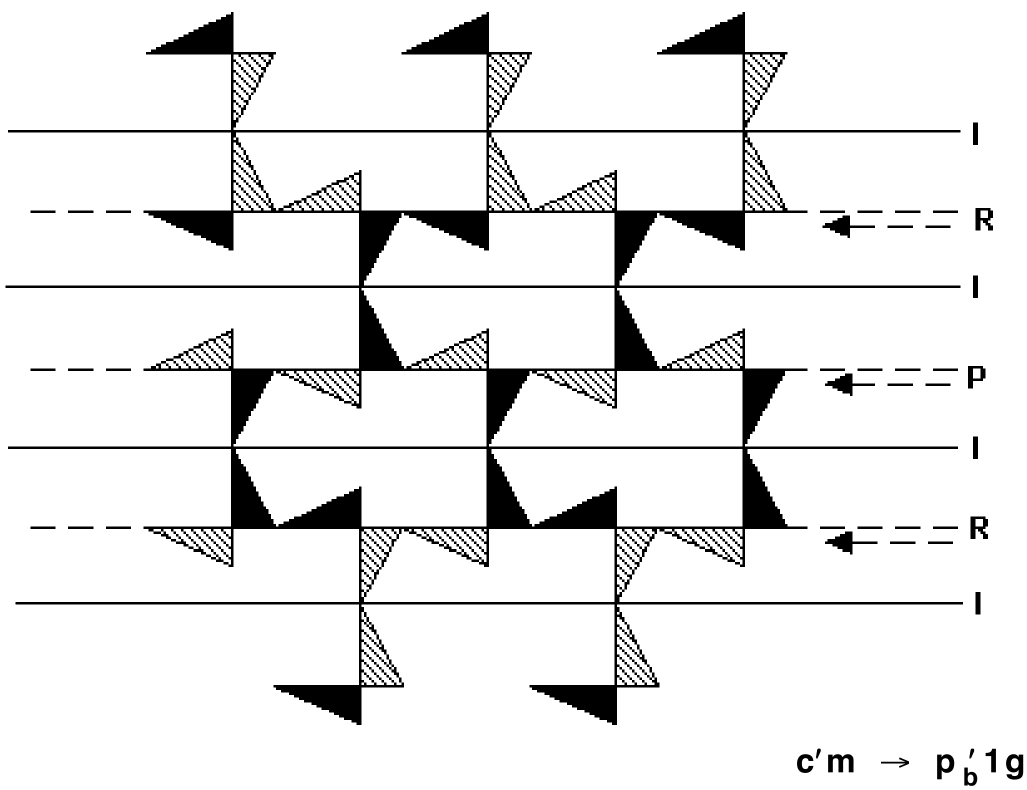

Fig. 6.29

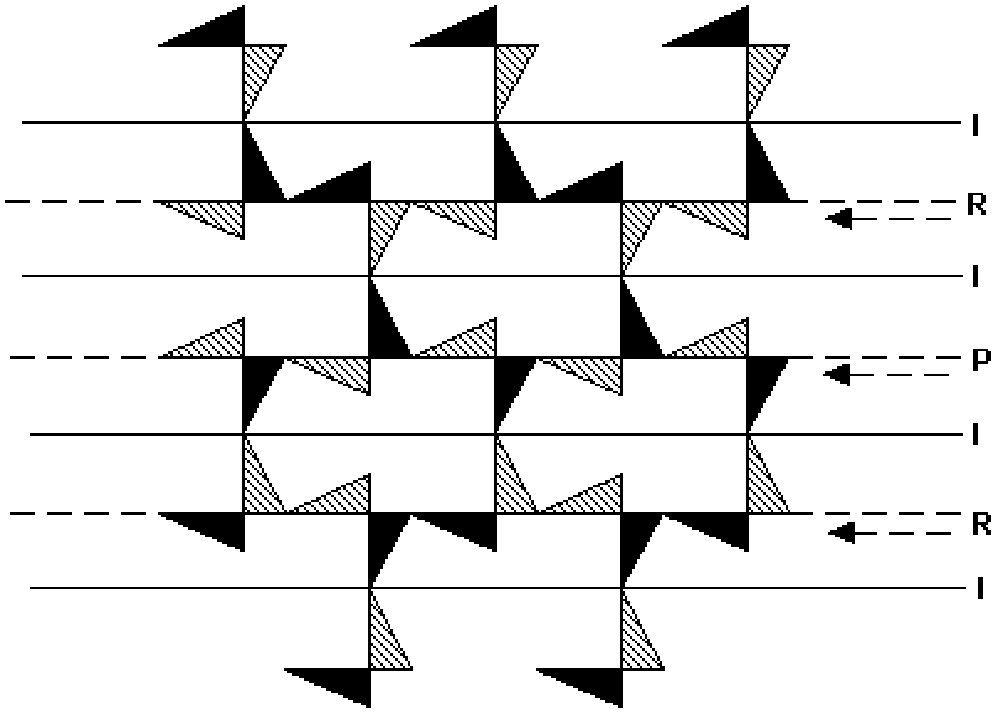

$p'_b1m \rightarrow p'_b1g$

Fig. 6.30

6.4.2 <u>Another 'game' to consider.</u> Let us revisit that $\mathbf{p'_b1}$ pattern in figure 6.1: since its underlying structure (before coloring) is that of a **cm**, it is reasonable to assume that some other colorings **may** produce **new cm**-like two-colored patterns. In figures 6.31-6.34 below we present a few failed attempts toward such additional **cm** types (some of which involve color **inconsistencies** leading this time to patterns belonging to the **p1** and **pm** groups rather than the **pg** group):

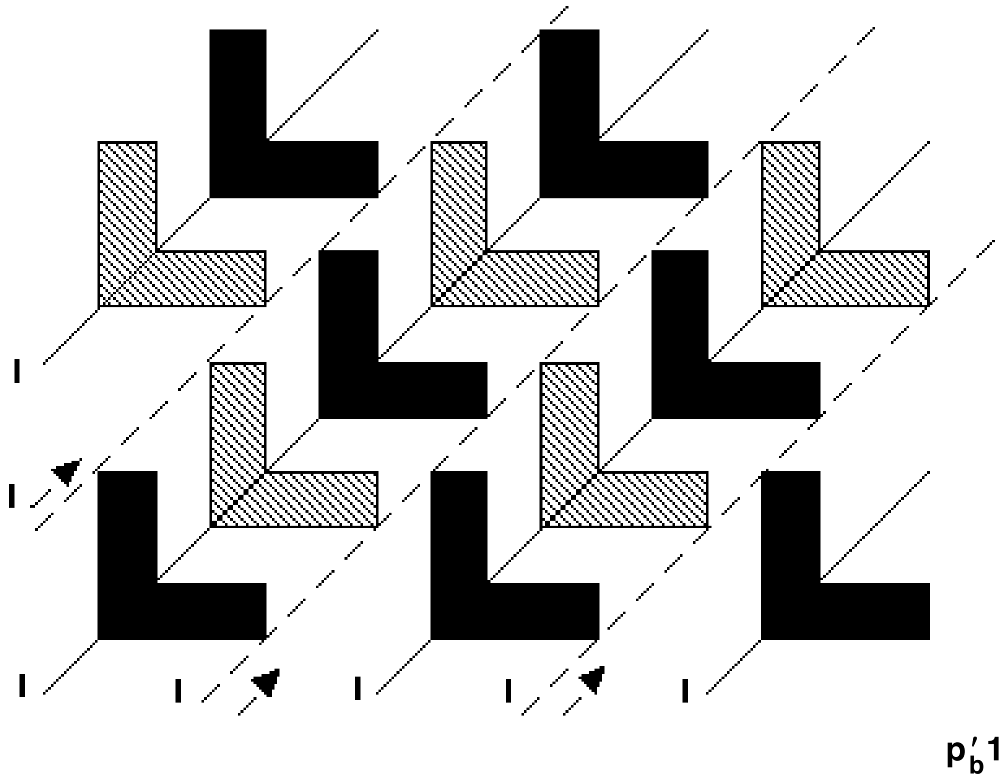

Fig. 6.31

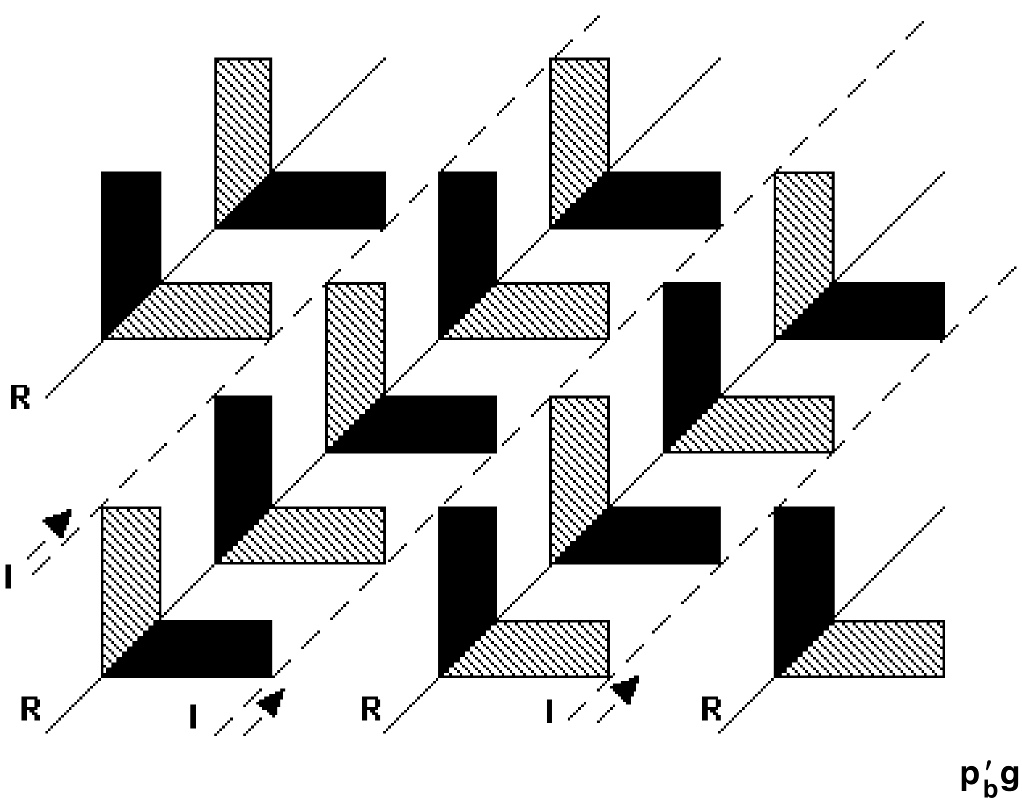

Fig. 6.32

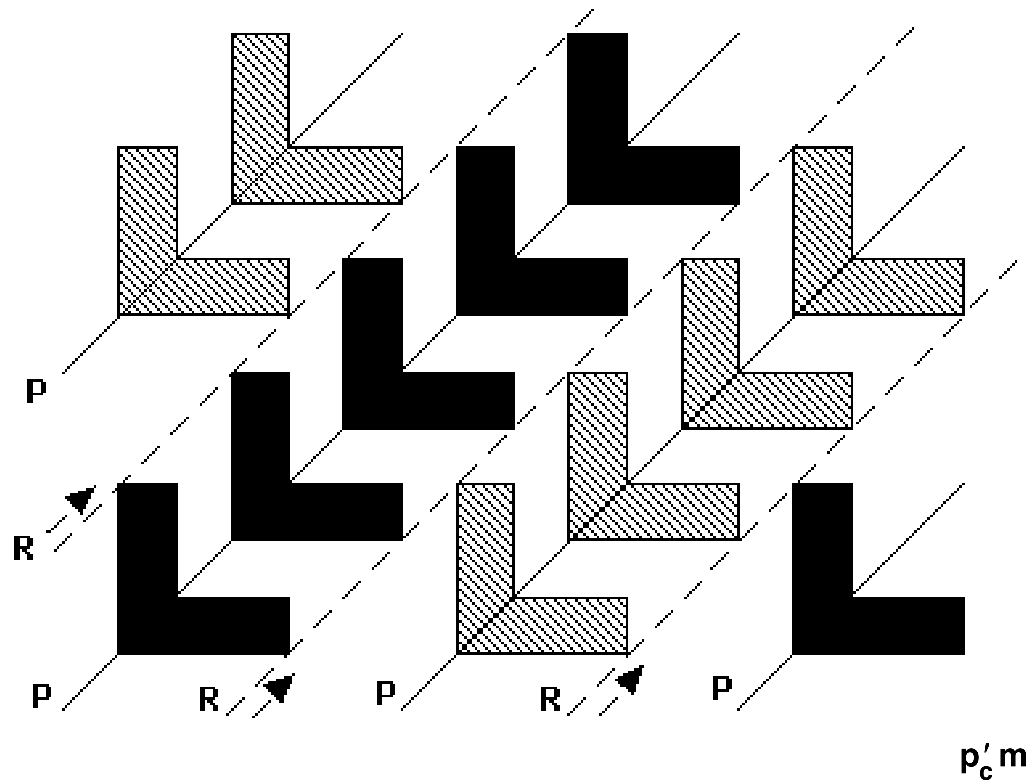

Fig. 6.33

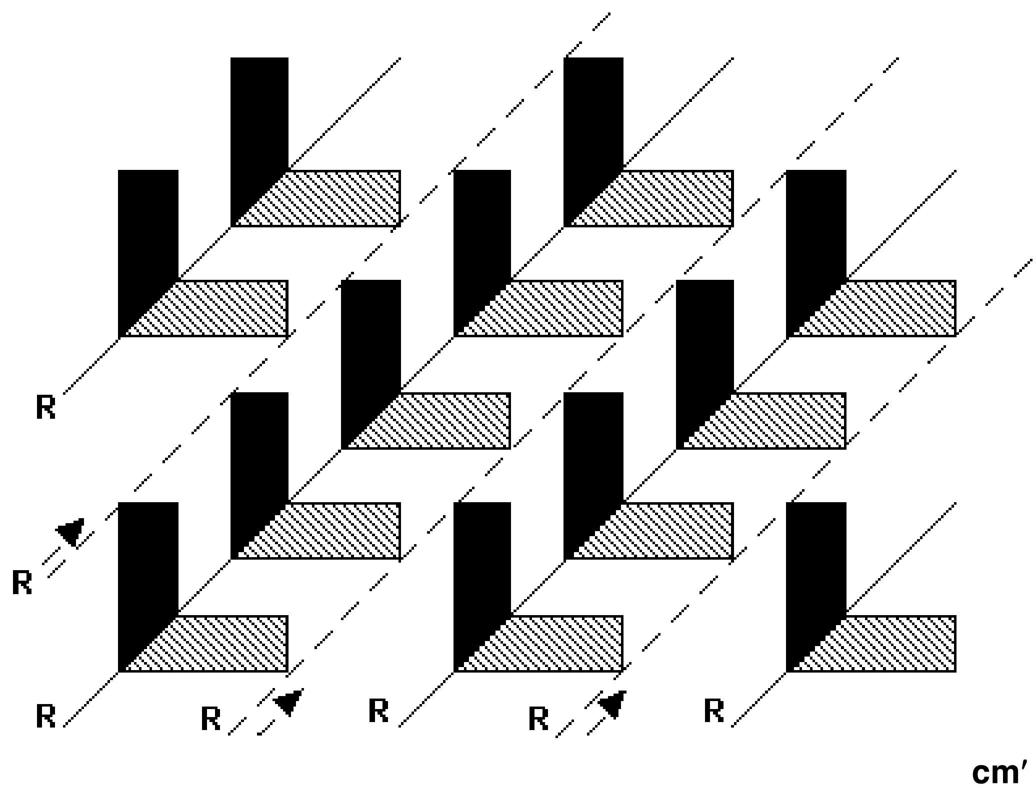

Fig. 6.34

So, while our first two colorings induced inconsistencies, yielding types **'lower'** than **cm**, the last two colorings provided **cm** types already known to us. Again, this begs the question: are there any other **cm**-like two-colored patterns besides the ones we have so far 'discovered'? The answer follows easily from the facts discussed right below in 6.4.3 and 6.4.4.

6.4.3 <u>No 'essential' hidden glide reflections.</u> The reason we got six rather than just three **pm**-like patterns in section 6.3 was the possibility of using a reflection axis for a (hidden) glide reflection of **opposite** effect on color. This is not quite possible in the case of a **cm**-like pattern ... simply because there cannot possibly be color-reversing translations **parallel** to reflection axes in such patterns!

To establish our claim above, let us first recall that a double application of a glide reflection yields a **color-preserving** translation parallel to it (5.4.1). Next, observe that the **smallest** possible translation vector parallel to the glide reflection axis has length equal to **2g**, where **g** > 0 is the length of the **shortest** glide reflection vector. To establish this observation we argue **by contradiction**, employing yet another 'proof without words':

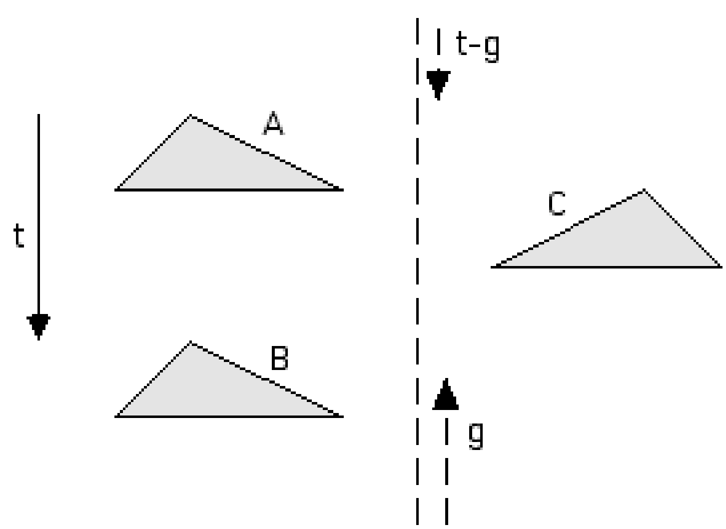

Fig. 6.35

[Assume that there is a **downward** translation vector of length **t** strictly **smaller** than **2g** (mapping A to B); apply then an **upward** glide reflection of length **g** (mapping B to C): the result is a downward glide reflection (mapping A to C) of length **t−g**, which is **shorter** than **g**, contradiction. (In case you like **inequalities** and **absolute values**, it's all a consequence of $0 < \mathbf{t} < \mathbf{2g} \Rightarrow |\mathbf{t}-\mathbf{g}| < \mathbf{g}$!)]

6.4.4 No (glide) reflections of both kinds. You may already have noticed another feature common to all two-colored **cm**-like patterns presented so far: in each example, all reflections have the **same effect on color**; and, likewise, all glide reflections have the same effect on color. This is **not** a coincidence! As figure 6.36 indicates, every two adjacent reflection axes -- therefore **all** reflection axes -- in a **cm**-like pattern **must** have the same effect on color:

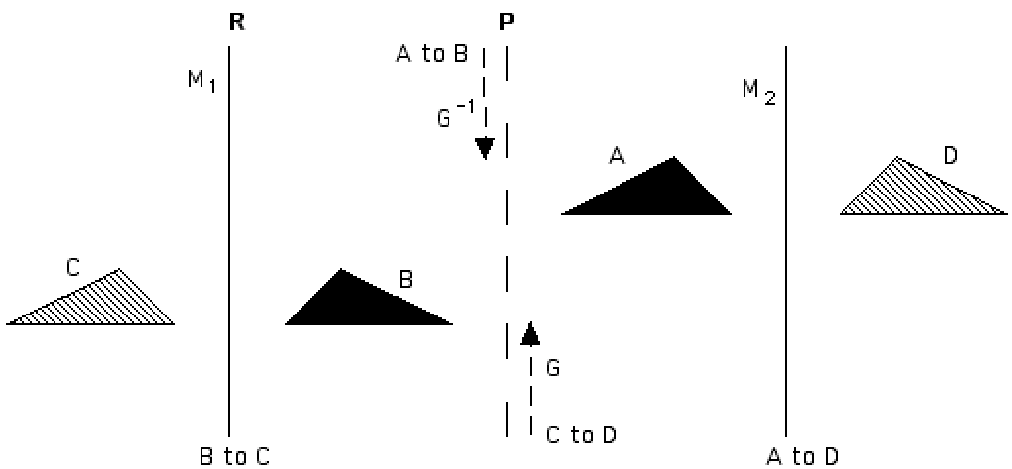

Fig. 6.36

[Assume that $\mathbf{M_1}$ **reverses colors** and that **G** preserves colors, the other three possibilities being treated in a very similar manner. Then $\mathbf{M_2}$ is the outcome of successive applications of $\mathbf{G^{-1}}$ (**downward** glide reflection), $\mathbf{M_1}$, and **G** (**upward** glide reflection). Employing the notation of 4.0.4, we may write $\mathbf{M_2 = G{*}M_1{*}G^{-1}}$, so that the 'multiplication rule' of 5.6.2 yields $\mathbf{P} \times \mathbf{R} \times \mathbf{P} = \mathbf{R}$ and therefore $\mathbf{M_2}$ **must reverse colors** (as figure 6.36 demonstrates).]

There is a similar argument (and picture) demonstrating the same fact for glide reflections: **all** axes have the **same** effect on color. At this point you may recall our 'innocent' comments in 4.4.6 to the effect that all reflection and glide reflection axes in a **cm** pattern **'look the same'**. It's a bit deeper than that: every two adjacent reflection axes (**M_1**, **M_2**) are **conjugates** (4.0.4) of each other by way of some **'in-between'** glide reflection (**G**); in simpler terms, there exists a glide reflection (**G**) **mapping** one (**M_1**) to the other (**M_2**), and that has the consequences discussed above (as well as in 4.0.4 & 4.0.5 and even 4.11.2). Similar facts hold true for the glide reflections of every **cm** pattern: every two adjacent glide reflection axes are mirrored to each other by some **'in-between'** reflection).

Putting everything discussed in the preceeding paragpaphs together we arrive at a **conjecture**: whenever $I_2 = I[I_1]$, where I, I_1, I_2 are isometries leaving a two-colored pattern invariant, I_1 and I_2 must have the same effect on color. As already indicated, our conjecture is not that difficult to prove -- via $I_2 = I*I_1*I^{-1}$ and the 'multiplication rules' of 5.6.2 -- so we will not delve into the details. But, please, remember this **important** fact that we will be using throughout this chapter: every two isometries of a **two-colored** pattern **mapped** to each other by a **third isometry** (and its inverse) **must** have the same effect on color (by way of being **conjugates** of each other).

The observation made here is in fact important enough to be assigned a name of its own, **Conjugacy Principle**; a principle that not only will help us to classify and understand wallpaper patterns from here on, but has already been employed in less pronounced ways: for example, it does lie behind the fact that **every other** reflection axis in a **pm**-like two-colored pattern (or glide reflection axis in a **pg**-like two-colored pattern) has the same effect on color! (Couldn't it be called the **Mapping Principle**, instead? Well, we prefer "Conjugacy Principle" because it resonates with the crucial role played by the **abstract algebraic structure** of wallpaper patterns -- a structure not discussed here, but rather prominent in the literature...) Beyond the Conjugacy Principle (studied in detail in section 8.0), (glide) reflections are further analysed in section 8.1.

6.4.5 Only four **cm** types! It is now easy to show that there are no **cm**-like two-colored patterns other than the ones already described in this section. Indeed if we view a **cm** two-colored pattern as a **'merge'** of a **pm** pattern (reflections) and a **pg** pattern (glide reflections), we see that there are only **two** possibilities for each **'partner'**: only **pm**, **pm′** for **pm** (6.4.4 rules out $\mathbf{p'_b1m}$ and **c′m**, while 6.4.3 rules out **p′m** and $\mathbf{p'_bg}$) and only **pg**, **pg′** for **pg** ($\mathbf{p'_b1g}$ is ruled out by 6.4.4). But two × two = four, and we can certainly write down the new (**cm**) types as **'products'** of the old ones (**pm**, **pg**):

$$\mathbf{cm} = \mathbf{pm} \times \mathbf{pg},\ \mathbf{cm'} = \mathbf{pm'} \times \mathbf{pg'},\ \mathbf{p'_cg} = \mathbf{pm'} \times \mathbf{pg},\ \mathbf{p'_cm} = \mathbf{pm} \times \mathbf{pg'}$$

Of course this 'multiplication' was first introduced in section 5.7, where we viewed **pmm2**s as 'products' of **pm11**s and **p1m1**s.

6.4.6 Further examples and symmetry plans.

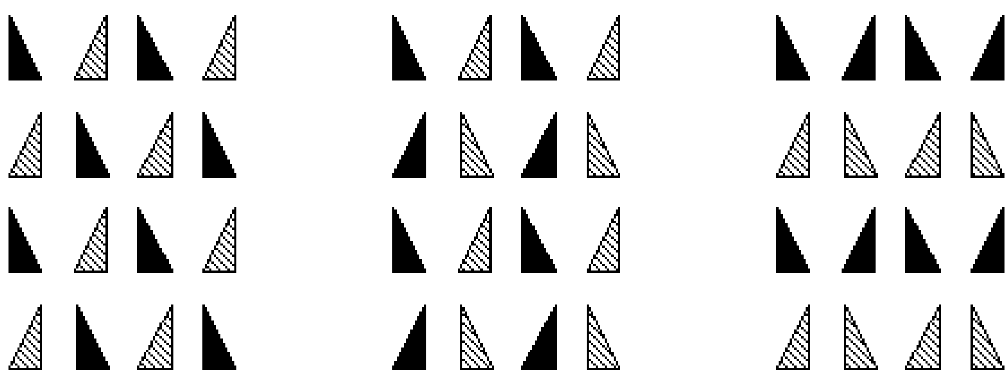

cm′ $\qquad$ $\mathbf{p'_cg}$ $\qquad$ $\mathbf{p'_cm}$

Fig. 6.37

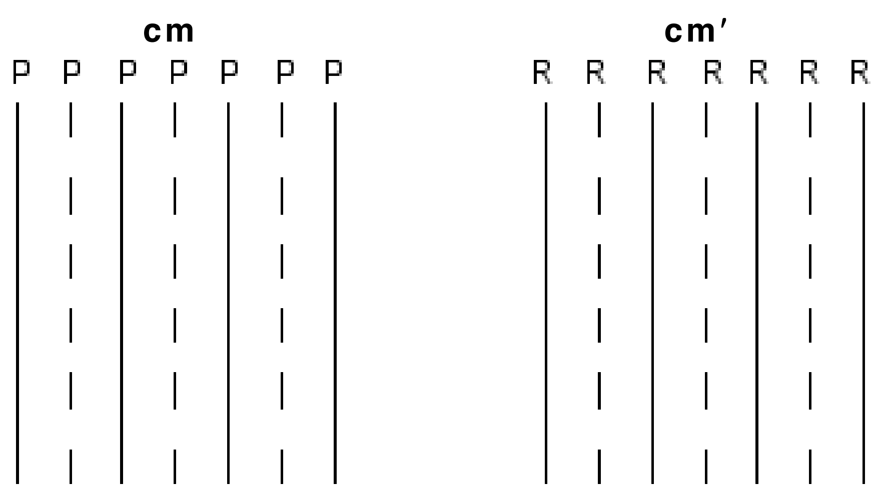

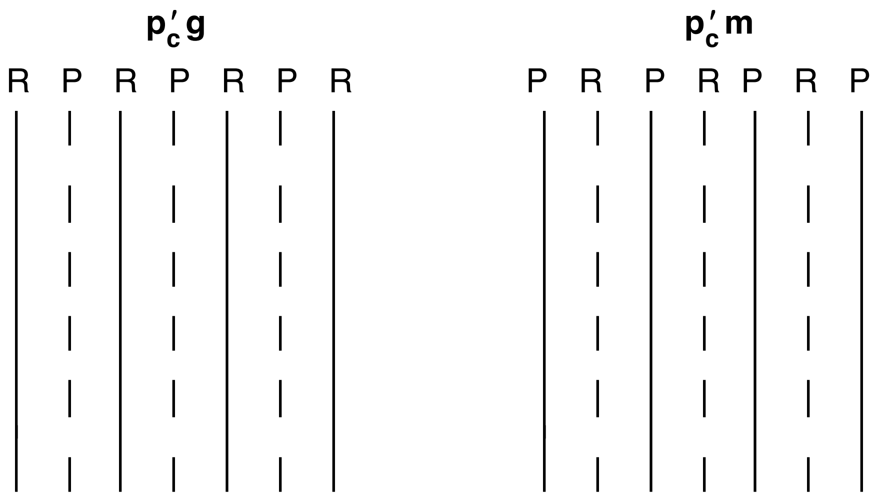

Fig. 6.38

6.5 p2 types ($p2$, $p2'$, $p'_b 2$)

6.5.1 <u>A good place to start!</u> 'Experimenting' a bit with the **p2** pattern in figure 6.5, we get a couple of 'genuine' two-colored ones:

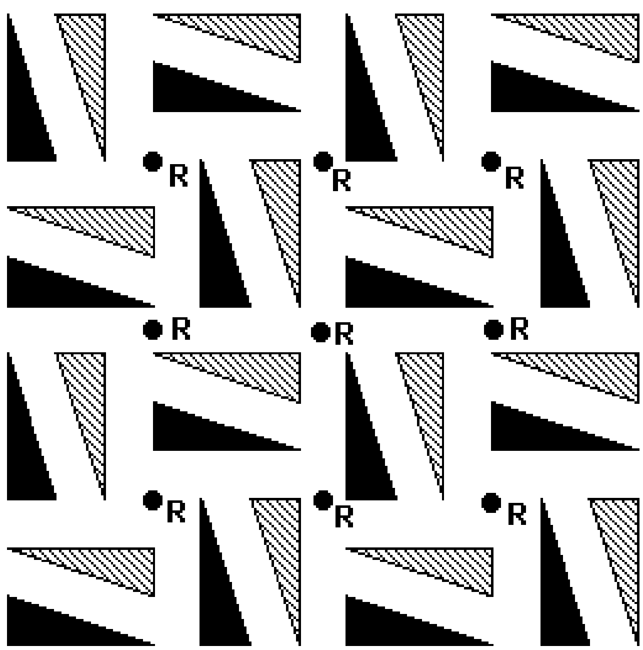

p2′

Fig. 6.39

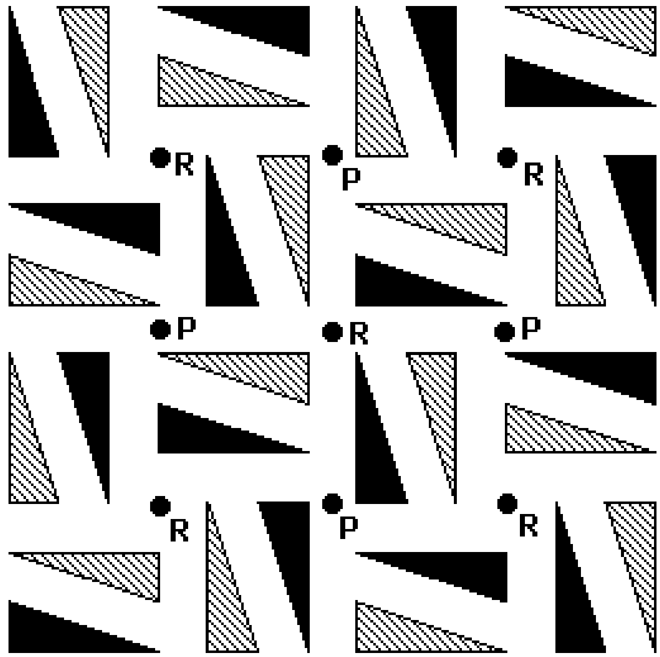

p'_b2

Fig. 6.40

The first type (**p2′**) has color-reversing half turns **only**, the second ($\mathbf{p'_b2}$) has **both** color-preserving and color-reversing ones.

6.5.2 <u>From **pg** to **p2**.</u> Let's revisit those 'root' patterns of 6.2:

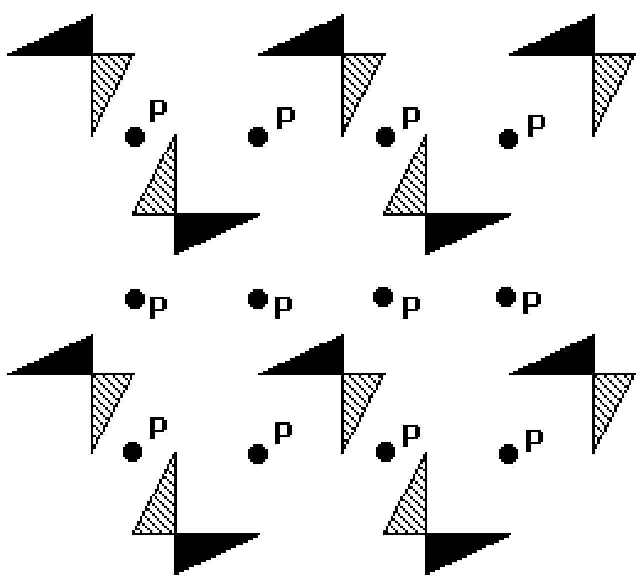

pg → p2

Fig. 6.41

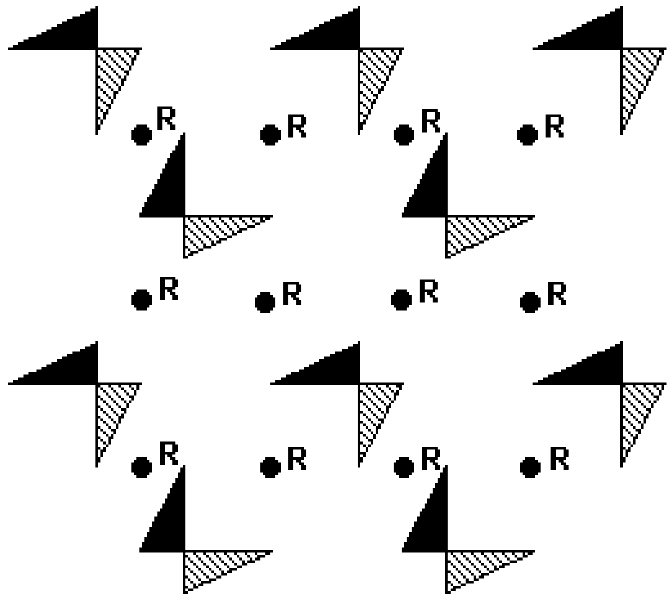

$pg' \rightarrow p2'$

Fig. 6.42

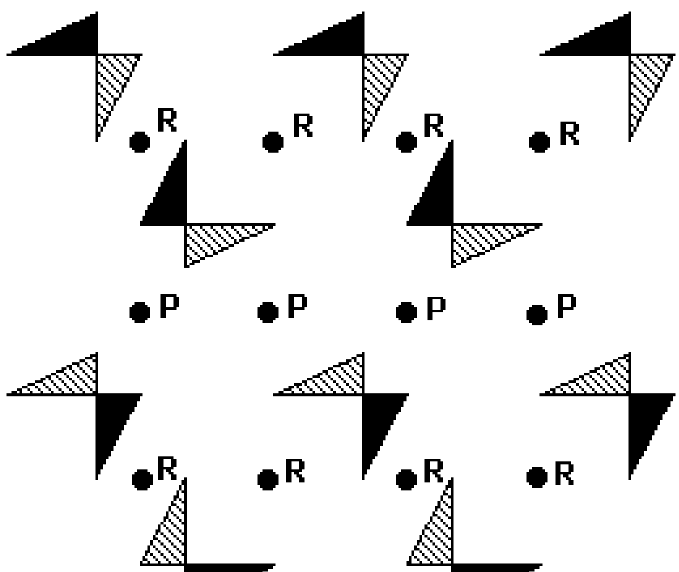

$p'_b1g \rightarrow p'_b2$

Fig. 6.43

What happened? By applying a 'secret' **vertical** reflection to **every other row** of a **pg**-like pattern, we end up -- in this case anyway -- with a **p2**-like pattern! This incident suggests a strong analogy between the two types, which we discuss right below.

6.5.3 Half turns and translations. Are there any more **p2**-like two-colored patterns? The answer is "no", and it strongly relies on figure 6.44, inspired in turn by figure 6.13:

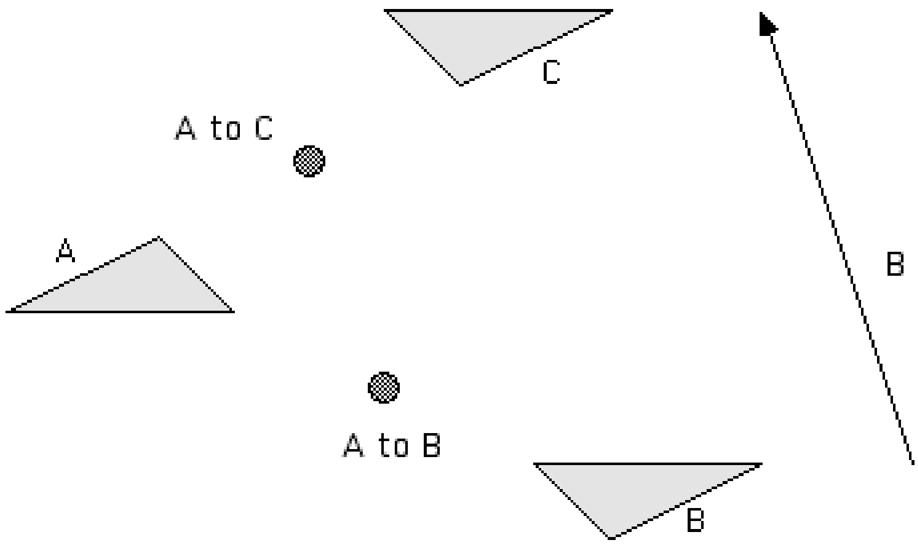

Fig. 6.44

What's the story here? Well, go back to section 6.2 for a moment and recall how we established the correlation between glide reflections of **both** kinds (color-preserving and color-reversing) and color-reversing translations: it all follows from the fact that the combination of a translation and a glide reflection is another glide reflection (figure 6.13); and that correlation proves (6.2.5) that there exist precisely three two-colored patterns in the **pg** family. In **exactly** the same way, figure 6.44 shows that the combination of a 180^0 rotation (mapping A to B) and a translation (mapping B to C) is another 180^0 rotation (mapping A to C). It follows, for example, that we cannot have a pattern with color-preserving half turns **only** and color-reversing translations: **P** $\times$ **R** = **R**, etc. (For a complete analysis of why there can only be three **p2** types follow 6.2.5 **case by case**, with 6.4.4 (Conjugacy Principle) in mind, replacing glide reflections by half turns.)

A few additional comments are in order. First of all, the fact illustrated in figure 6.44 (rotation $\times$ translation = rotation) holds true for **arbitrary** rotations, not just for 180^0 rotations: a rigorous proof will be given in section 7.6. More to the point, the close analogy between **pg** and **p2** is **also** based on the fact that, just as the combination of two **parallel** glide reflections is a translation (figure 6.21), the combination of two **180^0** rotations is indeed a translation: use the two half turns of figure 6.44 ‘in the reverse’ to see how rotating B to A and then A to C is equivalent to translating B to C! (Yes, this **rotation × rotation = translation** equation requires the two angles to be **180^0** or at least **equal** to each other **and** of **opposite** orientation; see figure 6.99 or 7.5.2 for details.)

6.5.4 Symmetry plans. Nothing but rotation centers this time:

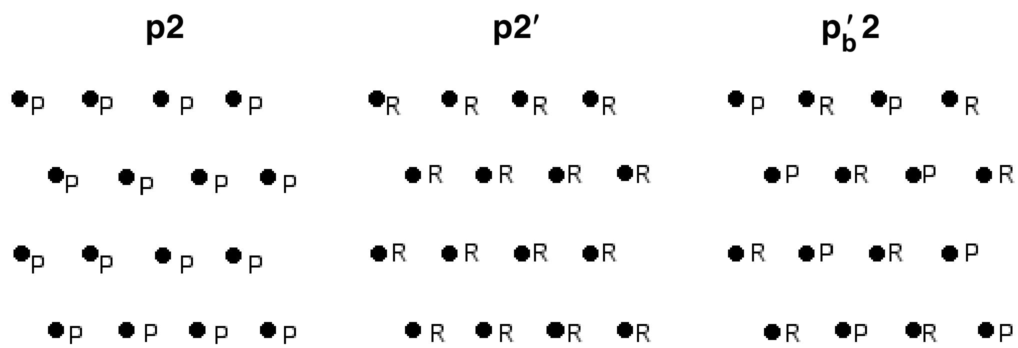

Fig. 6.45

6.5.5 Further examples. First our usual two-colored triangles:

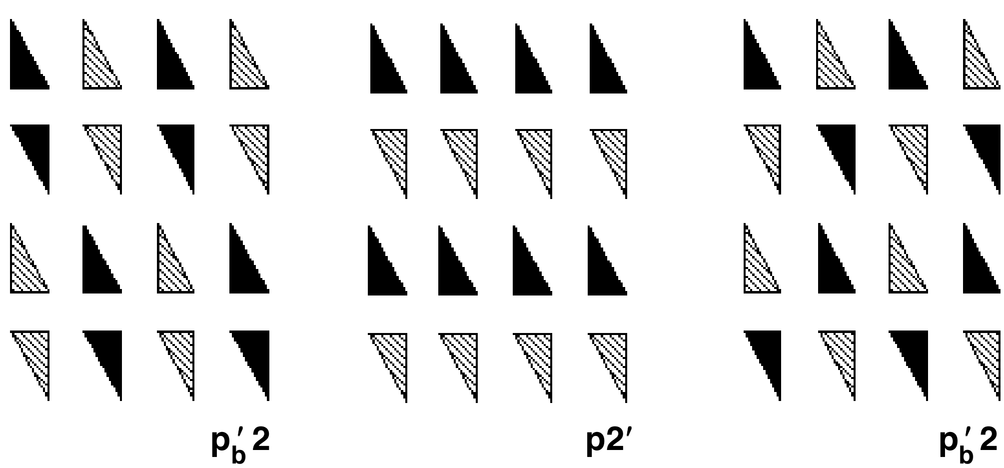

Fig. 6.46

You should probably compare figure 6.46 to figure 6.12!

And now a $\mathbf{p'_b2}$ example that many students misclassify thinking that it has glide reflection:

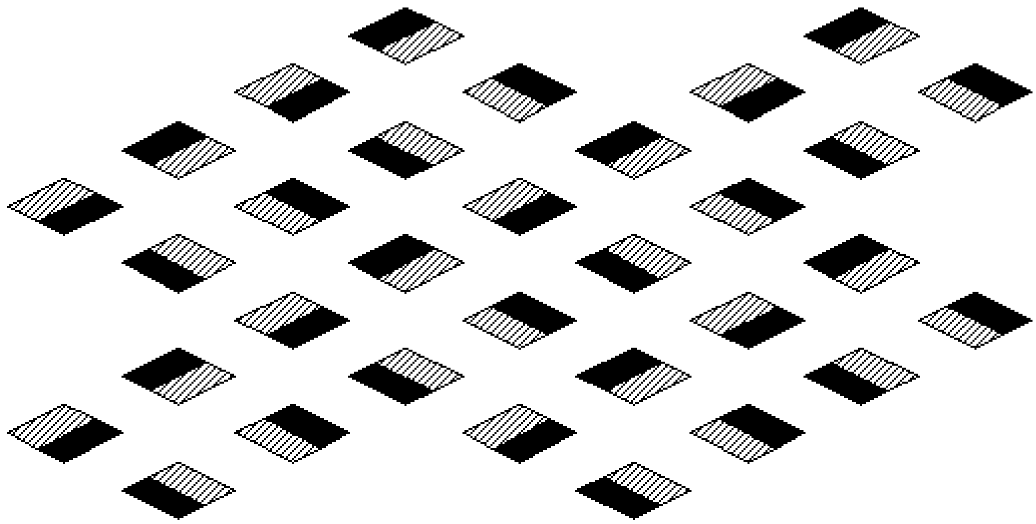

$\mathbf{p'_b2}$

Fig. 6.47

In an echo of the discussion in 4.5.1, we would like to point out that the half turn centers in figure 6.47 form **parallelograms** rather than rectangles (figures 6.41, 6.42, 6.43, 6.46) or squares (figures 6.5, 6.39, 6.40). This observation both **justifies** the 'general' arrangement (in parallelograms) of half turn centers in the **p2** symmetry plans (6.5.4) and **rules out** (4.8.2) the glide reflection in figure 6.47!

6.6 pgg types (pgg, pgg′, pg′g′)

6.6.1 From one to two directions. Let's now apply a 'secret' vertical **glide** reflection (6.5.2) of **both** kinds (color-preserving and color-reversing) to **every row** of a **pg** or **pg′**:

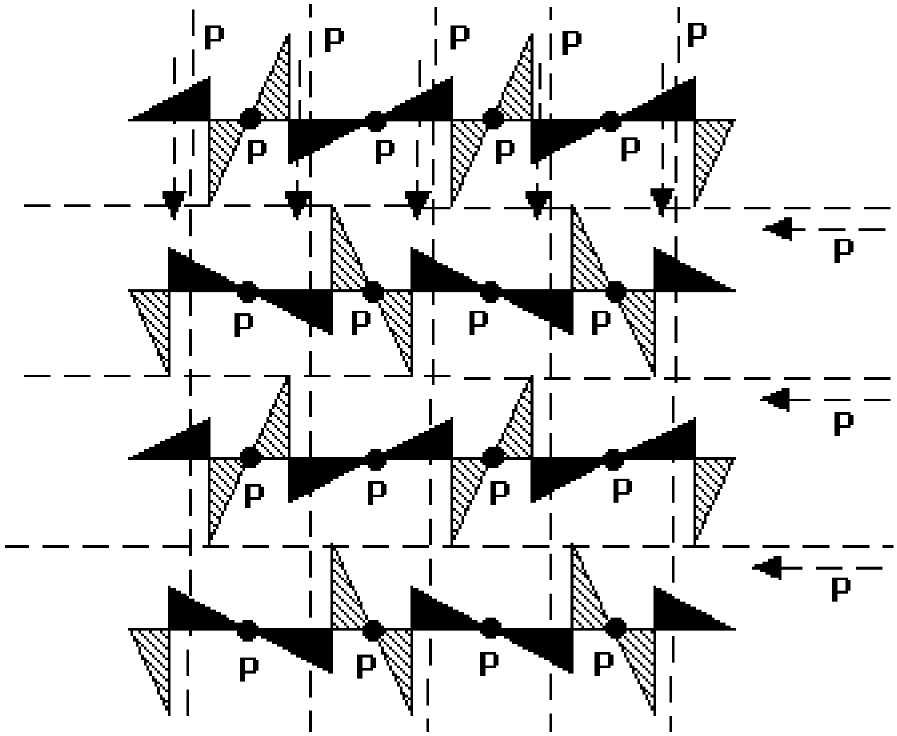

pg → pgg

Fig. 6.48

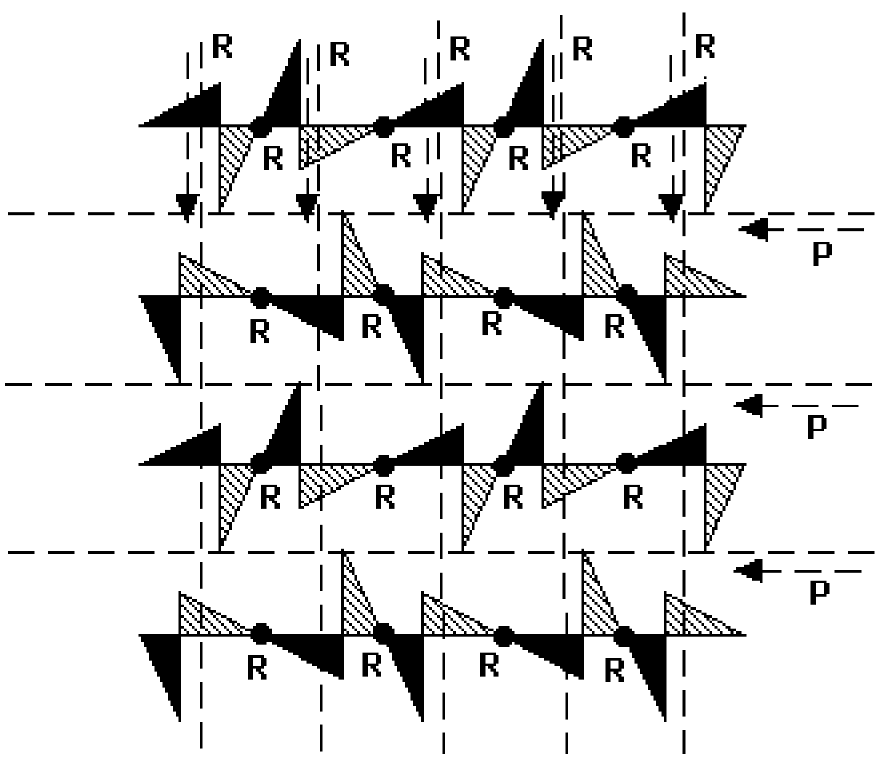

pg → pgg′

Fig. 6.49

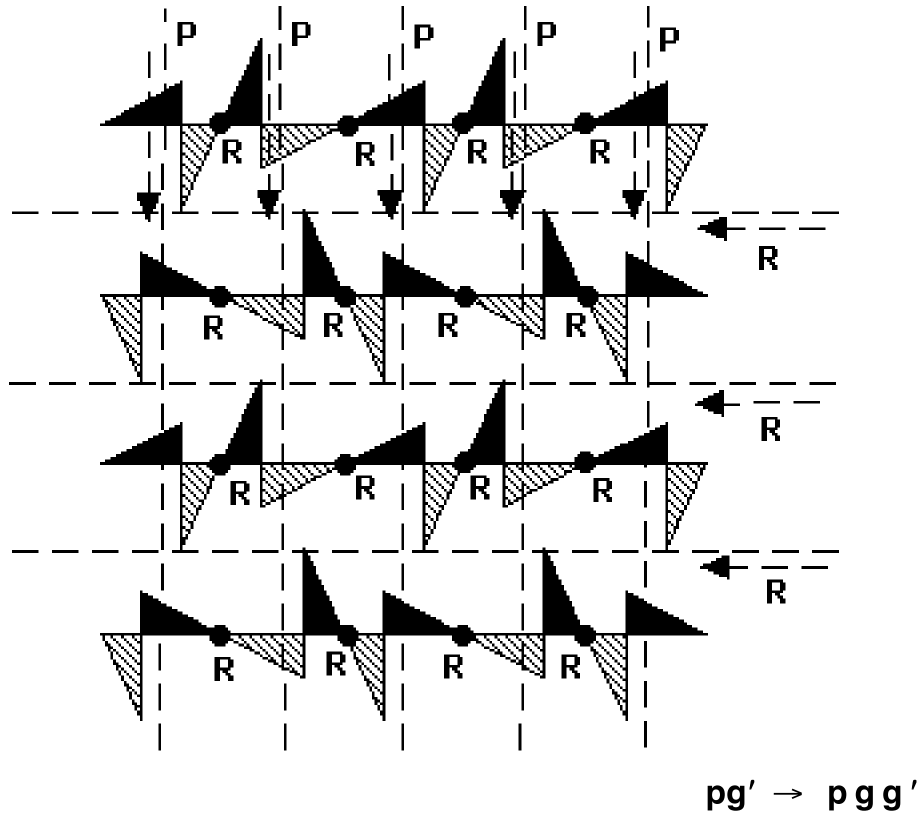

Fig. 6.50

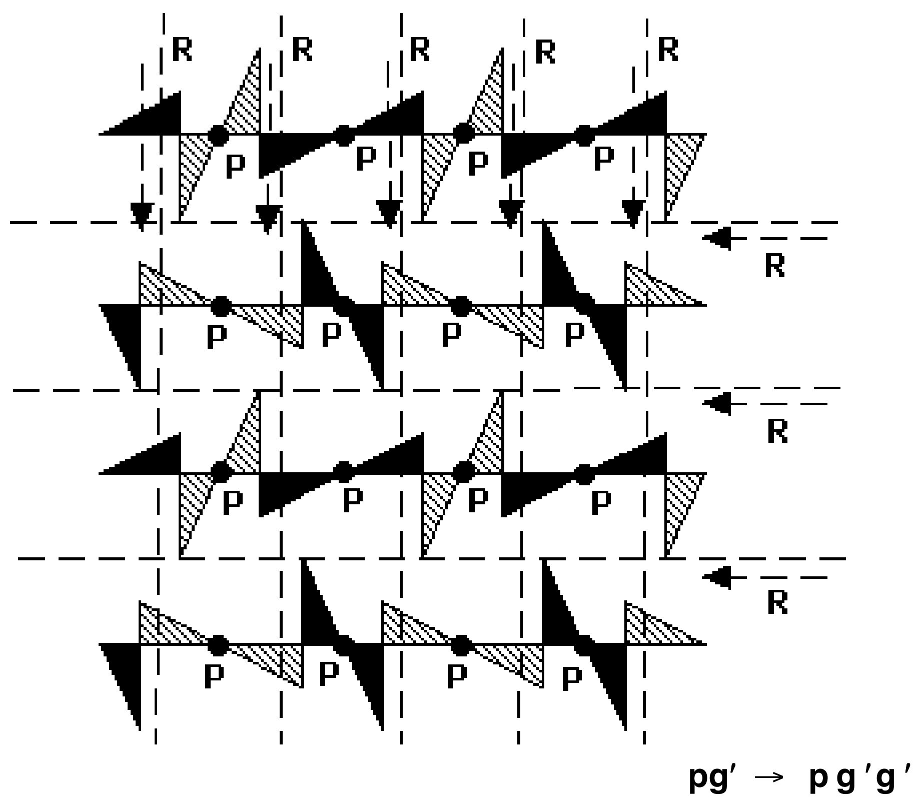

Fig. 6.51

So far so good: we obtained four two-colored patterns (from the 'root' **pg** and **pg′** patterns of figures 6.4 & 6.11 always) having glide reflection in **two** perpendicular directions, welcome additions to the **pgg** family; two of them (figures 6.49 & 6.50) **look** distinct but are the same mathematically (**pgg′**), with color-preserving glide reflection in one direction and color-reversing glide reflection in the other direction. But there will be 'casualties' caused by **color inconsistencies** as we apply this process to the $\mathbf{p'_b1g}$: right below you find two $\mathbf{p'_b2}$ patterns with color-inconsistent glide reflection (mappable in fact to each other by either color-preserving horizontal glide reflection or color-reversing vertical glide reflection):

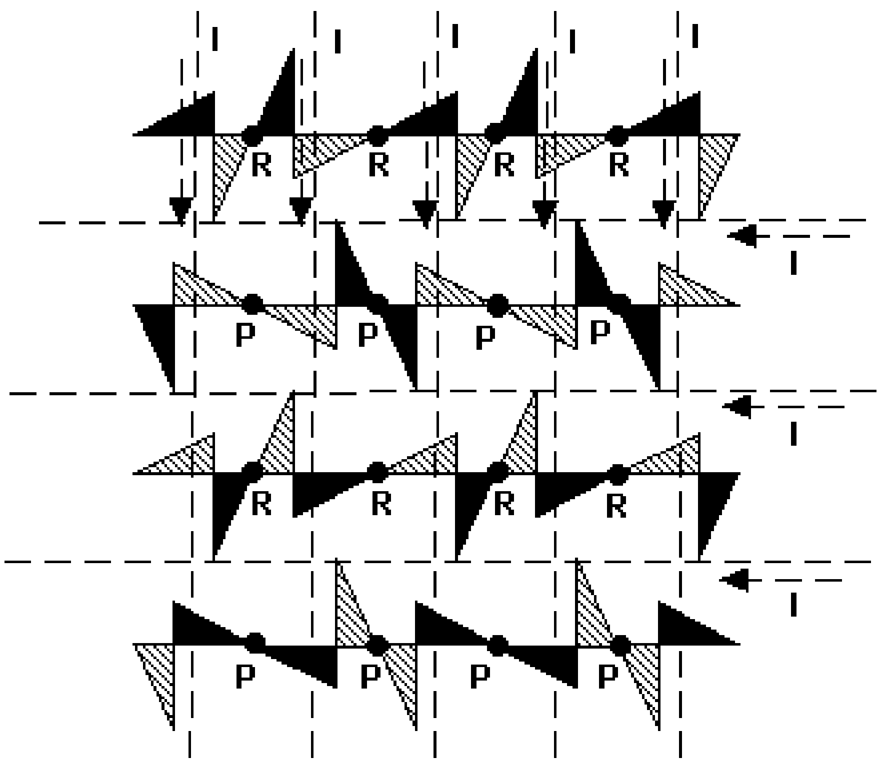

$\mathbf{p'_b1g \rightarrow p'_b2}$

Fig. 6.52

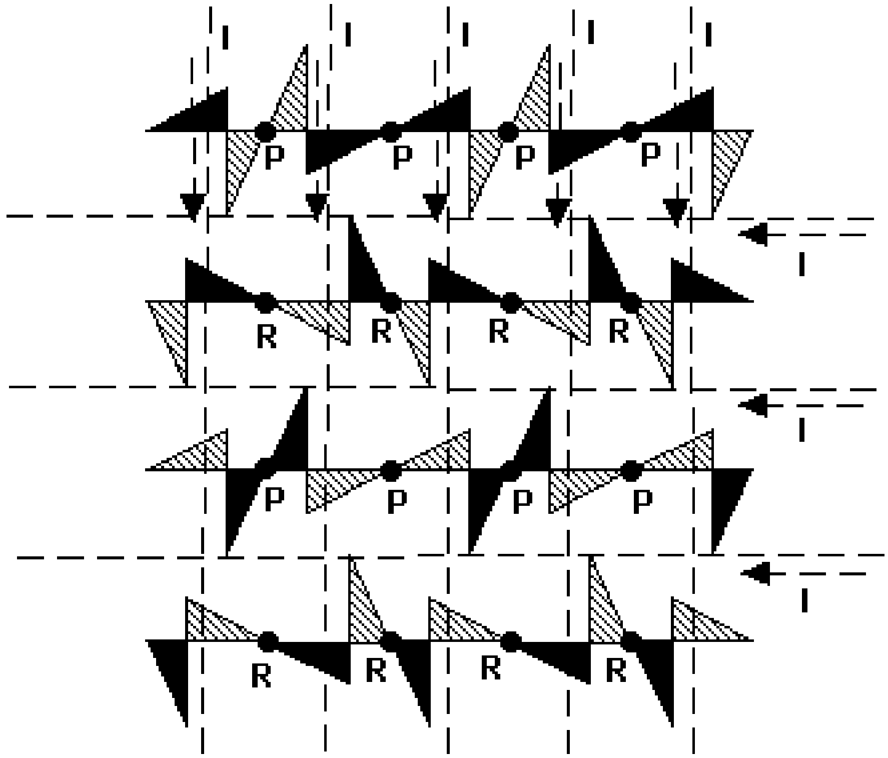

$p'_b1g \rightarrow p'_b2$

Fig. 6.53

6.6.2 Only three types indeed! Looking at the **pgg**-like patterns obtained so far, we notice that none of them has glide reflection of both kinds in the same direction: such a situation is indeed **impossible** because of what figures 6.54 & 6.55 tell us:

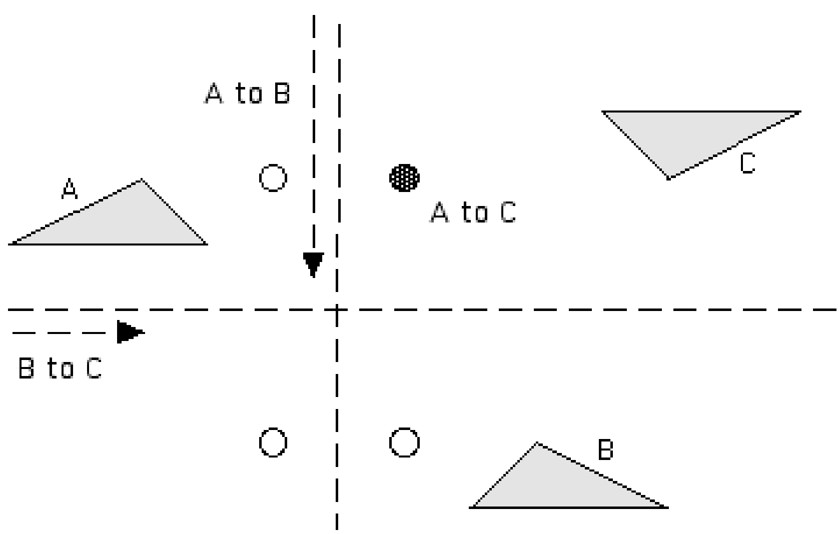

Fig. 6.54

This is a demonstration of a significant fact: the combination of two **perpendicular** glide reflections (mapping A to B and B to C) produces a **half turn** (mapping A to C)! We will go through a rigorous proof of a generalization of this in section 7.10, but you should try to verify an important aspect of this new theorem: depending on **which way** the gliding vector of each of the two glide reflections goes (north-south versus south-north and west-east versus east-west), as well as the **order** in which the two glide reflections are combined, we get **four** plausible centers (and half turns) out of **eight** actual possibilities; in our case, a **'symbolic' rule** yields (west-east) $\times$ (north-south) = northeast. (Notice also that the **distances** of the rotation center from the glide reflection axes are equal to **half** the length of the corresponding gliding vectors; as an important **special case**, the composition of two perpendicular **reflections** is a half turn centered at their intersection point. These facts throw new light into sections 2.6 (**pma2** border patterns) and 2.7 (**pmm2** border patterns), as well as several sections in chapter 4!)

Now figure 6.55, together with the preceding remarks, shows why color-preserving and color-reversing glide reflection axes of a **pgg**-like pattern **cannot** coexist in the same direction:

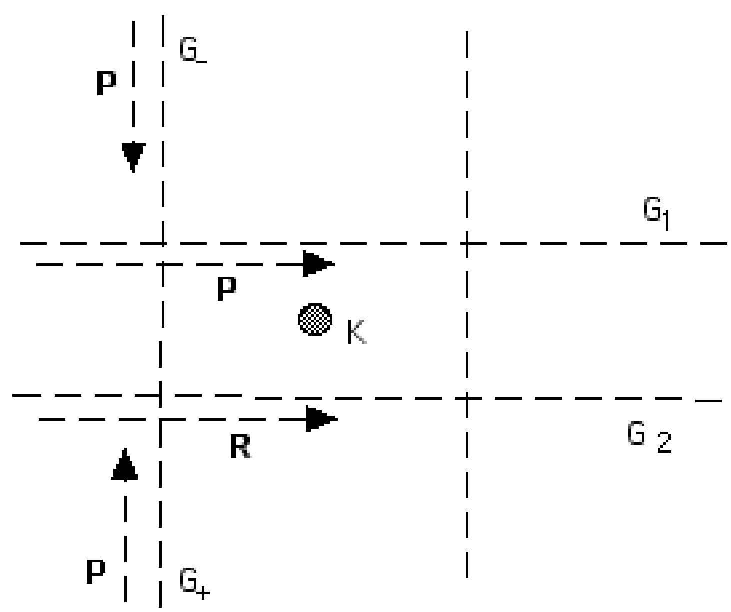

Fig. 6.55

Is the half turn (at) K color-preserving or color-reversing? In view of $\mathbf{K = G_1 * G_+}$ (G applied upwards (**P**) followed by G_1 (**P**)) and $\mathbf{K = G_2 * G_-}$ (G applied downwards (**P**) followed by G_2 (**R**)) we conclude that the half turn at K must be **both** color-preserving and color-reversing; that is, the situation featured in figure 6.55 ('mixed' horizontal axes) is **impossible**.

We conclude that each of the two **pg**-like 'factors' of a **pgg**-like pattern could be either a **pg** or a **pg′**, but **not** a $\mathbf{p'_b1g}$. This should allow for four possibilities, but since the outcome of this 'multiplication' is **not** affected by the **order** of 'factors', we are down to **three** types:

pgg = **pg** × **pg**, **pgg′** = **pg** × **pg′** = **pg′** × **pg**, **pg′g′** = **pg′** × **pg′**

6.6.3 <u>Another way of looking at it.</u> The discussion in 6.6.2 was very useful in terms of analysing the **structure** of the **pgg** pattern, but it is certainly not the easiest way to see that any two of its glide reflections parallel to each other must have the same effect on color. Indeed that follows **at once** from our **Conjugacy Principle** (6.4.4): every two **adjacent** parallel axes are mapped to each other by **any** half turn center lying **half way** between them! It might be a good idea for you to see how the Conjugacy Principle works in this **special case,** though: you should be able to provide your own proof, arguing in the spirit of figure 6.36.

In another direction now, let's revisit the **pgg** example of 4.8.3 and figure 4.43. We state there, with the Conjugacy Principle in mind (4.11.2), that it **appears** that there are **two** kinds of glide reflection axes in **both** directions: our reservations are now further justified by the impossibility of coloring that pattern in such a way that any two parallel glide reflections would have opposite effect on color!

6.6.4 <u>Further examples.</u> First, three **pgg**-like 'triangles' that you should compare to the **p2**-like patterns of figure 6.46:

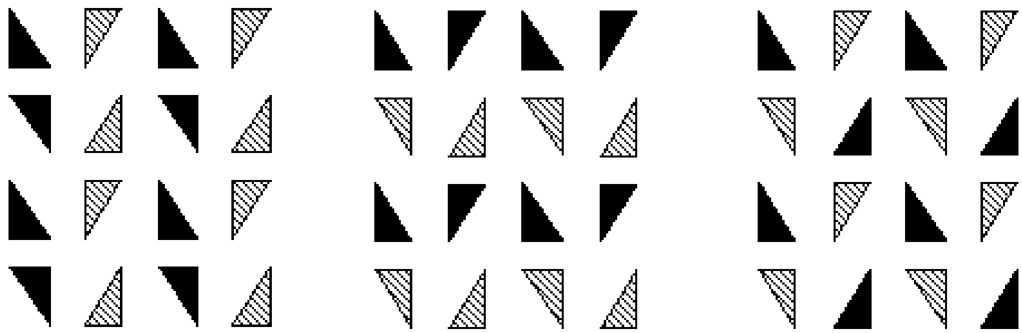

pg′g′ **pgg′** **pgg′**

Fig. 6.56

The ‘proximity’ between the two families (**pgg** and **p2**) is further outlined through the following curious example of a **pg′g′** that is a **close relative** of the **p2** example in figure 6.5:

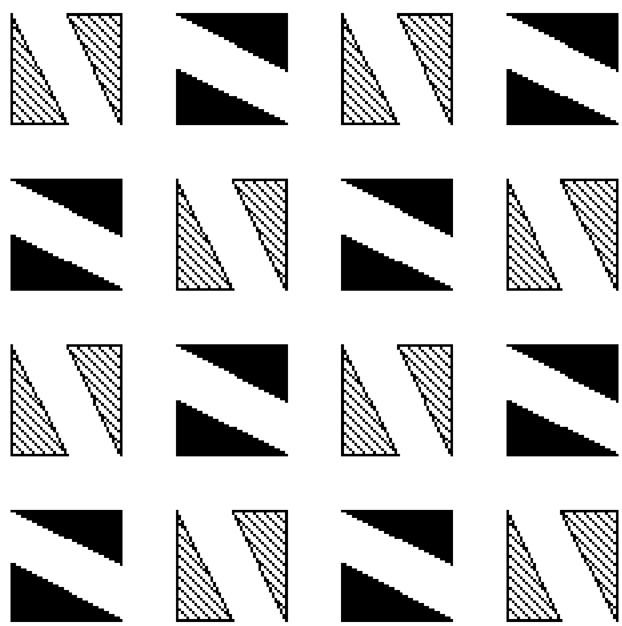

pg′g′

Fig. 6.57

This is an example that many would classify as a **p2**: after all, the rotations of **both** the **pg′g′** and the **p2** are color-preserving **only**. Well, the advice offered in 4.8.2 remains valid: after you locate **all** (hopefully!) the rotation centers, check for **‘in-between’ diagonal** glide reflection! Instead of applying this ‘squaring’ process to the **p2′** in figure 6.39 for a **pgg′**, we offer a fancy **pmg**-generated **pgg′**:

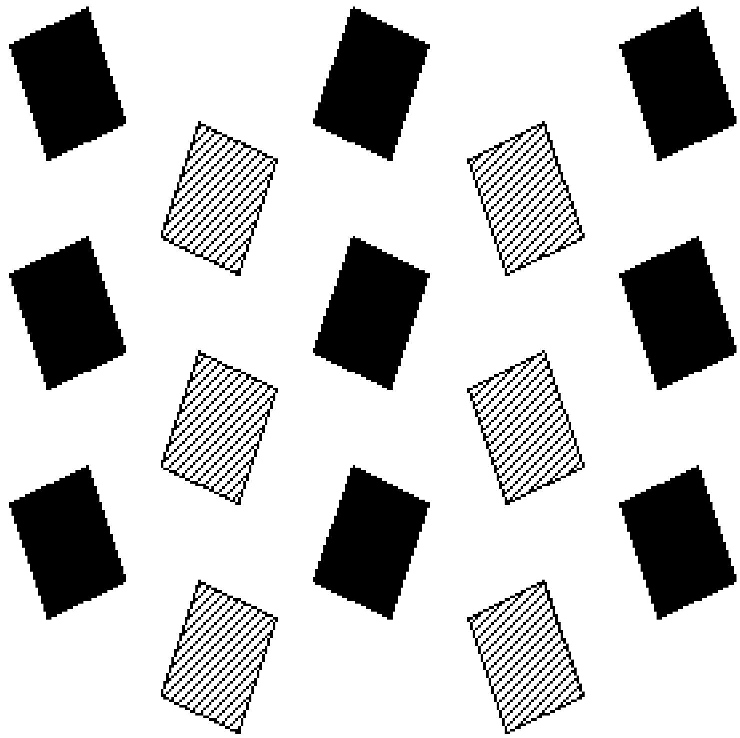

pgg′

Fig. 6.58

This pattern (**Laurie Beitchman**, Fall 1999) consists of **two pmg**s of distinct colors; its vertical and horizontal glide reflections reverse and preserve colors, respectively. Again, you may opt to find the glide reflection axes **after** you get **all** the half turn centers!

6.6.5 Symmetry plans. What follows captures our structural observations on the interplay between axes and centers (6.6.2):

pgg **pgg′** **pg′g′**

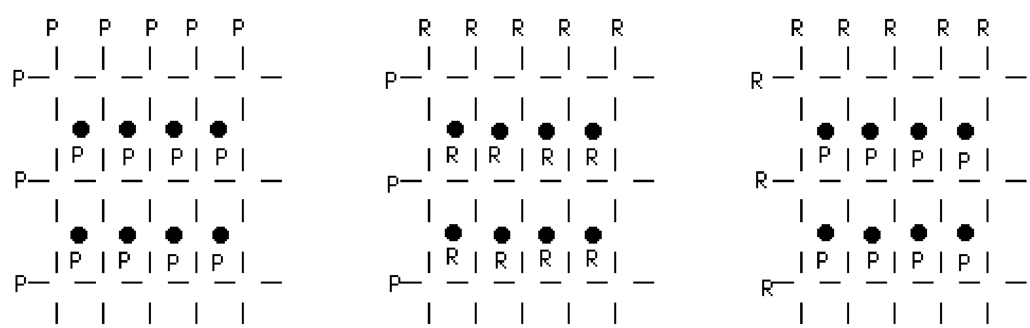

Fig. 6.59

You should compare these **pgg** symmetry plans to the **p2** symmetry plans in figure 6.45: parallelograms have now been **'ruled' by glide reflection** into rectangles, and the real reason is revealed in 8.2.2!

6.7 pmg types (pmg, p'_bmg, pmg′, pm′g, p'_bgg, pm′g′)

6.7.1 How many types at most? By now we know the game well enough to try to **predict** how many two-colored types can **possibly** exist within a family sharing the same symmetrical structure. In the case of the **pmg** (reflection in one direction, glide reflection in a direction perpendicular to that of the reflection), we are dealing with the **'product'** of a 'vertical' **pm** with a 'horizontal' **pg**. So it seems **at first** that we could have up to six × three = eighteen types ... but we also know that several cases will most likely have to be ruled out, as it has happened in the case of the **pgg**.

First, let's not forget the **pmg**'s 180^0 rotation and its centers, located -- special case of figure 6.55! -- **on** glide reflection axes and **half way** between every two adjacent reflection axes: arguing as in 6.6.3 (Conjugacy Principle), we see that all reflection axes of a **pmg** must have the **same effect** on color. (Alternatively, and closer in spirit to 6.4.4, we may appeal to the Conjugacy Principle by way of reflection axes mapped to each other by glide reflections rather than half turns!) This rules out **p'_b1m** and **c′m** for the **pm** 'factor', so we are down to **at most** four × three = twelve **pmg** types.

Next, observe that **'vertical'** hidden glide reflections and associated translations along reflection axes are fully **determined** by the **'horizontal'** glide reflections. Indeed the combination of any two **adjacent** glide reflections -- of **opposite** vectors, as in figure 6.21 -- produces the **shortest possible** (by figure 6.60 below) translation parallel to the reflection. It follows that there exists vertical color-reversing translation if and only if there exists horizontal glide reflection of both kinds.

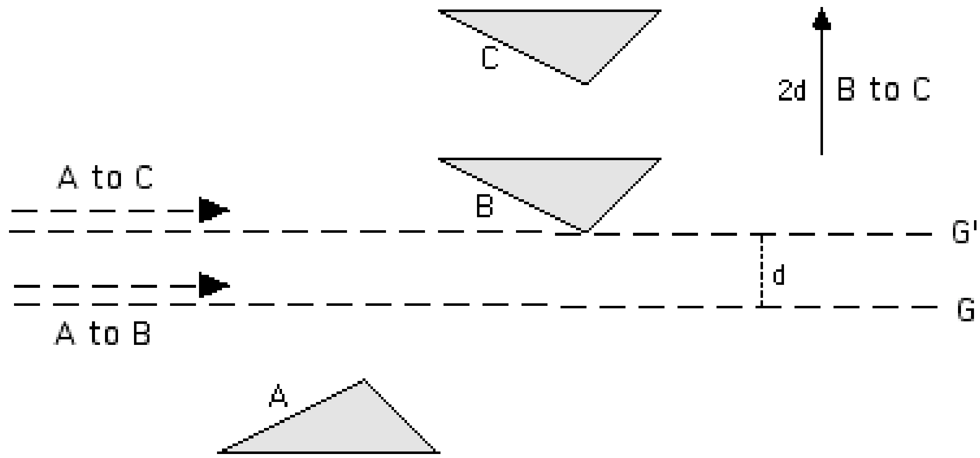

Fig. 6.60

[The combination of a glide reflection G (mapping A to B) and a translation of length 2d **perpendicular** to it (mapping B to C) produces a glide reflection G′ (mapping A to C) **parallel** to G, of **same** gliding vector and at a distance **d** from G; so if d (the distance between any two adjacent horizontal glide reflections) is assumed to be minimal then **2d** (the length of the resulting vertical translation) must be minimal, too.]

Putting everything together, we see that **all that matters** when it comes to the first factor (**pm**) of a **pmg** is whether its reflections preserve (**PP**) or reverse (**RR**) colors: color-reversing translations along reflection axes (and associated hidden glide reflections) **appear** to play no crucial role anymore **--** except that, as pointed out above, they do make their presence obvious indirectly, through the **pmg**'s second factor (**pg**)! Anyhow, there can be **at most** two × three = six **pmg**-like two-colored wallpaper patterns: two possibilities for the first factor (**PP**, **RR**) and three possibilities for the second factor (**PP**, **PR**, **RR**); see also 6.7.4.

There is no obvious reason to exclude any one of the resulting six possible types; and as we are going to see right below, each of them does show up, predictably perhaps, in concrete examples!

6.7.2 <u>Are they there after all?</u> Applying a 'secret' **reflection** to **every row** of our **pg** 'root' patterns, we **do** get six **pmg** types:

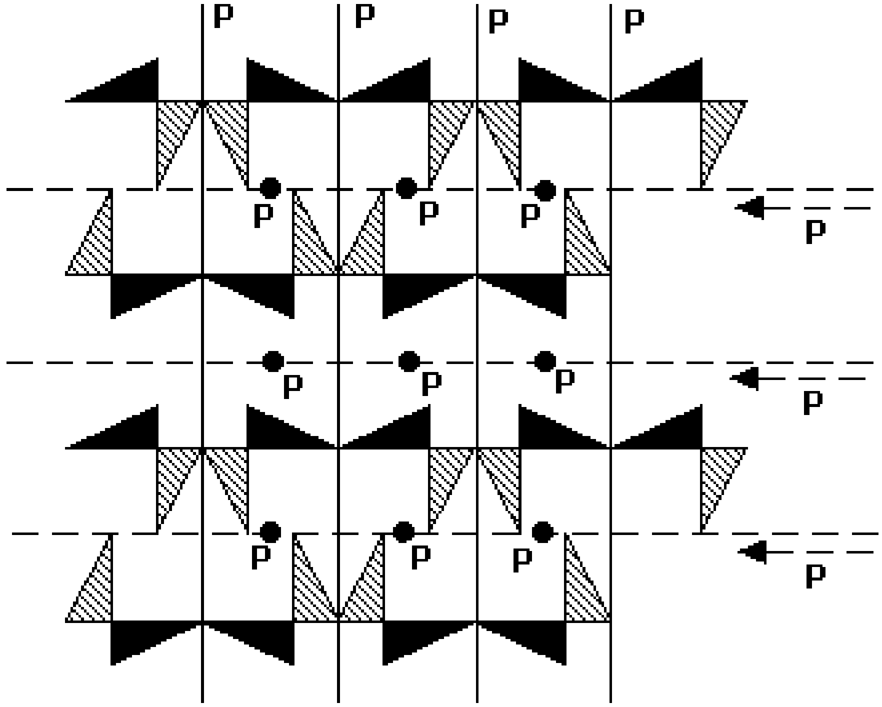

pg → pmg

Fig. 6.61

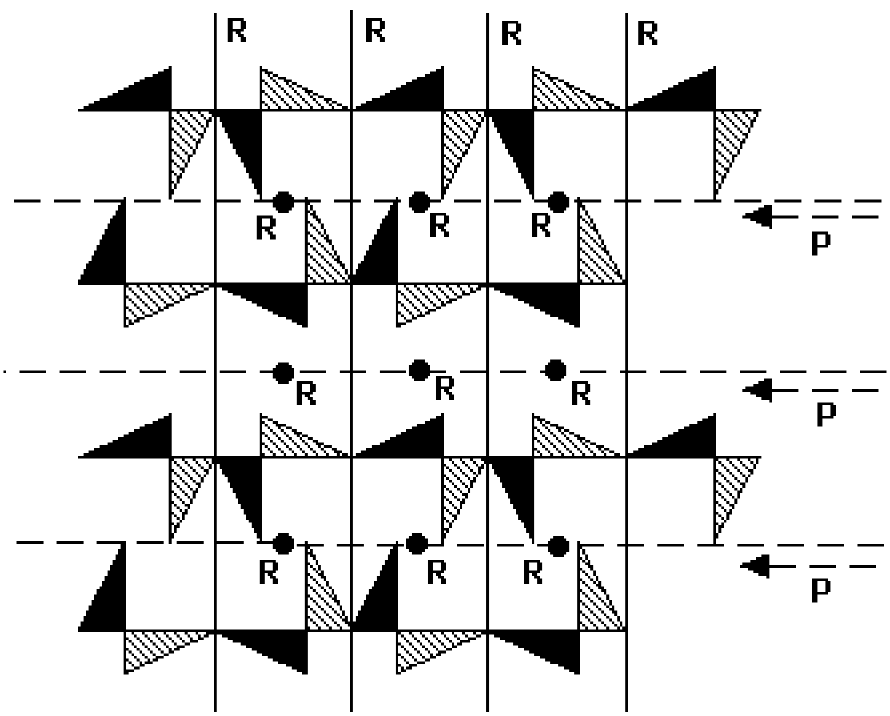

pg → pm′g

Fig. 6.62

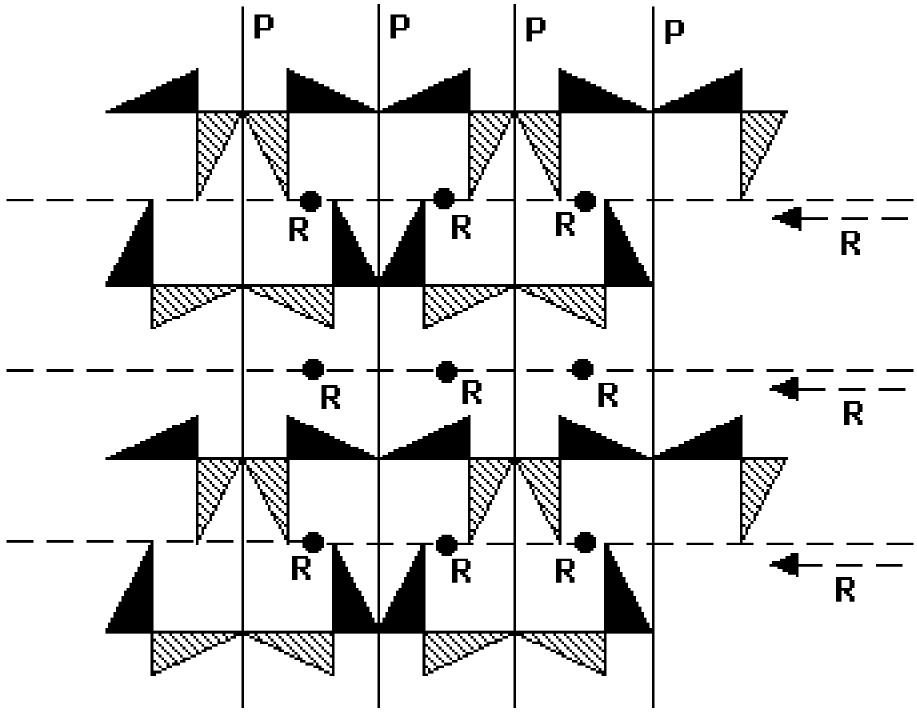

$\mathbf{pg' \rightarrow pmg'}$

Fig. 6.63

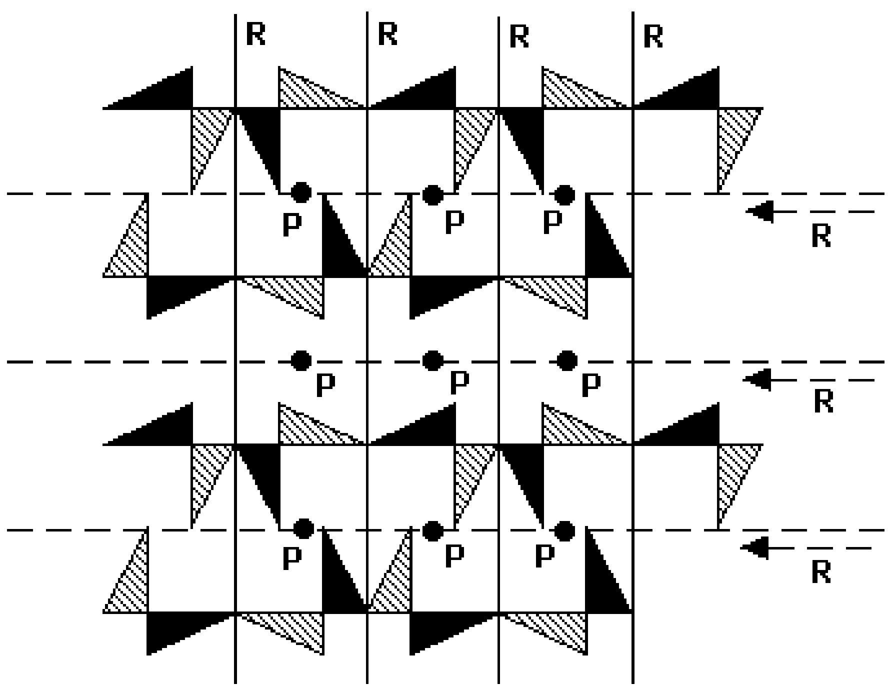

$\mathbf{pg' \rightarrow pm'g'}$

Fig. 6.64

So far there have been no surprises, save perhaps for the total absence of color-reversing translation -- provided in fact by the last two types, offspring of $\mathbf{p_b'1g}$ and rather more interesting:

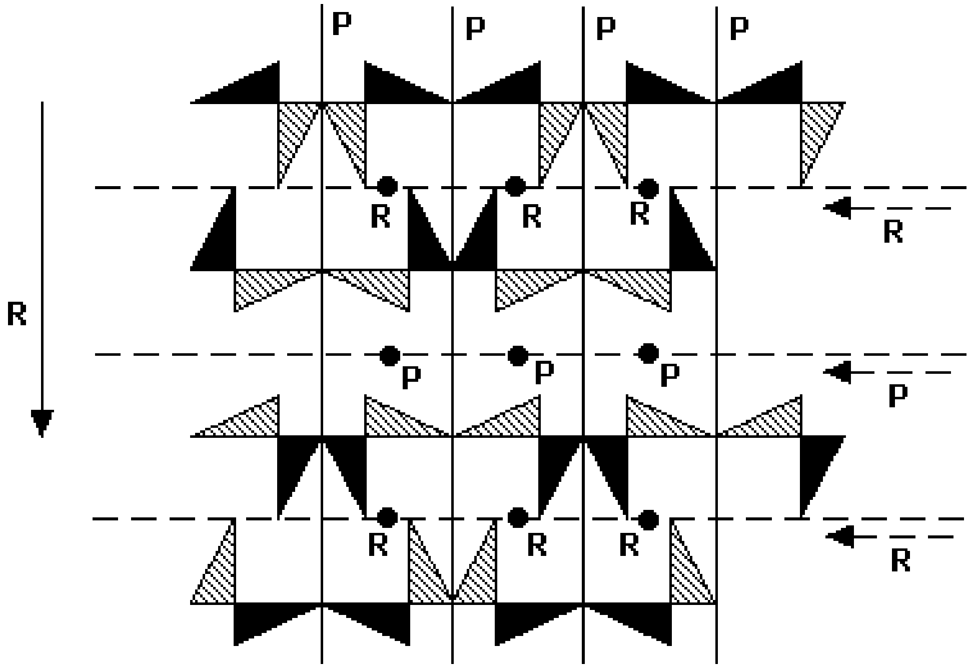

$\mathbf{p_b'1g \to p_b'mg}$

Fig. 6.65

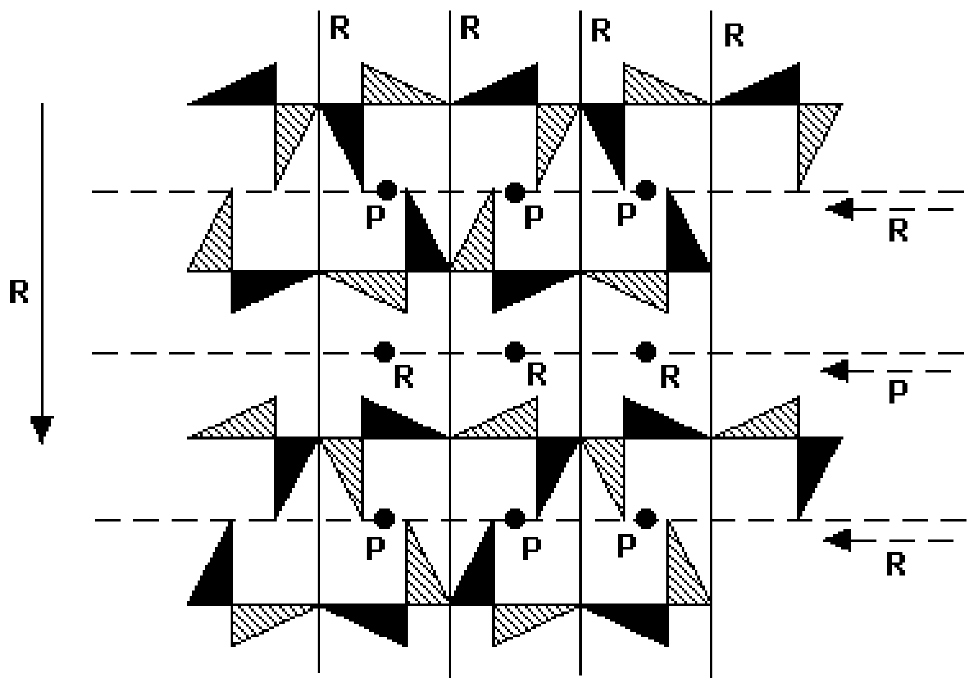

$\mathbf{p_b'1g \to p_b'gg}$

Fig. 6.66

This completes the **pmg** picture. The last two types, coming from the only **pg**-root with color-reversing translation (figure 6.9), have themselves color-reversing translation along the direction of the reflection ($\mathbf{p}'_\mathbf{b}$).

6.7.3 Examples. First, five types for six triangular colorings:

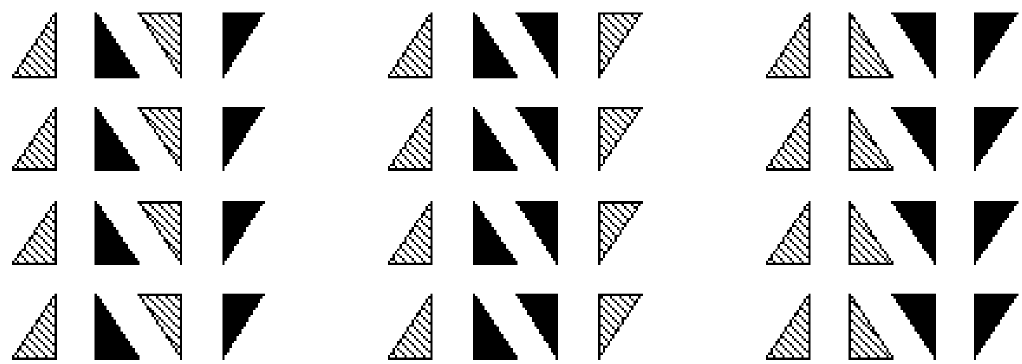

pm′g **pm′g′** **pmg′**

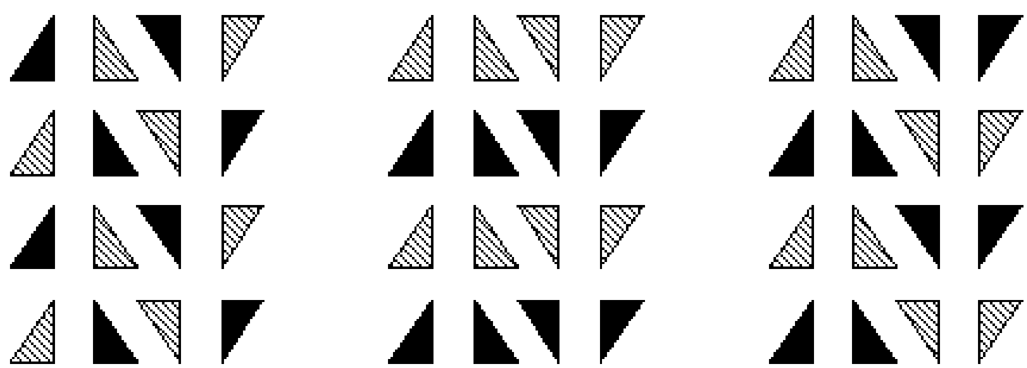

$\mathbf{p}'_\mathbf{b}\mathbf{gg}$ $\mathbf{p}'_\mathbf{b}\mathbf{mg}$ $\mathbf{p}'_\mathbf{b}\mathbf{mg}$

Fig. 6.67

And now an old **p4g** acquaintance (figures 6.2, 6.3, 6.10), revisited and (inconsistently) recolored as a $\mathbf{p}'_\mathbf{b}\mathbf{mg}$, calling for additional such **pmg**-like creations:

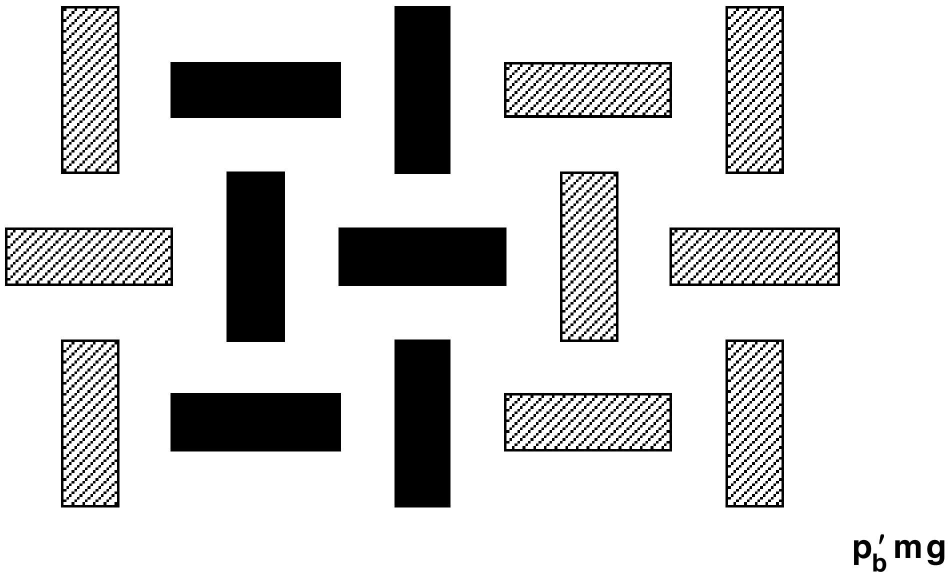

Fig. 6.68

6.7.4 <u>Symmetry plans.</u> Make sure you understand the complex interaction between reflection, glide reflection, and rotation:

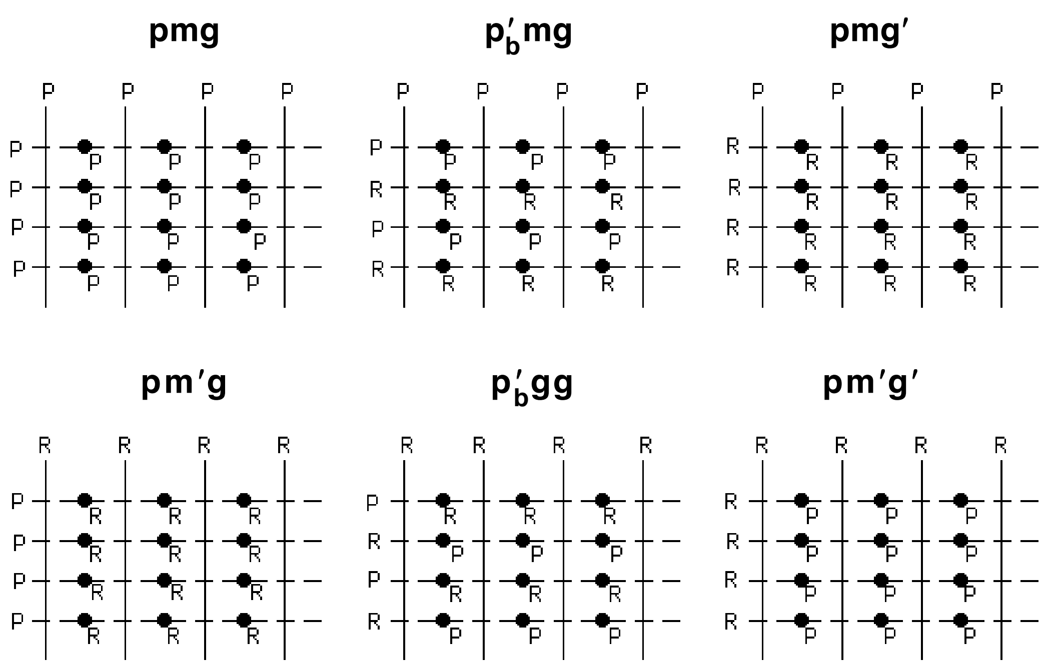

Fig. 6.69

Even though this is not exactly how we classified the **pmg**-like patterns, it is not a bad idea to express the six types as 'products' of simpler types; the main difficulty lies with the **pm** ‘factor’:

$$\mathbf{pmg} = \mathbf{pm} \times \mathbf{pg},\ \mathbf{p'_bmg} = \mathbf{p'm} \times \mathbf{p'_b1g},\ \mathbf{pmg'} = \mathbf{pm} \times \mathbf{pg'},$$
$$\mathbf{pm'g} = \mathbf{pm'} \times \mathbf{pg},\ \mathbf{p'_bgg} = \mathbf{p'_bg} \times \mathbf{p'_b1g},\ \mathbf{pm'g'} = \mathbf{pm'} \times \mathbf{pg'}$$

Of course the mysteries of the crystallographic notation and everything else make a bit more sense now, don’t you think? (Notice again the role played by the ‘vertical’ color-reversing translation in determining the first factor in our products: **p′m** or $\mathbf{p'_bg}$ in its presence (associated with a second factor of $\mathbf{p'_b1g}$), **pm** or **pm′** in its absence (associated with a second factor of **pg** or **pg′**).)

6.8 pmm types (pmm, $\mathbf{p'_bmm}$, pmm′, c′mm, $\mathbf{p'_bgm}$, pm′m′)

6.8.1 An easy guess this time. The **pmm** type may of course be viewed as the ‘product’ of two **pm**s. It can be shown as in 6.7.1 that it is easier to work with effect on color rather than types, and that we do not need to worry about the **pm**’s hidden glide reflections or color-reversing translations. With three possibilities (section 6.3) for **each** direction of reflection (**PP**, **PR**, **RR**), and the **order** of ‘factors’ in our ‘multiplication’ reduced to the **trivial** “vertical reflection versus horizontal reflection” issue, there seem to be **at most** six possible **pmm**-like types: **PP** × **PP**, **PP** × **PR**, **PP** × **RR**, **PR** × **PR**, **PR** × **RR**, **RR** × **RR**. Let’s see how many of those we can actually get -- if not all!

6.8.2 From the **pmg**s to the **pmm**s. Returning to old tricks, we will now try to get as many **pmm** types as possible by **‘perfect shiftings’** (4.4.2) of the **pmg** types we created in section 6.7; that is, we shift every other row by **half** the minimal horizontal translation.

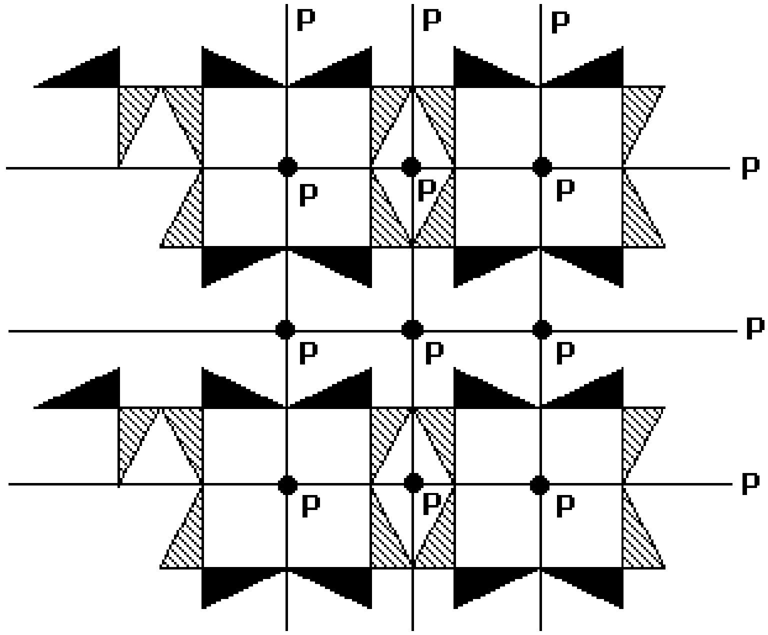

pmg → pmm

Fig. 6.70

Somewhat confused? It is not a bad idea to go back to figure 6.61 for a moment and compare the two patterns! Let's move on:

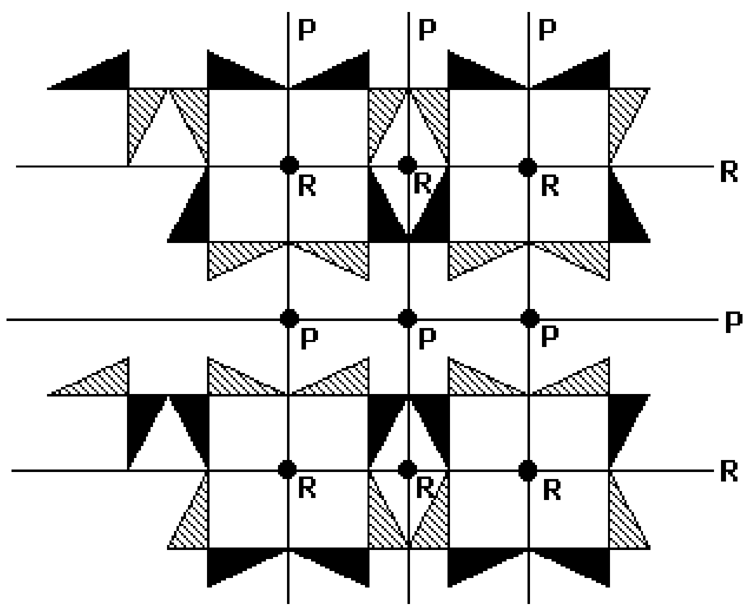

p'_bmg → p'_bmm

Fig. 6.71

Notice how the mixed horizontal **glide** reflections of the **p'_bmg** (figure 6.65) have turned into the mixed horizontal reflections of the

$\mathbf{p'_bmm}$, while all vertical reflections remained color-preserving: we started with **PP** × **PR** and ended up, predictably, with **PP** × **PR**.

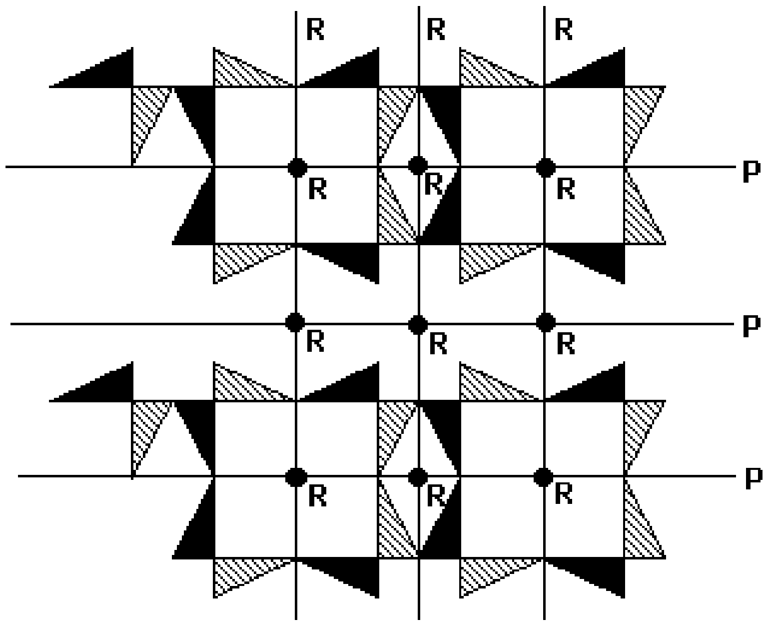

pm′g → pmm′

Fig. 6.72

No axis 'lost' its effect on color as figure 6.62 got 'perfectly shifted' into figure 6.72 (**RR** × **PP**). But look at our next step:

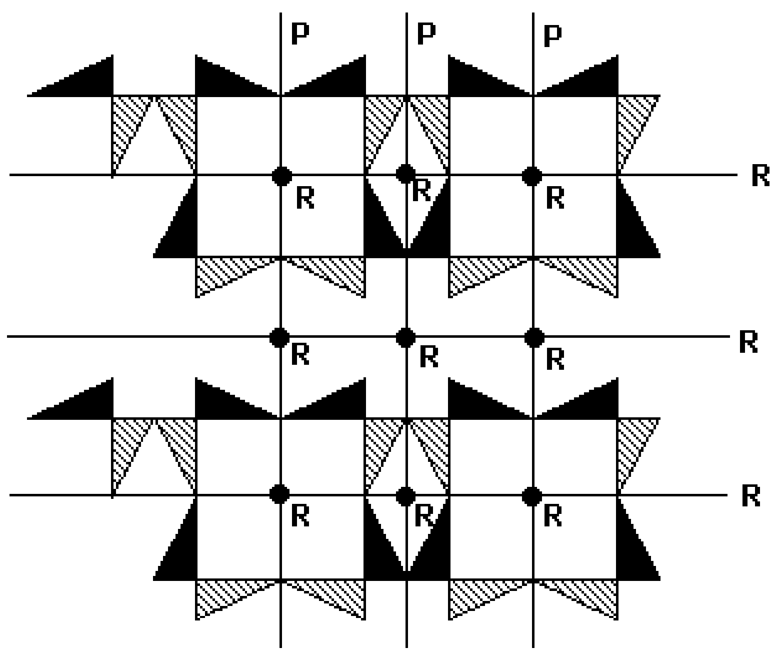

pmg′ → pmm′

Fig. 6.73

The two patterns in figures 6.72 & 6.73 **look** distinct, but mathematically they are the same (**RR** × **PP** versus **PP** × **RR**), even though they are related to two distinct **pmg**-like patterns: indeed the **pmg′** pattern of figure 6.63 (**PP** × **RR**) and the **pm′g** pattern of figure 6.62 (**RR** × **PP**) are **not** the same because the **pmg**'s two 'factors', unlike those of the **pmm**, are **not** equivalent (reflection × glide reflection as opposed to reflection × reflection).

Let's go on to a 'perfect shifting' of figure 6.66:

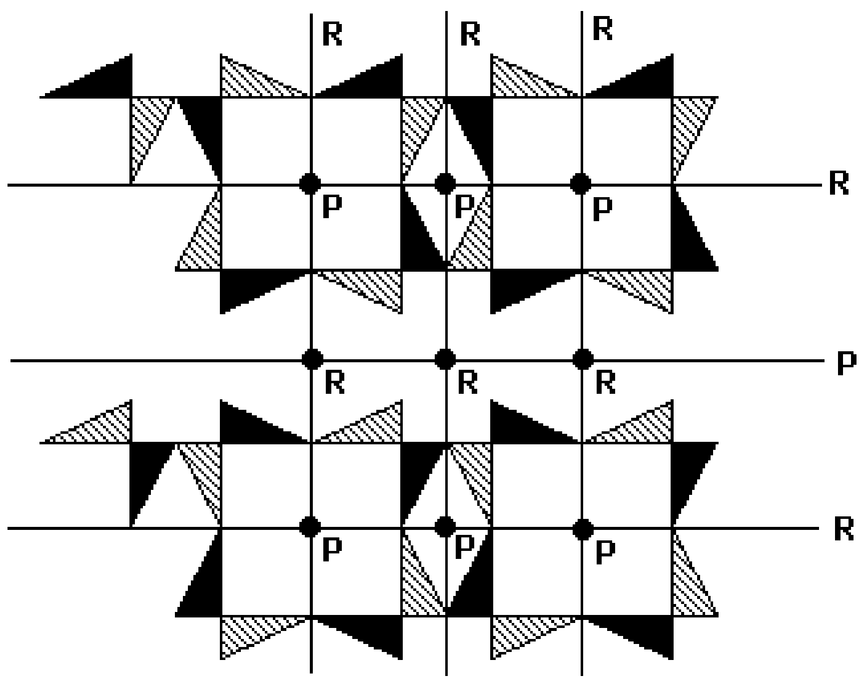

$\mathbf{p_b'gg \rightarrow p_b'gm}$

Fig. 6.74

This time we went from **RR** × **PR** to **PR** × **RR**: again 'no changes' (keeping in mind the equivalence between **RR** × **PR** and **PR** × **RR** in the **pmm** type, in accordance to our observations above on the equivalence between its 'vertical' and 'horizontal' directions).

Finally, a 'perfect shifting' of the **pm′g′** pattern of figure 6.64 leads, most predictably, to a **RR** × **RR** **pmm**-like pattern having color-reversing reflections **only**:

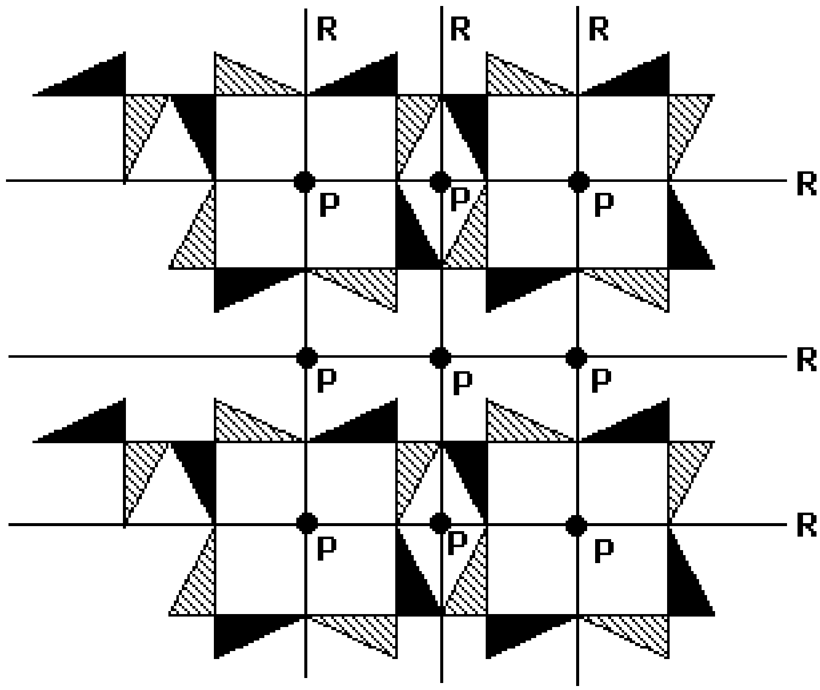

pm′g′ → pm′m′

Fig. 6.75

So we did get **five** out of six possible types, missing **PR** × **PR**: does this mean that there is no such **pmm**-like type? Certainly not:

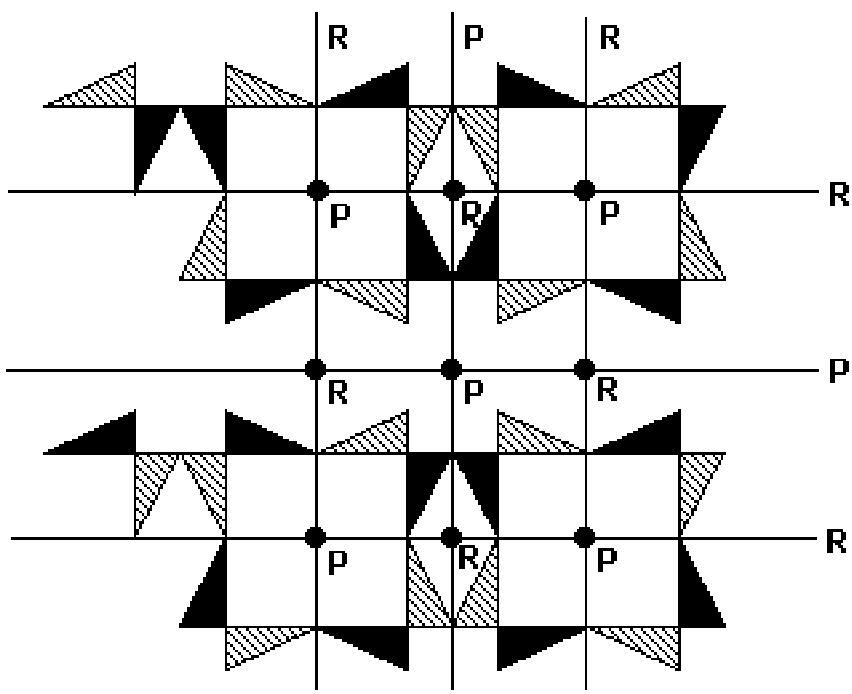

p_b'gm → c′mm

Fig. 6.76

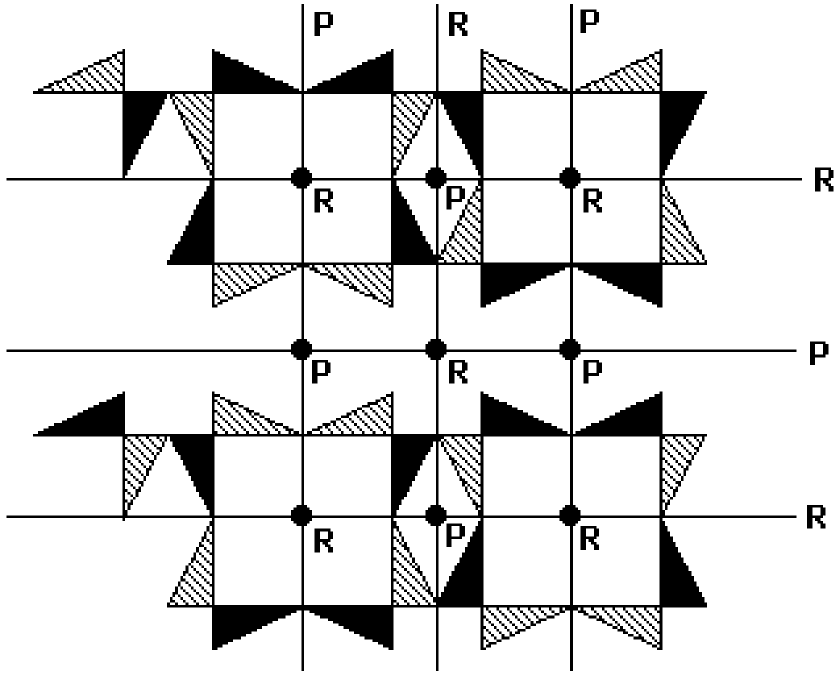

p_b'mm → c′mm

Fig. 6.77

What happened? **Shifting** now **columns** (rather than **rows**), and departing from two **pmm** (rather than **pmg**) types (figures 6.71 & 6.74), we did arrive at **two** 'distinct' representatives (figures 6.77 & 6.76, respectively) of the sought sixth **pmm**-like type!

6.8.3 Examples. A larger than usual collection of 'triangular patterns' indicating the **pmm**'s richness; notice how the last four examples have 'dropped' from **cmm** to **pmm** because of coloring.

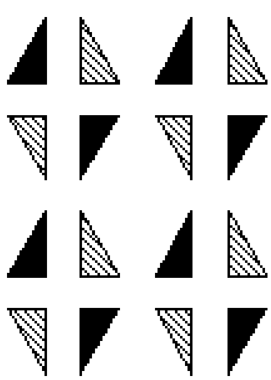

pm′m′

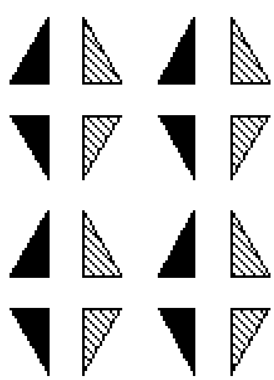

pmm′

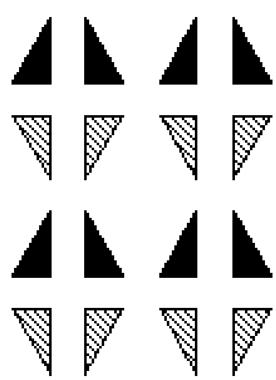

pmm′

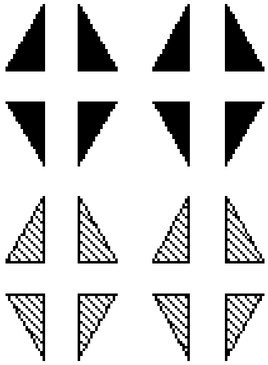

$p'_b mm$

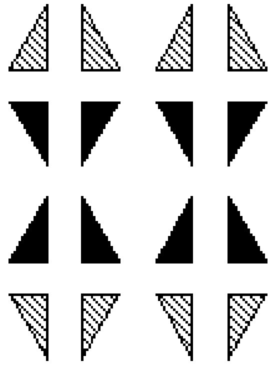

$p'_b mm$

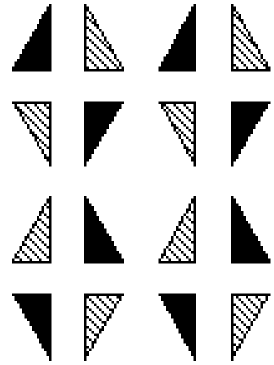

$p'_b gm$

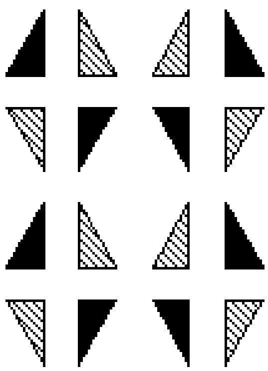

$p'_b gm$

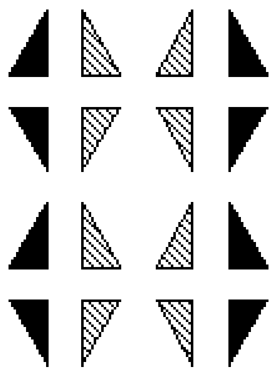

$p'_b mm$

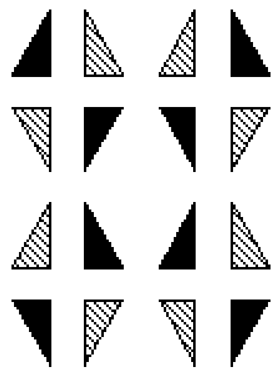

$c'm\ m$

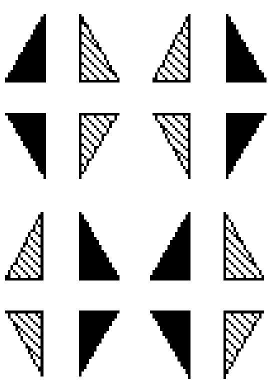

$c'mm$

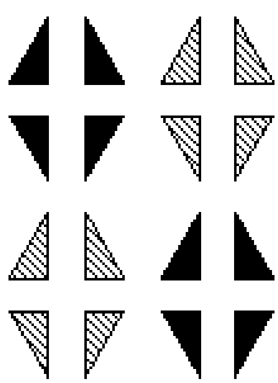

$c'mm$

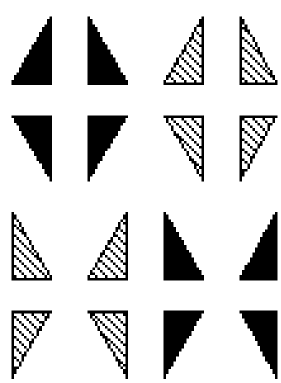

$p'_b mm$

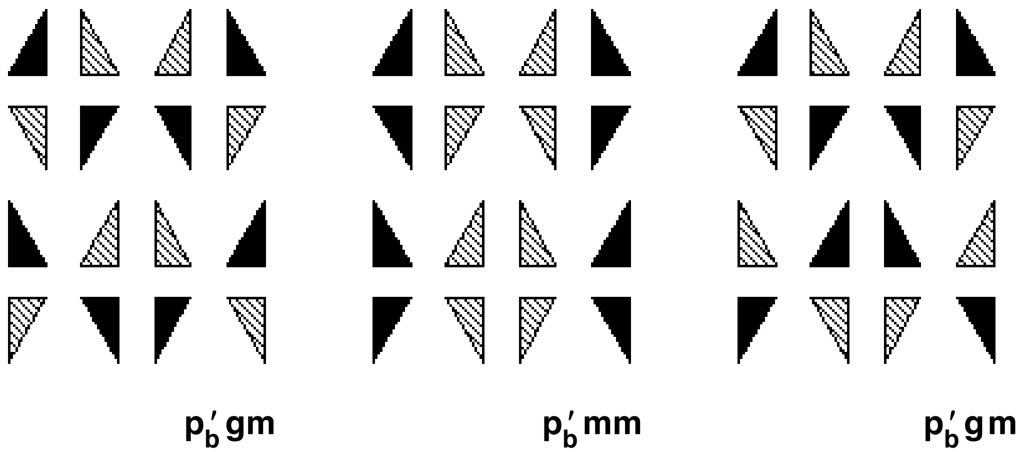

Fig. 6.78

6.8.4 Symmetry plans. No surprises here, just remember that all rotations are combinations of the two perpendicular reflection axes intersecting at their center (a **special case** of the fact illustrated in figure 6.54), hence their effect on color is determined by that of the reflections (and according to the 'multiplication' rules of 5.6.2).

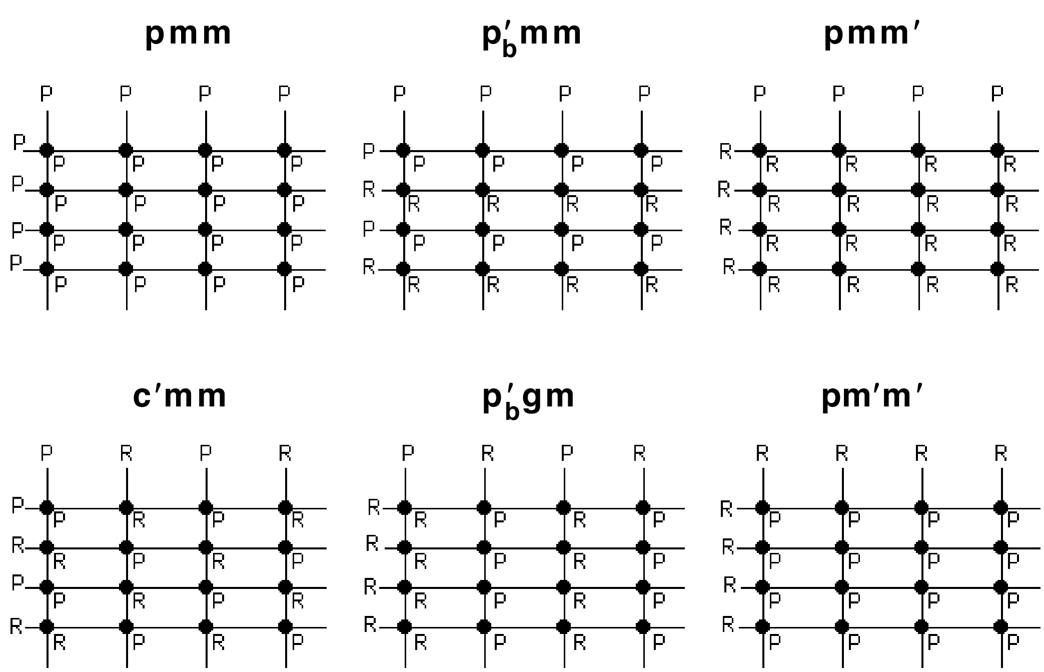

Fig. 6.79

We conclude by expressing each type as a 'product' of **pm** types:

$$\mathbf{pmm} = \mathbf{pm} \times \mathbf{pm},\ \mathbf{p'_b mm} = \mathbf{p'm} \times \mathbf{p'_b 1m},\ \mathbf{pmm'} = \mathbf{pm} \times \mathbf{pm'},$$
$$\mathbf{c'mm} = \mathbf{c'm} \times \mathbf{c'm},\ \mathbf{p'_b gm} = \mathbf{p'_b 1m} \times \mathbf{p'_b g},\ \mathbf{pm'm'} = \mathbf{pm'} \times \mathbf{pm'}$$

In connection to figure 6.79 (**pmm** symmetry plans) always, the 'first' factor corresponds to the 'vertical' direction and the 'second' factor corresponds to the 'horizontal' direction. Color-reversing translation is no longer crucial enough to be explicitly indicated; consistently with 5.5.1 and 6.5.3, it is to be found precisely in those directions in which there exist half turn centers of **opposite** effect on color. In particular the elusive **c′mm** is the only **pmm**-like type with color-reversing translation in **both** the vertical and horizontal directions, while **pmm** and **pm′m′** are the only ones with no color-reversing translation **at all**. More to the point, and arguing as in 6.7.1, we see that there exist vertical reflections of opposite color effect if and only if there exists horizontal color-reversing translation (and vice versa).

6.9 cmm types (cmm, cmm′, cm′m′, $\mathbf{p'_c mm}$, $\mathbf{p'_c mg}$, $\mathbf{p'_c gg}$)

6.9.1 How many types? Following the approach in 6.6.2, 6.7.1, and 6.8.1, we view a **cmm**-like pattern as a 'product' of two **cm**-like patterns. Having four possibilities for each 'factor' (**PP**, **PR**, **RP**, **RR**, where the **first** letter now stands for reflection and the **second** letter for in-between glide reflection), and keeping in mind that 'multiplication' is **commutative** (again the 'horizontal' versus 'vertical' non-issue), we see that there can be **at most** ten possible **cmm** types, defined by the 'products' **PP** × **PP**, **PP** × **PR**, **PP** × **RP**, **PP** × **RR**, **PR** × **PR**, **PR** × **RP**, **PR** × **RR**, **RP** × **RP**, **RP** × **RR**, **RR** × **RR**. Let's first check how many types we can get 'experimentally' (6.9.2), and then check how many types are in fact impossible (6.9.3).

6.9.2 Perfectly shifting the **pmm**s. We trace each new (**cmm**) type back to a **pmg** type, showing also the 'intermediate' **pmm** type (the perfect shifting of which led to the **cmm** type):

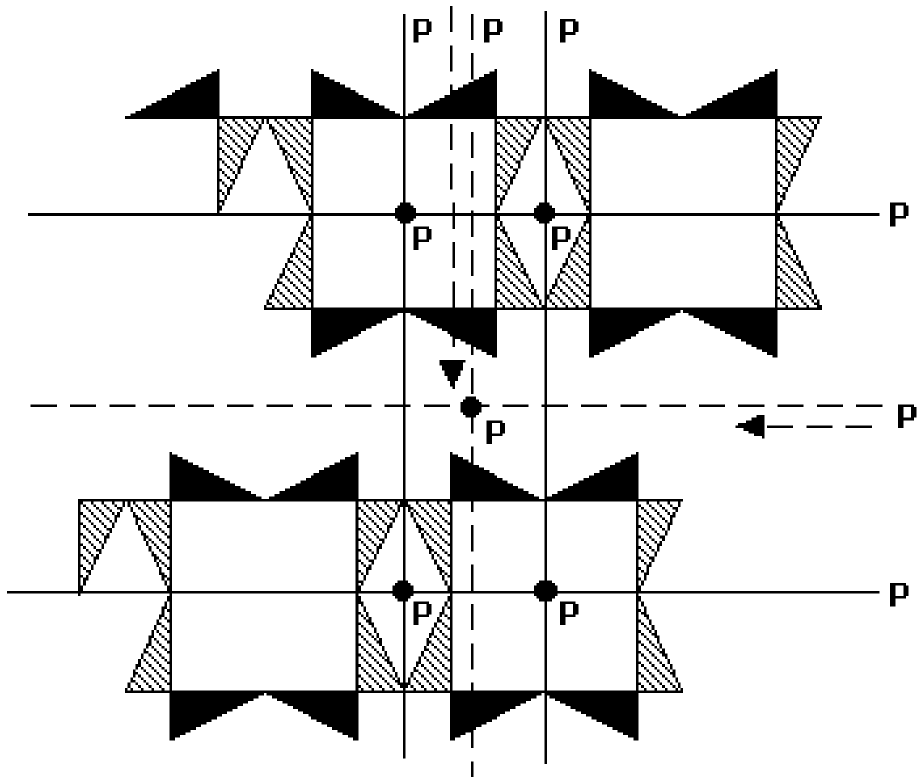

pmg → pmm → cmm

Fig. 6.80

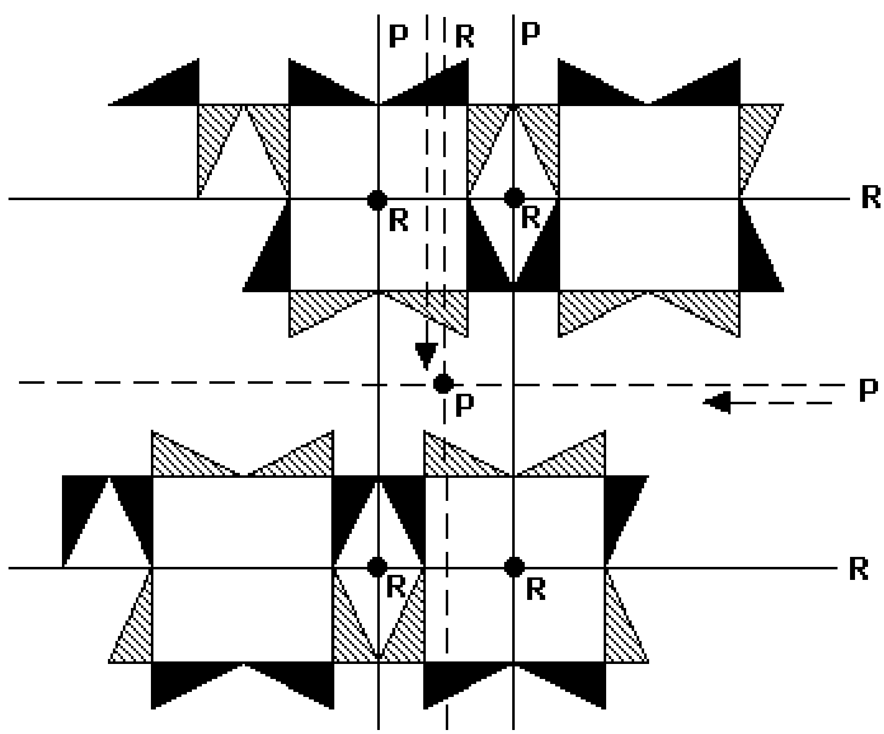

$p_b'mg \rightarrow p_b'mm \rightarrow p_c'mg$

Fig. 6.81

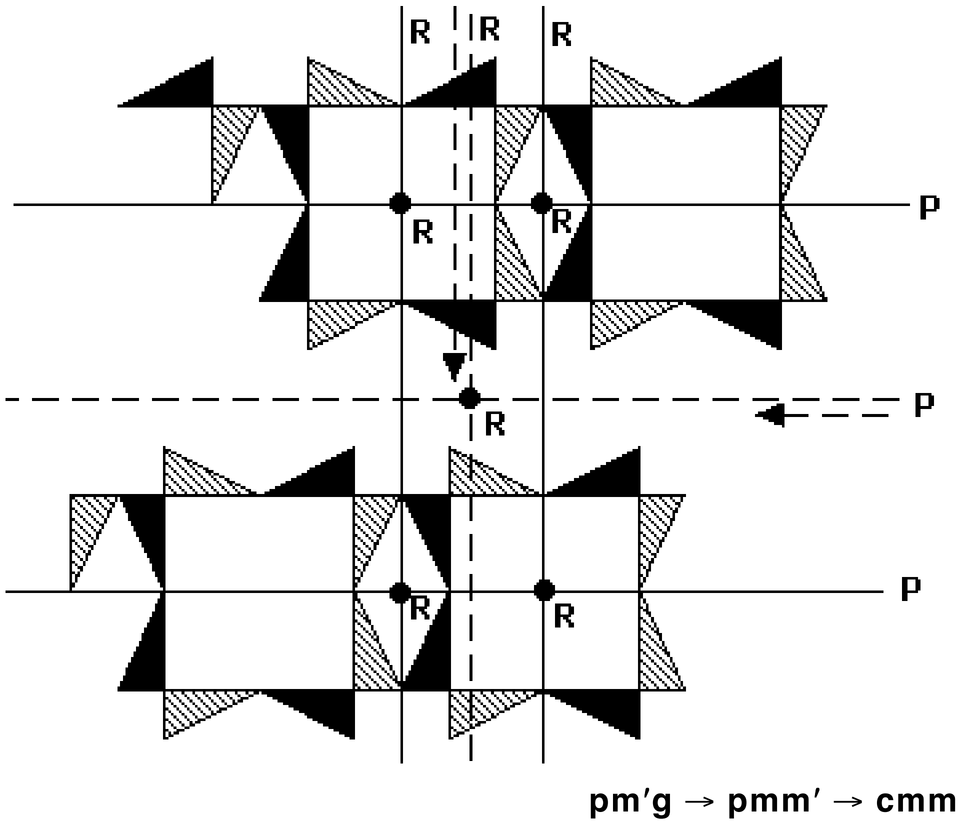

Fig. 6.82

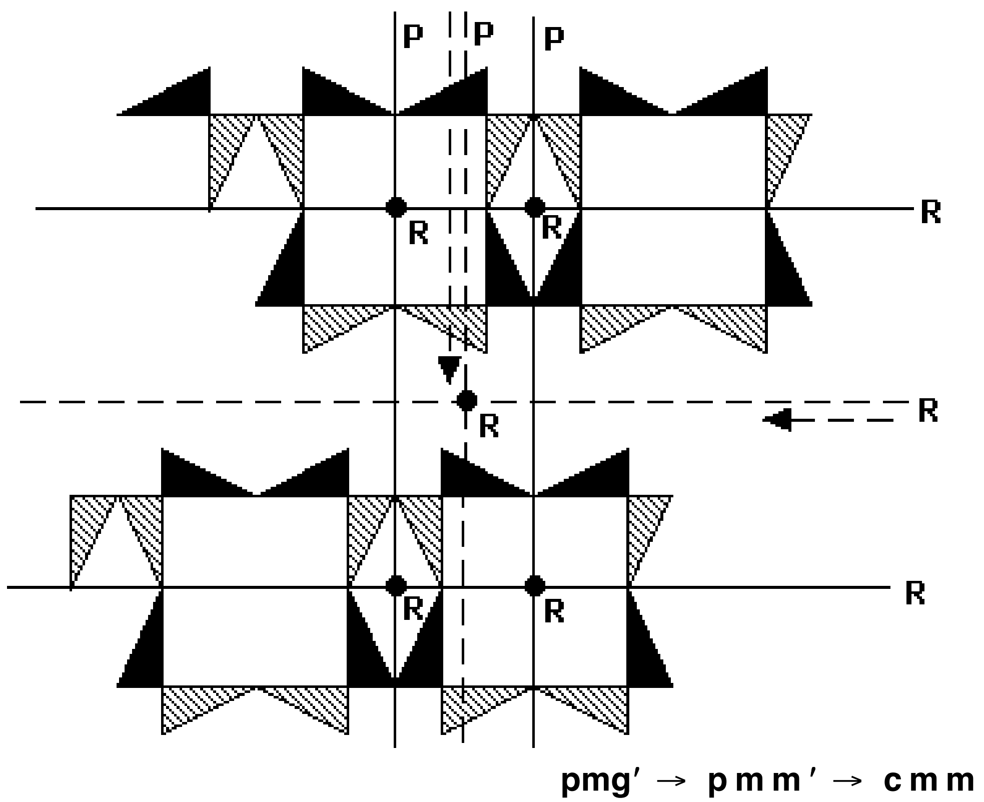

Fig. 6.83

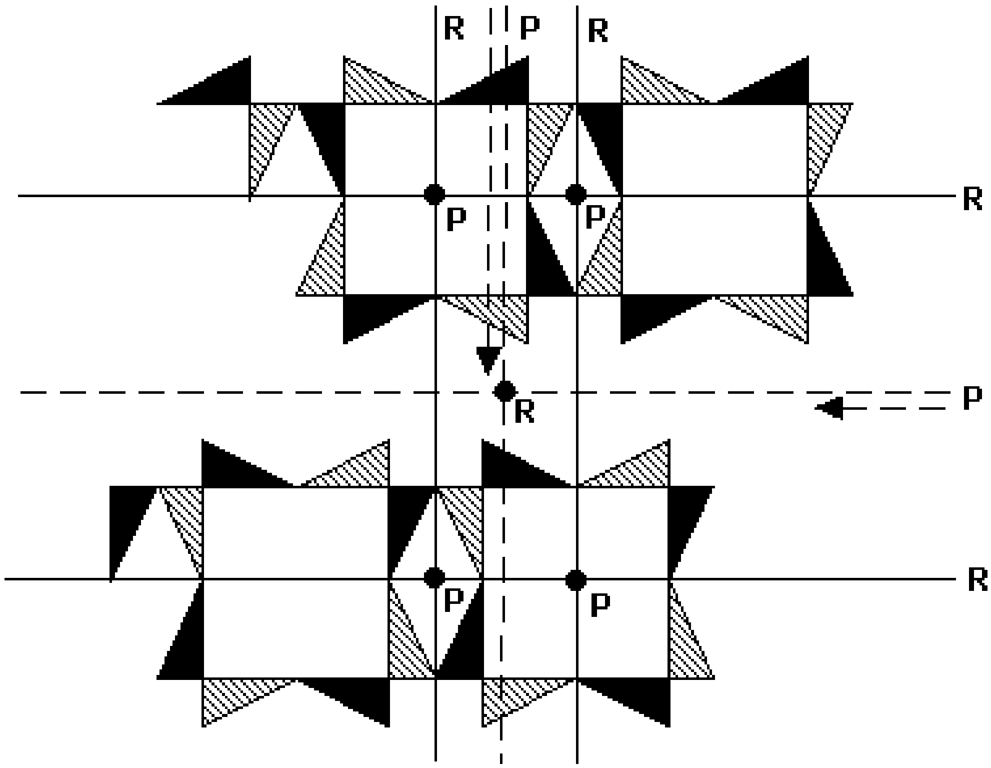

$p'_b gg \rightarrow p'_b gm \rightarrow p'_c gg$

Fig. 6.84

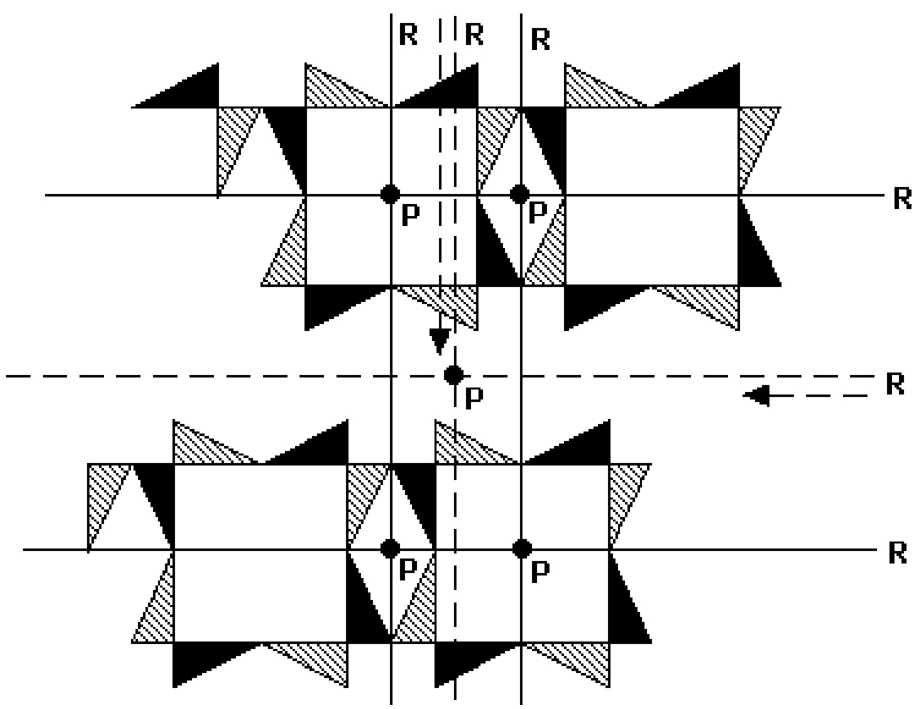

$pm'g' \rightarrow pm'm' \rightarrow cm'm'$

Fig. 6.85

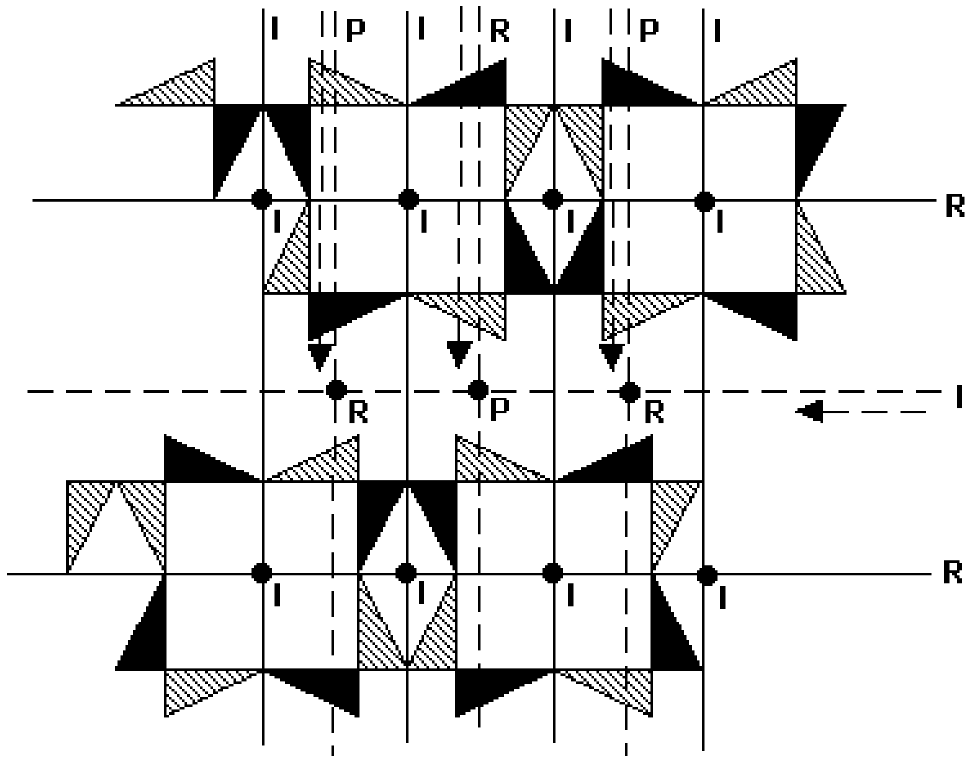

$p'_b gm \rightarrow c'mm \rightarrow p'_b gg$

Fig. 6.86

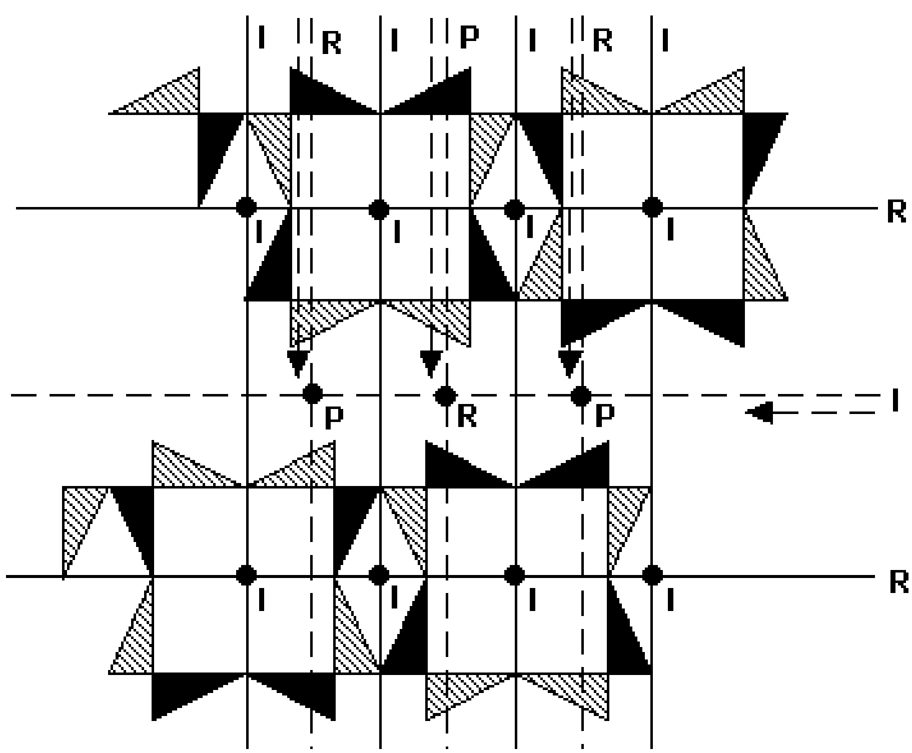

$p'_b mm \rightarrow c'mm \rightarrow p'_b gg$

Fig. 6.87

Due to not-that-obvious color inconsistencies, the last two patterns are of the same **pmg**-like type! Our shifting process has produced **five** out of at most ten possible types corresponding to the ten combinations listed in 6.9.1: **PP** × **PP** (**cmm**), **PR** × **RP** ($\mathbf{p'_c mg}$), **PP** × **RR** (**cmm′**), **RP** × **RP** ($\mathbf{p'_c gg}$), **RR** × **RR** (**cm′m′**). But this 50% rate of success is a bit too low in view of our experience with the other types! Is it possible that some or all of the remaining five combinations are in fact **impossible**?

6.9.3 Ruling out the non-obvious. It turns out that another four of the combinations in 6.9.1 are impossible (**PP** × **PR**, **PP** × **RP**, **PR** × **RR**, **RP** × **RR**), leaving thus only **one** question mark around **PR** × **PR**. Let's see for example why a situation such as **PP** × **PR** is impossible, using a version of the argument in 6.6.2 (figure 6.55):

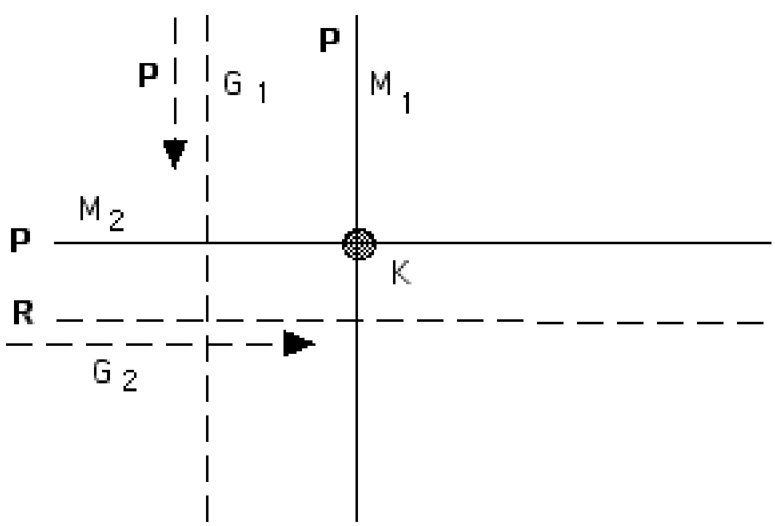

Fig. 6.88

Is the half turn (at) K color-preserving or color-reversing? In view of $\mathbf{K = M_2 * M_1 = M_1 * M_2}$ (reflection $\mathbf{M_1}$ (**P**) followed by reflection $\mathbf{M_2}$ (**P**) **or** the other way around) and $\mathbf{K = G_2 * G_1}$ (glide reflection $\mathbf{G_1}$ (**P**) followed by glide reflection $\mathbf{G_2}$ (**R**)) we conclude that the half turn at K must be **both** color-preserving and color-reversing, which is certainly **impossible**.

So, the **cmm** does not allow a ‘mixed’ combination of reflection and glide reflection in one direction **and** a ‘pure’ combination in the other direction. Unlike in 6.6.3, this impossibility cannot be deduced from the Conjugacy Principle; it is solely a consequence of the pattern’s structure and the way its isometries are **‘weaved’** into each other.

6.9.4 One more type! The question mark around **PR** × **PR** would not have been there at all were we blessed with photo memory: indeed the pattern in figure 6.2 has just what we were looking for, color-preserving reflections **and** in-between color-reversing glide reflections in **both** directions! Such patterns are known as $\mathbf{p'_c mm}$.

But here is another question: how could we **possibly** get a $\mathbf{p'_c mm}$ out of those ‘root’ **pg** patterns through our usual operations? This is something for you to wonder about as we are bidding farewell to our ‘roots’: even though the **p4m** types in section 6.12 may be viewed as special (‘square’) versions of the **pmm**, and likewise for **p4g** (section 6.11) and **cmm** (as our last example on $\mathbf{p'_c mm}$ indicates), the **pg** excursion cannot go on for ever, as color inconsistencies and worse stand on our way...

6.9.5 Examples. First a few ‘triangles’: **compare** with 6.8.3!

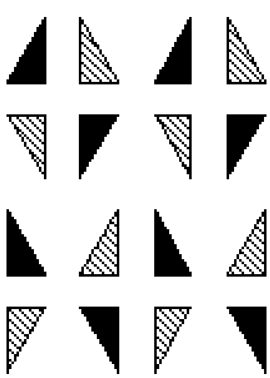
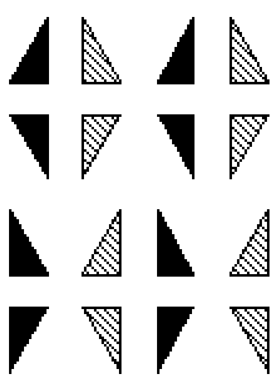
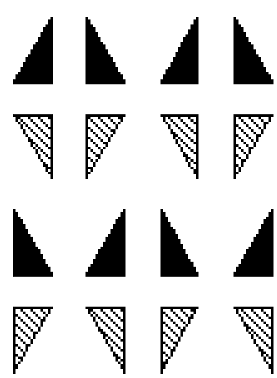

$\mathbf{p'_c gg}$ $\mathbf{p'_c mg}$ **cmm′**

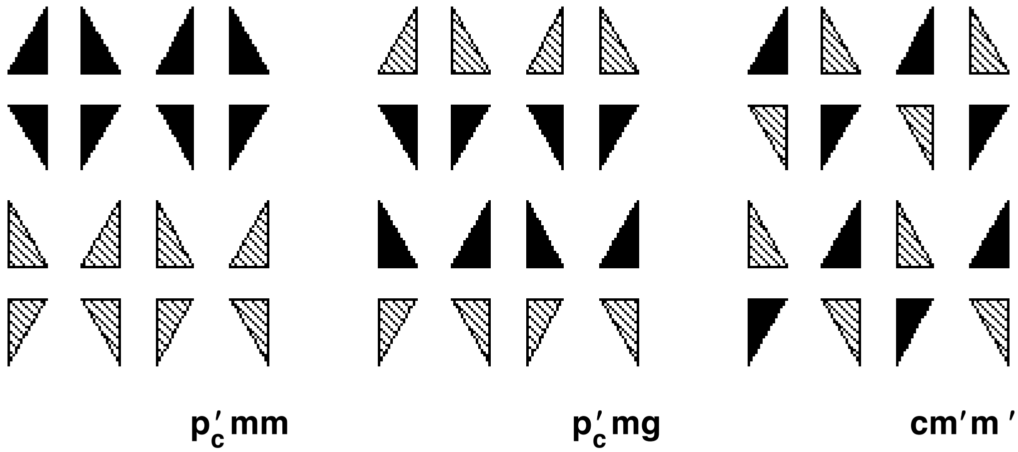

Fig. 6.89

And now a collection of examples in the spirit of 6.4.2, with or without **color inconsistencies** (and consequent **reductions** of symmetry from **cmm** to 'lower' types):

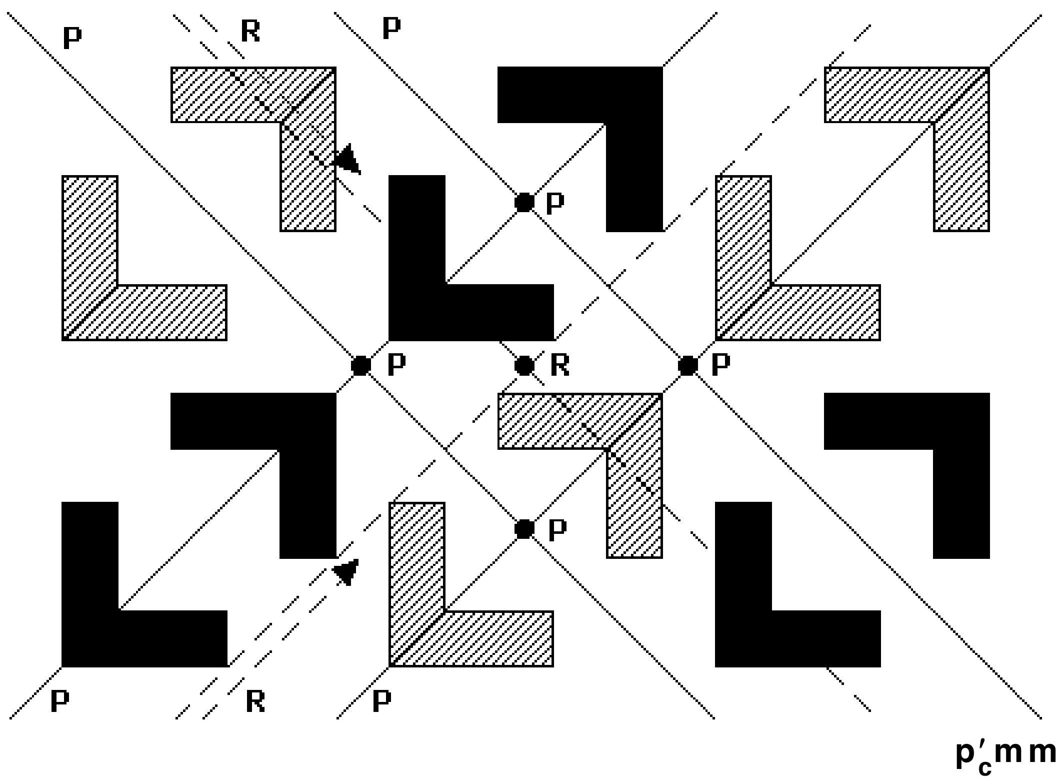

Fig. 6.90

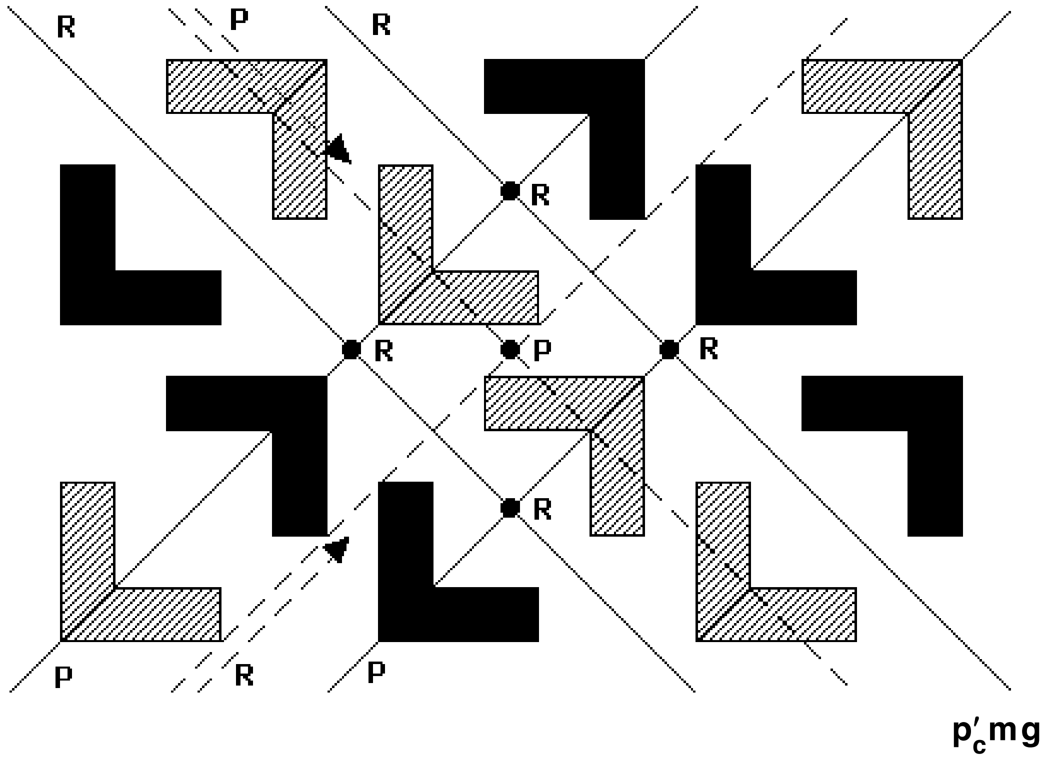

Fig. 6.91

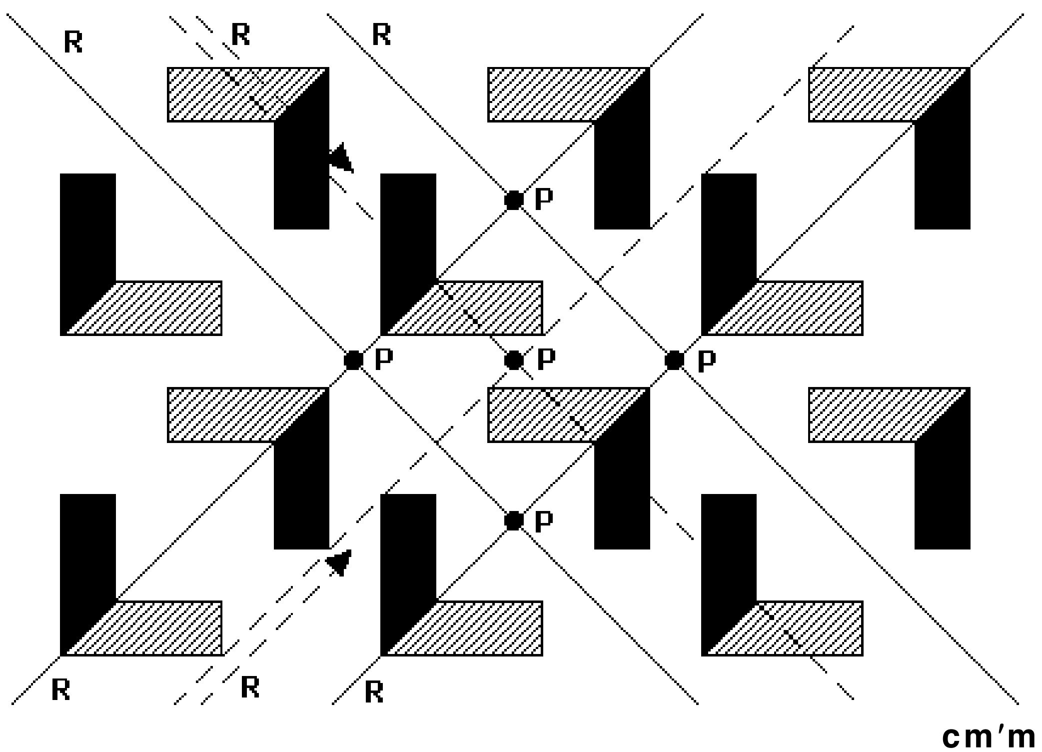

Fig. 6.92

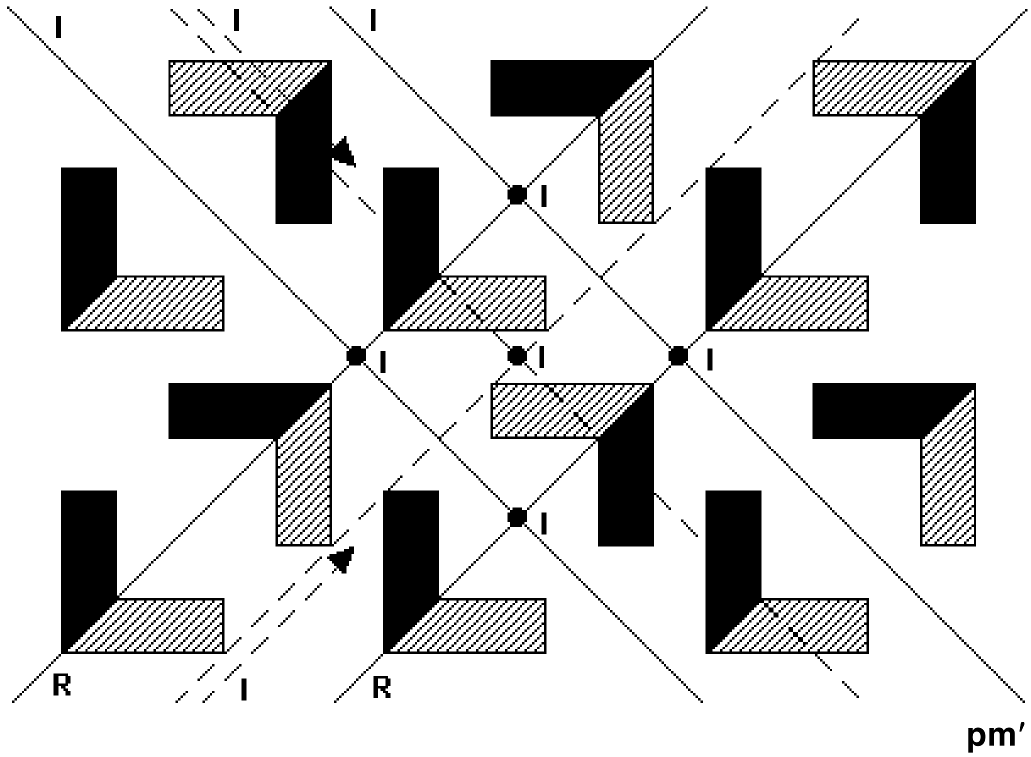

Fig. 6.93

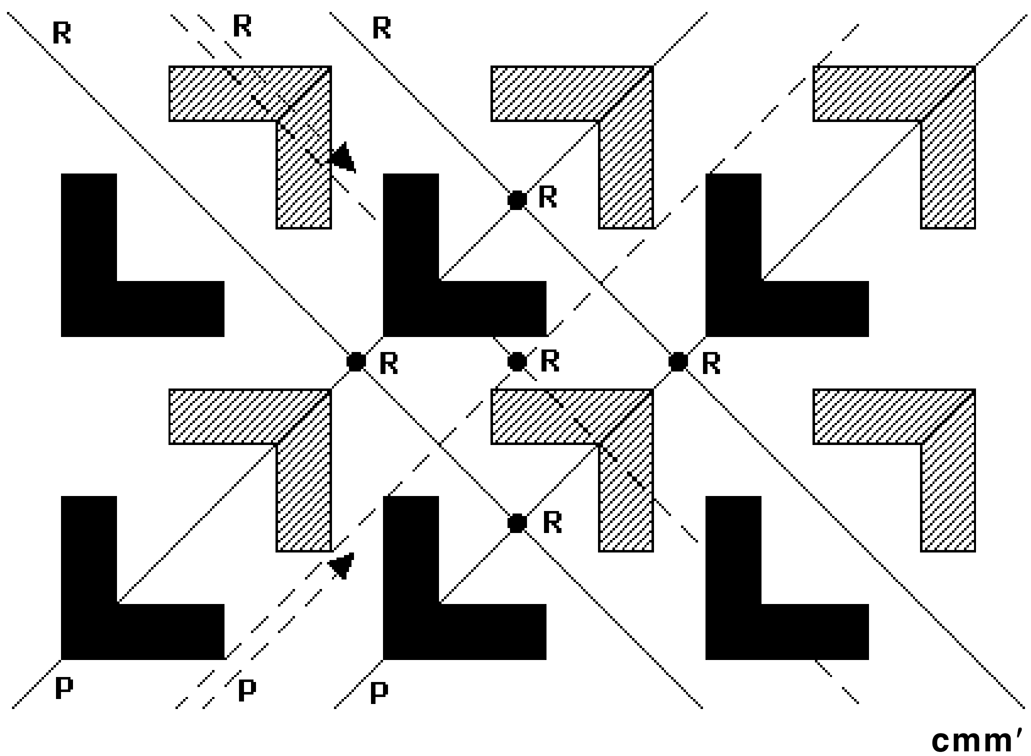

Fig. 6.94

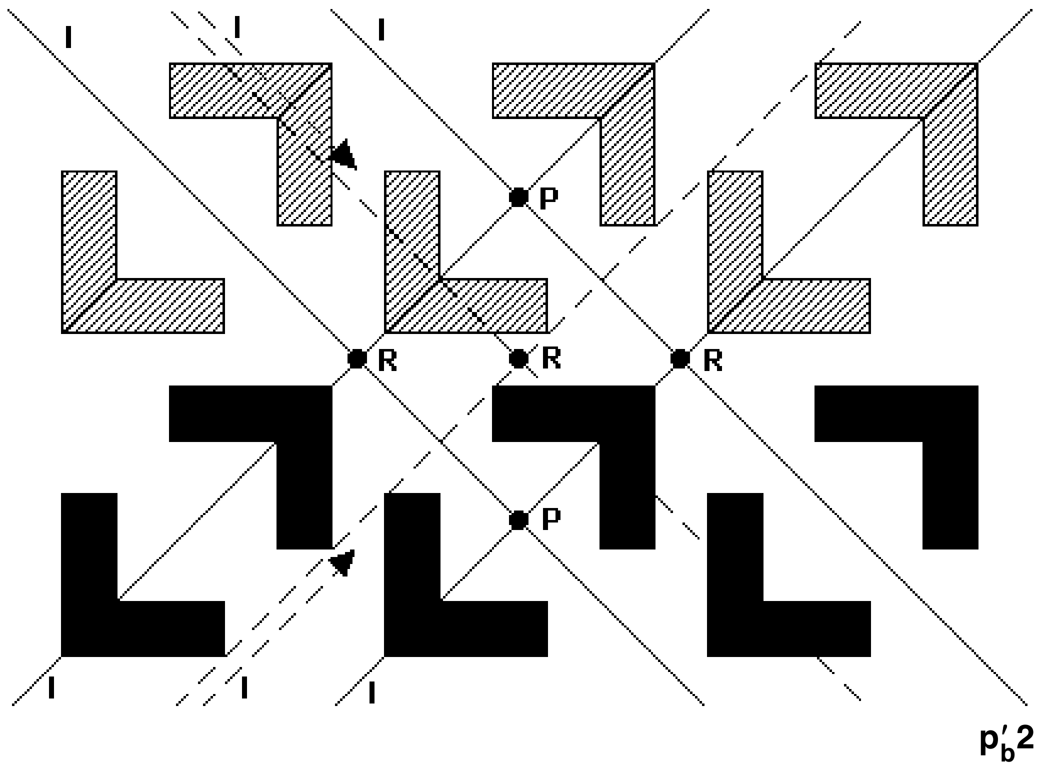

Fig. 6.95

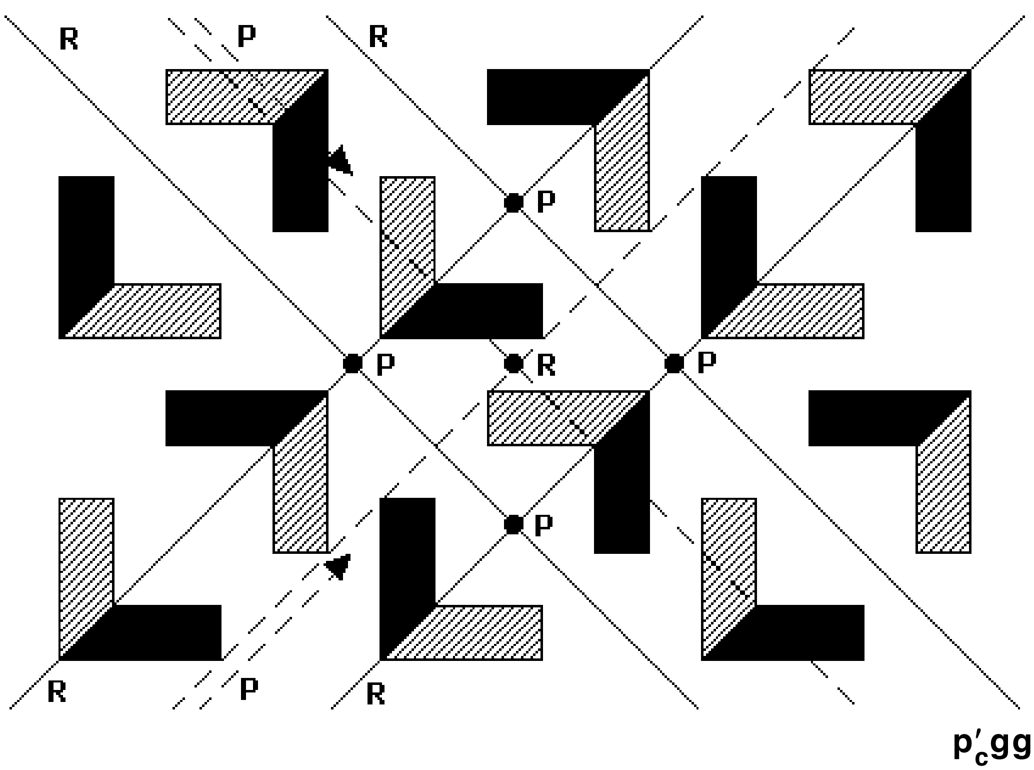

Fig. 6.96

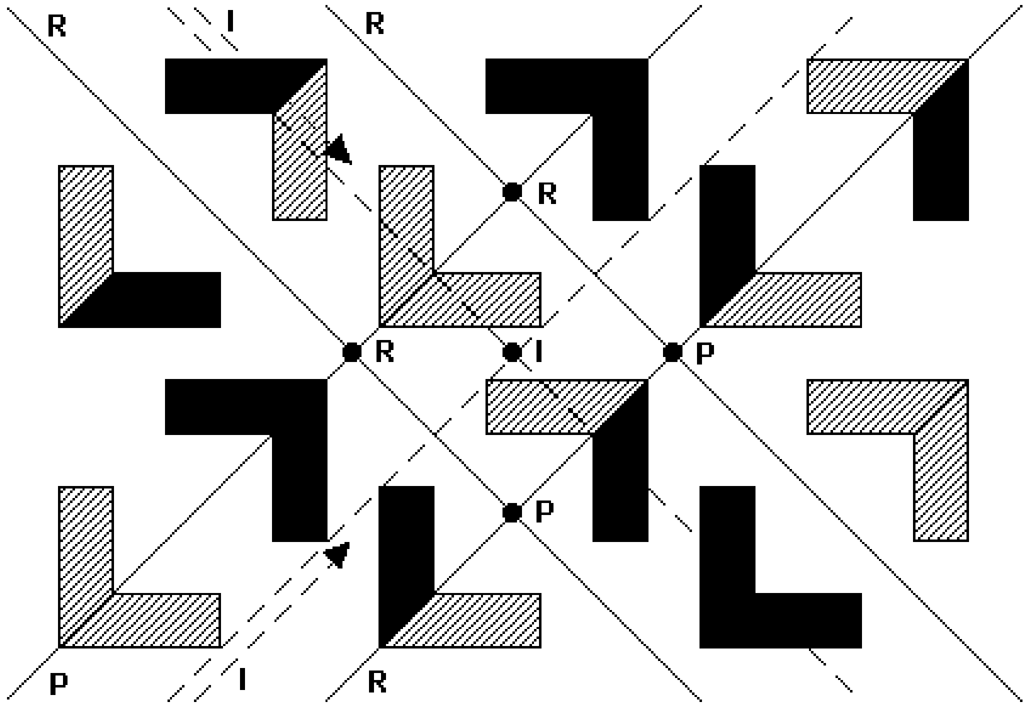

$p'_b gm$

Fig. 6.97

You should be able to derive more types out of the original **cmm** pattern of figures 6.90-6.97 using yet more imaginative colorings!

6.9.6 Symmetry plans. Notice the **location** and effect on color of rotation centers (**determined** by that of (glide) reflection axes).

cmm

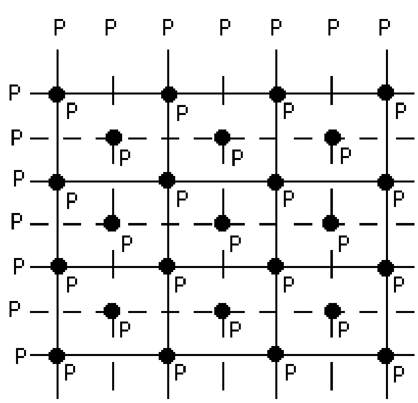

cm′m′

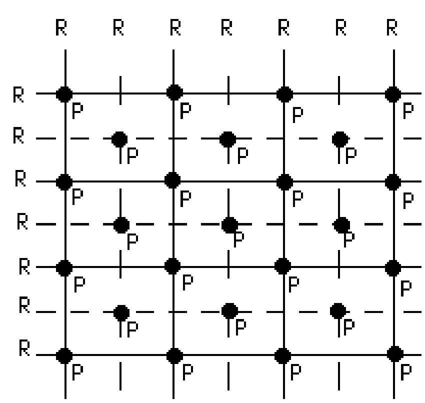

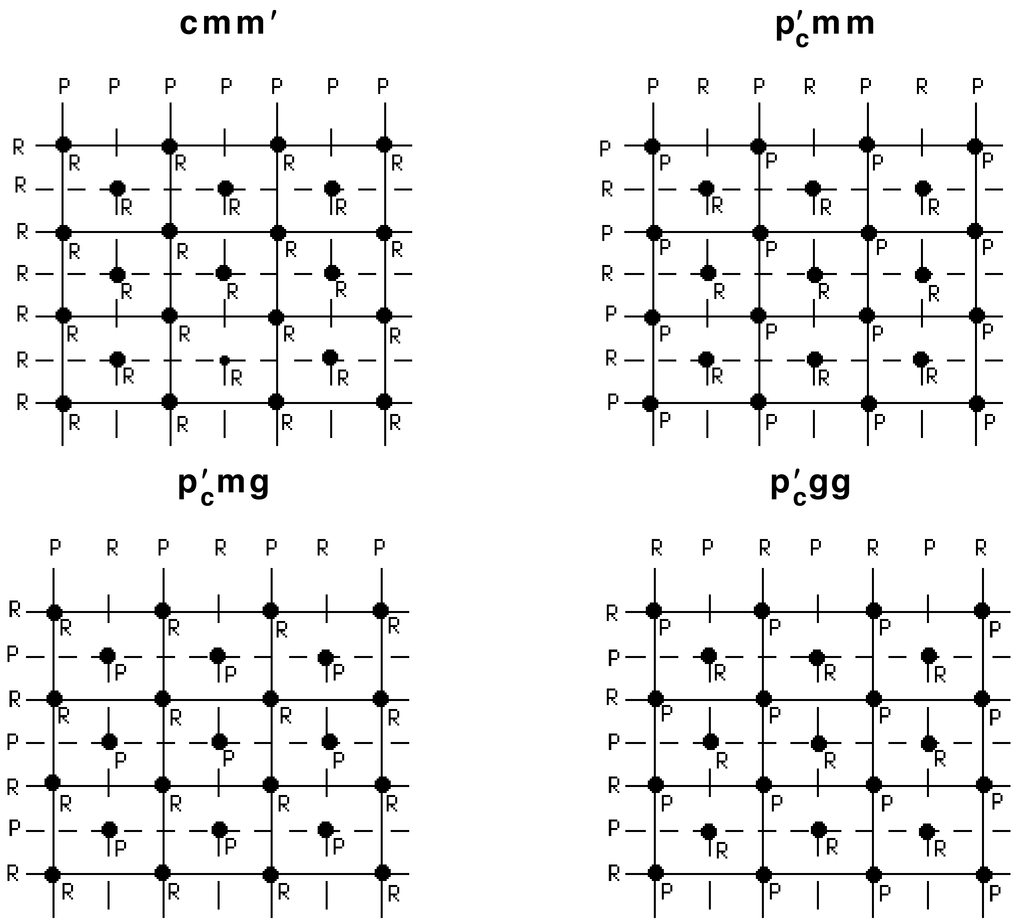

Fig. 6.98

A couple of remarks: the half turn centers found at the intersection of any two perpendicular **glide** reflection axes are ‘products’ of any one of the two glide reflections and a **reflection perpendicular** to it (as in the case of the **pmg**), **not** of the two glide reflections; and the length of the glide reflection vector is equal to the distance between two nearest half turn centers on a parallel to it (glide) reflection axis (as in the case of the **pmg**).

Finally, a ‘factorization’ of our **cmm** types into simpler ones:

$\mathbf{cmm} = \mathbf{cm} \times \mathbf{cm}$, $\mathbf{cm'm'} = \mathbf{cm'} \times \mathbf{cm'}$, $\mathbf{cmm'} = \mathbf{cm} \times \mathbf{cm'}$,
$\mathbf{p'_cmm} = \mathbf{p'_cm} \times \mathbf{p'_cm}$, $\mathbf{p'_cmg} = \mathbf{p'_cm} \times \mathbf{p'_cg}$, $\mathbf{p'_cgg} = \mathbf{p'_cg} \times \mathbf{p'_cg}$

You may also ‘factor’ the **cmm**s using either **pmm**s and **pgg**s or, in resonance with the remarks made above, **pmg**s in **both** directions!

6.10 p4 types ($p4$, $p4'$, p'_c4)

6.10.1 A look at fourfold rotations. We begin with a picture:

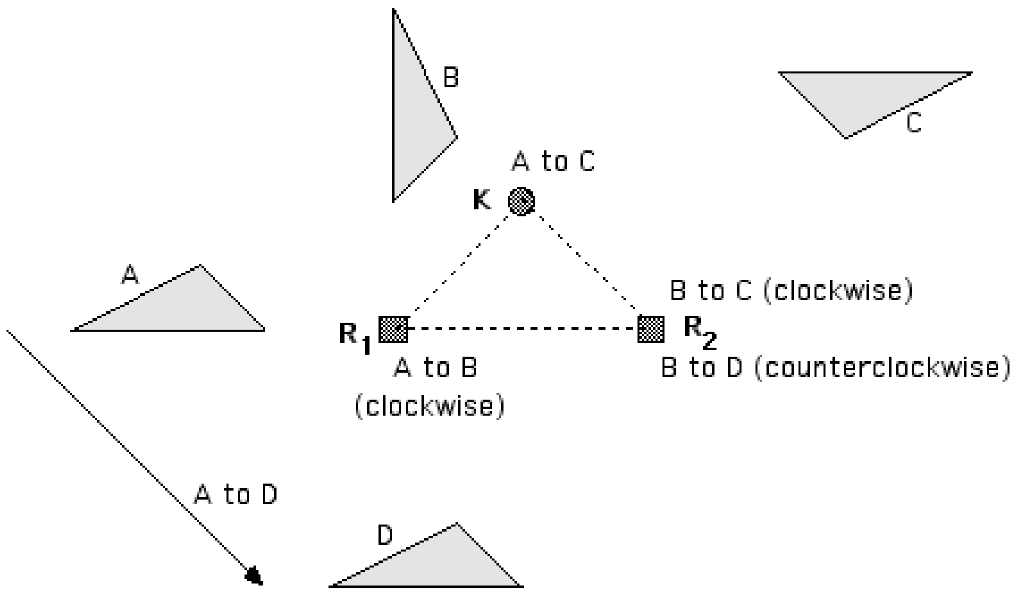

Fig. 6.99

That is, a **clockwise** $\mathbf{90^0}$ rotation centered at $\mathbf{R_1}$ (mapping A to B) followed by a **clockwise** $\mathbf{90^0}$ rotation centered at $\mathbf{R_2}$ (mapping B to C) result into a $\mathbf{180^0}$ **rotation** centered at **K** (mapping A to C); and a **clockwise** $\mathbf{90^0}$ rotation centered at $\mathbf{R_1}$ (mapping A to B) followed by a **counterclockwise** $\mathbf{90^0}$ rotation centered at $\mathbf{R_2}$ (mapping B to D) result into a **translation** (mapping A to D). Figure 6.99 offers of course illustrations rather than proofs (which are special cases of 7.5.1 and 7.5.2, respectively).

You can also use figure 6.99 ‘backwards’ to illustrate how the combination of a translation (mapping D to A) and a 90^0 rotation (mapping A to B) is another 90^0 rotation (mapping D to B).

6.10.2 The lattice of rotation centers revisited. Figure 6.99

throws quite a bit of light into the lattice of rotation centers featured in figure 4.5. Indeed it is not a coincidence that we always get **two** fourfold centers and **one** twofold center in an **isosceles right triangle** (90^0-45^0-45^0) configuration: you can see this rather special triangle being formed by the composition of the two fourfold rotations in figure 6.99; and it is true that **every** wallpaper pattern with 90^0 rotation is **bound** to have 180^0 rotation as well, with **all** the twofold centers ‘produced’ by fourfold centers as in figure 6.99.

6.10.3 Precisely three types. With all 180^0 rotations fully determined by 90^0 rotations, and an interplay between fourfold rotations and translations (figure 6.99) fully reminiscent of the one between the **pg**’s glide reflections and translations (figure 6.13) or the one between the **p2**’s half turns and translations (figure 6.44), it is easy to follow the approach in sections 6.2 (**pg**) or 6.5 (**p2**) and conclude without much effort that there exist **at most** three **p4** types: **p4** (**all** 90^0 rotations **preserve** colors), **p4′** (**all** 90^0 rotations **reverse** colors), and $\mathbf{p'_c4}$ (90^0 rotations of **both** kinds). As usual, we need to show that such types do indeed exist:

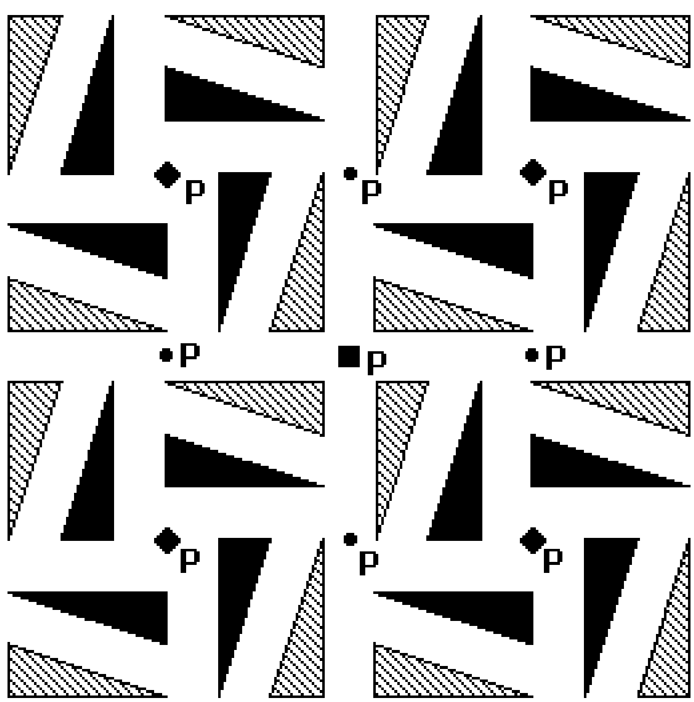

p4

Fig. 6.100

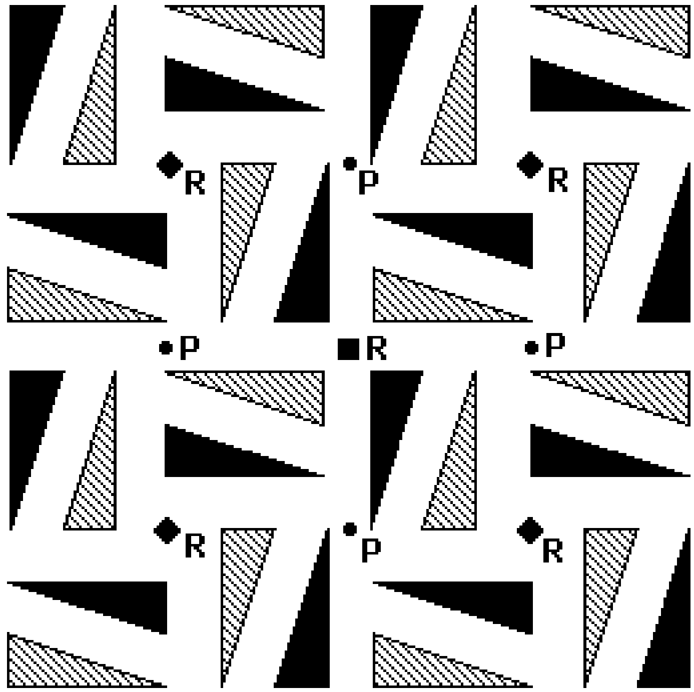

p4′

Fig. 6.101

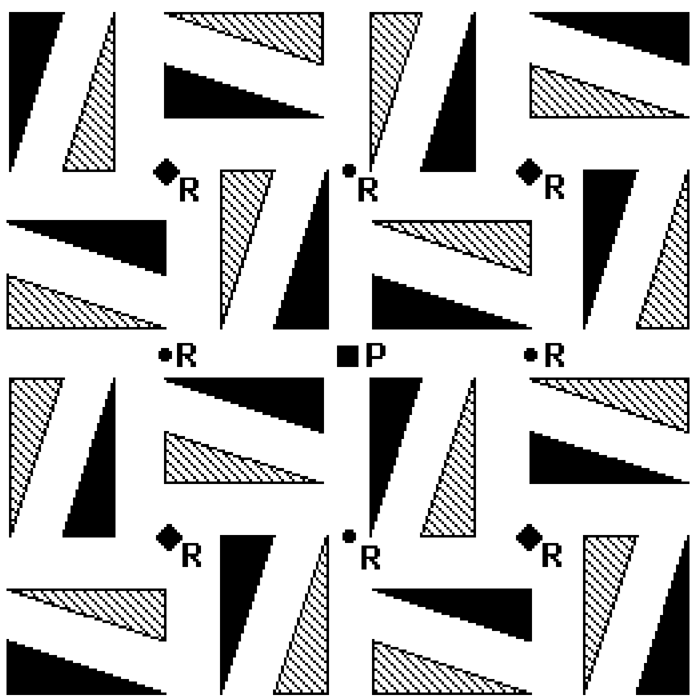

p'_c4

Fig. 6.102

We leave it to you to investigate the complex relationship between the **p4**-like patterns in figures 6.100-6.102 above and the **p2**-like patterns in figures 6.5, 6.39, and 6.40!

6.10.4 <u>Examples.</u> First a couple of 'triangles' and 'windmills':

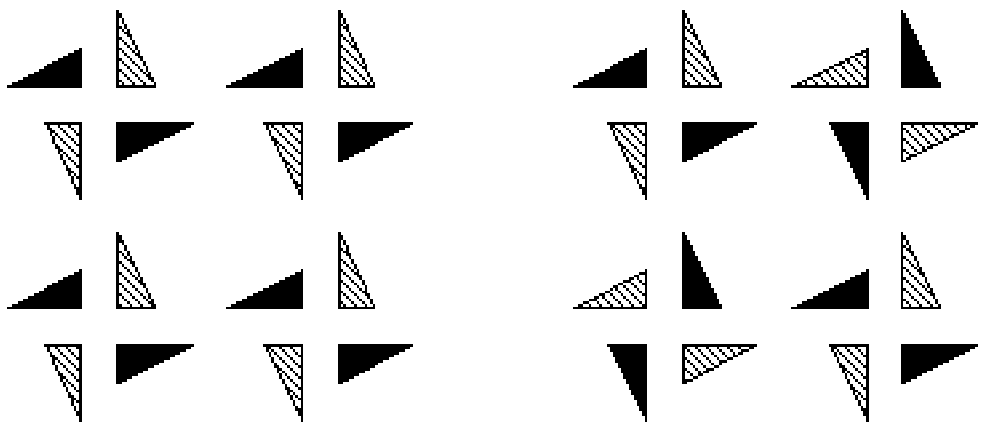

p4′ **p'_c4**

Fig. 6.103

Next, a rather complicated **p'_c4**, offspring of a **p4g** of which **all** reflections and glide reflections have been destroyed by coloring:

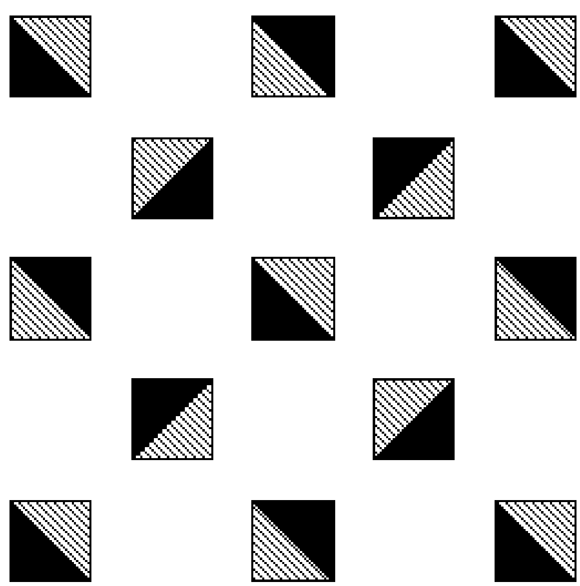

p'_c4

Fig. 6.104

6.10.5 <u>Symmetry plans.</u> We use 'straight' and 'slanted' squares for the **two kinds** of fourfold centers (4.0.4), and dots for the twofold centers (included for reference only, as 90^0 patterns can be classified based **solely** on the effect on color of their fourfold rotations).

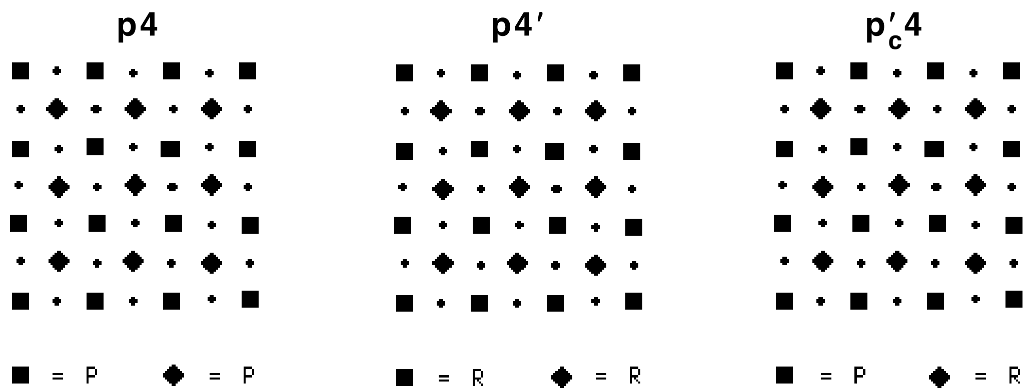

Fig. 6.105

Recall (4.0.3) that every fourfold center is **also** a twofold center by way of **double** application of the 90^0 rotation; this means that the resulting 180^0 rotation is color-preserving: **P** × **P** = **R** × **R** = **P**. Observe that, by the same 'multiplication' rules, **all** 'genuine' twofold centers must be color-preserving in **p4** and **p4′**, but color-reversing (**P** × **R** = **R**) in $\mathbf{p'_c4}$: this follows from our remarks in 6.10.1 and 6.10.2.

6.11 p4g types (p4g, p4′g′m, p4′gm′, p4g′m′)

6.11.1 <u>Studying the symmetry plan.</u> Of course a **p4g** may be viewed as a 'merge' of a **cmm** ('vertical'-'horizontal' direction) and a **pgg** ('diagonal' direction). This leads to a rather complex interaction between the two structures, severely limiting the number of possible two-colored **p4g**-like patterns and best understood by having a close look at the **p4g**'s symmetry plan:

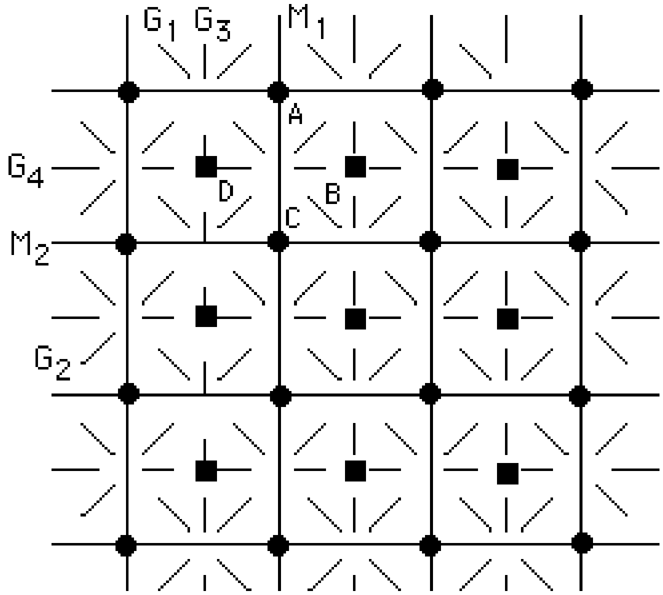

Fig. 6.106

Depending on their vector's direction, the diagonal glide reflections **G_1** and **G_2** produce **four** distinct **twofold** rotations, centered at A, B, C, D. (This relies on figure 6.54 and, primarily, on common sense: **where else** could the four centers be?) Of course B and D are centers for fourfold rotations, but, as pointed out in 6.10.5, such centers are also centers for **color-preserving** twofold rotations. A first consequence of this is that the **pgg**-like component of a **p4g** type can only be a **pgg** or a **pg′g′**: **G_1** and **G_2** must have the same effect on color, otherwise we get **color-reversing** twofold centers at B and D! Another consequence is that the **cmm**-like component of a **p4g** type can only (and **possibly**) be a **cmm** or a **cm′m′** or a **p'_cmg**: by figure 6.54 again, **M_1** and **G_4** combined produce a **color-preserving** twofold center at D, and so do **M_2** and **G_3**; this means that horizontal/vertical glide reflections (**G_4/G_3**) must have the **same** effect on color as vertical/horizontal reflections (**M_1/M_2**).

A further analysis of the symmetry plan rules out the **p'_cmg** as a possible **cmm** 'factor'. Indeed the **Conjugacy Principle** (and also a precursory remark in 4.11.2) tells us that the **fourfold** centers at B and D (**reflected** to each other by **M_1**) must have the same effect on color, hence the **twofold** center at C, produced by a combination of two fourfold rotations (figure 6.99), must be **color-preserving**. But then the two reflection axes **M_1** and **M_2**, which **also** produce the twofold rotation at C, must **both** be either color-preserving (**cmm**) or color-reversing (**cm′m′**). (One may also appeal directly to the **Conjugacy Principle**: $\mathbf{M_1}$ and $\mathbf{M_2}$ must have the same effect on color because they are rotated to each other by a 90^0 rotation at D!)

6.11.2 Precisely four types. We are already familiar with the **p4g** = **cmm** × **pgg** (but see 6.11.3 for a 'two-colored' version), and we had in fact produced a **p4′g′m** = **cmm** × **pg′g′** back in figure 6.10 (color-reversing 90^0 rotations, color-reversing 'diagonal' glide reflections (**pg′g′**), color-preserving 'vertical'-'horizontal' reflections and glide reflections (**cmm**)). One way to arrive at a **p4′gm′** = **cm′m′** × **pgg** is this: start with a **'p4′-unit'** like the one occupying the four central squares in figure 6.107, and then use color-reversing reflections to extend it to a full-fledged pattern:

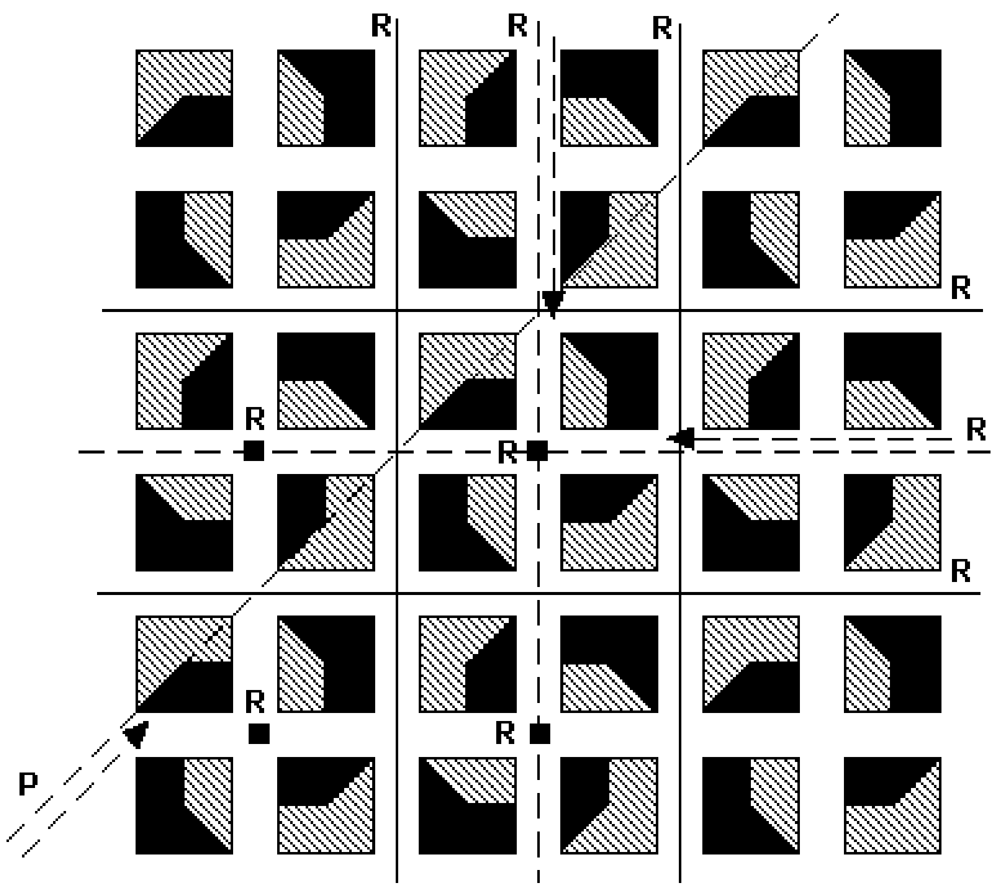

p4′gm′

Fig. 6.107

A variation on this approach, starting now with a **'p4-unit'**, yields the fourth type, **p4g′m′** = **cm′m′** × **pg′g′**:

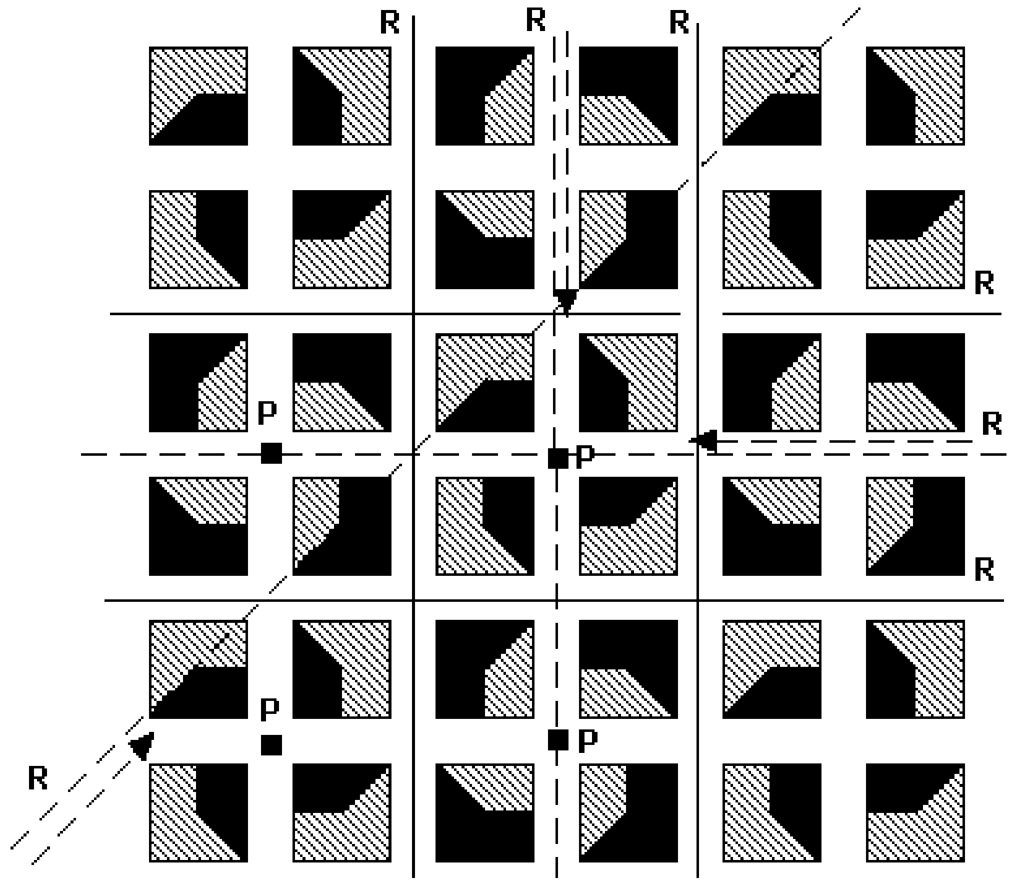

p4g′m ′

Fig. 6.108

Of course this approach would lead to the other two types if we used **color-preserving** mirrors around our starting unit. Notice also that, while there **seem** to be two kinds of fourfold centers in figures 6.107 & 6.108, their effect on color is the same in each case: for the reflection that maps them to each other makes them to have the same effect on color (**Conjugacy Principle**), even though it makes them look different (**heterostrophic**) at the same time.

6.11.3 Examples. Another way of getting **p4g**-like two-colored patterns is to start with a '**p4**-unit' or a '**p4′**-unit' and then extend it to a full pattern using **color-preserving** (by necessity) vertical-horizontal **translations** instead of reflections:

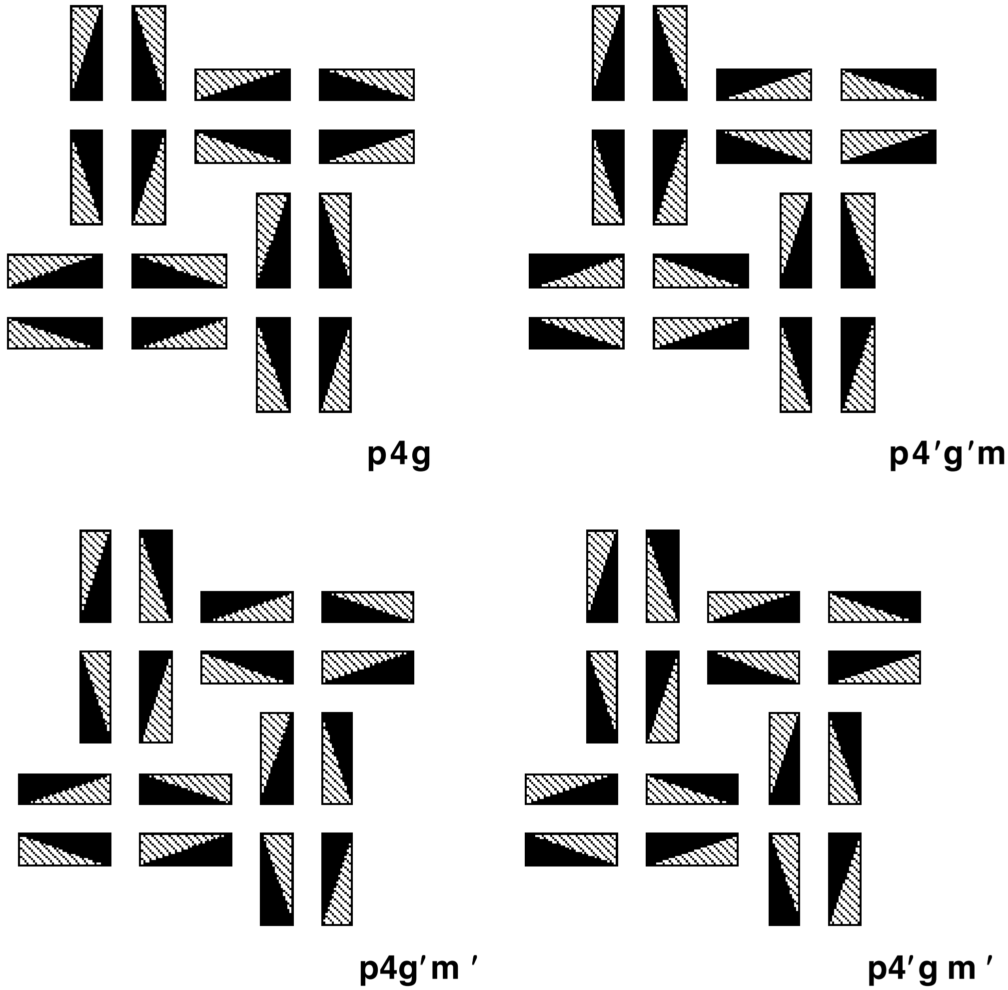

Fig. 6.109

6.11.4 Symmetry plans. Notice that a **p4g**-like pattern may be classified using **only** the underlying ‘vertical’-‘horizontal’ **cmm** (and, more specifically, its reflections) together with the effect on color of the fourfold centers (all of which are of **one kind** and therefore represented by the same type of square dot): this remark has some practical significance, as it is often **difficult** to ‘see’ a **p4g**-like pattern’s ‘diagonal’ **pgg** glide reflection. Notice by the way that the **g** or **g′** in the ‘names’ listed below stands for the diagonal (**pgg**) glide reflection, **not** for the vertical-horizontal (**cmm**) glide reflection. And do not forget that “diagonal”, “vertical”, and “horizontal” have always a lot to do ... with the way we ‘hold’ the pattern in question!

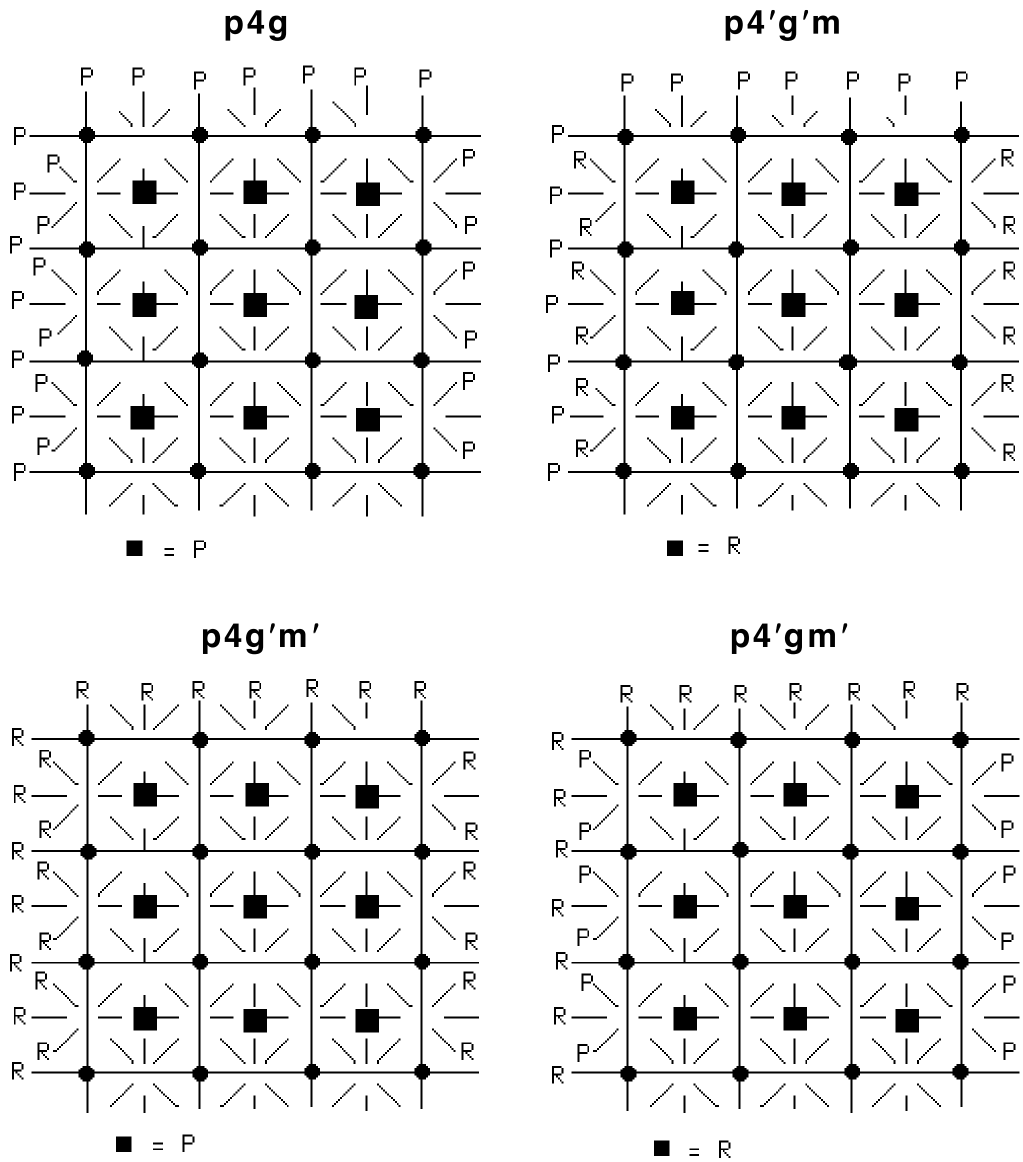

Fig. 6.110

6.12 p4m types (p4m, p4′mm′, $p_c'4mm$, $p_c'4gm$, p4′m′m, p4m′m′)

6.12.1 <u>Studying the symmetry plan.</u> Fortunately (a lot of fun) or unfortunately (a lot of work), we need to repeat the ‘break down’ process we applied to the **p4g** and its symmetry plan: that’s the only way to prove that there can only be six **p4m**-like two-colored patterns! So we start with a fresh look at the **p4m**’s symmetry plan:

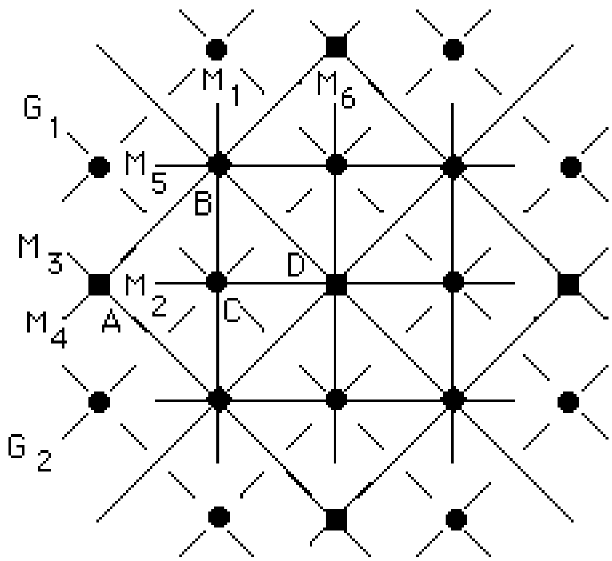

Fig. 6.111

We see that the **p4m** may be viewed as a 'product' of a 'vertical'-'horizontal' **pmm** and a 'diagonal' **cmm**. Every two adjacent horizontal or vertical axes **may** have opposite effect on color, but this is not possible for either any two **parallel** diagonal reflection axes or any two **parallel** diagonal glide reflection axes (by the very structure of **cm**(**m**)-like patterns, see 6.4.4); moreover, every two **perpendicular** diagonal axes (such as $\mathbf{G_1}$, $\mathbf{G_2}$ or $\mathbf{M_3}$, $\mathbf{M_4}$, for example) must have the same effect on color by the **Conjugacy Principle**: indeed they are **rotated** to each other by **fourfold** centers (such as A). We conclude, by revisiting 6.9.6 if needed, that the **cmm** 'factor' could only (and **possibly**) be one of **cmm**, **cm′m′**, $\mathbf{p'_c}$**mm**, or $\mathbf{p'_c}$**gg**. Moreover, every horizontal and every vertical reflection axis intersecting each other at a **fourfold** center (**twofold** center within the **pmm**), such as $\mathbf{M_1}$, $\mathbf{M_5}$ at B or $\mathbf{M_2}$, $\mathbf{M_6}$ at D, must have the same effect on color (**Conjugacy Principle** again). Therefore the **pmm** 'factor' could only (and **possibly**) be one of **pmm**, **pm′m′**, or **c′mm** (6.8.4).

Let's now have a closer look at how the two types 'merge' into the **p4m**. The 'genuine' **twofold** center C is produced by the combination of a glide reflection and a reflection perpendicular to it within the **cmm** 'factor' ($\mathbf{G_1}$, $\mathbf{M_4}$ or $\mathbf{G_2}$, $\mathbf{M_3}$), **as well as** by the combination of two perpendicular reflections within the **pmm** 'factor' ($\mathbf{M_1}$, $\mathbf{M_2}$). The implication of this **'weaving'** is that the **two perpendicular pairs** of diagonal (**cmm**) and vertical-horizontal (**pmm**) axes producing the same genuine twofold center **must** be of **same combined effect** on color: in the context of figure 6.111, ($\mathbf{M_4}$, $\mathbf{G_1}$) and ($\mathbf{M_1}$, $\mathbf{M_2}$) could **possibly** be nothing but **PP/PP**, **PP/RR**, **RR/PP**, **RR/RR** (if C preserves colors) or **PR/PR**, **RP/PR** (if C reverses colors). (Recall (6.9.1, 6.8.1) that the letter order in the latter case **is** crucial for **cmm** types (reflection, glide reflection) but **not** for **pmm** types (reflection, reflection).)

Converting our findings into 'type multiplication', we arrive at **six** possible combinations:

p4m = cmm × pmm, **p4′m′m = cmm × pm′m′**,
p4′mm′ = cm′m′ × pmm, **p4m′m′ = cm′m′ × pm′m′**,
p'_c4mm = p'_cmm × c′mm, **p'_c4gm = p'_cgg × c′mm**

6.12.2 Six types indeed. A good source of patterns verifying the five 'new' types above is chapter 5: employing the stacking process of chapter 4, we can often stack copies of a two-colored **pmm2**-like **border** pattern into a **p4m**-like two-colored wallpaper pattern:

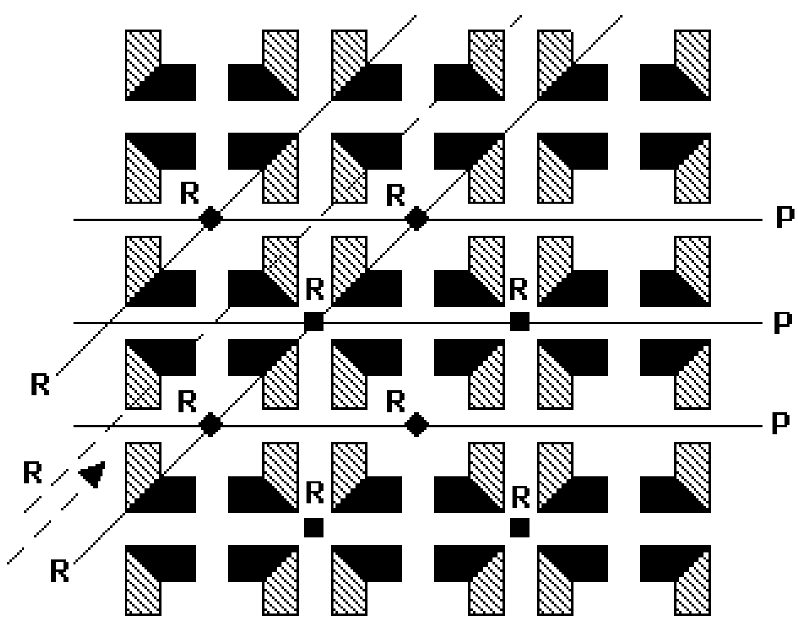

pmm2 → p4′mm′

Fig. 6.112

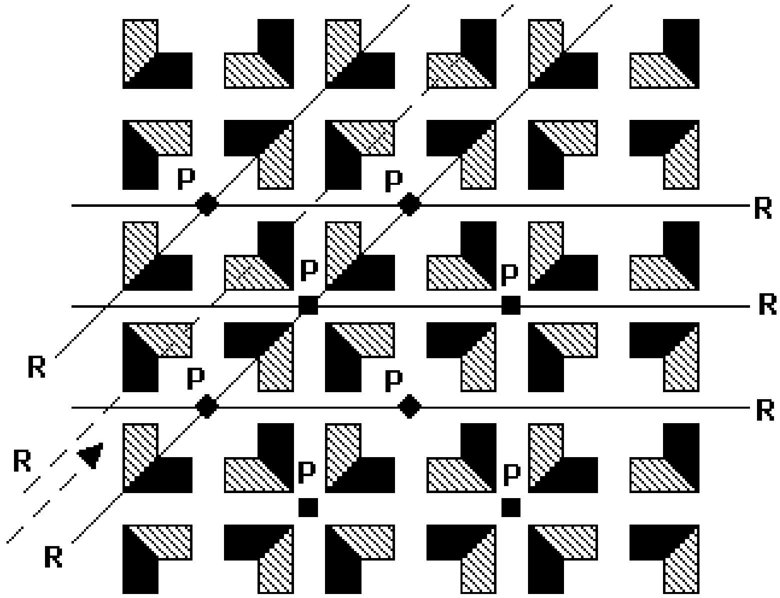

pm′m′2 → p4m′m′

Fig. 6.113

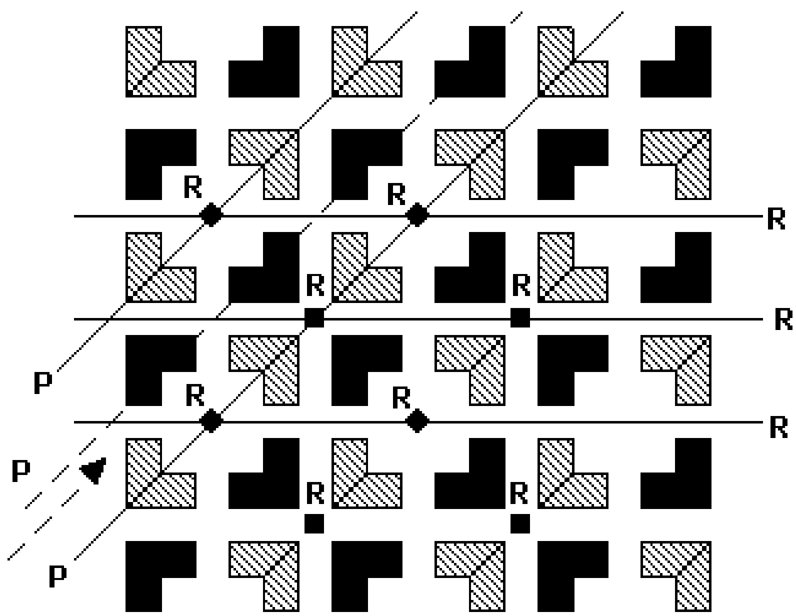

pm′m′2 → p4′m′m

Fig. 6.114

By now you can probably tell that the process is somewhat 'unpredictable': an **'one-colored'** type (**pmm2**, figure 5.31) led to a genuinely two-colored type (**p4′mm′**, figure 6.112), while distinct representatives of the same type (**pm′m′2**), one of them also from figure 5.31, led to two distinct **p4m** types (figures 6.113 & 6.114).

We move on to get the remaining two **p4m** types; the last one (figure 6.116) 'requires' a **perfectly shifted** stacking of yet another border pattern -- distinct from the one employed in figure 6.115 despite being of the same type (**p′mm2**) -- from figure 5.31:

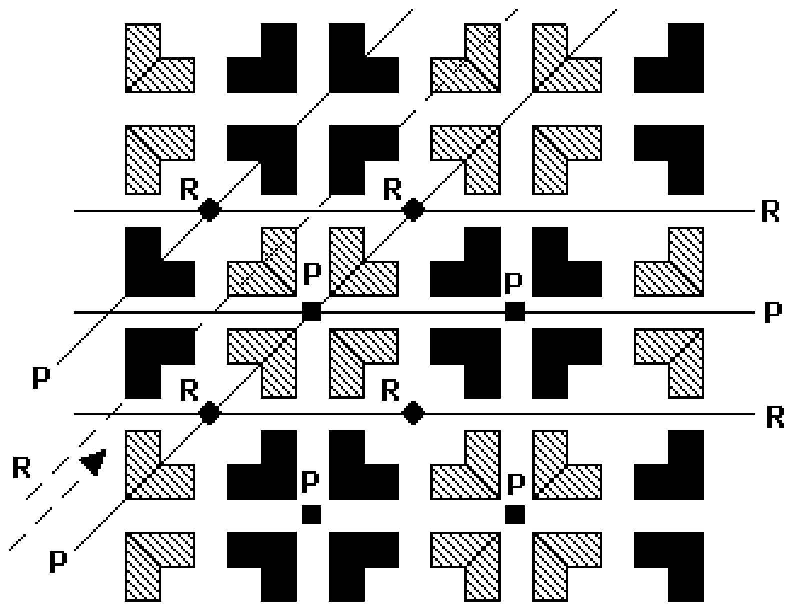

p′mm2 → p_c'4mm

Fig. 6.115

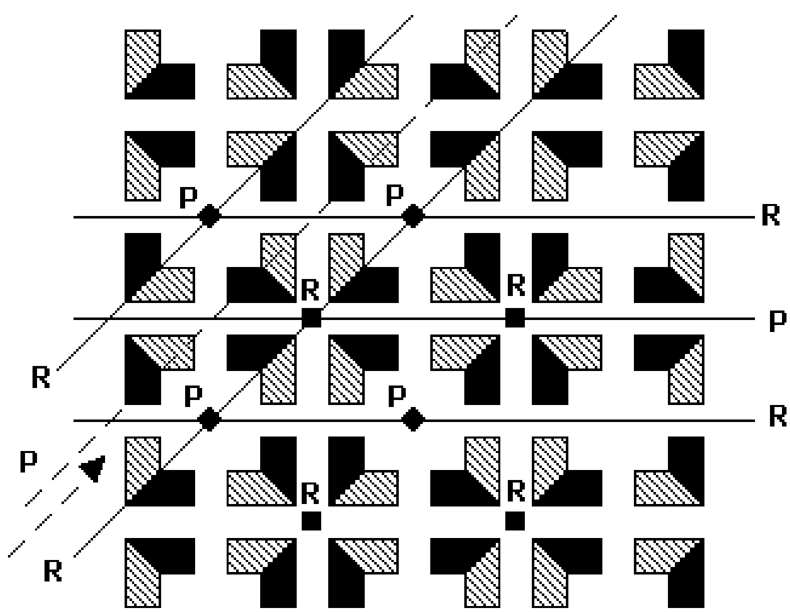

p′mm2 → p_c'4gm

Fig. 6.116

6.12.3 <u>Further examples.</u> Our ‘triangles’ have now been superficially merged into ‘squares’; notice the ‘two-colored’ **p4m**:

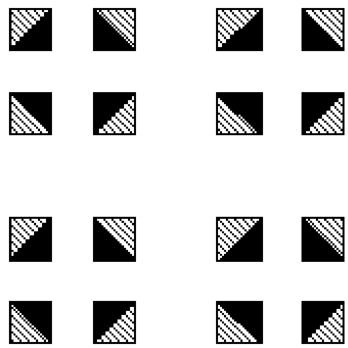

p4m

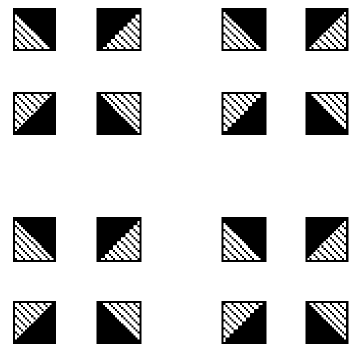

p4′mm′

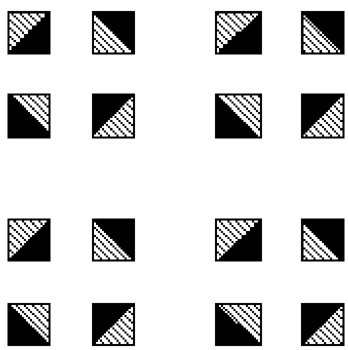

p4′m′m

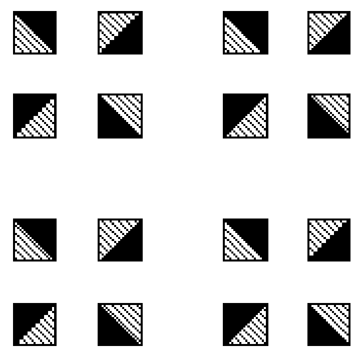

p4m′m′

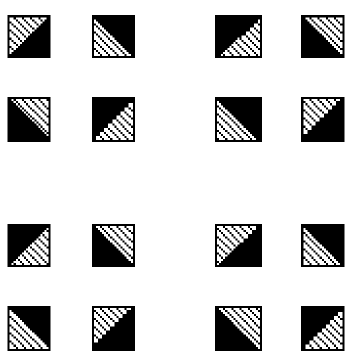

p'_c4mm

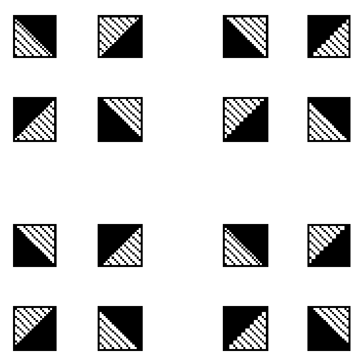

p'_c4gm

Fig. 6.117

6.12.4 <u>Hidden glide reflections revisited.</u> While color-reversing translations along reflection axes no longer matter (6.7.1), hidden glide reflections are now upgraded thanks to the second of the next two **p'_c4gm** examples provided by **Amber Sheldon** (Spring 1998):

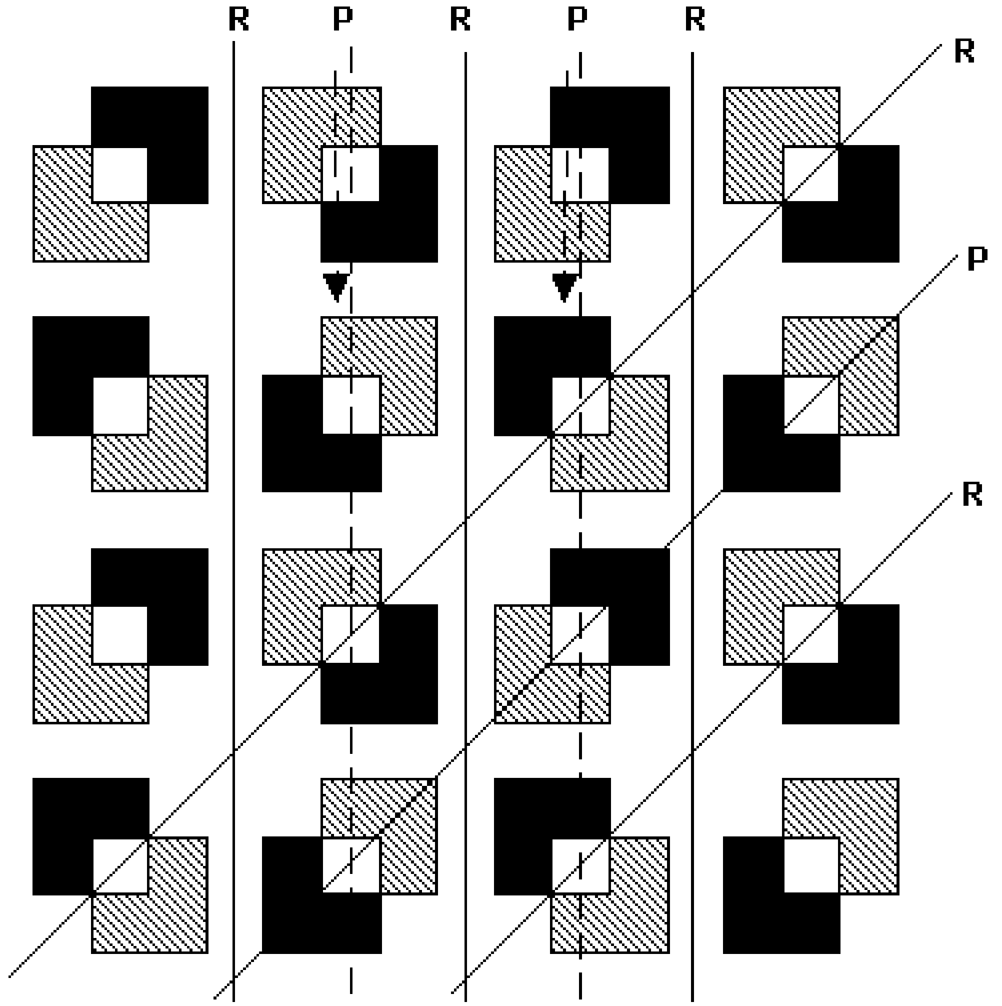

p'_c4gm

Fig. 6.118

This example is useful because it tells you once again that some patterns must be viewed **'diagonally'**: that is, the **cmm** direction (of in-between glide reflection) is vertical-horizontal rather than diagonal (as it has so far been the case with all our examples).

The next example is a clever variation on the previous one: **all** vertical-horizontal glide reflections are now **inconsistent** with color; and so is **every other** diagonal reflection, **but** the axes of **all** those diagonal reflections that are inconsistent with color **do** work for diagonal **glide reflections** (of vector shown below) that **are**

consistent with color! As a consequence of all this, we are now **back** to vertical-horizontal viewing and diagonal **cmm** subpattern (built, remarkably, on underlying structure of **pmm** type):

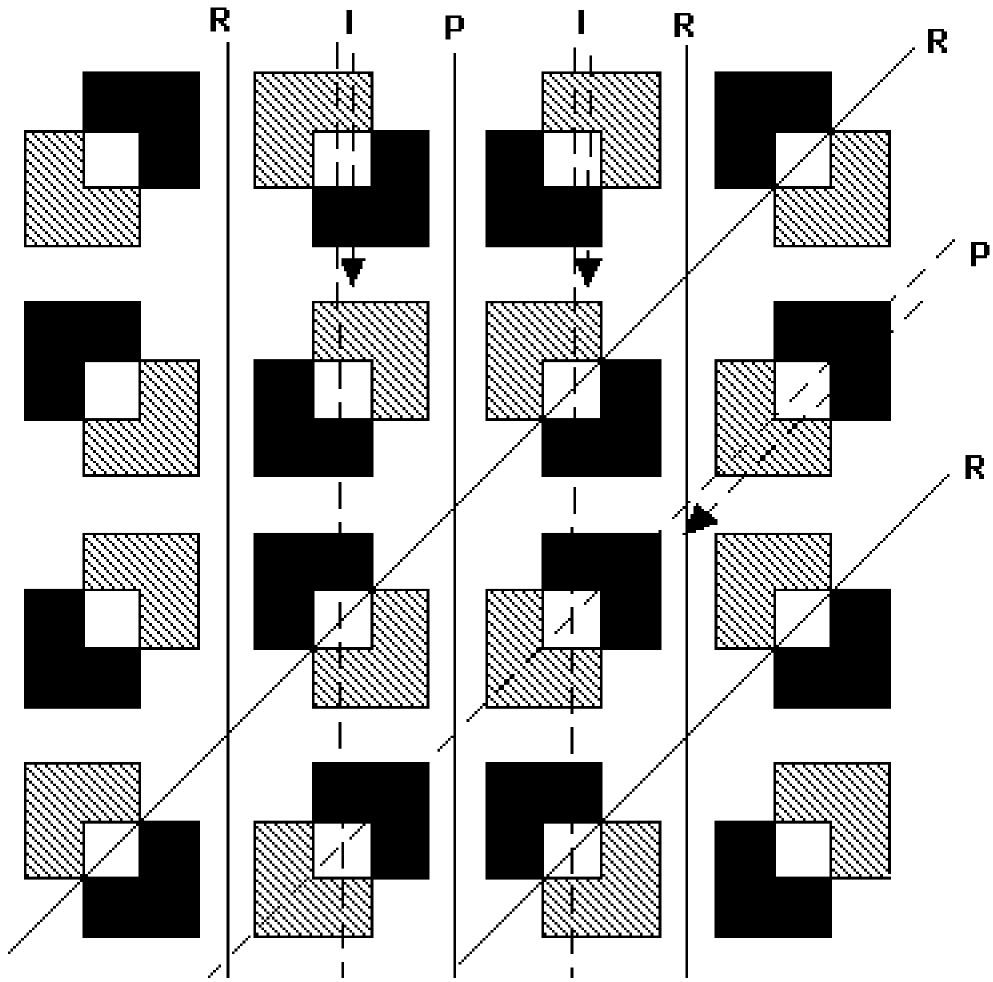

$\mathbf{p_c'4gm}$

Fig. 6.119

6.12.5 <u>Symmetry plans.</u> The two $\mathbf{p_c'4gm}$ patterns of 6.12.4 are fully indicative of the **pitfalls** associated with the classification of **p4m**-like patterns. We suggest the following way of 'reading' the symmetry plans listed below, particularly helpful in distinguishing between **p4′m′m** and **p4′mm′**: **first** decide what the **cmm** direction (of **in-between glide reflection**) is and determine what the **cmm** type is, **then** work on the **pmm** 'factor', and **finally** 'merge' the two factors following the **p4m**'s 'factorizations' at the end of 6.12.1.

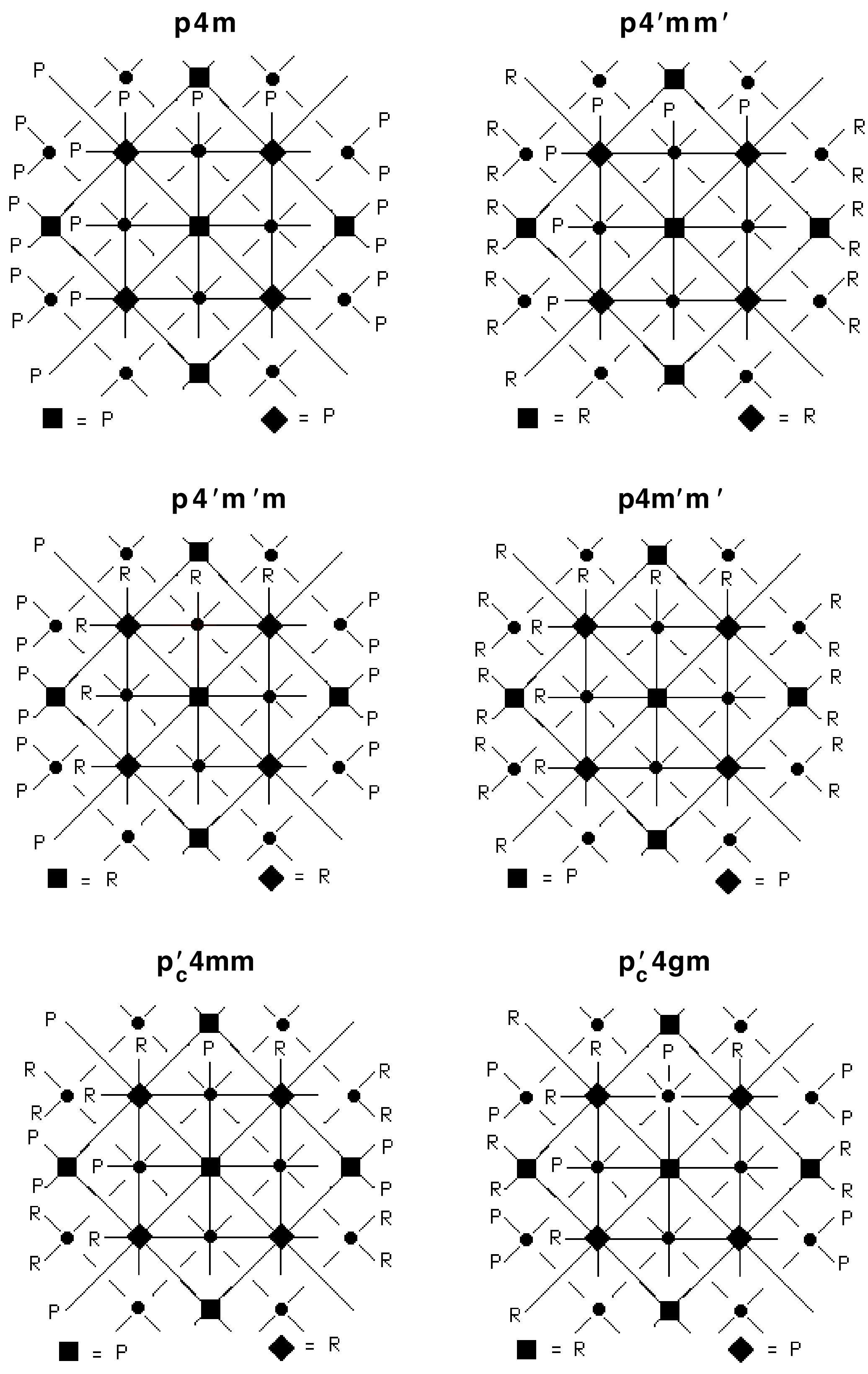

Fig. 6.120

Predictably, fourfold centers **preserve** colors precisely when they lie at the intersection of **four** reflection axes of **same** effect on color. Of course it is only in the last two types that different kinds of fourfold centers (**not** mapped to each other by any of the pattern's isometries) have **opposite** effect on color. (Again we have not marked the effect on color of the twofold centers, which are not essential for classification purposes; and that effect is in any case easily determined (within the **pmm** 'factor'), as twofold centers lie at the intersection of **two** reflection axes **only**.)

6.13 p3 types (p3)

6.13.1 No threefold color-reversing rotations. The assumption that there exists a 120^0 color-reversing rotation leads to an immediate **contradiction**: starting with a black point A, its image must be grey, then the image of the image must be black, and finally the third image, which is no other than the departing point A, must be grey! More generally, the same argument shows that no 'oddfold' rotation (in a **finite** pattern) can be color-reversing.

6.13.2 Farewell to color-reversing translations. As we show in section 7.6, and have indicated in 6.10.1 for the special case of 90^0, the combination of a rotation and a translation leads to a rotation of **same angle** but different center. It follows from 6.13.1 and the $\mathbf{P} \times \mathbf{R} = \mathbf{R}$ rule that **no** wallpaper pattern with 120^0 rotation (such as the **p3** or actually **every** type we are going to study from here on) can have **color-reversing** translation.

6.13.3 Only one type. In the absence of (glide) reflection, 6.13.1 and 6.13.2 imply that the **only** possible type in the **p3** group is the **p3** itself. Below we offer an example of a 'two-colored' **p3** pattern. Notice the **three** different kinds of 120^0 rotation centers (denoted by dots of different sizes): no two centers of different kind are mapped to each other by either a rotation or a translation. Notice also the **rhombuses** formed by rotation centers of the same kind: their importance will be made clear in later sections and chapters!

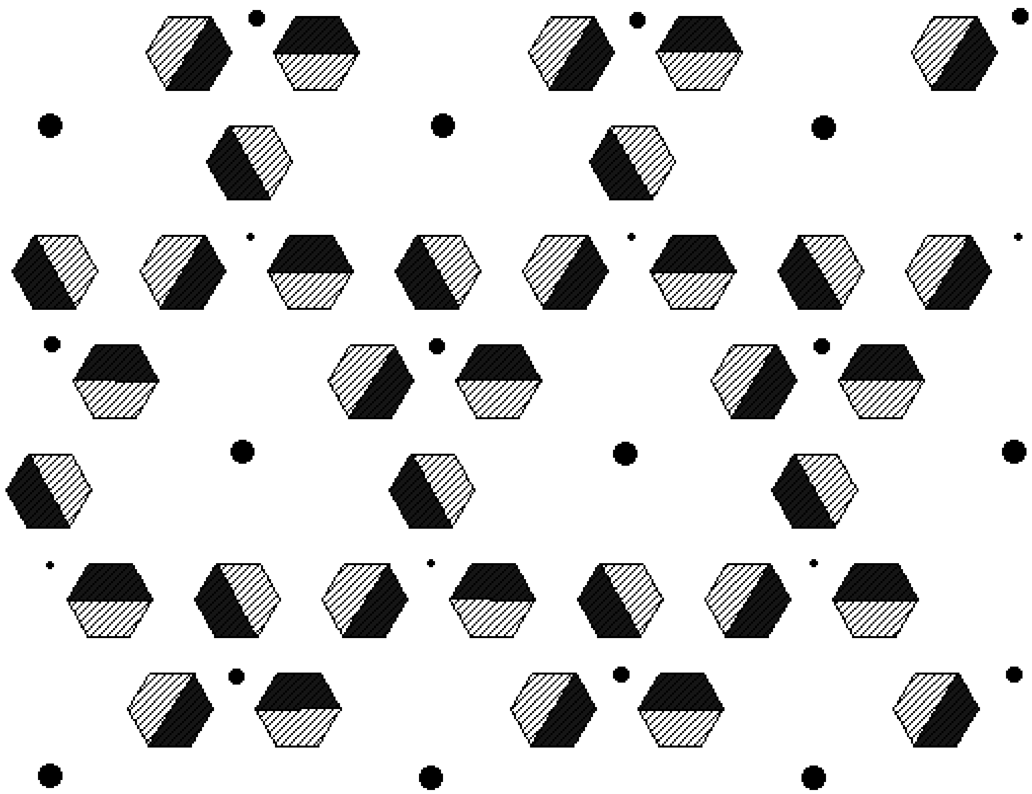

p3

Fig. 6.121

The pattern in figure 6.121 may not be the simplest two-colored **p3** in the world, but it should be compared to the **p31m** pattern in figure 6.122 below in order to illustrate a basic symmetry principle: **less** symmetry is often **harder** to achieve than **more** symmetry!

6.14 p31m types (p31m, p31m′)

6.14.1 <u>‘Products’ of three **cm**s.</u> The **p31m** has reflection and in-between glide reflection in three directions, hence it may be viewed as the ‘product’ of three **cm**s. Therefore all reflections within each one of the three directions must have the same effect on color and likewise all glide reflections within each of the three directions must have the same effect on color (6.4.4). **Moreover**, every two axes (be them glide reflection axes **or** reflection axes) of **non-parallel** direction must have the same effect on color: indeed any two such axes (intersecting each other at **60^0**) produce a **120^0 rotation** (see sections 7.2, 7.9, and 7.10); but this rotation **must** leave the pattern invariant, therefore it **must** be color-preserving (6.13.1), so that the two axes must have the **same** effect on color.

What all this means is that, in every **p31m**-like wallpaper pattern, **all axes** -- be them reflection or glide reflection axes -- must have the same effect on color. That is, either all axes **preserve** colors (**cm** × **cm** × **cm** = **p31m**) or all axes **reverse** colors (**cm′** × **cm′** × **cm′** = **p31m′**): no other possibilities!

6.14.2 Examples. First a ‘two-colored’ **p31m**:

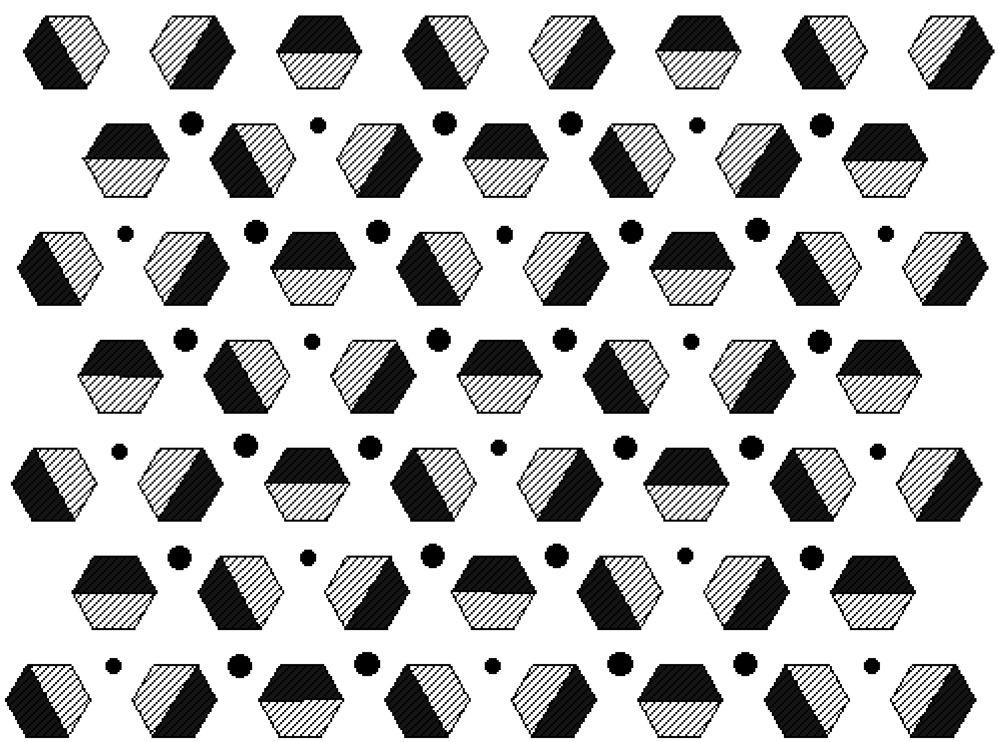

p31m

Fig. 6.122

We have marked the **two** different kinds of rotation centers by dots of different sizes. If you are at a loss trying to determine the **color-preserving** reflection axes, simply connect the **smaller** dots! As for glide reflection axes (**not** crucial for classification purposes), those pass not only half way between every two adjacent rows of **on-axis** centers (smaller dots), but also half way between every two adjacent rows of **off-axis** centers (larger dots).

Next comes an example of a **p31m′**:

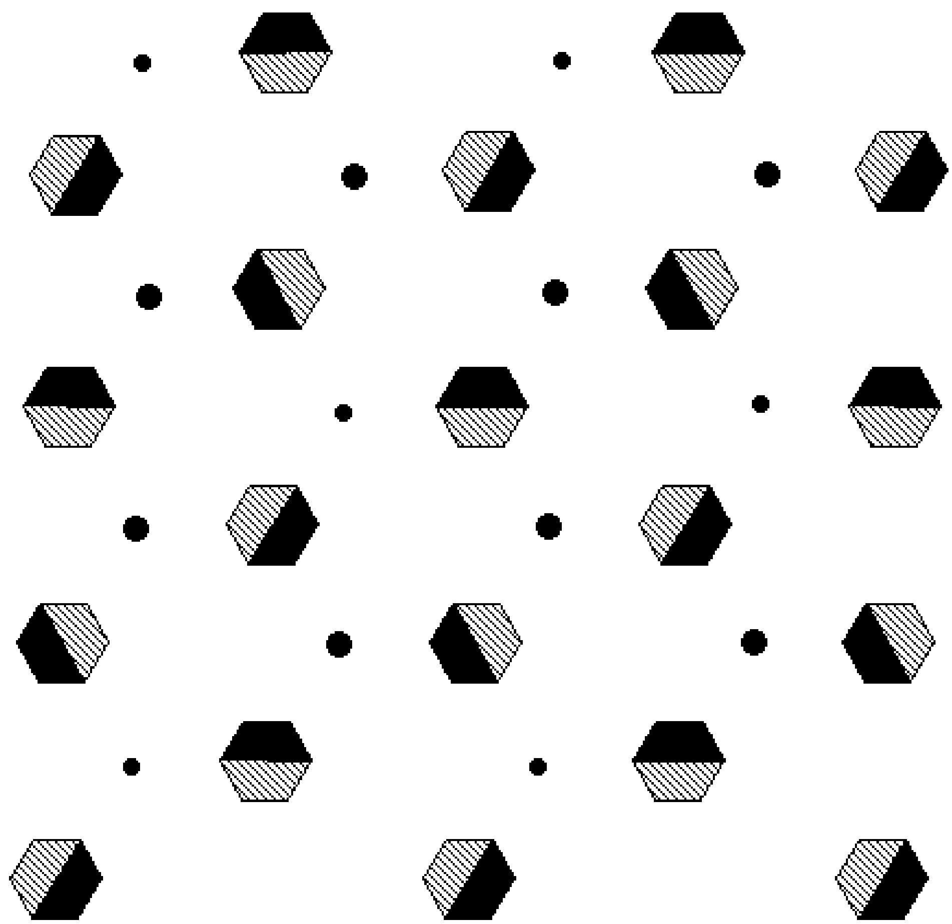

p31m′

Fig. 6.123

As in the case of figure 6.122, **color-reversing** reflection axes lie on lines formed by the smaller dots. And once again each on-axis center (smaller dot) is ‘surrounded’ by **six** off-axis centers (larger dots) symmetrically placed on the vertices of an invisible **hexagon**.

Finally, an example of a **p31m′**, ‘offspring’ of figure 4.69:

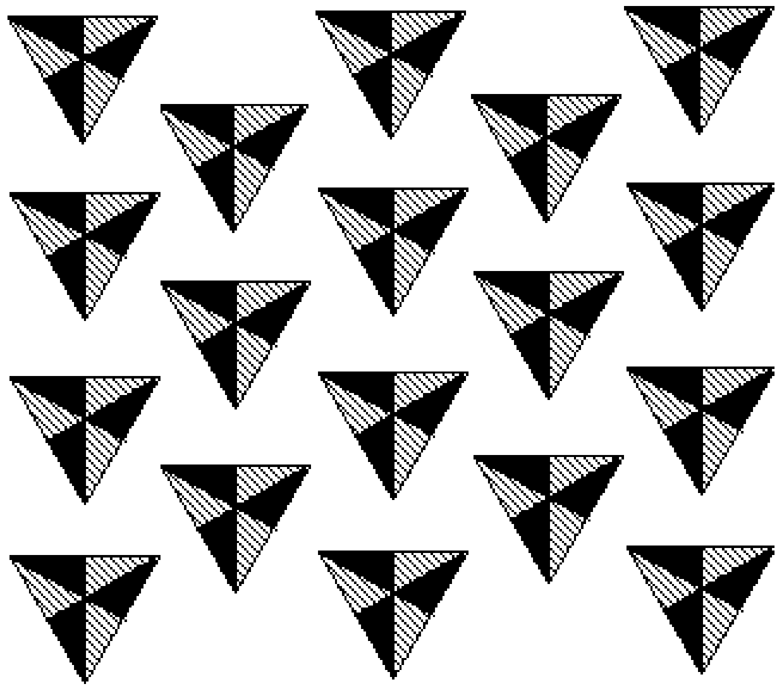

p31m′

Fig. 6.124

6.15 p3m1 types (p3m1, p3m′)

6.15.1 Three **cm**s again. As we indicated in 4.17.4, and will analyse further in chapters 7 and 8, the difference between the **p31m** and **p3m1** types is rather **subtle**, having in fact more to do with the glide reflection vector's length and the distances between glide reflection axes and rotation centers than with 'symmetry plan' structure (and the off-axis centers of the **p31m** specifically). It is clear in particular that **both** the **p3m1** and the **p31m** are 'products' of three **cm** patterns, and the entire **p31m** analysis of 6.14.1 is also applicable to the **p3m1** word by word. We conclude again that, depending on the (glide) reflections' **uniform** effect on color, there can only be two **p3m1**-like patterns, **p3m1** = **cm** × **cm** × **cm** (all (glide) reflections **preserve** colors) and **p3m′** = **cm′** × **cm′** × **cm′** (all (glide) reflections **reverse** colors).

6.15.2 Examples. We begin with a 'two-colored' **p3m1**:

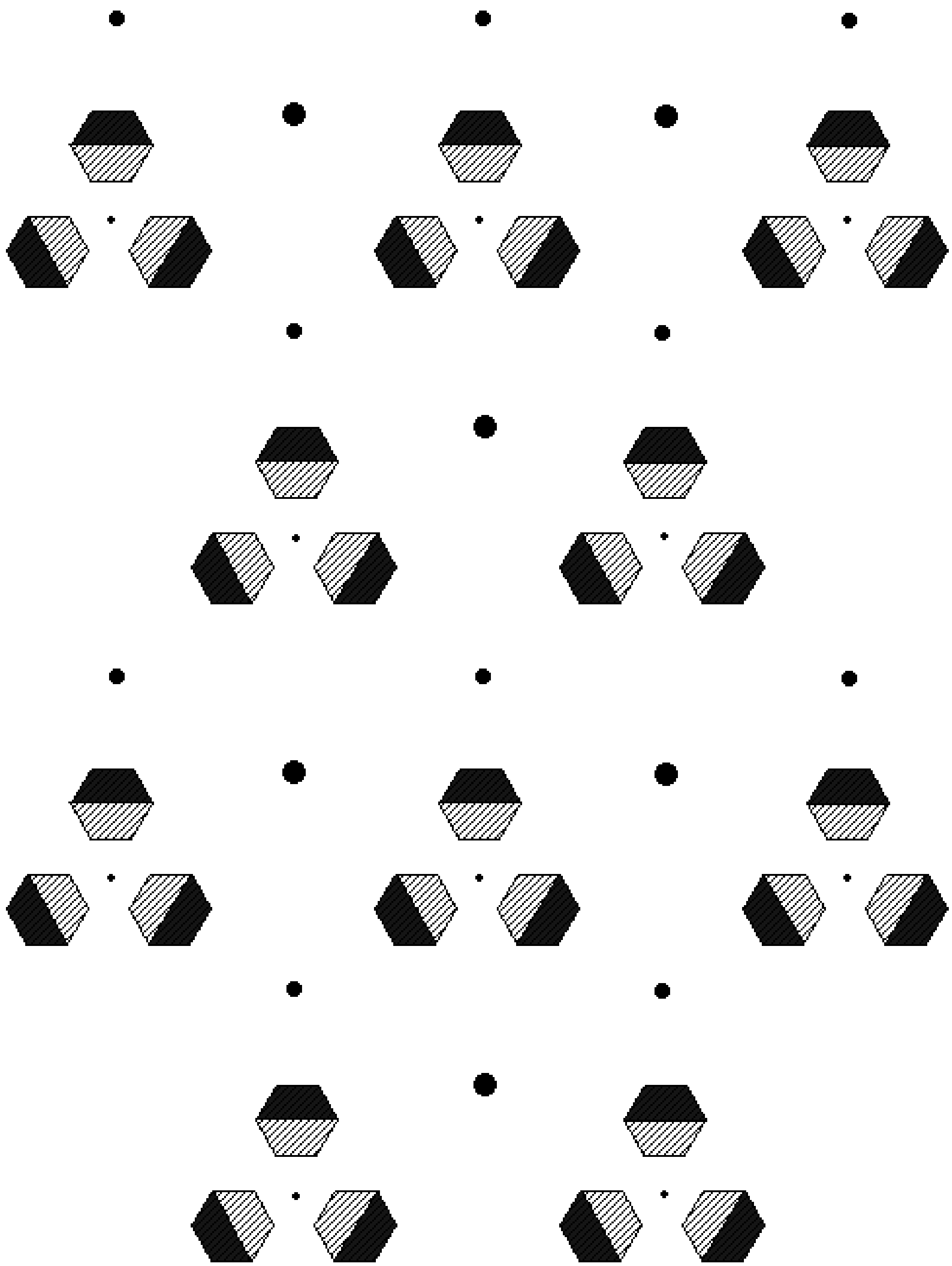

p3m1

Fig. 6.125

Next, a rather ‘exotic’ **p3m′** that probably celebrates the sacred concept of hexagon more than any other figure in this book:

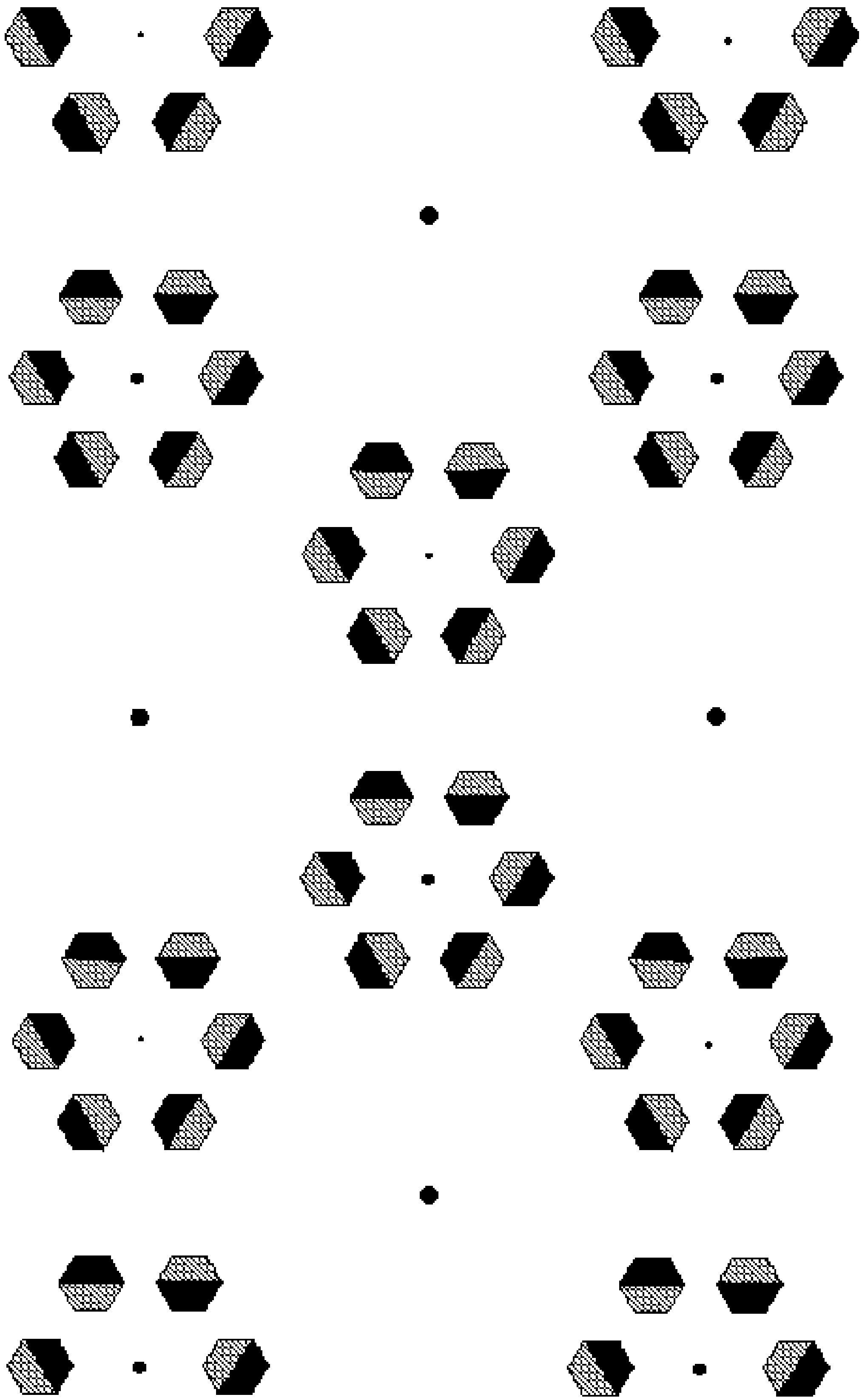

p3m′

Fig. 6.126

We are back to **three** kinds of rotation centers (**p3 structure**). (This is not obvious for the **p3m′** in figure 6.126, which at first glance **seems** to have only two kinds of threefold centers: do you see why the ‘hexagon middle’ centers are of two kinds?) As in figures 4.71 & 4.73, reflection axes are defined by any three **collinear** centers of **different** kind.

Finally, let’s **‘dilute’** (4.17.1) the **p31m′** pattern in figure 6.124 in order to get a ‘triangular’ **p3m′**:

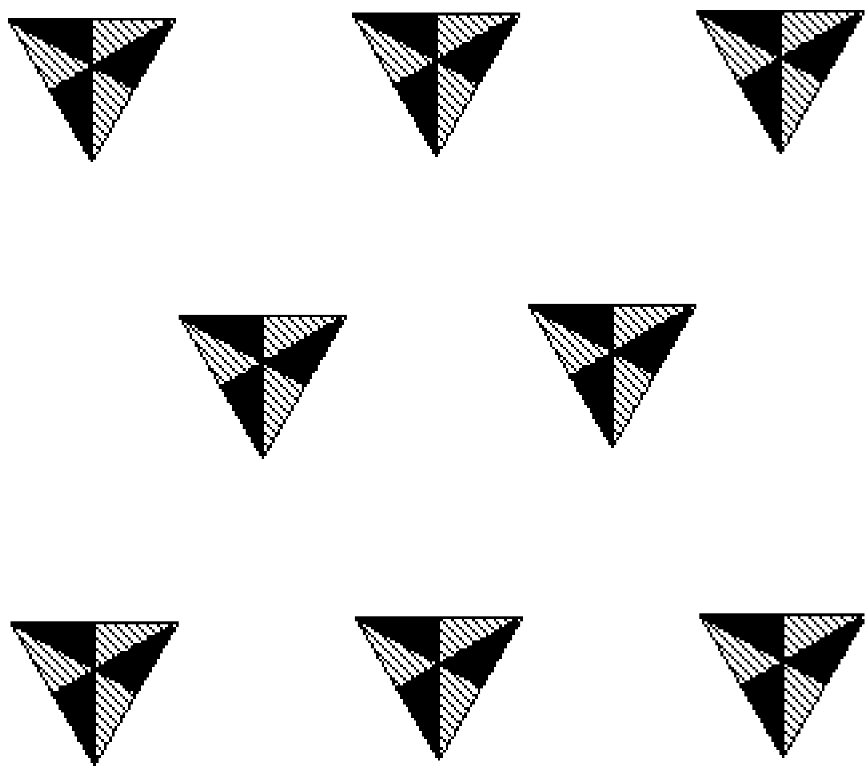

p3m′

Fig. 6.127

Observe here that rotating **all** triangles above about their center by **any** angle other than 60^0 or 120^0 or 180^0 turns the **p3m′** into a **p3**; exactly the same observation holds for the triangular **p31m′** of figure 6.124 (and in fact for all **p3m1**-like or **p31m**-like patterns)!

6.15.3 How about symmetry plans? You have probably noticed by now that we have not provided symmetry plans for **p3**, **p31m**, and

p3m1 types. They are not that crucial, because the classification is very easy within each type (two cases at most). Anyway, you will find symmetry plans for all sixty three two-colored types at the end of the chapter (section 6.18); before that, look also for the **p31m** and the **p3m1** ‘symmetry plans’ (inside the **p6m**) in section 6.17!

6.16 p6 types (p6, p6′)

6.16.1 The lattice of rotation centers. Let us first explain the arrangement of rotation centers (twofold, threefold, and sixfold) in **60^0** wallpaper patterns (both **p6**-like and **p6m**-like), shown already in figure 4.5 (**‘beehive’**), by way of the following demonstration:

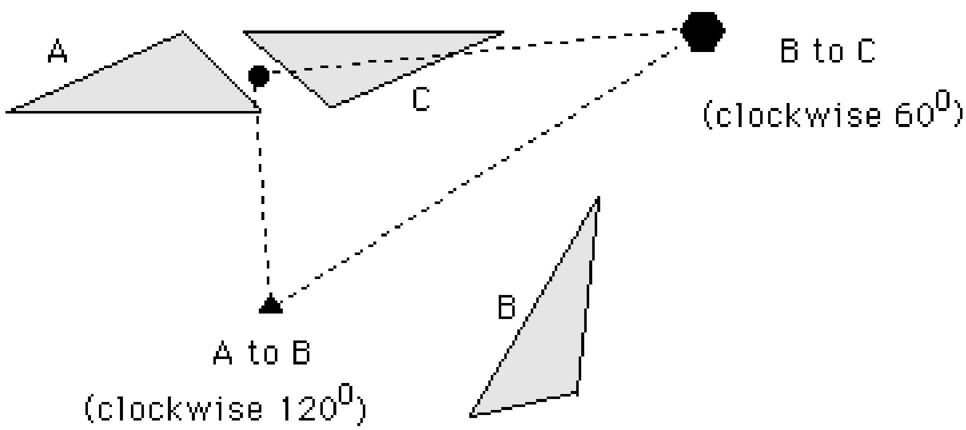

Fig. 6.128

We see that a **clockwise 120^0** rotation (mapping A to B) followed by a **clockwise 60^0** rotation (mapping B to C) results into a **180^0** rotation (mapping A to C). While a complete proof of this will be offered only in 7.5.4, figure 6.128 is rather convincing; especially in view of the fact that the three rotation centers are located at the three vertices of a **90^0-60^0-30^0** triangle, **exactly** as in figure 4.5!

You should use a demonstration similar to figure 6.128 in order to verify that the combination of two clockwise 60^0 rotations is a clockwise 120^0 rotation, that the combination of a 180^0 rotation and a clockwise 120^0 rotation is a counterclockwise 60^0 rotation, etc.

6.16.2 One kind of sixfold rotations at a time! Another fact valid for both **p6**-like and **p6m**-like types is that **no** 60^0 wallpaper pattern can possibly have **both** color-preserving and color-reversing sixfold centers. Indeed, should two 60^0 rotations of **opposite** effect on color coexist in a pattern, their combination would generate a **color-reversing** 120^0 rotation (see section 7.5 or proceed as in figure 6.99), which is impossible (6.13.1).

6.16.3 Only two types. In the **absence** of (glide) reflection and color-reversing translation (6.13.2), and in view of 6.16.2 above, we conclude at once that only two **p6**-like types are possible: one with **only color-preserving** 60^0 rotations (**p6**) and one with **only color-reversing** 60^0 rotations (**p6′**); no 'mixed' type like $\mathbf{p'_b2}$ (180^0) or $\mathbf{p'_c4}$ (90^0) is possible in the 60^0 case!

Of course all 120^0 rotations in either the **p6** or the **p6′** are color-preserving as usual. Then figure 6.128, together with the $\mathbf{P} \times \mathbf{P} = \mathbf{P}$ and $\mathbf{P} \times \mathbf{R} = \mathbf{R}$ rules, leads to an observation that may at times help you distinguish between **p6** and **p6′**: **all** 180^0 rotations in a **p6** pattern are color-preserving, and **all** 180^0 rotations in a **p6′** pattern are color-reversing. (Sometimes you may even **miss** the sixfold rotation and see only the twofold one, thus misclassifying a **p6′** or a **p6** as a **p2′** or a **p2**, respectively; more likely, you may only see the threefold rotation and misclassify a **p6** or a **p6′** as a **p3**!)

These remarks make it clear that the classification process within the **p6** type is rather simple, and the need for symmetry plans drastically reduced: therefore we follow the example set by the three previous sections, simply exiling the **p6** symmetry plans to the 'review' section 6.18.

6.16.4 Examples. First a 'two-colored' **p6** (with sixfold, threefold, and twofold centers represented by hexagons, triangles, and dots, respectively):

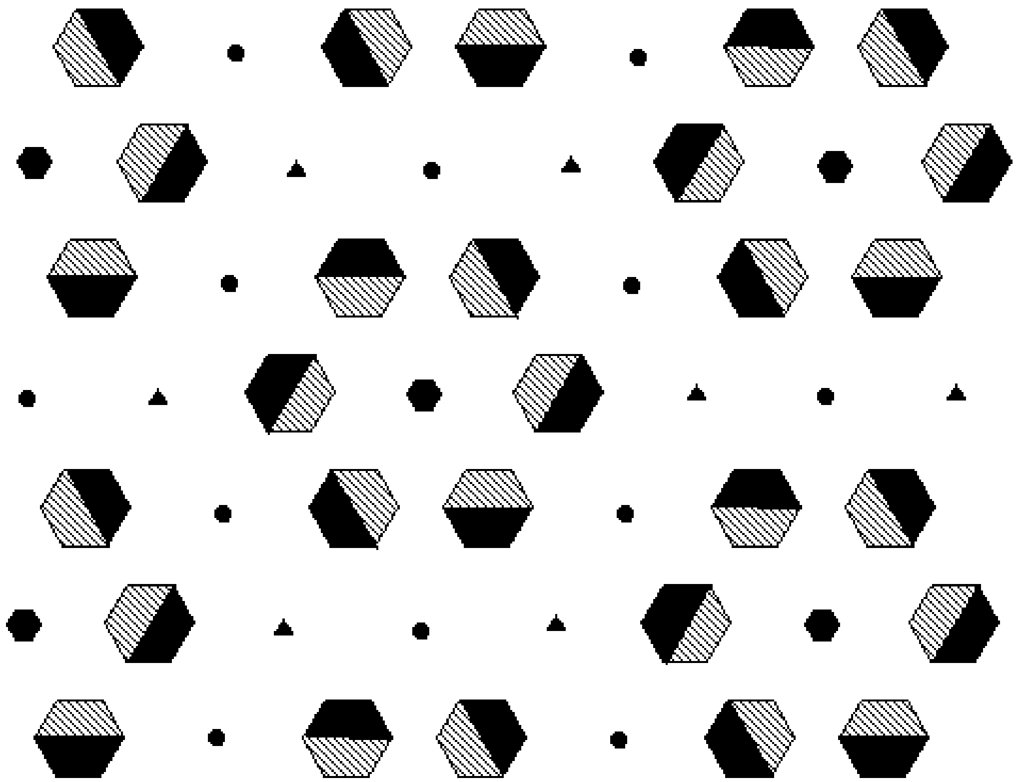

p6

Fig. 6.129

The 90^0-60^0-30^0 triangles of figure 6.128 are certainly ubiquitous. There are many other remarks one could make with regard to the positioning of the three kinds of rotation centers. One non-trivial remark is that every two rotation centers corresponding to equal rotation angles are **conjugate** in the sense of 6.4.4: at least one of the pattern's isometries (in fact a **rotation**) maps one to the other; in particular, this fact provides another explanation for the uniform effect on color within each kind of rotation. A related remark concerns the perfectly hexagonal arrangement of both twofold and threefold centers around every sixfold center. And so on.

We leave it to you to check that the **p6** pattern in figure 6.129 may be split into two identical **p6′** patterns the threefold centers of which are sixfold centers of the original **p6** pattern and vice versa! Further, here are two similar yet distinct **p6′** patterns (the second of which is sum of two copies of the **p31m′** pattern in figure 6.123):

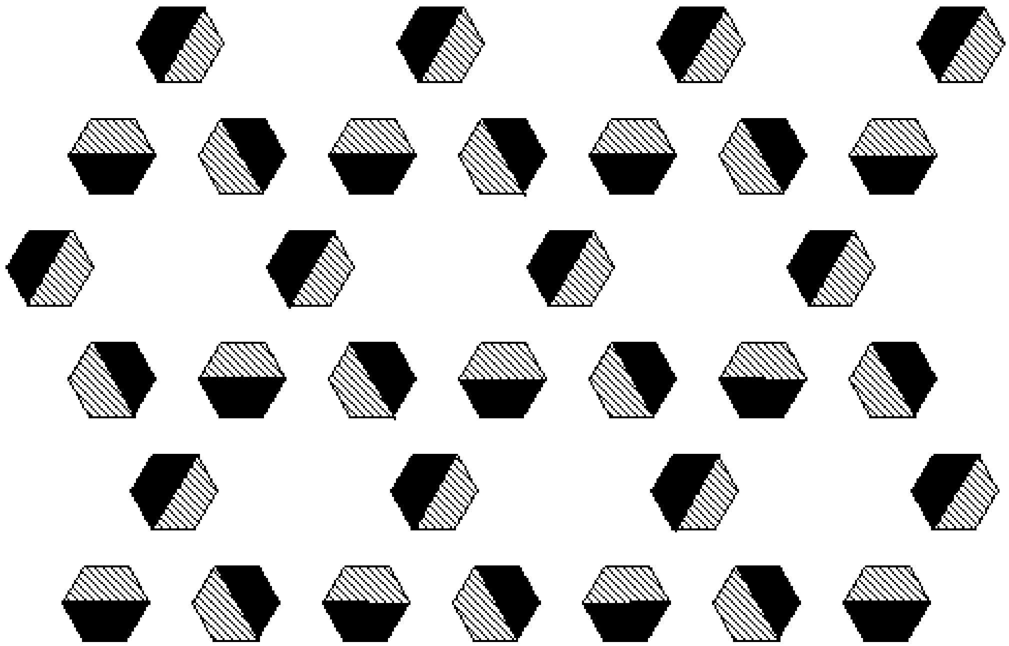

p6′

Fig. 6.130

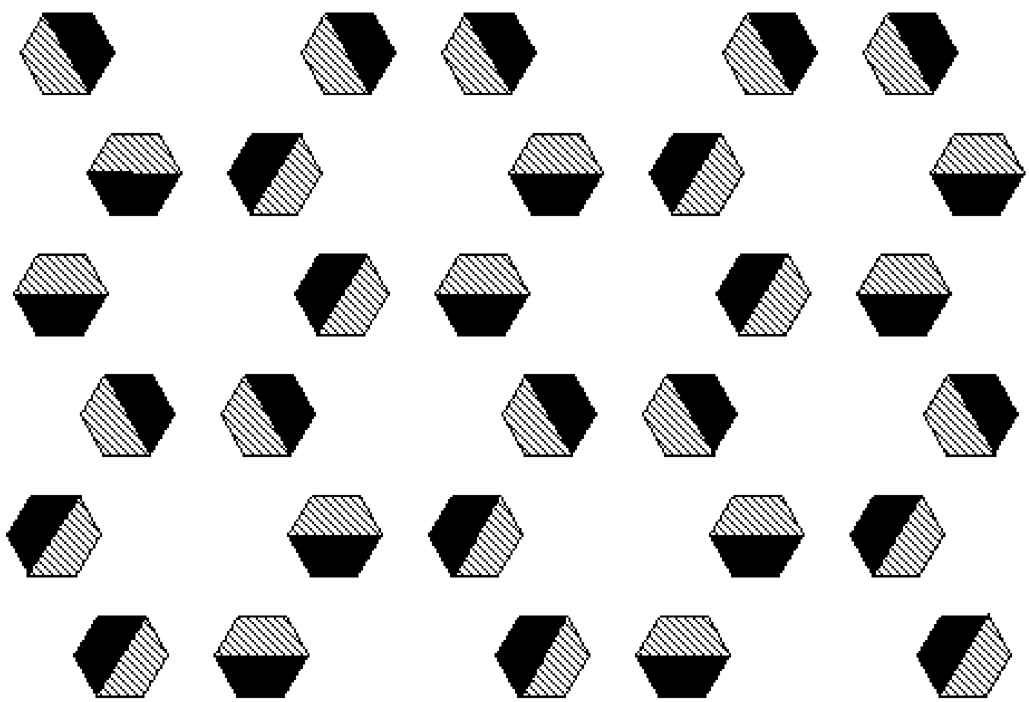

p6′

Fig. 6.131

6.17 p6m types (p6m, p6′mm′, p6′m′m, p6m′m′)

6.17.1 <u>A symmetry plan in two parts.</u> We begin with a very **visual** introduction to the most complex of wallpaper patterns:

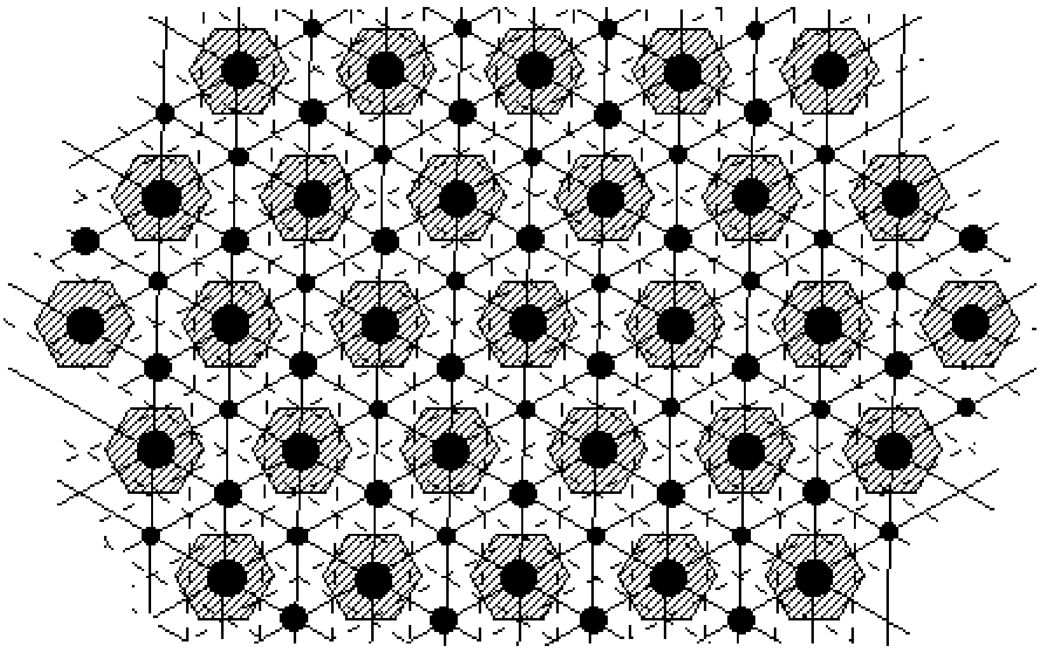

Fig. 6.132

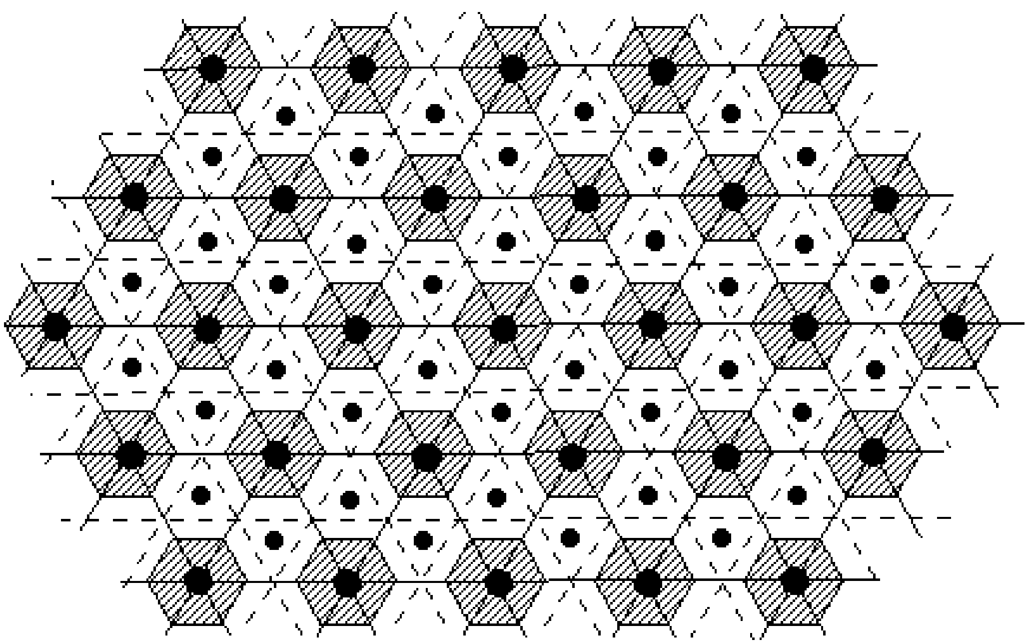

Fig. 6.133

Two pictures are worth two thousand words, one may say! All we did was to **'analyse'** a typical, hexagon-based **p6m** pattern into one **'p3m1'** pattern (with reflection axes passing through the **p6m**'s threefold centers and **hexagons' edges**, figure 6.132) and one **'p31m'** pattern (with reflection axes avoiding the **p6m**'s threefold centers and passing through the **hexagons' vertices**, figure 6.133). This is in fact the **'game'** we have been playing throughout most of this chapter, and some **'cheating'** was always involved! In the present case, for example, we do know that the 'off-axis' centers in figure 6.133 (**p31m** pattern) **do** in fact **lie** on the reflection axes of the **p3m1** pattern (figure 6.132); and that the 'distinct' on-axis centers of the **p3m1** pattern in figure 6.132 (small and medium sized dots) **are** in fact **mapped** to each other by the **p31m**'s reflection axes (figure 6.133). Moreover, the largest dots in both figures represent rotation centers for 60^0 rather than just 120^0, and so on. At the same time, the 'lower' patterns (**p3m1**, **p31m**) included in the 'higher' pattern (**p6m**) do **determine** its structure: for example, wherever two reflection axes (one from each 120^0 subpattern) cross each other at a $\mathbf{30^0}$ angle -- see figures 6.132 **and** 6.133 -- they do 'produce' a 60^0 rotation center (7.2.2). Conversely, the **p6m**'s properties are **inherited** by the **p3m1** and the **p31m** contained in it: for example, we may always 'use' a sixfold center as a threefold one; after all, a double application of a 60^0 rotation produces a 120^0 rotation (4.0.3). **In brief**, our **reduction** of the study of complex structures to that of simpler ones employed so far is **sound**, and we will appeal to it for one last time in 6.17.3.

6.17.2 <u>A complex structure indeed.</u> Figures 6.132 and 6.133 **together** make it clear that the **p6m**'s **sixfold** centers lie at the intersection of **six** reflection axes and that its **threefold** centers lie at the intersection of **three** reflection axes. Missing from both figures (and from 120^0 patterns!) are the **p6m**'s **twofold** centers, which nonetheless exist, located **half way** between every two adjacent hexagons; they are in fact located at the intersection of **one** reflection axis and **two** glide reflection axes **perpendicular** to hexagons' edges (figure 6.132) **and** at the intersection of **one** reflection axis and **two** glide reflection axes **parallel** to hexagons' edges (figure 6.133). We conclude that the **p6m**'s twofold centers lie at the intersection of **two** reflection axes and **four** glide reflection axes, still adhering to the **'p6 rule'** set by figure 6.128, and in full agreement with figure 4.5 as well. See also figure 8.42!

6.17.3 <u>Only four types!</u> Given the **p6m**'s complexity and what has happened in the case of other complex types (such as the **pmg** or the **p4m**), you would probably expect a long story here, too, right? Well, sometimes we get a break, rather predictable in this case: since the **p6m** is the 'product' of two **simple** (in terms of two-color possibilities) types, its study may not be that complicated after all. Indeed there can be **at most** two × two = four types, all of which **do** in fact exist (6.17.4): **p6m** = **p3m1** × **p31m** (both the **p3m1**'s and the **p31m**'s (glide) reflections preserve colors), **p6′mm′** = **p3m1** × **p31m′** (the **p3m1**'s (glide) reflection preserves colors and the **p31m**'s (glide) reflection reverses colors), **p6′m′m** = **p3m′** × **p31m** (the **p3m1**'s (glide) reflection reverses colors and the **p31m**'s (glide) reflection preserves colors), **p6m′m′** = **p3m′** × **p31m′** (both the **p3m1**'s and the **p31m**'s (glide) reflections reverse colors).

Our analysis so far is rather effective yet not terribly user-friendly. Taking advantage of the fact that one of the **p31m**'s (glide) reflection's directions is **'horizontal'** (figure 6.133) and that one of the **p3m1**'s (glide) reflection's directions is **'vertical'** (figure 6.132), we capture the preceding paragraph's findings in a simple diagram (and effective **substitute** for symmetry plan) as follows:

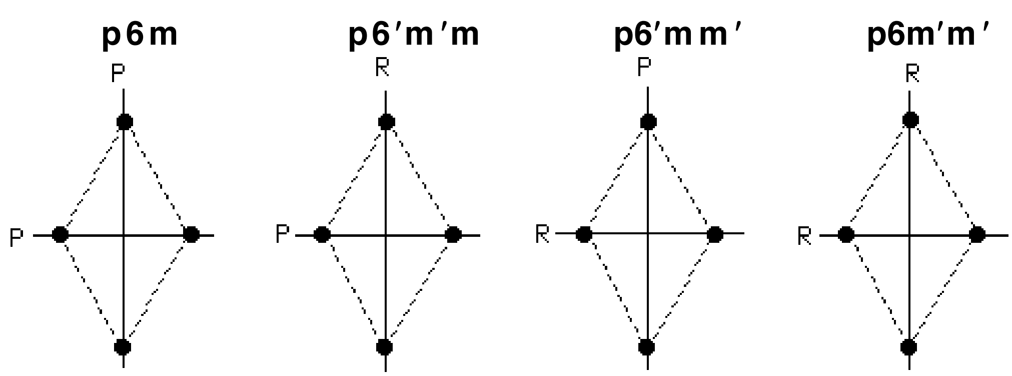

Fig. 6.134

So, once you decide that a two-colored pattern belongs to the **p6m** family (60^0 rotation plus 'some' reflection), locate all sixfold centers, pick four of them arranged in a (not necessarily 'vertical')

rhombus configuration as above, and then simply determine the effect on color of that rhombus' **short diagonal** (**p31m**) and **long diagonal** (**p3m1**). Notice that you do not need at all the effect on color of the **p6m**'s sixfold centers (represented by dots in figure 6.134), but you may still use them to **check** your classification: they of course have to **preserve** colors (**6**) in the cases of **p6m** and **p6m′m′**, and **reverse** colors (**6′**) in the cases of **p6′mm′** and **p6′m′m**.

6.17.4 Examples. First a **p6′mm′** and a **p6m′m′**:

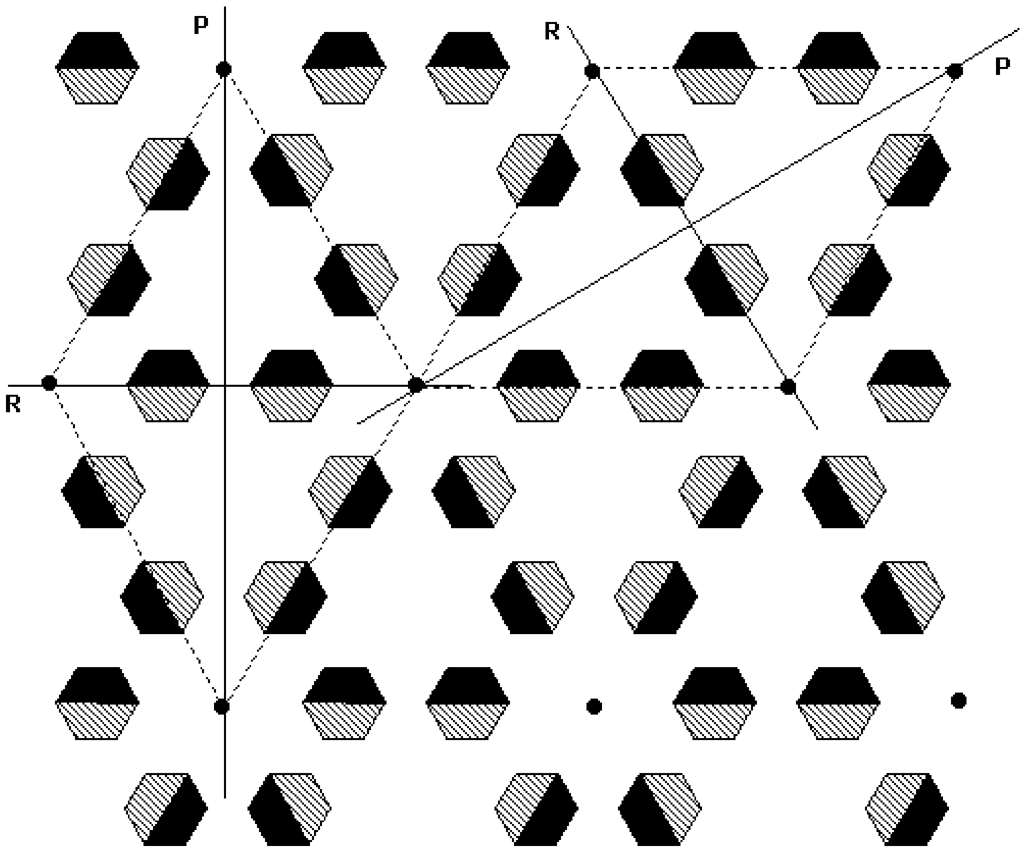

Fig. 6.135

We indicate **two** rhombuses of sixfold centers, one vertical and one non-vertical: the process is the same for both cases, the only thing that matters is the correct identification of the **long** and **short** diagonals. Make sure you can locate all the other isometries: threefold and twofold centers, in-between glide reflections, etc.

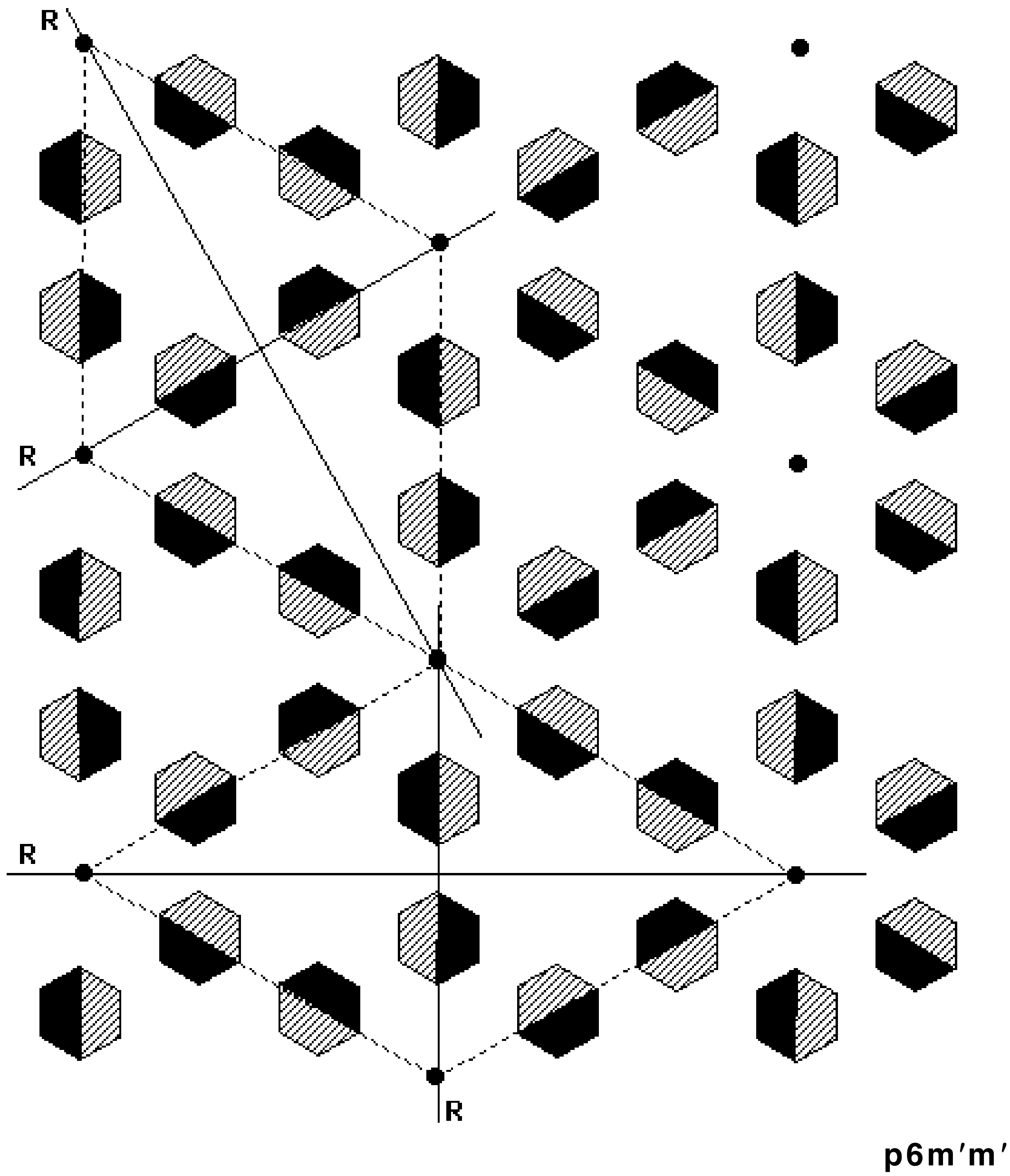

Fig. 6.136

In this example, closer than you might think to the previous one, we see that there is no **vertical** rhombus of sixfold centers. But we can still classify the pattern, using for example the **horizontal** rhombus at the bottom: **both** its diagonals **reverse** colors.

A slight yet necessary modification of the two-colored hexagons (and not only!) leads to examples of the remaining two **p6m** types, **p6′m′m** and ('two-colored') **p6m**. This time there is only one rhombus of sixfold centers shown per example:

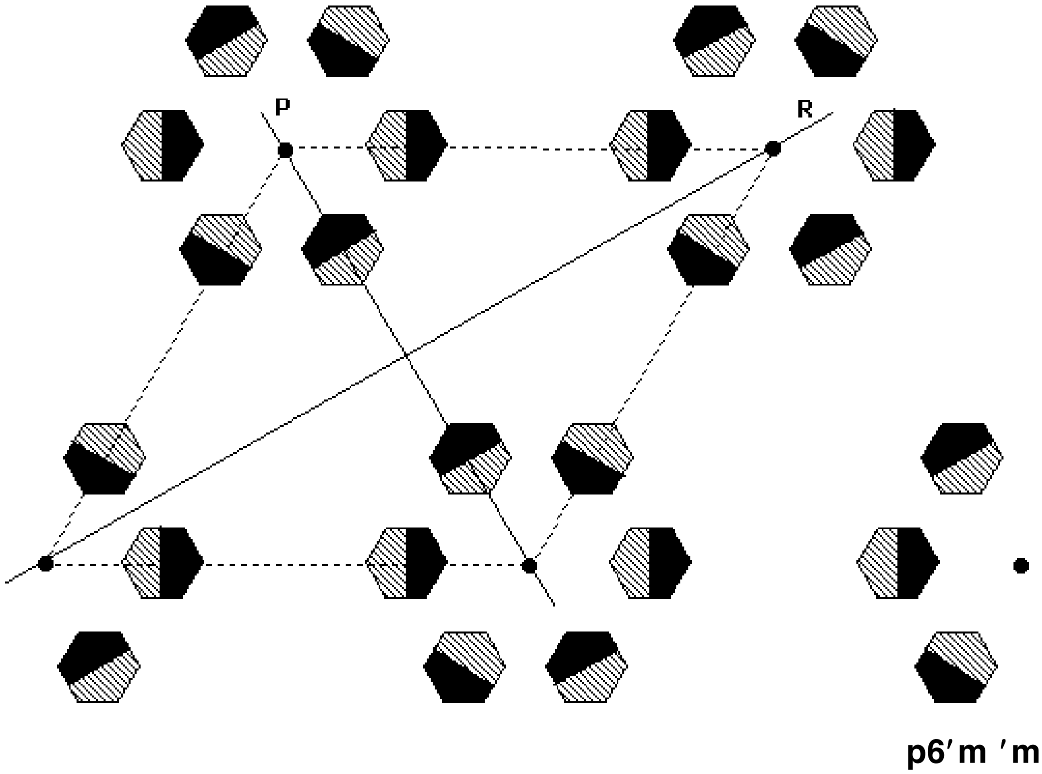

Fig. 6.137

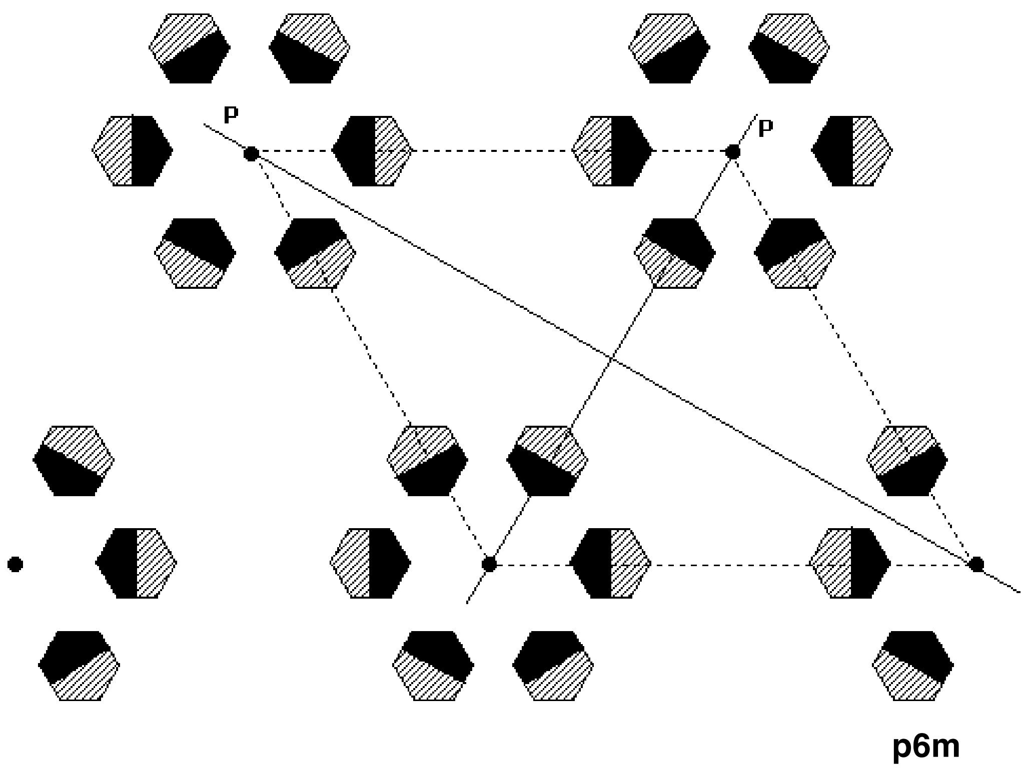

Fig. 6.138

Finally, some triangles inside the hexagons:

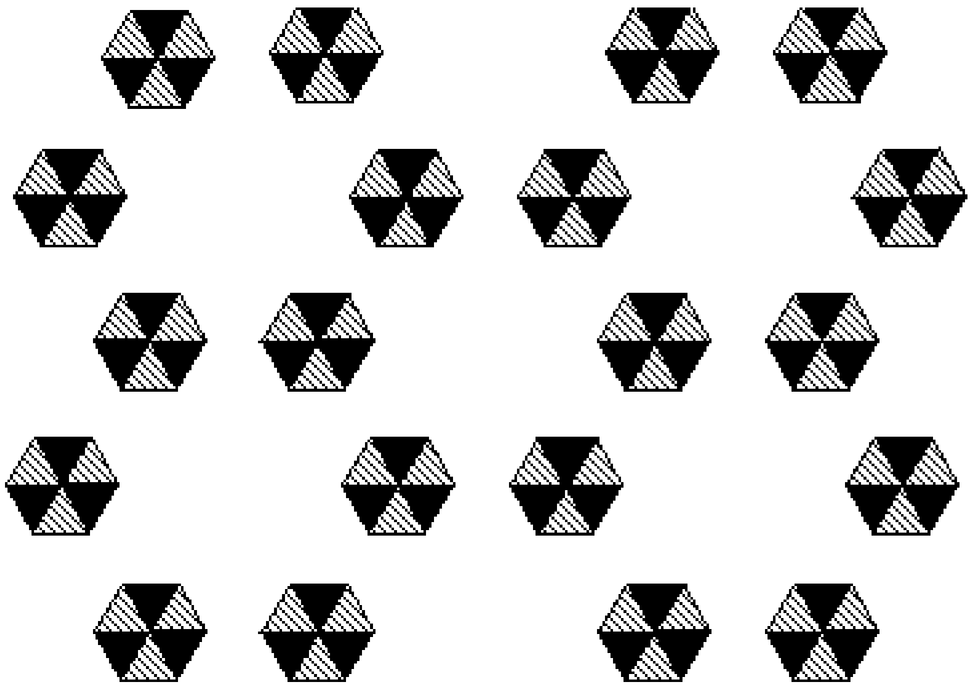

p6′m′m

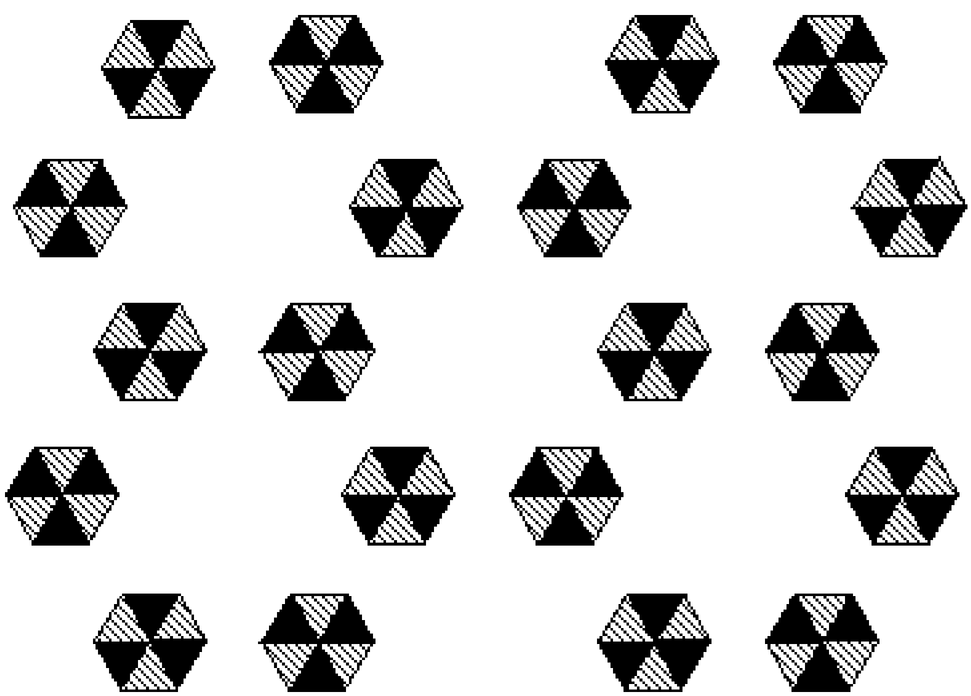

p6m′m′

Fig. 6.139

6.17.5 Reduction of symmetry revisited. You must have noticed that we provided no ‘triangular’ example of a **p6′mm′** in figure 6.139. While we leave it to you to decide whether or not such a particular example is possible, we compensate with the following variation:

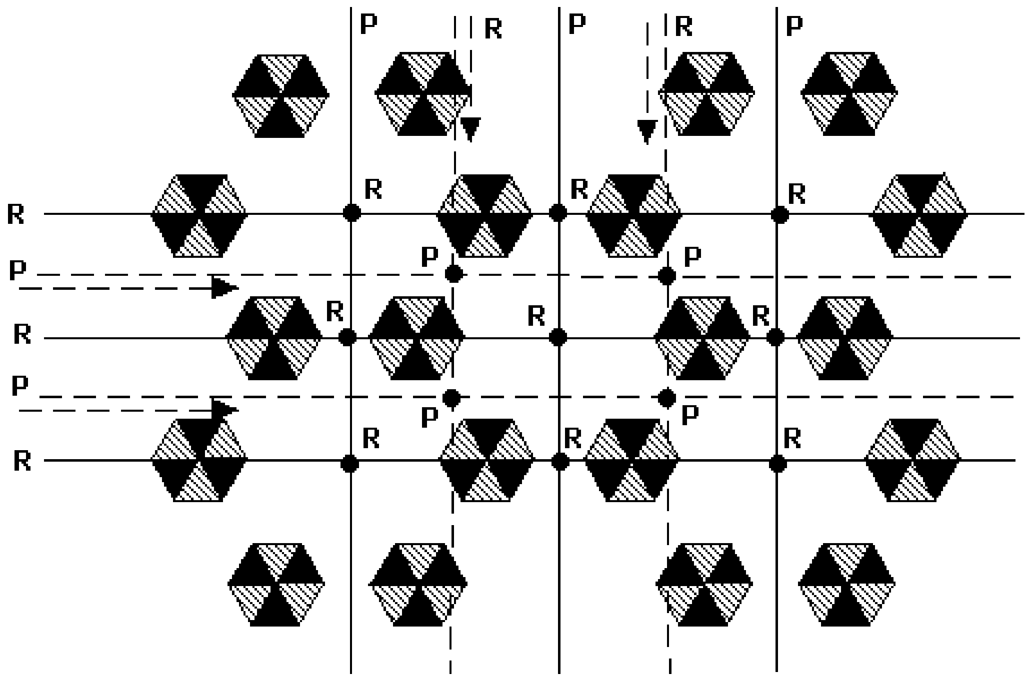

$p'_{c}mg$

Fig. 6.140

What happened? Quite simply, our coloring has rendered **all** the **p6m** isometries **but** the ones shown in figure 6.140 inconsistent with color. More specifically, only **one** direction of (glide) reflection has survived within each of the two 120^0 patterns hidden behind the **p6m**. As a result, all sixfold and threefold rotations are gone, but the twofold ones are left intact; to be more precise, all the sixfold centers have been **‘downgraded’** to twofold ones. It is certainly not difficult now to classify this ‘fallen’ pattern as a **cmm**-like type.

The **p6m** is a type that can generate many two-colored types (in all groups save for 90^0) by way of color inconsistency (just like the **p4g** of figure 4.57 has produced several 180^0 and 360^0 types). You should **experiment** on your own and **explore** its rich underground.

6.18 All sixty three types together (symmetry plans)

6.18.1 Reading and using the symmetry plans. As in section 4.18, we split the seventeen families of two-colored wallpaper patterns into **five groups** based on the angle of smallest rotation, indicating the **'parent types'** within each group in parenthesis; but the descriptions of the various patterns and types here are going to be visual rather than verbal, based on the symmetry plans developed throughout this chapter. As in section 5.9, isometries inconsistent with color are discarded: there are **no I**s in the symmetry plans!

In what follows, and as in the rest of the book, **solid** lines stand for **reflection** axes and **dotted** lines stand for **glide reflection** axes; once again, however, space limitations dictate the omission of all the glide reflection vectors and most translation vectors. Twofold, threefold, fourfold, and sixfold rotations are represented by dots, triangles, squares, and hexagons, respectively.

Recall at this point that all 120^0 rotations preserve colors (6.13.1) and that **all** reflections and glide reflections in two-colored 120^0 patterns must have the same effect on color (6.14.1): therefore in the respective symmetry plans a **P** or **R** to the symmetry plan's lower left or right indicates that **all** axes preserve colors or that **all** axes reverse colors, respectively. Along the same lines, rather than marking with a **P** or **R**, or even showing, every single (glide) reflection axis in each of the four **p6m** types, we limit ourselves to a single rhombus formed by sixfold centers (in the spirit of 6.17.3); a single unmarked **p6m** symmetry plan is shown **in full**.

Keep in mind that a symmetry plan not only provides the answer (as to what type a given two-colored wallpaper pattern belongs to), but it also may well **lead** to the answer; it shows, for example, how rotation centers are positioned with respect to (glide) reflection axes **and** vice versa: in some cases you may first locate the rotation centers, in other cases you may first find the (glide) reflection axes.

(I) 360^0 types (p1, pg, pm, cm)

p1

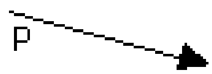

p'_b1

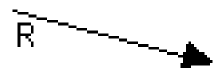

pg

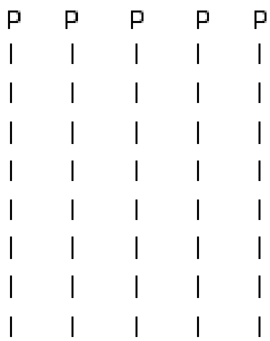

pg′

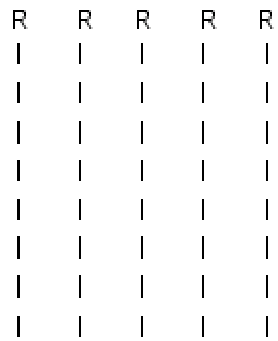

p'_b1g

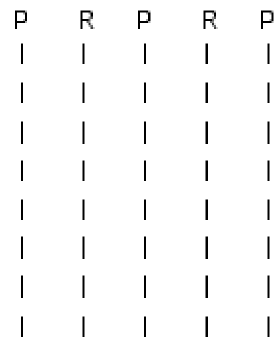

pm

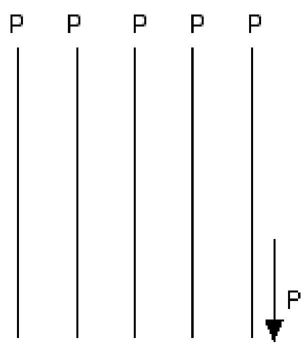

pm′

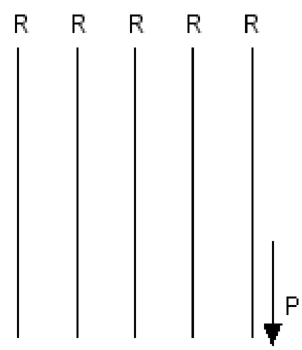

p'_b1m

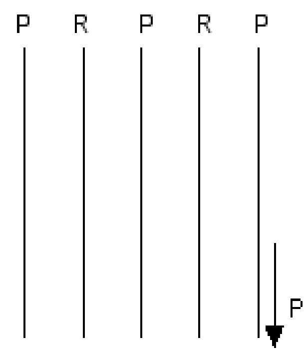

p′m

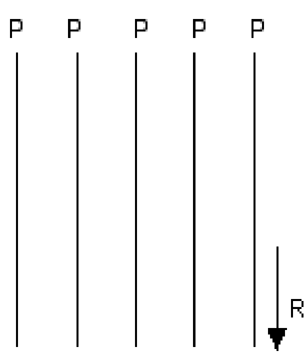

p'_bg

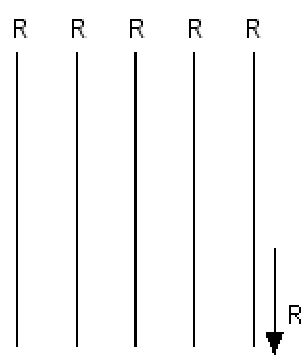

c′m

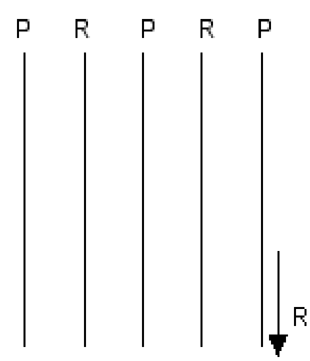

cm

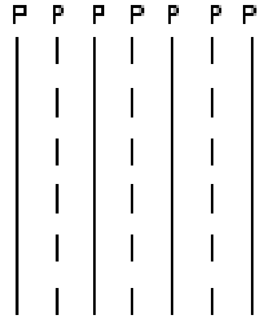

c m′

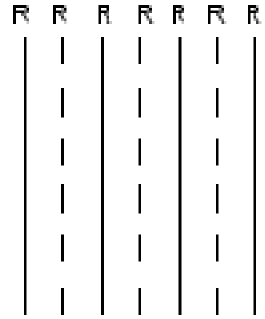

$p_c'g$

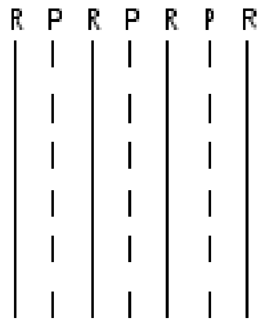

$p_c'm$

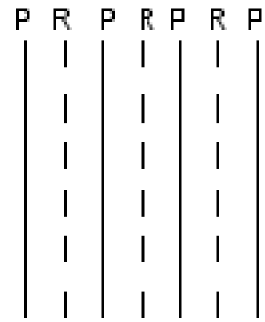

(II) 180^0 types (p2, pgg, pmg, pmm, cmm)

p2

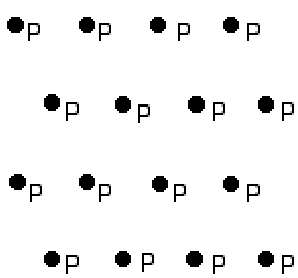

p2′

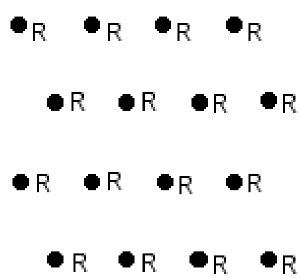

$p_b'2$

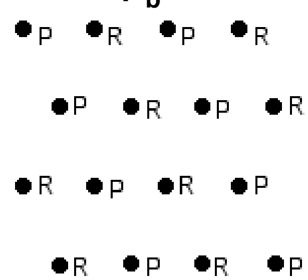

pgg

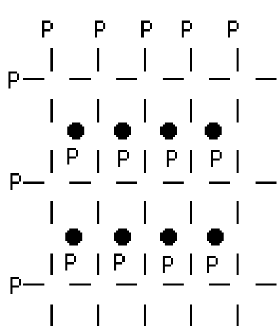

pgg′

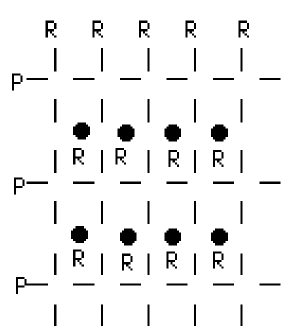

pg′g′

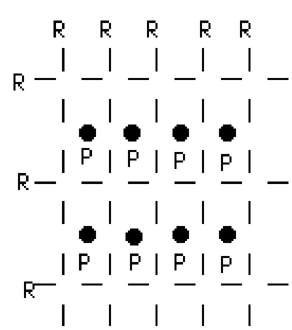

pmg

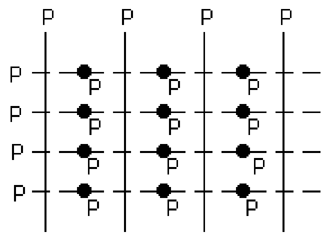

$p'_b mg$

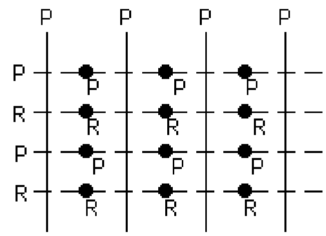

pmg'

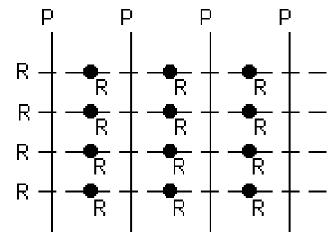

$pm'g$

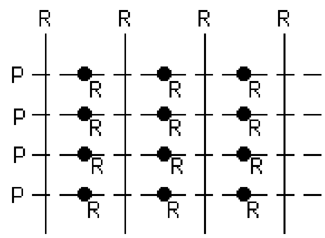

$p'_b gg$

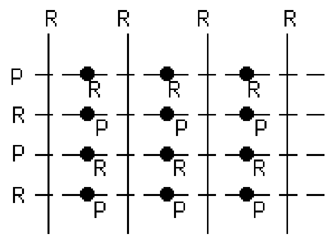

$pm'g'$

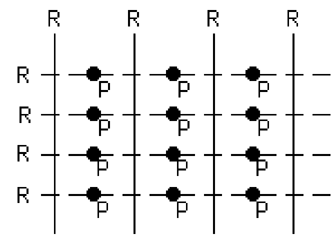

pmm

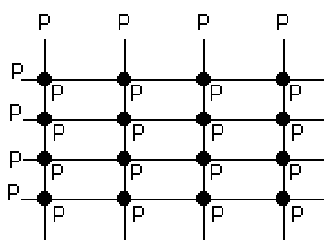

$p'_b mm$

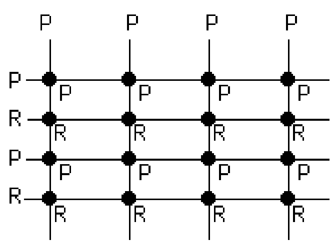

pmm'

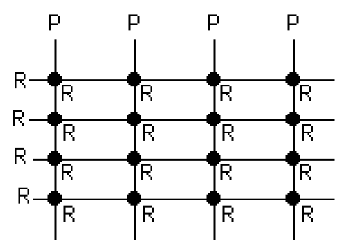

$c'mm$

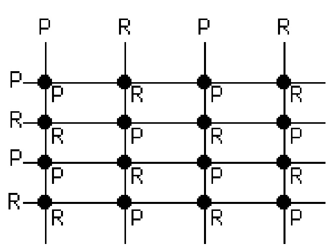

$p'_b gm$

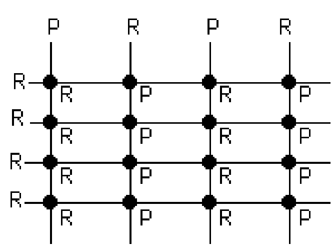

$pm'm'$

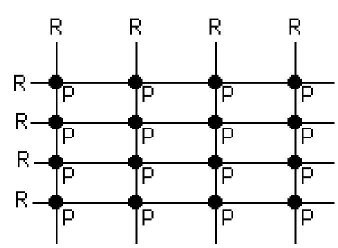

cmm

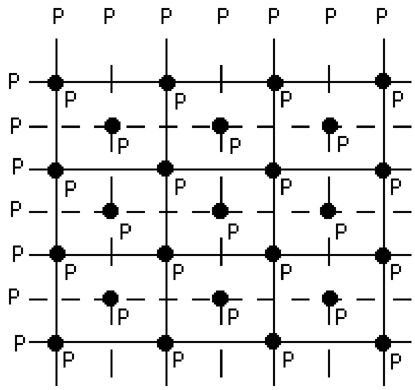

cm′m′

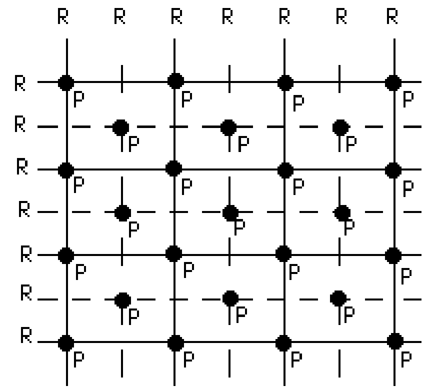

cmm′

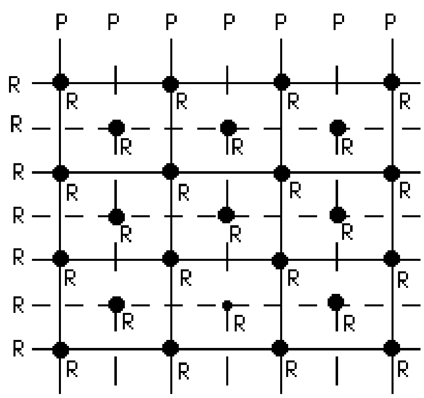

$p'_c mm$

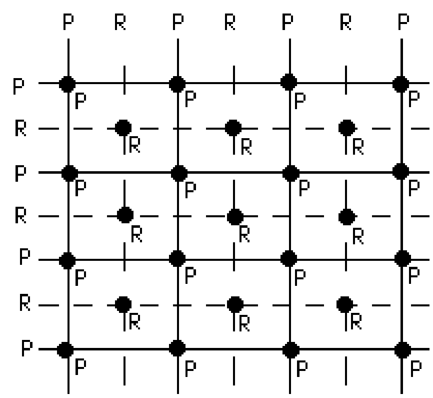

$p'_c mg$

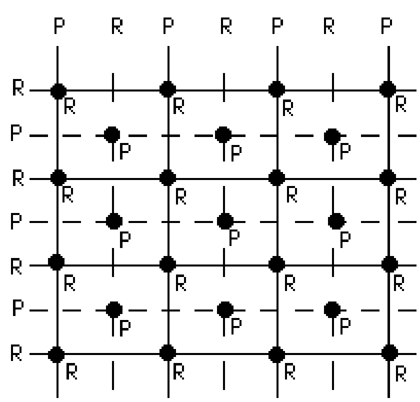

$p'_c gg$

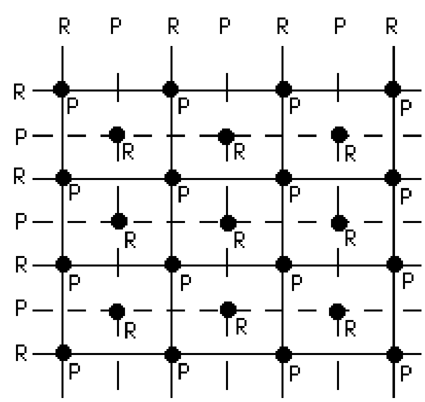

(III) 90^0 types (p4, p4g, p4m)

p4

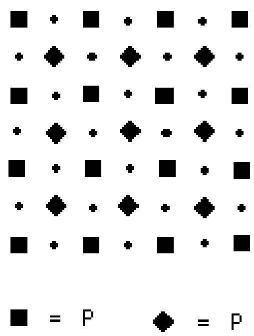

$p4'$

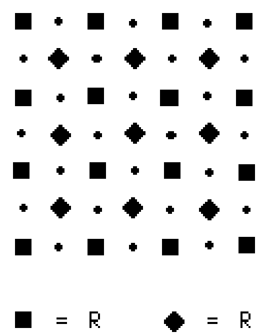

p'_c4

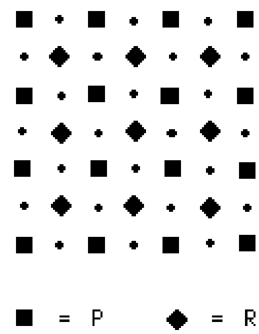

p4g

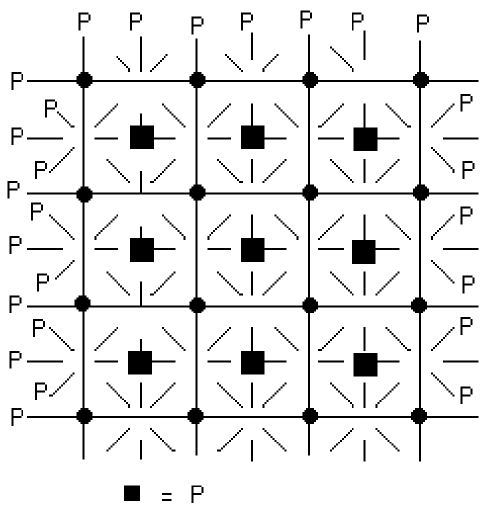

$p4'g'm$

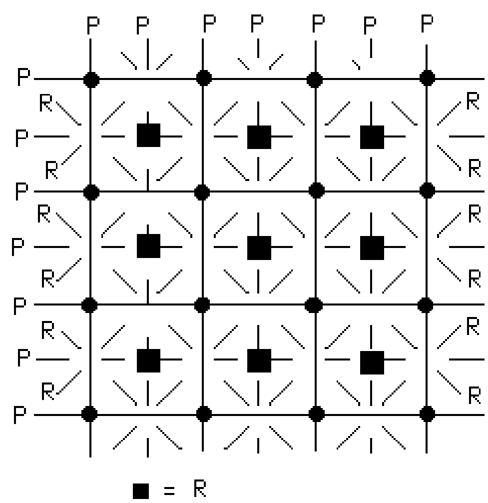

$p4g'm'$

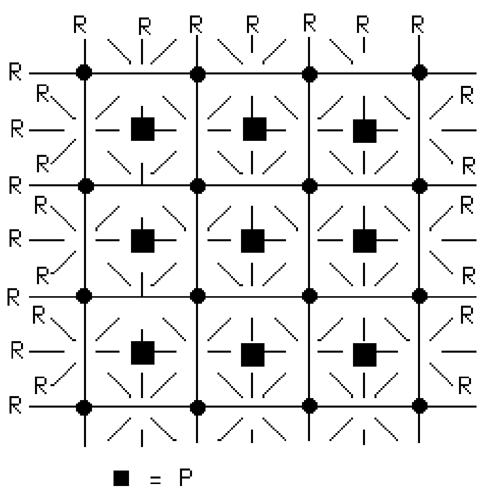

$p4'gm'$

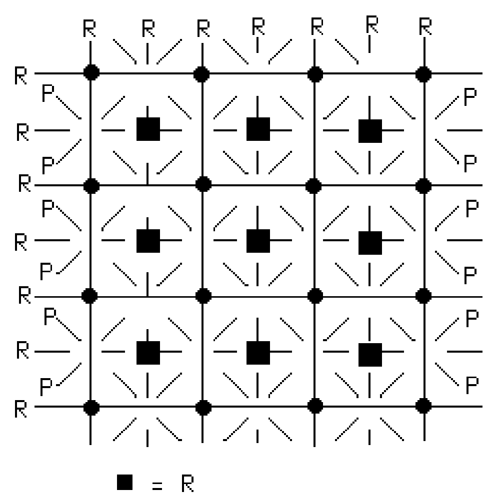

p4m

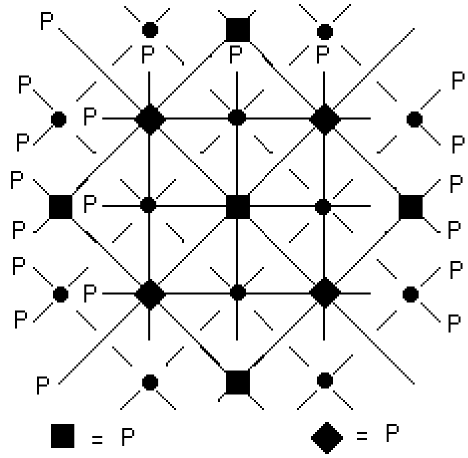

p4′m m′

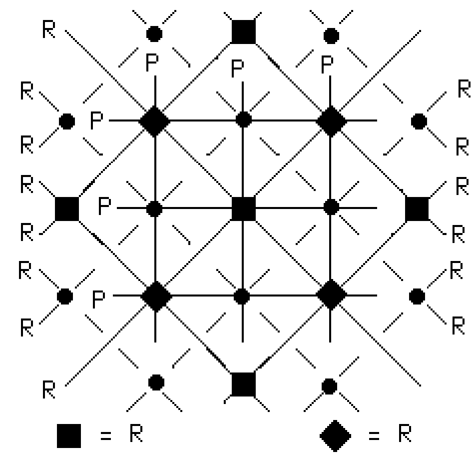

p4′m′m

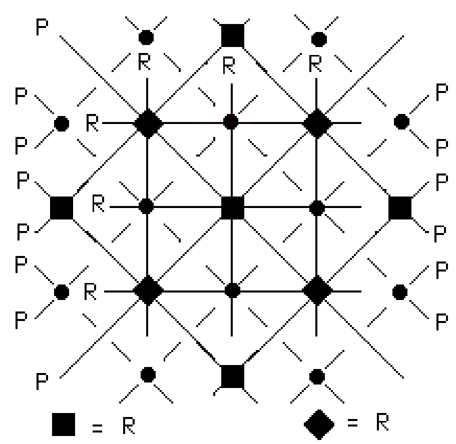

p4m′m′

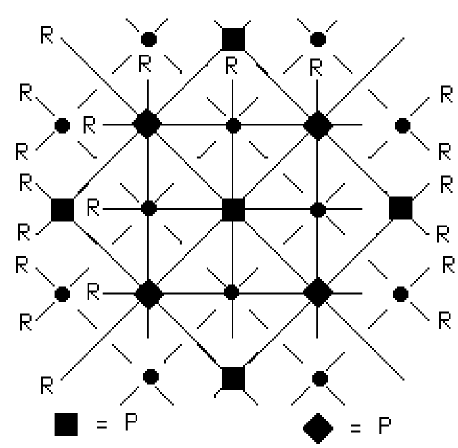

p'_c4mm

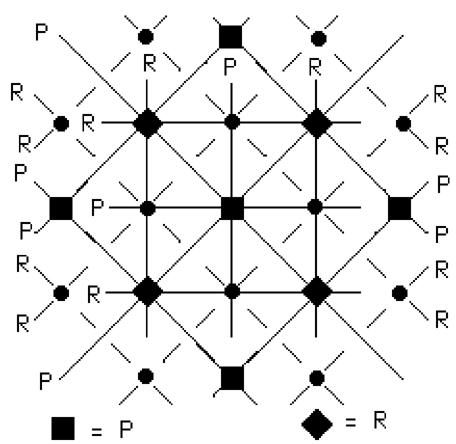

p'_c4gm

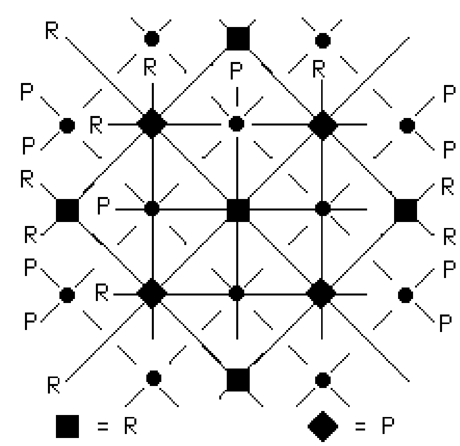

(IV-V) 120^0 (p3, p31m, p3m1) & 60^0 (p6, p6m) types

p6

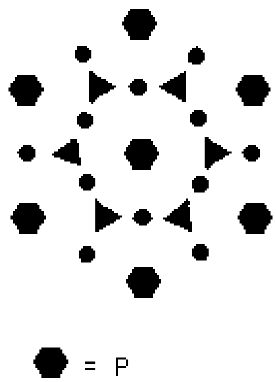

p3

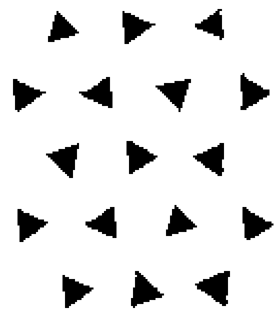

p6′

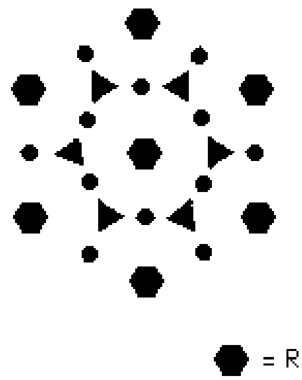

p31m

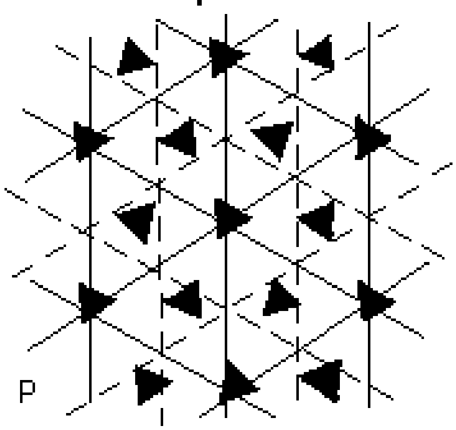

p31m′

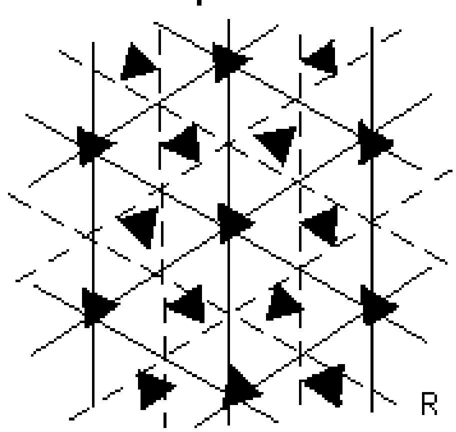

p3m1

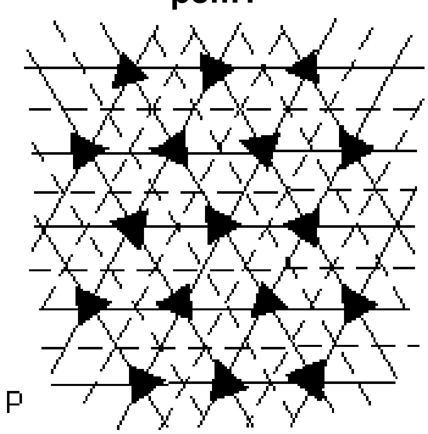

p3m′

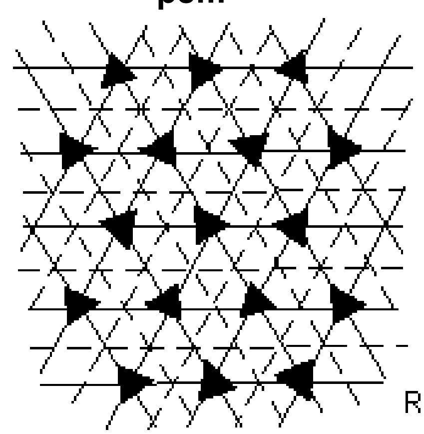

p6m

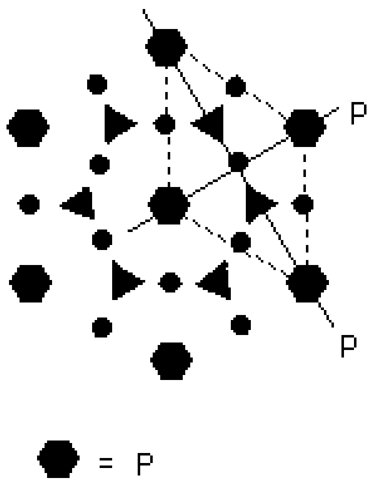

p6′m ′m

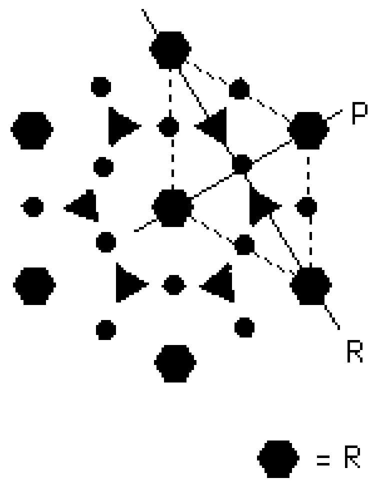

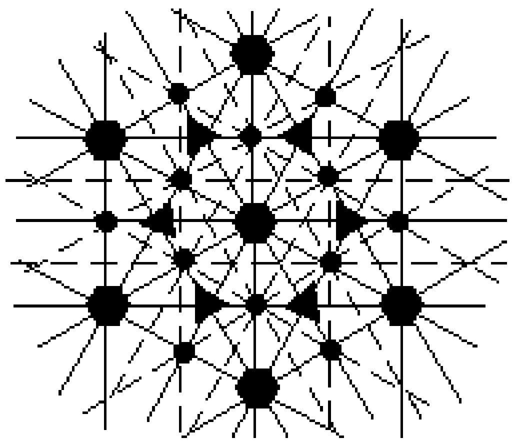

p6m′m ′

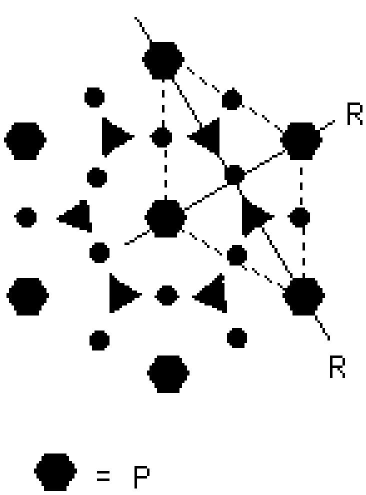

p6′m m ′

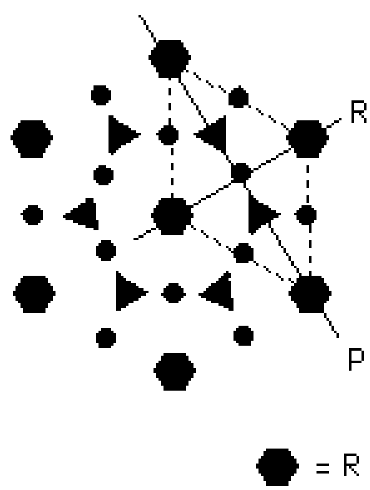

first draft: winter 2000

CHAPTER 7

COMPOSITIONS OF ISOMETRIES

7.0 Isometry 'hunting'

7.0.1 Nothing totally new. Already in 4.0.4 we saw that the composition (combined effect) of a rotation followed by a translation is another rotation, by the same angle but about a different center. And we employed this fact (in the special case of 180^0 rotation) in 6.5.3 (**'visual proof'** in figure 6.44) in our study of two-colored **p2** patterns. In fact we did run into several compositions of isometries in chapter 6: for example, figure 6.54 demonstrated that the composition of two perpendicular glide reflections is a 180^0 rotation; and we encountered instances of composition of two rotations in figures 6.44, 6.99, and 6.128.

Speaking of glide reflection, recall that its definition (1.4.2) involves the **commuting** composition of a reflection and a translation parallel to it. Moreover, we also pointed out in 1.4.2 that, in the composition of a reflection and a translation non-parallel to each other, whatever isometry that might be, the **order** of the two isometries does matter (figure 1.32). And we did indicate in figure 6.13 that the composition of a glide reflection (hence reflection as well) followed by a translation is a new glide reflection (about an axis parallel to the original and by a vector of different length).

7.0.2 'No way out'. Of course the most important point made in 1.4.2, if not in the entire book, is that the composition $I_2 * I_1$ of every two isometries I_1, I_2 **must** again be an isometry: indeed the distance between every two points P, Q is equal, because I_1 is an isometry, to the distance between I_1(P) and I_1(Q); which is in turn equal, because I_2 is an isometry, to the distance between $I_2(I_1(P)) = I_2 * I_1(P)$ and

$I_2(I_1(Q)) = I_2 * I_1(Q)$. In particular, the composition of every two isometries of a wallpaper pattern must be an isometry of it: this turns its set of isometries into a **group**. (More on this in chapter 8!)

So we do know that the composition $I_2 * I_1$ of any two given isometries I_1, I_2 is again an isometry. Since (section 1.5) there exist **only four** possibilities for planar isometries (translation, rotation, reflection, glide reflection), determining $I_2 * I_1$ should in principle be relatively simple. On the other hand, our remarks in 7.0.1 and overall experience so far indicate that there may after all be certain practical difficulties: formulas like the ones employed in chapter 1 may be too complicated for the mathematically naive (and not only!), while visual 'proofs' like the ones you saw throughout chapter 6 are not rigorous enough for the mathematician at heart. Therefore we prefer to base our conclusions in this chapter (and study of the **ten** possible combinations of isometries) on solid **geometrical proofs**: those are going to be as precise as algebraic proofs are, relying on the directness of pictures at the same time.

7.0.3 <u>A 'painted' bathroom wall.</u> Before we provide a detailed study of all possible combinations of isometries (sections 7.1-7.10), we present below a more **'empirical'** approach. Employing a 'standard' coloring of the familiar bathroom wall we seek to 'guess' -- **'hunt'** for, if you like -- the composition $\mathbf{T} * \mathbf{R_0}$ (clockwise 90^0 rotation followed by diagonal SW-NE translation, see figure 7.1) already determined in 4.0.4, dealing with other issues on the way. (The coordinate system of figure 4.3 is absent from figure 7.1, and the lettering/numbering of the tiles has given way to coloring.)

So, why the colors? First of all they help us, thanks to the **maplike** coloring, distinguish between neighboring tiles and keep track of where each tile is mapped under the various isometries of the tiling (and their compositions). Moreover, since the coloring is **consistent**, if the composition in question sends, say, **one** red tile to a green tile, then we know that it must send **every** red tile to some green tile: that helps us 'remember' (and even decide) where specific tiles are mapped by the 'unknown' isometry-composition (of the two isometries that we need to determine) without having to ‘keep notes’ on them. (All this assumes that you will take the time to color the tiles as suggested in figure 7.1, of course; but you do not have to, as long as you can keep track of where your tiles go!)

Most important, the colored tiles will help you rule out many possibilities. To elaborate, let’s first look at $\mathbf{T*R_0}$’s **color effect**:

$\mathbf{R_0}$	$\mathbf{T}$	$\mathbf{T*R_0}$
B → R	**R → G**	**B → G**
Y → G	**G → R**	**Y → R**
R → Y	**Y → B**	**R → B**
G → B	**B → Y**	**G → Y**

In other words, all we did was to rewrite $\mathbf{T*R_0}$ (in the language of color **permutations**) as **(RG)(BY)*(BRYG)** = **(BGYR)**. Now there exist many isometries whose effect on color is **(BGYR)**, such as the four 90^0 rotations around the red (**R**) square -- two of them ($\mathbf{R_1}$, $\mathbf{R_2}$) counterclockwise and two of them clockwise -- and the four diagonal glide reflections in figure 7.1: which one of these isometries, **if any**, is $\mathbf{T*R_0}$?

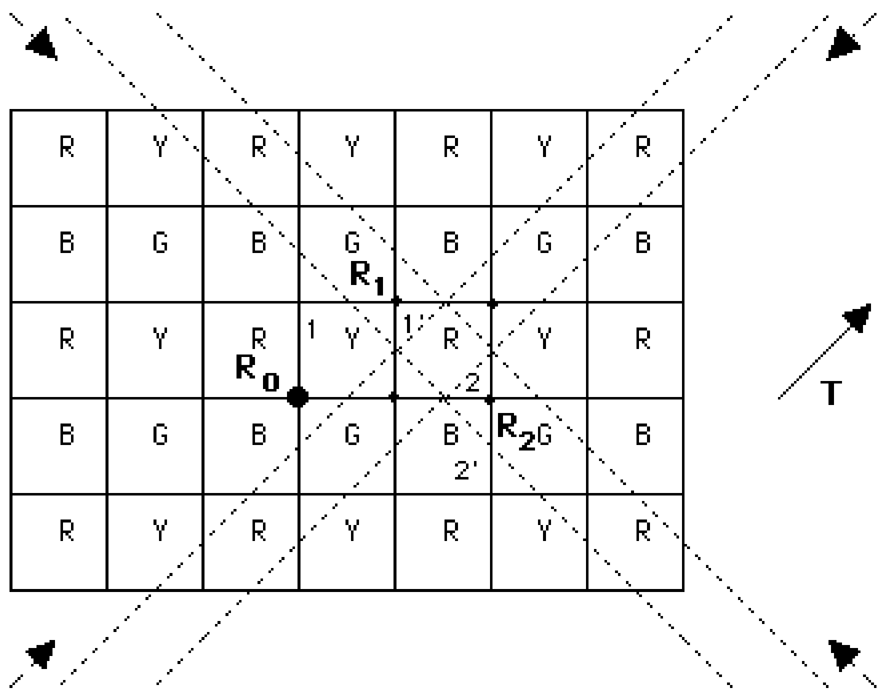

Fig. 7.1

Well, before we decide what $\mathbf{T*R_0}$ is, let's quickly observe what it **cannot** possibly be: since all translations, reflections, vertical or horizontal glide reflections, 180^0 rotations, and 90^0 rotations of first kind (i.e., centered in the middle of a tile) produce a color effect equal to either a product of two 2-cycles or a 2-cycle or the identity **P** (instead of a 4-cycle like **(BGYR)**), none of these isometries could possibly be $\mathbf{T*R_0}$. (For some examples, notice that the vertical reflection passing through $\mathbf{R_0}$ is **(BG)(YR)**, the left-to-right glide reflections passing through $\mathbf{R_0}$ are either **(BY)(GR)** or **(BR)(GY)**, minimal vertical translation is **(BR)(GY)**, 90^0 rotation about the center of any red or green square is **(BY)**, vertical or horizontal reflections passing through such centers are **P**, etc.) So, the only possibilities left are the ones that figure 7.1 'suggests'.

Now many students would naturally look at the outcome that we ruled out in 4.0.4, that is $\mathbf{R_1}$. To be more precise, at 4.0.4 we looked at **clockwise** 90^0 rotation at $\mathbf{R_1}$ (the translation of clockwise 90^0 $\mathbf{R_0}$ by **T**), which we can now rule out at once: its color effect is **(BRYG)**, not $\mathbf{T*R_0}$'s **(BGYR)**. But how about **counterclockwise** 90^0 rotation at $\mathbf{R_1}$, whose color effect is **(BGYR)**, after all? Well, looking (figure 7.1) at the yellow tile labeled #1, we see that $\mathbf{R_0}$ takes it to the green tile directly south of it, which is in turn mapped by **T** to the red tile labeled #1′ (figure 7.1); that's exactly where counterclockwise $\mathbf{R_1}$ moves tile #1, so it is **tempting** to guess that it equals $\mathbf{T*R_0}$: after all, the two isometries **seem** to agree not only in terms of color, but **position**, too! Well, the temptation should be resisted: for example, $\mathbf{T*R_0}$ moves the red tile #2 (formerly #1′) to the blue tile #2′ (by way of the yellow tile at the bottom center of figure 7.1), but counterclockwise $\mathbf{R_1}$ maps #2 to the blue tile directly north of it: if two isometries disagree on a single tile they simply cannot be one and the same.

So, are there any other 'good candidates' out there? Notice that counterclockwise $\mathbf{R_2}$ agrees with $\mathbf{T*R_0}$ on #2, but not #1, while $\mathbf{G_2}$ agrees with $\mathbf{T*R_0}$ on #1, but not #2. More promising is $\mathbf{G_1}$, which agrees with $\mathbf{T*R_0}$ on **both** #1 and #2: shouldn't the agreement on

two tiles allow us to conclude that these two isometries are equal? Well, at this point you need to go back to 3.3.4, where we discussed how and why "every isometry on the plane is uniquely determined by its effect on **any three non-collinear points**": replace points by **tiles**, and surely you will begin to suspect that $\mathbf{G_1}$ may not be the right answer after all; indeed this is demonstrated in figure 7.2, where we see that the blue tile #3 is mapped to a green tile #3′ by $\mathbf{T*R_0}$ but to a green tile #3″ by $\mathbf{G_1}$.

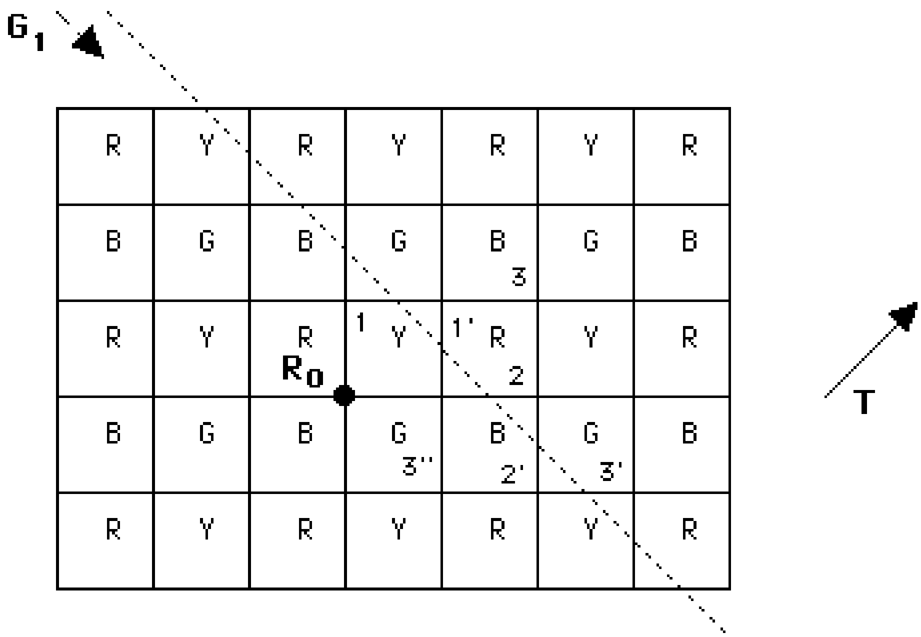

Fig. 7.2

Now a closer look at figure 7.2 reveals that $\mathbf{G_1}$, and, more generally, any glide reflection, had no chance at all: indeed, looking at the tile trio **123** and its image **1′2′3′**, we see that they are **homostrophic**, hence only a rotation could possibly work! But we have already tried a couple of rotations and none of them worked! Well, if you are about to give up on trial-and-error, if you feel lost in this forest of tiles and possibilities, chapter 3 comes to your rescue again: simply determine the center of a rotation that maps the **centers** of tiles #1, #2, #3 to the centers of the tiles #1′, #2′, #3′; this is in fact done in figure 7.3, where the rotation center is determined as the intersection of the three **perpendicular bisectors** 11′, 22′, and 33′. (Of course **just two** perpendicular bisectors would suffice, as we have seen in 3.3.5).

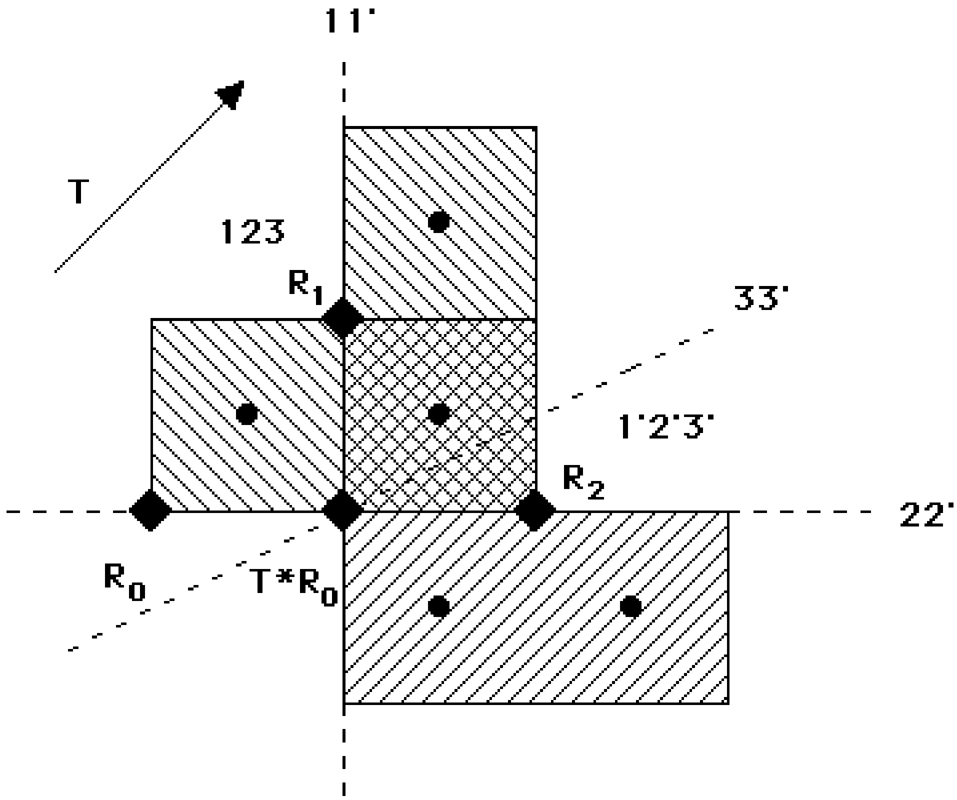

Fig. 7.3

So, it becomes clear after all that a clockwise 90^0 rotation maps the tile trio **123** (NW-SE shading) to the tile trio **1′2′3′** (NE-SW shading); that rotation **has** to be $\mathbf{T*R_0}$, and its center is located 'between' the three centers $\mathbf{R_0}$, $\mathbf{R_1}$, and $\mathbf{R_2}$ (all indicated by a black square in figure 7.3). We could very well have made the right guess earlier, but the chapter 3 method illustrated in figure 7.3 can **always** be applied after the first few guesses have failed! (An extra advantage is the replacement of $\mathbf{D_4}$ sets (squares) by $\mathbf{D_1}$ sets (trios of non-collinear squares), which facilitates isometry recovery.)

7.0.4 Additional examples. In figure 7.4 we demonstrate the determination of $\mathbf{R_0*G_1}$ and $\mathbf{G_1*R_0}$, where $\mathbf{R_0}$ is again a 90^0 clockwise rotation. In the case of $\mathbf{R_0*G_1}$, the color effect is just the identity **P = (BRYG)∗(BGYR)**: the details are as in 7.0.3 above. That immediately rules out all the rotations (save for one type of 180^0 rotation revealed towards the end of this section) and **'off-tile-center'** reflections: none of those isometries, in the case of the particular tiling and coloring, always, may preserve all the colors; less obviously, the same is true of **diagonal** glide reflections. What could it be, then? Working again with individual tiles #1, #2, and #3 (figure 7.4), we see them mapped by $\mathbf{R_0 * G_1}$ to the tiles #1′, #2′, and #3′: the two tile trios **123** and **1′2′3′** are **heterostrophic**, hence the outcome must be a **‘hidden’** glide reflection -- one of those glide reflections, first mentioned in 6.3.1, employing one of the tiling’s **reflection axes** and one of the tiling’s **translation vectors**. Either by applying the procedures of chapter 3 -- as in figure 7.3, but using midpoints instead of bisectors -- or by simple inspection, we find out that $\mathbf{R_0 * G_1}$ is indeed the hidden **vertical** glide reflection denoted in figure 7.4 by **MG′**: the importance of hidden glide reflections warrants the use of a separate notation!

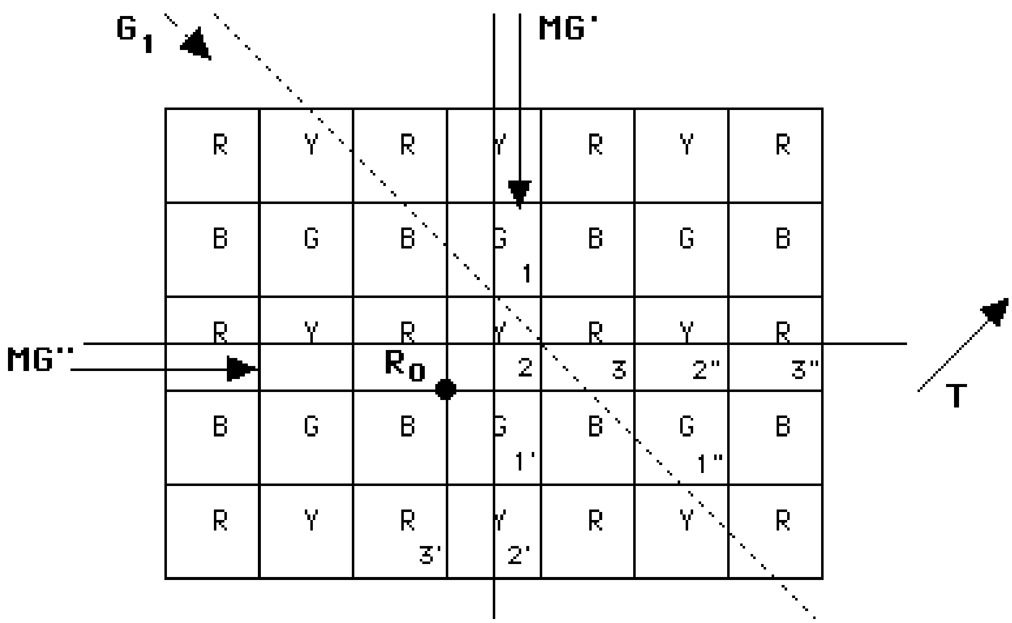

Fig. 7.4

A similar analysis, employing the tile trios **123** and **1″2″3″**, shows $\mathbf{G_1 * R_0}$ to be **MG″**, a **horizontal** hidden glide reflection (figure 7.4): rather predictably, $\mathbf{R_0 * G_1}$ and $\mathbf{G_1 * R_0}$ are differently positioned isometries of exactly the same kind. Notice the importance, in each case, of having used three non-collinear tiles: had we used only tiles #1 and #2 for $\mathbf{R_0 * G_1}$, or #2 and #3 for $\mathbf{G_1 * R_0}$, we would have ‘concluded’ that those glide reflections were mere translations!

Having seen the importance of order (of the two isometries) in combining isometries, we turn now to the relevance of **angle orientation**: we investigate, in figure 7.5, the compositions $\mathbf{R_3^+ * G_1}$ and $\mathbf{R_3^- * G_1}$, where $\mathbf{R_3^-}$ and $\mathbf{R_3^+}$ are counterclockwise and clockwise 90^0 rotations about the shown center $\mathbf{R_3}$, respectively.

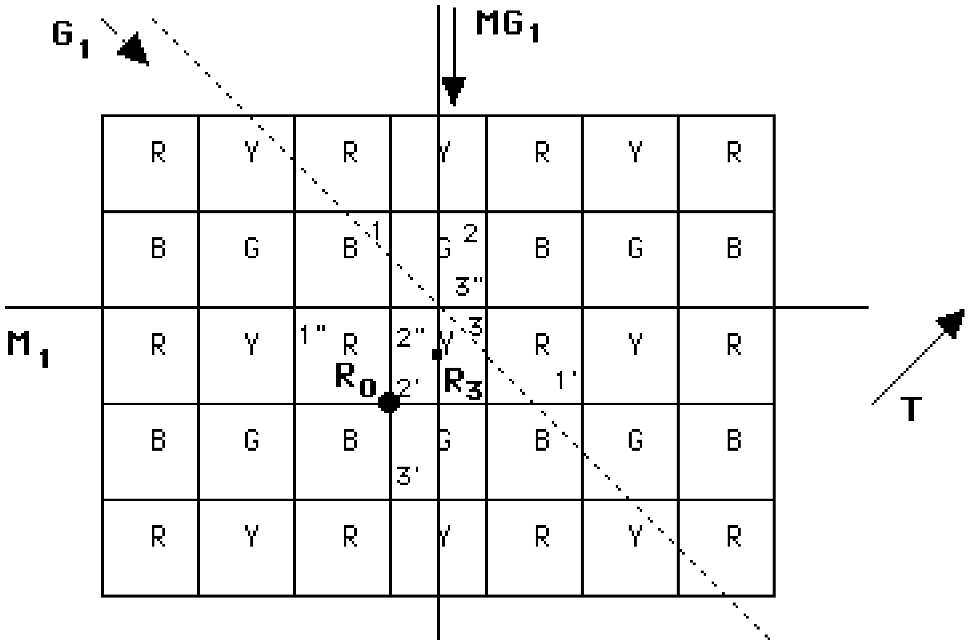

Fig. 7.5

Bypassing color considerations, but still using our ‘tile trios’ (**1′2′3′** for $\mathbf{R_3^+ * G_1}$, **1″2″3″** for $\mathbf{R_3^- * G_1}$), let’s look at the outcomes in figure 7.5. $\mathbf{R_3^+ * G_1}$ is a hidden glide reflection ($\mathbf{MG_1}$) sharing the same axis with $\mathbf{MG' = R_0 * G_1}$ (figure 7.4), but of smaller (half) gliding vector: yes, the **distance** from the rotation center to the glide reflection axis does play a crucial role! And $\mathbf{R_3^- * G_1}$ is a horizontal **reflection** ($\mathbf{M_1}$): as $\mathbf{R_3^-}$ **‘turns opposite’** of $\mathbf{G_1}$’s gliding vector, it ends up annihilating it -- while $\mathbf{R_3^+}$, ‘turning the same way’ as $\mathbf{G_1}$’s gliding vector, increases its length to that of $\mathbf{MG_1}$’s gliding vector!

How about compositions of glide reflections? Viewing, once again, a reflection as a glide reflection of zero gliding vector (1.4.8), we may first think of compositions like $\mathbf{M_1 * MG_1}$ and $\mathbf{MG_1 * M_1}$: those are rather easy in view of the discussion on perpendicular glide reflections in 6.6.2. For example, adjusting figure 6.54 to the present circumstances, we see that $\mathbf{M_1{*}MG_1}$ is the $\mathbf{180^0}$ rotation centered at the green tile right above $\mathbf{R_3}$, and this is corroborated by color permutations: **(BR)(GY)∗(BR)(GY)** = **P**. (Recall (4.0.3) that every fourfold center may also act as a twofold center, in this case preserving all colors!) Turning now to $\mathbf{M_1{*}G_1}$ (figure 7.6), **probably** a rotation in view of 6.6.2, we see that its color effect is **(BR)(GY)∗(BGYR)** = **(BY)**. The only **rotations** producing this color effect are $\mathbf{90^0}$ rotations centered **inside** a **green or red** tile (rather than at the common corner of four neighboring tiles); but there exist **many** such rotations, so it is best to once again resort to **position** considerations and numbered tiles!

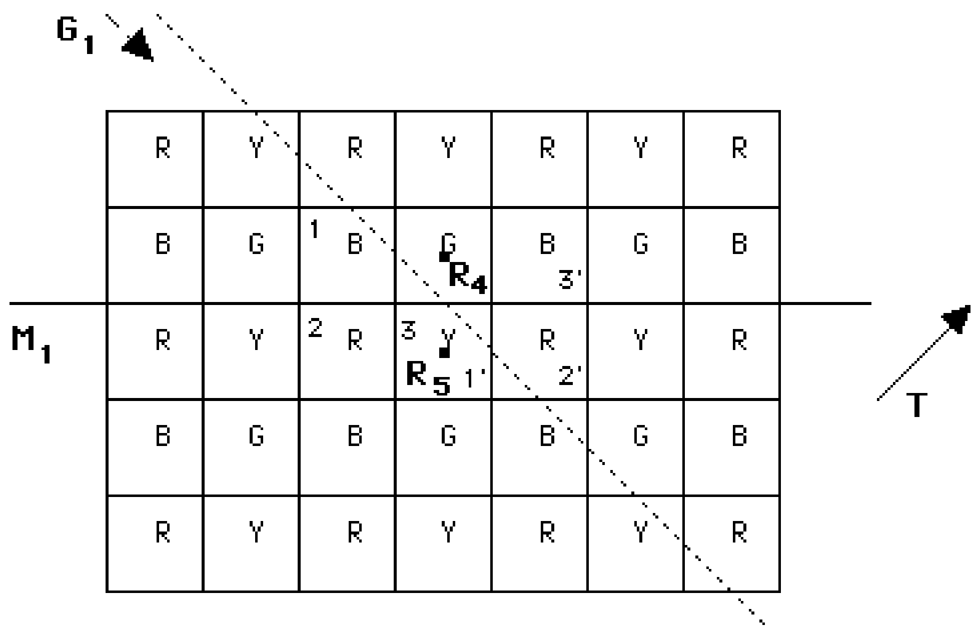

Fig. 7.6

Using three non-collinear tiles #1, #2, #3 (figure 7.6), we see that $\mathbf{M_1{*}G_1}$ maps the tile trio **123** to **1′2′3′**: these two trios are **homostrophic**, corroborating our guess that $\mathbf{M_1{*}G_1}$ is a rotation. And since we already know, through our **color** considerations above, that the composition in question must be a 90^0 rotation centered inside a green or red tile, the answer becomes obvious: $\mathbf{M_1{*}G_1}$ is the shown 90^0 **counterclockwise** rotation centered at $\mathbf{R_4}$. Work along similar lines will allow you to show that $\mathbf{G_1{*}M_1}$ is the **clockwise** 90^0 rotation $\mathbf{R_5}$ (of color effect **(GR)** = **(BGYR)∗(BR)(GY)**).

We could go on, looking not only at more combinations but at different colorings and types of tilings as well, but we would rather start looking at composition of isometries in a more systematic manner, just as promised in 7.0.2.

7.1 Translation $*$ Translation

7.1.1 Just the parallelogram rule. Composing two translations $\mathbf{T_1}$, $\mathbf{T_2}$, each of them represented by a vector, is like computing the combined effect of two forces (vectors) in high school Physics: all we need is the **parallelogram rule** as shown in figure 7.7 (and applied to a particular point P, where each of the two vectors has been applied).

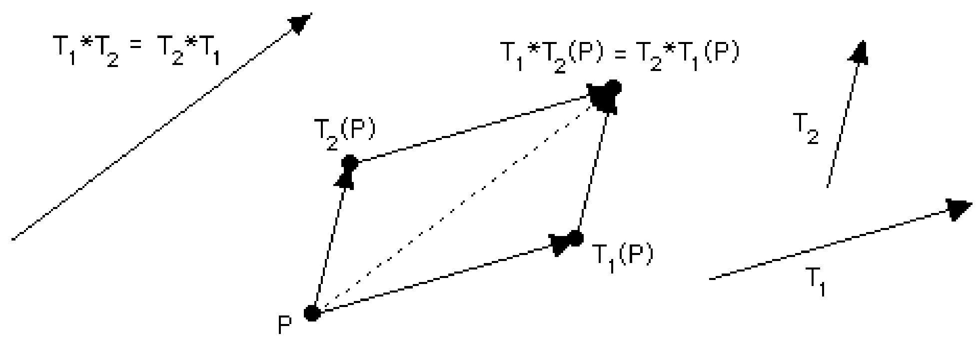

Fig 7.7

The composition is simply represented by the **'diagonal'** vector, and the equality $\mathbf{T_1*T_2 = T_2*T_1}$ is another way of saying that there are **two ways** of 'walking' (across the parallelogram's edges) from P to the diagonal's other end (figure 7.7). So, every two translations **commute** with each other, something that happens only in a few cases of other isometries (such as the composition of reflection and translation parallel to each other discussed in 1.4.2 and 7.0.1).

7.1.2 Collinear translations. When the translation vectors are collinear (parallel) to each other (as in the **border patterns** of chapters 2 and 5, for example), then the Physics becomes easier and the parallelogram of figure 7.7 is **flattened**. In fact, every two parallel vectors $\mathbf{T_1}$, $\mathbf{T_2}$ of lengths l_1, l_2 may be written as $\pm l_1\times\mathbf{T}$, $\pm l_2\times\mathbf{T}$, where $\mathbf{T}$ is a vector of length 1; the choice between + or – depends on whether or not $\mathbf{T}$ and the vector in question ($\mathbf{T_1}$ or $\mathbf{T_2}$) are of the same or opposite orientation (**sense**), respectively. The composition of the two translations is then reduced to addition of real numbers by way of $\mathbf{T_2}*\mathbf{T_1} = (\pm l_1 \pm l_2)\times\mathbf{T}$. Conversely, given any vector $\mathbf{T}$, not necessarily of length 1, all vectors parallel to it are of the form $l\times\mathbf{T}$, where l may be any positive or negative real number.

Combining 7.1.1 and 7.1.2, we may now talk about **linear combinations** of non-collinear translations $\mathbf{T_1}$, $\mathbf{T_2}$: those are sums of the form $l_1\times\mathbf{T_1}+l_2\times\mathbf{T_2}$, where l_1, l_2 are any real numbers ... and have already been employed in figures 4.10 & 4.11 (where we had in fact indicated, without saying so, that every translation in a wallpaper pattern may be written as a linear combination (with l_1, l_2 **integers**) of two particular translations).

7.2 Reflection ∗ Reflection

7.2.1 Parallel axes (translation). Back in 2.2.3, we did observe that the distance between every two **adjacent** mirrors in a **pm11** pattern is equal to **half** the length of the pattern's **minimal** translation vector. This makes full sense in view of the following 'proof without words':

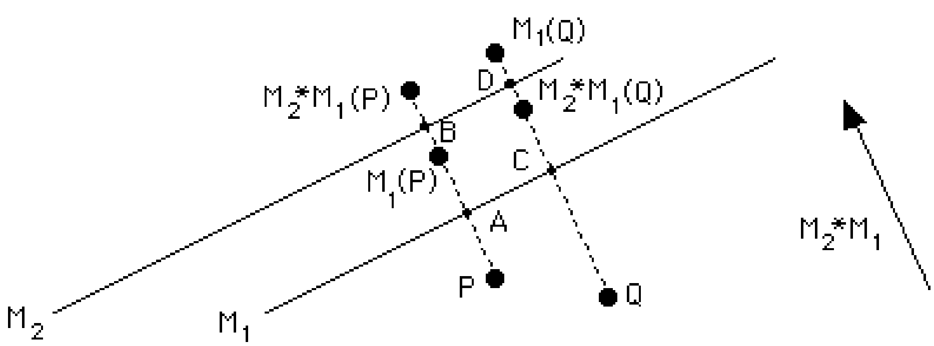

Fig. 7.8

Well, we can add a few words after all: with **d(X, Y)** standing for **distance** between points X and Y, we see that d(P, $\mathbf{M_2 * M_1}$(P)) = d(P, $\mathbf{M_1}$(P)) + d($\mathbf{M_1}$(P), $\mathbf{M_2 * M_1}$(P)) = 2 × d(A, $\mathbf{M_1}$(P)) + 2 × d($\mathbf{M_1}$(P), B) = 2 × d(A, B) = twice the distance between the parallel lines $\mathbf{M_1}$ and $\mathbf{M_2}$; likewise, d(Q, $\mathbf{M_2 * M_1}$(Q)) = d(Q, $\mathbf{M_1}$(Q)) – d($\mathbf{M_1}$(Q), $\mathbf{M_2 * M_1}$(Q)) = 2 × d(C, $\mathbf{M_1}$(Q)) – 2 × d($\mathbf{M_1}$(Q), D) = 2 × d(C, D) = twice the distance between the parallel lines $\mathbf{M_1}$ and $\mathbf{M_2}$. So, both P and Q moved in the same direction (**perpendicular** to $\mathbf{M_1}$ and $\mathbf{M_2}$, and **'from $\mathbf{M_1}$ toward $\mathbf{M_2}$'**) and by the same length (**twice** the distance between $\mathbf{M_1}$ and $\mathbf{M_2}$). We leave it to you to verify that the same will happen to any other point, regardless of its location (between the two reflection lines, 'north' of $\mathbf{M_2}$, 'way south' of $\mathbf{M_1}$, etc): always, the combined effect of $\mathbf{M_1}$ and $\mathbf{M_2}$ (in that **order**) is the **translation** vector $\mathbf{M_2 * M_1}$ shown in figure 7.8!

7.2.2 <u>Non-parallel axes.</u> We have not kept it a secret that the composition -- in this case **intersection** -- of two perpendicular reflections yields a half turn: we have seen this in 2.7.1 (**pmm2**), 4.6.1 (**pmm**), 4.9.1 (**cmm**), etc. Moreover, we have seen 120^0 centers (**p3m1**, **p31m**) at the intersections of three reflection axes (making angles of $\mathbf{60^0}$), 90^0 centers (**p4m**) at the intersections of four reflection axes (making angles of $\mathbf{45^0}$), and 60^0 centers (**p6m**) at the intersections of six reflection axes (making angles of $\mathbf{30^0}$). It is therefore reasonable to conjecture that every two reflection axes intersecting each other at an angle $\phi/2$ generate a rotation about their intersection point by an angle ϕ; this is corroborated right below:

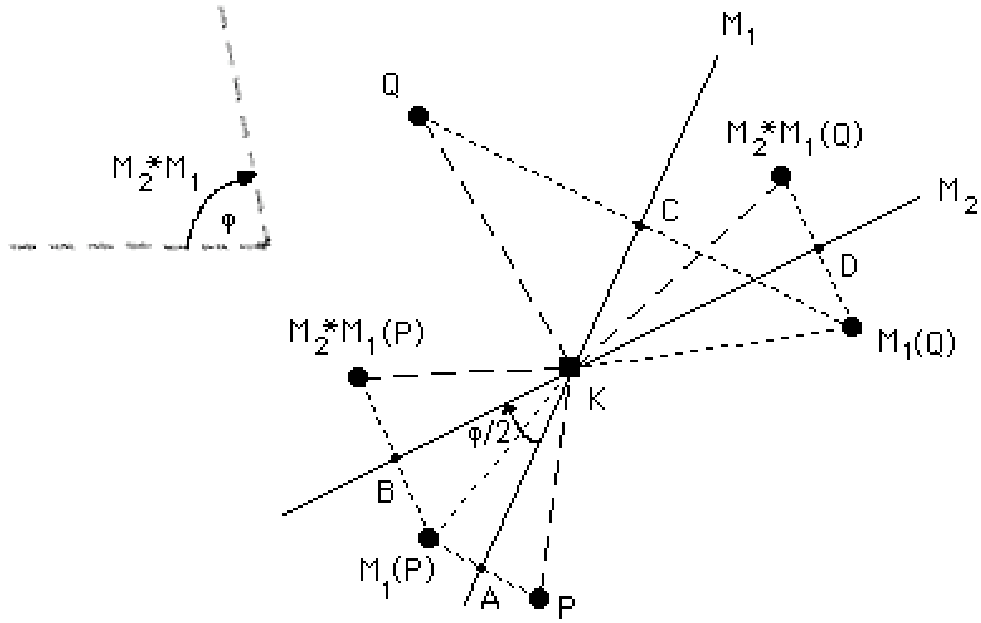

Fig. 7.9

To turn figure 7.9 into a proof, we must show, with **a(X, Y)** denoting the **angle** between lines KX and KY, that a(P, $\mathbf{M_2{*}M_1}$(P)) = 2 × a(A, B), a(Q, $\mathbf{M_2{*}M_1}$(Q)) = 2 × a(C, D), and so on. These equalities are derived **exactly** as the corresponding ones in 7.2.1, simply replacing **d** (distances) by **a** (angles). We leave it to you to verify that, no matter where P or Q is, the composition $\mathbf{M_2{*}M_1}$ is a rotation by the angle shown in figure 7.9: **twice** the size of the **acute** angle between $\mathbf{M_1}$ and $\mathbf{M_2}$, and going **'from $\mathbf{M_1}$ toward $\mathbf{M_2}$'** (which happens to be clockwise in this case).

7.2.3 The crucial role of reflections. Unlike translations, reflections do **not** commute with each other: it is easy to see that $\mathbf{M_1{*}M_2}$ is a vector opposite of $\mathbf{M_2{*}M_1}$ in 7.2.1, while $\mathbf{M_1{*}M_2}$ is an angle opposite (counterclockwise) of $\mathbf{M_2{*}M_1}$ in 7.2.2. A crucial **exception** occurs when $\mathbf{M_1}$ and $\mathbf{M_2}$ are perpendicular to each other: there is no difference between a clockwise 180^0 rotation and a counterclockwise 180^0 rotation sharing the same center (1.3.10)!

All the techniques and observations of this section, including that of the preceding paragraph, stress the closeness between

translation and **rotation**: each of them may be represented as the composition of **two** reflections, and the outcome depends only on whether the angle between them is zero (translation) or non-zero (reflection). It follows at once that every **glide reflection** may be written as the composition of **three** reflections. So we may safely say, knowing that there exist no other planar isometries (section 1.5), that every isometry of the plane is the composition of **at most three reflections**.

Conversely, the **traditional way** of proving that there exist only four types of planar isometries is to show **first** that every isometry of the plane **must** be the composition of at most three reflections: see for example ***Washburn & Crowe***, Appendix I. We certainly provided a classification of planar isometries not relying on this fact in section 1.5; but we will be analysing a translation or rotation into two reflections throughout chapter 7.

As a concluding remark, let us point out another difference between translation and rotation (and the way each of them may be written as a composition $\mathbf{M_2}*\mathbf{M_1}$ of reflections): in the case of a translation, we may vary the position of the parallel mirrors $\mathbf{M_1}$, $\mathbf{M_2}$ but not their distance or common direction; in the case of a rotation, we may vary the directions of $\mathbf{M_1}$, $\mathbf{M_2}$, but not their angle or intersection point.

7.3 Translation $*$ Reflection

7.3.1 Perpendicular instead of parallel. Of course we have already seen a most important special case of this combination in 1.4.2: when the translation and the reflection are parallel to each other, their **commuting** composition is useful and powerful enough to be viewed as an isometry of its own (glide reflection). Another important special case is the one that involves a translation and a reflection that are perpendicular to each other. We have encountered many such cases, the last one provided by 7.2.1: just think of the reflection $\mathbf{M_1}$ followed by the translation $\mathbf{M_2}*\mathbf{M_1}$, yielding the equality $(\mathbf{M_2}*\mathbf{M_1})*\mathbf{M_1} = \mathbf{M_2}*(\mathbf{M_1}*\mathbf{M_1}) = \mathbf{M_2}*\boldsymbol{I} = \mathbf{M_2}$; or of the translation

$\mathbf{M_2 * M_1}$ followed by the reflection $\mathbf{M_2}$, leading to the equality $\mathbf{M_2*(M_2*M_1) = (M_2*M_2)*M_1 = \mathit{I}*M_1 = M_1}$.

Our 'algebraic experimentation' (and appeal to 7.2.1) above suggests that the composition of a reflection **M** and a translation **T** perpendicular to each other is another reflection **parallel** to the original one; this is established below, via another appeal to 7.2.1:

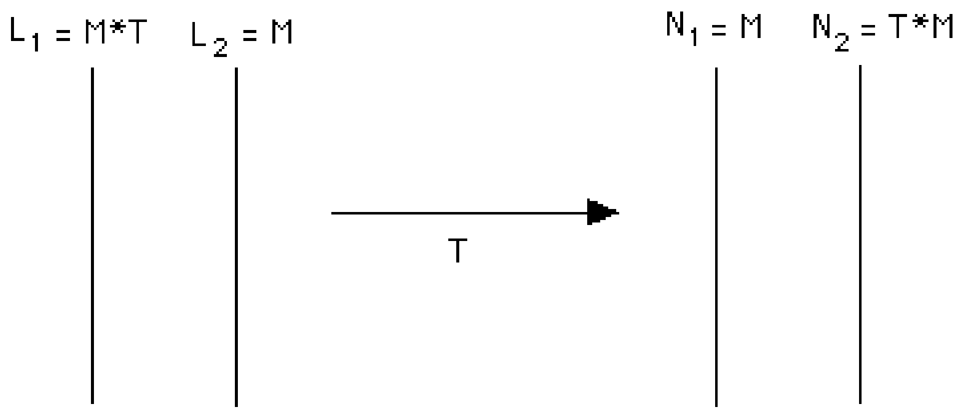

Fig. 7.10

What went on in figure 7.10? We computed **both** compositions $\mathbf{M*T}$ (left) and $\mathbf{T*M}$ (right), writing **T** as a composition of two reflections perpendicular to it (therefore **parallel** to **M**) and at a distance from each other equal to half the length of **T** (7.2.1): in the first case, with **T**'s **second** reflection $\mathbf{L_2}$ being **M**, $\mathbf{M*T}$ equals $\mathbf{L_2*(L_2*L_1) = L_1}$; and in the second case, with **T**'s **first** reflection $\mathbf{N_1}$ being **M**, $\mathbf{T*M}$ equals $\mathbf{(N_2*N_1)*N_1 = N_2}$. (As above, it is crucial that the square of a reflection is the identity isometry ***I***.)

So, we see that a reflection **M** and a translation **T** perpendicular to each other do not commute: when **T** comes first it moves **M** **'backward'** by $|\mathbf{T}|/2$ (figure 7.10, left), and when **T** follows **M** it moves it **'forward'** by $|\mathbf{T}|/2$ (figure 7.10, right); that is, $\mathbf{M*T}$ and $\mathbf{T*M}$ are **mirror images** of each other about **M**. You should try to verify these results, following the method, rather than the outcome, of 7.2.1 and figure 7.8.

7.3.2 Physics again! We come now to the general case of the composition of a reflection **M** and a translation **T**, assuming **M** and **T** to be neither parallel nor perpendicular to each other: it looks complicated, but an old trick from high school Physics is all that is needed! Indeed, **analysing T** into two components, $\mathbf{T_1}$ (perpendicular to **M**) and $\mathbf{T_2}$ (parallel to **M**), we reduce the problem to known special cases; in figure 7.11 you see how $\mathbf{M*T} = \mathbf{M*(T_1*T_2)} = \mathbf{(M*T_1)*T_2} = \mathbf{M'*T_2}$ turns into a **glide reflection** (of axis $\mathbf{M*T_1}$ (at a distance of $|\mathbf{T_1}|/2$ from **M**) and vector $\mathbf{T_2}$):

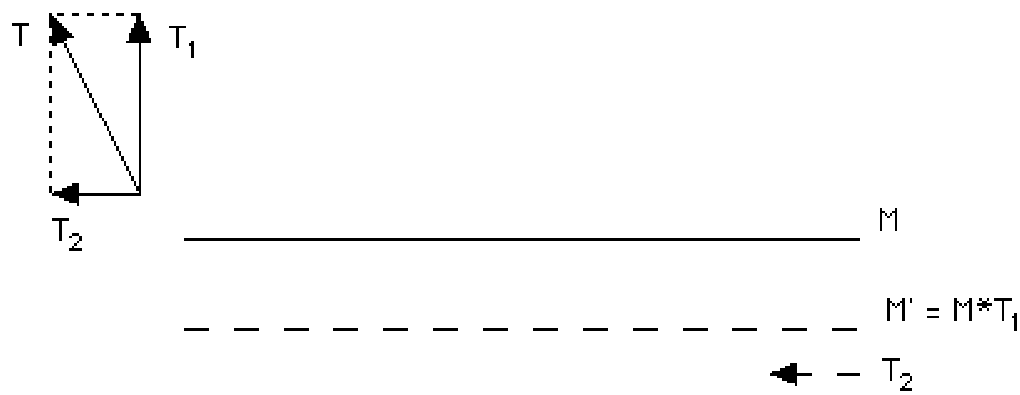

Fig. 7.11

Likewise, $\mathbf{T*M} = \mathbf{(T_2*T_1)*M} = \mathbf{T_2*(T_1*M)} = \mathbf{T_2*M''}$ is a glide reflection (not shown in figure 7.11) of vector $\mathbf{T_2}$ (no change here) and axis **M″** (mirror image of **M′** about **M**, as in 7.3.1). So, in general, the composition of a reflection **M** and a translation **T** is a glide reflection; and a closer look at this section's work shows that it is a reflection if and only if **M** and **T** are perpendicular to each other (that is, precisely when $\mathbf{T_2} = 0$).

7.4 Translation ∗ Glide Reflection

7.4.1 Just an extra translation. This case is so close to the previous one that it hardly deserves its own visual justification. Indeed, let $\mathbf{G} = \mathbf{M*T_0} = \mathbf{T_0*M}$ be the glide reflection, and let **T** be the translation. Then $\mathbf{G*T} = \mathbf{(M*T_0)*T} = \mathbf{M*(T_0*T)}$ and $\mathbf{T*G} = \mathbf{T*(T_0*M)} =$

$(\mathbf{T}*\mathbf{T_0})*\mathbf{M}$. Since $\mathbf{T_0}*\mathbf{T} = \mathbf{T}*\mathbf{T_0}$ is again a translation $\mathbf{T}'$, we have reduced this section to the previous one; and we may safely say that the composition of a translation and a glide reflection is another glide reflection, with their axes parallel to each other (and **identical** if and only if the translation is **parallel** to the glide reflection).

7.4.2 <u>Could it be a reflection?</u> We have run into compositions of non-parallel translations and glide reflections as far back as 6.2.5 and figure 6.13, while studying two-colored **pg** types: we could even say that the **pg**'s **diagonal** translations are 'responsible' for the perpetual repetition of the **vertical** glide reflection axes! And the interaction between the **pg**'s glide reflection and translation is also reflected in the fact that the only **pg** type ($\mathbf{p'_b1g}$) with both color-reversing and color-preserving glide reflection is the only **pg** type that has color-reversing translation (figures 6.4, 6.9, and 6.11).

But a similar observation is possible about two-colored **cm** types: the two types that have color-preserving reflection and color-reversing glide reflection ($\mathbf{p'_cm}$) or vice versa ($\mathbf{p'_cg}$) are precisely those that do have color-reversing translation (figures 6.25-6.28). Could it be that, the same way the **pg**'s 'diagonal' translation takes us from one 'vertical' glide reflection to another, the **cm**'s 'diagonal' translation takes us from 'vertical' reflection to 'vertical' glide reflection (which is to be expected in view of 7.3.2) **and** from 'vertical' glide reflection to 'vertical' reflection? In broader terms, could the composition of a glide reflection and a translation be **'exactly'** a reflection?

The answer is **"yes"**: a translation and a glide reflection may after all create a reflection! And this may be verified not only in the **cm** examples mentioned above, but also though a visit to our newly painted bathroom wall: for example, the composition $\mathbf{MG_1}*\mathbf{T}$ in figure 7.5 is the vertical reflection passing through $\mathbf{R_0}$. How does that happen? A closer look at the interaction between **T** and the hidden glide reflection $\mathbf{MG_1}$'s gliding vector $\mathbf{T_0}$ is rather revealing:

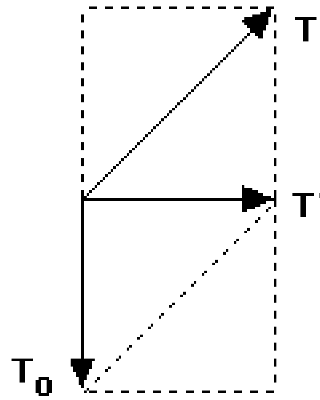

Fig. 7.12

A bit of ‘square geometry’ in figure 7.12 makes it clear that the composition $\mathbf{T}' = \mathbf{T_0} * \mathbf{T}$ is perpendicular to $\mathbf{T_0}$ (and $\mathbf{MG_1}$ as well). But we have already seen (combining 7.3.2 and 7.4.1) that $\mathbf{G} * \mathbf{T}$ is a reflection if and only if $\mathbf{T}'$ is perpendicular to $\mathbf{G}$: this is certainly the case in figures 7.12 & 7.5 (with $\mathbf{G} = \mathbf{MG_1}$).

In general, what relation between the glide reflection **G**’s vector $\mathbf{T_0}$ and the translation vector **T** is equivalent to $\mathbf{G} * \mathbf{T}$ (and therefore, by 7.3.2, $\mathbf{T} * \mathbf{G}$ as well) being a reflection? A bit of simple trigonometry (figure 7.13) shows that it all has to do with the **lengths** $|\mathbf{T_0}|$ and $|\mathbf{T}|$ of $\mathbf{T_0}$ and **T**, as well as the **angle** ϕ between $\mathbf{T_0}$ and **T**. Indeed, all we need is that for the angle $a(\mathbf{T_0}, \mathbf{T}')$ between $\mathbf{T_0}$ and $\mathbf{T}' = \mathbf{T_0} * \mathbf{T}$ to be $\pi/2$ (90^0). But in that case we end up with a **right** triangle of side lengths $|\mathbf{T}|$, $|\mathbf{T_0}|$, and $|\mathbf{T}'|$ and angles $\pi-\phi$ and $\phi-\pi/2$ (figure 7.13); it follows that $|\mathbf{T_0}| = |\mathbf{T}|\times\cos(\pi-\phi) = |\mathbf{T}|\times\sin(\phi-\pi/2)$, so that $|\mathbf{T_0}| = -|\mathbf{T}|\times\cos\phi$ or $|\mathbf{T}| = -|\mathbf{T_0}|/\cos\phi$, where, **inevitably**, $\pi/2 < \phi \leq \pi$.

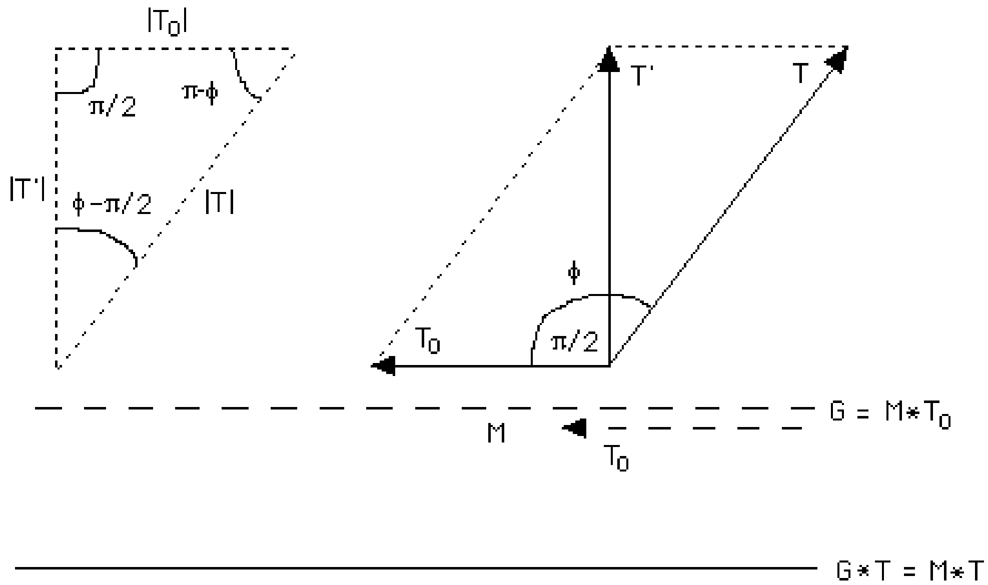

Fig. 7.13

So, to 'annul' the vector $\mathbf{T_0}$ of a glide reflection $\mathbf{G} = \mathbf{M}*\mathbf{T_0}$, all we need is to 'multiply' $\mathbf{G}$ by a translation $\mathbf{T}$ of length $|\mathbf{T}|$ that makes an angle ϕ with $\mathbf{T_0}$ such that $\mathbf{|T_0| = -|T|cos\phi}$. Observe that $\cos\phi < 0$, hence ϕ has to be an obtuse angle (forcing $\mathbf{T}$ to go **'somewhat opposite'** of $\mathbf{T_0}$); also, in view of $|\mathbf{T}| = -|\mathbf{T_0}|/\cos\phi$, the closer ϕ is to $\pi/2$ the longer $\mathbf{T}$ is: $\pi/2 < \phi \leq \pi$ yields $|\mathbf{T_0}| \leq |\mathbf{T}| < \infty$, with $|\mathbf{T}| = |\mathbf{T_0}|$ corresponding to $\phi = \pi$ ($\mathbf{T} = \mathbf{T_0^{-1}}$ and $\mathbf{G}*\mathbf{T} = \mathbf{T}*\mathbf{G} = \mathbf{M}$ -- the rather obvious 'parallel case').

In figures 7.12 & 7.5, $\phi = 135^0$ and $|\mathbf{T}| = -|\mathbf{T_0}|/\cos(135^0) = |\mathbf{T_0}|\sqrt{2}$.

7.5 Rotation * Rotation

7.5.1 Just like two reflections? Counterintuitive as it might seem as first, it turns out that determining the composition of two rotations is about as easy as determining the composition of two reflections. And you will be even more surprised to see that the key to the puzzle lies inside figure 7.10 (that does not seem to have anything to do with rotations)! On the other hand, a figure that is certainly related to rotations is 7.9: we demonstrated there how the composition of two intersecting reflections is a rotation; in this section we will play the game backwards, **breaking** rotations into two intersecting reflections.

So, let's first consider two clockwise rotations $\mathbf{R_A} = (A, \phi_1)$ and $\mathbf{R_B} = (B, \phi_2)$. To compute $\mathbf{R_B * R_A}$ we set $\mathbf{R_A} = \mathbf{M*L}$ and $\mathbf{R_B} = \mathbf{N*M}$, where **L**, **M** are reflection lines intersecting each other at A at an angle $\phi_1/2$ and **M**, **N** are reflection lines intersecting each other at B at an angle $\phi_2/2$; in particular, **M** is the line defined by A and B (figure 7.14), the **common reflection** destined to play the same **'vanishing'** role as in 7.3.1 (and figure 7.10). It is easy now to determine $\mathbf{R_B * R_A} = (\mathbf{N*M})*(\mathbf{M*L}) = \mathbf{N*L}$ as a **rotation** centered at C (composition of two reflections intersecting each other at C).

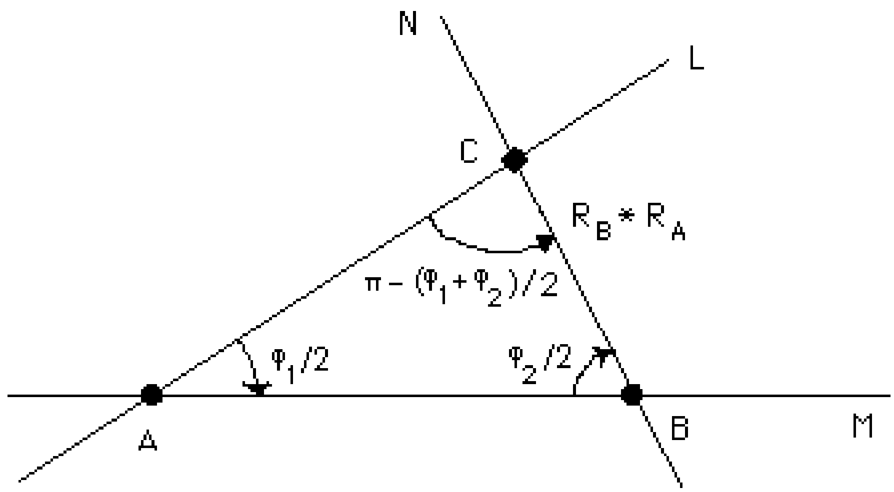

Fig. 7.14

So, it was quite easy to determine $\mathbf{R_B * R_A}$'s center, and there is nothing 'special' about it. But there is another potential surprise when it comes to $\mathbf{R_B * R_A}$'s angle: although both $\mathbf{R_A}$ and $\mathbf{R_B}$ are taken clockwise, $\mathbf{R_B * R_A} = \mathbf{N*L}$ ends up being counterclockwise (going from **L** toward **N**)! How about $\mathbf{R_A * R_B}$ then, with each of $\mathbf{R_A}$ and $\mathbf{R_B}$ taken counterclockwise this time? Or $\mathbf{R_B * R_A}$ with one rotation taken clockwise and the other counterclockwise, and so on? Taking **both** order and orientation into account, there exist eight possible cases (all based on **M**'s 'elimination'), shown in figure 7.15 (arguably the most important one in the entire chapter or even book):

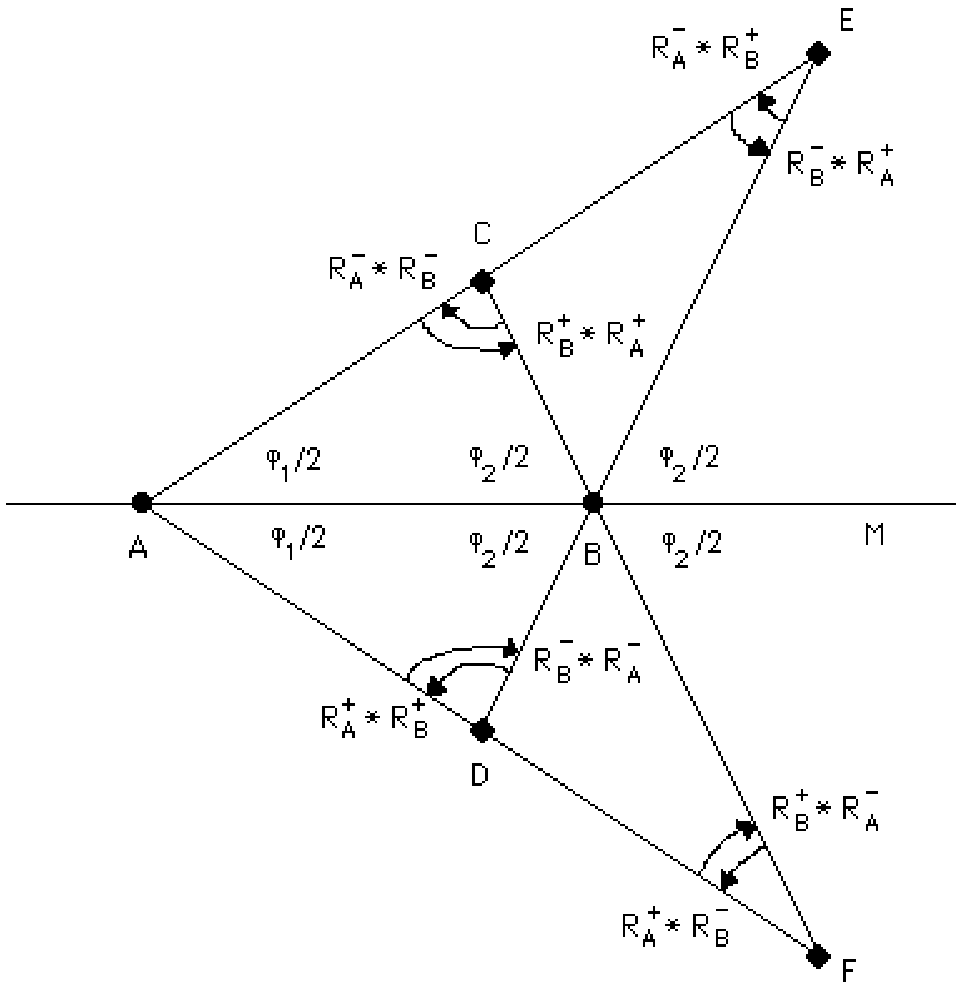

Fig. 7.15

As in 7.0.4, clockwise rotations are marked by a **+** superscript and counterclockwise rotations are marked by a **-** superscript, while the **arrows** pointing to each composition angle indicate its orientation. The example shown in figure 7.14 is therefore $\mathbf{R_B^+ * R_A^+}$; notice how each of the four centers C, D, E, F is **shared** by two compositions. Notice that the four rotations centered at C and D have angles equal to $2\times\angle ACB = 2\times(180^0-(\phi_1+\phi_2)/2) = 360^0-\phi_1-\phi_2$, which is **equivalent** to $\boldsymbol{\phi_1+\phi_2}$ (with **reversed** orientation, via $\phi_1 < 180^0$ and $\phi_2 < 180^0$); and the four compositions centered at E and F have angles equal to $2\times\angle CFA = 2\times(180^0-\angle CAF-\angle ACF) = 2\times(180^0-\angle CAD-\angle ACB) =$

$2\times(180^0-\phi_1-(180^0-(\phi_1+\phi_2)/2)) = 2\times(-(\phi_1/2)+(\phi_2/2)) = \boldsymbol{\phi_2-\phi_1}$ (which would have been $\boldsymbol{\phi_1-\phi_2}$ in case ϕ_1 was bigger than ϕ_2).

7.5.2 When the angles are equal. When $\boldsymbol{\phi_1 = \phi_2}$, our preceding analysis suggests that the angle between AE and BE (or AF and BF) in figure 7.15 is zero; but AE and BE are certainly **distinct**, passing through two distinct points A and B: indeed the two lines, making equal angles with **M**, should be **parallel** to each other, with E and F 'pushed' all the way to **infinity**! In simpler terms, when two rotations $\mathbf{R_A}$, $\mathbf{R_B}$ have **equal** angles of **opposite** orientation (one clockwise, one counterclockwise) their composition is a **translation** (composition of parallel reflections, see 7.2.1). [Notice (figure 7.15) that E and F act as centers precisely for those product rotations where one factor is counterclockwise and the other one is clockwise.]

Of course we do not need something as complicated and thorough as figure 7.15 to conclude that the composition of two rotations of equal, opposite angles is a translation: a simple modification of figure 7.14 suffices!

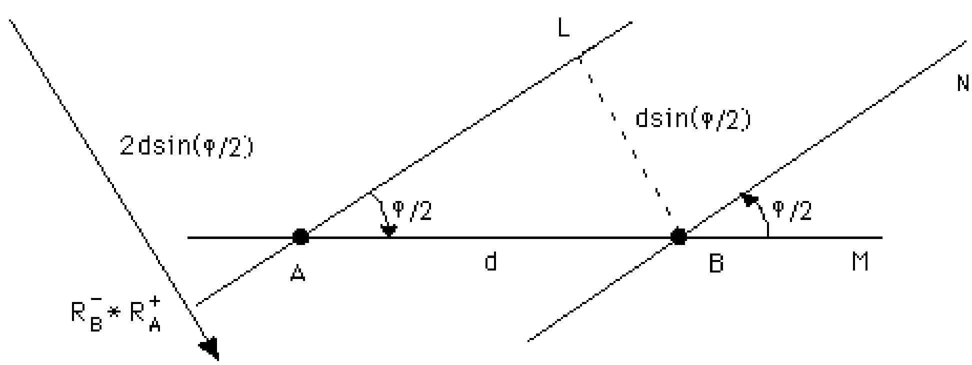

Fig. 7.16

With $\mathbf{R_A^+} = (A, \phi) = \mathbf{M*L}$ and $\mathbf{R_B^-} = (B, \phi) = \mathbf{N*M}$, **L** and **N** become parallel to each other (figure 7.16), therefore $\mathbf{R_B^-*R_A^+} = \mathbf{N*L}$ is a translation perpendicular to them (7.2.1). And since the distance between **L** and **N** is $|AB|\sin(\phi/2) = d\sin(\phi/2)$ (figure 7.16), the length of the translation vector is $2d\sin(\phi/2)$.

Once again, viewing a translation as a rotation the center of which is that mysterious 'point at infinity' (3.2.5) turns out to make a lot of sense!

7.5.3 The case of half turn. There is another way of destroying the **quadrangle** of figure 7.15: reduce it to a **triangle** by forcing the lines DE and CF to be one and the same, which would happen if and only if they are both perpendicular to **M** at B, that is if and only if $\boldsymbol{\phi_2} = \mathbf{180^0}$. Other than reducing the number of product rotations from eight to four, and the number of intersection points (rotation centers) from four to two, making one of the two rotations a half turn would not have any other consequences. But if **both** rotations are 180^0 then there are **no intersections** at all, and the number of compositions is further reduced from four to two: with angle orientation no longer an issue, both $\mathbf{R_A * R_B}$ and $\mathbf{R_B * R_A}$ are now **translations** of vector length 2d (figure 7.16 with $\phi = 180^0$).

7.5.4 An important example. How about the 'surviving' rotations of figure 7.15 when $\phi_1 = \phi_2$? Let's look at the case $\phi_1 = \phi_2 = \mathbf{60^0}$, where two sixfold centers at A and B generate counterclockwise and clockwise rotations of $\phi_1 + \phi_2 = \mathbf{120^0}$ at C and D (figure 7.17), as well as four translations that we will not be concerned with. With **M**, **N**, and **L** as in figure 7.14, and **N′**, **L′** being the mirror images of **N**, **L** about **M**, the four 120^0 rotations may be written as **N∗L**, **L′∗N′** (clockwise) and **L∗N**, **N′∗L′** (counterclockwise). Everything is shown in figure 7.17, and it is clear that the four centers A, B (60^0) and C, D (120^0) form a **rhombus**.

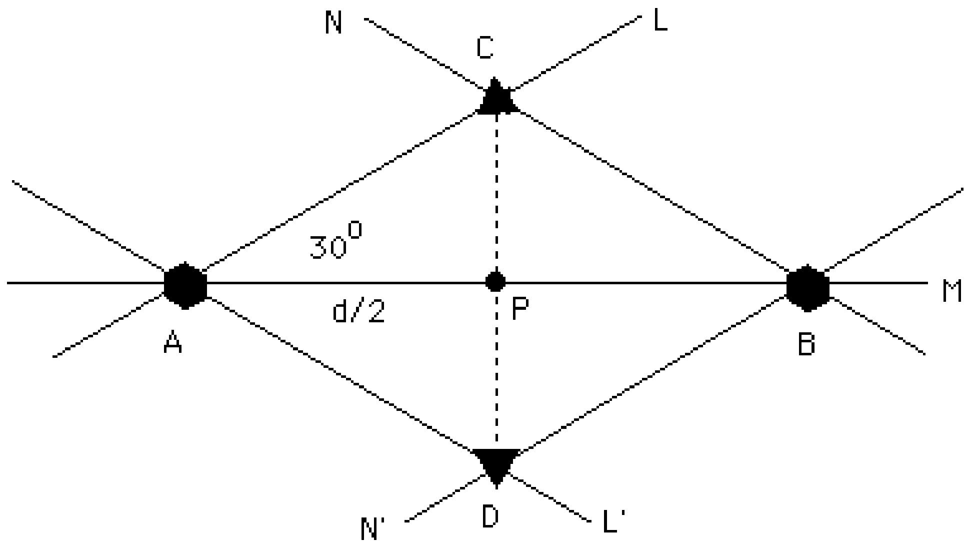

Fig. 7.17

So, any two sixfold centers A, B are bound to create two threefold centers C, D -- **but not vice versa**! What is the location of C (or D) with respect to A and B? With $|AB| = d$ and P the midpoint of AB, simple trigonometry in PAC establishes $|PC| = |AP|\tan 30^0 = d/(2\sqrt{3})$. It follows that $|CD| = d/\sqrt{3}$ and $|AD| = |AC| = \sqrt{|PA|^2 + |PC|^2} = \sqrt{d^2/4 + d^2/12} = d/\sqrt{3}$: the triangle ACD is **equilateral**! (Notice that ACBD will be a rhombus whenever $\phi_1 = \phi_2$, but ACD (and BCD) will be equilateral **if and only if** $\phi_1 = \phi_2 = 60^0$.)

All this begins to look rather familiar: didn't we talk about that rhombus of sixfold centers when we classified two-colored **p6m** types (6.17.3 & 6.17.4, figures 6.134-6.138)? The two rhombuses are **similar**, except that the one in 6.17.3 consists of **four** sixfold centers, while the one we just produced involves **two** sixfold and **two** threefold centers: where does the 6.17.3 rhombus come from? To answer this question, we simply adapt the quadrangle of figure 7.15 with $\boldsymbol{\phi_1 = 60^0}$ and $\boldsymbol{\phi_2 = 120^0}$; that is, we determine the 'total combined effect' of a sixfold center (A) and a threefold center (B), shown (figure 7.18) in the context of the **beehive**:

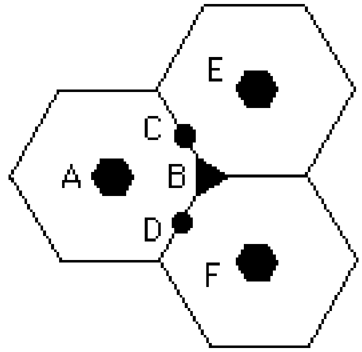

Fig. 7.18

Starting with centers A and B as above we produced two **180^0** ($\phi_1+\phi_2$) centers (C and D) and two **60^0** ($\phi_2-\phi_1$) centers (E and F). So, now we have three sixfold centers: where is the **fourth** one? Well, the answer lies in a combination of figures 7.17 and 7.18: sixfold centers E and F are bound (figure 7.17) to produce another threefold center B′, mirror image of B about EF; and then E (or F) and B′ will have to create the 'missing' sixfold center A′, A's mirror image about EF -- in the same way A and B produce E (and F) in figure 7.18!

Let's summarize the situation a bit: we may 'start' with two sixfold centers that create two threefold centers (figure 7.17), hence two additional sixfold centers (figure 7.18 plus discussion); or 'start' with one sixfold center and one threefold center that create two additional sixfold centers (figure 7.18), hence another threefold center (figure 7.17), and then a fourth sixfold center (figure 7.18 again). It seems rather clear that the first approach, summarized in figure 7.19 below, makes more sense:

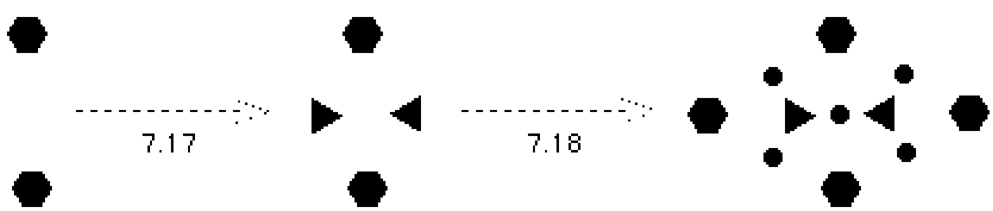

Fig. 7.19

Notice that we have removed not only the labels of the various centers, but the beehive as well: indeed, since we have created its lattice using **only** sixfold rotations, the lattice created in figure 7.19 is **also** the rotation center lattice of a **p6**; after all, the **p6** and the **p6m** are no different when it comes to their lattices of rotation centers (6.16.1).

The process of figure 7.19 can go on to create the full lattice shown in figure 4.5 (right); the next step involves compositions of **'peripheral'** sixfold and twofold centers, generating new threefold centers. The only question that remains is: could we have 'started' with **only one** sixfold center instead of two? The answer is "yes", provided that we seek some help from **translation**: as figure 7.18 shows, F is E's image under the pattern's **minimal** vertical translation (**T**); and, following 4.0.4 (Conjugacy Principle), **T**(E) = F **has** to be a sixfold center! [Attention: as in 4.0.4 again, **T**(E) is not the same as **T∗E** or **E∗T**, where **E** stands for the sixfold rotation(s) centered at E; we do **not** need **compositions** of translation and rotation (studied in the next section) to 'create' the beehive's lattice -- but we **do** need them to 'create' the bathroom wall's lattice (7.6.3)!]

7.6 Translation ∗ Rotation

7.6.1 A trip to infinity. What happens as A moves further and further westward in figure 7.14? Clearly **L** becomes 'nearly parallel' to **M** and the rotation angle ϕ_1 approaches zero; 'at the limit', when A has 'reached infinity', **L** and **M** are **parallel** to each other and the clockwise rotation $\mathbf{R_A}$ = **M∗L** becomes a **translation T** = **M∗L**:

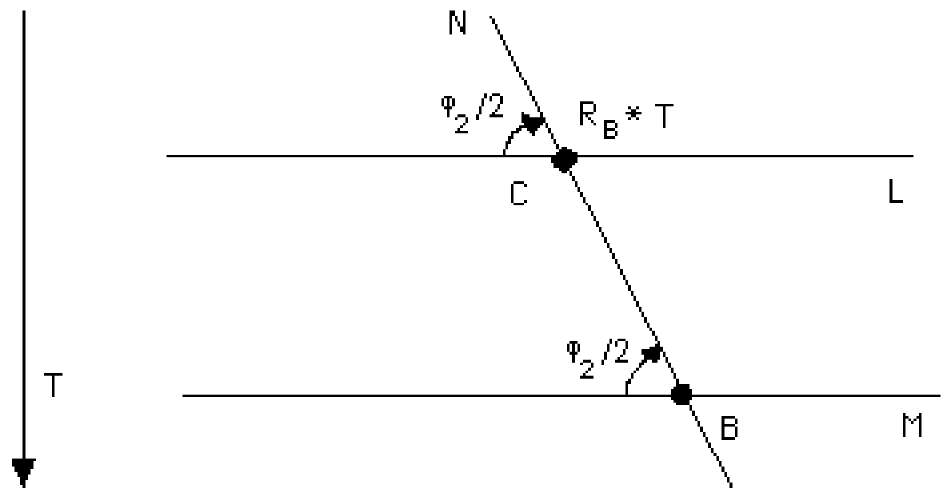

Fig. 7.20

Just as in figure 7.14, and with $\mathbf{R_B} = \mathbf{N*M}$ still a clockwise ϕ_2 rotation, the composition $\mathbf{R_B*T} = \mathbf{N*L}$ is now a **clockwise** rotation, centered at C, the point of intersection of **N** and **L**. Since **L** and **M** are parallel to each other, the angle between **L** and **N** is still $\phi_2/2$, therefore $\mathbf{R_B*T}$'s angle remains equal to ϕ_2. As for the location of $\mathbf{R_B*T}$'s center, that is fully determined via $|BC| = |\mathbf{T}|/(2\sin(\phi_2/2))$, a relation that has in essence been derived in figure 7.16.

7.6.2 Our old example. How does 7.6.1 apply to the composition $\mathbf{T*R_0}$ of 7.0.3? We demonstrate this below, in the context of figure 7.1, blending into it figure 7.20:

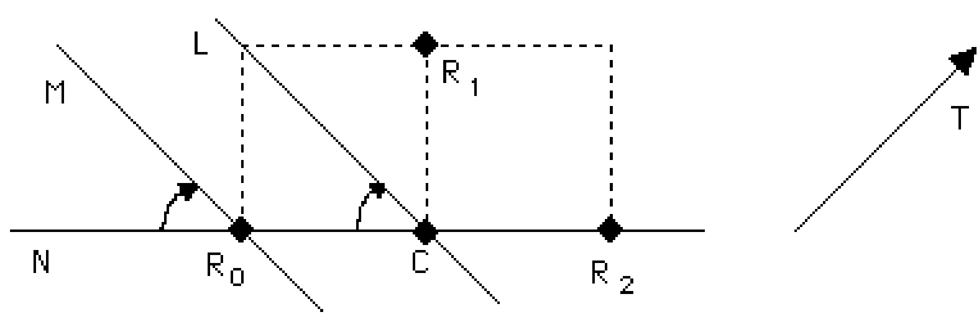

Fig. 7.21

With clockwise $\mathbf{R_0} = \mathbf{M*N}$ and $\mathbf{T} = \mathbf{L*M}$, $\mathbf{T*R_0}$ is equal to $\mathbf{L*N}$, a clockwise 90^0 rotation centered at C, intersection point of **L** and **N**.

7.6.3 An important pentagon. So, we have established that the composition of a translation **T** and a rotation **R** = (K, ϕ) is again a rotation by ϕ about another center. But, just as we did in 7.5.1, we observe here that the final outcome of the composition depends on the order in the operation (**R$*$T** versus **T$*$R**), the rotation's orientation (**R** clockwise versus **R** counterclockwise), and the translation's sense (**T** versus $\mathbf{T^{-1}}$). Again, there exist **eight** possible combinations sharing **four** rotation centers (C, D, E, F), all featured in figure 7.22 (that parallels figure 7.15, with $\mathbf{R_A}$ replaced by **T**):

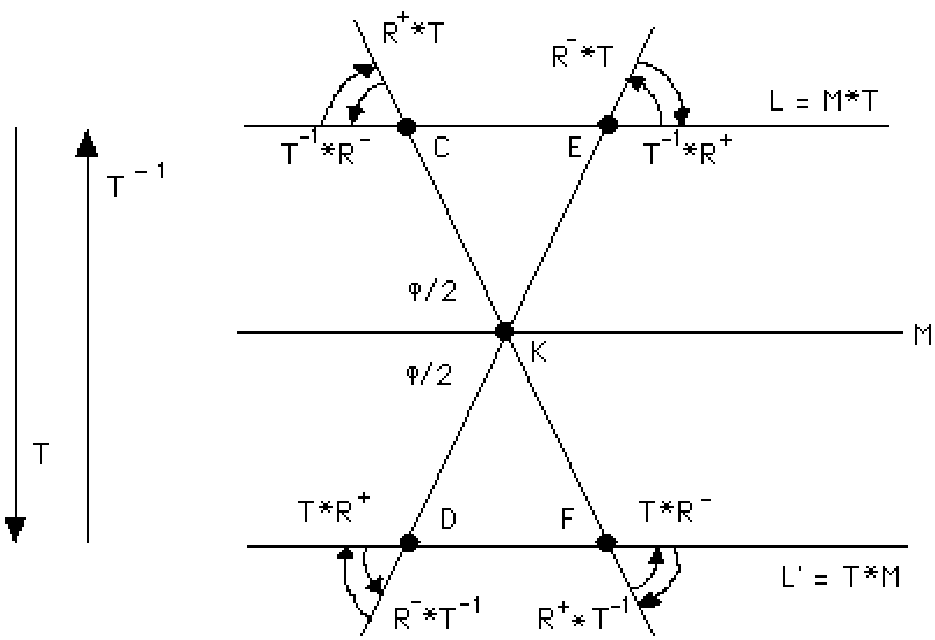

Fig. 7.22

As in figure 7.15, each angle's orientation is indicated by arrows pointing to it; all rotation angles are equal to ϕ, a fact that may be derived from our findings in 7.5.1 (with $\phi_1 = 0$ and $\phi_2 = \phi$), of course.

The five rotation centers (K, C, D, E, F) in figure 7.22 form a very symmetrical, non-convex **'pentagon'** -- a more 'scientific' term is ***quincunx*** -- that may remind you of the number **5**'s standard representation on **dice**! We have already seen it, certainly without noticing, in figure 7.19 (right): over there it stands for a 'formation' of twofold centers in a **p6** lattice, all of them obtained as compositions of **‘higher’** rotations. Should that lattice have been allowed to grow further, we would have certainly seen similar pentagons formed by sixfold centers, as well as rectangles formed by threefold centers; see also figure 4.2, and figure 7.25 further below. All those **p6** centers had been obtained by way of composition of **rotations**, starting from two sixfold centers -- or, if you prefer, **one** sixfold center and an image of it under translation. Now we derive the **p4** and the **p3** lattices of rotation centers **starting** from a ‘pentagon’: that is, we start with **one** fourfold or threefold rotation and **compose** it with the pattern’s **minimal ‘vertical’** translation, in the spirit of figure 7.22.

First, the **p4** lattice, shown initially in its **‘Big Bang’** (pentagonal) stage, then with some twofold centers created by the fourfold centers, and, finally, with additional fourfold centers created by one fourfold and one twofold center:

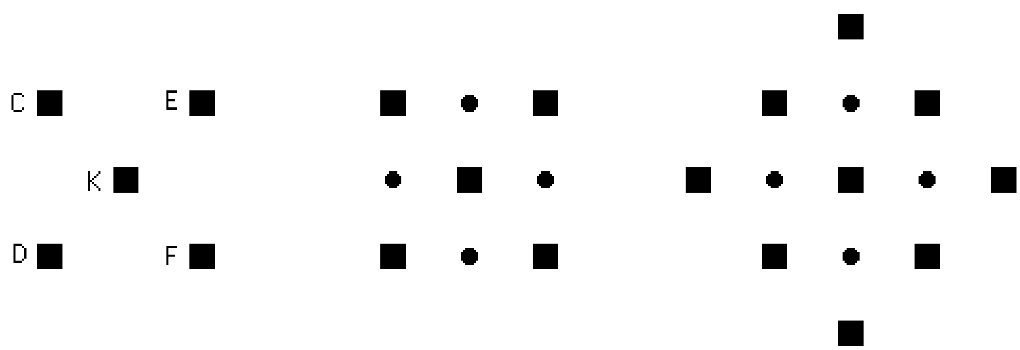

Fig. 7.23

Next comes the **p3** lattice, where threefold centers keep creating nothing but threefold centers:

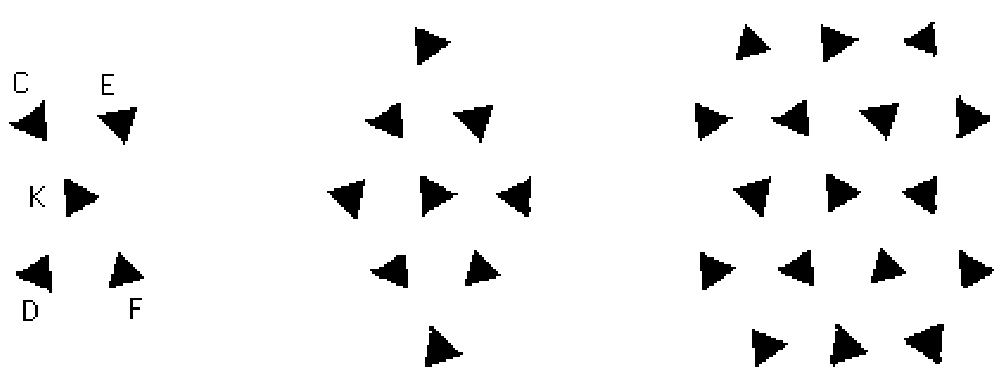

Fig. 7.24

How do these lattices relate to the ones shown in figures 4.59 (**p4**) and 4.68 (**p3**)? Looking at their 'fundamental pentagon' KCDEF (figure 7.22) in the context of those figures, as well as figures 7.23 & 7.24, we observe the following: the **p4** pattern has no translation taking K to any of the other four vertices, but it certainly has translations interchanging any two vertices among C, D, E, F (**'two kinds'** of fourfold centers, as indicated in figure 4.59); and the **p3** pattern has no translation interchanging any vertices from the 'first column' (C, D) with any vertices from either the 'third column' (E, F) or K (**'three kinds'** of threefold centers, as indicated in figure 4.68). Notice that these observations are fully justified by the pentagon's very 'creation': vector CD is by definition the pattern's **minimal** translation, and this rules out vector KF (but certainly **not** vector CF) in the case of **p4** (figure 7.23, left); CD's minimality also rules out vector CE (**hence** vector CF as well, for CE = CF−CD) in the case of **p3** (figure 7.24, left)!

Let's now look at the **p6**'s 'first three stages of creation', composing the 'first' rotation with a translation (as in the cases of **p4** and **p3**, figures 7.23 and 7.24, respectively) rather than another rotation (as in figure 7.19):

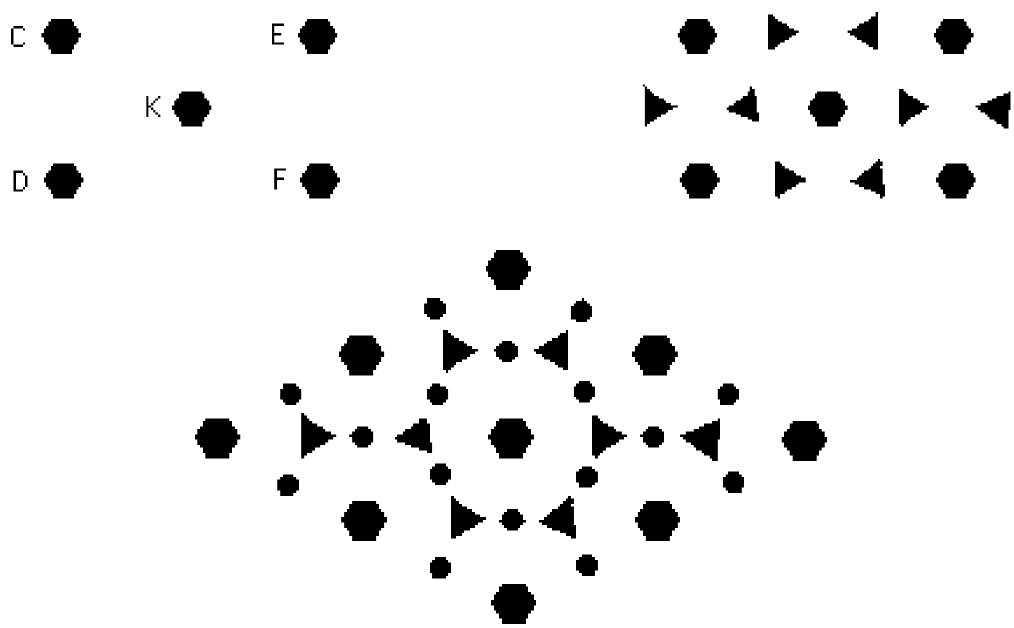

Fig. 7.25

This is of course an **alternative** way of looking at **p6**'s lattice: you can't miss the **four** copies of the rhombus in figure 7.19 packed inside the big rhombus of figure 7.25! But more illuminating is figure 7.25's pentagon, showing that there exists only **'one kind'** of sixfold centers: observe how any two of its vertices (labeled as in figure 7.22 always) are interchangeable via one of the **p6**'s translations -- indeed all edges but CE (and DF) are **'equivalent'** to either CD or 2×CD, while the above noticed CE = CF−CD allows CE (and DF) as well.

7.6.4 <u>When the pentagon collapses.</u> Exactly as in 7.5.3 and figure 7.15, a 180^0 rotation would make lines DE and CF one and the same in figure 7.22, allowing for only **one** intersection (and half turn center) with each of **L** and **L′**. So, $\phi = 180^0$ makes a trio of **collinear** points ($C \equiv E$, K, $D \equiv F$, with $|KC| = |KD| = |\mathbf{T}|/2$) out of the pentagon of figure 7.22. And yet there exists a 'starting pentagon' in every **p2** pattern, created by **one** half turn **R** and **two** non-parallel translations $\mathbf{T_1}$, $\mathbf{T_2}$:

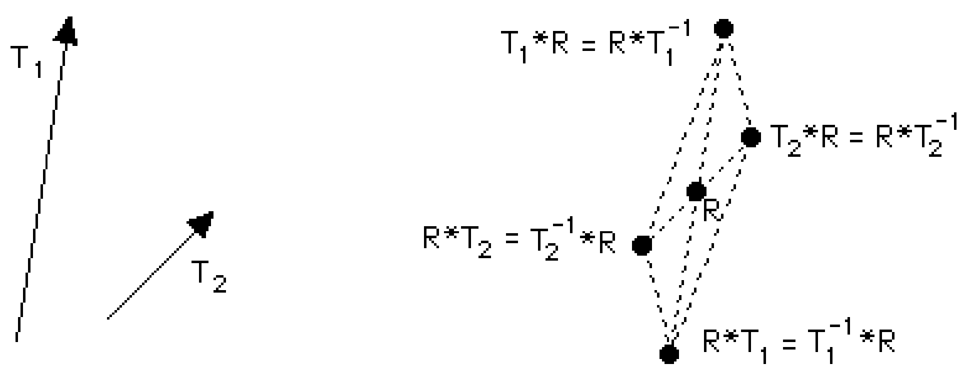

Fig. 7.26

We leave it to you to check the details in figure 7.26 and extend its **'oblique'** pentagon into the full **p2** lattice of half turn centers; keep in mind that many **new** half turn centers may **only** be created with the help of **translations**: after all the composition of any two half turns is a translation, not a half turn (7.5.3)!

Notice the importance of having two non-parallel, **'minimal'** translations available in the case of the **p2** pattern: assuming existence of translation in **one** direction only, plus 180^0 rotation, we are only guaranteed a **p112** (border) pattern -- half turn centers endlessly multiplied by the translation along a single line! On the other hand, the pentagon of rotation centers created by one threefold (**p3**) or fourfold (**p4**) or sixfold (**p6**) rotation and one minimal translation is bound (7.5.2) to produce translations in **three** (and eventually infinitely many) additional directions.

7.7 Rotation ∗ Reflection

7.7.1 When the center lies on the mirror. A comparison between the previous two sections shows that rotation and translation are of rather similar mathematical behavior. This is of course due to the fact that each of them is the composition of two reflections, a fact that also lies behind the proximity of this section and section 7.3; in particular, figure 7.27 below may be seen as a **'copy'** of figure 7.10:

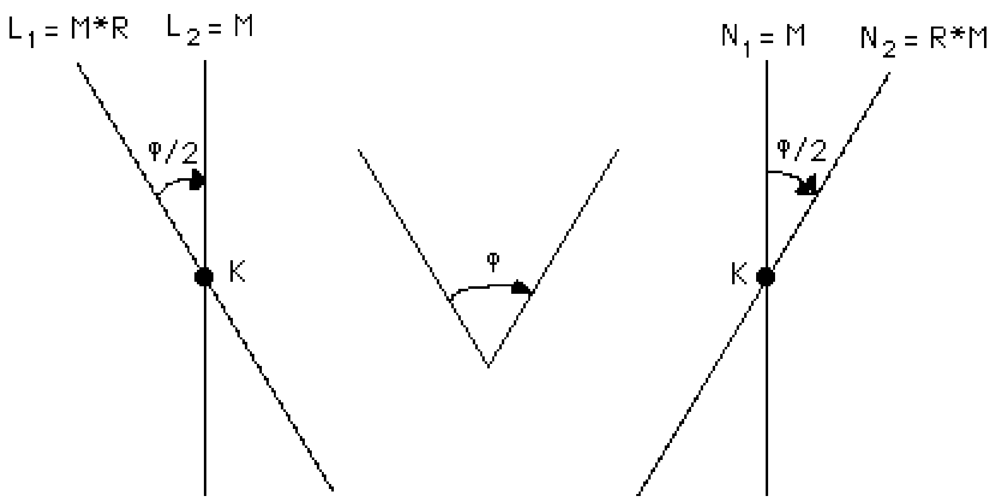

Fig. 7.27

On the left is the composition **M∗R** of a **clockwise** rotation **R** = (K, ϕ) followed by a reflection **M**, while on the right is **R∗M**; as figure 7.27 makes it clear, **R**'s center K lies on **M**. As in section 7.3 and figure 7.10, we analysed **R** as $\mathbf{L_2 * L_1}$ with $\mathbf{L_2} = \mathbf{M}$ in the first case, and as $\mathbf{N_2 * N_1}$ with $\mathbf{N_1} = \mathbf{M}$ in the second case; in both cases **M** cancels out, exactly as in figure 7.10.

Adopting (as in previous sections) the notations $\mathbf{R^+}$ and $\mathbf{R^-}$ for **R** taken clockwise and counterclockwise, respectively, we observe (in the context of figure 7.27 always) that $\mathbf{M}*\mathbf{R}^+ = \mathbf{R}^-*\mathbf{M} = \mathbf{L}_1$ and $\mathbf{M}*\mathbf{R}^- = \mathbf{R}^+*\mathbf{M} = \mathbf{N}_2$. So, the composition of a rotation and a reflection passing through the rotation center is always another reflection **'tilted'** by half the rotation angle, and still passing through the rotation center.

7.7.2 The general case. What happens when the rotation center does not lie on the reflection axis? This one looks a bit complicated! Perhaps some initial experimentation, in the context of a four-colored beehive this time, might help:

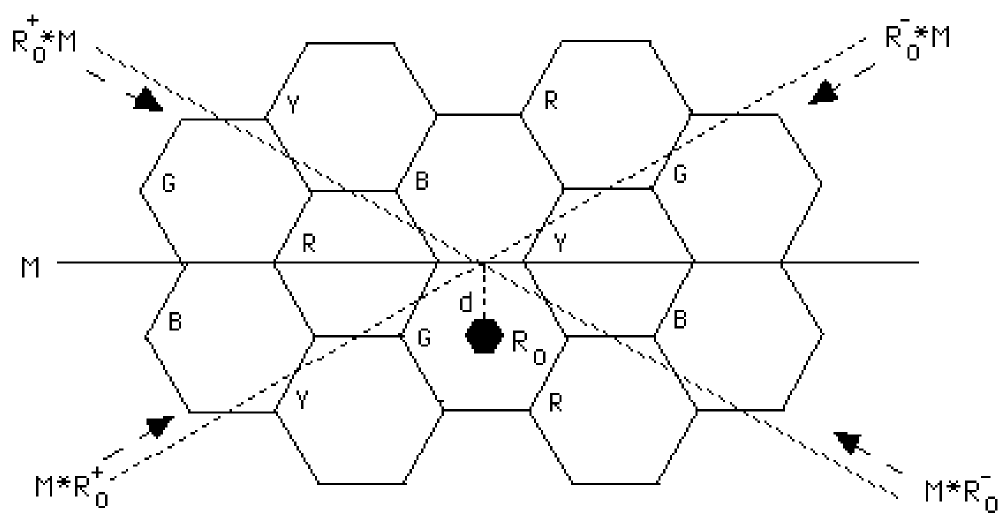

Fig. 7.28

Employing the methods of 7.0.3-7.0.4 if necessary, you may derive all **four** possible combinations between the reflection **M** and the sixfold rotation $\mathbf{R_0}$ in figure 7.28: they are **glide reflections** of gliding vectors of equal length, their **two** axes being mirror images of each other about **M**; at a more subtle level, observe how, in all four cases, the vector's **sense** is such that the glide reflection and the rotation **'turn the same way'**.

Let's now **justify** the outcome of the compositions in figure 7.28 through a specific example of the type $\mathbf{R}^+*\mathbf{M}$, where $\mathbf{R}^+ = (K, \phi^+)$ and K **not** on **M** (figure 7.29). We write $\mathbf{R}^+ = \mathbf{L}_2*\mathbf{L}_1$, where $\mathbf{L}_1$ is now

parallel to **M**, so that $\mathbf{R^+ * M} = (\mathbf{L_2 * L_1}) * \mathbf{M} = \mathbf{L_2} * (\mathbf{L_1 * M}) = \mathbf{L_2 * T}$, where **T** is a translation **perpendicular** to **M**, going from **M** toward $\mathbf{L_1}$ and of length **twice** the distance d between K and **M** (7.2.1).

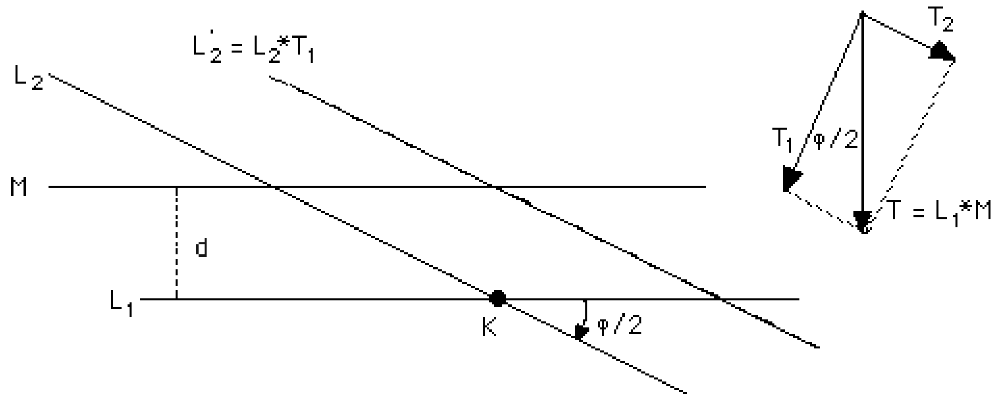

Fig. 7.29

From here on, we appeal to section 7.3: we write $\mathbf{T} = \mathbf{T_1 * T_2}$ with $\mathbf{T_1}$ **perpendicular** to $\mathbf{L_2}$ and $\mathbf{T_2}$ **parallel** to $\mathbf{L_2}$ (7.3.2), so that $\mathbf{L_2 * T_1}$ is a reflection $\mathbf{L'_2}$ parallel to $\mathbf{L_2}$ and at a distance $|\mathbf{T_1}|/2$ from it and 'backward' with respect to $\mathbf{T_1}$ (7.3.1); it follows at long last that $\mathbf{R^+ * M} = \mathbf{L_2 * T} = \mathbf{L'_2 * T_2}$ is indeed a glide reflection (of axis $\mathbf{L'_2}$ and vector $\mathbf{T_2}$). Since $a(\mathbf{T}, \mathbf{T_1}) = a(\mathbf{L_1}, \mathbf{L_2}) = \phi/2$ (because $\mathbf{T}$, $\mathbf{T_1}$ are perpendicular to $\mathbf{L_1}$, $\mathbf{L_2}$, respectively), $\mathbf{T_2}$'s length is $|\mathbf{T}| \times \sin(\phi/2) = 2d \times \sin(\phi/2)$: you may verify this in the case of figure 7.28, with $\phi = 60^0$ and $|\mathbf{T_2}| = d = r\sqrt{3}/2$, where r is the regular hexagon's side length.

7.7.3 <u>A sticking intersection point.</u> Figure 7.29 makes it visually clear that the intersection point of **M** and $\mathbf{L'_2}$ is K's projection on **M**. And figure 7.28 provides further evidence: the two glide reflection axes' **common** point is none other than $\mathbf{R_0}$'s projection on **M**! But how do we **prove** this fact? The proof is a bit **indirect**: starting from the four lines of figure 7.29, we let B be the point where the **perpendicular** to **M** at A (**intersection point** of **M** and $\mathbf{L'_2}$) intersects $\mathbf{L_2}$ (figure 7.30); and then we prove that B **has** to be the **same** as K (intersection point of $\mathbf{L_1}$ and $\mathbf{L_2}$) by showing |AB| to be equal to d (and **implying** that B lies on $\mathbf{L_1}$, too)!

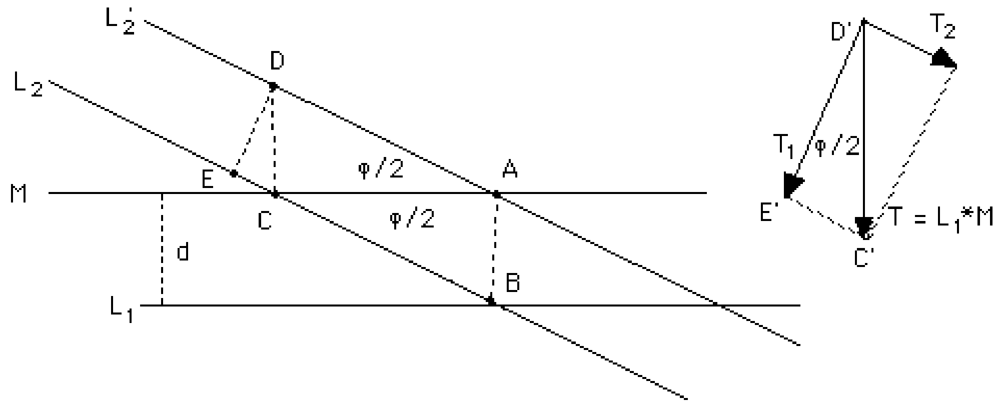

Fig. 7.30

To do this, we need two more lines: a line **perpendicular** to **M** at C (**M**'s intersection point with $\mathbf{L_2}$), intersecting $\mathbf{L'_2}$ at D; and a line **perpendicular** to $\mathbf{L'_2}$ at D that intersects $\mathbf{L_2}$ at E. Perpendicularities show then the angle CDE to be equal to $\angle$CAD = $\phi/2$ and the two right triangles EDC and E′D′C′ to be **similar** (figure 7.30). It follows that $\frac{|DE|}{|DC|} = \frac{|D'E'|}{|D'C'|}$, so that $|DC| = \frac{|DE| \times |D'C'|}{|D'E'|} = \frac{(|\mathbf{T_1}|/2) \times (2d)}{|\mathbf{T_1}|}$ = d. Now ABCD is by **assumption** ($\mathbf{L'_2}$ is parallel to $\mathbf{L_2}$, hence AD is parallel to BC) and **construction** (both AB and CD are perpendicular to **M**, hence parallel to each other) a **parallelogram**, therefore |AB| = |CD| = d.

We can finally state that the composition of a rotation **R** = (K, ϕ) and a reflection **M** at a distance d from K is a glide reflection **G** of axis passing through K's projection on **M** and gliding vector of length $2d \times \sin(\phi/2)$, intersecting **M** at an angle $\phi/2$.

7.7.4 <u>Could it pass through the center?</u> Figures 7.28 & 7.29 may for a moment give you the impression that the glide reflections produced by the combination of a rotation and a reflection cannot possibly pass through the rotation center: once again the case of **half turn** comes as a surprise! Not as a complete surprise though, as this situation (where the two glide reflection axes of figure 7.28 become one and the same) is characteristic of the **pma2** and **pmg**

patterns, where ‘vertical’ reflections ‘multiplied’ by half turns produce ‘horizontal’ glide reflection(s) passing through their centers: at long last, our **‘two as good as three’** observations in 2.6.3 begin to make full sense!

Notice, along these lines, that the relations $\mathbf{M}*\mathbf{R} = \mathbf{G}$ and $\mathbf{R}*\mathbf{M} = \mathbf{G}^{-1}$, where **R** is a **half turn**, yield (by way of ‘multiplication’ of each side by **R** and **M**, respectively, and $\mathbf{R}^2 = \mathbf{M}^2 = \boldsymbol{I}$) the relations $\mathbf{G}*\mathbf{R} = \mathbf{M} = \mathbf{R}*\mathbf{G}^{-1}$ and $\mathbf{M}*\mathbf{G} = \mathbf{R} = \mathbf{G}^{-1}*\mathbf{M}$: these represent special cases of the next two sections and also illuminate further, if not completely, the structure of the **pma2** and **pmg** patterns!

7.8 Rotation $*$ Glide Reflection

7.8.1 Just a bit of extra gliding. First a rather familiar example:

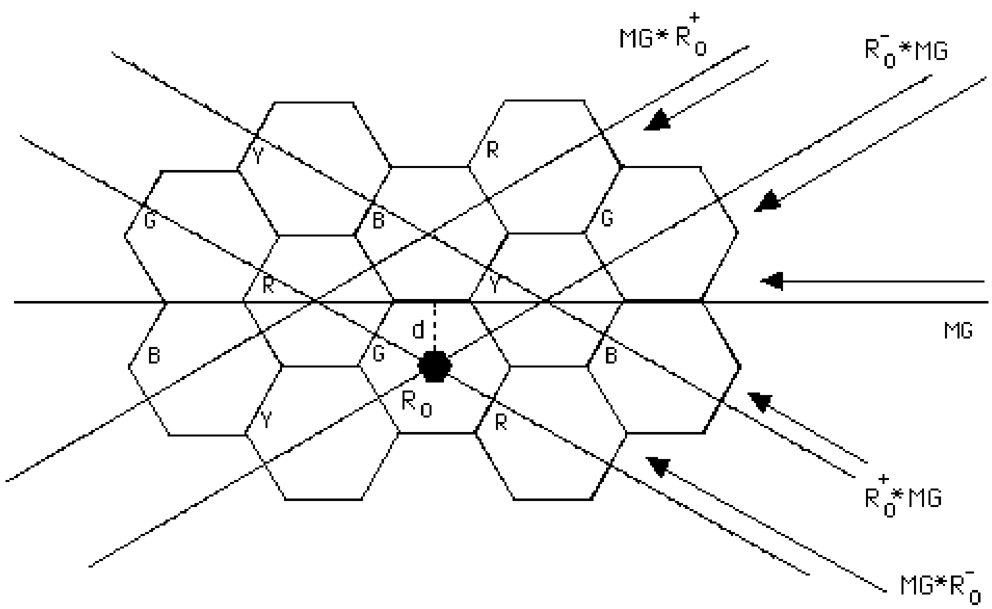

Fig. 7.31

What went on? There has been some slight **‘disturbance’** of figure 7.28, hasn’t it? All we did was to replace the reflection **M** by the hidden glide reflection **MG**, and then ... the glide reflection axes got scattered away from the safety of $\mathbf{R_0}$’s projection onto **M** ... into the four points of the horizon -- in fact two of them ended up passing through $\mathbf{R_0}$ itself, despite the rotation being 60^0 rather than 180^0 (7.7.4)!

To get a better understanding of the situation, it would be helpful to see what happens when **MG** is replaced by its inverse:

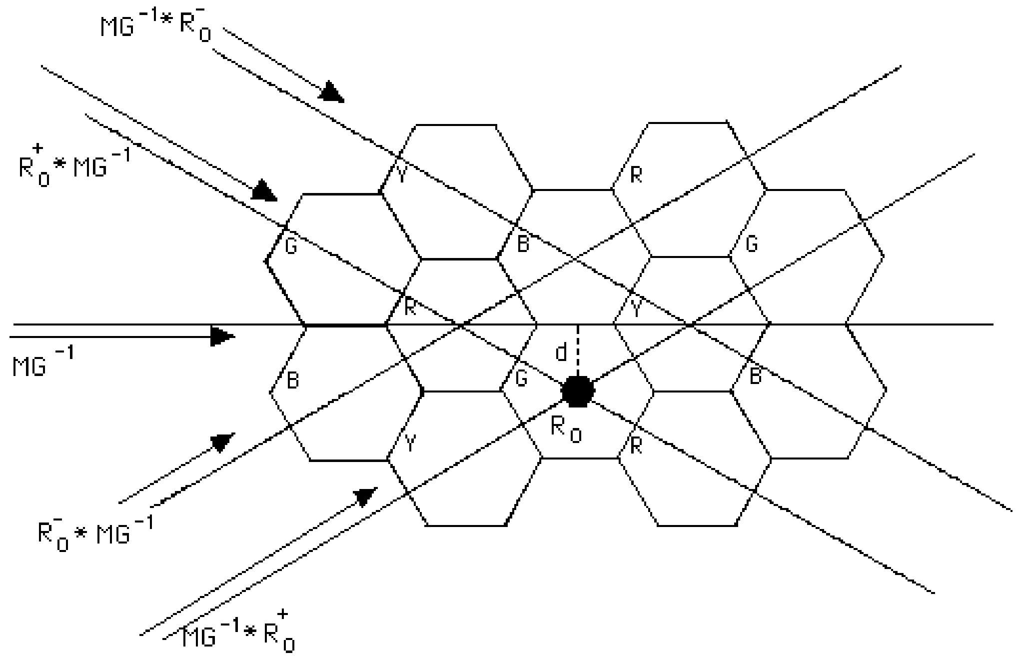

Fig. 7.32

In case that was not already clear through the comparison of figures 7.28 and 7.31, figure 7.32 certainly proves that the glide reflection vector has **'the last word'**: that should be intuitively obvious, and we go on to articulate it right below.

Let **R** be the rotation, and **G** = **M**∗**T** = **T**∗**M** the glide reflection. Then **R**∗**G** = (**R**∗**M**)∗**T** and **G**∗**R** = **T**∗(**M**∗**R**), where **R**∗**M** and **M**∗**R** are glide reflections: this section is just a blending of sections 7.4 and 7.7!

As an example, let us illustrate how we went from the $\mathbf{M*R_0^+}$ of figure 7.28 (section 7.7) to the $\mathbf{MG*R_0^+ = T*(M*R_0^+)}$ of figure 7.31:

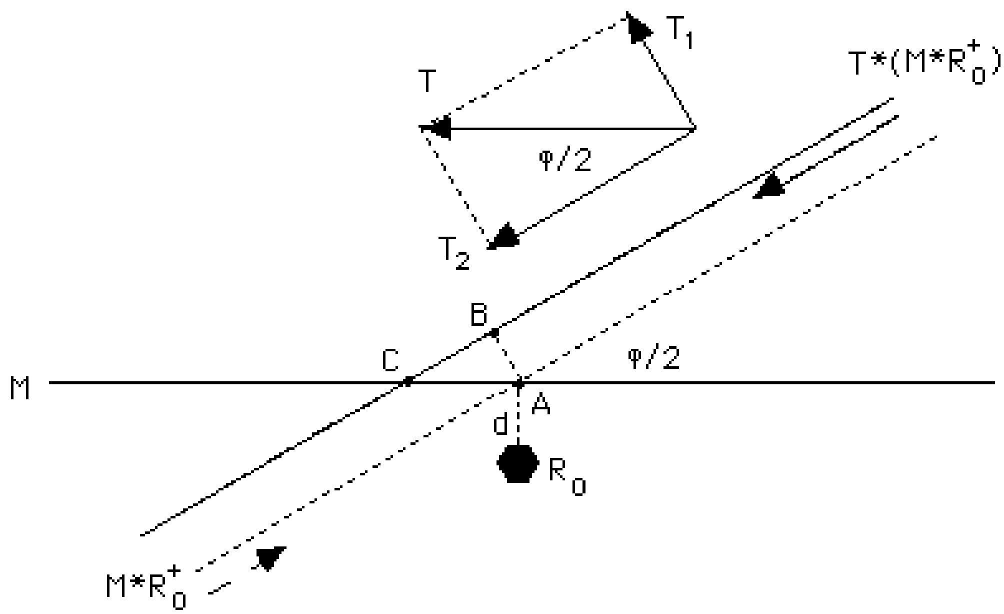

Fig. 7.33

All we had to do was to apply the idea of figure 7.11 and analyse **MG**'s gliding vector **T** into two vectors: one perpendicular to $\mathbf{M*R_0^+}$ ($\mathbf{T_1}$) that pulls $\mathbf{M*R_0^+}$'s axis **'forward'** by $|\mathbf{T_1}|/2$ (7.3.1), and one parallel to $\mathbf{M*R_0^+}$ ($\mathbf{T_2}$) that is easily **added** to $\mathbf{M*R_0^+}$'s vector (of **opposite** to $\mathbf{T_2}$'s sense in this case); the outcome is the glide reflection of figure 7.33, which is no other than figure 7.31's $\mathbf{MG*R_0^+}$, of course.

Figure 7.33 illustrates clearly why the glide reflection axes of figures 7.31 & 7.32 are still **parallel** to the glide reflection axes of figure 7.28, still making angles of 30^0 with **M**. Moreover, figure 7.33 determines exactly **where** they cross **M**: $|AC| = |AB|/(\sin(\phi/2)) = (|\mathbf{T_1}|/2)/(\sin(\phi/2)) = ((|\mathbf{T}|\sin(\phi/2))/2)/(\sin(\phi/2)) = |\mathbf{T}|/2$. (That's why the distance between the two **'crossing points'** in figures 7.31 & 7.32 is **equal** to $|\mathbf{T}|$ and, may we add, **independent of ϕ**!) Finally, figure 7.33 explains why there are vectors of two **distinct** lengths, $|\mathbf{T}| \times \cos(\phi/2) + 2d \times \sin(\phi/2)$ and $||\mathbf{T}| \times \cos(\phi/2) - 2d \times \sin(\phi/2)|$, in figures 7.31 & 7.32: $\mathbf{M*R_0^+}$ and $\mathbf{M*R_0^-}$ have gliding vectors of **equal length** $2d \times \sin(\phi/2)$ (7.7.2) but **distinct direction**, and the latter forces distinct lengths for the gliding vectors of $\mathbf{T*(M*R_0^+)}$ and $\mathbf{T*(M*R_0^-)}$; to recall our 'cryptic' expression from 7.7.2 (as well as

7.0.4), the longer vector is produced when the glide reflection and the rotation **'turn the same way'**.

7.8.2 Could it be a reflection? In the important special case where the glide reflection axis passes through the rotation center, d = 0 implies gliding vectors of length $|\mathbf{T}| \times \cos(\phi/2)$ for **all four** resulting glide reflections; their intersecting axes will still form a **rhombus** (as in figures 7.31 & 7.32), but the rotation center ($\mathbf{R_0}$) will now be in the **middle** of that rhombus (like fourfold center **D** combined with glide reflection $\mathbf{G_4}$ in figure 6.106 (**p4g**), for example). But the rhombus disappears when $\phi = 180^0$! In partial 'compensation', $|\mathbf{T}| \times \cos(180^0/2) = 0$ turns the glide reflections into **two** reflections crossing the original glide reflection at a distance of $|\mathbf{T}|/2$ from the half turn center: in case you didn't realize, that's the **pmg**'s story!

In general, when does a rotation turn a glide reflection into a reflection? Recall that we asked a similar question in 7.4.2: the answer remains the same here, and so does the way to get it. Indeed, with $\mathbf{R*G} = (\mathbf{R*(M*T_1)})\mathbf{*T_2}$ and $\mathbf{G*R} = \mathbf{T_2*((T_1*M)*R)}$, all we need is for $\mathbf{T_2}$ to be of **sense opposite** of $\mathbf{R*(M*T_1)}$'s (or $\mathbf{(T_1*M)*R}$'s) gliding vector (which is **bound** to happen for either **G** or $\mathbf{G^{-1}}$) **and** of **equal length** to it. Focusing on the latter condition, and referring to figure 7.33 and 7.7.2, we see that all we need is the equality $\mathbf{|T| \times \cos(\phi/2) = 2d \times \sin(\phi/2)}$ -- trivially valid in the case of **pmg** (with d = 0 and $\phi = 180^0$) and equivalent to $\mathbf{|T| = 2d \times \tan(\phi/2)}$ when $\mathbf{\phi \neq 180^0}$.

Of course we have already seen an example of $\mathbf{R*G} = \mathbf{M}$ in 7.0.4 and figure 7.5, where $\mathbf{R_3^-*G_1} = \mathbf{M_1}$: assuming that each tile has side length 1, $|\mathbf{T}| = 2d \times \tan(\phi/2)$ holds with $|\mathbf{T}| = \sqrt{2}/2$, $d = \sqrt{2}/4$ and $\tan(\phi/2) = \tan 45^0 = 1$. So, it is possible for the composition of a 90^0 rotation and a **'diagonal'** glide reflection to produce a reflection in the case of a **p4m** pattern; this also happens in the **p4g** pattern, as you should be able to verify (in figure 4.55 for example).

7.9 Reflection $*$ Glide Reflection

7.9.1 Only two centers. In the **pmg** pattern, the combination of a reflection **M** and a glide reflection **G** perpendicular to each other produces **two** half turns the centers of which lie on **G**'s axis and are **mirror images** of each other about **M**: this may either be checked directly (and by appeal to the discussions in 7.7.4 and 7.8.2 if necessary) or be derived as a special case of figure 6.6.2 (by making **one** of the glide reflection vectors zero). Could this be due to the **right angle**'s 'special privileges'? After all, there exist **four** possibilities altogether ($\mathbf{M*G}$, $\mathbf{G*M}$, $\mathbf{M*G^{-1}}$, $\mathbf{G^{-1}*M}$) that could create four distinct centers. Well, a look at 7.0.4 and figure 7.6 is not that promising for center diversity: over there we established $\mathbf{M_1*G_1} = \mathbf{R_4^-}$ and indicated that $\mathbf{G_1*M_1} = \mathbf{R_5^+}$, with $\mathbf{M_1}$ a 'horizontal' reflection and $\mathbf{G_1}$ a 'diagonal' glide reflection in a **p4m** pattern (bathroom wall); and a bit more work would show that $\mathbf{M_1*G_1^{-1}} = \mathbf{R_5^-}$ and $\mathbf{G_1^{-1}*M_1} = \mathbf{R_4^+}$ -- only **two** centers altogether!

Evidence for two rather than four centers is strengthened by a more 'exotic' (**p31m**) example:

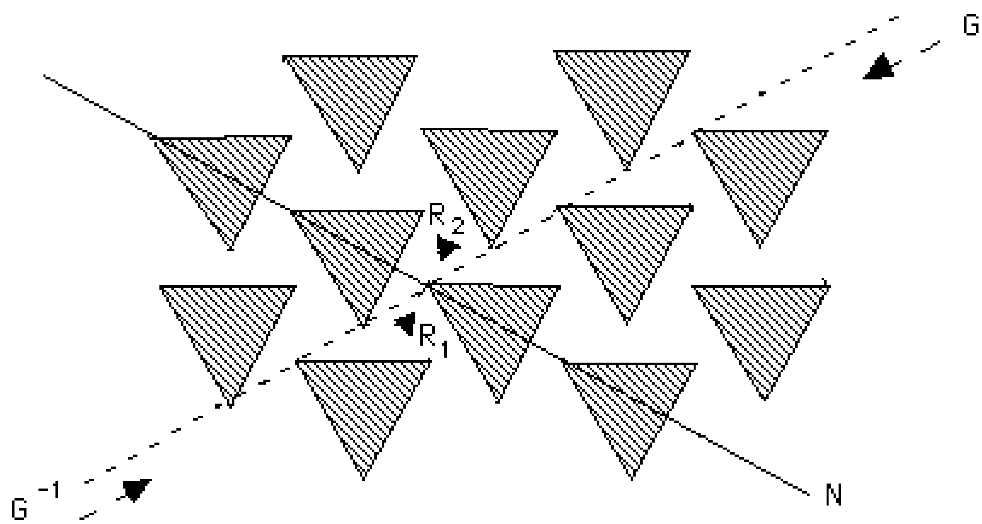

Fig. 7.34

You should be able to verify $\mathbf{N*G} = \mathbf{R_2^+}$, $\mathbf{G*N} = \mathbf{R_1^-}$, $\mathbf{N*G^{-1}} = \mathbf{R_1^+}$, and

$\mathbf{G^{-1}*N} = \mathbf{R_2^-}$: again, **four** compositions sharing **two** centers. (Notice here that $\mathbf{R_1}$ and $\mathbf{R_2}$ are among the **p31m**'s **'off-axis'** 120^0 centers (4.16.1), derived through the compositions above rather than as obvious compositions of intersecting reflections.)

7.9.2 <u>The way to the two centers.</u> Having 'only' two centers would make sense not only in view of the examples presented, but also in view of what we saw in 7.7.2: the combination of a reflection and a rotation produced two, not four, glide reflection axes. Moreover, having two rather than four centers will make perfect sense after the **'whole story'** is revealed in section 7.10!

So, having resigned to living with just two centers, how do we find them? How would we justify figure 7.34? Using $\mathbf{M_1}$ instead of $\mathbf{N}$ and setting $\mathbf{G} = \mathbf{M_2*T} = \mathbf{T*M_2}$, $\mathbf{G^{-1}} = \mathbf{M_2*T^{-1}} = \mathbf{T^{-1}*M_2}$, we notice that the four compositions of figure 7.34 may be written as $(\mathbf{M_1*M_2})*\mathbf{T}$, $\mathbf{T}*(\mathbf{M_2*M_1})$, $(\mathbf{M_1*M_2})*\mathbf{T^{-1}}$, and $\mathbf{T^{-1}}*(\mathbf{M_2*M_1})$; now $\mathbf{M_1*M_2}$ and $\mathbf{M_2*M_1}$ are rotations $\mathbf{R^+}$, $\mathbf{R^-}$ of same center K and angle ϕ (120^0 in this case) but opposite orientation, so we may **'blend'** figures 7.34 and 7.22:

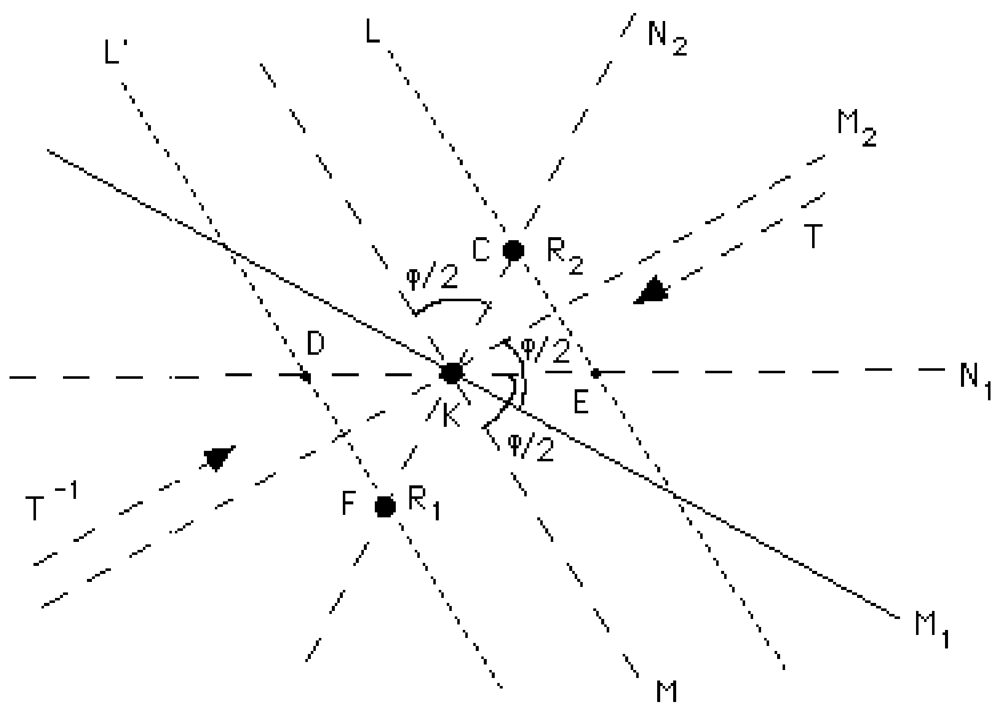

Fig. 7.35

So, with $\mathbf{N_1}$ = DE, $\mathbf{N_2}$ = CF, **M** perpendicular to **T** (therefore $\mathbf{M_2}$ as well), **L** and **L′** parallel to **M** with d(**M**, **L**) = d(**M**, **L′**) = |**T**|/2, and a($\mathbf{M}$, $\mathbf{N_1}$) = a($\mathbf{M}$, $\mathbf{N_2}$) = a($\mathbf{M_1}$, $\mathbf{M_2}$) = 60^0 (ϕ/2), the 'blending' of figures 7.22 and 7.34 is complete: center $\mathbf{R_1}$ (figure 7.34) corresponds to F (figure 7.22) and the rotations $\mathbf{R^+ * T^{-1}} = (\mathbf{M_1 * M_2}) * \mathbf{T^{-1}} = \mathbf{N * G^{-1}}$ and $\mathbf{T * R^-} = \mathbf{T} * (\mathbf{M_2 * M_1}) = \mathbf{G * N}$; and center $\mathbf{R_2}$ (figure 7.34) corresponds to C (figure 7.22) and the rotations $\mathbf{R^+ * T} = (\mathbf{M_1 * M_2}) * \mathbf{T} = \mathbf{N * G}$ and $\mathbf{T^{-1} * R^-} = \mathbf{T^{-1}} * (\mathbf{M_2 * M_1}) = \mathbf{G^{-1} * N}$. And there is a **bonus** as well: observe, focusing on **acute** angles always, that a($\mathbf{M_1}$, $\mathbf{N_2}$) = a($\mathbf{M_1}$, $\mathbf{M_2}$) + a($\mathbf{M_2}$, $\mathbf{N_2}$) = a($\mathbf{M}$, $\mathbf{N_2}$) + a($\mathbf{M_2}$, $\mathbf{N_2}$) = a($\mathbf{M}$, $\mathbf{M_2}$) = $\mathbf{90^0}$! In other words, $\mathbf{M_1}$ and $\mathbf{N_2}$ are **perpendicular** to each other: this is going to be important both in 7.9.3 below and in section 7.10.

Our analysis above has certainly explained how the composition centers are born, but there is one more question to answer: what do **'unused centers'** D (intersection of **L′** and $\mathbf{N_1}$) and E (intersection of **L** and $\mathbf{N_1}$) of figure 7.35 stand for? The answer is: they represent rotations **unrelated** to the given pair of reflection and glide reflection (and **not** 'belonging' to the **p31m** pattern of figure 7.34)! For example, one of the two rotations based on E is $\mathbf{R^- * T} = (\mathbf{M_2 * M_1}) * \mathbf{T} = \mathbf{M_2} * (\mathbf{M_1 * T})$, which is the composition of **another pair** of reflection ($\mathbf{M_2}$) and, by 7.3.2, glide reflection ($\mathbf{M_1 * T}$); it is of course crucial that we cannot replace $\mathbf{M_2 * M_1}$ by $\mathbf{M_1 * M_2}$ (7.2.3).

7.9.3 <u>A 'practical guide'.</u> The detailed discussion in 7.9.2 is certainly enlightening, but how would you describe to someone not terribly interested in mathematical rigor the **general** procedure for determining the composition of a reflection and a glide reflection? To be more precise, how would you lead that person to the center of the resulting rotation? That's really the only crucial question: for it is clear from the preceding discussion that the rotation angle is **twice** the **intersection angle** of the reflection and the glide reflection; and, once the center is known, the angle's orientation is easy to determine (by checking what happens at the **intersection point** of the reflection and the glide reflection, for example).

Removing all ‘redundant information’ from figure 7.35, we arrive at an easy answer to our question. Indeed, since $\mathbf{N_2}$ is perpendicular to $\mathbf{M_1}$ (7.9.2) and $\mathbf{L}$, $\mathbf{L'}$ are perpendicular to $\mathbf{M_2}$ with the intersection point K half way from $\mathbf{L}$ to $\mathbf{L'}$ (figure 7.35), the procedure for determining the rotation centers $\mathbf{R_1}$, $\mathbf{R_2}$ for the four possible compositions of 7.9.1 is simple: pick points K_1, K_2 on $\mathbf{M_2}$ so that $|KK_1| = |KK_2| = |\mathbf{T}|/2$, and then draw lines $\mathbf{L'}$, $\mathbf{L}$ perpendicular to $\mathbf{M_2}$ at K_1, K_2 respectively, and line $\mathbf{N_2}$ perpendicular to $\mathbf{M_1}$ at K; $\mathbf{R_1}$ and $\mathbf{R_2}$ are now determined as the intersections of $\mathbf{N_2}$ by $\mathbf{L}$ and $\mathbf{L'}$ (figure 7.36).

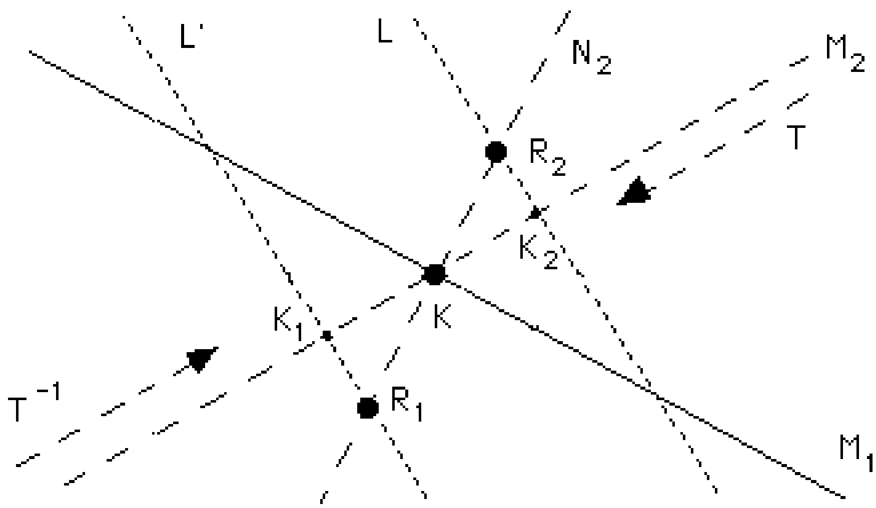

Fig. 7.36

Of course figure 7.36 **alone** does not tell us which center (between $\mathbf{R_1}$, $\mathbf{R_2}$) to use for any given combination of reflection and glide reflection. Some rules can be derived by referring to the discussion following figure 7.35, or perhaps by looking at figure 7.40 in section 7.10. But it is probably easier to follow the tip given above and determine the right center and angle orientation simply by checking where the intersection of the two axes is mapped. We illustrate all this in figure 7.37 below, where we verify the identities $\mathbf{M_1}*\mathbf{G_1} = \mathbf{R_4^-}$ and $\mathbf{G_1}*\mathbf{M_1} = \mathbf{R_5^+}$ of figure 7.6 (bathroom wall), which is reproduced in part, explicitly demonstrating the determination of centers $\mathbf{R_4}$ and $\mathbf{R_5}$: looking at the pair K, $\mathbf{M_1}*\mathbf{G_1}$(K), it becomes clear that the only rotation among $\mathbf{R_4^+}$, $\mathbf{R_4^-}$, $\mathbf{R_5^+}$, $\mathbf{R_5^-}$ that could map K to $\mathbf{M_1*G_1}$(K) is $\mathbf{R_4^-}$, therefore $\mathbf{M_1*G_1 = R_4^-}$; likewise, looking at the pair K, $\mathbf{G_1*M_1}$(K), we conclude that $\mathbf{G_1*M_1 = R_5^+}$.

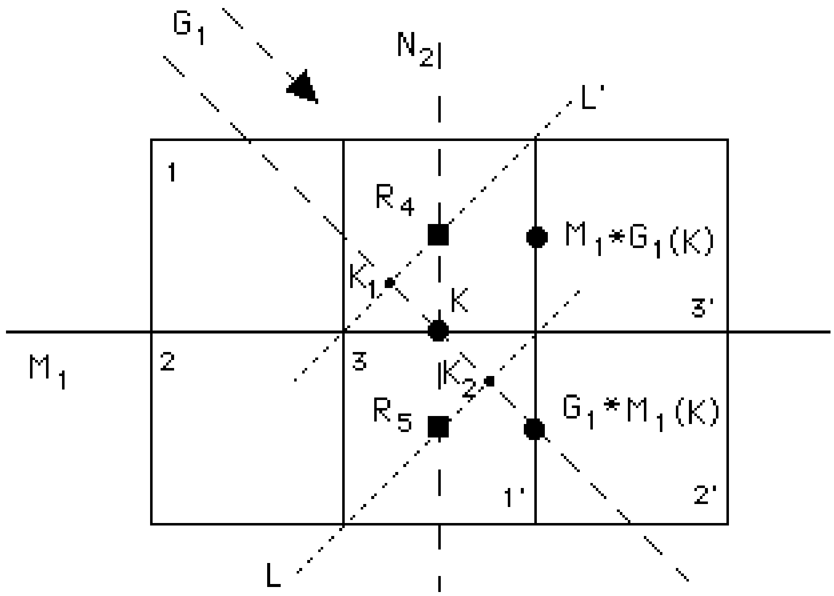

Fig. 7.37

7.9.4 <u>When the axes are parallel.</u> Everything we discussed so far in this section collapses in case $\mathbf{M_1}$ and $\mathbf{M_2}$, that is **N** and **G** are parallel to each other. Luckily, the compositions $\mathbf{N*G = (M_1*M_2)*T}$ and $\mathbf{G*N = T*(M_2*M_1)}$ are much easier to determine in this case; we derive these **translations** below, leaving $\mathbf{N*G^{-1}}$ and $\mathbf{G^{-1}*N}$ to you:

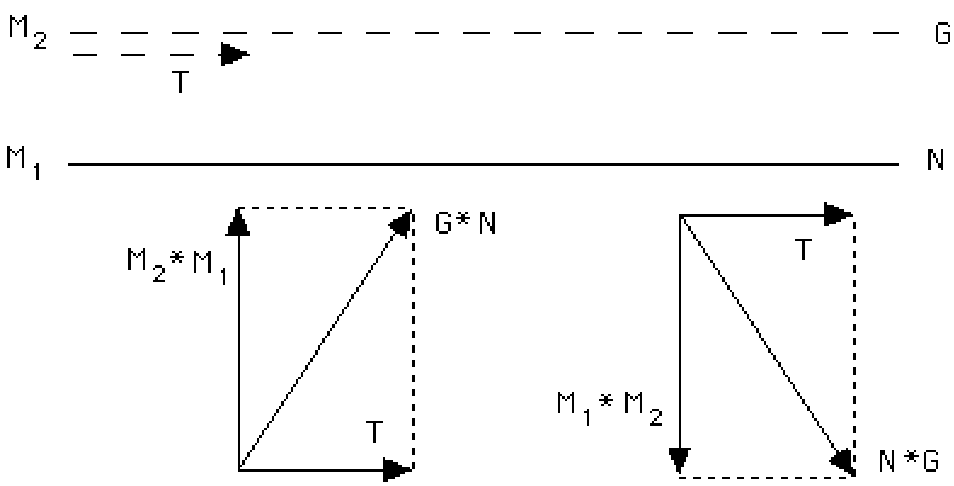

Fig. 7.38

Of course all this is strongly reminiscent of sections 7.3 and 7.4; and such compositions are prominent in **cm** (and **pm**) patterns, as well as all patterns containing them: **more** on this in chapter 8!

7.10 Glide reflection $*$ Glide Reflection

7.10.1 Parallel axes. This '**pg**' case is similar to the '**cm**' case of 7.9.4. Indeed $\mathbf{G_1*G_2} = \mathbf{T_1*(M_1*M_2)*T_2} = \mathbf{(T_1*T_2)*(M_1*M_2)}$ and $\mathbf{G_2*G_1} = \mathbf{T_2*(M_2*M_1)*T_1} = \mathbf{(T_2*T_1)*(M_2*M_1)}$ are '**diagonal**' translations:

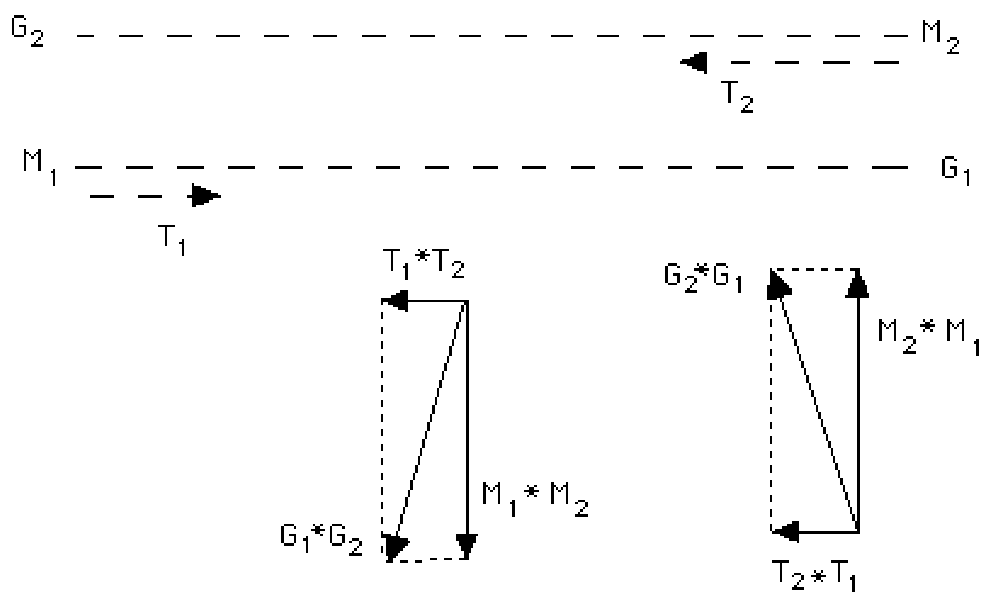

Fig. 7.39

Notice that the special case $\mathbf{T_1} = \mathbf{-T_2}$ (with $\mathbf{T_1*T_2} = \boldsymbol{I}$) has been employed in 6.3.2 (figure 6.21) in our investigation of two-colored **pm** patterns.

7.10.2 A good guess indeed! We now come to the much more involved case where $\mathbf{G_1}$ and $\mathbf{G_2}$ intersect each other at a point K. Luckily, most of the work has **already** been done in section 7.9!

Indeed, had you been asked to determine $\mathbf{G_1{*}G_2}$ (etc) yourself, you would probably look at figure 7.36 and think like this: "were $\mathbf{M_1}$ a glide reflection $\mathbf{G_1} = \mathbf{M_1{*}T_1}$ instead of a mere reflection, I would have treated it exactly as $\mathbf{G_2} = \mathbf{M_2{*}T_2}$; that is, I would draw lines **N**, **N′** perpendicular to $\mathbf{M_2}$ and at a distance of $|\mathbf{T_2}|/2$ to the left and right of K, and then I would look for the rotation center(s) at their intersection(s) with **L′** and **L**"; and surely you would already know that the composition is a **rotation** by an angle **twice** the intersection angle of $\mathbf{G_1}$ and $\mathbf{G_2}$! And you would be right on the mark:

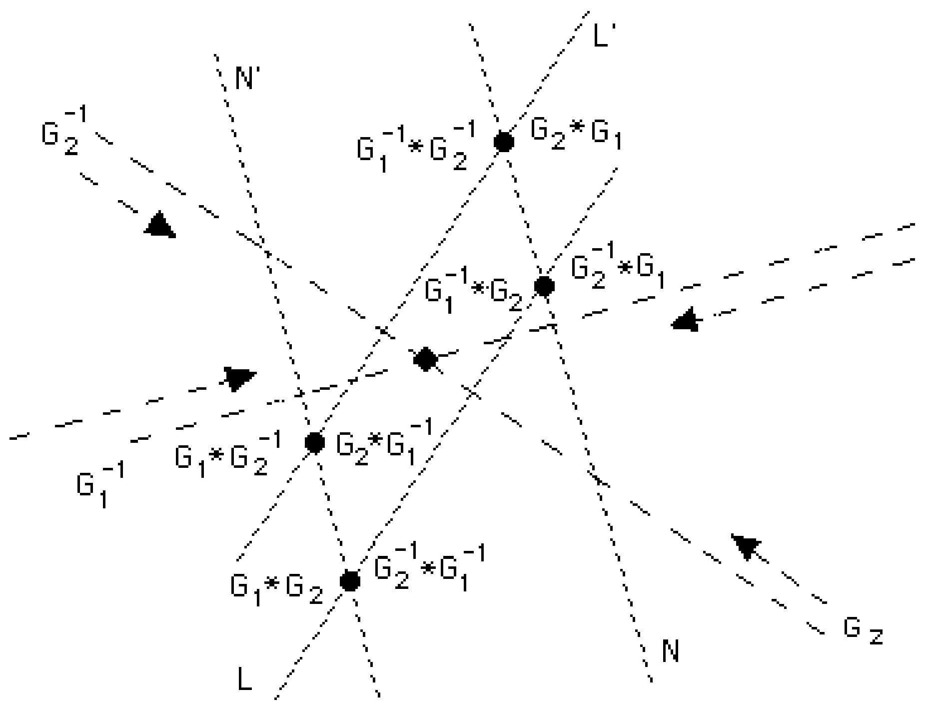

Fig. 7.40

Figure 7.40 offers an **exhaustive** overview of the situation, covering all **eight** possible combinations and **four** rotation centers: it is possible to develop rules about **'what goes where'**, but it is probably **smarter** to do what we suggested in 7.9.3 (and figure 7.37) when it comes to determining rotation centers and angle orientation!

In simple terms, draw two perpendiculars at each of the two axes and at distances equal to half the length of the respective gliding vector on each side of their intersection point, then look for the four intersections of the resulting two pairs of parallel lines (figure 7.40): observe that this **generalizes** figure 6.54, where the two axes are **perpendicular** to each other!

7.10.3 Where do they come from? Notice how we have **upgraded** from the two possible centers of figure 7.36 to the four possible centers of figure 7.40: this is hardly surprising if you notice that we did get an extra translation here (as the reflection turned into glide reflection) and if you recall how the addition of a translation increased the number of glide reflection axes from two (figure 7.28, **R∗M**) to four (figures 7.31 & 7.32, **R∗G**).

In 7.8.1, and figure 7.33 in particular, we explained how the additional translation leads to the two extra axes (when the reflection (figure 7.28) combined with the rotation is **upgraded** to glide reflection (figures 7.31 & 7.32)). We do something similar in figure 7.41 below, showing how **each** of the two rotation centers (**R_1**, **R_2**) generates **two** new rotation centers (**R_4**, **R_5** and **R_3**, **R_6**, respectively), the **same way** K generated **R_1** and **R_2** in figure 7.36:

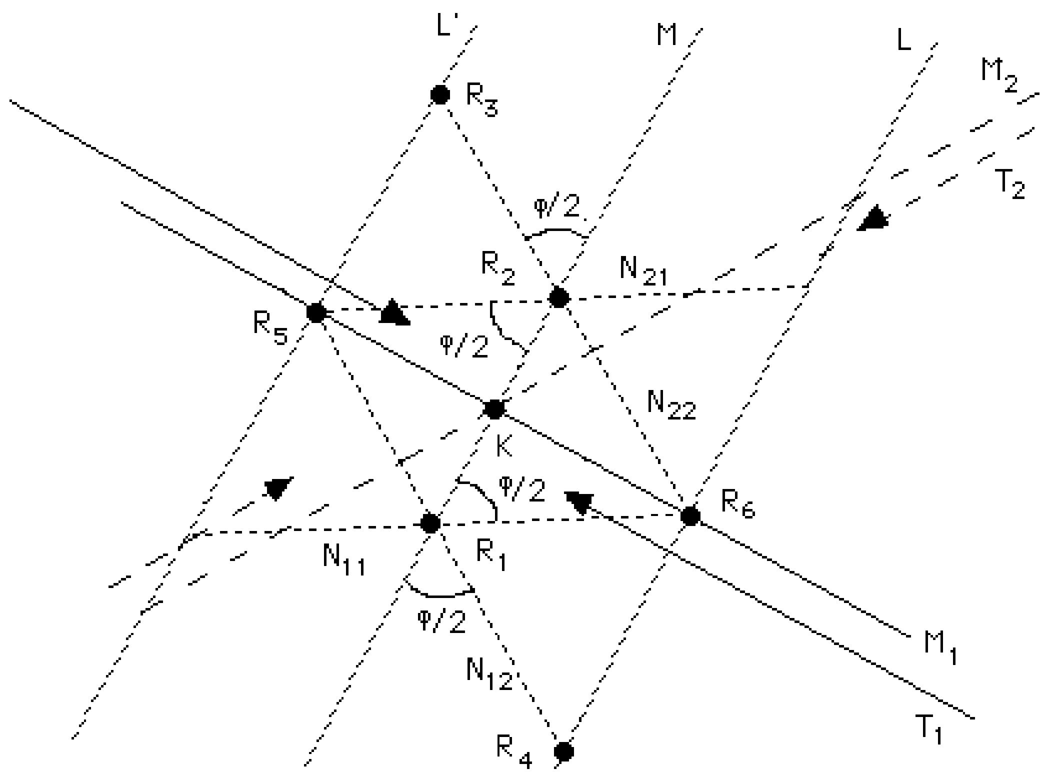

Fig. 7.41

Basically, all we had to do was to combine each of $\mathbf{R_1}$ and $\mathbf{R_2}$ with the **'added'** translation $\mathbf{T_1}$, exactly as in figures 7.22 **and** 7.35; and, for the same reason that line $\mathbf{N_1}$ was **'useless'** in figure 7.35, lines $\mathbf{N_{11}}$ and $\mathbf{N_{21}}$ play no role in figure 7.41: our rotation centers are created by the intersections of lines $\mathbf{N_{12}}$ and $\mathbf{N_{22}}$ with **L** and **L′**. (Notice however that $\mathbf{R_5}$ **also** lies on $\mathbf{N_{21}}$, while $\mathbf{R_6}$ **also** lies on $\mathbf{N_{11}}$: this is part of a **'coincidence'** discussed right below.)

Are you ready for a little **surprise**, at long last? Figure 7.41 is in fact an **'abstract detail'** of a **familiar** piece, namely figure 7.34! Indeed $\mathbf{M_2{*}T_2}$ is figure 7.34's glide reflection **G**, while $\mathbf{M_1{*}T_1}$ is figure 7.34's reflection **N** upgraded to a hidden glide reflection **MG**; everything is fully revealed in figure 7.42:

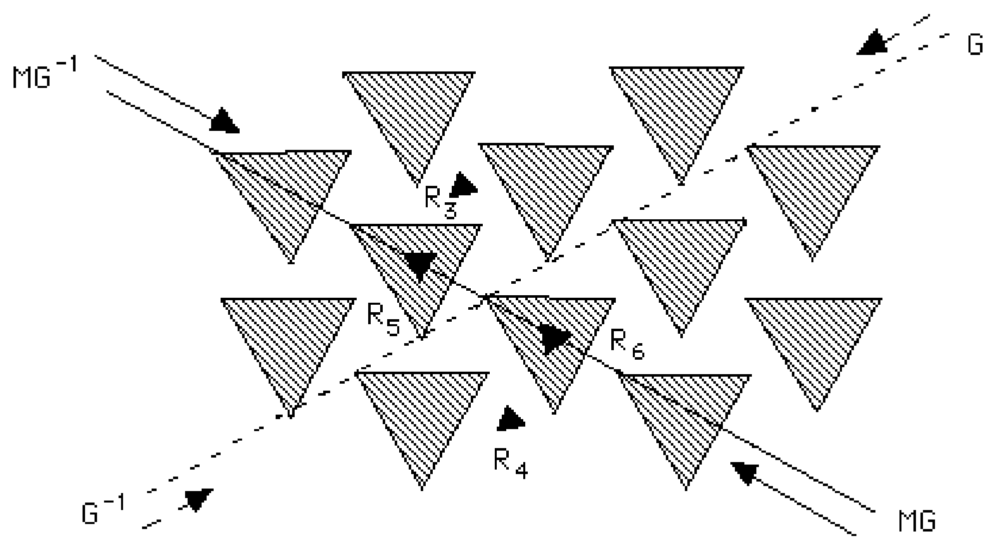

$MG{*}G = R_3^+$, $G{*}MG = R_4^-$, $MG{*}G^{-1} = R_5^+$, $G^{-1}{*}MG = R_6^-$,

$G^{-1}{*}MG^{-1} = R_3^-$, $MG^{-1}{*}G^{-1} = R_4^+$, $G{*}MG^{-1} = R_5^-$, $MG^{-1}{*}G = R_6^+$

Fig. 7.42

So, the 'coincidence' mentioned above reflects on the fact that $\mathbf{R_5}$ and $\mathbf{R_6}$ are **'on-axis'** 120^0 centers in figure 7.34's **p31m** pattern: figure 7.42 indicates that those centers are generated whenever two **'somewhat opposite'** glide reflections are combined; but it is more crucial to find out **'why'** those centers fall on the axes, and we do that next as a byproduct of a broader investigation.

7.10.4* <u>Some coordinates, at long last!</u> Our goal here is to determine the **location** of the four rotation centers (A, B, C, D) corresponding to 'all possible combinations' of the two given glide reflections $\mathbf{G_1}$, $\mathbf{G_2}$ **analytically** -- that is, using **cartesian coordinates** (for the first time since chapter 1)! To do that, we **'rotate'** figure 7.40 so that $\mathbf{G_1}$ is now our **x-axis** (y = 0), while $\mathbf{G_2}$ is a line of unspecified **slope m** (y = mx), and the intersection point of $\mathbf{G_1}$, $\mathbf{G_2}$ is the **origin** (0, 0); we also set $|\mathbf{T_1}| = 2d_1$ and $|\mathbf{T_2}| = 2d_2$, so that the perpendiculars to $\mathbf{G_1}$, **N** and **N′**, are now represented by the equations $x = d_1$ and $x = -d_1$, respectively (figure 7.43).

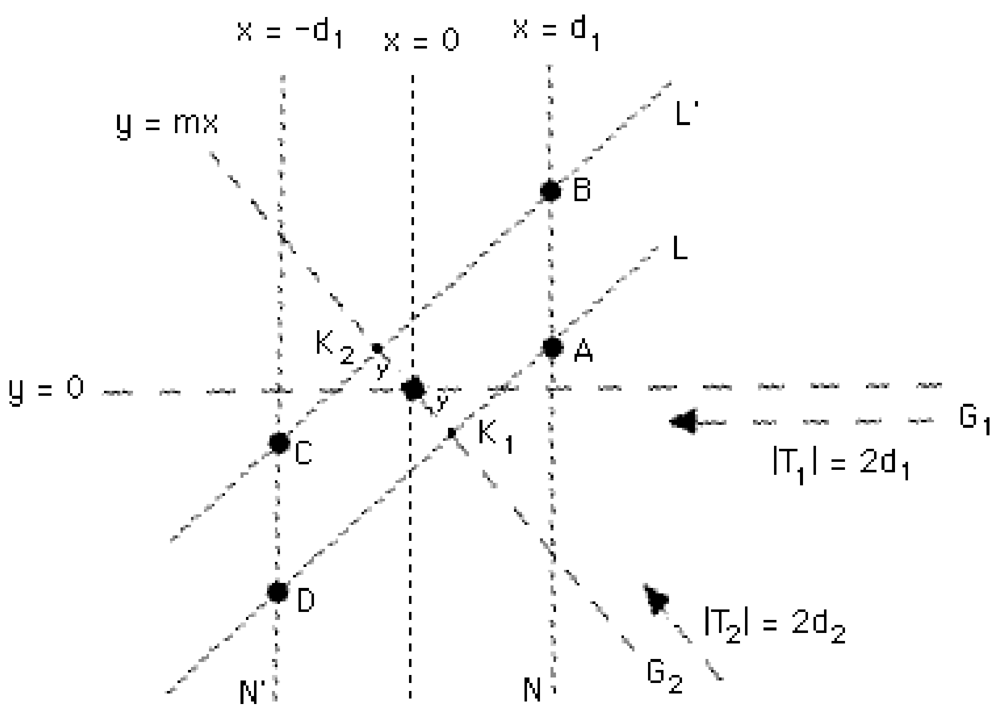

Fig. 7.43

The critical step is to determine the equations of the lines **L** and **L′**: being perpendicular to y = mx and **symmetric** of each other about (0, 0), they may be written as $y = (-1/m)x - k$ and $y = (-1/m)x + k$, respectively; k is a real number that we need to determine, and we do so by first determining the coordinates of K_1 and K_2, the intersection points of $\mathbf{G_2}$ with **L** and **L′**, respectively (figure 7.43).

Solving the systems $\mathbf{y = mx = (-1/m)x + k}$ and $\mathbf{y = mx = (-1/m)x - k}$, we obtain $K_1 = (\frac{-km}{m^2+1}, \frac{-km^2}{m^2+1})$ and $K_2 = (\frac{km}{m^2+1}, \frac{km^2}{m^2+1})$. We know that $|K_1K_2| = 2d_2$, so the **distance formula** leads to $\sqrt{(\frac{-km}{m^2+1} - \frac{km}{m^2+1})^2 + (\frac{-km^2}{m^2+1} - \frac{km^2}{m^2+1})^2} = 2d_2$, which is equivalent to $\frac{4k^2m^2}{(m^2+1)^2} + \frac{4k^2m^4}{(m^2+1)^2} = 4d_2^2$, $\frac{k^2m^2}{m^2+1} = d_2^2$ and, finally, $\mathbf{k = \pm\frac{d_2}{m}\sqrt{m^2+1}}$.

Knowing now the equations of **L** ($y = (-1/m)x - (d_2/m)\sqrt{m^2+1}$) and **L′** ($y = (-1/m)x + (d_2/m)\sqrt{m^2+1}$), it is **trivial** to determine the coordinates of their intersections with **N** ($x = d_1$) and **N′** ($x = -d_1$):

$$\mathbf{A = (d_1, \frac{-d_1-d_2\sqrt{m^2+1}}{m}),\quad B = (d_1, \frac{-d_1+d_2\sqrt{m^2+1}}{m}),}$$

$$\mathbf{C = (-d_1, \frac{d_1+d_2\sqrt{m^2+1}}{m}),\quad D = (-d_1, \frac{d_1-d_2\sqrt{m^2+1}}{m}).}$$

Now we can finally answer the question: when does the center of a rotation that is the composition of two glide reflections lie on one of the glide reflection axes? Working in the context of figure 7.43, always, we notice that there exist **two** distinct possibilities: two centers lying on $\mathbf{G_1}$ (if and only if their y-coordinate is 0), and two centers lying on $\mathbf{G_2}$ (if and only if their coordinates x and y satisfy $y = mx$). Indeed the first possibility may **only** occur for **both** B and D **at the same time**, and is equivalent to $\mathbf{d_1 = d_2\sqrt{m^2+1}}$; and the second possibility may **only** occur for **both** B and D **at the same time**, and is equivalent to $\mathbf{d_2 = d_1\sqrt{m^2+1}}$. (The roles of B, D and A, C are **switched** when we select **–** instead of **+** in the above derived formula for k, with the formulas for **L** and **L′** **swapped**.) Observe that we may in fact set $\mathbf{m = \tan\gamma}$, where $\gamma = \phi/2$ is the **acute** angle between the two glide reflection axes; with $m^2+1 = \tan^2\gamma+1 = \frac{1}{\cos^2\gamma}$, our condition becomes $|\mathbf{T_1}| = |\mathbf{T_2}| \times \cos\gamma$ **or** $|\mathbf{T_2}| = |\mathbf{T_1}| \times \cos\gamma$. [Notice that this condition is made all too obvious by figure 7.41, making all previous calculations above seem totally **redundant**; but our main goal was the determination of the composition center's **coordinates** in the **general case** (i.e., when the resulting rotation center lies on no glide reflection axis).]

In the case of the **p31m** pattern of figures 7.34 & 7.42, we may set, after rotating the coordinate system as above, $\mathbf{m = -\sqrt{3}}$; a bit of Geometry shows then that $|\mathbf{T_2}| = 2|\mathbf{T_1}|$, hence $d_2 = d_1\sqrt{m^2+1}$ and $|\mathbf{T_1}| = |\mathbf{T_2}| \times \cos\gamma$ are valid: **on-axis** rotations may therefore be seen as compositions of one genuine and one hidden glide reflection.

In the case of **perpendicular** glide reflections, $\lim_{m\to\infty} \frac{\sqrt{m^2+1}}{m} = 1$ (the fraction approaching 1 as m approaches infinity) and $d_1/m = 0$ yield the centers $(\pm \mathbf{d_1}, \pm \mathbf{d_2})$, corroborating figure 6.54 and contributing to our understanding of **pgg** and **cmm** patterns. In the case of the latter, the off-axis centers are always produced by one reflection and one glide reflection perpendicular to each other; any pair of perpendicular glide reflections produces four centers lying, as we indicated in 6.9.3, on intersections of **reflection** axes, hence **not** on **glide** reflection axes.

In the case of the **p4g** pattern of figure 7.44 (and 4.55), working with the shown horizontal and diagonal glide reflection axes and vectors, observe that $m = \tan 45^0 = 1$, $d_1 = a/2$, and $d_2 = a/(2\sqrt{2}) = d_1\cos 45^0$, so that $\frac{d_1+d_2\sqrt{m^2+1}}{m} = a$ and $\frac{d_1-d_2\sqrt{m^2+1}}{m} = 0$; here **a** stands for the length of the **horizontal** glide reflection vector (figure 7.44). The four intersection points (and fourfold centers) are $(a/2, 0)$, $(-a/2, 0)$, $(a/2, -a)$, and $(-a/2, a)$; the first two centers **do** indeed lie on the horizontal glide reflection axis:

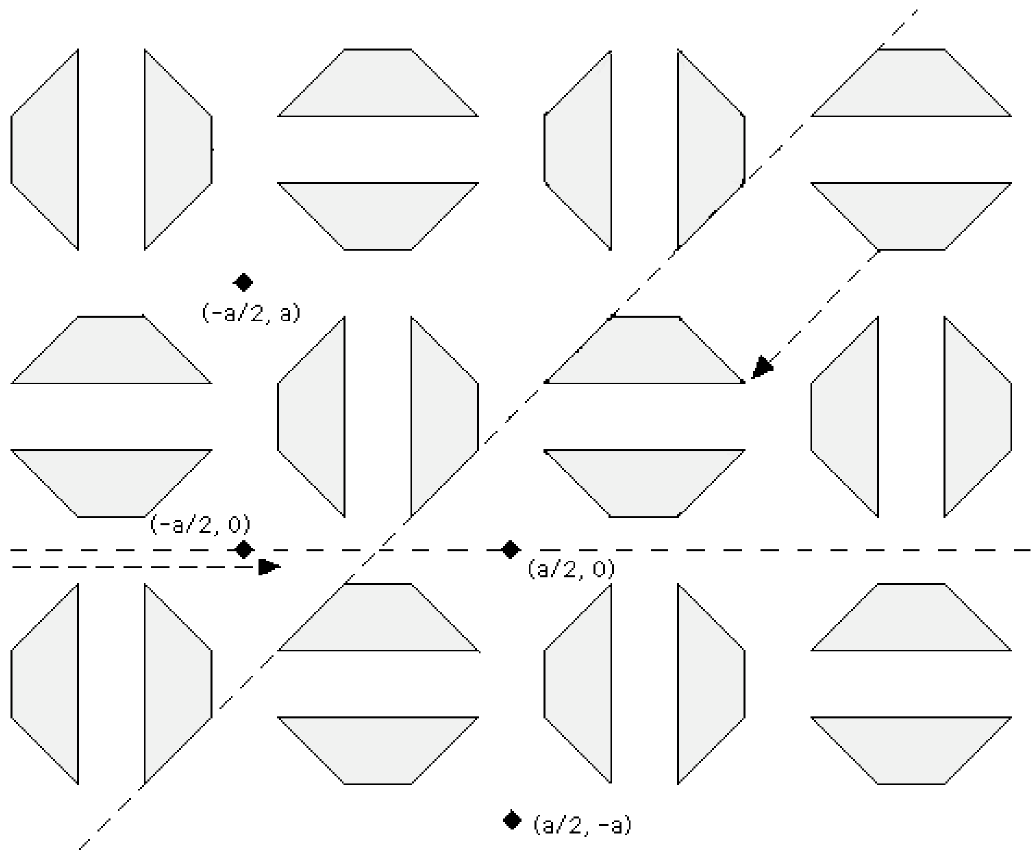

Fig. 7.44

first draft: summer 2001

CHAPTER 8

WHY PRECISELY SEVENTEEN TYPES?

8.0 Classification of wallpaper patterns

8.0.1 The goal. Back in section 2.8 it was rather easy to explain why there exist precisely **seven** types of **border** patterns. But we have not so far attempted to similarly **determine** the number of possible wallpaper patterns: we simply **assumed** that there exist precisely **seventeen** types of **wallpaper** patterns in order to investigate their two-colorings in chapter 6. And there was a good reason for this: unlike border patterns, wallpaper patterns may only be **classified** with considerable effort; in fact most known proofs would probably be too **advanced** mathematically for many readers of this book. Luckily, we are at long last in a position to fulfill our promise at the end of 4.0.6 and **justify** our assumptions on wallpaper patterns, classifying them in a purely **geometrical** manner: no tools beyond those already developed in earlier chapters will be needed.

Of course 'half' of our goal has already been achieved: chapter 4 provides some rather convincing evidence on the **existence** and **structure** of the seventeen types, and the latter has also been indirectly examined in chapters 6 and, to some extent, 7. What we need to reach now is a **negative** result: there cannot be any more types of wallpaper patterns other than the ones studied in chapter 4.

8.0.2 The tactics. The promised classification will be greatly facilitated by the **Crystallographic Restriction** of section 4.0, established in 4.0.6: the smallest rotation angle of a wallpaper pattern may only be 360^0 (none), 180^0, 120^0, 90^0, or 60^0. This fundamental fact allows us to **split** the entire classification process into **five** cases. Moreover, we will view each 90^0 pattern as

'built' on two 180^0 patterns, each of which will in turn be viewed as a **'product'** of two 360^0 patterns; and something quite similar will happen among 360^0, 120^0, and 60^0 patterns. This approach allows us to reduce potentially 'complicated' types to **simpler** ones.

As stated above, we will be looking for 'negative' results, trying to **rule out** various geometrical situations and, to be more specific, interactions among isometries. Therefore various facts on **compositions of isometries** explored in chapter 7 are going to be crucial. Moreover, looking at an isometry's **image** under another isometry will often be useful: that operation is closely related to the **Conjugacy Principle** of 6.4.4 (and 4.0.4 & 4.0.5), and needs to be further investigated before the classification begins.

8.0.3 <u>The Conjugacy Principle revisited.</u> First formulated in 6.4.4, the Conjugacy Principle essentially states that, given two isometries I and I_1, I_1's image under I, denoted by $I[I_1]$, is still an isometry, equal in fact to $I * I_1 * I^{-1}$ (and **not** $I * I_1$). In 6.4.4, figure 6.36, I was the glide reflection $\mathbf{G}$, I_1 was the reflection $\mathbf{M_1}$, and $I[I_1]$ was the glide reflection $\mathbf{M_2}$. In 4.0.4, figure 4.4, I was the translation $\mathbf{T}$, I_1 was the clockwise rotation $\mathbf{R} = (K, \phi)$, and $I[I_1]$ was the clockwise rotation $(\mathbf{T}(K), \phi)$. And in 4.0.5, figure 4.6, I was the clockwise rotation $\mathbf{R_1} = (K_1, \phi_1)$, I_1 was the clockwise rotation $\mathbf{R_2} = (K_2, \phi_2)$, and $I[I_1]$ was the clockwise rotation $(\mathbf{R_1}(K_2), \phi)$.

One should be careful about what exactly $I[I_1]$ stands for! The following example, where I is the glide reflection $\mathbf{G}$ and I_1 is the **counterclockwise** rotation $\mathbf{R} = (K, \phi)$ is rather illuminating:

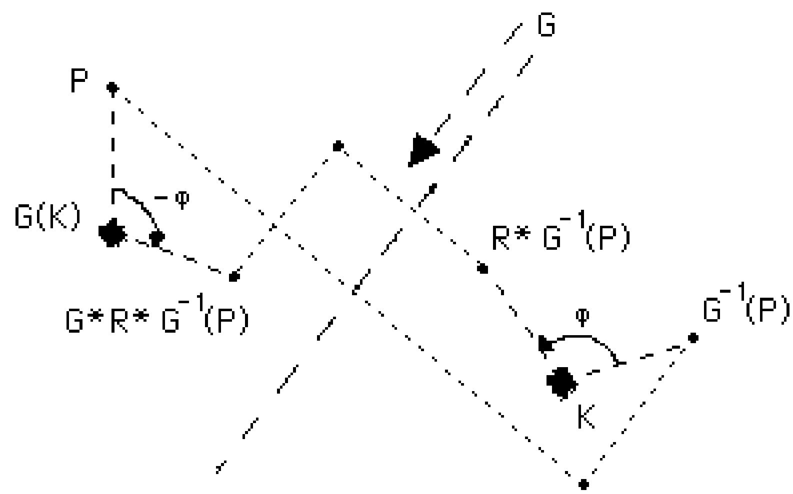

Fig. 8.1

As made clear by figure 8.1, $I[I_1] = I*I_1*I^{-1}$ is the **clockwise** rotation (**G**(K), $-\phi$): **G** glide-reflected not only **R**'s center, but also the **arrow** indicating its orientation! This **empirical** 'arrow rule' works rather well: for example, it indicates -- by placing the arrows and the angles in a circular context, if needed -- that **rotating** a rotation I_1 by another rotation I should **preserve** its orientation, regardless of whether I is clockwise or counterclockwise; you should be able to verify this claim by considering all possible combinations of clockwise and counterclockwise in figure 4.6.

So far we have not said anything about **proving** the various instances of the Conjugacy Principle. Well, **congruent triangles** simply give everything away in figure 4.6, while the presence of **three parallelograms** settles everything in figure 4.4. And in figure 8.1 above, where we are facing a seemingly more difficult situation, a seemingly cleverer but merely **generalizing** approach works: the triangle {P, **G**(K), $\mathbf{G*R*G^{-1}}$(P)} is the **image** of the **isosceles** triangle {$\mathbf{G^{-1}}$(P), K, $\mathbf{R*G^{-1}}$(P)} under **G**, therefore **congruent** to it; it follows that $\mathbf{G*R*G^{-1}}(P) = I*I_1*I^{-1}(P)$ is indeed the image of P under the **clockwise** rotation (**G**(K), $-\phi$) = $I[I_1]$, hence we may conclude that $I[I_1] = I*I_1*I^{-1}$ holds.

The method employed in figure 8.1 could also be employed back in figures 4.4 & 4.6: it requires no particular skill or ingenuity, just experience in arguing somewhat **abstractly**. But in figure 8.2 below -- an **'inverse'** of figure 8.1, for now we rotate a glide reflection instead of glide-reflecting a rotation -- there **seems** to be a complication: while K, P, and $\mathbf{R*G*R^{-1}}$(P) are clearly the images under **R** of K, $\mathbf{R^{-1}}$(P), and $\mathbf{G*R^{-1}}$(P), respectively, it is **not** obvious that P's image under the rotated reflection line **R[M]** is the same as $\mathbf{M*R^{-1}}$(P)'s image under **R**; notice that we do need this fact in order to show that the segment {**R[M]**(P), $\mathbf{R*G*R^{-1}}$(P)} is **both** equal in length to the segment {$\mathbf{M*R^{-1}}$(P), $\mathbf{G*R^{-1}}$(P)} and parallel to **R[M]**, therefore equal to the vector **R[T]**, as figure 8.2 suggests. (Recall at this point that isometries, and rotations in particular, map parallel lines to parallel lines (1.0.9).)

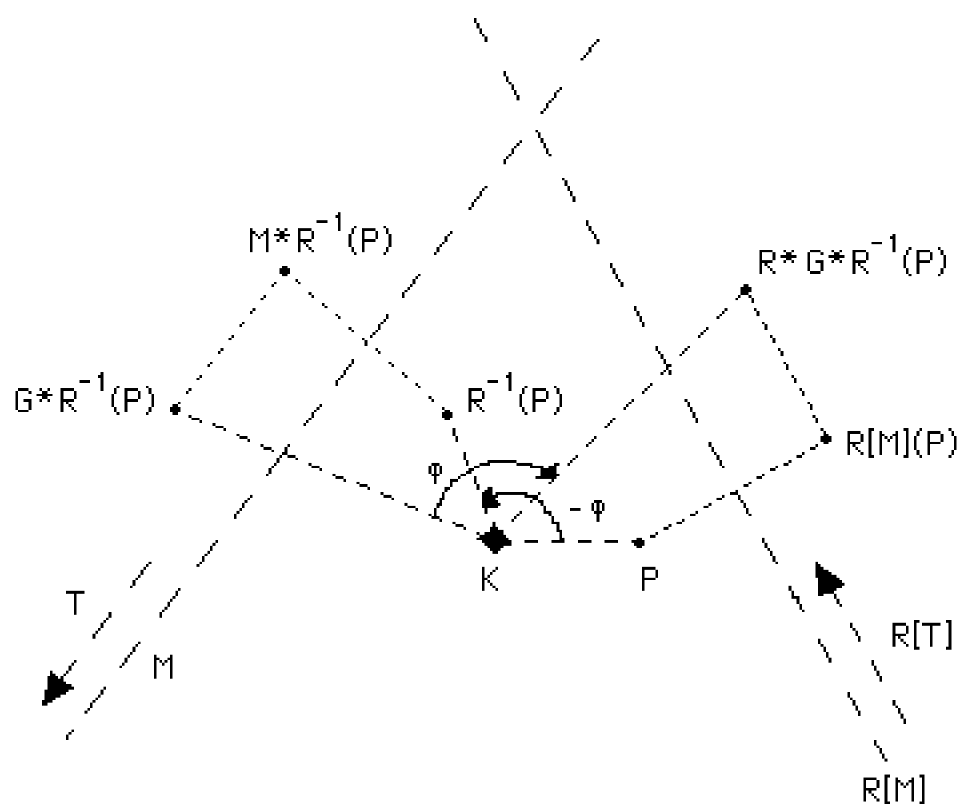

Fig. 8.2

So, how do we establish $\mathbf{R}(\mathbf{M*R^{-1}}(P))$ = **R[M]**(P)? While a 'standard' geometrical approach is possible, the following idea, extending the methods of this section and suggested by **Phil Tracy**, is much more efficient: simply **rotate** the axis **M** along with the quadrangle {K, $\mathbf{R^{-1}}$(P), $\mathbf{M*R^{-1}}$(P), $\mathbf{G*M*R^{-1}}$(P)} to **R**[**M**] and the

congruent quadrangle {K, P, $\mathbf{R}(\mathbf{M}*\mathbf{R}^{-1}(P))$, $\mathbf{R}*\mathbf{G}*\mathbf{R}^{-1}(P)$}; the desired equality $\mathbf{R}(\mathbf{M}*\mathbf{R}^{-1}(P)) = \mathbf{R}[\mathbf{M}](P)$ follows now from the observation that isometries preserve perpendicular bisectors -- in particular **R** rotates the perpendicular bisector **M** of {$\mathbf{R}^{-1}(P)$, $\mathbf{M}*\mathbf{R}^{-1}(P)$} to the perpendicular bisector **R**[**M**] of {P, $\mathbf{R}(\mathbf{M}*\mathbf{R}^{-1}(P))$}, so that $\mathbf{R}(\mathbf{M}*\mathbf{R}^{-1}(P))$ is indeed the mirror image of P about **R**[**M**].

We have just derived the most difficult case of the Conjugacy Principle, showing that the rotation of a glide reflection by an angle ϕ is another glide reflection **both** the axis and the vector of which have been rotated by ϕ: this will be useful in what follows, and so will be its 'inverse' on glide-reflected rotations (figure 8.1).

Here is a challenge for you concerning the image of a glide reflection under **another** glide reflection **not parallel** to it (a case that, unlike the previous ones, we do not need in the rest of this chapter): how would you 'justify' figure 8.3?

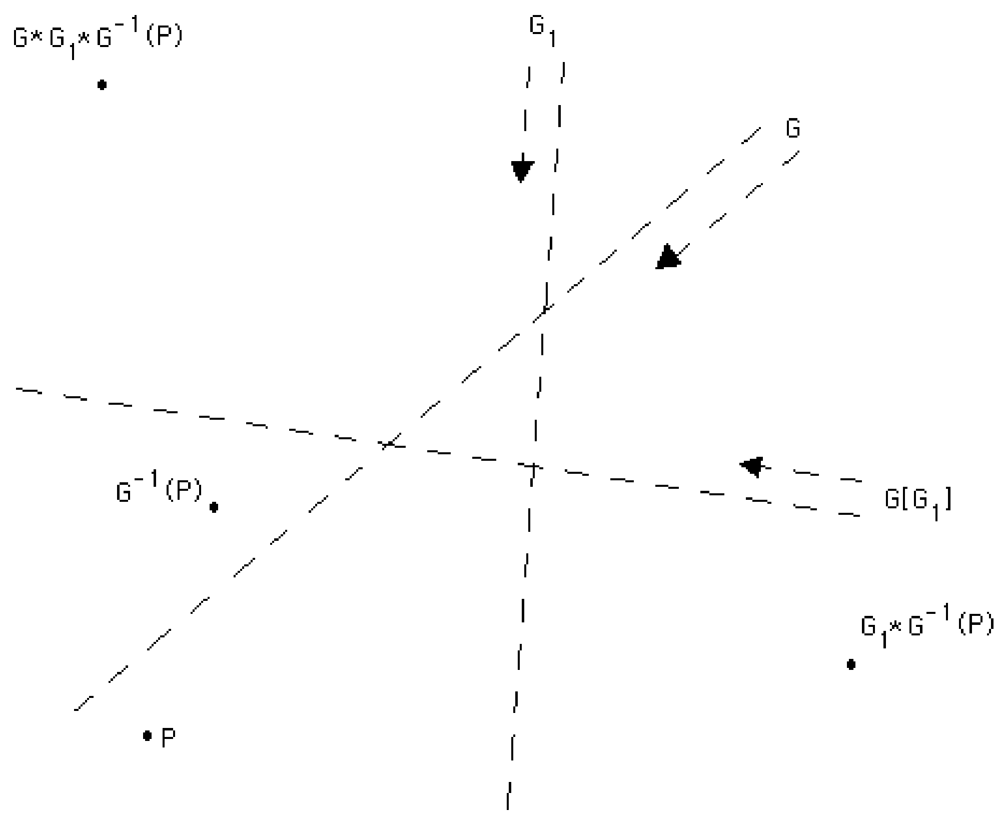

Fig. 8.3

Here is another useful instance of the Conjugacy Principle:

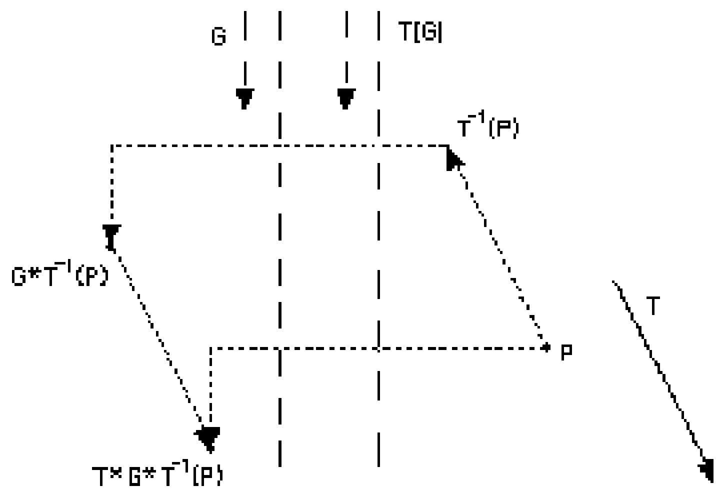

Fig. 8.4

A seasoned conjugacist by now, you should have no trouble understanding what happened in figure 8.4: you better do, it is destined to play a crucial role in what follows! (The few remaining cases and possibilities of the Conjugacy Principle are rather easier, and left to you to investigate; from here on we will assume it **proven** in full rigor and generality, but we will be explicitly stating where and how we use it throughout our classification of wallpaper patterns (sections 8.1-8.4).)

8.1 360^0 patterns

8.1.1 The basic question. The first question we will be asking in each of the coming sections is: does the pattern in question have (glide) reflection? In the case of a 360^0 pattern, a negative answer to this question implies a pattern that has **only** translation(s): that's our familiar **p1** pattern, and there is not much more to say about it than what we already discussed in sections 4.1 and 6.1.

8.1.2 <u>How many (glide) reflections?</u> An affirmative answer to the 'basic question' of 8.1.1 naturally raises the question: "how many kinds of (glide) reflection may coexist in a 360^0 pattern?" What we can say at once is that there **cannot** possibly be (glide) reflection in **two** distinct directions; indeed that is ruled out by the basic result of section 7.10 (which generalizes sections 7.2 and 7.9): any two (glide) reflections intersecting at an angle $\phi/2$ produce a **rotation** by an angle ϕ (7.10.2).

At the same time, the Conjugacy Principle yields infinitely many (glide) reflections derived out of the one that we started with. Indeed every wallpaper pattern has translation in **at least two** directions, in particular in a direction **distinct** from that of the given (glide) reflection; that translation **T**, as well as its **inverse** $\mathbf{T^{-1}}$, simply translate the given (glide) reflection **G** -- as suggested in figure 8.4 -- again and again in both directions, creating an **infinitude** of **parallel** (glide) reflections of **equal gliding vectors**: $\mathbf{T[G]}$, $\mathbf{T^2[G] = T[T[G]]}$, ... , $\mathbf{T^n[G] = T[T^{n-1}[G]]}$, ... and $\mathbf{T^{-1}[G]}$, $\mathbf{T^{-2}[G] = T^{-1}[T^{-1}[G]]}$, ... , $\mathbf{T^{-n}[G] = T^{-1}[T^{-n+1}[G]]}$, ... (figure 8.5):

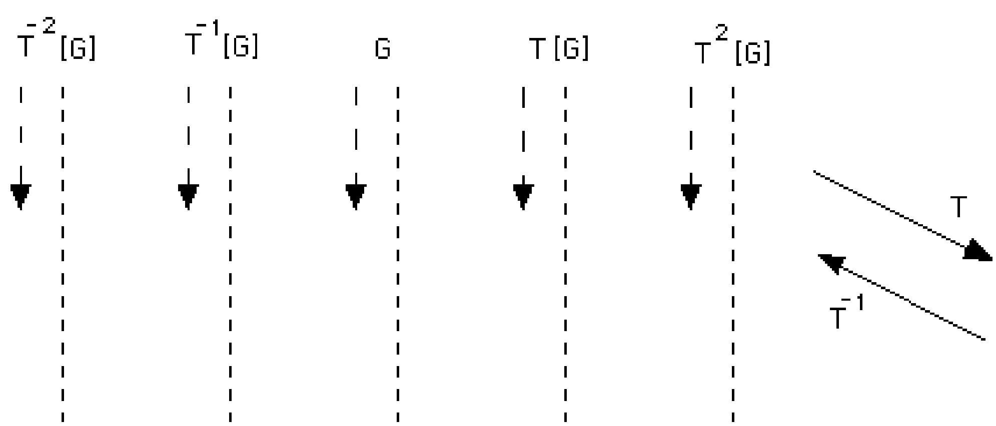

Fig. 8.5

8.1.3 <u>Another way to go.</u> Let's now employ composition of isometries (section 7.4) instead of the Conjugacy Principle, forming $\mathbf{T*G}$, $\mathbf{T^2*G = T*(T*G)}$, ... , $\mathbf{T^n*G = T*(T^{n-1}*G)}$, ... and $\mathbf{T^{-1}*G}$, $\mathbf{T^{-2}*G =}$ $\mathbf{T^{-1}*(T^{-1}*G)}$, $\mathbf{T^{-3}*G = T^{-1}*(T^{-2}*G)}$, ... , $\mathbf{T^{-n}*G = T^{-1}*(T^{-n+1}*G)}$, ... :

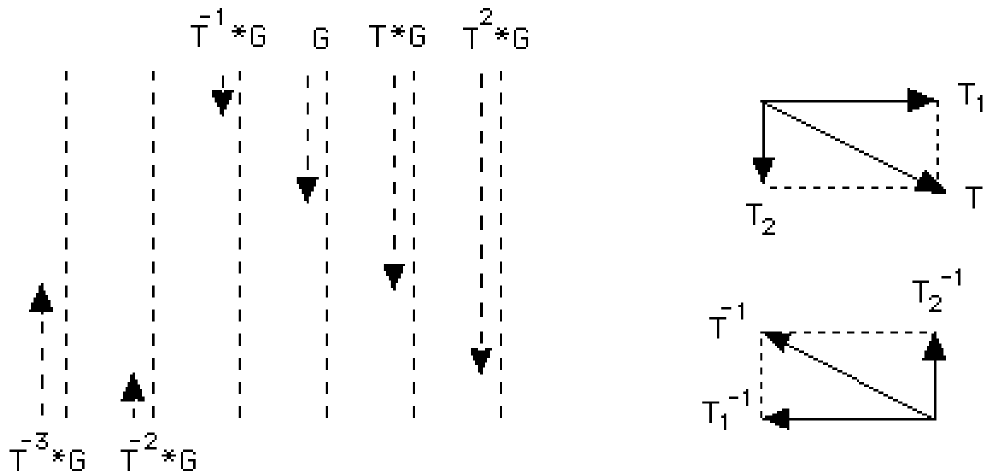

Fig. 8.6

Figure 8.6 certainly **looks** more complicated than figure 8.5, but it isn't; indeed it **essentially** consists, just like figure 8.5, of a **single** glide reflection, $\mathbf{G_0} = \mathbf{T^{-1}*G}$, with all others being **translated odd powers** of it: $\mathbf{G} = (\mathbf{T_1}/2)[\mathbf{G_0^3}]$, $\mathbf{T*G} = \mathbf{T_1}[\mathbf{G_0^5}]$, $\mathbf{T^2*G} = (3\mathbf{T_1}/2)[\mathbf{G_0^7}]$, ... and $\mathbf{T^{-2}*G} = (\mathbf{T_1^{-1}}/2)[\mathbf{G_0^{-1}}] = (-\mathbf{T_1}/2)[\mathbf{G_0^{-1}}]$, $\mathbf{T^{-3}*G} = \mathbf{T_1^{-1}}[\mathbf{G_0^{-3}}] = (-\mathbf{T_1})[(\mathbf{G_0^{-1}})^3]$, ... , where $\mathbf{T_1}$ and $\mathbf{T_1^{-1}} = -\mathbf{T_1}$ are **T**'s and $\mathbf{T^{-1}}$'s perpendicular-to-**G** components, respectively (figure 8.6). (In general, $\mathbf{T^m*G} = ((\frac{m+1}{2})\mathbf{T_1})[\mathbf{G_0^{2m+3}}]$, for **all** integers m; of course this equation is valid **only** for the **particular G** and **T** in figure 8.6!)

What we used above is the fact that every pattern having glide reflection based on axis **M** and **minimal** gliding vector **T** is bound to **also** have glide reflections (**M**, k**T**), where k is an **odd** integer (positive or negative); **no** even multiples of **T** are there because, as we saw as far back as 5.4.1 and 2.4.2 (**p1a1** border patterns), the **square** (and therefore every **even power**) of a glide reflection is a **translation** by a vector twice as long as the glide reflection vector. Conversely, every 'non-minimal' glide reflection combined with **T** and its powers brings us back to the minimal one, (**M**, **T**): in the context of figure 8.6, $\mathbf{G_0^{2m+3}} = \mathbf{T^{m+1}*G_0}$ for **all** integers m.

One last remark before we go on: the compositions $\mathbf{G*T^m}$ would not bring any additional glide reflections into figure 8.6. You may verify that using again the techniques of section 7.4; in algebraic terms, notice some curious identities such as $\mathbf{G}*\mathbf{T} = (\mathbf{T}^{-1}*\mathbf{G})^3$!

8.1.4 Can they coexist? In view of our remarks in 8.1.2 and 8.1.3, figures 8.5 and 8.6 may be merged into one as follows:

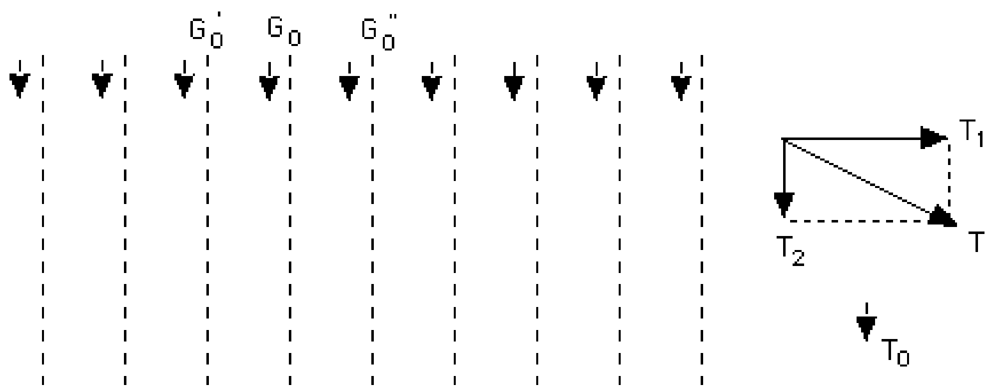

Fig. 8.7

In other words, we simply represent each one of infinitely many, parallel to each other glide reflections by its axis and **minimal** downward gliding vector $\mathbf{T_0}$, remembering that all **odd multiples** of $\mathbf{T_0}$ (positive/downward or negative/upward) produce valid glide reflections based on the same axis. And what we obtained after all these deliberations is the rather familiar symmetry plan of a **pg** pattern! (Note at this point that **T**'s components, $\mathbf{T_2} = \mathbf{G_0^2} = 2\times\mathbf{T_0}$ and $\mathbf{T_1} = \mathbf{G_0}*\mathbf{G'_0} = \mathbf{G''_0}*\mathbf{G_0}$, are valid translations of this **pg** pattern, too.)

It seems that there is no problem at all here, but ... there is a catch! Indeed each glide reflection in figure 8.7 is a translate (**copy**) of $\mathbf{G_0} = \mathbf{T}^{-1}*\mathbf{G}$ obtained in 8.1.3, but ... that's **not** the glide reflection **G** that we started with in 8.1.2! To wit: had we assumed **G** to be a glide reflection of **minimal** gliding vector in figure 8.5, we would be in trouble; for 'playing by the rules' led to a glide reflection $\mathbf{G_0}$ of gliding vector strictly smaller than that of **G** -- to be precise, **one third** the length of **G**'s gliding vector! And we have every right, in fact obligation, to **assume** the existence of a minimal gliding vector: if that is not the case, then, **squaring** glide reflections of arbitrarily small gliding vectors would imply the existence of a pattern with arbitrarily small translations, violating Loeb's **Postulate of Closest Approach** (4.0.4).

Looking back at 8.1.3 and figure 8.6, it becomes clear that what 'created' $\mathbf{G_0}$ and its 'smaller than minimal' gliding vector was $\mathbf{T_2^{-1}}$, the component of $\mathbf{T^{-1}}$ that is parallel to $\mathbf{G}$. At this point, you may ask: aren't we bound to always run into trouble, with $\mathbf{T_2^{-1}}$ always creating a glide reflection having a gliding vector **shorter** than $\mathbf{T_0}$?

Perhaps the best way to answer this question is to have a closer look at figure 8.7 and its 'apparently legal' **pg** pattern: what happens when we compose its minimal glide reflection $\mathbf{G_0}$ with $\mathbf{T}$? In simpler terms, what happens when $\mathbf{T_2^{-1}}$ is added to $\mathbf{G_0}$'s minimal vector $\mathbf{T_0}$? Since $\mathbf{T_2^{-1}} = -2\times\mathbf{T_0}$ (figure 8.7), the result is $\mathbf{T_0} + \mathbf{T_2^{-1}} = \mathbf{T_0} + (-2\times\mathbf{T_0}) = \mathbf{-T_0}$, which is $\mathbf{G_0^{-1}}$'s gliding vector: we 'jumped' from $\mathbf{T_0}$ to $\mathbf{-T_0}$ (as opposed to a still downward vector shorter than $\mathbf{T_0}$) only because $\mathbf{T_2}$ wasn't any shorter -- because $\mathbf{T_2}$ itself is **minimal** as the **vertical component** of **any** valid translation of the **pg** pattern in figure 8.7!

[More generally, $\mathbf{T_0} + m\times\mathbf{T_2} = (2m+1)\times\mathbf{T_0}$ for **all** integers m: the resulting gliding vector is, according to our discussion in 8.1.3, still 'legal', corresponding to a **valid** glide reflection. Even more generally, notice that $\mathbf{T_0} + \mathbf{t}$ is an **odd** ('legal') multiple of $\mathbf{T_0}$ if and only if the 'vertical' translation $\mathbf{t}$ is an **even** multiple of $\mathbf{T_0}$ (hence an arbitrary multiple of $\mathbf{T_2}$). Conversely, the composition of two vertical glide reflections of the form ($\mathbf{M}$, $k_1\times\mathbf{T_0}$) and ($\mathbf{M}$, $k_2\times\mathbf{T_0}$), where k_1 and k_2 are **odd** integers, is a **translation**, with k_1+k_2 **even**, of vertical component $(k_1+k_2)\times\mathbf{T_0}$: we can therefore say that all valid translations have a parallel-to-axis component of the form $k\times\mathbf{T_0}$, where k is an **even** integer.]

Putting everything together, and with our remarks in 8.1.7 further below also in mind, we get a **condition of existence** for **pg**, the pattern first studied in sections 4.3 and 6.2:

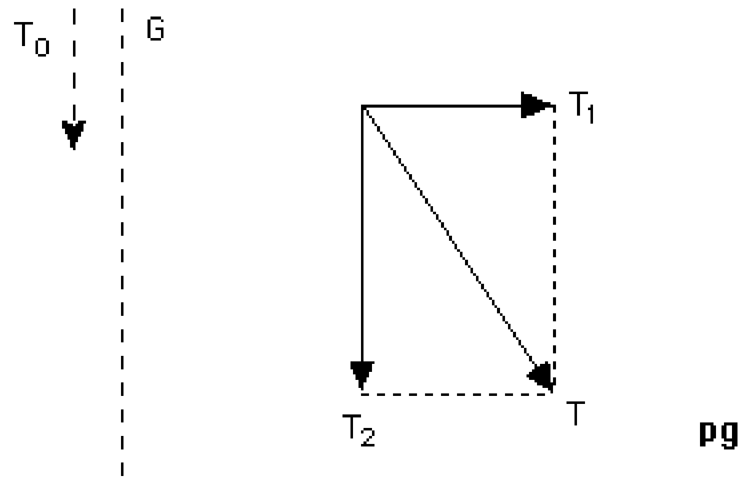

Fig. 8.8

In English: in a **pg** pattern, its translation's minimal parallel-to-the-gliding-axis component ($\mathbf{T_2}$) must be the double of its glide reflection's minimal gliding vector ($\mathbf{T_0}$).

8.1.5 <u>Two gliding vectors?</u> Unpleasant as that may sound, we are not completely through with our derivation of the **pg** pattern! Indeed, while we have fully justified and understood figure 8.7's infinitely many, parallel and 'equal' glide reflections, running at equal distances from each other, we never ruled out the existence of **another** glide reflection **half way** (Conjugacy Principle) between the axes of figure 8.7!

Luckily, that is not difficult to do: if $\mathbf{t_1}$, $\mathbf{t_2}$ are minimal gliding vectors for the glide reflection axes $\mathbf{M_1}$, $\mathbf{M_2}$, respectively (and with $\mathbf{M_1}$, $\mathbf{M_2}$ parallel to each other by necessity), then their **squares** $2\times\mathbf{t_1}$ and $2\times\mathbf{t_2}$ are **translations** parallel to ($\mathbf{M_1}$, $\mathbf{t_1}$) and ($\mathbf{M_2}$, $\mathbf{t_2}$); so, by 7.4.1, ($\mathbf{M_1}$, $\mathbf{t_1}-2\times\mathbf{t_2}$) and ($\mathbf{M_2}$, $\mathbf{t_2}-2\times\mathbf{t_1}$) are **valid** glide reflections. The minimality assumptions on ($\mathbf{M_1}$, $\mathbf{t_1}$) and ($\mathbf{M_2}$, $\mathbf{t_2}$) lead then -- after switching from the two **collinear** vectors to their lengths -- to the inequalities $|t_1-2t_2| \geq t_1$ and $|t_2-2t_1| \geq t_2$, which **seem** to hold concurrently **if and only if** $t_1 = t_2$ (i.e., $\mathbf{t_1} = \pm\mathbf{t_2}$, making the two glide reflections 'equal' to each other). Our argument is illustrated in figure 8.9, where $t_1 \neq t_2$ leads to a violation of the minimality assumption about $\mathbf{t_1}$ being the minimal vector for $\mathbf{M_1}$:

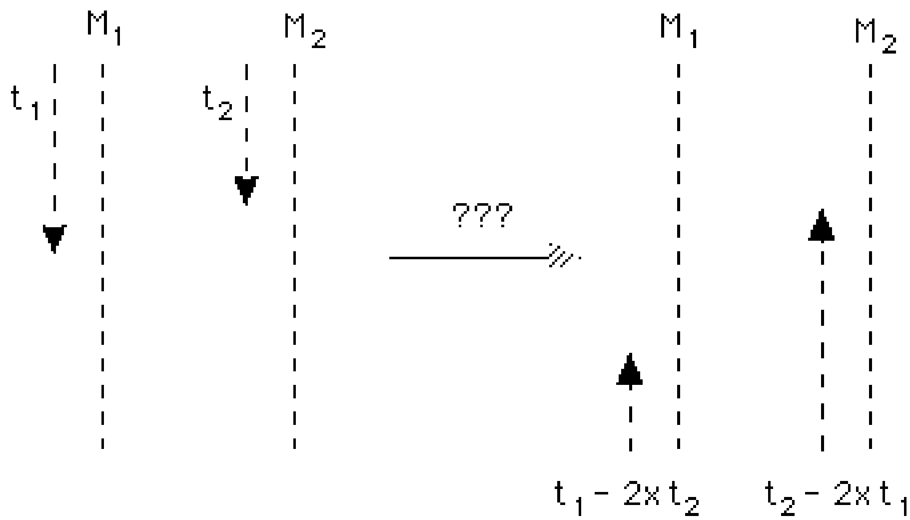

Fig. 8.9

Well, didn't we go a bit **too fast** with the algebra in the preceding paragraph? Let's see: squaring both inequalities we end up with $-4t_1t_2 + 4t_2^2 \geq 0$ and $-4t_1t_2 + 4t_1^2 \geq 0$, that is $t_2^2 \geq t_1t_2$ and $t_1^2 \geq t_1t_2$ or, equivalently, $t_2(t_2-t_1) \geq 0$ and $t_1(t_1-t_2) \geq 0$; now **if** $t_2 > 0$ and $t_1 > 0$, we may safely conclude $t_2-t_1 \geq 0$ and $t_1-t_2 \geq 0$, therefore $t_1 = t_2$ as above. Observe however that it is **possible** to have $t_2 = 0$ and $t_1 > 0$ **or** $t_1 = 0$ and $t_2 > 0$! (**Or** $t_1 = t_2 = 0$, of course.)

What is the geometric relevance of our algebraic observations? What corresponds to a glide reflection of minimal gliding vector of length **zero**? Luckily we are well prepared for this question, and the answer is: **reflection**! To be precise, a glide reflection employing a reflection axis, what we already know as a 'hidden glide reflection'.

8.1.6 A closer look at reflection. We have certainly seen as far back as in 1.4.8 that a reflection **M** may be viewed as a glide reflection of gliding vector zero. A natural question to ask would be the following: what is **M**'s **next shortest** gliding vector? This question makes a lot of sense in view of what we have already discussed in this section: if **T** is the minimal gliding vector of a glide reflection **G**, then the next shortest vector is 3×**T** (8.1.4).

Alternatively, we may look at $\mathbf{T_0}$, the shortest **non-zero** gliding vector of a (glide) reflection. In the case of a genuine glide reflection and a **pg** pattern, we have seen in figure 8.8 and 8.1.4 that $\mathbf{T_0} = \mathbf{T_2}/2$, where $\mathbf{T_2}$ is always the translation's **minimal** vertical component. When it comes to reflection, we observed in 6.3.4 (figure 6.23), while studying two-colored **pm** patterns, how the existence of a vertical reflection **M** does indeed **guarantee** 2×$\mathbf{T_2}$ as a valid vertical translation. That means that 2×$\mathbf{T_2}$ **must** be a gliding vector for the hidden glide reflection associated with **M**, albeit **not necessarily** the shortest non-zero one ($\mathbf{T_0}$). Indeed a review of our examples in chapters 4 and 6 would certainly show that $\mathbf{T_0} = 2\times\mathbf{T_2}$ holds for **cm** patterns only; in **pm** patterns it gives way to $\mathbf{T_0} = \mathbf{T_2}$!

Leaving the **cm** aside for now, we could derive the symmetry plan for the **pm** (almost a **'special case'** of **pg**, studied in sections 4.2 and 6.3), arguing as in 8.1.2 through 8.1.4; we prefer to simply record the **pm**'s 'condition of existence':

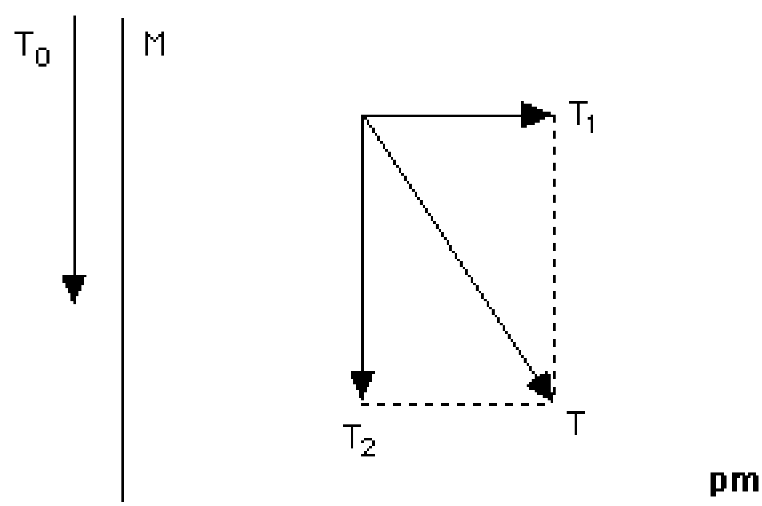

Fig. 8.10

In English: in a **pm** pattern, its translation's minimal parallel-to-the-gliding-axis component ($\mathbf{T_2}$) must be equal to the shortest non-zero gliding vector associated with its reflection ($\mathbf{T_0}$).

The next natural question: is $\mathbf{T_0} = k\times\mathbf{T_2}$ possible for $1 < k < 2$ in the presence of reflection? (Notice that $k > 2$ is impossible by 6.3.4, while $k < 1$ would contradict the minimality of $\mathbf{T_2}$ at once: a gliding vector for a vertical reflection **must** in addition be a vertical translation vector -- **and** vice versa, of course, as noted above.) The answer is negative: with **both** $2\times\mathbf{T_2}$ (6.3.4) and $k\times\mathbf{T_2}$ being vertical translations, their **difference** $(2-k)\times\mathbf{T_2}$ must **also** be a vertical translation, violating the minimality of $k\times\mathbf{T_2} = \mathbf{T_0}$ via $\mathbf{0 < 2-k < k}$. We illustrate our argument for $\mathbf{k = 5/4}$ in figure 8.11 below:

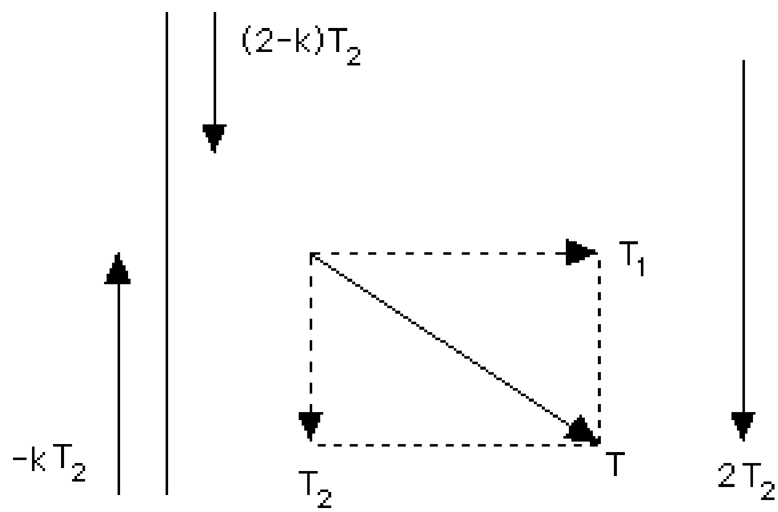

Fig. 8.11

8.1.7 Back to glide reflection. We have already seen in 8.1.4 and figure 8.8 that the **pg** pattern satisfies the relation $\mathbf{T_0} = (1/2)\times\mathbf{T_2}$; at the same time, looking at the **cm** examples of chapters 4 and 6 we see that the vertical glide reflection's minimal gliding vector is **equal** to the translation's minimal vertical component: $\mathbf{T_0} = \mathbf{T_2}$! Now we rule out all other possibilities (for a **glide** reflection **G**) in $\mathbf{T_0} = k\times\mathbf{T_2}$, namely $k < 1/2$, $1/2 < k < 1$, $1 < k < 2$, and $k \geq 2$.

Ruling out $k < 1/2$ is the easiest of the four: indeed $2\times\mathbf{T_0} = 2k\times\mathbf{T_2}$ is a vertical translation, therefore minimality of $\mathbf{T_2}$ yields $2k \geq 1$.

We illustrate the case $1/2 < k < 1$ for $\mathbf{k = 3/4}$ in figure 8.12:

assuming $\mathbf{T_0} = k\times\mathbf{T_2}$ with $1/2 < k < 1$, we notice that $\mathbf{T'_2} = 2\times\mathbf{T_0} - \mathbf{T_2} = (2k-1)\times\mathbf{T_2}$ is **also** the vertical component of a **valid** translation, namely $\mathbf{T'} = (-\mathbf{T})*(2\times\mathbf{T_0}) = (-\mathbf{T_1})*(-\mathbf{T_2})*(2k\times\mathbf{T_2}) = (-\mathbf{T_1})*((2k-1)\times\mathbf{T_2})$; but this contradicts the minimality of $\mathbf{T_2}$ via $\mathbf{0 < 2k-1 < 1}$.

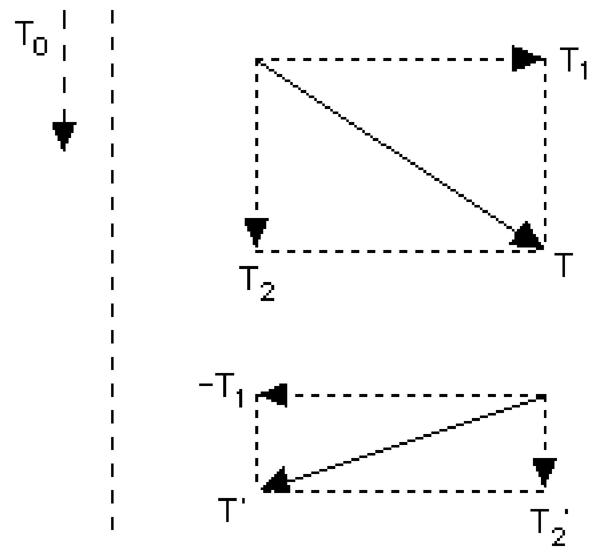

Fig. 8.12

As in the case of reflection (8.1.6, figure 8.11), the case $1 < k < 2$ is ruled out by appeal to the minimality of $\mathbf{T_0}$. Thanks to 7.4.1 the argument remains intact, except that 6.3.4 must be extended to glide reflection; in figure 8.13 we employ the Conjugacy Principle in order to show that $2\times\mathbf{T_2} = \mathbf{T}*(\mathbf{G[T]})$ is **still** a valid vertical translation:

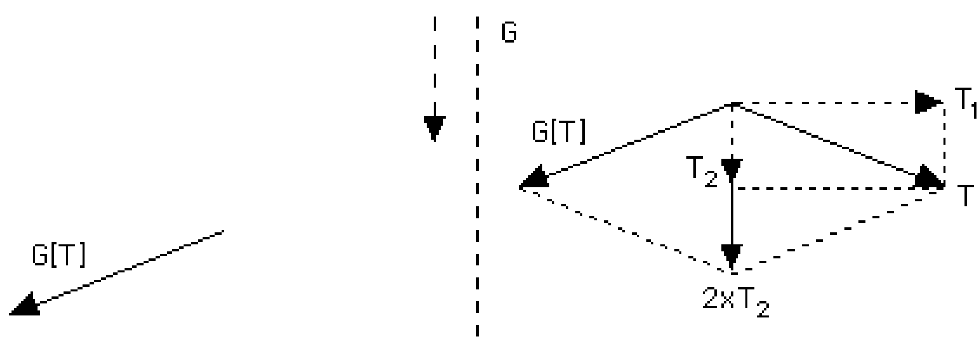

Fig. 8.13

Here is a **'direct'** approach to the matter (and in the spirit of figure 6.23), corresponding to 8.1.6 and figure 8.11 (and **k = 5/4**), that you should ponder on your own:

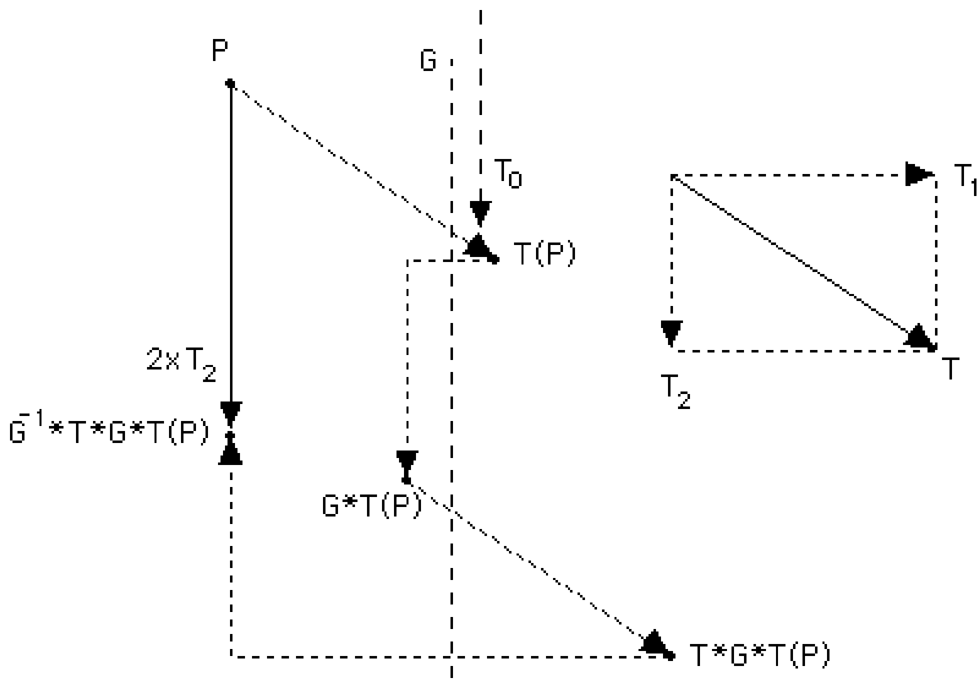

Fig. 8.14

Finally, we need to rule out the case $k \geq 2$. Since $2\times\mathbf{T_2}$ is a valid translation (figure 8.13), $\mathbf{T'_0} = \mathbf{T_0} - 2\times\mathbf{T_2} = (k-2)\times\mathbf{T_2}$ is **also** a gliding vector, corresponding (7.4.1) to the glide reflection $\mathbf{G}*(-2\times\mathbf{T_2})$; this contradicts the minimality of $\mathbf{T_0}$ via $\mathbf{0 \leq k-2 < k}$. (To be more precise, **k = 2** yields a contradiction by turning the glide reflection into a **reflection**.)

So, while glide reflection is more ‘complicated’ than reflection, we have obtained a result **similar** to the one in 8.1.6: the glide reflection’s minimal gliding vector $\mathbf{T_0}$ is either **half** of or **equal** to the translation’s minimal vertical component $\mathbf{T_2}$. (We stress again in passing a major difference between reflection and glide reflection: the former may employ **all multiples** of $\mathbf{T_0}$ as gliding vectors, the latter only the **odd multiples** of $\mathbf{T_0}$.)

8.1.8 <u>The last case.</u> Summarizing, we point to a few useful facts already established:

-- two parallel glide reflections of distinct minimal gliding vectors may coexist if and only if one of them is a reflection (8.1.5)

-- the smallest non-zero gliding vector (**T_0**) of a reflection **M** may only be either equal or double the translation's minimal parallel-to-**M** component (**T_2**) (8.1.6)

-- the smallest gliding vector (**T_0**) of a glide reflection **G** may only be either equal or half the translation's minimal parallel-to-**G** component (**T_2**) (8.1.7)

In addition, we derived the **pg** (glide reflection only, **$T_0 = T_2$**/2) and **pm** (reflection only, **$T_0 = T_2$**) patterns (figures 8.8 & 8.10), corresponding to the equalities $t_1 = t_2 > 0$ and $t_1 = t_2 = 0$ of 8.1.5, respectively. Two natural questions would then be whether or not there exists a **reflection-only** pattern satisfying **T_0** = 2×**T_2** and whether or not there exists a **glide-reflection-only** pattern satisfying **T_0** = **T_2**.

The first possibility is ruled out as follows:

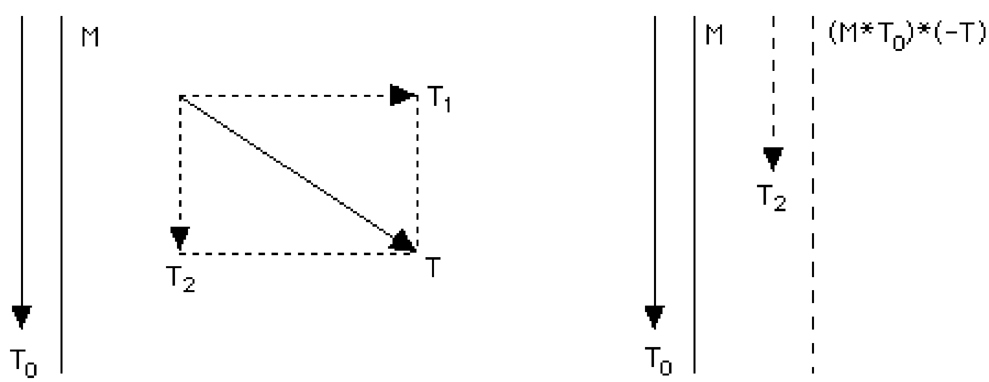

Fig. 8.15

Treating **$M*T_0$** as a glide reflection and applying 7.4.1, we see that its composition with **T^{-1}** = **–T** produces a **glide** reflection based on an axis at a distance of |**T_1**|/2 to the right of **M** and of gliding vector **T_0–T_2** = **T_2** (figure 8.15): this violates either **T_0**'s minimality (in case $(\mathbf{M}*\mathbf{T_0})*\mathbf{T}^{-1}$ is indeed a reflection) or our assumption that **all** axes are **reflection** axes.

The second possibility is ruled out as follows:

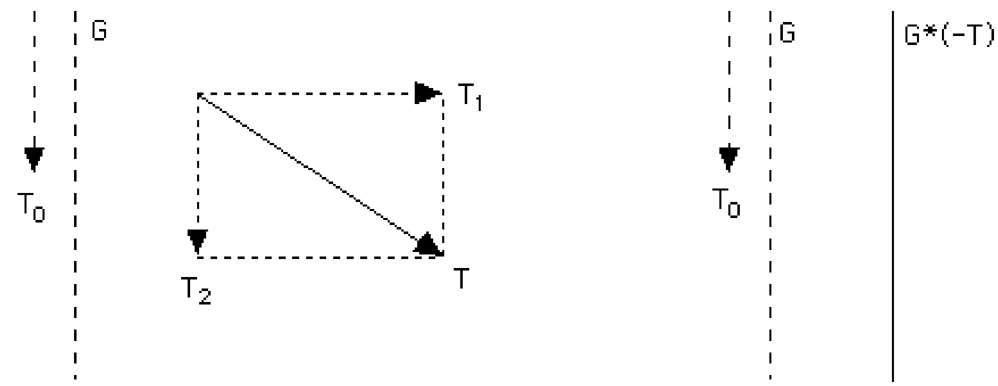

Fig. 8.16

Employing ideas from section 7.4 as in figure 8.15, we see that $\mathbf{G}*\mathbf{T}^{-1}$ is a **reflection** based on an axis at a distance of $|\mathbf{T_1}|/2$ to the right of **G** (figure 8.16), again contradicting our starting assumption.

So, the only possibilities that remain are the ones corresponding to the case $t_1 > 0$, $t_2 = 0$ (or vice versa) of 8.1.5: reflection **and** glide reflection in one and the same pattern, at long last! Let $\mathbf{T_0^G}$ be the minimal gliding vector of the glide reflection **G**, and let $\mathbf{T_0^M}$ be the minimal **non-zero** gliding vector associated with the reflection **M**. With $\mathbf{T_2}$ being always the translation's minimal parallel-to-**M**-and-**G** component, there exist, in theory, four possibilities:

(I) $\mathbf{T_0^G} = \mathbf{T_2}/2$, $\mathbf{T_0^M} = \mathbf{T_2}$

(II) $\mathbf{T_0^G} = \mathbf{T_2}/2$, $\mathbf{T_0^M} = 2\times\mathbf{T_2}$

(III) $\mathbf{T_0^G} = \mathbf{T_2}$, $\mathbf{T_0^M} = \mathbf{T_2}$

(IV) $\mathbf{T_0^G} = \mathbf{T_2}$, $\mathbf{T_0^M} = 2\times\mathbf{T_2}$

It is easy to rule out (I) through (III). In (I) the composition of the reflection and the glide reflection yields a valid translation of 'vertical' component $\mathbf{T}_0^{\mathbf{G}} = \mathbf{T}_2/2$, contradicting $\mathbf{T}_2$'s minimality. In (II) the square of the glide reflection produces a valid translation $\mathbf{T}_2$ that contradicts the minimality of $\mathbf{T}_0^{\mathbf{M}} = 2\times\mathbf{T}_2$. And in (III) the axis of **G** ends up being a **reflection** axis for $\mathbf{G}*\mathbf{T}_2^{-1}$ -- recall that any gliding vector associated with a reflection axis is in fact a valid **translation** vector.

So the **only** remaining possibility is (IV), which is more or less already known to correspond to the only 360^0 pattern not 'formally' derived so far (good old **cm** of sections 4.4 and 6.4) and whose 'condition of existence' is given below:

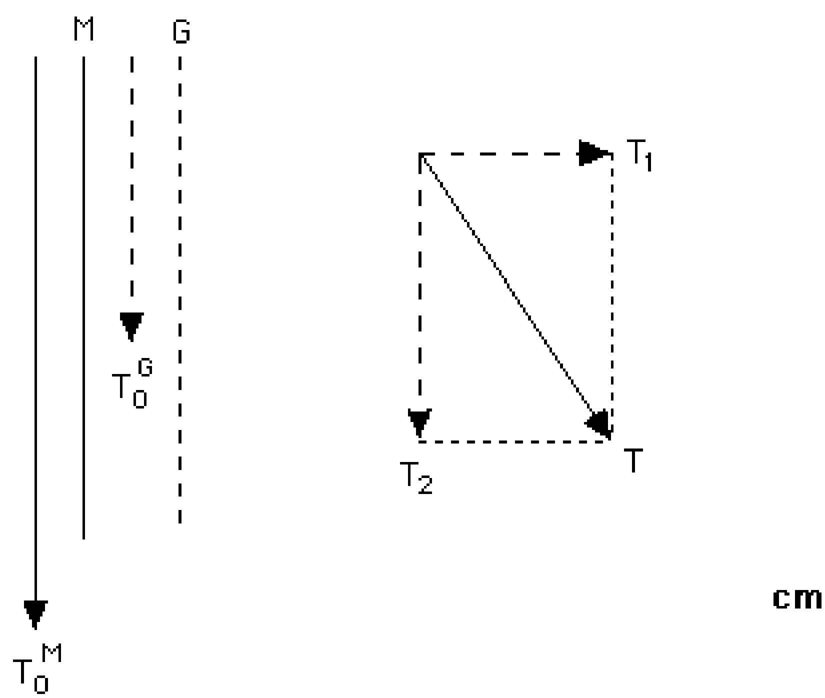

Fig. 8.17

Indeed we may verify figure 8.17 by reviewing old **cm** examples from chapters 4 and 6. No contradictions are to be found, glide reflection axes will never be good for reflection, whatever is supposed to be minimal will indeed remain minimal, etc. Of course $\mathbf{T}*\mathbf{M} = \mathbf{G}$, while $\mathbf{T}_1$ and $\mathbf{T}_2$ are **not** valid translations.

8.1.9 Brief overview. We have finally demonstrated why, in the presence of (glide) reflection and in the absence of rotation, only three types of wallpaper patterns are possible (**pg**, **pm**, **cm**); those are **'defined'** in figures 8.8, 8.10, and 8.17, respectively, and are **characterized** by the relations $\mathbf{T_0^G} = \mathbf{T_2}/2$ (**pg**), $\mathbf{T_0^M} = \mathbf{T_2}$ (**pm**), and $\mathbf{T_0^G} = \mathbf{T_2}$ & $\mathbf{T_0^M} = 2\times\mathbf{T_2}$ (**cm**). (The fact that these relations are indeed characterizations of the patterns in question follows from a closer look at our work in this section.) Together with the **p1** type (8.1.1), there exist therefore precisely **four** 360^0 wallpaper patterns.

In view of the characterizations and 'definitions' cited above for the three non-trivial 360^0 patterns, we need to **question** somewhat our discussion of the **cm** type in 6.4.5, where we viewed it as a **'merge'** of **pg** and **pm**: **cm** has definitely its own structure, and it's more than a **pg** and a **pm** 'under the same roof'! Please have a look at the two-colored **cm** examples of figure 6.37 and notice how the removal of every other **row** yields a **pm** pattern, while the removal of every other **column** yields a **pg** pattern; in both cases the removal of half of the pattern **doubles** the vectors **T** and $\mathbf{T_2}$ but leaves $\mathbf{T_0^G}$ and $\mathbf{T_0^M}$ unchanged, altering $\mathbf{T_0^G} = \mathbf{T_2}$ & $\mathbf{T_0^M} = 2\times\mathbf{T_2}$ to $\mathbf{T_0^M} = \mathbf{T_2}$ (row removal, **pm**) or $\mathbf{T_0^G} = \mathbf{T_2}/2$ (column removal, **pg**).

One **important fact** to keep in mind: $\mathbf{T_2}$ (and hence $\mathbf{T_1} = \mathbf{T}-\mathbf{T_2}$ as well) is a valid translation in both the **pg** and **pm** patterns, but **not** in the **cm** pattern; differently said, a translation's projection onto the (glide) reflection direction (and its perpendicular) may **not** be a valid translation **if and only if** the 360^0 pattern is a **cm**.

The "if" part above is established through figure 8.17 and related comments. The "only if" follows from the observation that, in **any** pattern, the vertical component of **any** translation $\mathbf{T'}$ must be an **integral** multiple of $\mathbf{T_2}$; but in both the **pm** and the **pg** the $\mathbf{T_2}$ is a valid translation, and so would be any integral multiple of it! (If the vertical component of $\mathbf{T'}$ equals $k\times\mathbf{T_2}$ with k non-integer then the vertical component of the valid translation $\mathbf{T'} - m\times\mathbf{T}$, where m is the closest integer to k, would violate the minimality of $\mathbf{T_2}$.)

8.2 180^0 patterns

8.2.1 <u>The **p2** lattice.</u> In the absence of (glide) reflection, a 180^0 pattern is fully determined by an infinitude of half turn centers propagated by two non-parallel, **'shortest possible'** translations $\mathbf{T_1}$, $\mathbf{T_2}$. This is demonstrated in figure 8.18, echoing figure 7.26 and related discussion in 7.6.4: please refer there for details.

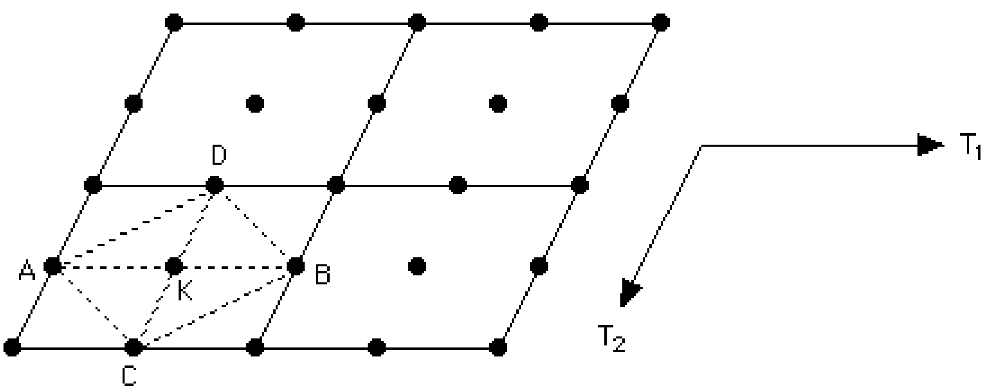

Fig. 8.18

The rows and columns of half turn centers of the **p2** pattern in figure 8.18 would be **orthogonal** to each other in case there was some (glide) reflection (as in 8.2.3-8.2.6 below): indeed in such a case $\mathbf{T_1}$ and $\mathbf{T_2}$ would be **perpendicular** and **parallel**, respectively, to the (glide) reflection axis (as in figures 8.8, 8.10, and 8.17). Of course we do **not** need any (glide) reflection in order to make $\mathbf{T_1}$ and $\mathbf{T_2}$ perpendicular to each other and **'rule'** the 180^0 centers: see for example figures 4.28, 4.30, 6.39, and 6.40 in sections 4.5 and 6.5!

8.2.2 <u>Ruling the centers.</u> In the case you are not convinced by our argument above concerning the **'alignment'** of half turn centers by (glide) reflection, figure 8.19 offers another approach to the matter:

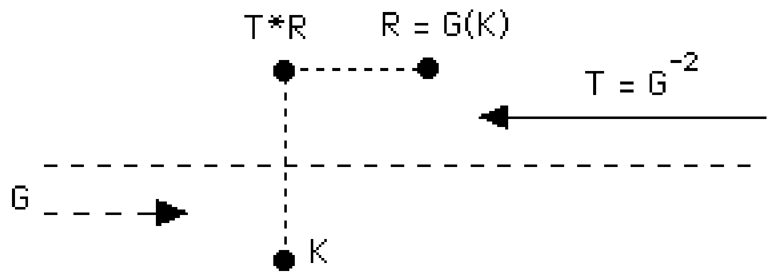

Fig. 8.19

Miraculously, **G** not only glide-reflects K into a new center **G**(K) (Conjugacy Principle), but it also ends up **mirroring** it into another working center right across its axis: how did that happen? Well, as figure 8.19 suggests, the inverse of **G**'s square is a **'backward'** translation **T**; composing **T** with the half turn **R** centered at **G**(K), and with **T** going **second** (7.3.1, 7.6.4), creates a new rotation center **half way** between **G**(K) and **T**(**G**(K)), which is K's mirror image!

Such observations are going to be crucial in what follows: assuming some (glide) reflection from here on, we will see how the 'ruled', orthogonalized lattice(s) of half turn centers are built, classifying 180^0 patterns at the same time. A solid departing point is to assume (glide) reflection in the pattern's 'vertical' direction: that **forces** (glide) reflection in the 'horizontal' direction as well, and in ways dictated by the laws that govern isometry composition; what is clear, in view of our results in section 8.1, is that there are precisely **three** possibilities for the vertical 'factor' (**pm**, **pg**, **cm**).

8.2.3 <u>Starting with a **pm** and an on-axis center.</u> We begin by assuming a **pm** vertical factor **and** the existence of one **180^0 center** K **on** one of the reflection axes. By the Conjugacy Principle, that center is translated all over that axis by multiples of $\mathbf{T_2}$; and then all the centers on that axis are translated across to **every other** reflection axis by multiples of $\mathbf{T_1}$:

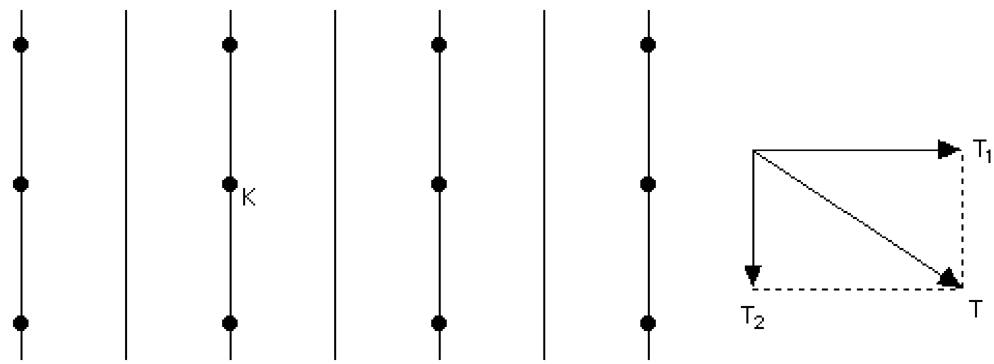

Fig. 8.20

Next come the compositions of the 'already existing' half turns with $\mathbf{T_1}$ and $\mathbf{T_2}$, creating 'new' centers at distances of $|\mathbf{T_1}|/2$, $|\mathbf{T_2}|/2$ from the 'old' ones (7.6.4), inevitably lying on the reflection axes (which may be viewed as having been created by the same compositions):

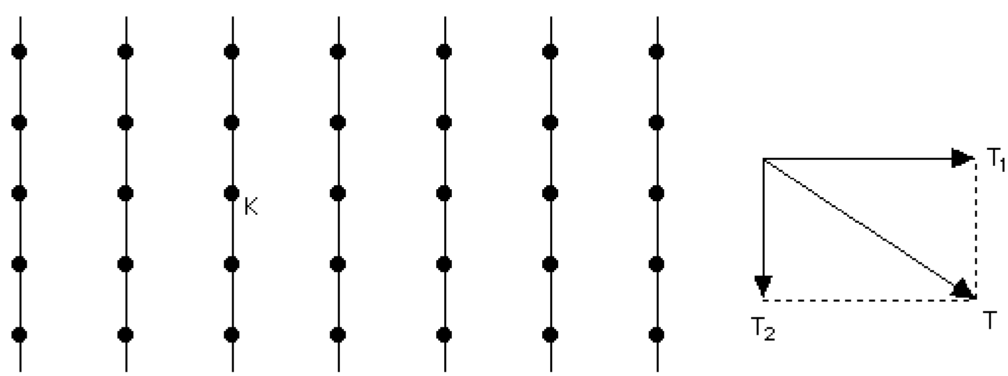

Fig. 8.21

Finally, the compositions of 180^0 rotations and reflections create 'new' reflection axes perpendicular to the existing ones and passing through the half turn centers (7.7.1):

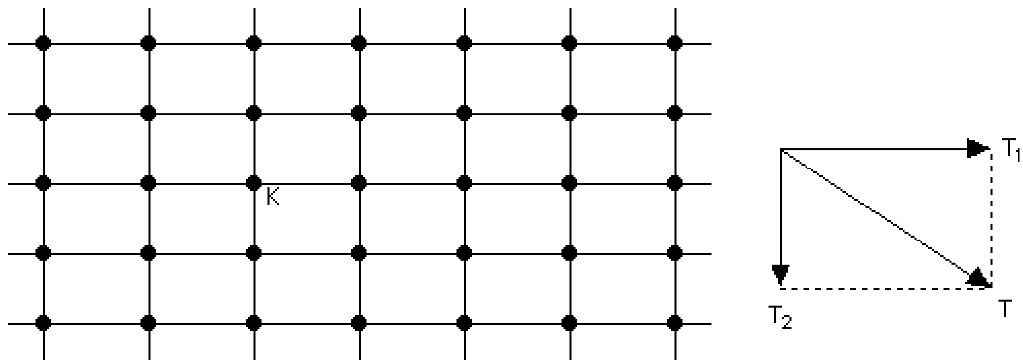

Fig. 8.22

What you see in figure 8.22 is the familiar **pmm** = **pm** × **pm** pattern of sections 4.6 and 6.8: no new isometry compositions are possible, everything is **'complete'** and **'settled'**. Assuming minimality of $\mathbf{T_1}$ and $\mathbf{T_2}$, **T** is the pattern's **shortest** 'diagonal' translation; in particular, no translation (or any other isometry) may swap any two of the centers located at the corners of any given **smallest rectangle** in figure 8.22: this justifies our reference to **'four kinds'** of half turn centers in 4.6.1.

8.2.4 Starting with a **pm** and an off-axis center. Let's now assume a vertical **pm** factor and a 180^0 center K that does **not** lie on any of the vertical reflection axes. By the Conjugacy Principle, K must lie **half way** between two adjacent axes, **rotating** them onto each other; arguing then as in 8.2.3, we see that K is 'multiplied' by $\mathbf{T_1}$ and $\mathbf{T_2}$ into the group of centers shown in figure 8.23:

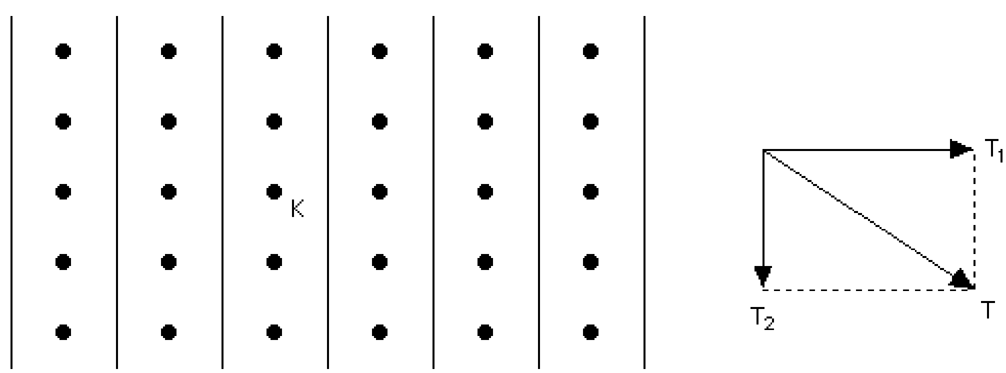

Fig. 8.23

Next, each composition of a 180^0 rotation and a reflection creates a glide reflection perpendicular to the reflection and passing through the rotation center (7.7.4), and of gliding vector of length $2x(|\mathbf{T_1}|/4)\times\sin(180^0/2) = |\mathbf{T_1}|/2$ (7.7.3). We end up with the 'complete' pattern of figure 8.24, which is the **pmg** = **pm** × **pg** of sections 4.7 and 6.7:

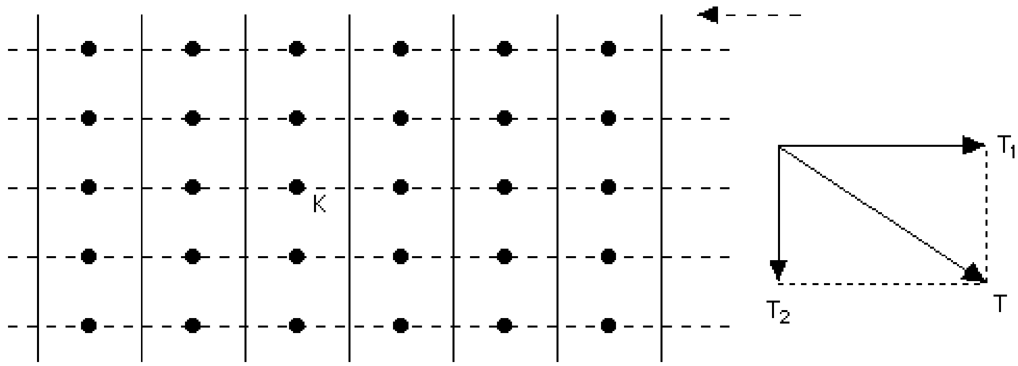

Fig. 8.24

Indeed the pattern's horizontal factor is a **pg**, with its minimal gliding vector being half of **T**'s horizontal component (8.1.4).

8.2.5 <u>Starting with a **pg** and an on-axis center.</u> Let's now assume the existence of a **pg** in the vertical direction **and** the existence of a 180^0 center K **on** a glide reflection axis. Exactly as in 8.2.3, the standard translations $\mathbf{T_1}$ and $\mathbf{T_2}$ 'multiply' the half turn centers (still lying **on** the glide reflection axes); and, reversing the process of 8.2.4, each composition of a 180^0 rotation and a glide reflection of gliding vector $\mathbf{T_2}/2$ produces a reflection perpendicular to the glide reflection and at a distance of $(|\mathbf{T_2}/2|)/2 = |\mathbf{T_2}|/4$ from the rotation center (7.8.2). We end up with a horizontal **pm** factor and, **again**, a **pmg** pattern:

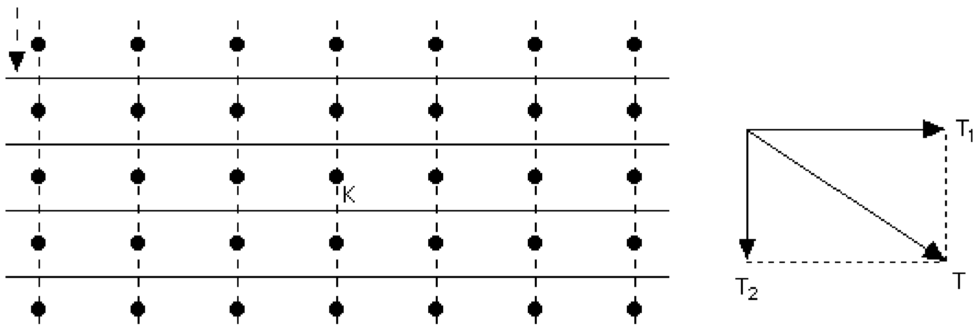

Fig. 8.25

Most certainly, the **pmg** patterns shown in figures 8.24 & 8.25 are mathematically indistinguishable. Looking at any '**smallest rectangle** of rotation centers' (as we did in 8.2.3), we see the four corners split into **two** pairs (4.11.2) of centers (lying on opposite sides) that may be swapped by **both** the pattern's reflection and the pattern's glide reflection.

8.2.6 Starting with a **pg** and an off-axis center. Assuming this time a vertical **pg** factor and a 180^0 rotation center K that does **not** lie on any glide reflection axis, we follow previous considerations in order to once more arrive at an 'aligned' **p2** lattice 'coexisting' with the **pg** pattern. As in 8.2.4, the Conjugacy Principle shows that K, and therefore all other centers created out of it via $\mathbf{T_1}$ and $\mathbf{T_2}$, must lie half way between two adjacent glide reflection axes. Next, we appeal to 7.8.1 and 7.8.2 in order to see that each composition of a 180^0 rotation with a **vertical** glide reflection of gliding vector $\mathbf{T_2}/2$ lying at a distance $|\mathbf{T_1}|/4$ from its center creates a **horizontal** glide reflection of gliding vector of length $2\times(|\mathbf{T_1}|/4)\times\sin(180^0/2) = |\mathbf{T_1}|/2$ at a distance of $(|\mathbf{T_2}/2|)/2 = |\mathbf{T_2}|/4$ from the rotation center (figure 8.26). The outcome is a horizontal **pg** factor and the familiar **pgg** = **pg** × **pg** pattern of sections 4.8 and 6.6.

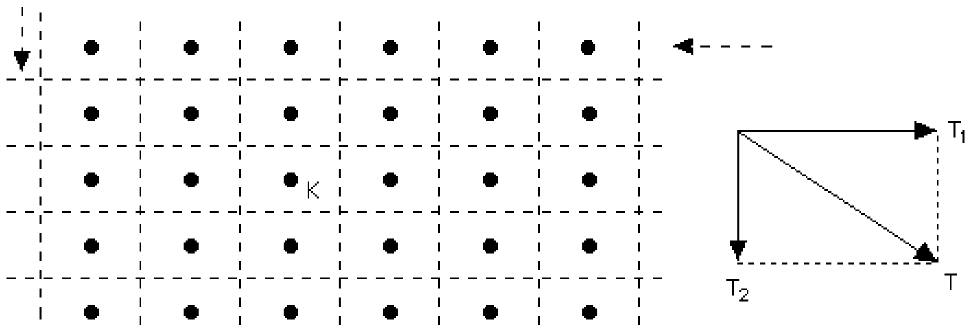

Fig. 8.26

Notice how the half turn centers in figure 8.26 are mirrored across glide reflection axes, precisely as shown in 8.2.2. Of course we did not directly appeal to glide reflection in order to get the **pgg** lattice; but notice that the **pgg**'s glide reflections allow **'travel'** along the **diagonals** of that smallest rectangle of half turn centers: this confirms our remark about **two** kinds of **pgg** centers in 4.11.2!

8.2.7 Starting with a **cm** and a 'reflection' center. We have just verified in 8.2.3-8.2.6 that we may start with a **pm** vertical factor and end up with either a **pm** or **pg** horizontal factor, or that we may start with a **pg** vertical factor and end up with either a **pg** or **pm** horizontal factor. It seems that there is no way we can get a **cm** horizontal factor starting with either a **pm** or a **pg** in the vertical direction: for one thing, you may verify that there is **no way** we can insert a horizontal **in-between** (glide) reflection in figures 8.22 and 8.24-8.26 without creating, by way of isometry composition, **non-existing** (glide) reflection in the vertical direction.

In fact the coexistence of the **cm** with either the **pm** or the **pg** may be ruled out by our **crucial** remark at the end of 8.1.9: the **cm** **requires** a translation the vertical and horizontal components of which are not translations, which is **impossible** in either **pm** or **pg**!

So, let's **start** with a vertical **cm** and see what we get in the horizontal direction. (By symmetry between the two directions, we may **only** anticipate a horizontal **cm**; but we still have to verify that this **is** possible, after all, and also see in **how many** ways it is possible.) By the Conjugacy Principle, a 180^0 center K may only lie

on either a reflection or a glide reflection axis. Leaving the latter case for 8.2.8, we begin with K on a **reflection** axis, paralleling the 'center creation' process of 8.2.3 and figure 8.20:

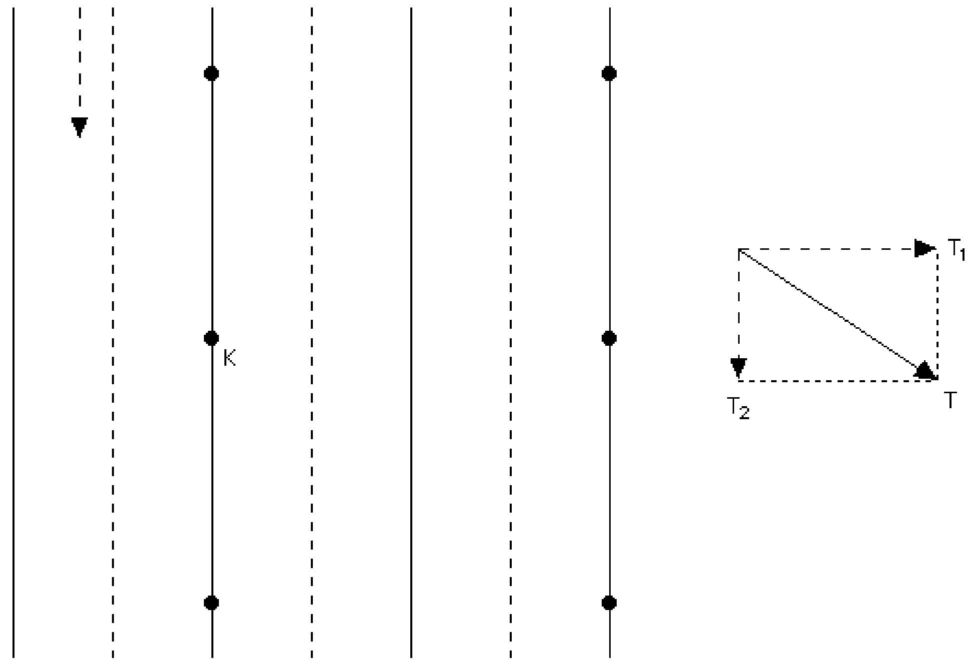

Fig. 8.27

The 180^0 centers featured in figure 8.27 are precisely those created out of K by way of **translation** and the Conjugacy Principle: recall at this point that the **cm**'s **minimal** vertical and **minimal** horizontal translations are $2\times\mathbf{T_2}$ and $2\times\mathbf{T_1}$, respectively (8.1.8).

Next we **compose** the 'already existing' centers with the translations $2\times\mathbf{T_2}$ and $2\times\mathbf{T_1}$ (in the spirit of 7.6.4 and figure 8.21) in order to get 'new' centers, still on reflection axes **only** (figure 8.28); alternatively, we could get the same centers by employing the glide reflections and 8.2.2:

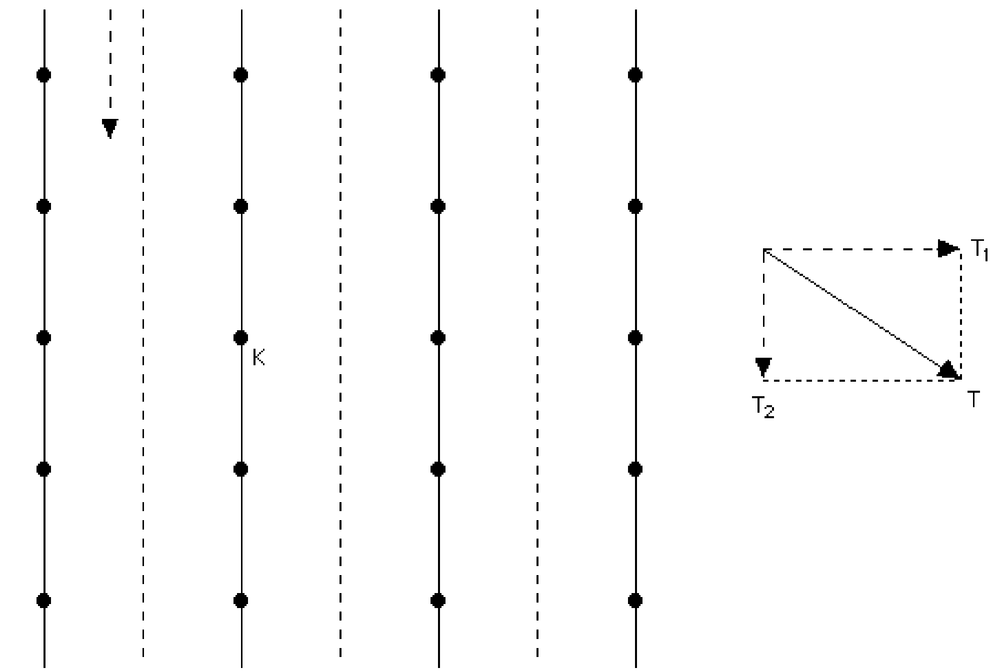

Fig. 8.28

Now the vertical reflections **'turn'** into horizontal reflections, exactly as in figure 8.22:

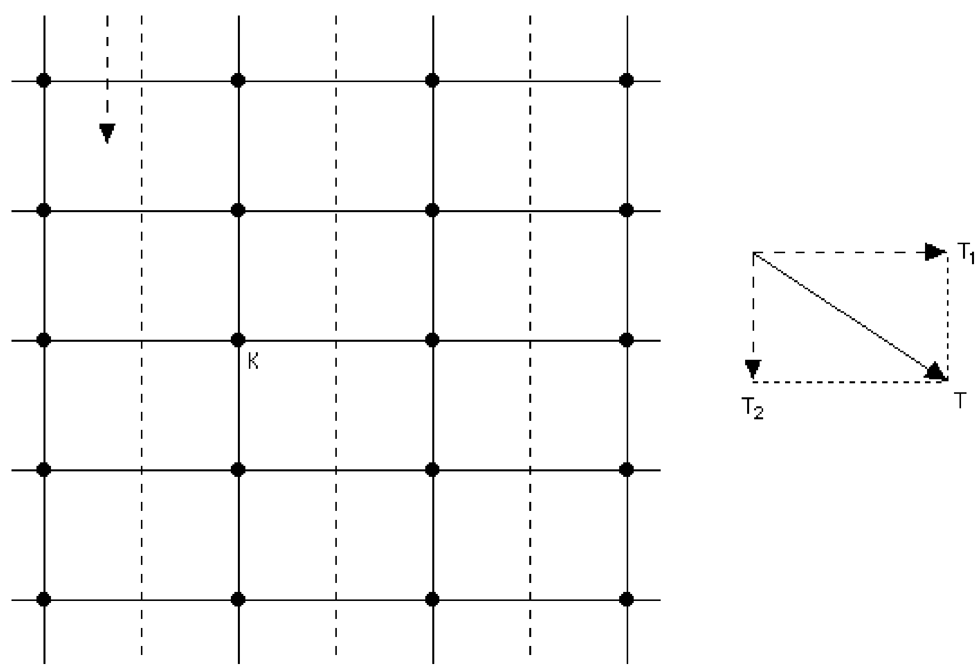

Fig. 8.29

Next come the horizontal glide reflections, ‘created’, as in 8.2.6 and figure 8.26, by compositions of vertical glide reflections with 180^0 rotations the centers of which do not lie on the glide reflection axes. To be more specific, the composition of every vertical glide reflection of gliding vector $\mathbf{T_2}$ with a half turn center at a distance of $|\mathbf{T_1}|/2$ from it (figure 8.29) produces a horizontal glide reflection of gliding vector of length $2\times(|\mathbf{T_1}|/2)\times\sin(180^0/2) = |\mathbf{T_1}|$ at a distance of $|\mathbf{T_2}|/2$ from the rotation center (7.8.1):

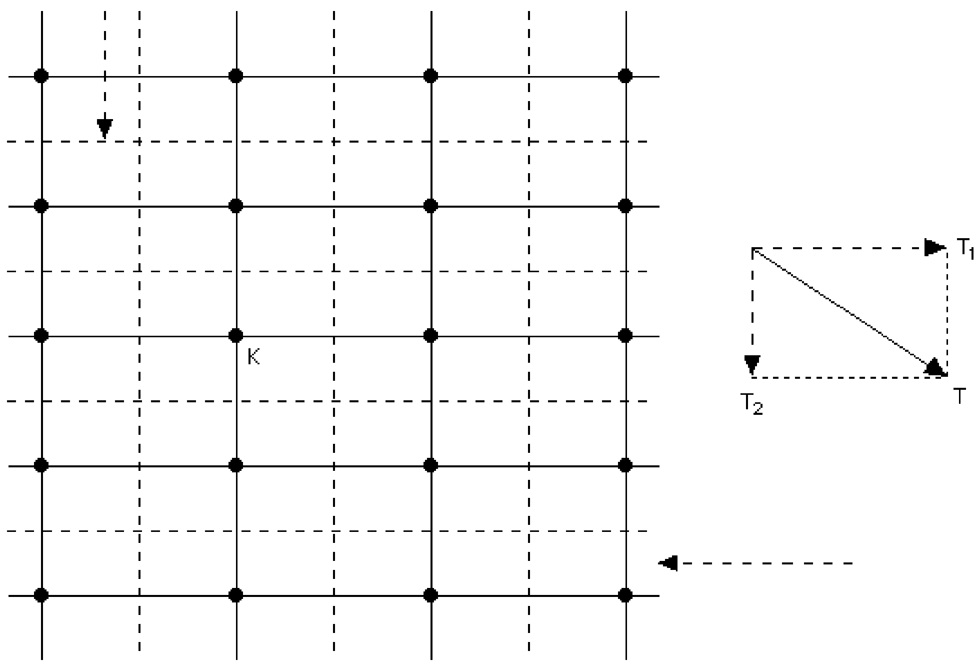

Fig. 8.30

Finally, every composition of a vertical glide reflection (of gliding vector $\mathbf{T_2}$) with a horizontal reflection produces a 180^0 center lying at the intersection of two glide reflection axes, and so does every composition of a vertical reflection with a horizontal glide reflection (of gliding vector $\mathbf{T_1}$). We demonstrate this in figure 8.31 below, relying either on section 7.9 or on figure 6.6.2: the shown half turn center and 180^0 rotation equals both $\mathbf{M_1}*\mathbf{G_2}$ and $\mathbf{M_2}*\mathbf{G_1}$, lying on $\mathbf{G_2}$ and at a distance $|\mathbf{T_2}|/2$ from its intersection with $\mathbf{M_1}$, as well as on $\mathbf{G_1}$ and at a distance $|\mathbf{T_1}|/2$ from its intersection with $\mathbf{M_2}$.

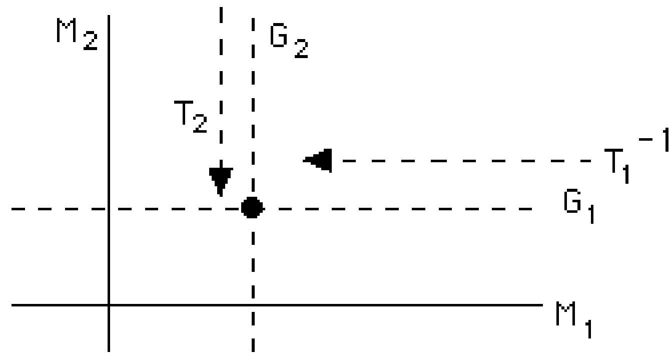

Fig. 8.31

Alternatively, we could at long last have used the **diagonal** translation **T** and its **compositions** with 'existing' centers at the intersections of reflection axes (figure 8.30) to get the 'new' centers at the intersections of glide reflection axes. One way or another, we have finally arrived at the 'standard' **cmm** = **cm** × **cm** pattern of sections 4.9 and 6.9, as no more centers or axes can be created:

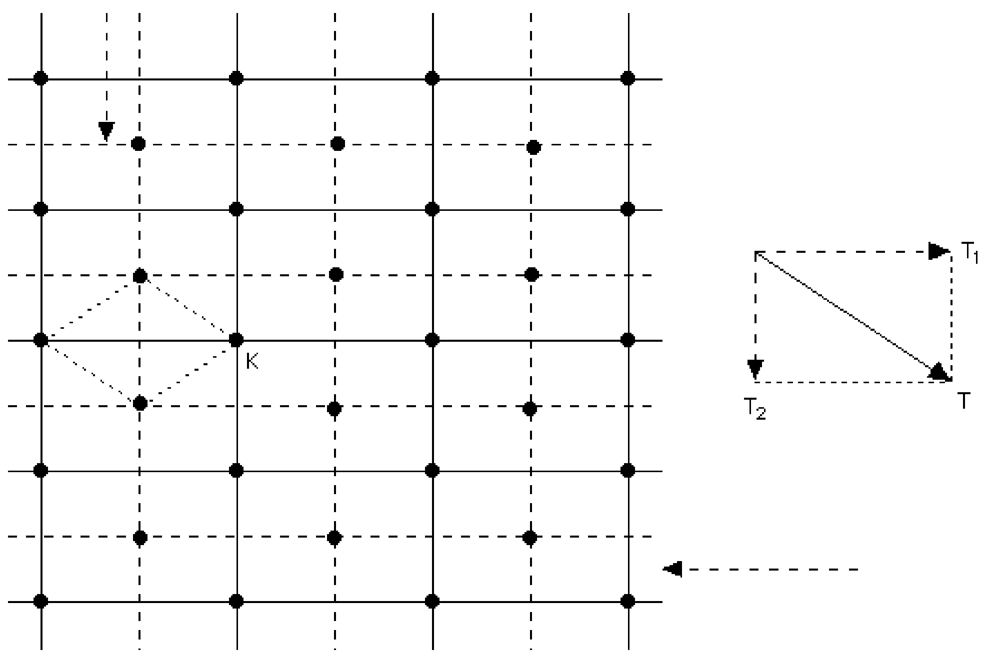

Fig. 8.32

Comparing the lattice of half centers in figure 8.32 (**cmm**) to the ones in figures 8.22 (**pmm**), 8.24 & 8.25 (**pmg**), and 8.26 (**pgg**), we can certainly say that this new lattice 'has been cut in half'; or, if you prefer, while the minimal translation **T** remained the same, we moved from the ‘minimal rectangle’ of centers of the **pmm**, **pmg**, and **pgg** patterns to the **cmm**’s **‘minimal rhombus’** of centers, which is **twice** as large in area as that rectangle (figure 8.32).

8.2.8 Starting with a **cm** and a ‘glide reflection’ center. What happens in case the ‘creating center’ K lies on a vertical **glide** reflection axis? The answer may disappoint, but hopefully not astonish, you: we end up with exactly the **same cmm** pattern of figure 8.32, completing in fact the classification of 180^0 patterns! We leave it to you to check the details, providing just one **possible** ‘intermediate stage’ in figure 8.33: horizontal reflections have just been ‘created’ as compositions of vertical glide reflections and 180^0 rotations lying on them (as in 8.2.5); in the next stage, intersecting reflection axes will create all ‘missing’ half turn centers, etc.

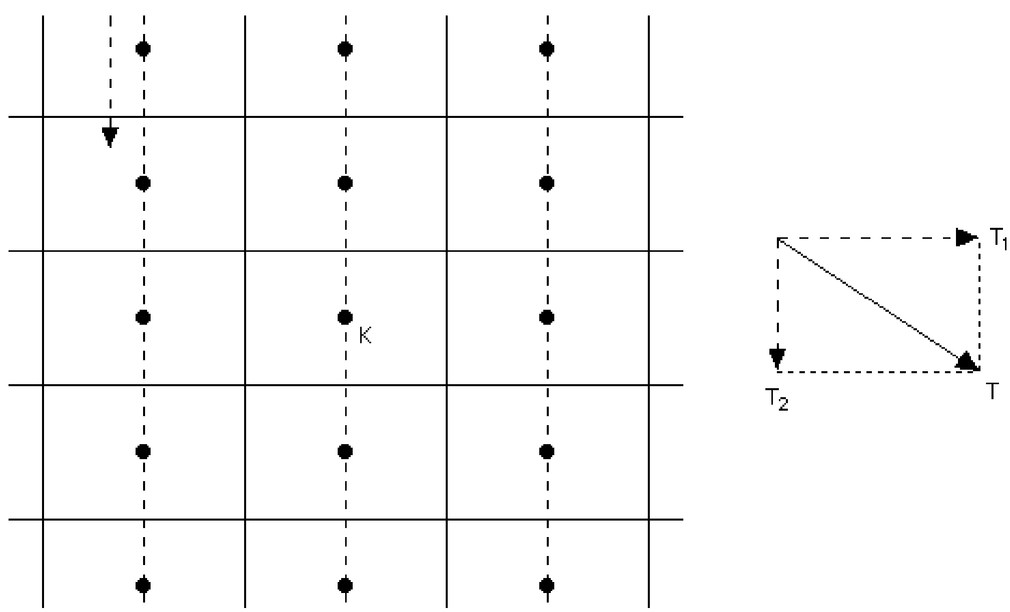

Fig. 8.33

Of course there was no way we were going to get anything but a **cm** in the horizontal direction (as already pointed out in 8.2.7). Still, we had to check that the horizontal **cm** factor would be the **same** in the two possible cases examined (half turn center on reflection axis or half turn center on glide reflection axis) in terms of translations, gliding vectors, etc; and figure 8.33 certainly makes that clear.

8.3 90^0 patterns

8.3.1 The lattice and the possibilities. It took us some time to 'build' the lattice of rotation centers for 180^0 patterns, be it with the help of translations only (**p2**, 7.6.4) or with the added assistance of (glide) reflection (**pgg**, **pmg**, **pmm**, **cmm** -- section 8.2). On the other hand, as we have seen in section 7.6, **just one** minimal translation suffices to build that lattice in the cases of 90^0, 120^0, and 60^0 patterns (starting from a **single** rotation center, always). This difference has dramatic consequences: unlike 180^0 lattices, all other lattices are **uniquely** determined and are **independent** of the (glide) reflection possibilities; in fact, as we will see below, it is now the lattice of rotation centers that **determines** the possible (glide) reflection interactions rather than the other way around!

To begin, observe that the lattice of rotation centers determines the **possible directions** of (glide) reflection in the case of a 90^0 pattern. Indeed the image of any segment AB, where A and B are two **closest possible** 90^0 centers, under **any** isometry could only run in **two** directions (figure 8.34); by 3.2.4, those yield at most **four** possible directions of (glide) reflection: images of AB under any two (glide) reflections are parallel if and only if their axes are either parallel or perpendicular to each other!

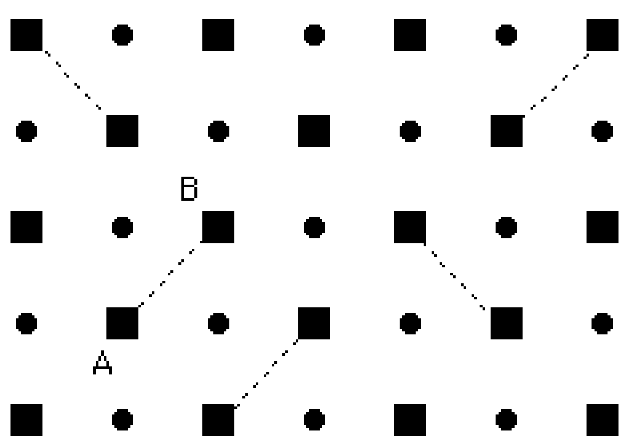

Fig. 8.34

Before we proceed into investigating the (glide) reflection structure of any given 90^0 pattern, we must of course ask: is there **any** (glide) reflection in the given pattern? If not, then the pattern only has 90^0 (and 180^0) rotation and translation, and it's no other than the familiar **p4** pattern of sections 4.12 and 6.10. Its structure has been discussed in 7.6.3 and it is also going to be further investigated in 8.3.2 below ... precisely because it is destined to play a very important role **even** in the presence of (glide) reflection!

8.3.2 Two fateful translations. Assuming from now on that our 90^0 pattern has (glide) reflection, let us notice first that sections 7.8 and 7.10 imply **precisely four** directions of (glide) reflection (indicated in fact in figures 8.34 and 8.35): **at least** four because the composition of a glide reflection with a 90^0 rotation generates another glide reflection making an angle of 45^0 with the original (section 7.8); and **at most** four because any two glide reflections intersecting each other at an angle smaller than 45^0 would generate a rotation by an angle smaller than 90^0 (section 7.10).

Further, the Conjugacy Principle implies that we must have the **same** type of **360^0 subpattern** in the 'vertical' and 'horizontal' directions (mapped to each other by the 90^0 rotation), and likewise for the two 'diagonal' directions; in particular, this **rules out** the **pmg** as a **180^0 subpattern**. Still, we are left, **in theory**, with **nine** combinations among **pmm**, **pgg**, and **cmm** 'factors'.

The way to eliminate most of these nine possibilities with very little work relies on the characterization of the **cm** pattern at the end of 8.1.9 **and** on the structure of the **p4** lattice investigated in 7.6.3 (and figure 7.23). Blending everything into figure 8.35 below, we examine whether or not the valid translations **t** and **T** may be analysed into valid translations in the diagonal and vertical-horizontal pair of directions, respectively:

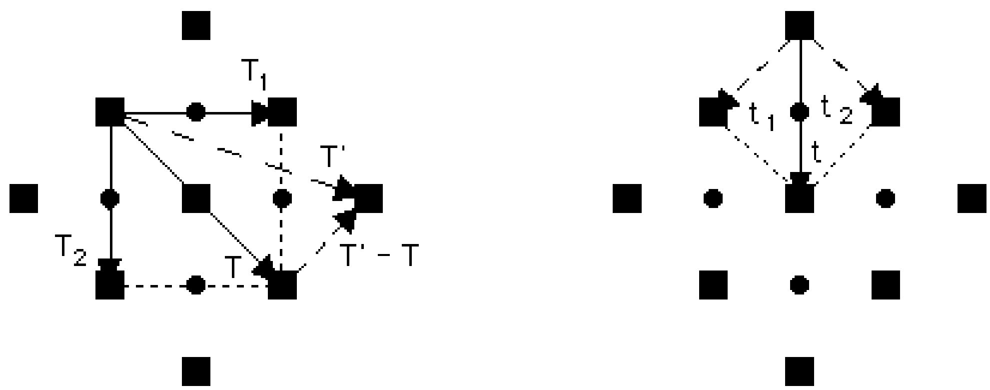

Fig. 8.35

On the right, the minimal vertical translation **t** may **certainly** be written as $\mathbf{t}_1+\mathbf{t}_2$, where $\mathbf{t}_1$ and $\mathbf{t}_2$ are **not** valid **diagonal** translations. On the left, we see that valid translations such as **T** may be analysed into sums of two valid **vertical** and **horizontal** translations (like the **minimal** translations $\mathbf{T}_1$ and $\mathbf{T}_2$), while 'non-analysable' translations such as **T′** are **not** valid to begin with (otherwise **T′ – T** would be a **valid** translation violating the minimality of $\mathbf{T}_1$ or $\mathbf{T}_2$); in fact some further analysis would easily show that **every** valid translation may only have **valid** vertical and horizontal components. (Here is a way to confirm that: observe that we may introduce a coordinate system so that all rotation centers have **integer** coordinates, the twofold centers one even and one odd, the fourfold centers either two even coordinates (**'even'** centers) or two odd coordinates (**'odd'** centers); a translation would then be valid if and only if it 'connects' two odd centers or, **equivalently**, two even centers -- that is if and only if it is of the form $<2k, 2l> = k \times \mathbf{T}_1 - l \times \mathbf{T}_2$, where $\mathbf{T}_1 = <2, 0>$ and $\mathbf{T}_2 = <0, -2>$.)

In view of our crucial remark in 8.1.9, two conclusions follow at once: **one**, in the pattern's vertical-horizontal directions we may only have a **pmm** (two perpendicular **pm**s) or **pgg** (two perpendicular **pg**s) subpattern; **two**, in the pattern's diagonal directions we may only have a **cmm** subpattern (two perpendicular **cm**s).

Focusing first on the diagonal (**cmm**) directions, we notice that the Conjugacy Principle allows for **two** possibilities: reflections passing either through the **fourfold** centers (figure 8.36, left) or through the **twofold** centers (figure 8.36, right).

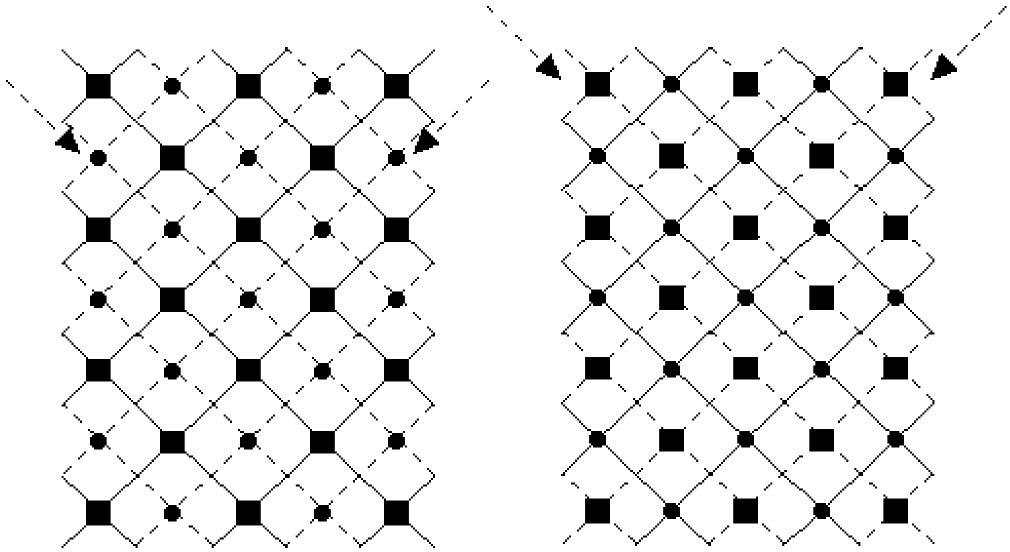

Fig. 8.36

Before examining the vertical-horizontal possibilities (**pmm** and **pgg**), let's have another look at the lattice of rotation centers in figure 8.36: while every two twofold centers may be mapped to each other by either a fourfold rotation (applied twice if necessary) or a translation, and every two fourfold centers on the right may be mapped to each other by some isometry (including a reflection or glide reflection), there exist fourfold centers on the left that may **not** be mapped to each other by any isometries; this is destined **not** to change (by the addition of vertical-horizontal isometries in figure 8.36), so the distinct notation for 'even' and 'odd' fourfold centers employed as early as in figure 4.5 is justified after all!

In theory, **each** of the two emerging 90^0 patterns of figure 8.36 should allow for **two** possibilities, **cmm** × **pmm** and **cmm** × **pgg**, bringing the maximum number of possible 90^0 patterns (with (glide) reflection) to **four**. But the actual situation is even simpler: by 7.7.1, we can only have either **none** or **four** reflections passing through a **fourfold** center; and this fact eliminates at once the **pgg** possibility on the left side and the **pmm** possibility on the right side of figure 8.36! So we are finally limited to **cmm** × **pmm** on the left and **cmm** × **pgg** on the right:

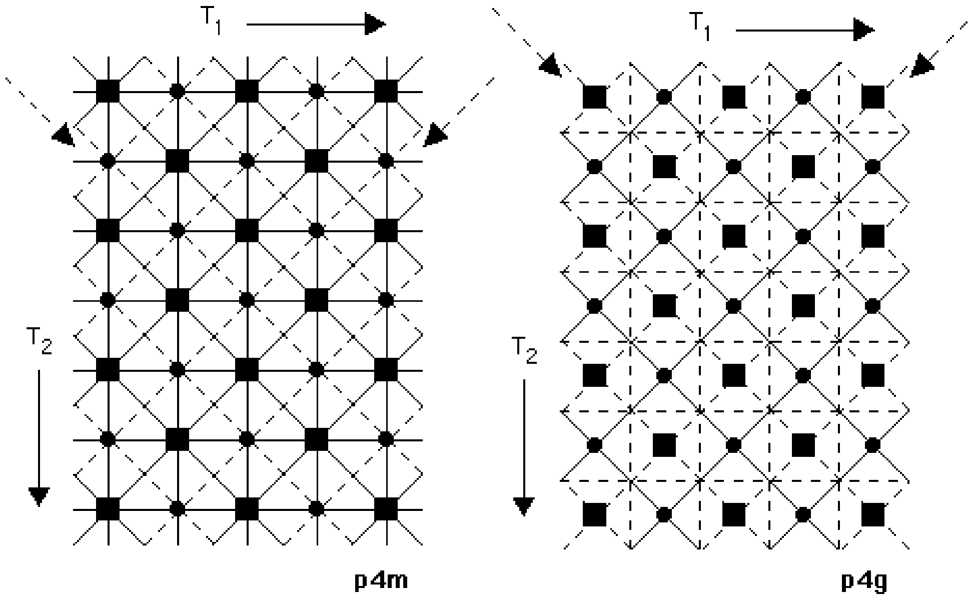

Fig. 8.37

But these patterns are the familiar **p4m** of sections 4.10 and 6.12 (left) and, after rotation by 45^0, **p4g** of sections 4.11 and 6.11 (right): the classification of the 90^0 patterns is now complete.

8.4 120^0 and 60^0 patterns

8.4.1 Two families, one lattice. The reason we are studying 120^0 patterns and 60^0 patterns in the same section is that, to a large extent, these two types share the same lattice of rotation centers. Let's have a look at the two lattices in figure 7.24 (**p3**, smallest rotation 120^0) and figure 7.25 (**p6**, smallest rotation 60^0): if we ignore the 180^0 centers of the latter and view its 60^0 centers as 120^0 centers, then it would indeed be identical to the former!

8.4.2 Six possible directions. Let's now look at the **p3** lattice and the possibilities for (glide) reflection, observing that a valid (glide) reflection direction in the **p6** lattice **must** provide a valid (glide) reflection direction in the **p3** lattice, and, although not obvious, vice versa (8.4.4). We argue as in 8.3.1 and figure 8.34, showing the underlying **hexagons** for clarity (figure 8.38); this time there are **three** possible directions for the image of AB, associated (via 3.2.4 again) with **six** possible directions of (glide) reflection:

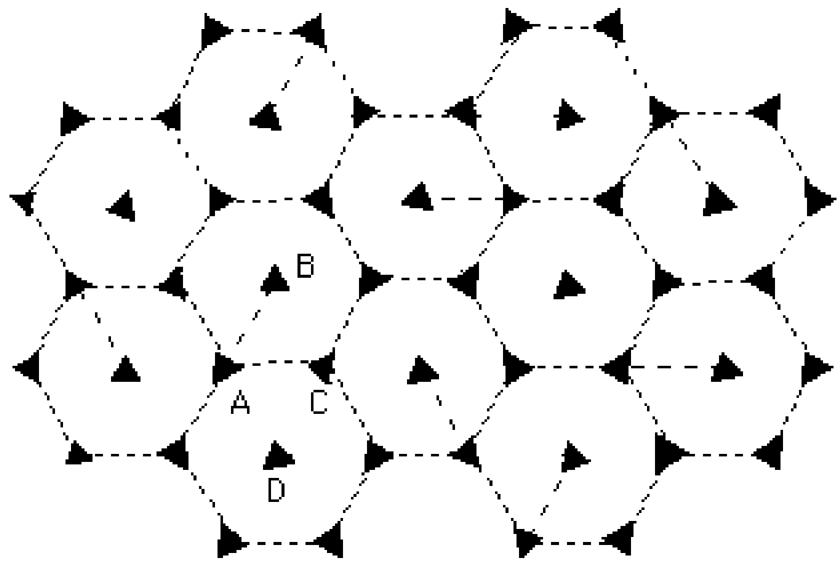

Fig. 8.38

Employing the methods of chapter 3 or otherwise, you should be able to see that the six possible directions are determined by pairs of either opposite vertices or opposite sides of any fixed hexagon (see figure 8.38). Assuming there is (glide) reflection, we need to decide, as we did in 8.3.2 for 90^0 patterns, **which type** among **pg**, **pm**, and **cm** we could get in each of the six directions; and, by the Conjugacy Principle (which **rotates** (glide) reflection axes by 120^0), we actually need to check only **two** directions (one perpendicular to AB and one parallel to AB), and in just **one** stroke at that:

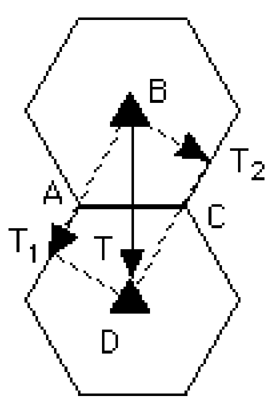

Fig. 8.39

What figure 8.39 offers is an analysis of the pattern's **minimal** (by 7.6.3) translation **T** into two components **parallel** to the two glide reflection directions, **none** of which is a valid translation: by 8.1.9, we can only have a **cm** 'factor' in **each** of those directions!

8.4.3 Threefold types. In the absence of any (glide) reflection, a 120^0 pattern may only be the familiar **p3** pattern of sections 4.15 and 6.13, also investigated (in fact **derived**) in 7.6.3. If there is (glide) reflection, then it has to exist through a **cm** subpattern in precisely **three** of the six directions derived in 8.4.2. Specifically, and referring to figures 8.39 & 8.17, there exist two possibilities: **one**, a **cm** subpattern in the direction of $\mathbf{T_2}$ (plus that **rotated** by 120^0 both ways), with reflection axes at a distance of $|\mathbf{T_1}|$ from each other and in-between glide reflection of gliding vector $\mathbf{T_2}$ (figure 8.40, right); **two**, reversing the roles of $\mathbf{T_1}$ and $\mathbf{T_2}$ in figure 8.17, a **cm** subpattern in the direction of $\mathbf{T_1}$ (plus that rotated by 120^0 both ways), with reflection axes at a distance of $|\mathbf{T_2}|$ from each other and in-between glide reflection of gliding vector $\mathbf{T_1}$ (figure 8.40, left).

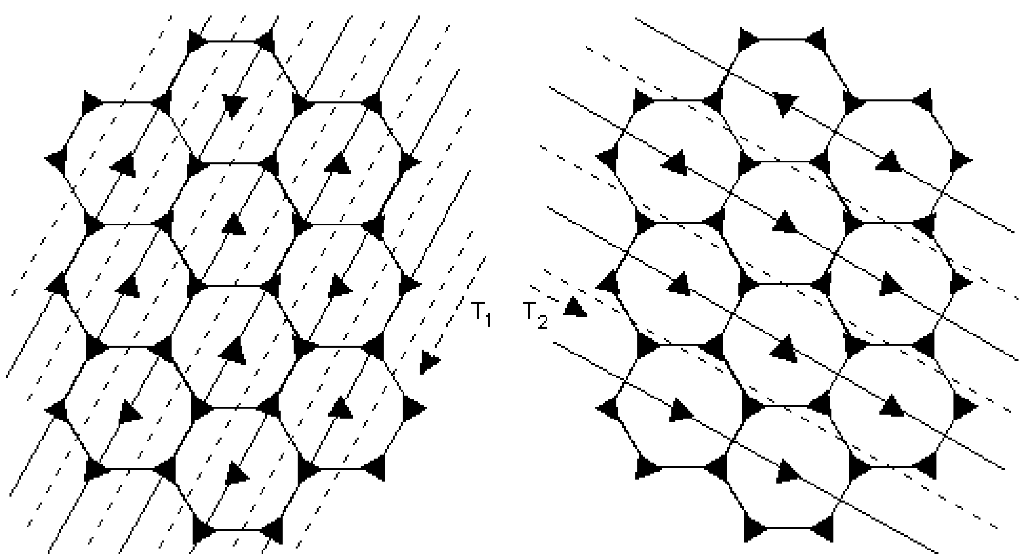

Fig. 8.40

A comparison between figure 8.36 (90^0 pattern generation) and figure 8.40 (120^0 pattern generation) is now appropriate: in figure

8.36, the direction of the two **cm** subpatterns was **uniquely** determined by the lattice, but there were **two** possible locations of the axes with respect to the centers; in figure 8.40, there are **two** possible **directions** of the three **cm** subpatterns, but the location of the axes with respect to the centers is **uniquely** determined within each of the two possible directions.

The **cm** subpatterns of figure 8.40 may now generate the two familiar 120^0 patterns shown in figure 8.41 (without the underlying hexagons or the gliding vectors): **p3m1** on the left (studied in sections 4.17 and 6.15) and **p31m** on the right (studied in sections 4.16 and 6.14); the classification of 120^0 patterns is now complete.

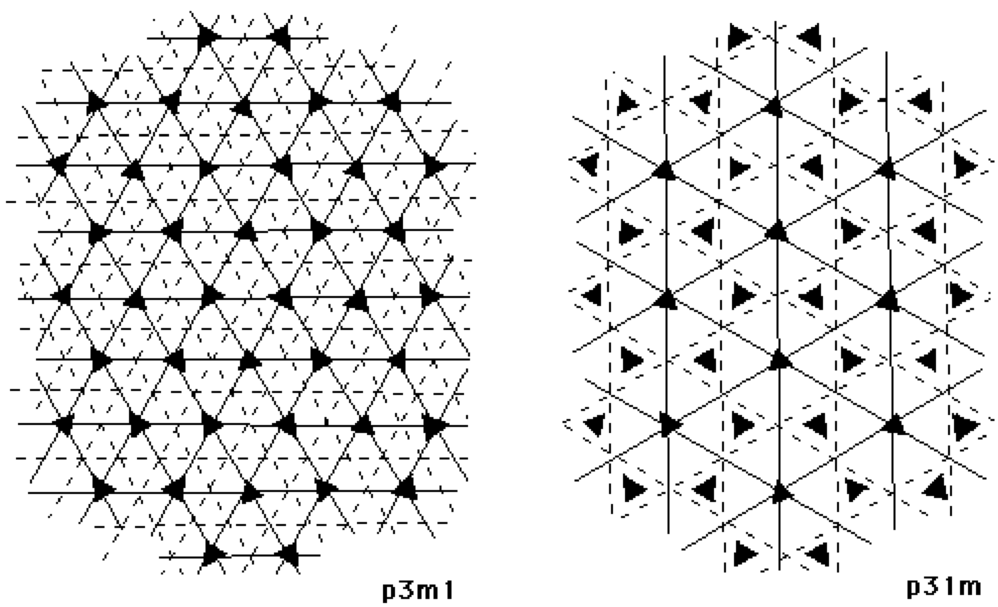

Fig. 8.41

Looking at figure 8.41 (or 8.40 for more clarity), we see that, remarkably, every two off-axis centers of the **p31m** may be mapped to each other by one of the pattern’s isometries (notably (**glide**) **reflection**), while there exist indeed **‘three kinds’** of centers in the **p3m1** (with no isometry swapping centers of different kind), and likewise in the **p3** (7.6.3): this confirms old observations from chapter 4! (Similar stories for 90^0 patterns: every two fourfold centers of a **p4g** are **‘conjugate’** of each other (thanks to (glide) reflection again), which is **not** true in either the **p4m** or the **p4**.)

8.4.4 Sixfold types. The last step of the classification is the easiest! Indeed, in the absence of any (glide) reflection there can only be the **p6** pattern of sections 4.14 and 6.16, also investigated (and **derived**) in 7.6.3. And in the presence of (glide) reflection, we need **all six** directions of 8.4.2, and it is still possible to show that we **must** have a **cm** subpattern in **all six** directions: all we need to do is make B and D **sixfold** centers in figure 8.39; and all other arguments and facts of 8.4.3 may also be extended, leading to the **p6m** pattern of sections 4.13 and 6.17 as the **'merge'** of **p3m1** and **p31m** featured in figures 6.132 & 6.133 (and figure 8.41 as well)! Here it is in its full glory, with $\mathbf{T_1}$ and $\mathbf{T_2}$ playing the **same roles** as in 8.4.2 & 8.4.3 (and figure 8.40) -- and all **'old'** glide reflections mapping **sixfold** centers to **sixfold** centers):

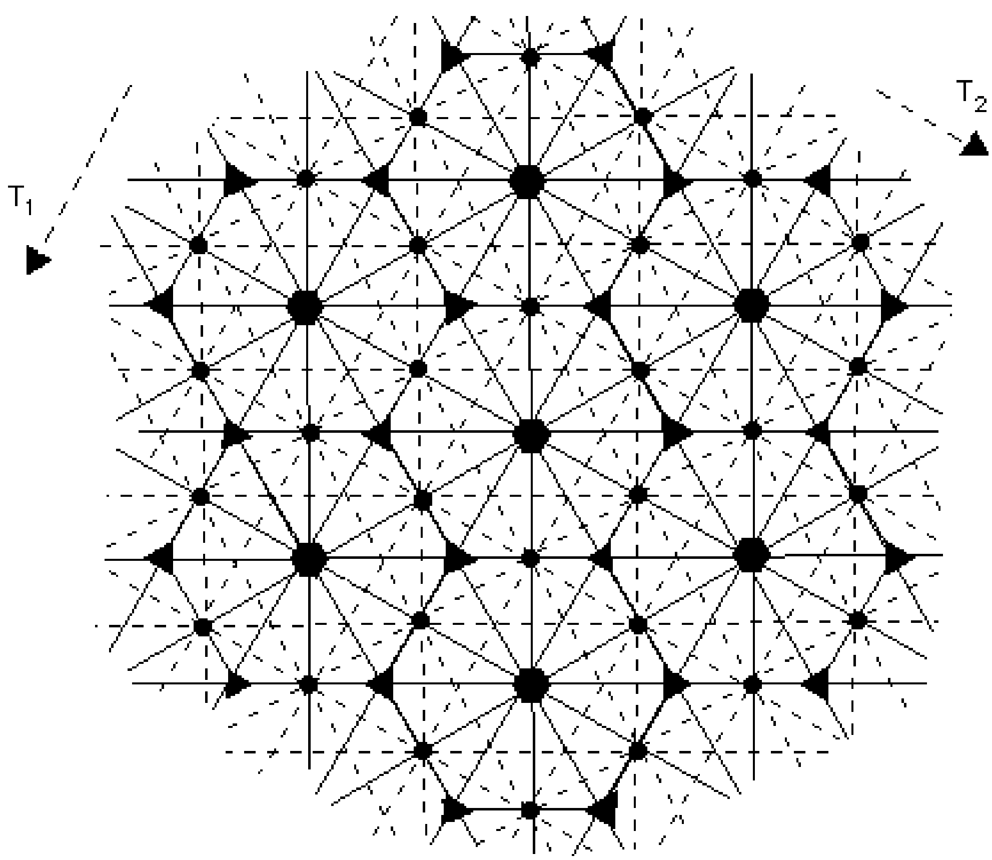

Fig. 8.42

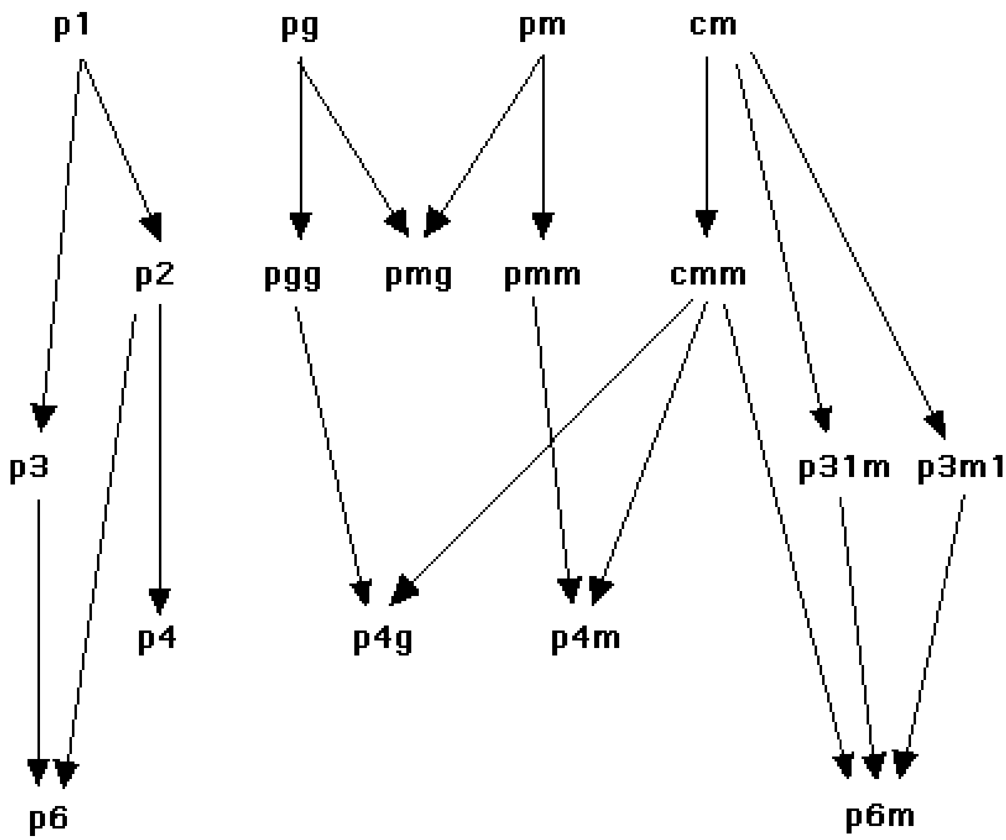
p1
pg
pm
cm
p2
pgg
pmg
pmm
cmm
p3
p31m
p3m1
p4
p4g
p4m
p6
p6m

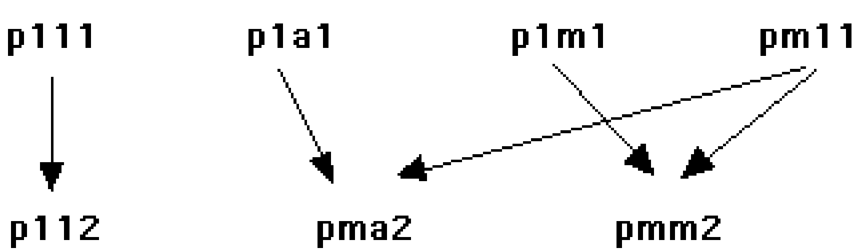
p111
p1a1
p1m1
pm11
p112
pma2
pmm2